# Investigation into the molecular function of the neuronal Hu RNA binding protein, HuCsv1

Peter James McCarthy

Discipline of Biochemistry,
School of Molecular and Biomedical Sciences,
University of Adelaide

A thesis submitted in fulfilment of the requirements for the Degree of Doctor of Philosophy

March 2011

## Table of Contents

## Acknowledgements

It is at once incredibly frustrating and completely fitting that the acknowledgements would be the most difficult part of the thesis to write. Not because it is difficult to think of people to acknowledge, but because it's hard to put into words how significant the role they've played has been in my getting to this point. Nevertheless, I'll do my best.

My first acknowledgement is for my sister Sarah. You have seen more than your fair share of my ups and downs throughout this PhD (and in general) and through it all have been an endless source of support, encouragement and inspiration. Both you and Mattt have been so important, especially through the home stretch of writing this thesis, and to you I am forever grateful.

Secondly, a very special acknowledgement for Ana, without whom it's fair to say I probably wouldn't ever have gotten to this point in the first place. Your drive and dedication to being the best at what you do is both humbling and inspiring. The love and support you gave me are what made this whole PhD possible and will always be a part of me.

Thirdly, to my mum and dad, who despite being very different people have always been role models for me as people who say what they mean, work hard to be the best at what they do and look after those they love.

I'd like to acknowledge my PhD supervisor Kirk Jensen for giving me an opportunity to do this PhD work in his lab and for teaching me to discern good science from bad science and helping me identify qualities that make good students, post-docs and supervisors. I sincerely believe that with this knowledge I can only be a better scientist.

Finally, I'd like to thank all the great people I've met and worked with throughout my time at the School of Molecular and Biomedical Sciences. Particularly Sophie, who made every day a good day in the lab, no matter how good or bad my experiments were going and whose friendship is one of the best things I take away from my time in the Jensen lab.

Sincerely,
P.

## Declaration of Originality

[*With the exception of this declaration*], this work contains no material which has been accepted for the award of any other degree or diploma in any university or other tertiary institution to Peter James McCarthy and, to the best of my knowledge and belief, contains no material previously published or written by another person, except where due reference has been made in the text. I give consent to this copy of my thesis, when deposited in the University Library, being made available for loan and photocopying, subject to the provisions of the Copyright Act 1968. I also give permission for the digital version of my thesis to be made available on the web, via the University's digital research repository, the Library catalogue, the Australasian Digital Theses Program (ADTP) and also through web search engines, unless permission has been granted by the University to restrict access for a period of time.

Signed,

Peter James McCarthy

## Abstract

Of the four Hu genes found in most vertebrates (HuA, HuB, HuC and HuD), all except HuA exhibit mRNA and protein expression that is essentially restricted to post-mitotic neurons of the developing and adult nervous systems. Spatial and temporal examination of individual "neuronal Hu" (nHu = HuB, HuC and HuD) proteins in brain tissue suggests nHu proteins may play a functional role during neuronal differentiation; as RNA-binding proteins, the nHu proteins may participate in gene regulatory events that are essential for acquisition of the neuronal phenotype.

We have identified a number of candidate mRNA targets of the nHu proteins. Our data suggest that the majority of these mRNAs interact with nHu proteins through sequences present in their 3′ untranslated regions (UTRs). From this 3′UTR target subset, several mRNAs were selected for further examination based on reported roles for their encoded proteins during axonogenesis, a critical developmental process during which nascent neurons grow and extend axons that eventually connect to and form synaptic connections with other neurons. The mRNAs chosen encode for cytoskeleton-modifying proteins; Cofilin, Vasodilator-Stimulated Phosphoprotein (VASP) and the Rho GTPase Cdc42.

The primary aim of the work reported in this thesis was to characterise the effect of interactions between the neuronal Hu protein HuC, and the CLIP-identified 3′UTRs listed above. To do this, the 3′UTR sequences were cloned into reporter vectors (both fluorescent and luciferase reporter-based) to produce reporter protein-encoding messages that included a putative target 3′UTR. These vectors were then used in co-transfection experiments with or without HuC and measurements of reporter protein and mRNA abundance obtained. Interestingly, despite initial speculation that HuC might be involved in directly regulating protein expression from target mRNAs, no significant effect of HuC on protein production from any of the 3′UTR-reporter mRNAs tested was observed. However and quite unexpectedly, measurement of 3′UTR-reporter mRNA abundance from co-transfection assays revealed a potential role for HuC in modulating alternative polyadenylation site choice for one of the CLIP-identified 3′UTR sequences. Regulation of mRNA polyadenylation site choice may be a novel mechanism by which nHu proteins post-transcriptionally control gene expression during neuronal development.

# Hu RNA-Binding Proteins

## Identification

### Auto-antigens in paraneoplastic neurological disorders

Hu RNA-binding proteins were identified over a decade ago as autoimmune targets in patients suffering from a paraneoplastic neurological disorder (PND) called Hu syndrome. Paraneoplastic neurological disorders are the result of an autoimmune response that specifically targets the nervous system, often leading to fatal neuronal degeneration [1]. Paraneoplastic neurological disorders occur when a systemic cancer, (such as small cell lung carcinoma, in the case of Hu-syndrome) mis-expresses a neuronal protein [2]. Importantly, under normal conditions, the nervous system is one of a handful of tissues that is largely isolated from the systemic immune system (others include tissues of the visual and reproductive systems). It is thought that the resulting immune-privileged status of these tissues evolved to protect organs that are critical for the survival and reproduction and are unable to undergo significant repair after injury, against damaging effects of inflammation that occur during an immune response [1]. However, by excluding the nervous system from exposure to the systemic immune system, tolerance of the immune system to neuronal auto-antigens is not acquired during development. As such, when expressed outside the brain, onconeural proteins are recognised as foreign antigens and invoke a powerful immune response. As a consequence, progression of the PND-associated cancer is generally limited and PND sufferers only present when the autoimmune response causes loss of nervous system function. How the systemic autoimmune response gains access to the normally immune privileged nervous tissue is still not fully understood. It is believed that loss of blood barrier integrity, potentially caused by a chemical agent or localised inflammatory incident is necessary to allow entry of the systemic immune system into nervous tissues [3]. Once the systemic immune system, which is primed to recognise and destroy the onconeural antigen, gains access to the nervous system, rapid neurodegeneration ensues, which is ultimately fatal.

Importantly, a hallmark feature of PNDs is the generation of auto-antibodies that specifically recognise the onconeural antigen [4], (reviewed in [1]). Both serum and spinal fluid from PND patients contain high titres of these antibodies, which have been used to identify and clone a number of neuronal proteins including the Hu proteins [2]. Early descriptions of the Hu-antigen involved probing protein purified from particular organs with Hu patient antisera [5], [6].

In 1985, Graus *et al* published the first description of anti-Hu immunoglobins in *Neurology*. In this paper, serum and cerebrospinal fluid (CSF) from patients with small cell lung carcinoma (SCLC) and sub-acute sensory polyneuropathy was used to probe protein extract from cerebrocortical neurons by Western blot [5]. Both the CSF and serum were shown to contain high titre autoantibodies reactive to proteins in the 35-40 kDa molecular weight range. The antibodies were designated anti-Hu antibodies from the first two letters of the patient's last name, Hu. Subsequent investigations demonstrated the presence of anti-Hu antibodies in the serum of patients suffering a variety of neuropathies including sensory neuronopathy, motor neuron dysfunction, cerebellar dysfunction, limbic encephalopathy, brainstem encephalopathy and autonomic nervous system failure [4],[6], [7]. These observations provided the first clues about the restricted expression of neuronal Hu proteins, indicating they were likely expressed throughout both the central and peripheral nervous systems.

## Cloning the first Hu gene - *HuD*

In 1991, the first Hu gene was identified through cloning from a human cerebellar λ ZAP cDNA expression library that was screened using Hu syndrome patient antisera [8]. The encoded protein was designated HuD and was shown to be expressed solely within tissue of the nervous system. The predicted amino acid sequence indicated the protein product was approximately 40kDa in size and contained three RNA-binding domains known as RNA recognition motifs (RRMs).

While the function of the protein was unknown, HuD was shown to be highly homologous to a (then) recently described RNA-binding protein present in *Drosophila* called ELAV (pronounced *Ela-vee*). Interestingly, the expression of *elav* (short for embryonic lethal, abnormal visual system, the phenotype of flies lacking this protein) had been shown to be restricted to the nervous system in developing and adult *Drosophila* [9], [10], specifically within committed neuronal cells [10], [11]. Furthermore, and quite intriguingly, *elav*-null *Drosophila* lines are embryonic lethal due to structural defects in the central nervous system [12]. Looking at later developmental stages, temperature sensitive mutants indicated that ELAV is autonomously required during development of the optic lobe and other neuronal tissues [12], [13].

Indeed, aside from cloning the first auto-antigen responsible for Hu-syndrome, demonstration of the homology between HuD and Elav was arguably the most significant finding of the paper from Szabo *et al*. The strong sequence conservation between HuD and ELAV combined with similar

tissue-specific expression invited speculation that, like ELAV, HuD plays an important role during the development of the nervous system of higher organisms.

## The Family of Hu RNA-binding proteins

Following the cloning of *HuD*, PND patient antisera-based cDNA library screening as well as degenerate PCR approaches revealed the presence of three more Hu genes in vertebrates, named *HuC*, *HuB* and *HuR* [8], [14], [15], [16], [17], [18], [19]. As with *HuD*, the expression of *HuC* and *HuB* was also found to be essentially restricted to the nervous system of both developing and adult vertebrates [8], [14], [16], [18]. Notably, expression of *HuB* was also detected in mouse testis [17] and *Xenopus* ovaries and during very early stages of *Xenopus* embryogenesis [18]. However, unlike the three neuronal Hu genes (nHu = HuB, HuC, HuD), expression of *HuR* (also known as *HuA*) was found ubiquitously in all vertebrates tested [18], [19]. As such, the Hu protein family members can be further divided into neuronally-expressed and ubiquitously-expressed sub-families.

A complete list with a brief description of each homolog is provided in Table 1.

### Hu RNA-binding proteins – homology, structure and isoforms

HuR is considered to be the ancestral member of the vertebrate Hu protein family, showing the least genetic divergence from ELAV [20]. Of the neuronal family members, HuC shows the least divergence from ELAV, followed by HuD and HuB. This is likely the order in which duplication of an ancestral Hu gene occurred, giving rise to the neuronal Hu family members. All four Hu proteins show a high degree of sequence homology ranging from 70-80% [20].

Like ELAV, the predicted protein structure of all four Hu proteins contains three RNA recognition motifs (RRMs) (figure 1a). The first two RRMs (approximately 90 residues each) are located in tandem less than 100 amino acids from the N-terminus of the protein. The third RRM is present at the very C-terminal end of the proteins and is separated from the second RRM by a "spacer" domain that can be alternatively spliced (figure 1b). Importantly, while not predicted to assume any defined tertiary structure, the spacer domain has been shown to confer nucleocytoplasmic shuttling activity [21], [22], [23].

While the HuR gene produces only a single HuR protein isoform, alternative splicing within the spacer domain-encoding region of the neuronal Hu mRNA results in the production of up to ten different highly conserved splice isoforms [20] (figure 2a-c). By way of example, conservation of the amino acid sequences across the alternatively spliced spacer region of HuC from several

different vertebrate species is presented in (figure 3). Interestingly, studies in our lab have found that alternative splicing in the spacer domain affects the steady-state subcellular distribution of Hu proteins within the cell. At steady-state, HuR and smallest splice isoforms of the neuronal Hu proteins are found predominantly within the nucleus. However, the introduction of additional amino acids sequences to the spacer domain through alternative splicing causes an increase in cytoplasmic localisation [24]. The role of the spacer region in mediating subcellular localisation is discussed below. For now it is sufficient to state that the small changes in protein size resulting alternative splicing are not responsible for altered subcellular distribution of the protein. Rather, the spacer region contains sequences that specifically dictate where in the cell a given Hu protein will predominate.

In addition to alternative splicing within the spacer domain, alternative transcription start sites have been identified for HuB and HuC leading to the production of mRNAs with different 5´UTR lengths and different N-termini (Supplementary figure 1 at end of chapter). The length of 3´UTR sequences for HuR and HuB have also been found to be variable as a result of alternative polyadenylation site usage (Supplementary figure 2 at end of chapter). Clearly then, within the family of four Hu RNA-binding proteins, complexity in possible Hu protein expression is introduced through alternative processing of encoding pre-mRNAs.

## Hu proteins - Functional protein domains

### *RNA recognition motifs (RRMs)*

The RRM is an evolutionarily conserved protein domain found in prokaria, eukaria and even some viruses [25]. The ~90 amino acid residue structure folds into an αβ sandwich structure with a four stranded antiparallel β-sheet against which two α-helices are packed [25]. The β-sheets are ordered β4-β1-β3-β2. RNA binding is dependent on two separate consensus sequences called RNP1 and RNP2 located within the β1 and β3 strands respectively [26], [27], [28]. Both consensus sequences are composed of predominantly positively charged and aromatic residues (RNP1 – Lys/Arg-Gly-Phe/Tyr-Gly/Ala-Phe/Tyr-Val/Ile/Leu-X-Phe/Tyr) (RNP2 = Ile/Val/Leu-Phe/Tyr-Ile/Val/Leu-X-Asn-Leu) (X = any amino acid) and have been shown to be both necessary and sufficient for RNA-binding activity of the motif (reviewed in [29], [30], [31]).

The core consensus binding sequences of RNP1 and RNP2 (β-strands 1 and 3 respectively) do not themselves confer strong sequence specificity in RNA binding [25]. Specificity in sequence recognition is provided by base-specific hydrogen bonding between the bases in the bound RNA and amino acid residues present within the β-strands 2 and 4, that surround the RNA-binding pocket but are not part of either RNP consensus sequence [25]. Furthermore, in isolation single RRMs can bind RNA sequences of up to 6 nucleotides in length with varying degrees of affinity (mM to nM range). However, in combination, multiple RRMs allow proteins to recognise longer nucleotide sequences with affinities in the sub-nanomolar range [32].

Importantly, while classically regarded as RNA-binding domains, RRMs are also well-documented protein-protein interfaces ([25] and references therein). However, unlike the highly conserved RNA interface, crystallographic analysis of protein-protein interactions through RRMs shows a diverse array of possible conformations to elicit binding [25].

***RRMs 1 and 2 co-operate to bind uracil-rich RNA sequences.***

Examination of the nucleic acid binding properties of Hu proteins has revealed a general preference for uracil-rich RNA sequences [16], [17], [33], [34], [35], [36]. Deletion analysis of HuR, HuC and HuD has shown that uracil-binding activity is conveyed primarily by the first two RRMs (Abe 1996 Nucleic Acids Res, [35], [36], a result that is supported by NMR studies using the first two RRMs of HuC [37]. In 2001, crystal structures of the first two RRMs of HuD in complex with one of two 11nt uracil-rich RNA sequences were solved [38]. The data revealed the two β-sheets of RRMs 1 and 2 form a cleft within which the target mRNA is bound. The arrangement of the RRMs places the two α-helices of each RRM on the opposite side of the β-sheet to RNA binding. The data identified key molecular interactions between amino acids within the RNP1 and RNP2 consensus sequences and uracil residues within the RNA sequence allowing for the loose prediction of a consensus RNA recognition sequence of N-Y-U-N-N-U-U-Y (where N = any nucleotide and Y = any pyrimidine U or C). Subsequent crystal structures of the first two RRMs of HuR bound to an 11-nt synthetic oligoribonucleotide (5′-AUUUUUAUUUU-3′) agree with the HuD RRM1-2 crystal structure [39].

***RRM3 acts independently binding adenylate-rich RNA sequences and potentially mediates protein-protein interactions***

Interestingly, unlike RRMs 1 and 2, RRM3 appears to preferentially bind adenylate-rich sequences and has been shown to specifically bind the poly(A) tail of target mRNAs [34], [36], [40]. RRM3 has also been suggested to serve as a protein-protein interaction domain, enabling

Hu proteins to form multimeric Hu complexes [41], [42], [43]. In a recent study, cooperative assembly of multimeric HuR complexes was demonstrated using a uracil-rich sequence from the TNFα 3′UTR [42]. Interestingly, in their paper, Fialcowitz-White *et al* show that deletion of the third RRM of HuR significantly reduces the incidence of HuR complex formation on the target mRNA sequence, suggesting that RRM3 is possibly involved in the assembly of HuR oligomers. This finding is supported by data from another study in which both yeast two-hybrid and co-immunoprecipitation were used to show HuD proteins interact and can form dimeric and trimeric complexes and that this ability was strongly reduced when the third RRM of HuD was deleted [41]. Importantly, Kasashima *et al* also show that interactions between Hu proteins are not solely dependent on an RNA intermediate and that some interaction is able to occur even in the absence of RNA, albeit to a lesser extent. Furthermore, they also show that interactions between Hu proteins are not necessarily homomeric, with GST-tagged versions of all three neuronal Hu proteins able to bind $^{35}$S-labelled HuD, even in the presence of RNAse A. Finally, similar results have been obtained in studies of ELAV, which also indicate ELAV can form homomeric complexes via the third RRM [44] through residues that are conserved in the Hu protein family [45]. Importantly, using a yeast-2-hybrid system, Toba *et al* showed that protein-protein interactions mediated by RRM3 rely on amino acid residues not directly involved in RNA binding. Indeed, the residues necessary for protein-protein interactions are arranged on the opposite side of the RRM to the RNA interface. In addition to this, specific replacement of residues at the RNA interface of RRM3 with corresponding residues from RRM2 (which was shown not to mediate protein-protein interactions) did not reduce the ability of the hybrid RRM3 to interact with wildtype RRM3. This experiment suggests that changing the RNA-sequence specificity of one RRM3 domain, does not affect its ability to interact with other RRM3 domains. From these experiments, Toba *et al* proposed that RNA-binding activity of RRM3 would not be sterically blocked by multimerisation and that while ELAV-ELAV interactions required the presence of RNA, this requirement was more likely due to conformational changes in RRM3 following mRNA binding that promoted protein-protein interactions, rather than the RNA merely acting as a scaffold for multiple bound ELAV proteins.

***The spacer domain - Nucleocytoplasmic shuttling of Hu proteins***

Observation of nucleocytoplasmic shuttling of Hu proteins was first made for HuR [21]. Using heterokaryon assays, Fan *et al* showed that HuR transiently overexpressed in human HeLa cells was able to translocate out of the nucleus and localise to the nucleus of a mouse fibroblast cell (NIH3T3) following fusing of the two cell's cytoplasms, such that the nuclei occupied the same cytoplasmic space. In subsequent work, Fan et al showed that this activity was dependent on the

presence of the short (~55 amino acids) spacer domain that links RRM2 to RRM3 [22]. Through further characterisation, a 32 amino acid region within the spacer domain that is enriched in basic residues (204 – RRFGGPVHHQAQRFRFSPMGVDHMSGLGVNVP – 238) was shown to be the minimal shuttling sequence able to confer both nuclear localisation and nuclear export activity on HuR. This sequence was designated as the HNS, short for HuR Nucleocytoplasmic Shuttling sequence (figure 1b).

Following identification of the HNS, the HuR import and export pathways were identified. The CRM-1 dependent nuclear export pathway was the first identified mechanism by which HuR is exported from the nucleus. Export via CRM-1 occurs through interactions between CRM-1 and hydrophobic amino acids (typically leucine) present within its "cargo" protein or intermediate proteins, which in turn bind to the "cargo" protein [46]. Common nuclear ligand proteins that facilitate CRM-1 -dependent nuclear export are pp32 and pp32 and Acidic-Protein-Rich-In-Leucine (APRIL) (reviewed in [47]). HuR has been shown to use the CRM-1 dependent export pathway, through specific interactions with pp32 and APRIL [48]. Notably, CRM-1 –dependent nuclear export can be blocked by treatment with the anti-fungal antibiotic leptomycin B, which blocks CRM-1/cargo interactions [49]. Interestingly, treatment of cells with leptomycin B does not completely block nuclear export of HuR [48]. This observation led to the identification of a separate export pathway involving a direct interaction between HuR and transportins 1 and 2 [50], [51]. Transportins are members of the importin β family of nuclear transporters and serve in both the import and export of another RNA-binding protein, hnRNP A1, to and from the nucleus [52], [53]. Nuclear import of HuR is also mediated by transportin 2 [54]. In both cases, transportin 2 interacts directly with the HNS sequence [50], [51].

***Alternative splicing in the spacer domain of neuronal Hu proteins***

In the neuronal Hu proteins, alternative splicing introduces additional sequence within the spacer domain, generating a number of protein isoforms (figure 2a-c). Importantly, the insertion of additional sequence occurs within the region identified as the HNS in HuR. To date, little has been reported on the outcome of alternative nHu mRNA processing in terms subcellular localisation or function. However, studies in our lab have found that the insertion of sequences within the HNS by alternative splicing leads to a switch in steady-state subcellular distribution of nHu proteins [24]. Specifically, nHu splice isoforms for which no additional sequence is included in the HNS region localise in a similar manner to HuR, showing significant nuclear abundance at steady-state. Conversely, the introduction of additional sequences into the HNS regions of HuC and HuD by alternative splicing leads to much higher cytoplasmic abundance at steady-state.

This suggests that the included sequences, which contain a number of leucine residues, have some influence over the nucleocytoplasmic shuttling properties of the HNS.

There are two general mechanisms by which the introduced sequences could affect steady-state subcellular distribution of nHu proteins:

- Increasing nuclear export of longer nHu splice variants
- Decreasing nuclear import

In the first case, the prevalence of leucine residues within the introduced sequences may facilitate more efficient export of longer nHu splice variants from the nucleus, by enabling CRM-1-dependent export without the requirement for (or with reduced requirement for) the binding of nuclear ligands such as pp32 or APRIL.

In the second case, it is also possible that once outside the nucleus, the introduced sequences mediate protein-protein interactions or are specifically post-translationally modified in a way that results in greater cytoplasmic retention. Recently, the spacer domain of the longest HuD splice variant (HuDsv1), which includes the most interrupting sequence within its HNS-like sequence was found to interact with the eukaryotic translation initiation factor eIF4A [40], [23]. Using an alanine-substitution mutagenesis screen in combination with co-immunoprecipitation, the authors identified a single amino acid within the HNS region (F278) necessary for interaction with eIF4A. They went on to show that the F278A mutation abolished the ability of HuDsv1 to enhance cap-dependent translation in an *in vitro* luciferase-based reporter assay. Interestingly, F278 is present in the HNS-region of all Hu proteins, suggesting this interaction on its own is unlikely to cause the specific retention of longer splice variants in the cytoplasm. Importantly, the authors did not identify the reciprocal HuD-interaction site of eIF4A and thus, were unable to test whether loss of eIF4A binding to wildtype HuDsv1 also results in reduced translation enhancement by HuD. Nor did they test other nHu splice variants, such as HuDsv4, which includes the phenylalanine residue present at position 278 in HuDsv1 but does not include sequences within the HNS added by alternative splicing. As such, it is possible that in addition to interacting with eIF4A, sequences unique to the longer HuD splice variant mediate further interactions that facilitate enhancement of translation. Specific interaction of longer splice variants with the components of the translation machinery is an obvious mechanism by which the stay of nHu proteins in the cytoplasm could be lengthened.

## A review of the current literature regarding Hu protein function

### HuR, a regulator of mRNA stability

To date, HuR has been the most heavily studied of the Hu RNA-binding proteins. Interestingly, from this research, a substantial amount of data has been published that indicates HuR is an important regulator of mRNA stability in the cytoplasm, despite its considerable steady-state nuclear presence. Specifically, HuR has been reported to stabilise several rapidly turned-over mRNAs through direct binding to classical mRNA destabilising elements called AU-rich elements present within the target message 3´UTR [55], [56], [21], [57]. AU-rich elements are characterised by a localised high incidence of adenosine and uracil residues within a short (50-150nt) nucleotide region of a 3´UTR (reviewed in [58]. Many AREs can be identified by the presence of AUUUA pentameric or UUAUUUA(U/A)(U/A) nonameric sequences. However, a number of AREs have been identified that do not contain these sequences and are simply A/U-rich [59], [58], [60]– *and associated online database - http://brp.kfshrc.edu.sa/ARED/*. Finally, not all A/U-rich sequences cause mRNA destabilisation [59], [58].

AREs that destabilise mRNAs do so by serving as binding sites for specific RNA-binding proteins that actively recruit the message to the exosome [61]. In the exosome, degradation of ARE-containing mRNA then occurs in a two-step process [62], [63]. In the first step, the polyadenylate tail undergoes rapid deadenylation, shortening to approximately 30-60nts. Following deadenylation, the remaining mRNA sequence rapidly decays. AREs are typically found in mRNAs whose expression is tightly controlled, such as those encoding proteins involved in proliferation, responses of the immune system and responses to cell stress [60]. The presence of AREs in these mRNAs ensures their rapid turnover, preventing prolonged or premature production of their encoded proteins.

The first observations of HuR-mediated mRNA stabilisation were made for the ARE-containing mRNAs of VEGF [55], c-fos [56], [21], and GM-CSF [21]. A number of important observations were made in these papers. Firstly, Fan and Steitz demonstrated that stabilisation of the c-fos and GM-CSF mRNAs was specific to HuR and could not be mediated by another RRM-containing RNA-binding protein (hnRNP A0) that had previously been reported to interact with AU-rich elements and is expressed at similar levels to HuR in the cell line (HeLa) tested [21]. Secondly, Fan and Steitz showed that mRNA stabilisation was contingent on the presence of RRM3, with a total loss of mRNA stabilisation in experiments using an HuR overexpression construct lacking

the third RRM. When taken in context with the observation that RRM3 preferentially interacts with poly(A) sequences [34], [36], [40]this finding sets up a simple model in which HuR binding to AREs within target mRNAs promotes mRNA stabilisation in a mechanism involving an interaction with the poly(A) tail. In support of this model, Fan and Steitz state (*although no data was provided*) that HuR had no effect on the decay kinetics of ARE-containing target RNA that lacked a poly(A) tail [21]. Finally, the work by Peng *et al*, showed that modulation of HuR cytoplasmic localisation resulted in observable changes in c-fos mRNA stability. Specifically, increased presence of HuR in the cytoplasm was directly associated with increased stability of the c-fos mRNA. This finding was seminal to subsequent papers correlating changes in the expression of putative HuR target mRNAs with HuR relocalisation from the nucleus to the cytoplasm in response to specific cellular stimuli [64], [65], [66], [67], [68]and others.

Subsequent reports on HuR-mediated mRNA stabilisation implicate HuR in the regulation of half-life and translation for a number of mRNAs with uracil-rich 3´UTRs. Target messages that feature most prominently in the literature are generally mRNAs that encode protein products known to play important roles in the development and progression of cancer. These include protooncogenes such as c-fos and c-myc [21], [69], [70] as well as regulators of the cell cycle and apoptosis including cyclin B1, cyclin D1, cdk1, mdm2, and $p21^{Cip/Waf}$ [64], [71], [72], [73], [74], and common cancer markers cox-2 and VEGF [55], [75], [76], [77]. Importantly, much the literature describing HuR targets does not include definitive identification of HuR-mRNA interactions. Instead, changes in HuR expression and/or subcellular localisation are simply correlated with altered behaviour of putative target mRNAs because of the presence of AU-rich sequences within their 3´UTRs [78], [79]. Much of this is driven by the (overwhelming) observation that HuR expression is increased in a number of cancer cell lines [80], [81], [82], [79], just to list a few. Given the reported association of HuR with several known cancer related mRNAs, reports demonstrating increased cytoplasmic localisation of HuR coincident with increased mRNA/protein abundance of putative mRNA targets have been used as evidence to support a functional role of HuR in the regulation of these mRNAs, when no biological function has yet been ascribed. As such, while HuR has been clearly shown to increase the half-life of a number of mRNAs whose 3´UTRs contain uracil-rich sequences, caution is required when correlating changes in HuR expression or subcellular localisation with altered behaviour of potential target mRNAs.

## Activation of HuR

A common theme to the majority of papers examining HuR function is the requirement for some form of external stimuli to trigger changes in HuR activity (reviewed in [83]). In a large proportion of cases, such triggers come in the form of cell stress paradigms including hypoxia [55], [84], UV irradiation [85], [66], [86], γ-irradiation [72]oxidative stress [87], [88]and nutrient deprivation [89], [90]. In all cases, an increase in the cytoplasmic presence of HuR is observed and found to result in physiologically relevant changes in expression from target mRNAs whose products are involved in responses to cell stress and or DNA damage. However, more recent examination of HuR in such paradigms has revealed direct post-translational modifications of HuR, particularly by phosphorylation, which are necessary for its reported functions ([83] and references therein).

### *Activation by cell stress*

The most complete example of how phosphorylation of HuR regulates its function comes from two paradigms in which DNA damage triggers a biological response by HuR. The story begins with the observation that following DNA damage, HuR levels in the cytoplasm rapidly increase [64]. At the molecular level, DNA damage causes the activation of checkpoint kinase 2 (Chk2 – a key inhibitor of cell cycle progression in response to DNA damage) [91], [87]), which directly phosphorylates HuR on serine and threonine residues present within RRMs 1 and 2 [87]. Phosphorylation of HuR at these residues is associated with the release of the ARE-containing mRNAs encoding SIRT1 (an anti-apoptotitic factor [92] and cyclins D1 and A (regulators of cell cycle progression [93], [94] from binding by HuR and a concomitant increase in binding by HuR to the 3´UTRs of mRNAs encoding ProTα (a regulator of gene expression in response to oxidative stress – [95] and p21 (an inhibitor of cell cycle progression [96], [87]. This result reveals that specificity of mRNA-target binding by HuR (and conceivably other Hu proteins) can be directly modulated by post-translational modifications to its RNA-binding domains.

Importantly, phosphorylation of HuR by chk2 **does not** influence HuR subcellular localisation [87]. Instead, movement of HuR into the cytoplasm can be regulated by another cell cycle associated kinase, cdk1 (cell cycle dependent kinase) [86], [68]. In its active state (unphosphorylated), cdk1 promotes cell cycle progression through the G2/M phase transition [97]. However, under conditions in which cell cycle progression is not desired (such as in response to DNA damage or cell stress), cdk1 is phosphorylated, resulting in the inhibition of its kinase activity and subsequent cell cycle arrest.

In their paper, Kim *et al* show that active cdk1 directly phosphorylates HuR at a serine residue (S202) present within the spacer domain [86]. Phosphorylation of HuR by cdk1 results in the predominantly nuclear localisation of HuR characteristic of healthy, cycling cells. Contrastingly, inactivation of cdk1 prevents phosphorylation of HuR within its spacer domain leading to increased abundance of HuR within the cytoplasm, as is seen in cells following DNA damage or cell stress. As such, the paper identifies a key post-translational modification of HuR, within its spacer domain, that regulates its nucleocytoplasmic shuttling activity. In normal, mitotically active cells, Kim *et al*, propose that cdk1 could influence HuR subcellular localisation throughout the cell cycle and suggest that this activity could be a requirement for modulating the expression of HuR-target mRNAs encoding cell cycle regulators.

However, the findings of the Kim paper have even greater significance in terms of understanding the regulation of HuRs response during cell stress. As well as phosphorylating HuR in response to DNA damage, chk2 directly phosphorylates cdk1, rendering it inactive and promoting cell cycle arrest. By inactivating cdk1, chk2 phosphorylation indirectly regulates HuR subcellular localisation, preventing its phosphorylation by cdk1, resulting in increased levels of HuR in the cytoplasm. As such, the findings of the Adbelmohsen and Kim papers reveal a mechanism by which the responses of HuR to DNA damaging cell stress are linked to a network of signalling pathways that control cell cycle progression and responses to DNA damage. Notably, the serine residue (S202) in HuR phosphorylated by cdk1 is conserved in the spacer domains of all the neuronal Hu proteins in mouse (figure 1 and figure 2a-c). As such, it is possible that the subcellular distribution of neuronal members of the Hu family could also be influenced by phosphorylation at this residue.

## Other roles for HuR

### *De-repression of miRNA-mediated translation silencing*

In addition its role as an mRNA stabilising agent, HuR has been show to be involved in regulating microRNA (miRNA) control of mRNA expression. Under normal cellular conditions, translation of the mRNA encoding cationic amino acid transporter (CAT-1) is repressed through the binding of microRNA 122 (miR-122) and subsequent sequestration into P-bodies (processing bodies) within the cytoplasm [90]. Recruitment of this mRNA to P-bodies is associated with a dramatic reduction in mRNA translatability and increased rate of mRNA decay [98]. Interestingly, repression of the CAT-1 mRNA is relieved in response to amino acid deprivation (and other

stresses) in a manner that was found to be dependent on HuR [90]. Specifically, in response to stress, HuR was shown to translocate to the cytoplasm and interact with the 3´UTR of the CAT-1 mRNA, at a site independent from the binding sites of miR-122. Interaction with HuR resulted in translocation of the CAT-1 mRNA from translationally silent P-body complexes to actively translating polysomes. Importantly, in the absence of miR-122 binding sites, HuR had no effect on the expression of the CAT-1 mRNA indicating HuR itself did not stimulate increased CAT-1 mRNA translation. From these data it is possible that the effect of HuR on relieving miR-122-mediated translational repression of the CAT-1 mRNA occurs through some effect of HuR in antagonising factors that restrict the miRNA-bound CAT-1 mRNA to P-bodies.

To date, the findings presented by Bhattacharya *et al*, are the first (and only) example of a mechanism by which increased expression of an HuR target-mRNA is the result of an HuR-dependent relief from miRNA-mediated repression. However, given these finding it may be pertinent to reassess the interpretation of previously described HuR-mediated mRNA stabilisation experiments in which mRNA stability and translation increase following activation of HuR.

***A developmentally important regulator of gene expression***

Finally, two recently published mouse HuR knockout papers indicate HuR is essential during embryonic development and in post-natal life [99], [73].

Katsanou *et al* (and Ghosh *et al*) report that in mice, HuR knockout results in a complicated embryonic lethal phenotype that shows roles for HuR in a number of important developmental stages. HuR was shown to be necessary for proper differentiation of the extraembryonic tissues that form the placenta and vascularisation of the growing embryo. Conditional knockouts in which extraembryonic tissues retain wildtype HuR expression levels progress further than obligate HuR knockouts but are still embryonic lethal with serious defects in limb outgrowth and patterning, bone ossification and development of the spleen.

Analysis of mRNA expression by microarray revealed ~400 differentially expressed genes comparing $HuR^{-/-}$ and $HuR^{+/-}$ mouse embryonic fibroblasts. Unsurprisingly, the most frequent gene ontology terms associated mRNAs within the identified genes fell in categories for cell proliferation, anatomical structure specification and developmental morphogenesis. From this list, differential expression of 19 out of 23 mRNA considered functionally relevant to the defects observed in the $HuR^{-/-}$ mice were confirmed by qRT-PCR. Of these 6 were confirmed to interact

with HuR in $HuR^{+/+}$ MEFs by RNA-IP experiments specifically immunoprecipitating HuR. The apparently small number of putative HuR target mRNAs identified in this paper underscores the difficulty associated with trying to determine RNA-binding protein function by examining general changes in gene expression in a whole organism knockout with complex developmental abnormalities. While this paper did not identify a mechanism by which loss of HuR results in the identified developmental abnormalities, the knockout phenotypes demonstrate HuR plays an important role in regulated gene expression throughout embryogenesis.

Ghosh *et al* employed a more simple approach to examine loss of HuR function in a whole organism model. In their paper, they used a tamoxifen-inducible HuR knockout mouse line to globally ablate HuR expression in postnatal (8 week old) mice. Loss of HuR expression was confirmed following treatment with tamoxifen. As seen in obligate HuR knockouts, postnatal loss of HuR was not conducive with survival and conditional HuR-/- mice died within 10 days of tamoxifen treatment. Notably, in this post-natal knockout model loss of HuR expression resulted in a comparably simpler phenotype to that of Katsanou *et al*. A profound loss of cells in the bone marrow, thymus, spleen and lymph nodes indicated a significant effect on haematopoiesis and was supported by a strong reduction in average circulating white blood cell counts. Interestingly, detailed analysis of cell types present within the bone marrow revealed no obvious reduction in haematopoietic stem cell (HSC) numbers. However, lineage-specific progenitor cells that derive from HSCs (*eg* lymphoid, myeloid, erythroid and B-cell progenitor cells) were noticeably depleted. Similar results were observed in the thymus (location of T-cell progenitors) and in the crypts of the small intestine (location of intestinal epithelial progenitor cells). Loss of progenitor cells types was associated with high amounts of apoptosis in the affected tissues. The cause of progenitor cell loss was shown to be cell-autonomous by transplanting bone marrow from uninduced knockout mice (ie HuR gene still present and expressed) into congenic wildtype mice (γ-irradiated). Following treatment with tamoxifen, progenitor cell numbers in the bone marrow and thymus of mice that received bone marrow from the tamoxifen-inducible line were reduced to a similar extent to that observed in the non-transplanted tamoxifen-inducible mice. Contrastingly, no reduction in intestinal epithelial progenitor cells number was observed in these animals.

Subsequent examination of global changes in gene expression in bone marrow of knockout mice by microarray showed a clear upregulation of proapoptotic genes and cell cycle inhibitors. Notable in these results was the activation of the p53 pathway as evidenced by increased

expression of p53 and its downstream target $p21^{Cip1/Waf1}$ (an inhibitor of cell cycle progression [96]), contrasted by reduced expression of mdm2 (a critical negative regulator of p53 – [100]). Changes in mRNA expression levels of p53, $p21^{Cip1/Waf1}$ and mdm2 were mirrored in western blot analysis of respective protein expression. Examination of the mdm2 3´UTR revealed the presence of a number of ARE-like sequences. RNA-IP of HuR from wildtype MEFs demonstrated HuR associates with the mdm2 mRNA. Comparison of mdm2 mRNA half-life in wildtype versus knockout MEFs following actinomycin treatment to block transcription showed the mdm2 mRNA half-life was reduced in knockout cells. Finally, proliferation of MEFs from tamoxifen-inducible HuR knockout mice was shown to be reduced following treatment with tamoxifen (along with a reduction in HuR expression). However, loss of proliferation could be rescued by overexpression of mdm2 in tamoxifen treated cells. In total these results strongly implicate disregulation of the p53 proapoptotic pathway, through loss of HuR-mediated control of mdm2 expression, in the loss of mitotically active progenitor cells of HuR knockout mice.

The results from the Ghosh paper indicate regulation of apoptosis by HuR is most critical in actively dividing cells as no effect was reported for terminally differentiated or slowly dividing stem cell populations. Interestingly, HuR expression is clearly higher in the actively dividing precursor cell populations compared to the surrounding differentiated tissues in tissue samples presented within the paper. As such, high HuR expression appears to be correlated with high mitotic activity a finding that is corroborated by a subsequent study that showed HuR expression is strongly reduced in senescent cells [101]. The data from the Ghosh paper supports a model in which HuR expression is necessary in these cells to avoid induction of apoptosis. This result is in some sense ways contradictory to the results from the Katsanou paper, which showed no evidence of apoptosis in $HuR^{-/-}$ embryos up to 8dpc. Given cell division is a requisite part of embryogenesis it is hard to understand any cell division was possible at all in these embryos. As such, the role of HuR in protecting progenitor cells from apoptosis may be a specialised function that is served through different mechanisms in stem cell and terminally differentiated cell types.

## Conclusions on HuR function in light of the current literature

In summary, the current literature indicates HuR is an RNA-binding protein that specifically interacts with uracil-rich sequences present within the 3´UTR of target mRNAs. In specific cases, HuR has been shown to directly influence the stability, expression and localisation of target messages. In terms of its roles within the cell, the current data indicates HuR is involved in post-transcriptionally regulating gene expression controlling cell cycle progression, cellular responses to stress and apoptosis. In this role, HuR appears to act in a predominantly pro-survival manner. Genetic investigation into the consequences of disregulated HuR expression during development suggest HuR is fundamentally required for the survival of mitotically active cells, in particular stem cell-derived progenitor cell lineages of both mesodermal (bone marrow) and endodermal (intestinal epithelium) origin, in agreement with it's pro-survival activity identified in more molecular studies. This role appears somewhat cell type specific, as less lineage restricted stem cell types (such as HSCs, ESCs etc) do not show disregulated apoptosis, suggesting a difference in the regulation of apoptotic pathways (such as the p53 pathway) between these two mitotically active cell types. It is possible then, that expression of HuR is an important determinant of progenitor cell identity; assuming some level of control over cell cycle and survival pathways to allow lineage-restricted progenitor cells to maintain active cell division in a context where other stem cell-like properties have been lost. The results from recent HuR-knockout mouse studies warrant further investigation into the control of cell cycle and apoptosis pathways between stem, progenitor and terminally differentiated cell types of a common lineage (such as hematopoietic cells), in the context of HuR with a view to distinguishing how and when regulation of these pathways by HuR becomes important.

## A review of the current literature regarding the function of the neuronal Hu proteins

As shown, research into the function of the ubiquitously expressed Hu protein, HuR has been aided significantly by the identification of stimuli that cause changes in its localisation and RNA-binding activity. Studies into the function of the neuronal Hu proteins (nHu = HuB, HuC and HuD) have also tried to identify biological triggers that result in differential modulation of nHu behaviour. Examination into the timing of nHu expression both at the cellular level and within the whole organism in combination with transgenic models for gain and loss of nHu expression strongly suggest nHu proteins are important in the assumption and maintenance of neuronal identity. However, while studies focusing on nHu proteins at a molecular level implicate them in a variety of biological processes that affect mRNA metabolism, a mechanism that convincingly unifies these processes in a model of nHu protein function is still yet to evolve.

### Developmental expression of the neuronal Hu RNA-binding proteins

From the work identifying nHu proteins, it was clear that neuronal Hu protein expression occurs throughout the central and peripheral nervous systems of both developing and mature vertebrate organisms. However, experiments examining the timing of neuronal Hu protein expression during embryonic development may provide important clues about its biological role.

Development of the vertebrate nervous system begins with the formation of the neural plate. The neural plate forms along the midline of the vertebrate embryo shortly after gastrulation. Once formed, the neural plate develops two bilateral neural folds that run along the rostro-caudal axis of the plate. Through a process called neurulation the neural folds fuse along the midline forming the neural tube [102]. The space within the tube is referred to as the ventricular space. Neuronal progenitor cells originate from the layer of cells lining the ventricular space. As such, the neural tube gives rise to cells that go on to form both the central nervous system (brain and spinal cord) and peripheral (sympathetic) nervous system [102].

#### *Neuronal Hu proteins: early markers of neuronal identity*

The Drosophila homolog of nHu proteins, ELAV is first expressed in newly born neurons concomitant to their birth from neuronal precursor cells [11]. As such, ELAV is widely regarded as one of the earliest markers of post mitotic neurons in Drosophila. Examination of nHu gene

expression during development indicates they too are one of the first neuron-specific gene products expressed in newly born neurons.

Early work examining nHu protein expression in the developing chick embryo using a neuronal Hu-specific monoclonal antibody (16A11 – Santa Cruz) revealed nHu protein expression in neurogenic cells of the neural tube [103]. Using a short (1-2hr) BrdU pulse label followed by immediate fixation and co-staining for nHu proteins, Marusich *et al* showed that nHu protein expression was predominantly evident in post-mitotic (BrdU-negative) cells in the neural tube and was maintained during and after their migration out of the neural tube to form the spinal cord, brain and ganglia of the peripheral nervous system. Quite significantly though, nHu immunoreactivity was also observed in a few cells that were also BrdU-positive both in the neural tube and in neurogenic, but mitotically active neural crest cells cultured from avian neural tube, *in vitro*. Given the short duration of BrdU labelling and immediate fixation there after, this result suggested that nHu expression occurs either shortly before or concomitant to the exit of neuronal precursor cells from the cell cycle.

In zebrafish, detection of nHu expression by *in situ* hybridisation reveals HuC is expressed by cells of the neural plate, even before formation of the neural tube [104], [105]. Following neurulation, expression of HuC and HuD was observed in the neural tube and [105] in all subsequent neuronal structures derived from it. Subsequent examination of nHu expression during chick and *Xenopus* neurogenesis has revealed the same staging and order of expression [106], [18] with HuC expressed first, followed by HuD and finally by HuB. Notably, in the Xenopus study, timing of nHu expression was only determined by Northern Blot and thus no information was provided regarding the location or identity of cells expressing either gene [18].

Similarly, in the developing mouse cortex, nHu expression is observed in cells transitioning from precursor to differentiated neuron [107], [108]. The cortex is comprised of multiple layers of neurons all arising from the differentiation of neuronal precursor cells at the rostral end of the neural tube. During this process, asymmetric division of the precursor cells present within the ventricular zone (lining the ventricular space) results in the production of two daughter cells. One of the daughter cells remains in the ventricular zone and retains neuronal precursor cell properties, while the other moves into the subventricular zone (away from the ventricle) where it may undergo a limited number of cell divisions before differentiation into an immature migratory neuron [109]. These migratory neurons transition radially away from the ventricular

zone towards the pial layer, which envelopes the entire developing brain, and form the layers of the cortex.

In their paper [107], Miyata *et al* examined nHu protein expression in the developing cortex using the same 16A11 antibody developed and used in the Marusich *et al* paper from 1994 [103]. Miyata *et al*, observed nHu expression in mitotically active cells, present within the subventricular zone, derived from neuronal precursors within the ventricular zone. These mitotically active $nHu^+$ cells gave rise to immature migratory neurons that would go on to populate the growing cortical layers. This result showed that in mouse, nHu expression comes on concomitant to the assumption of neuronal identity and also differentiates the mitotically active neuronal precursor cells within the subventricular zone from those present within the ventricular zone, which can also contribute to other non-neuronal cell types present within the nervous system (glial cell lineages).

Compounding the studies of nHu expression in the early embryo, a similar phenomenon is observed within proliferative centres of neuronal tissues later in development. The first example of this was noted in studies of neurogenesis in the ependymal and subependymal zones of the avian songbird brain [110]. The ependymal zone is a well described neurogenic niche containing mitotically active neuronal precursor cells, in a variety of vertebrate organisms including birds, mice and humans [111]. In their study, Barami *et al* showed that nHu expressing cells are present within the ependymal and subependymal zones. Using a [$^3$H]thymidine DNA labelling experiment similar to the BrdU pulse labelling experiment to that of the Marusich paper [103], they also found that nHu expression occurred within the first few hours of lineage restriction from mitotically active precursor cell to immature neuron.

Similarly, in mice nHu expression is detected in the subventricular zone [112], a neurogenic niche in mammalian brains [113]. In their paper, Sakakibara *et al* compared the mRNA and protein expression of a neuronal precursor specific marker, *musashi-1* to that of nHu proteins. They found that the expression of musashi-1 and nHu proteins in neurogenic regions was *essentially* mutually exclusive; supporting the idea that musashi-1 is a true marker of neuronal precursor cells. However, in their immunofluorescence data it is clear that nHu protein expression was also detected in a few cells that were also positive for musashi-1 staining [114] and [112].

Finally, as observed in other vertebrates, sequential expression of nHu during mouse neurogenesis has also been reported, although the specific order of expression is different [20]. *In situ* hybridisation analysis of specific nHu mRNA expression in the developing mouse cortex (embryonic day 14) indicates HuB is expressed first, in cells still located within the subventricular zone. Expression of HuB was also observed throughout the cortical layers, although expression appeared to be reduced at the outermost layers. Conversely, expression of HuC was predominately restricted to the outer-most layers of the developing cortex, at the cortical plate, where terminally differentiated cortical neurons reside. [20]. Timing of the expression of HuB and HuC was similar in the developing cerebellum. HuB expression was again found to be essentially restricted to the external granular layer (EGL), which contains neuronal precursors and immature neurons. Interestingly, HuC expression was also detected in the EGL, however, strong expression was found in regions containing mature, differentiated neuronal cells, exclusive to HuB. In combination, the data from these two neurogenic brain regions suggest that HuB expression occurs first during neuronal differentiation and that expression of HuC occurs subsequent to this in more differentiated neurons. Expression of HuD in both the developing cortex and cerebellum was less restricted, occurring in regions of terminally differentiated neurons (such as the cortical plate) and in intermediate regions between the location of precursors and differentiated neurons. It is conceivable that HuD expression occurs in developing neurons as they transition from HuB expressing immature neurons to differentiated HuC expressing neurons. Interestingly, Okano *et al* showed that in the adult mouse brain, HuC is expressed essentially pan-neuronally [20]. As such, of the three family members, HuC appears to be the fundamental marker of differentiated neuronal cells. Expression of HuB and HuD was found to occur differentially in specific neuronal regions, in combination with HuC. However, in several terminally differentiated neuronal cell types, including cerebellar Purkinje cells and hippocampal dentate neurons, HuC is the only nHu expressed. These data suggest two important features of nHu protein expression in mouse. Firstly, the pan-neuronal expression of HuC suggests it is fundamentally required by all neurons. Secondly, different combinations of nHu proteins may be required for specification of particular neuronal cell sub-types.

## Conclusions for work examining the developmental expression of nHu family members

When taken together, these data show that, like ELAV, neuronal Hu proteins are one of the earliest markers of post mitotic neuronal cells. Given the timing of nHu expression relative to developmental stage, and from short pulse BrdU and [$^3$H]thymidine DNA labelling experiments, the switching on of nHu gene expression appeared to be an important step in the assumption and maintenance of neuronal identity. Furthermore, the pan-neuronal expression of HuC suggests it plays an important role in all neuronal cell types, while different combinations of the other family members may add diversity and levels of redundancy to nHu protein function across different neuronal sub-types.

## Consequences of gain or loss of nHu expression

The idea that nHu expression motivates the assumption and maintenance of neuronal identity is supported by transgenic studies into the effects of gain and loss of nHu expression in neuronal cells.

### *Gain of nHu expression causes neuronal differentiation*

Transient overexpression of nHu proteins in cells with neuronal potential has been shown to result in the assumption of neuronal-like characteristics including the expression of neuronal markers and extension of neuronal processes (neurites/axon-like structures). One of the first examples of this effect followed transfection of HuBsv2 into a human embryonic teratocarcinoma cell line, hNT2 [115]. hNT2 cells undergo neuronal-like differentiation following treatment with retinoic acid [116] as evidenced by increased expression of HuB [117]and another neuronal marker, neurofilament M (NF-M), exit from the cell cycle and extension of neurite-like processes [116]. In their paper, Antic *et al* showed that this process could be replicated in the absence of RA by transfection of HuBsv2 into hNT2 cells. Furthermore, RA-induced neuronal differentiation was shown to be blocked in cells transfected with antisense oligonucleotides specific for HuB [115].

Similar results were obtained with PC12 cells [23], [118], [119], which can be induced to a neuronal-like phenotype upon treatment with nerve growth factor (NGF). As with hNT2 cells, nHu expression in PC12 cells increases following NGF treatment and cells assume a more neuron-like morphology. In the absence of NGF, this effect could be recapitulated by transfection of PC12 cells with vectors encoding any of the three nHu proteins (HuB, HuC or HuD), but not with HuR. Furthermore, this effect was blocked in cells expressing antisense oligonucleotides against HuD [119].

Additionally, Akamatsu *et al* tested the ability of HuC to trigger neuronal differentiation of *in vivo* neuronal precursor cells within the neural tube of E9.5 mouse embryos. Twenty-four hours after electroporation of a FLAG-tagged HuC construct into one side of the neural tube, expression of neuronal markers including neurofilament-M and Tuj-1 in FLAG-HuC overexpressing cells was upregulated, where no upregulation was observed on the contra-lateral side of the neural tube for which FLAG-HuC expression was absent.

***Neuronal differentiation by neuronal Hu requires nuclear export and RNA-binding activity***

In their paper, Kasashima *et al* also characterised the spacer domain of HuD and subsequently identified a region responsible for nuclear export in the second half of this region. Their findings were in agreement with those of Fan and Steitz in their identification of the HNS region of HuR [22]. Kasashima *et al* went on to show that the ability of HuD to induce a neuronal-like phenotype was contingent on its ability to shuttle into the cytoplasm as deletion mutants lacking the identified nuclear export region were unable to induce a neuronal phenotype. Importantly, cells expressing the mutant nHu proteins were still able to undergo NGF-induced neuronal differentiation indicating the co-expression of mutant forms of HuD was not inhibitory to this process [23].

Akamatsu *et al* also carried out deletion analysis of HuC, although in their strategy they tested overexpression of HuC proteins from which either the first two RRMs plus the spacer domain or the final RRM plus the spacer domain were deleted. They also tested point-mutants in which key residues within the RNP1 and RNP2 of the first two RRMs were mutated to aspartic acid, abolishing RNA-binding activity. In separate experiments they showed that the ability of the mutant HuC proteins to bind RNA or induce the neuronal phenotype was strongly reduced compared to wildtype nHu. This result, particularly for the RNP1/RNP2 point mutants, suggested that induction of the neuronal phenotype by nHu proteins was also dependent on their capacity to bind RNA. In agreement with the Kasashima paper, NGF-induction of neuronal differentiation in PC12 cells expressing just RRM3 of HuC was unaffected, with cells still assuming a neuronal morphology [118].

The results from these nHu overexpression studies support a role for nHu proteins in the assumption of neuronal identity in the transition from neuronal precursor cell to neuron, as observed *in vivo*. However, identification of a mechanism for this activity is still lacking. The results from examination of nHu mutants deficient in RNA-binding activity or nuclear export activity indicate both RNA-binding and nuclear export are necessary for this effect. Interestingly, a recently published paper that revisited nHu-induced differentiation of PC12 cells has identified a role for HuD in enhancing cap-dependent mRNA translation, with direct consequences on its ability to cause NGF-independent neuronal differentiation [40]. The authors show that both the spacer domain and RRM3 are required for interaction between HuD and polysomes. They go on to show and that this interaction occurs through binding of the eukaryotic translation initiation factor eIF4A to sequences within the spacer domain of HuD. Using an *in vitro* reporter

translation assay HuD is shown to stimulate reporter translation but that this activity is lost for HuD mutants unable to bind eIF4A. Furthermore, while HuD mutants lacking RRMs 1 and 2 show reduced activity (in terms of stimulating translation and differentiation), RRM3 mutants are unable to stimulate translation and cannot induce NGF-independent neuronal differentiation. This is proposed to indicate that poly(A) binding activity (which they demonstrate is mediated by RRM3) is also required for stimulation of translation and NGF-independent differentiation. As such, the results from this recent paper suggest that at least part of the function of nHu proteins following their expression in newly born neurons, is in the regulation of mRNA translation, with direct outcomes on cell identity.

***Loss of HuD expression impairs neuronal differentiation***

In 2005, characterisation of an HuD knockout mouse was published [120]. The mice were shown to be viable with no gross morphological defects. Furthermore, other than a transient developmental delay in extension of neurites from several sensory nerve ganglia, no major perturbations in the development of the nervous system were noted. Comparison of brain, sensory and spinal cord structures in adult $HuD^{-/-}$ mice compared to wildtype also revealed no obvious morphological abnormalities. However, two interesting observations were made in adult $HuD^{-/-}$ mice. Firstly, while the delay to development of sensory nerve ganglia in embryos appeared only transient, adult $HuD^{-/-}$ mice displayed a clasping phenotype when suspended by their tails, a hallmark feature of motor/sensory defects arising from incorrect wiring between the cortex and basal ganglia [121], [122], [123]. Secondly, motor coordination of $HuD^{-/-}$ mice was severely impaired as evidenced by poor performance in rotarod tests relative to wildtype mice. As such, $HuD^{-/-}$ mice appear to have subtle defects in either the development or wiring of neuronal connections important for sensory and/or motor function, which are not apparent in gross morphological examination of the nervous system.

Importantly, $HuD^{-/-}$ mice did show evidence of an important functional role for HuD expression in neuronal differentiation. Firstly, analysis of BrdU incorporation into cells lining the ventricle and within the subventricular zone revealed a significant increase in the number of mitotically active cells (neuronal precursor cells) in $HuD^{-/-}$ mice compared to wildtype. Secondly, *in vitro* cultures of primary cortical cells from $HuD^{-/-}$ mice were shown to produce more neurospheres (individual colonies derived from a single proliferative precursor cell) than cultures from wildtype mice. Furthermore, dissociation and replating of primary neurospheres to yield secondary neurospheres produced the same result. Finally, differentiation of cultured neurosphere colonies by withdrawal of growth factors from the culture media revealed neurospheres from $HuD^{-/-}$ mice produced significantly fewer Tuj-1-positive neurons compared

to wildtype. These data indicate that in the absence of HuD, neuronal precursor cells are less competent to undergo neuronal differentiation, resulting in an apparent increase in the number of proliferative cells.

The results from the $HuD^{-/-}$ mouse highlight an important and complicating point regarding the study of nHu proteins in whole organisms. While BrdU incorporation and *in vitro* neurosphere culture assays suggest HuD is involved in the transition of neuronal precursor cells into differentiated neurons, the lack of any persistent gross morphological changes in the nervous system of $HuD^{-/-}$ mice suggests significant functional redundancy exists within the family. Importantly, the identification of moto-sensory defects in $HuD^{-/-}$ mice may point to a specific role for HuD in particular subsets of neurons. Indeed, while expression of nHu family members occurs pan-neuronally, variation in expression patterns of each family member across different neuronal tissues have been documented [20]. Notably, unpublished results for an HuC knockout mouse line are similar to the results for the $HuD^{-/-}$ mouse in terms of essentially normal gross morphology of the central and peripheral nervous systems. This supports the idea that nHu proteins can act redundantly in overall neuronal specification (Robert Darnell, *pers comm.*). It will be interesting to see what the results of an HuC/HuD double knockout mouse model will be.

In conclusion, studies examining the effect of gain or loss of nHu expression in neuronal and neuronal-like cells support a role for nHu proteins in promoting and/or maintaining neuronal identity. However, the mechanism(s) by which nHu proteins fulfil this role have yet to be elucidated.

## Insight into neuronal Hu protein function from studies of ELAV

The *Drosophila* homolog of the vertebrate Hu proteins, ELAV, is first expressed in newly born neurons concomitant to their birth from neuronal precursor cells [11]. Genetic ablation of ELAV expression results in impaired development of the nervous system and embryonic lethality [12]. Tissue-specific manipulation of ELAV expression (ablation in neuronal tissues and overexpression in non-neuronal tissues) shows ELAV is both necessary and sufficient for the production of neuronal tissue-specific splice isoforms of several ubiquitously expressed mRNAs [124], [125], [126]. These lines of evidence suggest ELAV expression plays a crucial role in the assumption and maintenance of neuronal identity during the development of the *Drosophila* nervous system, potentially as a regulator of neuron-specific alternative mRNA processing.

In 2003, Soller *et al* identified an ELAV binding region within the terminal intron (intron 6) of the alternatively processed pre-mRNA of *erect wing* (*ewg*) [126] (figure 4a). The region, spanning approximately 150nt is particularly enriched in uracil residues, and also contains a canonical polyadenylation signal (using an AAUAAA hexanucleotide sequence). Strongest ELAV binding within the identified binding region was detected within a polypyrimidine tract immediately 3´ of the hexanucleotide sequence that is recognised by mRNA cleavage and polyadenylation specific factors [127], [128], [129]. In non-neuronal tissues, the terminal intron of *ewg* is not processed and remains in the final mRNA constituting the 3´ untranslated region (UTR). Soller *et al* show that binding of ELAV inhibited 3´-end formation of the intron, preventing cleavage of the mRNA at the polyadenylation site located within intron 6. Through inhibiting cleavage at the intron-contained poly(A) site, ELAV promotes the production of longer pre-mRNA variants that contain the necessary downstream splice acceptor site to facilitate neuronal tissue-specific splicing of intron 6 from the *ewg* pre-mRNA. Interestingly, Soller *et al* show that ELAV physically interacts with at least one cleavage and polyadenylation specific factor (dCstF64) in a manner that does not require the presence of RNA. However, they went on to demonstrate that the mechanism by which ELAV prevented 3´-end processing in intron 6 did not involve inhibition of dCstF64 binding to its target sequence. As such, it is possible that interaction of ELAV with dCstF64 inhibits dCstF64 function, possibly by blocking interactions with other factors necessary for cleavage and polyadenylation.

In subsequently published experiments, Soller *et al* present evidence showing ELAV is also able to form large homomeric complexes of up to 12 individual ELAV molecules upon binding to intron 6 of the *ewg* pre-mRNA [44]. They do not indicate how multimerisation affects ELAV-

mediated regulation of 3´-end processing although possibilities such as increased binding affinity/specificity are pointed out along with an idea that multimerisation might assist in splicing of intron 6 by bringing splice sites into closer proximity.

In total, the work of Matthias Soller and Kalpana White in these two papers suggests ELAV is able to regulate 3´-end processing of target mRNAs most likely through specific interactions with cleavage and polyadenylation specific factors. It also implicates the formation of multimeric ELAV complexes in this process. These functions are linked to important developmental outcomes of ELAV expression in the developing Drosophila nervous system and potentially reveal a critical mechanism by which ELAV regulates gene expression choices important in defining the identity of neurons.

## Evidence of a role for nHu in 3´-end processing

Interestingly, nHu proteins have been reported to serve a similar function in the formation of alternative gene products from the calcitonin/calcitonin gene-related peptide pre-mRNA [130].

***Enhanced use of an early polyadenylation site produces calcitonin mRNA in non-neuronal cells***

The calcitonin/CGRP gene contains six exons. In non-neuronal cells, a polyadenylation signal sequence present in exon 4 is cleaved and polyadenylated resulting in the production of an mRNA encoding calcitonin (figure 4b). Importantly, splicing of intron 3a (between the third and fourth exons of the calcitonin mRNA) in non-neuronal cells has been shown to be an inefficient process due to the use of a sub-optimal branch acceptor site in intron 3a [131]. However, splicing of intron 3a in non-neuronal cells is enhanced by a uracil-rich sequence present immediately 3´ of the polyadenylation sequence used by the calcitonin mRNA transcript, which has been shown to promote cleavage and polyadenylation at this polyadenylation site [132]. In subsequent work, binding of the ubiquitously expressed RNA-binding protein TIAR was shown to occur at this uracil-rich sequence and promote non-neuronal splicing of the calcitonin/CGRP pre-mRNA [133]. However, a clear mechanism to explain how TIAR achieved this outcome was not elucidated.

***Skipping of exon 4 in neuronal cells depends on neuronal Hu proteins***

In a follow up paper to their published work on the role of TIAR in controlling splicing decisions of the calcitonin/CGRP gene, Zhu *et al* present evidence showing neuronal Hu proteins also bind the uracil-rich enhancer sequence [130]. However, nHu proteins (in this paper HuB and HuC) were shown to have the opposite effect of TIAR on mRNA processing, reducing splicing of exon 3a and biasing pre-mRNA processing towards generation of the neuron-specific CGRP mRNA (figure 4b). In their experiments they compare the ability of HuC to cause CGRP-type mRNA processing when co-transfected with a TIAR-REV fusion protein that tethers TIAR immediately upstream of the uracil-rich enhancer sequence. In this scenario, HuC is unable to influence exon usage and the non-neuronal mRNA processing pattern prevails. They then compare this result to an experiment in which HuC is also expressed as an HuC-REV fusion protein and co-transfected with TIAR-REV. In this case, the neuronal mRNA processing pattern is observed. Finally they compare these results to the effect of the REV protein alone, co-transfected with TIAR-REV. The REV protein alone is also able cause the neuronal mRNA processing pattern with approximately the same strength as the HuC-REV fusion protein. They interpret this result as indicating that nHu proteins promote neuronal splicing of the CGRP/calcitonin pre-mRNA simply through

physically competing with TIAR1 for occupancy on the uracil-rich sequence and preventing it from enhancing splicing of intron 3a, thus promoting non-neuronal splicing.

Importantly, several key pieces of information are lacking in this story, which prevents definitive conclusions to be made about nHu protein function in the calcitonin/CGRP alternative splicing decision. For starters, other than suggesting HuC competes with TIAR1 for binding to the identified uracil-rich enhancer sequence, Zhu *et al* do not pursue the effect of HuC binding to the calcitonin/CGRP pre-mRNA. However, the biggest deficiency in this story is the lack of information indicating how TIAR1 specifically promotes splicing of intron 3a. Without this information it is difficult to conclude how competition between nHu proteins and TIAR1 for binding to the uracil-rich enhancer sequence would affect alternative splicing of the calcitonin/CGRP gene. Notably, from their earlier work, Zhu *et al* had proposed that in non-neuronal cells, TIAR is required for production of the calcitonin mRNA either through blocking exon skipping (*ie* blocking use of the downstream splice acceptor site used by intron 3b) or by enhancing splicing of intron 3a [133]. In building on this idea, they suggest that in neuronal cells, nHu proteins might sterically inhibit binding of TIAR to the uracil-rich enhancer sequence. Consequently, because of the sub-optimal branch acceptor site used by intron 3a, in the absence of TIAR1-mediated splicing enhancement, splicing of intron 3b is favoured, leading to the production of the CGRP mRNA.

However, what's intriguing about this story is the connection between an alternative splicing decision (either intron 3a or 3b), an alternative polyadenylation site, and a uracil-rich sequence that has been observed to recruit factors that have some influence (direct or otherwise) on use of the alternative polyadenylation site present immediately upstream.

Generally speaking, relative to other splicing events that occur during pre-mRNA processing, splicing of the penultimate exon to the terminal exon involves a number of unique interactions that do not occur in upstream splicing events. Central to this are interactions between factors that bind to the splice acceptor site at the start of the terminal exon and factors binding to the polyadenylation signal at the end of the exon (reviewed in [134], which are critical in the recognition of the terminal exon. Enhancement of these interactions promotes terminal exon recognition, while perturbation of these interactions can lead to skipping of the terminal exon and splicing to alternative, downstream exonic sequences.

Zhu *et al* do mention testing for a role of TIAR1 in enhancement of polyadenylation site use in the terminal exon (exon 4) of the calcitonin mRNA in their initial paper [133]. However, from data not shown, they state TIAR1 did not directly influence cleavage or polyadenylation at the early polyadenylation site using an *in vitro* cleavage and polyadenylation assay. Interestingly, in their most recent paper on nHu proteins, Zhu *et al* provide evidence that unlike TIAR1, nHu proteins **does** reduce cleavage and polyadenylation at specific polyadenylation sites, through interactions with proximal uracil-rich sequences [135]. Furthermore, they show that this reduction occurs through direct interactions with cleavage and polyadenylation machinery.

## nHu proteins influence poly(A) site usage through interactions with cleavage and polyadenylation factors

In their 2007 paper, Zhu *et al* use a number of *in vitro* and cell culture assays to demonstrate nHu proteins block cleavage and polyadenylation through interactions with proximal uracil-rich sequences. They compare this activity using four pre-mRNA sequences that have uracil-rich sequences surrounding the AAUAAA hexanucleotide sequence of the polyadenylation signal. Of the four pre-mRNAs (calcitonin exon 4 poly(A) site, SV40 late poly(A) site, APRT poly(A) site and growth hormone poly(A) site) nHu proteins were found to block cleavage and polyadenylation in two cases (SV40 late and calcitonin exon 4).

Similarly to ELAV, Zhu *et al* go on to show a direct interaction between nHu proteins and cleavage and polyadenylation stimulating factors (CPSF160 and CstF64) by GST-pull down and co-IP experiments from mouse brain lysates. Notably, they do not indicate whether they control for the presence of RNA intermediates in these assays. Conceivably, some amount of interaction could be detected simply through binding of both proteins to a common RNA molecule. In the absence of RNAse treatment of lysates prior to co-IP/pull down experiments, one cannot rule this possibility out.

However, in contrast to the ELAV study, they also show that bacterially expressed GST-tagged HuB reduces binding of CstF64 to an *in vitro* transcribed, $^{32}$P-labelled, calcitonin exon 4 pre-mRNA in HeLa cell nuclear extracts. This result somewhat contradicts the reported evidence from Soller and White, in which recombinant ELAV did not reduce binding of dCstF64 to target mRNA sequences. Notably, it is possible this difference is caused by differences in the method used to assay binding of CstF64 in the presence of nHu proteins (Soller and White used neuronal nuclear extracts from flies overexpressing HA-tagged dCstF64, while Zhu *et al* use non-neuronal

nuclear extracts with endogenous levels of CstF64). Regardless, in both cases, further investigation is required to identify the mechanism by which interactions between nHu proteins and cleavage and polyadenylation specific factors influence the process of polyadenylation site choice and addition of the polyadenylate tail.

Again, the data presented by Zhu *et al* in this paper does not fully satisfy and further evidence is required to be confident that the effects observed in their assays are relevant to an *in vivo* context. The primary deficiency is the absence of a connection between the regulation of polyadenylation site usage for the calcitonin exon 4 reporter in their *in vitro* studies [135] and the splicing decision that controls production of either calcitonin or CGRP mRNA from the calcitonin/CGRP gene as examined in their earlier paper [130]. Importantly, the CGRP/calcitonin exon 4 sequence used in these assays did not include the uracil-rich enhancer sequence identified as being important in the regulation of exon 4 polyadenylation, as discussed in their earlier paper [130]. As such, these data may suggest that binding of nHu proteins occurs in multiple locations along the CGRP/calcitonin pre-mRNA and thus, potentially exerts multiple effects on alternative splicing.

Finally, the data presented by Zhu *et al*, is somewhat unique with respect to the majority of papers published that examine Hu protein function (both neuronal and non-neuronal). To date, work on neuronal Hu proteins has mainly focused on effects involving regulation of translation (discussed later in this thesis). While there are a number of very good reasons for this; the data provided by Zhu *et al*, in combination with recently emerging evidence that global changes in 3´-end processing are associated with the transition of cells from precursor to differentiated cell types (discussed below), suggest consideration should be given to testing nHu proteins for a role in 3´-end formation of target mRNAs.

## Alternative polyadenylation site choice during development

Regulation of mRNA expression through molecular interactions occurring in the 3´ untranslated region (3´UTR) is a powerful and well-described biological phenomenon. Interactions between *trans*-acting factors such as RNA-binding proteins and micro-RNAs (miRNAs), and cis-elements within 3´UTRs have been shown to regulate a number of processes, including mRNA half-life, mRNA subcellular localisation, and the ability of mRNA to attract the translational machinery and initiate protein production. All of these post-transcriptional gene regulatory events have important effects on cell survival, growth, identity and function (for review see [136], [137], [138] and references there in).

### *Tissue-specific trends in polyadenylation site choice*

Intrinsic to the influence of trans-acting factors on mRNA dynamics is, the presence of the 3´UTR sequence to which they bind. Interestingly, roughly half of mammalian mRNAs can be alternatively polyadenylated, leading to the production of mRNA isoforms that differ in terms of the length of their 3´UTR sequences [139]. A recent large-scale bioinformatic comparison of alternatively polyadenylated mRNAs across 42 different tissues has revealed particular features of tissue-specific polyadenylation that had not previously been reported [140]. Firstly, tissues show a general bias towards use of more proximal (5´ with respect to the mRNA) or more distal (3´ with respect to the mRNA) polyadenylation sites. Secondly, preferential use of either proximal or distal poly(A) sites is correlated with expression of specific cleavage and polyadenylation factors.

Notably, neuronal tissues were specifically highlighted as generally biasing towards use of distal (3´) poly(A) sites. This bias was strongly correlated with neuron-specific changes in the expression of five specific factors with known roles in cleavage and polyadenylation. They include: τCstF64, a paralog of the cleavage stimulator factor CstF64 and major component of the cleavage and polyadenylation specific machinery [141], [142]; pyrimidine tract binding protein (PTB), a repressor of alternative splicing in neuronal tissues [143]and modulator of binding by CstF64 at polyadenylation sites [144]; nPTB, a highly homologous, neuronal-specific isoform of PTB [145]; U1A, an inhibitor of poly(A) polymerase [146]; and PC4, a negative regulator of mRNA cleavage through direct interactions with CstF64 [147]. Zhang *et al* found that expression of PTB and U1A was consistently lower in neuronal tissues compared to non-neuronal tissues. Conversely, expression of τCstF64, PC4 and nPTB was consistently higher in neuronal tissues. Based on the published activities of these five proteins in combination with their observed

expression profiles, Zhang *et al* proposed that expression of tissue specific combinations of cleavage and polyadenylation components (primarily focussing on neuronal tissues as an example) was likely instrumental in setting up the observed differences in poly(A) site choice. Importantly, this paper was the one of the first to conclusively demonstrate that tissues can be profiled by the length of their 3´UTRs.

***Correlation between polyadenylation site choice and differentiation***

In a subsequent publication from the same group, genome-wide examination of alternatively polyadenylated mRNAs during mouse embryonic development revealed the frequency of use of distal polyadenylation sites (examined globally) tends to increase as development proceeds [148]. In support of these findings, a similar study comparing alternative polyadenylation site usage in activated versus quiescent mouse primary CD4+ T-lymphocytes (as a model for proliferative versus non-proliferative cells of the same cell-lineage) revealed use of proximal polyadenylation sites predominates in proliferating cells while the respective distal site is preferred in non-proliferating cells [149]. Both papers present similar justifications for the developmental importance of increased 3´UTR length, citing the obvious potential for increased regulation of mRNA expression by trans-acting factors to sequences present in longer 3´UTRs.

The paper from Ji *et al* does take things a bit further though; correlating changes in polyadenylation site choice with gene ontology terms [148]. They show the timing of 3´UTR lengthening during development correlates with the timing of increases in expression of genes involved in morphogenesis and differentiation, and the timing of decreased expression of genes involved in proliferation. Furthermore, using the C2C12 myoblast cell-line as an *in vitro* differentiation model, they show that frequency of polyadenylation at proximal poly(A) signals is reduced by differentiation of C2C12 cells to myotubes compared to undifferentiated C2C12 myoblasts. Taking this observation further still, they analyse expression of genes encoding components of the human pre-mRNA 3´-processing complex (guided by proteomic identification of these components in another paper [150]. This analysis reveals significant downregulation of several genes with known roles in polyadenylation including all components of the cleavage stimulatory factory complex (CstF). Interestingly, expression of τCstF64 was found to be upregulated, an observation that strengthens the idea that this paralog of CstF64 plays an important role as a positive regulator of distal poly(A) site use.

In combination with their other results, Ji *et al* propose a model in which use of proximal polyadenylation sites is weakened as differentiation progresses. In their model, weakening of

proximal polyadenylation sites is caused in two ways. Firstly, a general mechanism for promoting use of proximal polyadenylation sites exists in undifferentiated cells (cells positioned earlier in the process of differentiation), which relies on expression of specific, general cleavage and polyadenylation factors (as noted in their first paper; [140]). As differentiation proceeds, expression of components of the basal cleavage and polyadenylation machinery is reduced or switched resulting in reduced cleavage and polyadenylation at proximal sites. Secondly, expression of tissue-specific *trans*-acting factors that interact with mRNAs and influence cleavage and polyadenylation factors favouring particular distal (or proximal) poly(A) site choices

## Neuronal Hu proteins: trans-acting factors involved in neuron-specific polyadenylation site choice?

The connections between cell identity and 3´UTR length, as governed by alternative polyadenylation, are interesting given the available data for nHu expression during development and recently observed effects on specific polyadenylation decisions. Neuronal Hu expression is one of the earliest markers of immature neurons, and its expression is linked to the assumption of neuronal identity. Development of the nervous system through the differentiation of precursor cells to mature, post-mitotic neurons is associated with increased use of distal poly(A) sites in alternatively polyadenylated mRNAs. Experimental data suggests nHu proteins can influence polyadenylation site choice through interactions with components of the basal cleavage and polyadenylation machinery [135], [130]. These observations are supported by a similar observation in their homolog ELAV [126], [44]. As such, evidence is available which does support the idea that one role of neuronal Hu proteins during development of the vertebrate nervous system, is as a regulator of alternative polyadenylation site choice, with important consequences on gene expression that defines the identity of the newly born neuronal cells.

## A role for neuronal Hu proteins in regulation of target-mRNA translation?

While recent work suggests a role for nHu proteins in regulation of pre-mRNA processing, it is of critical importance to note that up until quite recently, data concerning nHu protein function was almost exclusively centred around a role for these proteins in the regulation of stability and/or translation of target mRNAs [117], [151], [115], [152], [119], [153], [154], [155], [156], [67], [157], [158], [40]. The idea that nHu proteins regulate protein production from target mRNA sequences stems largely from correlation with observed effects of HuR on mRNA stability and

translation, and with early observations of an association between nHu proteins and the translation machinery in differentiated neuronal cells [117], [151].

***Correlating neuronal Hu proteins with mRNA translation***

An association between nHu proteins and the translational machinery was first revealed by immunofluorescence and density gradient separation techniques in terminally differentiated neurons and neuronal-like cell lines [117], [151]. From these early studies, nHu proteins were reported to reside predominantly in the cytoplasm, in discrete, mRNA containing cytoplasmic foci (often referred to as cytospeckles or cytoplasmic granules) predicted to be large ribonucleoprotein complexes (denoted as mRNPs). In 1999, the first correlation between mRNA binding by a neuronal Hu protein and translation of a target mRNA was made, from evidence revealing transfection of HuB into hNT2 cells (a neuronal-like immortalised cell line) resulted in increased association of the neurofilament-M mRNA with polysomes [115]. Furthermore, formation of polysome-associated nHu-positive mRNPs was dependent on the microtubules and the actin cytoskeleton as disruption of these networks using specific drugs abolished the polysome-mRNP association [151].

The connection between nHu proteins and the cytoskeleton identified by Antic *et al* [151] is significant. Subsequent examination of nHu protein localisation within neuronal cells has revealed nHu proteins are present within actively growing axons, in association with microtubules [159], [160], (*KB Jensen unpublished results, see figure 5*). Aronov *et al* showed that localisation of nHu proteins to growing axons of differentiated P19 cells is dependent on the microtubule motor protein KIF3A. In their paper, nHu proteins localise to axons in mRNPs containing the mRNA encoding tau (a protein involved in microtubule assembly and stability). In the absence of KIF3A, nHu-tau mRNP localisation is lost. In previous work, the same group identified a sequence within the 3´UTR of the tau mRNA responsible for its localisation to axons [161]. This sequence (called the ALS – Axon Localisation Sequence) also contains a putative nHu binding site which had been reported to stabilise tau mRNA [152]. Importantly, Aronov et al show that the tau ALS sequence is sufficient to direct the axonal localisation of a reporter mRNA consisting of the coding sequence for GFP, fused to the ALS sequence from the tau mRNA [161], [159]. Furthermore, they show that the GFP-tau ALS message is specifically translated in "hot spots" within the axon. Their paper is one of the first to describe localised translation of an mRNA in axons. In their paper, Smith et al present data indicating growth cone localised nHu proteins co-localise with ribosomes and GAP-43 protein. Based on previous work showing an association between nHu proteins (particularly HuD) and the GAP-43 mRNA results in increased

GAP-43 expression [162], [163], [119], [153], Smith *et al* propose that nHu proteins recruit GAP-43 mRNA to ribosome present within the axonal growth cone, to facilitate its translation.

The connection between the binding and co-localisation of nHu proteins with an axonally localised mRNA that undergoes local translation within axons, and interaction between nHu proteins and the translation machinery, sets up a very interesting hypothesis, that nHu proteins are involved in regulating the local translation of target mRNAs within neuronal axons. But why would axonally localised translation be important during neuronal development?

## Local translation in axons during axon growth

Local translation is a fundamental requirement of axons during their growth. Following neuronal polarisation; the process by which an immature neuron specifies the site of its axon on the cell body, neurons extend an axonal process away from the cell body that eventually meets with a target cell and forms a synaptic connection. This process is known as axon migration. Growth of the nascent axon occurs at its tip, a region of the axon known as the growth cone. The growth cone is a highly dynamic and motile structure from which filopodia and lamellipodia extend, driving growth cone motility.

The surface of the growth cone contains a host of adhesion molecules and extracellular signal receptor proteins that respond to local signalling cues (attractants or repellents – collectively known as chemotactic factors). Chemotactic signalling at the growth cone directly modulates the arrangement of its cytoskeleton. Attractive signals cause stabilisation of filopodia and subsequent extension towards the source of the attractant. Conversely, repulsive signals cause filopodial retraction, blocking the growth cone from migrating towards the source of the repellent. By controlling extension and retraction of growth cone filopodia, chemotactic factors effectively steer the migrating growth cone as it extends from the cell body to its eventual synaptic location.

Growth cone steering in response to numerous chemotactic factors depends on local translation within the growth cone [164]. Interestingly, examination of translation in migrating growth cones has revealed a number of cytoskeleton-modifying proteins are specifically and rapidly translated at the growth cone following stimulation by signalling cues [164], [165] [166], [167], [167].

In response to an asymmetric gradient of chemoattractants such as netrin-1 or brain-derived neurotrophic factor (BDNF), translation of growth cone-localised mRNA encoding β-actin is specifically increased [168], [167]. The greatest increase occurs on the side of the growth cone closest to the source of attractant indicating localised β-actin synthesis promotes motility towards attractive cues. Furthermore, translational upregulation is blocked using anti-sense oligonucleotides that bind to the 3´UTR of the β-actin mRNA, implicating this region of the message in localised translation.

Conversely, exposure of the growth cone to an asymmetric gradient of chemorepellent, such as slit-2 or semaphorin-3A, causes local translation of proteins involved in cytoskeleton disassembly, [169], [166]. These proteins include the RhoGTPase RhoA and cofilin1 [169], [166], both of which are regulators of actin filament disassembly, as well as β-thymosin, an actin monomer sequestration factor [170]. This evidence supports the notion that the retraction of growth cone filopodia and subsequent repulsion from chemorepellents is caused by local changes in cytoskeletal stability, resulting from local translation of cytoskeleton-modifying proteins. In combination with the cytoskeleton-promoting effects of chemoattractants, these observations have lead to the formulation of a model in which asymmetric translation of cytoskeleton-modifying factors within the growth cone, in response to chemotactic factors, cause changes in the migratory path of the motile growth cone [171].

## Regulation of locally translated mRNAs

Execution of localised mRNA translation *a priori* relies on cellular mechanisms to localise specific mRNAs and control their translation. To ensure translation of mRNAs occurs locally, mRNAs must be repressed during transport to the site of their eventual translation. Once localised, this repression must be alleviated, presumably through signalling that releases the mRNA from translational repression. Importantly, RNA-binding proteins are central players in both the localisation and translational regulation of locally translated mRNAs (reviewed in [172]).

### *RNA-binding proteins control mRNA localisation and translation*

Evidence that RNA-binding proteins regulate mRNA localisation and translation can be found for many cellular processes that rely on localised gene expression (for review see [138]. In neurons, two well-characterised RNA-bind proteins include ZBP-1 and FMRP.

ZBP-1 binds the β-actin mRNA through an interaction with a highly conserved 54-nt sequence element present within the 3´UTR [173]. In complex with β-actin mRNA, ZBP-1 has been found in elongating axons and is observed to move into the growth cone upon stimulation with the chemoattractant netrin-1 [167]. Binding of ZBP-1 to the β-actin mRNA blocks translation initiation; this block is relieved following phosphorylation of ZBP-1 by Src kinase [174]. Importantly, Src-dependent phosphorylation of ZBP-1 has been shown to be triggered by BDNF signalling [175], which as discussed is a known chemoattractant.

Regulation of mRNA translation by FMRP occurs through its interaction with mRNAs containing a particular stem-loop secondary structure called a G-quartet [176]. Through interactions with kinesins (microtubule associated motor proteins) FMRP localises bound mRNAs in dendrites [177]. FMRP also recruits an eIF4E binding protein, CYFIP1, which blocks translation of FMRP-bound mRNAs [178].

From these, and other studies, ZBP-1 and FMRP are clearly able to serve multiple functions that act in concert to ensure regulated temporal and spatial expression of target mRNAs with important consequences in neuronal development. Importantly, of the numerous mRNAs known to localise specifically to neuronal growth cones, identification of the factors and mechanisms involved in their localised translation has only been achieved in a handful of cases. Given the importance of axon guidance in the development and function of the nervous system, greater insight of the players and processes involved in controlling axon guidance is required to understand how neurons make the connections that lead to a functional nervous system and how these processes may be used in the development of therapies for medical conditions arising when connections are lost.

## GAP-43, an example of neuronal Hu regulation of a growth cone localised mRNA?

As it stands, there is currently limited data available that actually shows regulation of an axonally-localised mRNA, in the growth cone, by neuronal Hu proteins. Of that evidence, most of it is correlative at best, linking discrete observations of effects of nHu proteins on the translation or stabilisation of particular mRNAs, to functional roles of the mRNA-encoded protein in neuronal function or development (as clearly demonstrated in this review – [179]. The nHu target mRNA that has received the most coverage is the mRNA encoding GAP-43. GAP-43 is a growth cone localised phosphoprotein involved in transducing signals that regulate the cytoskeleton [180]. The mRNA encoding GAP-43 has been shown to associate with nHu proteins in mRNPs that localise to the growth cone and associate with ribosomes [160]. Interactions between the GAP-43 mRNA and nHu proteins are reported to occur through AU-rich elements present in the GAP-43 3´UTR [162], causing it to be stabilised in a manner dependent on RRM3 [119], [153]. These data have been extrapolated to explain observed increases in GAP-43 translation following treatments that cause concurrent increases in expression of nHu proteins. Specifically, concurrent increases in nHu and GAP-43 protein expression is observed in regions of mouse brain associated with learning and memory following tasks that stimulate these neuronal regions [156], [181]). Furthermore, stimulation of several cell lines with phorbol esters has been reported to cause an increase in cytoplasmic localisation of nHu proteins [67], [182], specifically to the cytoskeleton, concurrent with increased translation of GAP-43 mRNA [67]. Phorbol esters are general activators of the PKC family. Other research indicates phosphorylation of nHu proteins by PKC family members affects subcellular localisation and ability to cause mRNA stabilisation [67], [182], [183], demonstrating modulation of nHu protein function could occur from input by extra and intracellular signalling pathways involving PKC isoforms.

## Taking investigation of nHu protein function further

While the nHu protein-GAP-43 mRNA story is interesting in itself, it still has a long way to go before the observations therein provide a convincing picture of a biologically relevant interaction. Several elements of that story are still missing, including mechanistic elucidation of how nHu protein interactions with the GAP-43 mRNA affect its stability or translation or localisation, and some evidence to demonstrate how post-transcriptional regulation of the GAP-43 mRNA by nHu proteins influences biological processes the GAP-43 protein is involved in. Furthermore, in isolation the GAP-43 story is a single example of a message for which interactions with nHu proteins are implicated in its localisation and expression. While the biological outcomes of this interaction may be fascinating, it is not possible to confidently define neuronal Hu protein functionality based on a single mRNA target. This is especially true given that examination of nHu protein function has identified potential roles for these proteins at numerous levels of mRNA regulation, from mRNA processing to regulation of mRNA stability, localisation and/or translation. Importantly, the greatest weakness of the nHu protein literature in general, is the lack of a clearly defined list of *bone fide* mRNA targets of nHu proteins. A broader understanding of which mRNA sequences are targeted by nHu proteins would in many ways be expected to assist researchers in identifying their particular biological function(s). *A priori*, it would be expected that if nHu proteins do play important roles in particular biological processes such as the assumption of neuronal identity or outgrowth and/or directed migration of neuronal axons (for example), then they would interact with a variety of mRNAs whose encoded products are directly involved in these processes. Identification of a cohort of mRNA targets, all encoding proteins involved in a particular biological outcome does two things. Firstly, it rationalises experimentation by providing a specific biological context within which to assay outcomes of nHu protein-target mRNA interactions at both a cellular and molecular level. Secondly, it enables a more complete understanding of how nHu proteins regulate specific biological processes (as a hypothetical example; neuronal differentiation) by providing numerous examples of mRNA interactions that act in concert to arrive at a particular biological outcome.

To try and overcome the lack information regarding bone fide mRNA targets of nHu proteins we have applied a cross-linking and immunoprecipitation technique called CLIP [184] to identify *in vivo* mRNA targets of nHu RNA-binding proteins.

## Identifying mRNA targets of nHu proteins: CLIP

CLIP, is cross-linking and immunoprecipitation protocol designed to specifically isolate and purify *in vivo* RNA-protein interactions [184], [185]. CLIP employs ultraviolet irradiation to generate covalent cross-links between RNA-binding proteins and their RNA targets in live cells or tissues to effectively capture *bone fide* interactions prior to cell lysis and immunoprecipitation of the complexes. Unlike other cross-linking agents, ultraviolet irradiation relies on particular chemical properties of RNA and the protein domains that bind them to cause covalent cross-linking, providing some level of specificity in the reaction. Furthermore, cross-linking occurs with relatively low efficiency and is only effective across very small distances (*ie* within Angstroms), greatly increasing the probability of identifying true molecular interactions. Covalent cross-linking prior to lysis has been shown to be an important step in avoiding "artificial" interactions between RNAs and proteins that can occur following lysis [186].

Following cross-linking and subsequent lysis, lysates are treated with RNAse T1 and RNAse A to produce RNA fragments that are approximately 60-70 nucleotides long. This "clipping" of the RNA produces a CLIP "tag" that is of sufficient length to unambiguously identify the parental RNA from which it is derived, but short enough to allow one to determine the approximate location of protein binding within the RNA. Following this, immunoprecipitation isolates the RNA-proteins complexes of interest and a series of rigorous purification steps are used to isolate the covalently linked RNA-protein complexes away from non-covalently associated RNA-protein complexes. Once purified, the cross-linked protein-RNA complexes are subject to protease digestion of the target protein and the RNA cloned through a series of steps including directional 5' and 3' RNA linker ligation, cDNA synthesis, and amplification by PCR. The result is a set of CLIP-tags which can then sequenced. Finally, sequenced CLIP-tags are aligned with their respective genome sequence, revealing not only the identity of the mRNA from which the tag originated, but also the region of the mRNA bound by the RNA-binding protein of interest.

## CLIP identifies *bone fide*, *in vivo* RNA targets

CLIP was originally developed in Dr. Robert Darnell's lab as a means of identifying RNA targets of a PND auto-antigen Nova-1 [184],[185]. Previous work had shown Nova-1 was an RNA binding protein able to regulate neuron-specific alternative splicing of several mRNAs [187], [188]. However, using CLIP, Ule *et al* were able to identify 340 separate CLIP-tags. The data from these tags agreed with previously published data characterising the Nova binding element, and revealed Nova-1 binding sites in intronic, exonic and 3´UTR sequences. Furthermore, of the

CLIP-identified mRNA targets, 34 were shown to have 2 or more CLIP tags. Approximately three quarters of these targets were found to encode proteins present at the neuronal synapses. Finally, a Nova-1 knockout mouse line was used to validate 7 CLIP-identified target mRNAs, showing changes in their splicing pattern relative to wildtype mice.

Importantly, despite the relatively small number of CLIP-tags sequenced, this paper was instrumental in demonstrating the utility of CLIP, not only in identifying *bone fide* mRNA targets, but also in its capacity to reveal the location and nucleotide content of binding sequences. This information was directly useful in predicting effects of Nova-1 binding on several target sequences.

However, the true power of CLIP is revealed when used in combination with recently developed, high-throughput sequencing techniques (HITS-CLIP), which enable complete and exhaustive sequencing of CLIP-tag libraries (reviewed in [189]). The ability to exhaustively sequence CLIP-libraries allows for identification of RNA-protein interaction "hot spots", or sites at which many individual binding events are captured within a single experiment. By normalising the abundance of overlapping CLIP-tags to expression levels of the target mRNA, it is possible to rank identified binding sequences in terms of their absolute representation within a library. This information is useful in two ways; firstly, it allows for a rough triaging of identified interactions in terms of their potential biological importance. (*Notably, it is also entirely possible that some interactions may have very important biological consequences, without necessary being highly ranked following this normalisation. However, it provides a starting point for functional analysis of RBP-RNA interactions.*) Secondly, it eliminates bias towards binding events that are highly represented because of high levels of expression of a particular target mRNA. In this way, high throughput sequencing allows straightforward identification of highly specific interactions occurring between RNA-binding proteins and lowly abundant mRNAs.

To date, HITS-CLIP has been used in only a limited number of published studies identifying RNA targets of both RNA-binding proteins (Nova2 – [190], FOX2 – [191], SFRS – [192], Ago – [193]) and miRNAs [193], [194]. Nevertheless, the results of these studies have provided key insights into RNA regulation by RNA-binding proteins and miRNAs on a genome-wide scale. In combination with bioinformatic and biochemical approaches, HITS CLIP has demonstrated that RNA-binding proteins regulate biologically coherent RNA networks [190], [191], [192]). Furthermore, through identification of specific binding sites within mRNAs, HITS CLIP has

helped reveal previously unknown functions of RNA-binding proteins [190] as well as previously unrealised regulatory mechanisms; for example, where a single RNA-processing factor specifically regulates expression of a cohort of other RNA processing factors to effect global mRNA regulatory effects that define cellular identity [192]. In summary, CLIP is an incredibly useful biological tool enabling the identification of biologically relevant RNA-protein (and RNA-miRNA) interactions to be carried out with a high degree of confidence. This is evidenced by the high degree of accord between identified mRNA targets and experimentally proven functional outcomes as seen on both small and large-scale CLIP experiments.

## Using CLIP to identify mRNA targets of nHu RNA-binding proteins

As a starting point for examining nHu protein function during neuronal development, several small-scale CLIP experiments were performed in our lab. Each experiment used different sources of neuronal tissue including P4 mouse brain and 4 and 24 hours post-fertilisation (hpf) zebrafish embryos. Based on expression data, the P4 mouse brain and 24hpf zebrafish CLIP will contain mRNA targets of potentially all three nHu proteins. Conversely, the 4hpf zebrafish CLIP should only contain mRNA targets of HuB, which is present as a maternally deposited protein at this early time point [195]. The use of zebrafish for these experiments was motivated by morpholino-knockdown experiments occurring at the time looking at the effects of loss of HuC or HuD expression during zebrafish development. It was anticipated that the data from the CLIP experiments might help in rationalising phenotypes obtained from these experiments and that effects of specific nHu proteins on particular mRNA targets could then be tested in a true *in vivo* context. Connection of these two experimental systems was never made though because of difficulties encountered in morpholino-knockdown experiments. However, the data from the CLIP experiments provided a valuable resource as a guide for potential mRNA targets of nHu proteins.

### Information gleaned from nHu CLIP experiments

A brief breakdown of the results from each CLIP experiment is provided in figure 6. In total 611 CLIP tags were sequenced from the 4hpf CLIP experiment, of which, 439 aligned to gene encoding positions in the zebrafish genome (Zv8 zebrafish genome assembly – Wellcome Trust Sanger Institute). For the 24hpf zebrafish CLIP experiment, 478 CLIP-tags were sequences, with 271 aligning to gene encoding sequences in the Zv8 zebrafish genome assembly (figure 6a). Importantly, alignment of zebrafish CLIP-tags to known gene-encoding sequences was hampered

by incomplete mapping of genes to the Zf8 zebrafish genome assembly, which is still lacks widespread annotation. Conversely, for the mouse CLIP experiment, of the 124 CLIP tags sequenced, 110 could be aligned to mapped genes in the mouse genome (NCBI Build 37, considered "essentially complete") (figure 6d).

Importantly, a number of general features of mRNA binding by nHu proteins were consistently observed across all three CLIP experiments. These included, a high proportion of nHu target sequences occurring in 3´UTR and to a lesser extent intronic regions and a preference for uracil-rich sequences (in agreement with previous observations of nucleotide preference for Hu proteins) (figure 6b-d)

***mRNA binding by nHu proteins***

The results from the nHu CLIP experiments indicate nHu proteins interact most frequently with uracil-rich sequences present in 3´UTR and intronic sequences. From both of the zebrafish CLIP experiments, interactions with 3´UTR sequences are most strongly represented. In the 4hpf CLIP experiment, 84% the of 439 CLIP tags that aligned to gene encoding regions of the zebrafish genome, occurred in 3´UTRs, with the remainder occurring in either intronic (7%) or coding (8%) sequences (figure 6b). Similarly for the 24hpf CLIP experiment, of the 271 CLIP tags assigned to a gene-encoding region of the zebrafish genome, 66% occurred in 3´UTRs, with a further 31% corresponding to intronic sequences (figure 6c). In both cases, the percentage of nucleotide representation per tag indicated a strong preference for uracil-rich sequences at an average of ~45% uracil content per CLIP tag (figure 7a and 7b). The remaining three possible nucleotides were represented approximately equally. The P4 mouse CLIP experiment indicated a higher incidence of mRNA binding occurring at intronic sequences of target mRNAs. Of 118 gene-aligned CLIP-tags, 33% were found to occur in 3´UTRs, while ~50% were shown to be intronic (figure 6d). CLIP-tags from the P4 mouse brain CLIP showed a similar enrichment in uracil-residues as observed in the zebrafish CLIP experiments. Furthermore, in this case, while uracil residues were prominent in sequenced CLIP-tags (30%), equal incidence of cytosine residues (30%) was also seen (figure 7c). It is important to note, for the P4 mouse brain CLIP experiment, averaged nucleotide content was determined from **the entire library of sequenced tags** and is **not** a representation of nucleotide content per tag. Information on the nucleotide content per CLIP tag was not available at the time of thesis completion. As such, this information is only really indicative of general nucleotide content and is not informative about the average percentage content of specific nucleotides for each tag, which may be significantly higher or lower than indicated.

## nHu CLIP results guide functional experiments into nHu protein function

The results from the three nHu CLIP experiments indicated nHu proteins are potentially involved in a variety of biological functions. The presence of nHu binding sites in intronic sequences of target mRNAs suggests a role in the regulation of pre-mRNA processing. However, the high prevalence of CLIP-tags occurring in 3´UTRs of target mRNAs agreed with the overarching idea that nHu proteins are involved in post-transcriptional regulation of target mRNA translation, stability or localisation. As such, it was decided that application of CLIP-derived data to experiments testing nHu protein function would focus on this aspect of nHu protein biology.

## HYPOTHESIS

Neuronal Hu proteins are involved in local translation of mRNA targets at the growth cone of migrating axons.

***A subset of mRNA targets known to localise to the axonal growth cone***

A common theme between the three CLIP experiments was the identification of CLIP-tags in the 3´UTRs of mRNAs encoding cytoskeletal components and cytoskeleton-modifying proteins. A selection of CLIP-tags corresponding to mRNAs pertinent to the work covered in this thesis is shown in figure 7d.

Importantly, growth cone localisation of protein and/or mRNA for several of these CLIP-identified nHu mRNA targets had previously been reported. In itself, the correlation between binding of nHu proteins to the 3´UTR of growth cone-localised mRNAs, and the observed growth cone localisation of nHu proteins was difficult to ignore. Compounding this correlation, in addition to being growth cone localised, protein products of several of these mRNAs had already been implicated in regulation of cytoskeletal dynamics (within axonal growth cones) in response to chemotactic signalling molecules. A selection of these mRNAs includes; the small RhoGTPase cdc42 [196], [197], the actin depolymerising factor Cofilin1 [198], [169], vasodilator-stimulated phosphoprotein (VASP) [199], β-actin [167], a regulator of growth cone adhesion MARCKS [200] and a regulator of microtubule growth CLASP1 [201]. Furthermore, growth cone-localised translation of Cofilin and β-actin mRNAs, in response to chemotactic factors, had also recently been demonstrated [169], [167]. Given the dependence of axon guidance on local translation, particularly of cytoskeleton-modifying factors in the growth cone, in response to chemotactic factors, the data from the CLIP experiments was compelling and drove the formulation of a hypothesis that nHu proteins play a role in the localised translation of mRNA targets at the growth cone of migrating axons, through interactions in the 3´UTR of target messages.

## Work covered in this thesis

The primary aim of this project was to investigate the molecular mechanisms by which nHu proteins influence target mRNAs. The data from the CLIP experiments and associated correlative information outlined above, had identified a specific biological context on which to base these investigations. Specifically, that nHu proteins regulate growth cone localised mRNAs as part of a role in the process of axon migration. However, at the time of commencing this work, very little information was available that indicated a specific mechanism by which neuronal Hu proteins influenced target mRNAs. While effects on mRNA translation appeared likely, a host of possible mechanisms existed by which this could occur. Furthermore, co-localisation of nHu proteins with the cytoskeleton, particularly microtubules, invited the possibility that nHu proteins are involved in the specific localisation of target mRNAs. Several possible roles can be imagined for this function including; serving as a scaffold between specific mRNAs and cytoskeleton-associated motor proteins that translocate cargo to the axonal growth cone, or a role in repressing target mRNA translation, or ensuring mRNA stability during translocation to ensure bound mRNAs are translated at the correct location and under the right conditions (such as in response to extracellular signals). As such, the work undertaken with these reporter assays was largely pioneering in its aim to identify molecular mechanisms by which nHu proteins affect their target mRNAs.

### A cell culture-based assay for nHu protein function

As a starting point for this project, a cell culture-based reporter assay was devised to compare the translation of mRNAs carrying a CLIP-identified 3´UTR sequence, in the presence or absence of a specific neuronal Hu protein. The primary objective of this reporter assay system was to determine whether or not nHu proteins exert an effect (either positive or negative) on target mRNA translation, through binding to sequences present within the 3´UTR. If an effect of nHu proteins on translation of a target mRNA was revealed, the 3´UTR-reporter assay system would then be used to identify sequences within the 3´UTR that modulate this effect, functional elements within the nHu protein critical for its role in regulating mRNA translation and any other molecular interactions (*ie* nHu-nHu or nHu-protein X/miRNA X/etc) that participated in the ultimate effect on target mRNA translation.

***Key features of the 3´UTR-reporter assays***

To assay for changes in target mRNA translation due to nHu proteins, reporter constructs were generated in which the 3´UTR sequence of a CLIP-identified target mRNA was placed immediately downstream of a sequence encoding a particular reporter protein. The details for 3´UTR-reporter assay design are given in the relevant results chapters. However, it is necessary to point out from the outset that the 3´UTR-reporter assays went through several rounds of optimisation. In total, three different reporter proteins were tested; these include a destabilised variant of the enhanced green fluorescent proteins (d2EGFP), and the bioluminescent proteins, firefly and renilla luciferase. Evolution of the reporter assay design was guided by results obtained through experimentation, and is explained in the relevant results sections.

***Immortalised cell lines versus primary neuron cultures***

Furthermore, 3´UTR reporter assays were carried out in a variety of immortalised cell lines. Given the primary aim of the 3´UTR-reporter assays, it was decided that the simplest way to test for an effect of nHu proteins on translation of target mRNAs would be to overexpress a specific nHu protein, along with a single target mRNA sequence, in cells with little to no nHu protein expression, and then assay for differences in reporter protein expression. While these cell lines lack many of the features (both molecular and morphological) of true neuronal cultures (such as primary cultures of E18 rat hippocampal neurons), they would allow for identification of changes in reporter mRNA translation occurring as a direct result of co-expression with a specific nHu protein. In addition to this, the ease of culturing and transfecting the cell lines used compared to primary neuronal cultures was a distinct advantage. Depending on the results from the cell line-based reporter assays, experiments to test the involvement of specific sequences within 3´UTR-reporter mRNAs in nHu protein-mediated effects could be extended into a primary neuron culture system. A neuronal system would also be important for identification neuron-specific interactions between nHu proteins and factors involved in functional changes to target mRNA translation. A protocol for the dissection and culturing of E18 rat hippocampal neurons was optimised, along with a low efficiency calcium phosphate-based transfection method. The details of these experiments are included in a supplementary chapter (Appendix 1).

***HuCsv1 – the most likely regulator of mRNA translation?***

Finally, 3´UTR-reporter assays were carried out using the nHu protein HuC splice variant 1 (referred to as HuCsv1 in this thesis). The decision to use HuCsv1 was made based conclusions drawn from several lines of evidence. Firstly, according to expression data from mouse, HuC is

the only pan neuronal nHu family member, and in some neurons, the only nHu family member expressed [20]. As such, while HuB and HuD are conceivably more specialised in their functions; serving roles in specific cell types, or under specific conditions, it seemed likely that HuC would be capable of performing any and all functions necessary of a nHu protein, in the development of a neuron. Secondly, earlier examination of the subcellular localisation of all 10 nHu splice isoforms, conducted in our lab, indicated that of the four HuC splice variants, HuCsv1 showed the greatest level of cytoplasmic localisation, appearing almost exclusively cytoplasmic at steady-state and significantly more cytoplamsic than any of the other three HuC splice isoforms [24]. For reporter assays testing for a role of nHu proteins in the regulation of target mRNA translation, the use of an HuC splice variant that showed the greatest level of cytoplasmic localisation in these assays made the most sense, as these proteins would be expected to act predominantly in the cytoplasm (or sub-domains therein, such as axonal growth cones) in a role specific to this location; namely, regulation of mRNA translation. Finally, semi-quantitative RT-PCR analysis of all three neuronal Hu family members (and their splice variants) was carried out using mRNA obtained from E18 rat hippocampi. The results of this experiment showed that HuCsv1 is one of the more abundant nHu family members expressed in this tissue (Appendix 1 – figure 9). Notably, HuBsv2 HuCsv2 and HuDsv1 and sv2 were also highly expressed, while expression of the shorter splice variants was significantly lower for all three family members. High expression of HuCsv1, relative to other splice variants in this cell type, in combination with the conclusions listed above provided the final justification for using HuCsv1 in these assays.

## Preamble to the results

In not knowing how nHu proteins might influence target mRNAs, early observations were taken at face value. These observations suggested that nHu proteins had a modest negative effect on target mRNA translation for several of the assayed 3´UTR-reporters. Importantly, during the course of the 3´UTR-reporter experiments reported herein, the assays used to examine nHu protein function underwent several rounds of refinement and optimisation. These refinements were guided by results obtained at each stage of experimentation and in the end yielded results that were not anticipated at the beginning of the project. As such, this thesis presents an evolution of ideas regarding possible functional roles of nHu proteins, driven by results from experiments designed to test nHu protein function. Ultimately, rather than providing an answer to the original hypothesis, the data presented in this thesis, in combination with recent insights into RNA-binding protein biology, has lead to the formulation of a new hypothesis in regards to a functional role for at least one neuronal Hu protein family member.

| Gene | Other names | Reported expression |
|---|---|---|
| *elav* | *Elav* | Very early neurons, most mature neurons [10] [201] |
| | *RBP9* | CNS neurons from 3rd instar, cytoplasm of cystocytes and later in oocytes |
| *HuA* | *HuR* | Ubiquitous [19] |
| | *mHuA, Mel-G1* | Ubiquitous [20] |
| | *cHuA* | Almost ubiquitous [106] |
| | *elrA* | Ubiquitous [18] |
| | *zHuA* | Ubiquitous [105] |
| *HuG* | *zHuG* | Ubiquitous [105] |
| *HuB* | *Hel-N1* | Foetal and adult brain [202] |
| | *mHuB, Mel-N1* | Early neurons, adult brain [20] |
| | *elrB, Xel-1* | Neurons, testis, ovary, early maternal transcripts [18] [203] |
| *HuC* | *mHuC* | All mature neurons [20] |
| | *cHuC* | Early neurons (following cHuD expression), mature neurons [106] |
| | *elrC* | Late neural progenitors, early and mature neurons [204] [205] [18] [203] |
| | *zHuC* | Very early neurons, mature neurons [104] |
| *HuD* | - | Foetal and adult brain [202] |
| | *mHuD* | Some early neurons, adult brain [20] |
| | *cHuD* | Early and mature neurons [106] |
| | *elrD* | Fairly early neurons, mature neurons [18] [203] |
| | *zHuD* | Fairly early neurons, mature neurons [105] |

Legend: *Drosophila* | Human | Mouse | Chick | *Xenopus* | Zebrafish

Table 1. A list of names by which the neuronal Hu proteins (HuB, HuC and HuD) and non-neuronal Hu proteins (HuA and HuG) have been reported as throughout the literature is provided. A brief description of their specific expression pattern is also provided.

A

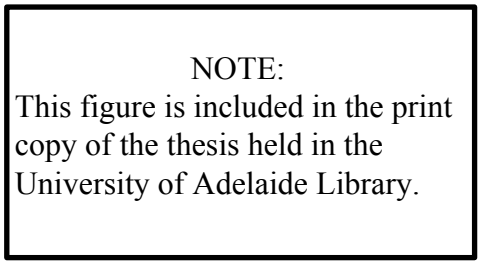


Modified from Okano H.J. & Darnell R.B. J Neurosci. 17(9) :3024. (1997)

B

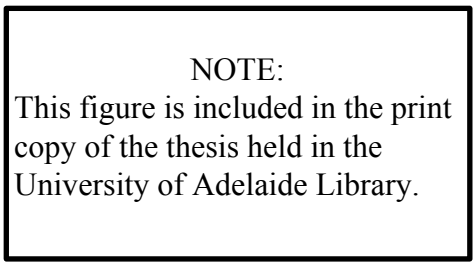


Modified from Lisbin M.J. et al. Genetics. 155(4) : 1789. (2000)

Figure 1a. Amino acid sequence comparison of all four mouse Hu proteins. The longest nHu protein splice variants are shown (HuBsv2, HuCsv1, HuDsv1). Conserved residues are highlighted in black. Hu family members show 70-80% sequence homology in protein sequence. Sequences encoding RNA Recognition Motifs are indicated by green lines. The HuR Nucleocytoplasmic shuttling Sequence is indicated by the red dashed line.

Figure 1b. Sequential arrangement of RRMs in all Hu proteins. RRMs 2 and 3 are separated by an alternatively spliced spacer domain which contains sequences necessary for nucleocytoplasmic shuttling of all Hu proteins, referred to as the HuR Nucleocytoplasmic shuttling Sequence (HNS - indicated in red box)

Asterisk denotes conserved serine residue, known to be phosphorylated by cdk1.

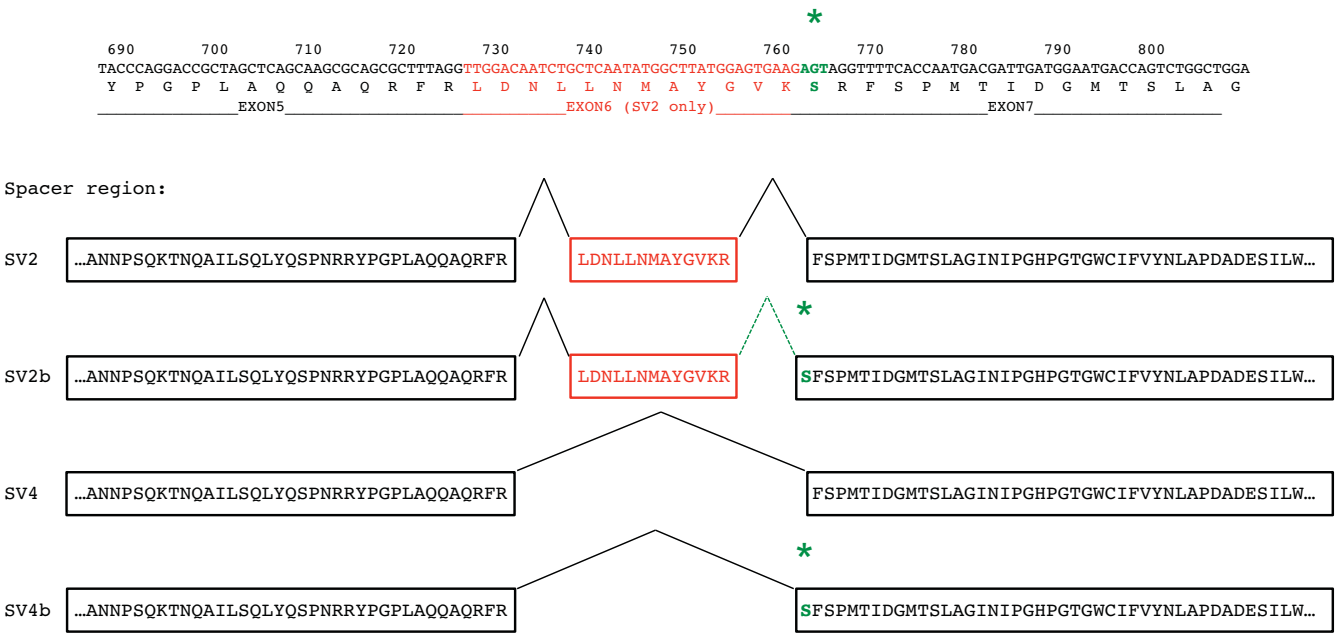


Figure 2a. Alternative splicing in the spacer region of HuB results in the inclusion of a short leucine-rich sequence (exon6). This splice variant is called HuBsv2. Skipping of exon6 produces HuBsv4.

Use of an alternative splice acceptor site at the 5´-end of exon7 results in the inclusion of an additional serine residue (sequence in green indicated by asterisk) in the exon7 encoded protein sequence. A number of ESTs in the UCSC genome data base support the expression of an HuBsv2 variant containing this additional serine (referred to as HuBsv2b). A single EST (AY035378) indicates splicing to produce HuBsv4 can also lead to the inclusion of this serine residue (referred to as HuBsv4b).

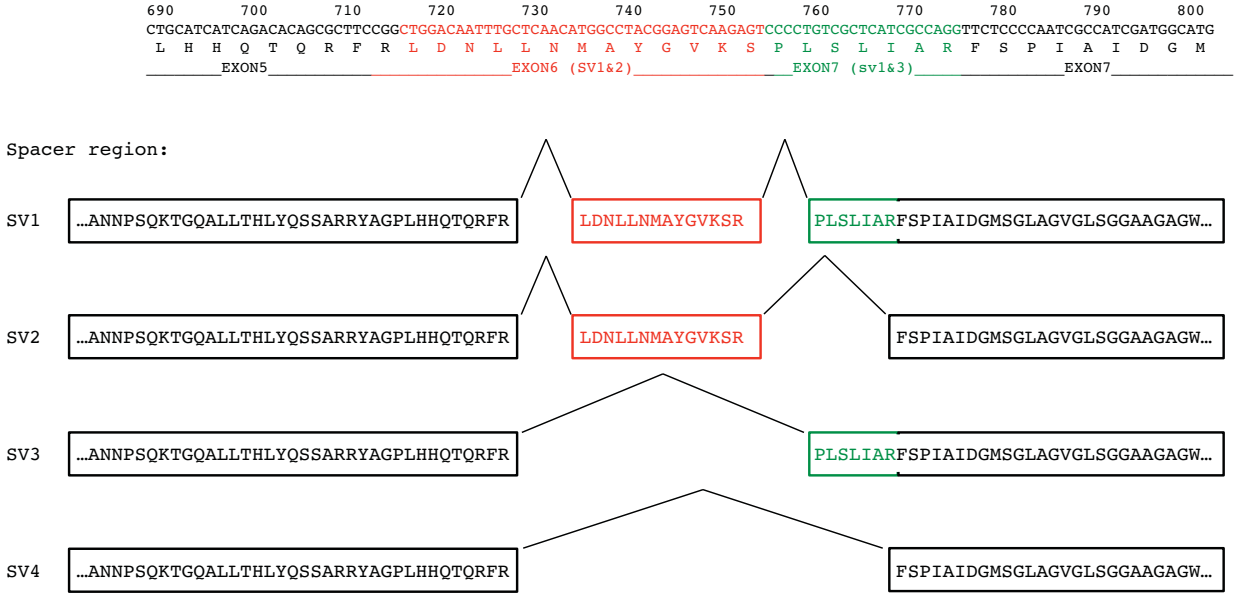


Figure 2b. Alternative splicing in the spacer region of HuC. Splicing of exon5 to exon6 is requisite for HuCsv1 and HuCsv2 production. Alternative splice acceptor sites in exon7 distinguish the two isoforms, as indicated. Exon6 is skipped in both HuCsv3 and HuCsv4 and the two products arise from differential use of the two splice acceptor sites in exon7.

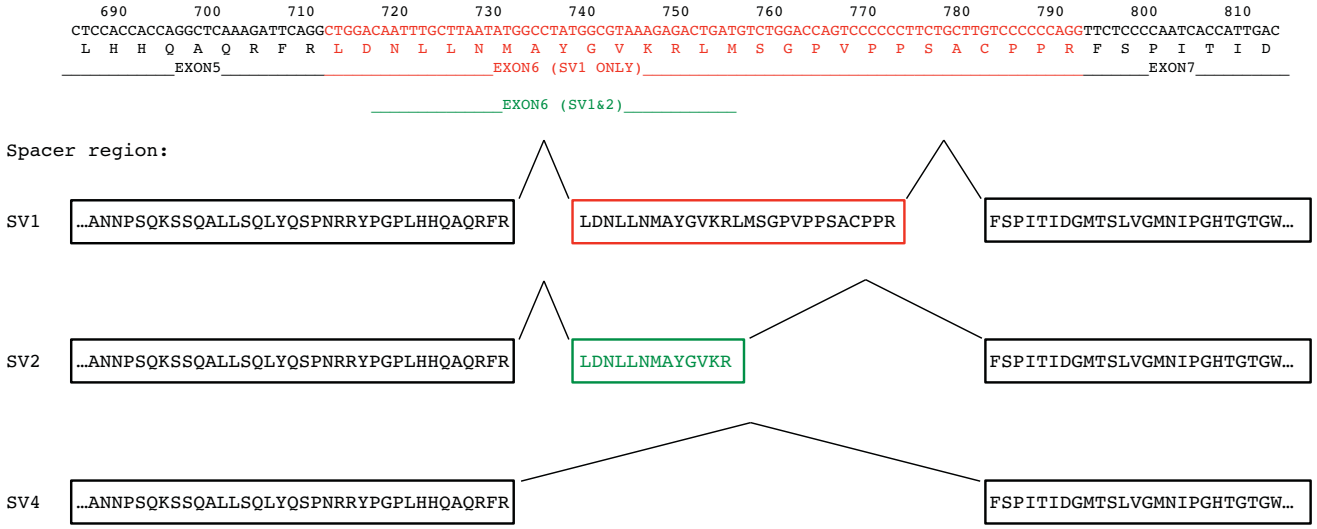


Figure 2c. Alternative splicing in the spacer region of HuD. Splicing of exon5 to exon6 is requisite for HuDsv1 and HuDsv2 production. However, unlike HuC, alternative splice donor sites in exon6 splice to a common splice acceptor site in exon7 as indicated. HuDsv4 is produced by skipping of exon6.

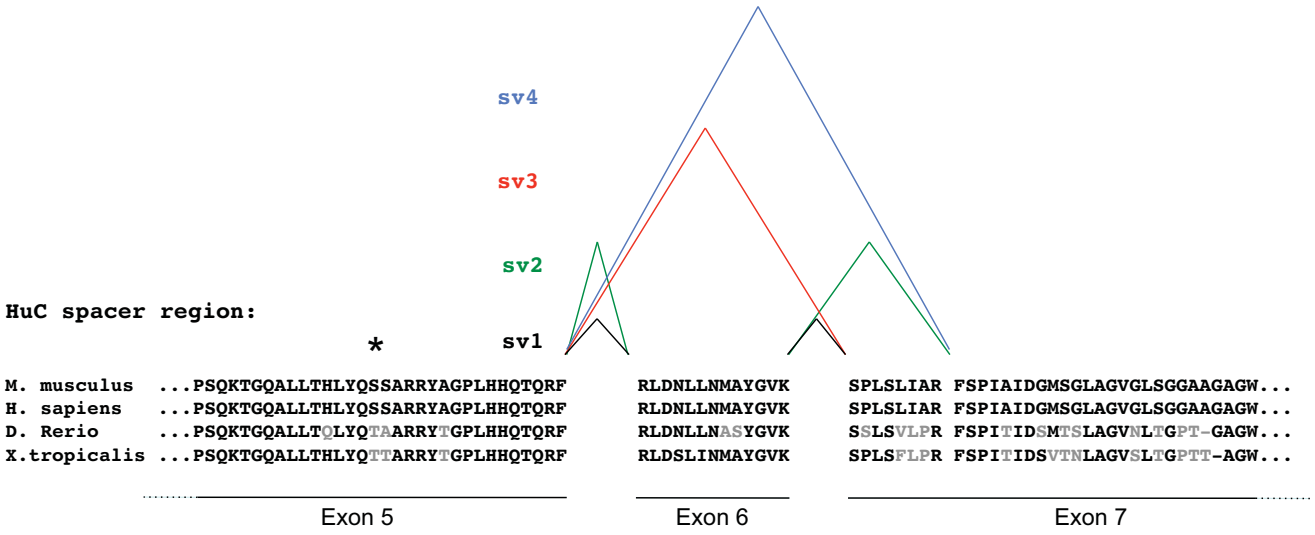


Figure3. The amino acid sequence and alternative splicing in the spacer region of HuC is highly conserved between vertebrates. Conserved residues are shown in **bold** text. Non-conserved residues are shown in grey.

Asterisk denotes a predicted phosphorylated serine (mouse/human) or threonine (zebrafish/Xenopus) based on conservation with HuR based on results from Kim HH, Genes Dev. 22(13): 180 (2008)

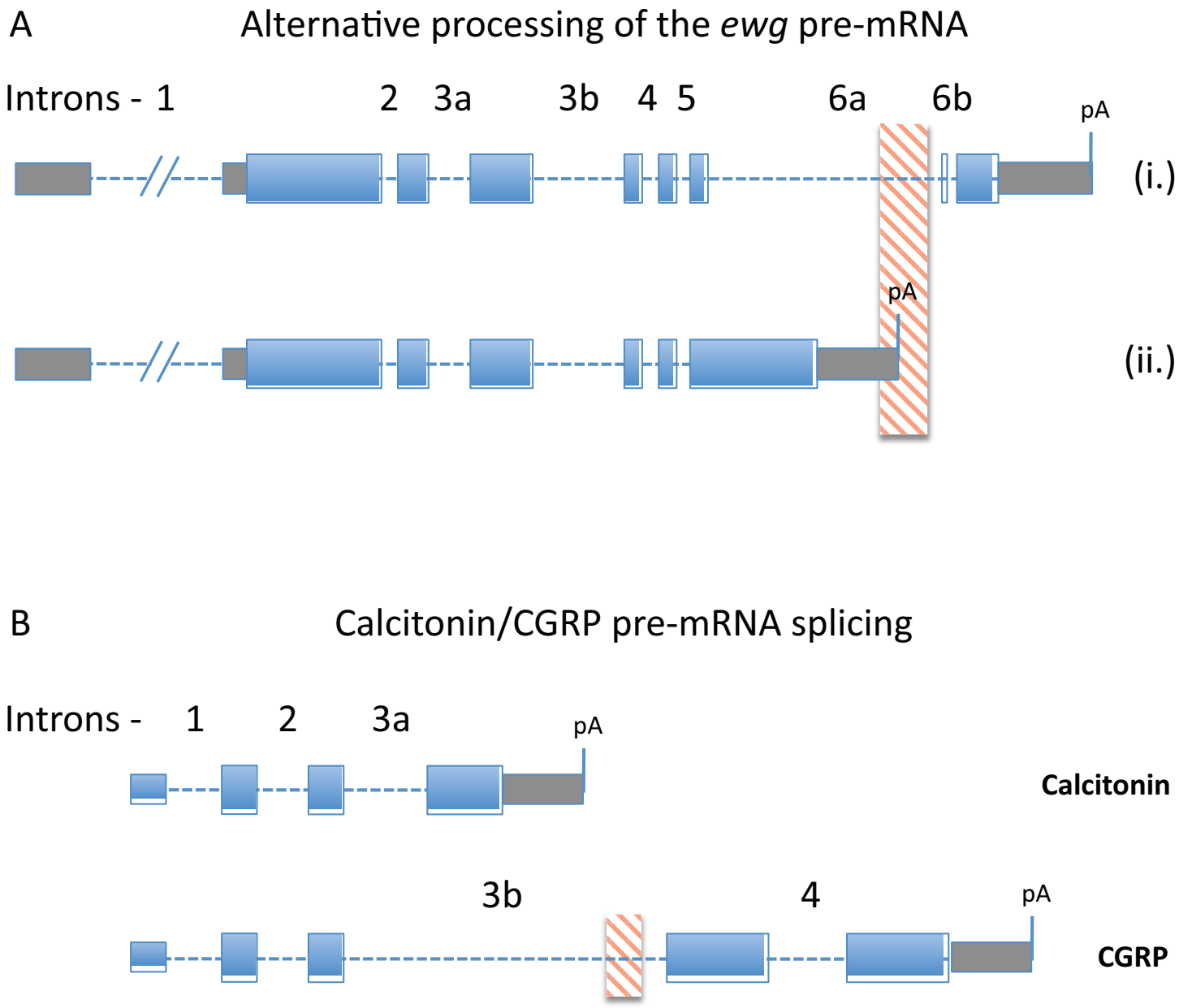


Figure 4a. Alternative splicing of the *ewg* pre-mRNA. Binding of ELAV to a uracil-rich region (red and white striped box) present in intron 6a prevents use of an early polyadenylation site (present in intron 6a) facilitating splicing of intron 6a and production of the longer, neuron-specific *ewg* mRNA splice isoform (indicated as i.).

Figure 4b. Alternative splicing of the CGRP/calcitonin mRNA. Non-neuronal splicing to produce the calcitonin-encoding mRNA transcript is indicated first. Binding of TIAR to a uracil-rich sequence immediately 3´ of the polyadenylation site of the calcitonin mRNA (indicated by the red and white striped box in intron 3b of the CGRP mRNA) promotes splicing of intron 3a and thus production of the calcitonin mRNA. Binding of nHu proteins to this same uracil-rich sequence has been reported to block splicing of intron 3a in favour of splicing intron 3b.

A

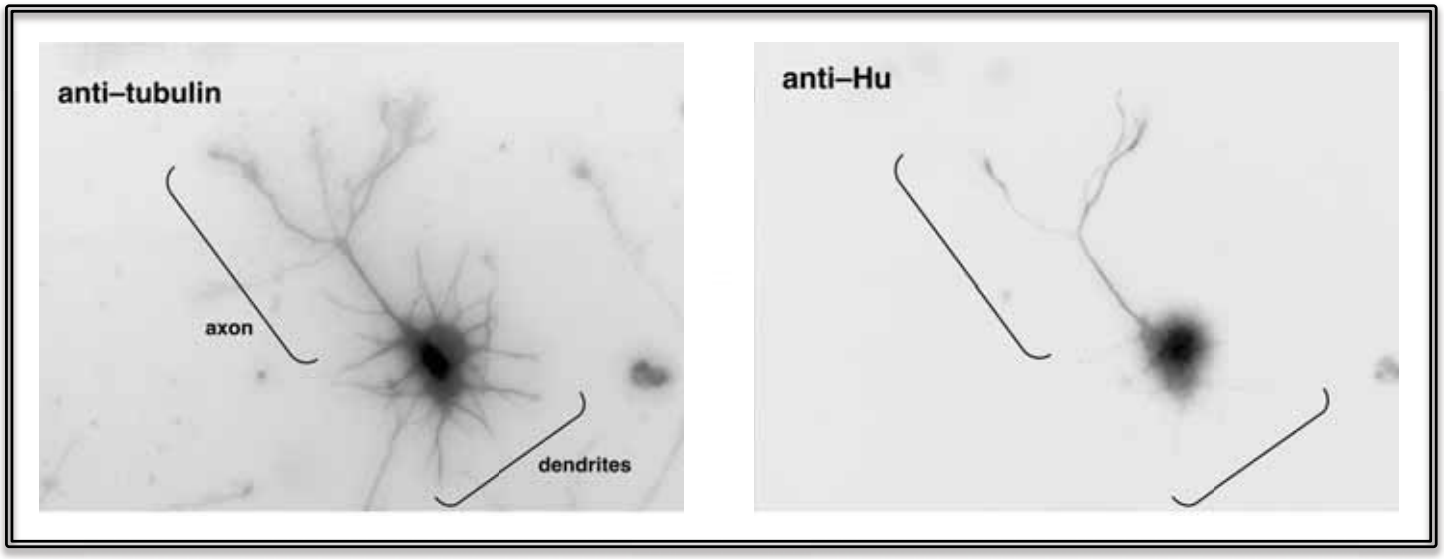


B

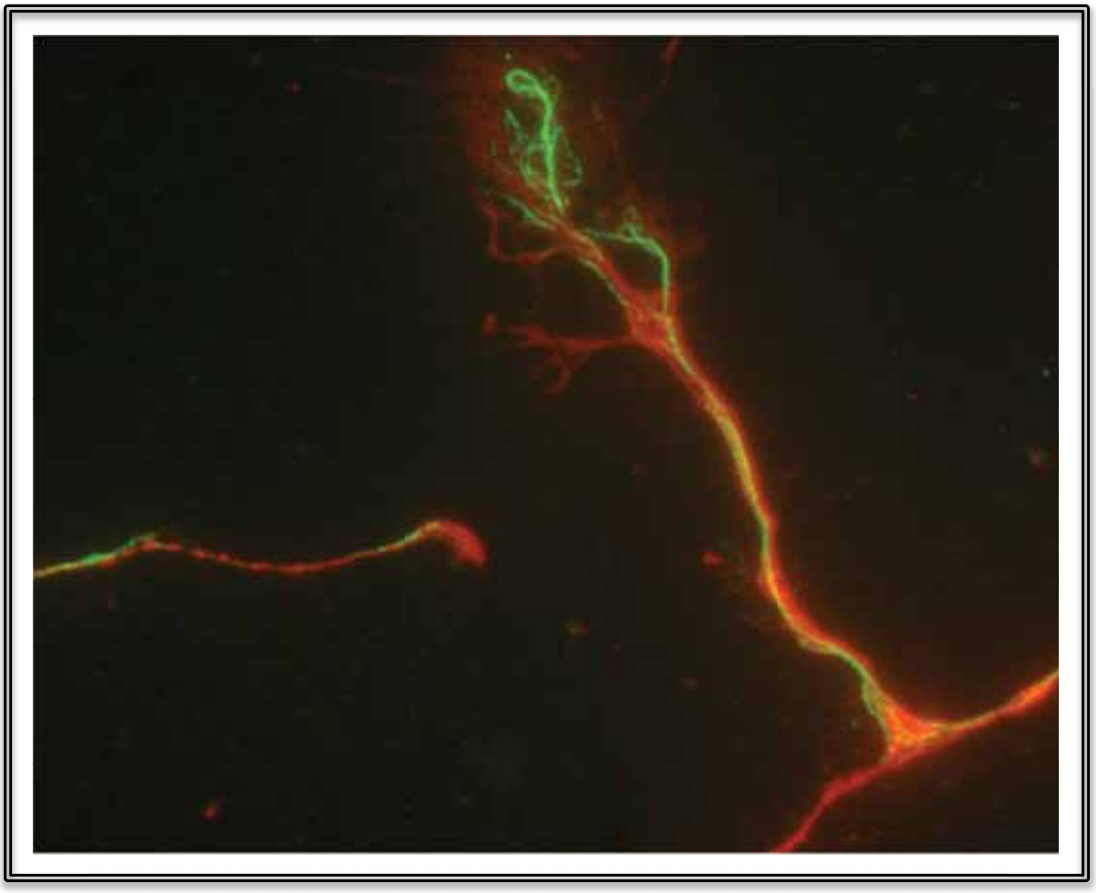

Figure 5a. Unpublished immunofluorescence images of an E18 rat hippocampal neuron ground for 3 days in vitro (DIV) and then fixed and stained for acetylated α-tubulin (left) and nHu protein expression (right).

Figure 5b. Higher magnification image of shows nHu protein (green) co-localising with microtubules (red) at the axonal growth cone of an E18 rat hippocampal neuron.

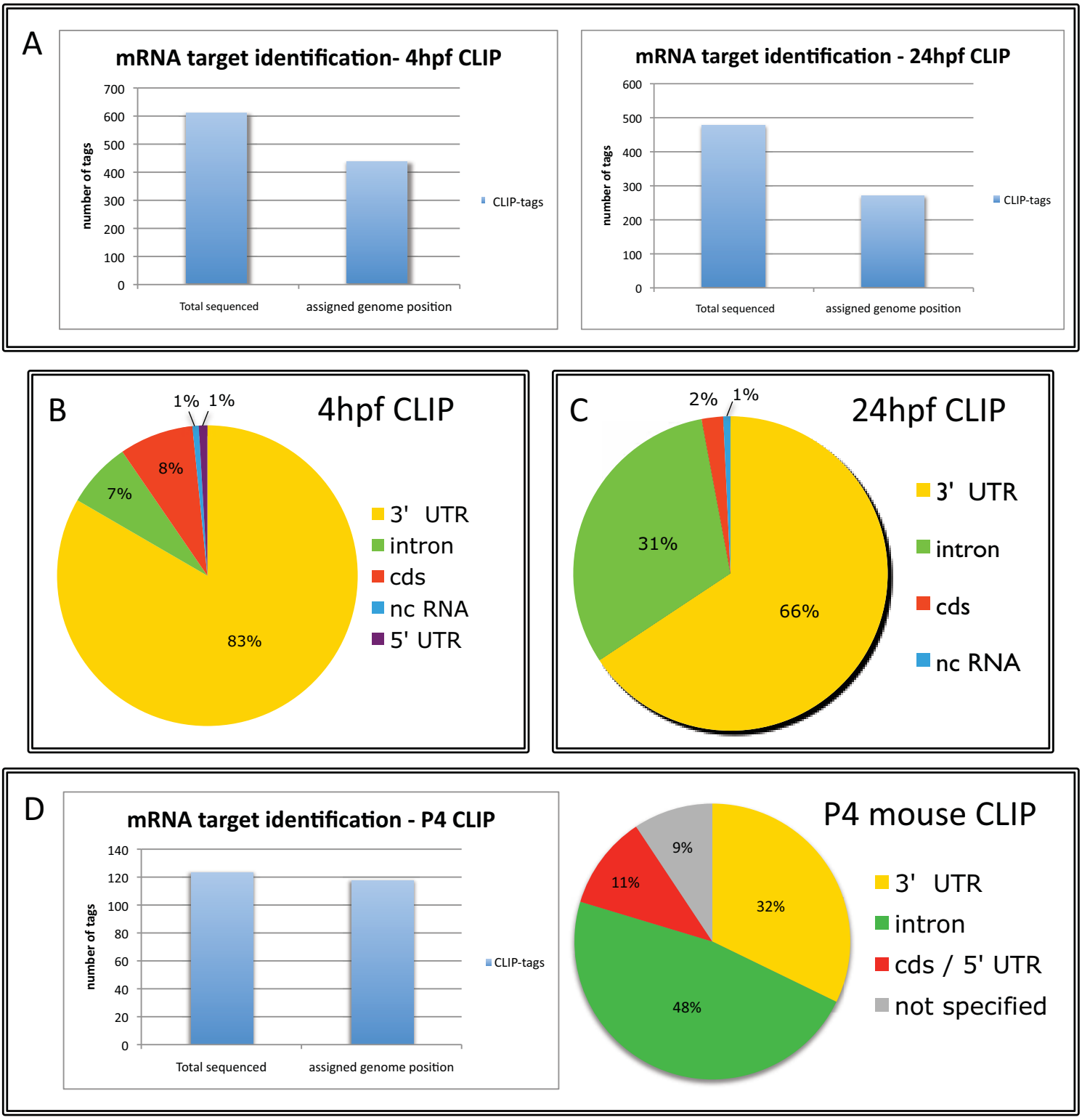


Figure 6. Unpublished CLIP data from 4hpf and 24hpf zebrafish and P4 mouse brain CLIP experiments.

6a. Number of CLIP tags sequenced versus number of tags for which alignment to a position within a gene encoding region of the zebrafish genome could be made.

6b and 6c. Percentage of CLIP tags from zebrafish CLIP experiments binding to specific regions within target mRNAs. cds = coding sequence, nc RNA = non-coding RNA

6d. Data from P4 mouse brain CLIP experiments.

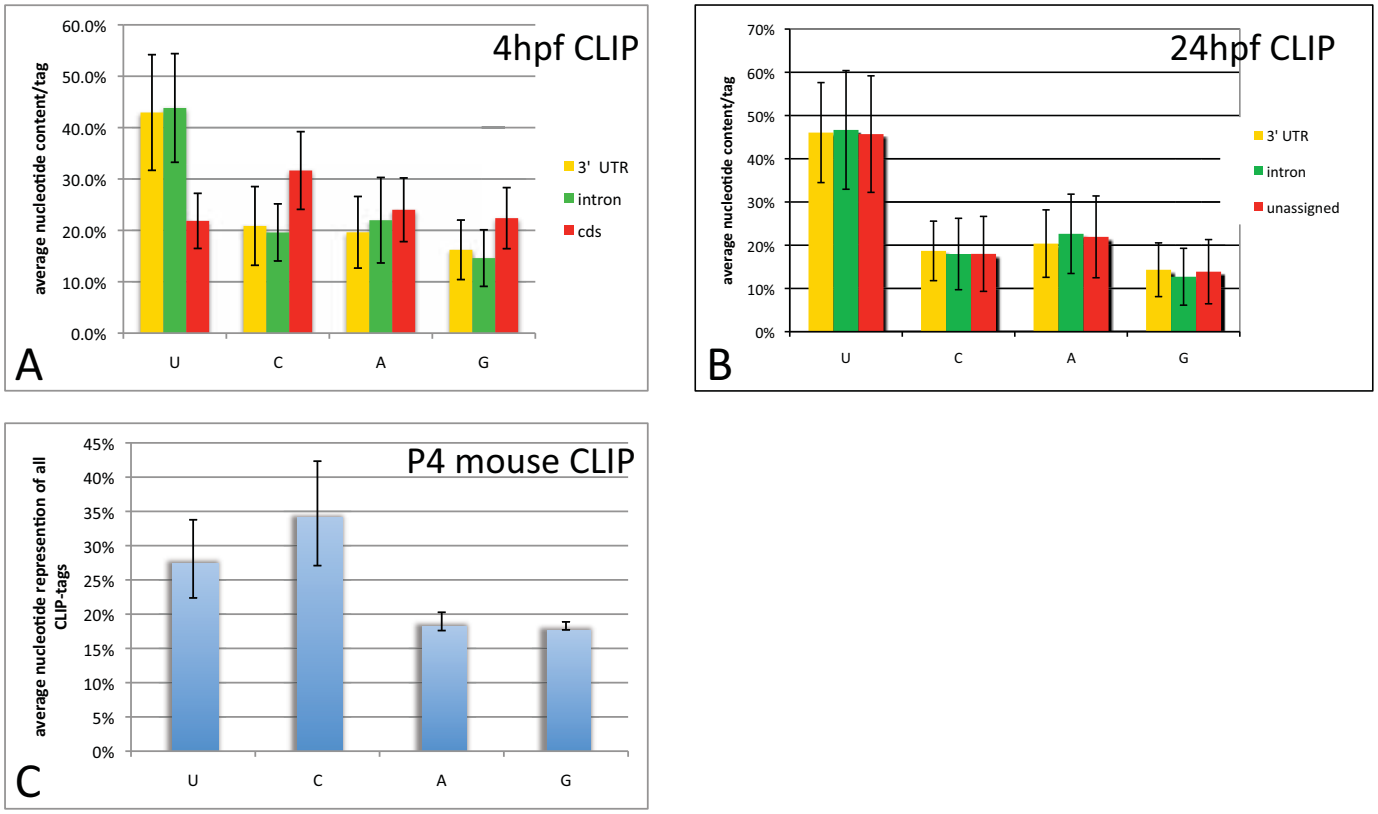


Figure 7. Unpublished CLIP data from 4hpf and 24hpf zebrafish and P4 mouse brain CLIP experiments.

7a and 7b. Averaged nucleotide content per CLIP tag from zebrafish CLIP experiments

7c. Averaged nucleotide content from entire library of sequenced CLIP-tags obtained from the P4 mouse brain CLIP experiment. Nucleotide content per tag was not available at the time of thesis completion.

| Target mRNA | | CLIP tag sequences | CLIP experiment |
|---|---|---|---|
| cdc42-v1 | CLIP tag 1 | TGTAGTCAAGATAACCTCGCTCTTACAGACTTTAAACCCT GAATAGAACCAAGTTTCATACTGTAACACAGGTGCTATTA TGGATCAAAGTTGGTTTGATTTCCAGTCTTTCCCCCCT | 4hpf zebrafish CLIP |
| cdc42-v2 | CLIP tag 1 | TTGCTTTGGACTTTATTTCGTCTTACTGTTATTAAGAGCAG ACCAAG | 24hpf zebrafish CLIP |
| cofilin | CLIP tag 1 | CCCTCTTATTTTATTTTGAGCAAGTTATTTTAAT | 24hpf zebrafish CLIP |
| | CLIP tag 2 | AAACGTCTAGTTAAGTTTATTTTCTAAGTTTGTGTGTGTT GCGACTAGGTATAGTACAAAGTCACACATTGTTATCGGA CC | 24hpf zebrafish CLIP |
| | CLIP tag 3 | ACACCCCTACTCCGTATCCCTCCCCATCCCATGCTGCCAA | mouse P4 CLIP |
| | CLIP tag 4 | ATACTACTCCCCTTTCCCTCTTATTTTATTTTTGAG | 4hpf zebrafish CLIP |
| | CLIP tag 5 | TATAGTACAAAGTCACACATTGTTATCGGACCATTCTGGG AACACGATCTACTCCCCTTTCCCTCTG | 4hpf zebrafish CLIP |
| VASP | CLIP tag1 | CTCTCTCCTTGTTTACTTTGACATATTTAGTTTTTTTTCCAC TTAATATTTTTGCT | 24hpf zebrafish CLIP |

Figure 7d. A selection of CLIP identified mRNAs that encode cytoskeleton modifying factors. The CLIP-tag sequence identified by CLIP is shown along with an indication of which CLIP experiment the mRNA was identified in. The CLIP tags for all four of the indicated mRNAs correspond to sequences in the respective mRNAs 3´UTR.

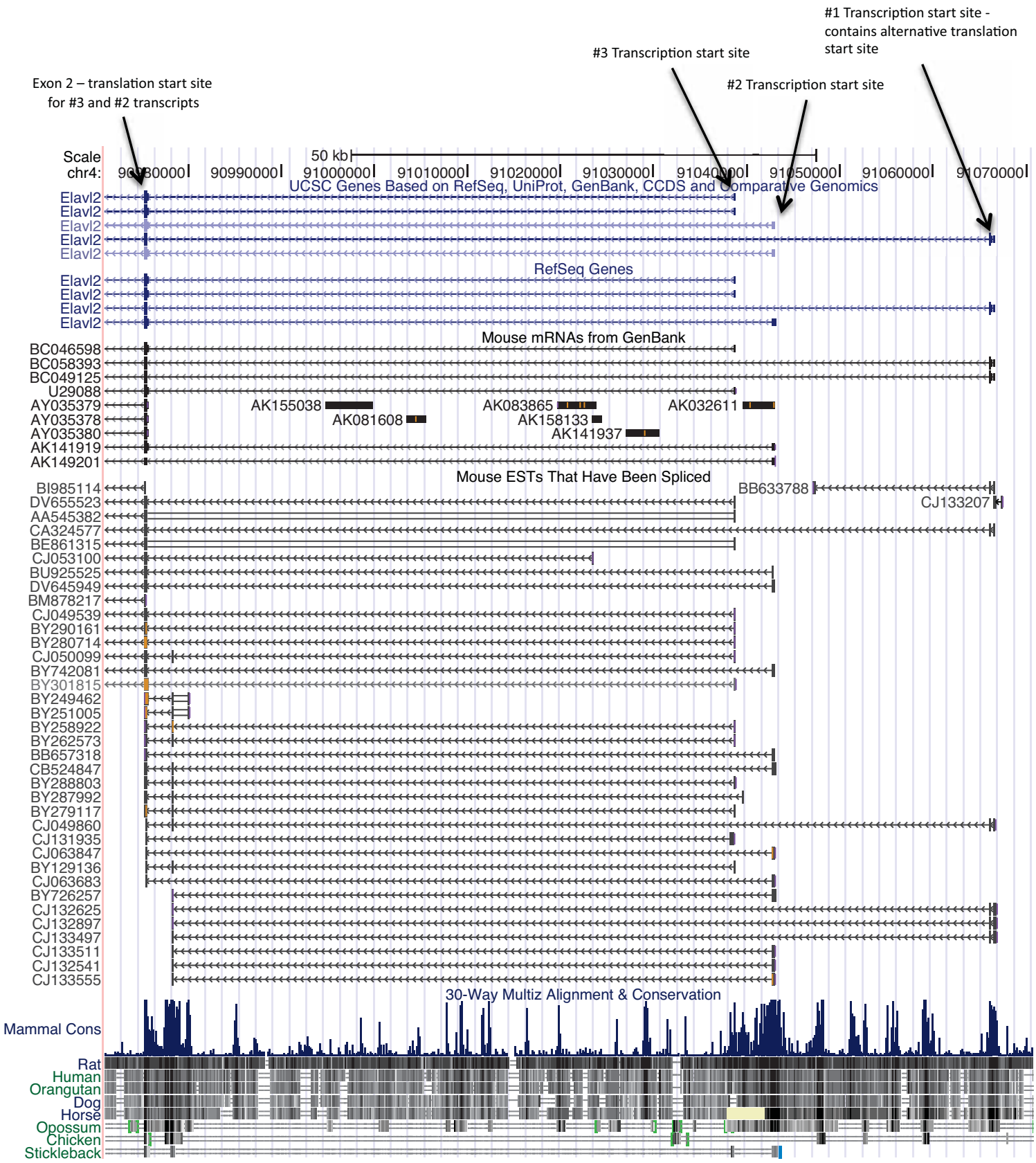


Supp Figure 1. Alternative transcription and translation start sites of mouse HuB.

Exon 2 contains the translation initiation AUG (with Kozak sequence) for HuB transcripts originating from the #2 and #3 transcription start sites. HuB transcripts originating from the #1 transcription start site contain an alternative translation initiation site (AUG + Kozak sequence) and thus produce proteins with alternative N-terminal sequences. All three transcripts have unique 5´UTRs.

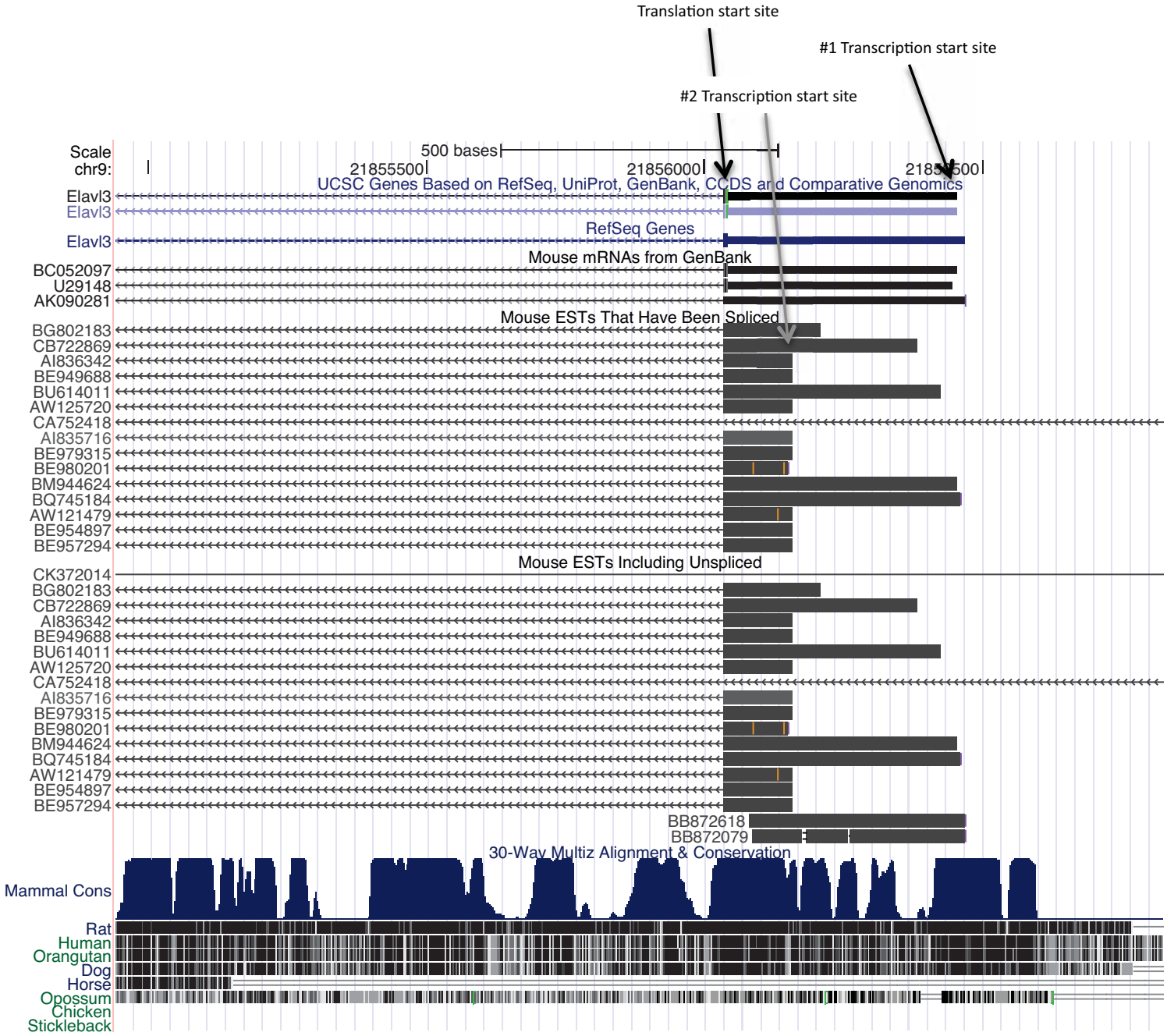


Supp Figure 1b. Alternative transcription and translation start sites of mouse HuC.

Exon 1 contains the translation initiation AUG (with Kozak sequence) for all HuC transcripts. Alternative transcription start sites yield 2 different mRNAs with unique 5´UTRs.

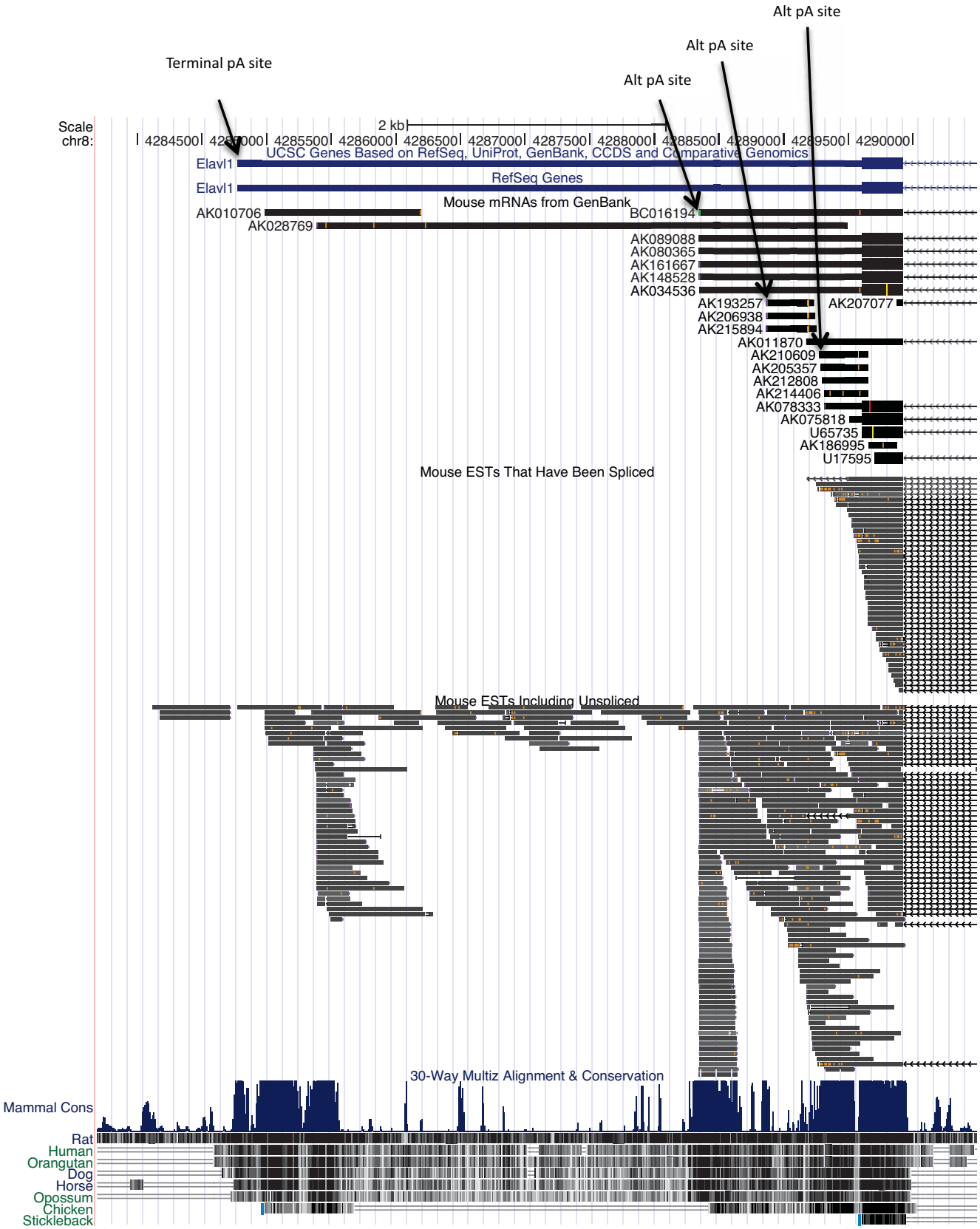


Supp Figure 2a. Alternative polyadenylation site usage of mouse HuR.

Indicated sites all use canonical (AAUAAA or AUUAAA) hexanucleotide sequences at the indicate pA site

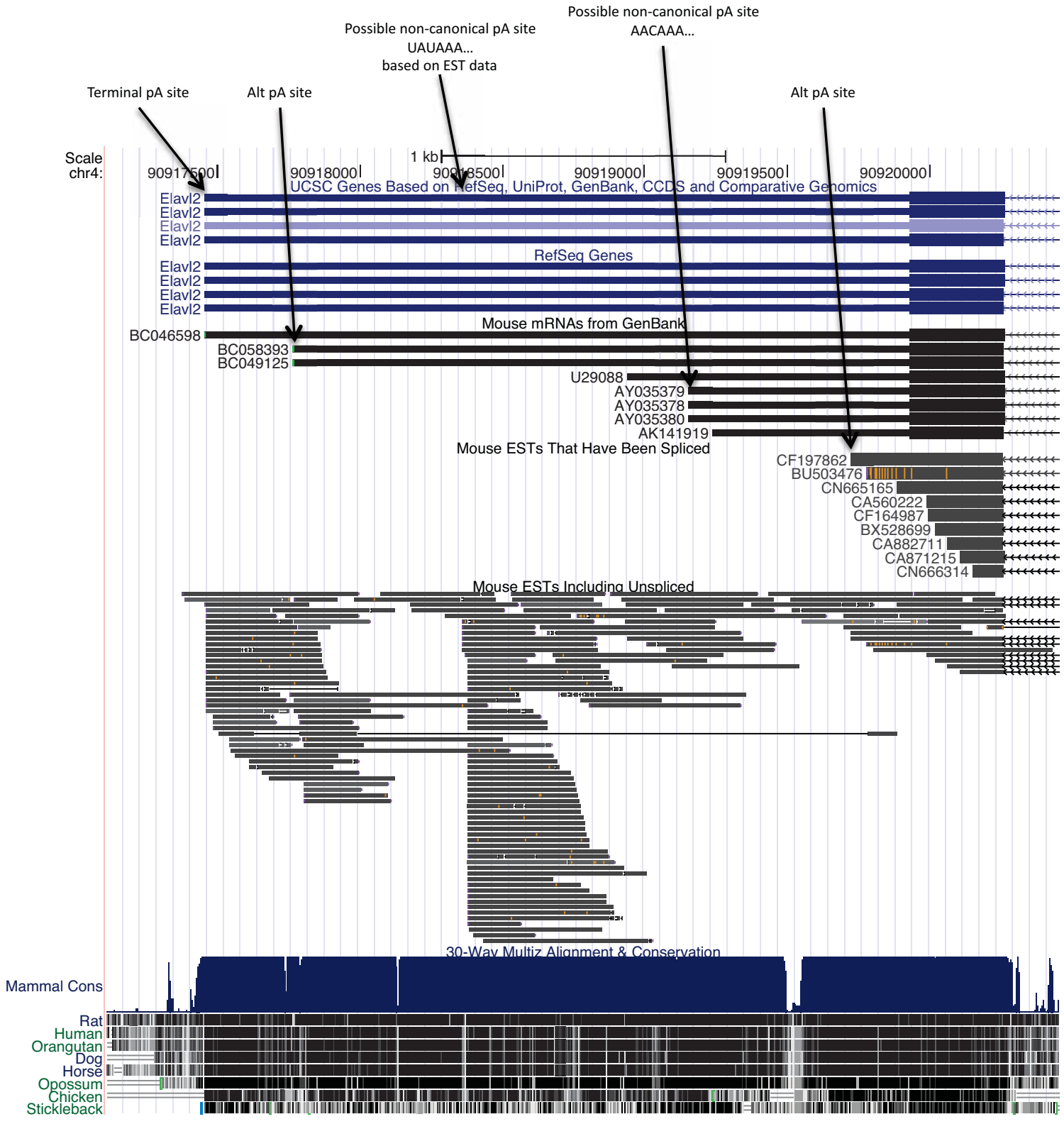


Supp Figure 2b. Alternative polyadenylation site usage of mouse HuB.

All sites use canonical (AAUAAA or AUUAAA) hexanucleotide sequences unless otherwise indicated.

All alignments current on 12th August 2010.

# Fluorescence-based Reporter Assays

## Introduction

Can we understand nHu function by looking at 3´UTR sequences (identified by nHu-CLIP experiments as nHu targets) in reporter assays? Hypothesis – nHu can affect target mRNA half-life or protein production through interactions with specific 3´UTR elements. To test this hypothesis, CLIP-identified 3´UTRs were incorporated into a reporter system.

The first generation of 3´UTR-reporter assays employed a destabilised variant of the enhanced green fluorescent protein (d2EGFP) as the reporter protein. Initially just two CLIP-identified 3´UTR sequences were incorporated into a d2EGFP overexpression vector, as 3´UTR sequences for the d2EGFP mRNA, with the unmodified d2EGFP vector (*ie* no added 3´UTR sequence) serving as a "non-target" negative control. 3´UTR-reporter vectors were co-transfected with either an HuCsv1 encoding vector (or empty vector control) into HEK293T cells, and d2EGFP expression with or without HuCsv1 overexpression compared using quantitative fluorescent western blot.

## Basic experimental rational

Basing the first generation of 3´UTR-reporter vectors on a fluorescent reporter protein was intended to facilitate multiple lines of investigation into effects of nHu proteins on target mRNAs. The primary focus of these experiments was to determine whether HuCsv1 influenced (either positively or negatively) reporter protein production from reporter mRNAs that incorporated specific 3´UTRs identified in nHu CLIP experiments. This work would be conducted in non-neuronal immortalised cell lines, such that the investigator could control both the amount of nHu protein expression and the amount of 3´UTR-reporter placed in transfected cells. This would allow for direct examination of effects arising from interactions between reporter mRNA and a specific nHu protein. However, the reporters could be directly transfered to a neuronal context, such as cultured rat E18 hippocampal neurons, where in addition to serving as an indicator of mRNA translatability, the fluorescent reporter protein could also serve as an indicator of mRNA subcellular localisation. Furthermore, neuronal cells could potentially be used to identify neuron-specific factors involved in nHu functions.

For the non-neuronal cell line assays, an effect on reporter protein expression by nHu would be determined by quantitative fluorescent western blotting. Specifically, the human kidney cell line HEK293T would be co-transfected with a vector encoding an N-terminally myc-tagged HuCsv1 (pmHuCsv1 – a pcDNA3 overexpression vector backbone carrying the coding sequence for HuCsv1), along with a reporter vector encoding a destabilised variant of enhanced green fluorescent protein (d2EGFP, Clontech) immediately followed by the 3`UTR of a putative target 3`UTR. The amount of d2EGFP reporter protein expressed in this condition would then be compared to the amount expressed when the reporter vector was co-transfected with an empty pcDNA3 vector (-HuCsv1 condition). Any effect of HuCsv1 on reporter protein expression would be seen as a difference in the amount of d2EGFP in a given amount of cell lysate, normalised to the total amount of β-actin protein (as a loading control), between the +HuCsv1 and –HuCsv1 conditions. As a "non-target" negative control, the d2EGFP reporter vector with no added 3´UTR sequence would be used to demonstrate any effect of HuCsv1 on d2EGFP expression from a specific 3`UTR-reporter vector was 3`UTR-dependent.

## Designing the EGFP-based 3´UTR reporter constructs

### *The 3´UTR-reporter vector backbone – pCI*

The reporter vector backbone used for the 3´UTR-reporter constructs was the CMV-promoter driven expression vector, pCI (Promega), designed for transgene expression in mammalian cells. Importantly, pCI vectors incorporate a chimeric intron immediately upstream of the reporter protein coding sequence. It has been empirically shown that the presence of a functional intron within the vector-encoded transgene transcript, improves transgene expression [207], [208], [209]. This occurs primarily as a result of improved transgene mRNA stability and translation, which is proposed to occur as a result of the mRNA having undergone proper mRNA processing and export. Both of these processes leave molecular marks on processed mRNAs in the form of bound protein complexes. These marks are informative about the nuclear history of a message and are interpreted by cytoplasmic factors involved in mRNA translation in a manner that affects both message stability and translatability. In the case of these 3´UTR-reporter assays, it was entirely possible that interactions between HuCsv1 and putative target mRNA sequences would not occur unless the reporter mRNA had been properly processed. As such, it was deemed to be of critical importance that 3´UTR-reporter transcripts be processed and exported into the cytoplasm in the same context as endogenous mRNAs. By using the pCI vector backbone, all 3´UTR reporter constructs could be generated with a common excisable intron. In this way, the synthesis and early processing of the putative target 3´UTR-reporter mRNAs in these assays would approximate that of typical mammalian messages and thus endow the reporter mRNA with a nuclear history consistent with that of a properly synthesised, processed and exported message.

### *The reporter protein – destabilised EGFP*

Another potentially critical issue in the design of the reporter assay was the overall stability of the reporter protein. Detection of an effect by HuCsv1 on expression of reporter proteins translated from mRNA carrying a putative nHu target 3´UTR depends on the ability to observe a difference in the total amount of reporter protein produced in the presence versus absence of HuCsv1. If the reporter protein is not rapidly turned over, then a build up may occur that could prevent observation of more modest effects on reporter expression by HuCsv1. As such, a destabilised variant of the enhanced green fluorescent protein was used to report expression from messages carrying putative nHu target 3´UTRs. Destabilisation of EGFP is caused by the incorporation of a PEST sequence (from mouse ornithine decarboxylase) at the carboxy-terminal

end of the protein, which targets the d2EGFP protein for ubiquitylation that ultimately results degradation by the proteosome. The half life of d2EGFP is ~2hrs, as determined by inhibiting translation using cyclohexamide followed by interrogation of cell fluorescence by FACS and by western blotting (*pd2EGFP-N1 vector data sheet*). By using a destabilised reporter it was hoped excessive accumulation of the reporter protein, which might interfere with detection of HuCsv1 mediated effects on reporter expression, could be avoided.

The 3´UTR-reporter vector backbone was constructed by sub-cloning the d2EGFP sequence from pd2EGFP-1 (Clontech) into pCI (Promega) as outlined in the materials and methods. The 3´UTR-reporter vector backbone is referred to as pCI_d2EGFP and is shown in figure 8.

## Selecting target 3´UTR sequences to test

Finally, consideration was given to the candidate nHu target 3´UTR sequences chosen for the reporter assay. In choosing nHu CLIP-identified 3´UTR sequences to test, several criteria were used. In particular, emphasis was placed on target mRNAs encoding proteins known to localise specifically to the growing axon of neurons and with a demonstrated role in modulating cytoskeleton dynamics within migratory axonal growth cones in response to chemotactic factors. As discussed in the introduction, a number of candidate targets were identified that encode for proteins involved in axonogenesis and axon guidance during development. From this list, two candidate nHu target 3´UTRs were selected; one from the Rho GTPase *cdc42* and one from the actin depolymerising factor *cofilin1*.

### *The Rho GTPase, Cdc42*

Cdc42 is a member of the Rho GTPase family. Rho GTPases in general act as molecular switches relaying both intra and extra-cellular signals to effect changes in actin cytoskeletal organisation. They have been shown to play important roles in various cellular processes such as cytokinesis, cell polarisation, cell migration and the formation of membrane processes including lamellipodia and filopodia [210], [196]. In neurons, cdc42 is required for polarisation, the process by which neurons specify their axon [197]. Following polarisation, cdc42 is an important regulator of responses by the migrating axonal (and dendritic) growth cone to chemotactic signalling cues [211].

Interestingly, alternative splicing of the penultimate exon of the cdc42 pre-mRNA to two distinct terminal exons results in the production of two highly similar cdc42 protein isoforms. With

respect to the cdc42 coding sequence, splice isoforms differ in only the final 30 nucleotides (terminal 10 amino acid residues) (figure 9a). However, the resulting splice isoforms have distinct 3´UTR sequences (figure 9b). Notably, while the canonical cdc42 splice variant (referred to as cdc42-v1 in this thesis) is reportedly expressed ubiquitously [212], the alternatively spliced cdc42 variant (referred to as cdc42-v2 in this thesis) is found to be uniquely expressed within neuronal tissues and was originally identified from a human fetal brain cDNA library [212], [213]. Comparison of mRNA expression levels of cdc42-v1 and cdc42-v2 in neuronal tissues reveals they occur at roughly similar levels, [214].

At the time, while there was clear evidence of a variety of roles for cdc42 important for neuronal development (a thorough review of the available literature on the role of cdc42 in neuronal development is available from [215]), the consequences of alternative splicing for the cdc42 gene were not completely understood. However, recent work identifying previously unidentified palmitoylated proteins from rat embryonic cortical neurons and synaptosomal membrane fractions using a proteomic approach revealed cdc42-v2 as a target for palmitoylation [214]. Palmitoylation is a type of post-translational modification whereby the 16-carbon saturated fatty acid; palmitate, is linked to cysteine residues via a thioester bond. The addition of a fatty acid residue to a protein enables the protein to be tethered to membranes. How and where proteins are tethered in membranes is influenced by the particular type of lipid modification the protein carries with ramifications for both protein localisation and function within a cell. Addition of lipid-modifications to cdc42 proteins facilitates their recruitment into the membrane, which enables them to target actin cytoskeleton polymerisation to discrete sites proximal to their position in the plasma membrane [216].

In their work, Kang *et al* found that palmitoylation was dependent on the final 10 amino acids of cdc42-v2 that make it unique compared to the cdc42-v1 isoform. They also showed that palmitylation did not occur for the cdc42-v1 isoform, which has previously been shown to carry a different lipid modification (prenylation). Functional analysis of cdc42-v2 palmitoylation in cultured rat embryonic neurons revealed a requirement for this form of post-translational modification in the formation of dendritic spines, small, actin-rich processes that extend out from the main dendritic branch that are involved in synapse formation. Importantly, the requirement for cdc42-v2 in spine formation appeared to be at the time when small filopodia (spine precursors) extend out from the main dendritic branch and explore the local environment for potential pre-synaptic connections. This observation suggests that palmitoylated cdc42

(cdc42-v2) may play a specific role in growth cone/filopodial dynamics during neuronal development.

***The cdc42-v2 3´UTR***

As well as leading to the production of two distinct cdc42 protein isoforms, alternative splicing of the 3´-end of the *cdc42* gene results in the generation of two mRNAs with distinctive 3´UTR sequences. Interestingly, the 3´UTR sequences of both cdc42-v1 and cdc42-v2 were identified as target sequences of neuronal Hu protein in the zebrafish CLIP experiments. The cdc42-v2 3´UTR was identified in the 24 hours post-fertilisation (hpf) zebrafish CLIP experiment, a developmental time point at which the full complement of neuronal Hu proteins is expressed in zebrafish and neuronal connections are still being made. The cdc42-v1 3´UTR was identified in the 4hpf zebrafish CLIP experiment, a time point at which the only neuronal Hu protein present is HuB [195] and embryos have not yet begun zygotic transcription nor have they completed gastrulation and thus, have not yet begun development of the nervous system. Given that cdc42-v2 had been identified as a nervous system-specific cdc42 variant [212], [213] the 3´UTR for cdc42-v2 was chosen for analysis in the 3´UTR-reporter assays.

For the fluorescence based 3´UTR-reporter assays the *cdc42-v2* 3´UTR was cloned from rat embryonic day 18 (E18) total brain cDNA and thus is referred to as **rcdc42-v2** in this thesis. The rat cdc42-v2 3´UTR was cloned (in preference to zebrafish) to accommodate potential future experiments examining the 3´UTR-reporter in a cultured rat hippocampal neuron system. Primer sequences used to amplify the target sequence are shown in table 2 along with restriction enzyme sites incorporated onto the ends of the amplified sequence to facilitate cloning into the pCI_d2EGFP vector backbone. Notably, the 3´UTR cloning primers amplify the complete rcdc42-v2 3´UTR, including the terminal canonical polyadenylation hexanucleotide sequence (AUUAAA) and predicted cleavage site, but not the downstream G/U-rich sequences required for polyadenylation at the 3´UTR-encoded terminal polyadenylation site. As such, polyadenylation of the rcdc42-v2 3´UTR-reporter mRNA was ensured by the presence of the SV40 late polyadenylation signal within the pCI vector backbone, 3´ of the included rcdc42-v2 3´UTR sequence. In total, the resulting mRNA transcript was ~2.1kb reporter mRNA (~960nt of 3´UTR sequence) + polyadenylate tail (~50-200nt) (figure 10). An upstream (early) polyadenylation signal containing a canonical, AAUAAA hexanucleotide sequence is also present within the first 80nt of the 3´UTR. Use of this early polyadenylation signal is supported by available EST data (UCSC database).

## The actin depolymerising factor, Cofilin1

Cofilin1 belongs to a family of **a**ctin **d**e-polymerising **f**actors collectively known as ADFs. There are a total of three ADFs found in vertebrates: ADF, cofilin1 (non-muscle) and cofilin2. It is generally true for vertebrate organisms that both ADF and cofilin1 are primarily expressed within the nervous system while cofilin2 is expressed in muscle [217]. Functionally, ADFs bind to the minus end of F-actin filaments inducing a conformational change that results in unidirectional disassembly of actin monomers from the filament. In this way, ADFs are major actin cytoskeleton remodelling proteins that have been found to play important roles in actin-dependent cellular processes including cell and growth cone migration, cytokinesis, and both phago and endocytosis [218], [219].

Of particular interest to this thesis was Cofilin1, the 3´UTR of which was identified as a target sequence of neuronal Hu proteins in the P4 mouse brain, 4hpf and 24hpf zebrafish CLIP experiments (figure 7d). *In vitro* primary neuron culture-based studies, examining factors influencing the growth and behaviour of actively migrating axonal growth cones, have shown Cofilin1 is required for development and elongation of the axon [197], and in turning responses of growth cones to a variety of chemotactic factors involved in proper guidance of migrating growth cones during wiring of the nervous system [220] [221] [169]. Of particular note are the results from a series of experiments examining the molecular basis of axonal growth cone turning in response to the chemorepellent molecule, Slit2 [169]. Using an *in vitro* primary neuron culture system to study migrating axonal growth cones isolated from Xenopus retinal ganglion cells, Piper *et al* show that the repulsive effect of Slit2 on growth cone steering is caused by a decrease in cytoskeletal F-actin within growth cones, which importantly, is dependent on local protein translation. Intriguingly, they show that concomitant to a decrease in F-actin within growth cones responding to Slit2, a local increase in Cofilin1 protein is also observed that is similarly dependent on local, *de novo* protein synthesis. The importance of this finding cannot be overlooked. In combination with research showing the *cofilin1* mRNA is specifically localised to growth cones in a manner that is proposed to be dependent on sequences present within it's 3´UTR [222], [223], [224], the results from the Piper *et al* paper strongly implicate local translation of Cofilin1 in the responses of migrating growth cones to local chemotactic factors, important for the proper wiring of vertebrate nervous systems. That the *cofilin1* 3´UTR is detected as a neuronal Hu protein target in both the P4 mouse brain and 24hpf zebrafish embryo CLIP experiments was seen as strong evidence of a role for nHu proteins in some form of post-transcriptional regulation of the *cofilin1* mRNA. In combination with the data of Piper and others

and our observations of neuronal Hu protein localisation in axons and growth cones of E18 rat hippocampal neurons actively undergoing axonogenesis, a role for nHu proteins in the regulation of cofilin1 mRNA localisation or local translation appeared highly possible.

***The cofilin 3´UTR***

The *cofilin1* 3´UTR was cloned from rat embryonic day 18 (E18) total brain cDNA and thus is referred to as **rCofilin** in this thesis. Primer sequences used to amplify the target sequence are shown in table 2 along with restriction enzyme sites incorporated onto the ends of the amplified sequence to facilitate cloning into the pCI_d2EGFP vector backbone. As with the rcdc42-v2 3´UTR sequence, the cloning primers used to amplify the rCofilin 3´UTR include the terminal canonical polyadenylation hexanucleotide sequence (AAUAAA) in the amplified sequence but not any of the downstream polyadenylation signal elements (cleavage site or downstream G/U-rich sequences). As such, polyadenylation of the rCofilin 3´UTR-reporter mRNA would occur using the SV40 late polyadenylation signal present within the pCI vector backbone and result in an mRNA product of ~1.9kb (~730nt of 3´UTR sequence) + polyadenylate tail (50-200nt in length) (figure 10). No upstream (early) canonical polyadenylation signals are present within the rCofilin 3´UTR and no evidence of alternative polyadenylation sites is found in the available EST data for the rat, mouse or human genomes.

***The non-target control 3´UTR***

Finally, the pCI_d2EGFP vector backbone was used as a non-target control reporter to show that any effect of HuCsv1 on putative target 3´UTR-reporters was dependent on the presence of a CLIP-identified 3´UTR sequence. The resulting control reporter message is approximately 1.3kb in length (~150nt of 3´UTR sequence immediately distal to the d2EGFP stop codon) and terminates at the vector encoded SV40 late polyadenylation signal (figure 10).

## Advantages and limitations of the reporter assay

While the reporter assay design did take steps to try and recapitulate as faithfully as possible the production and presentation of candidate target 3´UTR sequences for interaction with neuronal Hu proteins, several limitations were still present that could in principle influence the utility of the assay for examining nHu function. These limitations are outlined below.

***Reporter transgene versus target coding sequence***

Firstly, one obvious limitation comes from using a fluorescent reporter transgene (d2EGFP) rather than the protein actually encoded by the target message. While the advantages of ease of

detection in live transfected cells, availability of high quality antibodies for detection by western/immunofluorescence and added control over the experiment by ensuring the only unique sequence present within the reporter mRNA is the 3´UTR itself support the use of a fluorescent reporter protein such as EGFP, the turnover dynamics of the original target message-encoded protein are lost. This could present a problem in a situation where, the (target mRNA) encoded protein has a significantly higher rate of turnover compared to the fluorescent reporter. In this case, any effect of HuCsv1 on target expression may be masked because the transgenic reporter protein is not turned over rapidly enough to reveal any difference between the +HuCsv1 and –HuCsv1 conditions. To address this issue, a destabilised EGFP variant, d2EGFP was used as the reporter protein. The half-life of this protein is relatively short (~2hr) and was the best available solution for any potential issue arising from prolonged reporter protein stability. Importantly, neither cdc42-v2 nor cofilin is described as a being a rapidly turned over protein in the literature, nor do either contain any classical protein turnover domains such as a PEST sequence or ubiquitylation sites. Given the lack of any information suggesting either protein is rapidly degraded, the 2hr half-life of d2EGFP was presumed to be short enough to either approximate or be shorter than the half-life of either cdc42-v2 or cofilin.

***A neuronal versus non-neuronal cell system***

Secondly, the experimental design is predicated on the idea that it would be possible to observe nHu RNA-binding protein activity using the 3´UTR target reporter system described, when used in a heterologous cell system. The advantage of using a non-neuronal cell line in this assay is that such a cell line will lack endogenous nHu proteins, and thus, a single neuronal Hu protein can be tested in the context of a given reporter, making it much easier to ascribe specific biological function to a given neuronal Hu protein.

However, it is entirely possible that nHu proteins operate within a specific molecular environment and that any regulatory activity of nHu proteins is carried out in concert with other regulatory factors such as other RNA-binding proteins, mRNA translation machinery or regulatory factors (such as miRNAs), which may or may not be present within the cell line chosen for these experiments. Given the primary aim of the experiment was to test the function of a specific neuronal Hu protein, the simplest system with which to do that was one in which no other nHu proteins were present. If, following testing, it appeared that no obvious effect of nHu on target 3´UTR reporter mRNA then alternative, more neuron-like, conditions could be sought out.

***Multiple factors affecting assay sensitivity***

Finally, assay sensitivity was expected to be a potential issue and one that could only be resolved through empirical testing of different assay conditions. There were a number of parameters that could affect assay sensitivity, including: the amount of d2EGFP reporter protein necessary for reliable fluorescent immunodetection from a western blot, the kinetics of 3´UTR-reporter mRNA and HuCsv1 protein expression, the ratio of HuCsv1 protein to 3´UTR-reporter mRNA necessary for maximum HuCsv1 activity within the assay, and finally, the robustness of HuCsv1 influence on a target 3´UTR-reporter mRNA. These issues are discussed below.

**Fluorescent western blotting**

Fluorescent immunodetection of the d2EGFP reporter (and HuCsv1) protein levels was used in preference to more classical enzymatic detection methods (such as Enhanced Chemiluminescence (ECL) exposed to film) for a number of reasons. The most significant reason was that in terms of the relationship between signal and protein abundance, fluorescent detection methods have a significantly larger dynamic range over which fluorescence intensity is linearly related to abundance of the protein of interest. Under the conditions used for these reporter assays, fluorescent detection of protein abundance from western blots has been empirically shown to be linear over 3.6 orders of magnitude, compared to just 1.5 orders of magnitude for ECL detection ([225]). As such, fluorescent immunodetection from western blots is considerably more robust in terms of capacity to quantify abundances of a given protein of interest and sensitivity to differences in abundance, when compared to enzymatic detection methods. Using the most quantitative and robust method of western blotting to measure differences in d2EGFP protein abundance within the 3´UTR-reporter assays was obviously desirable, as from the outset there was no way of knowing how nHu proteins might affect expression of the d2EGFP reporter and if any effect was observed, what the magnitude of that effect might be.

In addition to being highly quantitative, fluorescent western blotting is also readily amenable to multiplexing. The ability to detect multiple proteins simultaneously simplifies workup of the data by eliminating the need to strip and re-probe blots. Under the conditions used for these reporter assays, it was possible to detect of up to three different proteins of interest from the same blot at the same time.

**Molar amounts of HuCsv1 protein to 3´UTR-reporter mRNA**

One potential trade-off to the advantages of fluorescent western blotting over enzymatic methods was a reduction in assay sensitivity when detecting low abundance proteins. Enzyme-based detection methods such as ECL have been reported to be up to twice as sensitive (comparing absolute lower limit of detection) than the fluorescent detection method used in these experiments [225]. Where this becomes important is in considering how much 3´UTR-reporter mRNA is necessary to yield detectable amounts of d2EGFP protein. It was anticipated that in order to see an effect of HuCsv1 on any given HuCsv1-targetted 3´UTR-reporter message, there must be a significant molar excess of HuCsv1 protein to reporter mRNA. Depending on the functional outcome of an interaction between nHu proteins and a given target mRNA, failure to ensure a molar excess of HuCsv1 to 3´UTR-reporter mRNA could obscure any functional effects of HuCsv1 on reporter activity. The most obvious situation where this could be a problem would be where HuCsv1 negatively regulates the expression of a specific target message. In cells co-transfected with HuCsv1 and the 3´UTR-reporter, excess unregulated reporter mRNA would generate greater levels of reporter protein and effectively mask the repressive effect of the neuronal Hu protein on its target mRNA.

Compounding the potential issue of lower sensitivity of the fluorescent western method was the short half-life of the d2EGFP reporter protein. While the advantages of this reporter have been discussed, greater instability of the reporter protein was expected to directly translate to reduced abundance and thus reduced signal on western blots. In light of these factors, a balance had to be struck between providing enough 3´UTR-reporter mRNA to express d2EGFP at detectable levels and while maintaining a molar excess of HuCsv1 protein.

In addressing the issue with reporter mRNA abundance, two preliminary experiments were conducted. In the first experiment, a range of control 3´UTR-reporter vector amounts were tested to get a feel for how much reporter vector was necessary in order to detect the d2EGFP reporter by fluorescent western blot. By fixing this parameter from the outset, a range of pmHuCsv1 vector amounts could be tested in subsequent co-transfection assays to try and determine how much pmHuCsv1 vector was necessary to provide levels of HuCsv1 protein that resulted in changes in expression from either of the two putative target 3´UTR-reporters.

***Testing amounts of 3´UTR-reporter vector***

In the first experiment (figure 11), the control 3´UTR vector was tested at a range of amounts from 2µg to 0.25µg. In each well (6-well tray) of ~$2x10^5$ 293T cells, the total amount of DNA co-

transfected was maintained at 2μg using the empty pcDNA3 vector (-HuCsv1 condition). Cells were transfected using 6μL of FuGENE to maintain a 3:1 ratio of FuGENE to DNA and left for 20hr post-transfection prior to cell lysate collection. 10μg of each whole cell extract was loaded into a 12% bis-tris polyacrylamide gel and separated by SDS-PAGE. Following transfer of separated proteins to a PVDF membrane, total protein abundance for d2EGFP and βactin (loading control) were determined by fluorescent western blot using antibodies specific for EGFP and β-actin, as detailed in the Materials and Methods with corresponding species-specific fluorescently tagged secondary antibodies. Detection and quantification of fluorescence intensity for each protein of interest was carried out using the Typhoon Trio Variable Mode Imager (GE Healthcare) and associated Image Quant 1.0 software.

Relative abundance of the d2EGFP reporter was determined by normalising the raw fluorescence values for d2EGFP to those of β-actin (fluorescent signal arising from the relevant secondary antibody). The results of this experiment (figure 11) showed that EGFP expression was detectable at all amounts tested, although there was not a linear response to dosage (the lower amounts tested – 0.25μg and 0.5μg, appeared slightly stronger than expected relative to the behaviour of the larger amounts). This was likely due to the difficultly in measuring low amounts of reporter protein by fluorescent western. From these results, 0.25μg of 3´UTR reporter vector was used in subsequent transfections.

***A small dose-response test of pmHuCsv1 with 3´UTR-reporter constructs***

In the second experiment (figure 12a-b), a small range of pmHuCsv1 vector amounts was tested with each of the 3´UTR-reporter vectors. In this case, 0.25μg of either 3´UTR-reporter vectors was co-transfected with 0μg, 1μg or 2μg of pmHuCsv1. In terms of molar amounts of plasmid, 1μg of pmHuCsv1 provides a minimum 3-fold molar excess of pmHuCsv1 vector to 3´UTR-reporter vector (1μg pmHuCsv1 = 234.34fmol versus 0.25μg = 78.69fmol of control 3´UTR-reporter – pCI_d2EGFP). Given these plasmids use the same CMV-promoter to drive transgene expression, a molar excess of pmHuCsv1 compared to 3´UTR-reporter vector would be expected to translate into a molar excess of HuCsv1 protein to 3´UTR-reporter mRNA.

Where required, the total amount of plasmid transfected was made up to 2.25μg with empty pcDNA3 vector DNA. Cells were transfected using 7μL of FuGENE and left for 20hrs prior to collection of whole cell lysates. As a control, 0.25μg of each 3´UTR-reporter vector was also transfected with 0.75μL of FuGENE (3:1 ratio) to compare differences in reporter expression when co-transfected with other vectors versus singly. Samples from each transfection were

separated by SDS-PAGE using 4-12% bis-tris polyacrylamide gels and processed for fluorescent western blot (figure 12a) as in the previous experiment.

The results from this experiment showed a modest reduction in the amount of β-actin-normalised d2EGFP reporter protein from both the rcdc42-v2 and rCofilin 3′UTR-reporter when co-transfection with HuCsv1 (figure 2b). Furthermore, the effect appeared to be somewhat dose-dependent, with lysates from cells that received 2μg of pmHuCsv1 having less overall d2EGFP expression than cells that received 1μg pmHuCsv1. The results for the target 3′UTR-reporters suggested that the amount of HuCsv1 protein expressed by co-transfected cells was sufficient to cause a measurable effect of HuCsv1 on d2EGFP expression. Notably, based on these results it was conceivable that the maximum effect of HuCsv1 had not been observed in these experiments and that higher amounts of pmHuCsv1 (or lower amounts of 3′UTR-reporter vector) could lead to greater reductions in d2EGFP reporter protein expression.

However, while no obvious effect of HuCsv1 was observed for the control 3′UTR-reporter in the 1μg pmHuCsv1 condition, expression of d2EGFP in the 2μg pmHuCsv1 condition did appear to be slightly reduced (~1.5-fold reduction compared to -HuCsv1) (figure 12b). This observation invited the possibility that at higher levels of HuCsv1 overexpression, a non-specific effect on general translation was occurring that resulted in reduced d2EGFP expression from the non-target 3′UTR-reporter. Given this result, the stronger reduction in d2EGFP abundance from either of the experimental reporters in the 2μg pmHuCsv1 condition could not be completely attributed to a uniquely 3′UTR-specific effect of HuCsv1.

A variety of potential mechanisms exist to explain how high levels of HuCsv1 protein might lead to general reductions in protein expression. It is possible HuCsv1 interacts with one or more components of the general translation machinery and that high HuCsv1 protein expression leads to sequestration of these factors, causing a reduction in translation activity within cells independent of any mRNA sequence-specific activity of HuCsv1. Alternatively, it is possible that at high HuCsv1 concentrations HuCsv1 could begin to engage in mRNA interactions not specifically directed by the presence of a genuine U-rich target sequence, which could then lead to reduced message translation. Regardless of how this effect occurred, it appeared from this experiment that high levels of HuCsv1 expression could yield effects on 3′UTR-reporter expression, which were not sequence-specific.

## Results from replicate experiments: does HuCsv1 have a negative effect on protein production from target 3´UTR-reporters?

Following on from these preliminary experiments, a series of replicate experiments were carried out to test a range of pmHuCsv1 amounts against each 3´UTR-reporter. The aim of these experiments was to obtain enough replicate data sets to allow statistical analysis of changes in d2EGFP reporter expression to confirm or refute the 3´UTR-specific effect of HuCsv1 on reporter expression observed in the preliminary experiment. In four independently repeated experiments, 0.25µg of either the control 3´UTR vector, rcdc42-v2 3´UTR or rCofilin 3´UTR-reporter vectors were co-transfected into HEK293T cells with increasing amounts of pmHuCsv1 (up to 2µg). The total amount of DNA transfected was always 2.25µg/well, obtained by supplementing transfection cocktails with empty pcDNA3 vector where required. In these experiments, lower amounts of the pmHuCsv1 vector were tested against each reporter to more finely examine the dose response of 3´UTR-reporters to HuCsv1 (figure 13). The complete range of pmHuCsv1 amounts tested included 0µg, 0.25µg, 0.5µg, 1µg and 2µg. Whole cell extracts from transfected cells were collected 20-28hrs after transfection and expression of HuCsv1, d2EGFP and β-actin in each transfection condition was determined using fluorescent western blotting. In all graphs presented, the amount of expression of either HuCsv1 or d2EGFP is shown normalised to the reported abundance of β-actin for the same sample. The averaged results for normalised d2EGFP and HuCsv1 abundance from the four replicate experiments are presented for each 3´UTR-reporter (figure 14a, 15a and 16a).

## Fluorescent western approach yields poor reproducibility between experimental replicates.

The take home message from these experiments was that obtaining consistent results between different fluorescent western blots was incredibly difficult. Specifically, while the general trend of a 3´UTR-specific effect of HuCsv1 in negatively affecting expression of d2EGFP from the rcdc42-v2 3´UTR-reporter (at lower pmHuCsv1 amounts) can be seen, the large variation in normalised d2EGFP abundance between experiments as well as large variations in the degree to which d2EGFP expression was reduced at specific pmHuCsv1 amounts, prevented any meaningful statistical analysis. A summary of the results is provided herein.

***Results for the control 3´UTR-reporter***

The standard deviation values for the averaged results show just how much variation in normalised d2EGFP and HuCsv1 abundance there was between experiments. While the averaged results for the control 3´UTR-reporter indicate that HuCsv1 does not affect d2EGFP reporter expression at any dose, the huge variation in β-actin-normalised d2EGFP values between each experiment render the averaged values effectively meaningless (figure 14a). Adjusting the normalised d2EGFP abundances within each experiment so they are relative to the 0μg pmHuCsv1 condition (*to look at changes in d2EGFP expression as the amount of HuCsv1 present increases*) does help to reduce the magnitude of variation between experiments to some degree (figure 14b). With this additional normalisation it is possible carry out some statistical analysis of changes in d2EGFP abundance at different amounts of HuCsv1. Interestingly, what this reveals is that at the lowest amount of pmHuCsv1 tested (0.25μg), a modest but significant increase in d2EGFP expression is observed ($p<0.03$). At higher pmHuCsv1 amounts this effect is lost and no statistically significant difference in d2EGFP expression is observed compared to the 0μg pmHuCsv1 condition.

In terms of HuCsv1 function, the significance of the observed increase at 0.25μg pmHuCsv1 is not clear. That the effect is only seen at the lowest amount of pmHuCsv1 tested is curious, as it would be expected that if HuCsv1 were able to influence expression of d2EGFP from the control 3´UTR-reporter this effect would be consistent across the range of pmHuCsv1 amounts tested, and would possibly also be sensitive to increasing HuCsv1 expression. Furthermore, in the first experiment (of the four replicates) there is no evidence of an increase in d2EGFP expression at the 0.25μg pmHuCsv1 condition. In this case, expression of the d2EGFP reporter is unaffected up to 0.5μg of pmHuCsv1. At the 1μg pmHuCsv1 condition an increase in d2EGFP expression is observed, which is comparable to that observed at the 0.25μg condition of the other three experiments. However, the effect is reversed at the 2μg pmHuCsv1 condition and HuCsv1 appears to have a negative effect on d2EGFP expression (~30% reduced compared to 0μg pmHuCsv1) as was seen in the preliminary experiment (figure 12b).

One possibility could be that in the first experiment HuCsv1 expression was much lower overall and only became comparable at the "1μg" pmHuCsv1 condition. However, looking at HuCsv1 expression normalised to β-actin across the four experiments (figure 14c), this does not seem to be the case. In fact, of the four experiments HuCsv1 expression (normalised to β-actin) is relatively high at all amounts of pmHuCsv1.

In light of these points, it was difficult know whether the small increase in d2EGFP observed in the 0.25μg pmHuCsv1 condition was an indication of a real biological effect of HuCsv1 on the control 3′UTR-reporter or either some artefact of the transfection protocol or simply a chance co-incidence within the data. Looking at the entire range of pmHuCsv1 amounts as a whole, there is no obvious increase or reduction in d2EGFP expression from the control 3′UTR-reporter. Furthermore, looking at the raw d2EGFP and β-actin values from the control 3′UTR-reporter co-transfections of each experiment, the averaged raw d2EGFP and β-actin values across all HuCsv1 conditions were reasonably consistent (figure 17a-c). This indicated that within individual experiments, expression of the control 3′UTR across transfections was fairly consistent (d2EGFP results) and that there was little variation in gel loading or sample preparation (β-actin results).

***Results for the rcdc42-v2 3′UTR-reporter***

From the averaged β-actin-normalised d2EGFP results (figure 15a), a slight trend towards reduced d2EGFP expression was apparent as HuCsv1 abundance increased. However, the large variation in values within the averaged data prevented any useful statistical analysis of these changes. Furthermore, while normalisation to show **changes** in d2EGFP abundance relative to 0μg pmHuCsv1 generally reduced variation in the averaged results for the control 3′UTR-reporter; the same cannot be said for the rcdc42-v2 3′UTR-reporter (figure 15b). The reason for this is that the rcdc42-v2 3′UTR-reporter was not entirely consistent in the way it behaved with respect to increasing amounts of HuCsv1, across the four experiments presented. The biggest inconsistencies are apparent for the 0.5μg and 2.0μg pmHuCsv1 conditions across the experimental replicates (*ie* Expts 1-4) and in the results from the fourth experiment. For the 0.5μg condition, across the first three experiments, d2EGFP abundance varies from 10% to 90% relative to 0μg pmHuCsv1 (figure 15b). For the 2.0μg condition; the expression of d2EGFP in the third experiment is ~3-fold lower than in either the first or second experiment. The result for the 2μg condition in the third experiment is not intuitive as in this case the expression of HuCsv1 (normalised to β-actin) is the lowest relative to the other experiments conducted. Compounding these inconsistencies, the results from the fourth experiment completely contradict those from the first three with expression of d2EGFP from the rcdc42-v2 3′UTR-reporter increasing with increasing amounts of HuCsv1.

The clear difference in the response of the rcdc42-v2 3′UTR-reporter to HuCsv1 in the fourth experiment is not readily explained. While no overt differences exist the in materials used, protocols followed or the way in which cells and lysates were handled for this experiment

(relative to the previous three replicates) technical problems such as differences in protein transfer (from gel to membrane) or detection may offer an explanation. In the face of the data from the previous three replicates and preliminary experiment, the results from the fourth experiment appear to be strongly outlying to the general trend of reporter behaviour from the rcdc42-v2 3´UTR-reporter in the presence of HuCsv1. While somewhat dissatisfying, treating this data set as an outlier and excluding it from statistical analysis **does** somewhat improve the averaged results for two of the four pmHuCsv1 amounts tested (figure 15b, graph ii). Looking at β-actin-normalised d2EGFP expression from cells co-transfected with 0.25μg pmHuCsv1 relative to 0μg HuCsv1, an ~20% reduction in expression is seen, which more importantly, is approaching statistical significance ($p$<0.072 – homoschedastic Student's t-test). Furthermore, when co-transfected with 1μg pmHuCsv1 the effect is even greater with an ~2-fold reduction seen in d2EGFP expression relative to the 0μg pmHuCsv1 (figure 15b graph ii). This reduction is very significant with a $p$-value of 0.005, suggesting that despite the problems with reproducibility within the data set as a whole, these two data points provided a glimpse of a potential effect of HuCsv1 on a putative target 3´UTR sequence. Comparing the 0.25μg and 1μg pmHuCsv1 conditions to the 0μg pmHuCsv1 condition showed that the presence of HuCsv1 in cells co-transfected with the rcdc42-v2 3´UTR reporter construct led to a reduction in expression of the d2EGFP reporter protein. This result was in agreement with the observed effect of HuCsv1 on the rcdc42-v2 3´UTR reporter from the preliminary experiment (figure 12a) and indicated that an interaction between HuCsv1 and the rcdc42-v2 3´UTR could result in either reduced translatability or stability of the targeted mRNA. Importantly, it was noted that this tentative interpretation did not fit with all of the available data for the rcdc42-v2 3´UTR (omission of the fourth data set). As such, further testing was carried out in an effort to more convincingly demonstrate (or disprove) the observed negative effect of HuCsv1 on d2EGFP expression from the rcdc42-v2 3´UTR-reporter.

***Results for the rCofilin 3´UTR-reporter***

The behaviour of the rCofilin 3´UTR-reporter is even more inconsistent across the four experiments. Looking at the β-actin-normalised values (figure 16a), in the first experiment HuCsv1 does not appear have any great effect on d2EGFP expression at any amount of pmHuCsv1 tested. However, in the second and fourth experiment d2EGFP expression clearly increases with increasing amounts of co-transfected pmHuCsv1, up to 1μg. Interestingly though, in both experiments d2EGFP abundance appears to reduce in the 2μg pmHuCsv1 condition. On their own, these two experimental results could suggest that HuCsv1 could have a different role in an interaction with the rCofilin 3´UTR, apparently serving to increase either mRNA

translatability or possibly mRNA half-life. Contrary to this hypothesis though, the results from the third experiment show a strong negative effect of HuCsv1 on expression of d2EGFP from the rCofilin 3´UTR-reporter at all amounts of pmHuCsv1 co-transfected. Furthermore, because of the huge variation in reporter behaviour in response to HuCsv1 between the four experiments, normalising d2EGFP expression relative to β-actin and setting the 0µg pmHuCsv1 condition to 1, does not reveal any greater similarities in reporter behaviour in response to HuCsv1 (figure 16b).

## Conclusions

That the control 3´UTR-reporter behaved reasonably consistently within experiments was encouraging and along with the lack of any strong effect on d2EGFP expression in response to HuCsv1, supported its use as a "non-target" control. However, the lack of consistency and/or reproducibility in terms of raw and normalised d2EGFP and HuCsv1 amounts (and raw β-actin amounts) between experiments, presented a significant hurdle in terms of being able to make any statistical analysis of changes in d2EGFP expression for the control 3´UTR-reporter and either of the two experimental 3´UTR-reporters. Furthermore, of the five experiments carried out in total (including the preliminary experiment – figure 12), two showed some reduction in d2EGFP expression in the presence of the highest amount of pmHuCsv1 tested (2μg condition from preliminary experiment – figure 12; and Expt 1 figure 14). As such, while the averaged results did not suggest HuCsv1 had a direct effect on d2EGFP expression from the control 3´UTR-reporter, it remained possible that under certain conditions; such as high HuCsv1 overexpression, HuCsv1 could exert a negative effect on translation, either through some effect on the general translation machinery or simply through low affinity "non-specific" interactions with the reporter sequences that would only become obvious when the amount of HuCsv1 protein present in the cell was sufficiently high.

For the putative HuC target 3´UTR-reporters, the rCofilin reporter data is the best example of just how much variation and inconsistency there was within the fluorescence-based 3´UTR-reporter assay system. Consequently, very little could be concluded about how this reporter was affected by the presence of HuCsv1. However, the results for the rcdc42-v2 3´UTR-reporter were somewhat encouraging showing that (inconsistencies aside) the presence of HuCsv1 caused a reduction in the expression of the d2EGFP reporter. This result was in-line with the initial hypothesis that neuronal Hu proteins could (in some cases) regulate target mRNA translation as part of a role in facilitating localised or signal-dependent translation. Thus, a tentative interpretation of the rcdc42-v2 3´UTR-reporter results was that through an interaction with the rcdc42-v2 3´UTR, HuCsv1 reduced protein expression from the reporter mRNA.

## Why is there so much variation in HuCsv1 and 3´UTR-reporter expression between experiments?

A potentially key source of variation within the 3´UTR-reporter data presented was the kinetics of HuCsv1 protein and 3´UTR-reporter (mRNA and protein) expression within a given experiment. Specifically, the 3´UTR-reporter mRNA and protein (d2EGFP) have each a synthesis rate and rate of degradation. Similarly, the HuCsv1 protein has a particular synthesis and degradation rate. One possible explanation for the observed variation in β-actin-normalised expression of HuCsv1 and 3´UTR reporter (d2EGFP) within the data presented, was that the length of incubation time following transfection (~24hr) was not sufficient to allow the 3´UTR-reporter mRNA/protein and HuCsv1 protein to reach steady-state levels of expression. Indeed, if the expression of any of these components had not reached steady state within the 24hr time period, then potentially large variation could be observed.

At the simplest level, following transfection of the 3´UTR-reporter and pmHuCsv1 plasmids, expression of the 3´UTR-reporter mRNA *should* have a head start over expression of the HuCsv1 protein. As a result, in all cases there would be an initial burst of d2EGFP protein expression from 3´UTR-reporter mRNAs that had not had an opportunity to interact with HuCsv1. Depending on the time taken for all components of the reporter assay to reach steady state, there is potentially a large window in which expression of the d2EGFP reporter protein would not faithfully reflect any effect on HuCsv1 on 3´UTR-reporter expression.

A more complex and potentially confounding factor is that the rCofilin and rcdc42-v2 3´UTR sequences may significantly alter the degradation rate of the reporter mRNAs or the rate of d2EGFP translation from these mRNAs (compared to the control mRNA) in a manner independent of HuCsv1. As such, it was possible that the length of time cells were incubated for (following transfection) may need to be altered (even individualised to suit each reporter), such that the 3´UTR-reporter mRNA and d2EGFP protein and HuCsv1 protein all had enough time to reach steady state. As a first step to examining this possibility, a time course transfection experiment with all three reporters was conducted.

## A time course experiment to profile HuCsv1 and 3´UTR-reporter expression

The time course was carried out at 4-hour intervals from 24 hours to 48hrs. Cells were transfected in 6-well plates (~$2x10^5$ cells/well) with one of the three 3´UTR-reporter constructs and 1µg of either pmHuCsv1 or empty pcDNA3 vector.

The results from the time course experiment appeared to support the idea that longer transfection times **were necessary** to observe a 3´UTR-dependent effect of HuCsv1 on d2EGFP expression from the reporter messages tested. Indeed, there appeared to be no consistent effect of HuCsv1 on expression of the control 3´UTR-reporter across the entire time course (figure 18a). Meanwhile, a reduction in d2EGFP expression from the rCofilin 3´UTR-reporter in the presence of HuCsv1 was observed from the 35hr time-point onwards (figure 18b). Likewise for the rcdc42-v2 3´UTR-reporter, a small reduction in d2EGFP expression was observed up to the 28hr time-point, after which time the magnitude of the reduction increased (figure 18c).

On the face of it, the results from this experiment suggested that longer incubation times (compared to those initially tested) might be required before an effect of HuCsv1 on candidate target 3´UTR sequences could be observed in this reporter assay format. Notably, in cells lacking HuCsv1, d2EGFP protein expression for both of the candidate target 3´UTR-reporters continues to increase across the entire time course (figure 18b and 18c), indicating reporter protein expression from both of these vectors had yet to reach steady state within the 48hr post-transfection time frame tested. This was not the case for the control 3´UTR-reporter, which appeared to have reached steady state (d2EGFP protein levels) from the first time point (24hr) examined, in the presence and absence of HuCsv1 (figure 18a). As such, in order to most accurately measure the negative effect of HuCsv1 on d2EGFP expression from the candidate target 3´UTR-reporters, it would have been necessary to extend the time course, to empirically define the time point at which reporter protein expression had reached a steady state.

However, two important features of the westerns blots from this experiment indicated that technically, the fluorescent reporter assay design itself, may account for a substantial portion of the variation in results observed in the 3´UTR-reporter data. Firstly, HuCsv1 abundance appeared to decline from the 28hr time point and only recovered in the 40hr, 44hr and 48hr time points, where they match the abundances seen at the 24hr time point (figure 19). This expression profile of HuCsv1 was not what would have been expected in that, over the time

course, HuCsv1 abundance would be predicted to steadily increase up to some point and then level off once at steady state.

Secondly, raw β-actin abundance clearly increases (approximately 3-fold) from the 24hr time point to the 40hr time point when it appears to plateau (figure 22a, b and c). This effect was certainly not expected within the western data. For each sample, Bradford assays were carried out to determine total protein concentration and all lanes loaded with equal concentrations of total protein (*data not shown*). One possible interpretation of this result was that HuCsv1 was exerting a positive effect on the expression of β-actin (protein). However, given the expression of d2EGFP from the control 3´UTR-reporter also appeared to increase over the time course (see gel photo in figure 19) and β-actin-normalised d2EGFP abundance from this reporter was *approximately* equal across the entire time course (indicating any increase in β-actin expression was matched by the "non-target" d2EGFP – figure 18a), an effect of HuCsv1 on β-actin expression seemed less likely. A more likely scenario was that localised differences in the efficiency protein transfer from polyacrylamide gel (following electrophoresis) onto the PVDF membrane resulted in artifactual differences in perceived protein abundance as assayed by fluorescent western blot. Such an occurrence may also have explained the unexpected expression profile of HuCsv1 in this experiment. To test this, a second, identical western blot was carried out, using the same time course samples as presented above, to double-check the results and eliminate the possibility of errors occurring due to gel-to-gel variation.

***Duplicate gels, different results***

Strikingly, the results for the control 3´UTR-reporter from the replicate western blot directly contradict the results from the first blot. In this case, d2EGFP expression from the control 3´UTR-reporter is unaffected by co-expression with HuCsv1 up until the 35hr time point, where upon a strong and essentially consistent reduction in expression is observed in samples from cells co-transfected with pmHuCsv1 (figure 20a). Furthermore, the expression profile of d2EGFP from the control 3´UTR-reporter (figure 20a) and HuCsv1 (figure 21) are also clearly different from the first data set obtained. Expression of d2EGFP from the control 3´UTR-reporter (in the absence of HuCsv1) increases over time, peaking around 35hrs post-transfection. For HuCsv1, peak expression is observed around 32hr post-transfection. The lack of congruence between the two duplicate gels makes any interpretation of d2EGFP or HuCsv1 protein expression across the time course difficult. Interestingly, some increase (~ 2-fold) in raw β-actin expression over the time course is again observed (figure 22a, c and d graph ii). However, this increase is smaller than observed in the first gel (figure 22a graph i) and this time is clearly **not** mirrored by

d2EGFP expression from the "non-target" control 3´UTR-reporter (as evidenced by the increase in β-actin-normalised d2EGFP expression from this reporter over time – figure 20a). As for the expression of d2EGFP and HuCsv1, the lack of consistency between the duplicate western blots prevents any firm conclusions from being drawn as to whether the changes in β-actin expression over time represent some technical problem inherent to the assay or a genuine biological effect of HuCsv1 on β-actin expression.

Notably, the results for the rCofilin 3´UTR-reporter roughly agreed with those from the first time course blot. Although unlike the first blot, a small reduction in d2EGFP expression (in the presence of HuCsv1) was observed up until the 35hr time point, where upon the magnitude of reduction was greatly increased (figure 20b). The rcdc42-v2 3´UTR-reporter results were also similar to those in the first blot, with a modest reduction in d2EGFP expression observed up to the 35hr time point, however in this blot with the exception of the 40hr time point, the magnitude of this effect did not increase over increasing incubation times (figure 20c).

### Conclusions from the time course experiment

The initial motivation for conducting the time course experiment was well reasoned. In principle, having HuCsv1 protein and both the 3´UTR-reporter protein and mRNA reach steady state levels prior to analysis by western blot would play an important role in achieving consistency in observed protein expression between experiments. The idea behind the time course experiment was that it would empirically identify the amount of incubation time required for transfected cells in order to reach steady state levels of reporter and HuCsv1 protein. This time point could then be applied to a series of replicate experiments (as presented earlier in this chapter) with the aim of obtaining more consistent data from the reporter assays and thus ascertaining whether HuCsv1 did in fact have a statistically significant (negative) influence on expression of either the rcdc42-v2 or rCofilin 3´UTR-reporters.

However, rather than achieving this, the results from the time course experiment indicated that the fluorescence-based reporter assay design employed was technically too difficult. As such, further investigation into a possible general negative effect of HuCsv1 on translation was not carried out using this assay. A discussion of the technical issues associated with this assay is presented below.

## Technical limitations of the fluorescence-based reporter assay and their effect on experimental reproducibility and reliability

### Inconsistent results due to experimental workup

There are a number of reasons why firm conclusions cannot be made from the data obtained using the fluorescence-based 3´UTR-reporter assays. From a statistical perspective; there were generally not enough experimental repeats, within data sets there were often large inconsistencies in the response of 3´UTR-reporters to HuCsv1, between experiments there was inconsistency in the magnitude of effect of HuCsv1 on 3´UTR-reporters, and in numerous cases responses to HuCsv1 were observed for the control 3´UTR-reporter where no response was expected. Importantly, problems with reproducibility within these assays appeared to largely come down to technical issues. At the forefront of these issues are differences in experimental readout caused by the entire work up from cell lysis to western blot.

Following lysis, samples undergo several handling steps before any data can be retrieved. These include determination of total protein content by Bradford assay and subsequent preparation and loading of samples for SDS-PAGE. Failure to accurately determine protein concentrations for all samples or load equal amounts of protein leads to differences in protein abundance between samples within gels, influencing the consistency of raw protein abundances quantified for each sample.

Following this, gel-to-gel variation in separation characteristics of samples introduces another point at which inconsistency can arise. For instance, differences in shape and spread of protein bands and the extent of separation prior to transfer to the membrane, even slight, potentially affect the quantification of raw protein abundances. Compounding this, the transfer of electrophoretically separated proteins to the PVDF membrane is another point at which variation can occur. Even small differences in efficiency of transfer between experiments have the potential to impact on perceived protein abundances. These differences can exist at both the level of the whole gel and within discrete regions within gels. Imperfections in transfer within specific parts of the gel can be caused by localised differences in transfer buffer amounts due to incomplete wetting of whatman paper stacks (semi-dry transfer method) or air bubbles trapped within transfer stacks. Accidental stretching of gels when placed down on membranes prior to transfer can cause localised distortion of band shape. Finally, while immunodetection of proteins should prevent errors in terms of limitations in how much d2EGFP, HuCsv1 or β-actin

protein can be detected in any given sample, differences in background signal from blot-to-blot as well as time between probing and scanning of membranes may both influence the consistency of protein abundances relative to each other.

It is certainly true that the impact of some of the issues identified here could be greatly reduced by carrying out experiments carefully and methodically. However, the point being made is that the work up from cell lysate to quantification of protein abundances by western blot is complicated and contains numerous steps at which variation between experiments can be introduced, even when following a strict experimental protocol. For the most part, sample preparation, electrophoretic separation and detection by western blotting were carried out as consistently as possible, something that is reflected in the quality of the western blots produced and internal consistency of raw actin abundances within gels (figure 17c and 22a). However, even when specifically trying to maintain consistent technique between experiments, significant differences in results are observed, something that is most clearly exemplified by the replicate western blots from the time course experiment (22a-c).

## Replicate western blots show significant differences in raw and normalised protein abundances

The best example of how unexpected variation between experimental replicates can be introduced through the western blotting process comes from the duplicate blots generated from the time course experiment. In this case, obvious variation in protein abundances, both raw and normalised, was observed for identical samples between blots. As a first example of this, there are clear differences in raw actin abundances between gels in terms of both actual quantified abundance (*ie.* the amount of fluorescent signal observed for β-actin from a given sample between two duplicate gels – for example compare raw β-actin abundance for the 40hr time point between blots 1 and 2 for any of the three reporters – figure 22a, b or c) and abundance of actin of one sample relative to another (*ie*. comparing raw β-actin abundance within a gel between two time points figure 22a-c). One example of this can be seen comparing the difference in actin abundance between the 24hr and 40hr time points from both blots. From the first western blot, an ~3-fold increase in actin abundance is observed between the 24hr and 40hr time point for all 3´UTR-reporters tested. Whereas, in the second blot only an ~2-fold increase in actin abundance is observed between the same time points. These differences are hard to rationalise given:

- Total protein concentrations for each sample were determined by Bradford analysis and equal amounts of total protein loaded per well
- The same amount of protein for each sample was loaded in the two different duplicate gels
- The same type of gel, transfer materials and conditions (*ie* PVDF membrane, transfer apparatus, transfer time and voltage, etc) were used for the two duplicate gels.

Similarly to the actin quantification, raw HuCsv1 abundance shows large differences between duplicate time points from separate gels (figure 23a-c compare graphs i and ii).

Notably, because of the number of samples collected for the time course experiment, it was necessary to run two gels for each duplicate (figures 19 and 21). One gel contained samples from the 24hr to 35hr time points, while the second contained samples from the 40hr to 48hr time points. Looking at the raw HuCsv1 abundances it is clear that large variation in terms of relative abundance of protein from one gel to another can be seen even when (in addition to the points listed in bullet points above):

- The gels were run using the same type of gel
- The gels were run at the same time
- The gels were transferred, immunoblotted and scanned simultaneously.

In the case of the first blot, a 20 to 40-fold increase in raw HuCsv1 abundance is seen between the "early" gel (24hr to 35hr time points) and the "late" gel (40hr to 48hr time points). Contradicting this, in the second blot, raw HuCsv1 abundances appear to be reasonably consistent from the 32hr time point onwards as was expected given the same amount of pmHuCsv1 vector was transfected into all +HuCsv1 samples.

The biggest problem with the gel-to-gel variation observed is that the resulting β-actin-normalised values for both HuCsv1 and d2EGFP are different. In some cases, it is possible to overcome this problem by carrying out a second normalisation to compare changes in normalised d2EGFP and HuCsv1 abundances (relative to a single data point within a data set) between experiments, as was done for the four replicate westerns presented first in this chapter (figures 14 – 16). While there is nothing inherently wrong with this type of normalisation, it prevents comparison of actual protein expression levels between experiments. Importantly, this normalisation is only useful when the differences in actin-normalised protein abundance

(d2EGFP or HuCsv1 in this case) are similar. When this is not the case, as is seen in comparing the actin-normalised HuCsv1 abundances from the two duplicate western blots from the time course experiment (figure 19 versus figure 21) then further normalisation is of no benefit. Importantly, given the amounts of sample loaded for each of the duplicate westerns from the time course were identical (original protein concentrations were used), the exact same protocols, immunodetection reagents and PVDF membrane were used, and no evidence of protein degradation is apparent in the second blot, any difference in actin-normalised d2EGFP or HuCsv1 expression should be low. As such, the only explanation for this kind of variation is that differences were introduced through gel-to-gel or blot-to-blot variation. The fact that such differences are possible under conditions where all experimenter-controlled parameters have been kept as consistent as possible, challenges the utility of the fluorescent western blot as a useful quantitative tool in these 3´UTR-reporter assays.

### Variation in transfection efficiency between experiments

Finally, differences in transfection efficiency between experiments would also have the potential to cause variation in normalised d2EGFP and HuCsv1 abundances. This is primarily because normalisation was carried out using endogenously expressed β-actin rather than a co-transfected internal control. It was believed that normalisation to β-actin would be suitable in these experiments because within experiments, comparisons were being made against approximately equal numbers of cells, transfected and lysed at the same time using the same reagents. However, comparison of actin-normalised HuCsv1 and d2EGFP abundances from experimental replicates (figures 14 - 16) highlights the point that actin-normalised protein amounts are not consistently reproduced across replicate transfections. While it is not possible to say why this is the case in all examples, differences in transfection efficiency could easily account for some of this variation. By using a co-transfected internal control for normalising HuCsv1 and d2EGFP protein abundances, it would have been possible to eliminate this potential source of variation.

Admittedly, it is curious that such differences in transfection efficiency might occur, at least across the four replicate experiments presented at the start of this chapter (figures 14 - 16). The protocol for transfection was standardised across the four repeats in terms of amounts of cells and plasmid used in each transfection and the same source of plasmid DNA for each vector was used each time (high concentration/high purity cesium chloride prepared plasmid). However, differences in the number of passages the 293T cells had been through for each transfection,

small differences in time of transfection following plating (these would have differed by no more than 8hrs for any given experiment) or differences in nutrient media quality could affect the rate of cell division or fitness of cells which would have a direct effect on the cells' competence for transfection.

## Final Conclusions

### HuCsv1 a negative regulator of target mRNA expression?

While no solid conclusions were drawn from the fluorescence-based 3´UTR-reporter assays regarding HuCsv1 function, the data suggested that co-expression of HuCsv1 with the rcdc42-v2 3´UTR-reporter may result in a reduction of d2EGFP reporter protein production (figure 15b graph ii and accompanying table). There are several possible explanations for this effect:

1. HuCsv1 specifically binds to the rcdc42-v2 3´UTR and somehow down-regulates reporter protein translation.
2. HuCsv1 specifically binds to the rcdc42-v2 3´UTR and lowers the reporter mRNAs half-life, which would lead to a reduction in reporter protein production.
3. HuCsv1 affects the production of the mature rcdc42-v2 3´UTR-reporter mRNA in such a way that reduces reporter protein output.

However, before any of these possible functions could be tested, a new 3´UTR-reporter assay format would be required that could overcome the technical problems associated with the fluorescence-based reporter approach. Given the results thus far suggested that HuCsv1 was working as a negative regulator of protein expression from targeted mRNAs, the new reporter assay system would remain geared towards assaying changes in protein output from 3´UTR-reporters.

### Redesigning the 3´UTR-reporter assay

In designing a new 3´UTR-reporter assay system, the challenges encountered by the fluorescence-based reporter assays were addressed. As a start, a new reporter assay system would ideally involve less handling steps between cell lysis and data collection so as to minimise variation introduced by experimental (or experimenter) inconsistencies in sample preparation. Furthermore, and as part of reducing handling, the new assay system would be of significantly higher throughput so as to facilitate the analysis of greater numbers of samples per experiment. This feature would be important on two levels. Firstly, higher throughput would allow for the analysis of replicate transfections for a single data point within an experiment. This in itself would be a huge improvement over fluorescent western-based detection methods as it would allow for greater statistical confidence in the results for each data point and enable the

investigator to differentiate between inconsistencies occurring because of a problem (technical or otherwise) with a single sample, and true changes in reporter activity within a single data point. Secondly, higher throughput would allow for a greater number of CLIP-identified 3´UTRs to be tested per assay. By increasing the number of 3´UTRs tested, it would be possible to determine whether the negative effect of HuCsv1 observed for the rcdc42-v2 3´UTR-reporter was specific to that 3´UTR, or indicative of a general, more universal role for HuCsv1.

The new assay design would also incorporate a co-transfected internal control rather than relying on normalisation to endogenously expressed proteins. It was expected that using a co-transfected internal control would make the assay more robust, overcoming issues associated with differences in transfection efficiency between experiments and allowing for more reliable comparison of normalised 3´UTR-reporter protein expression, between experiments.

Finally, the new 3´UTR-reporter assay system would ideally be more sensitive. Using an assay with a lower limit of detection (compared to the fluorescence-based assay) would allow for the transfection of smaller amounts of 3´UTR-reporter vector and thus, lower amounts of 3´UTR-reporter mRNA. Reducing the amount of reporter plasmid transfected was seen as advantageous for several reasons. Primarily, changes in 3´UTR-reporter expression observed in the fluorescence-based assays were generally small (~2-fold reductions in d2EGFP expression at most – figures 15a and 15b graph ii). By using a more sensitive system in which lower amounts of reporter plasmid could be transfected, these relatively small changes in reporter expression would not be lost. Indeed, these changes may even be found to be greater if, under conditions using in the fluorescence-based reporter assay, the amount of reporter plasmid had been saturating endogenous translation control machinery. Additionally, and as discussed already, it was desirable to ensure the reporter assay used conditions in which HuCsv1 protein was in molar excess compared to 3´UTR-reporter mRNA. Co-transfection of lower amounts of 3´UTR-reporter plasmid (relative to pmHuCsv1) was expected to ensure reporter assays were conducted under conditions where HuCsv1 protein was in molar excess of the 3´UTR-reporter.

Examination of literature dealing with analysing the role of proteins on mRNA translation revealed a method of investigation with all of the features deemed desirable. Luminescence-based reporter assays, which use the a firefly luciferase reporter and a co-transfected renilla luciferase internal control, have been widely used in reporter-based assays to address functional studies similar to this study looking at the role of neuronal Hu proteins. As such, the use of

fluorescence-based reporters in this investigation was subsequently dropped, in favour of applying the dual luciferase-based reporter system to address the effect of HuCsv1 on CLIP-identified mRNAs.

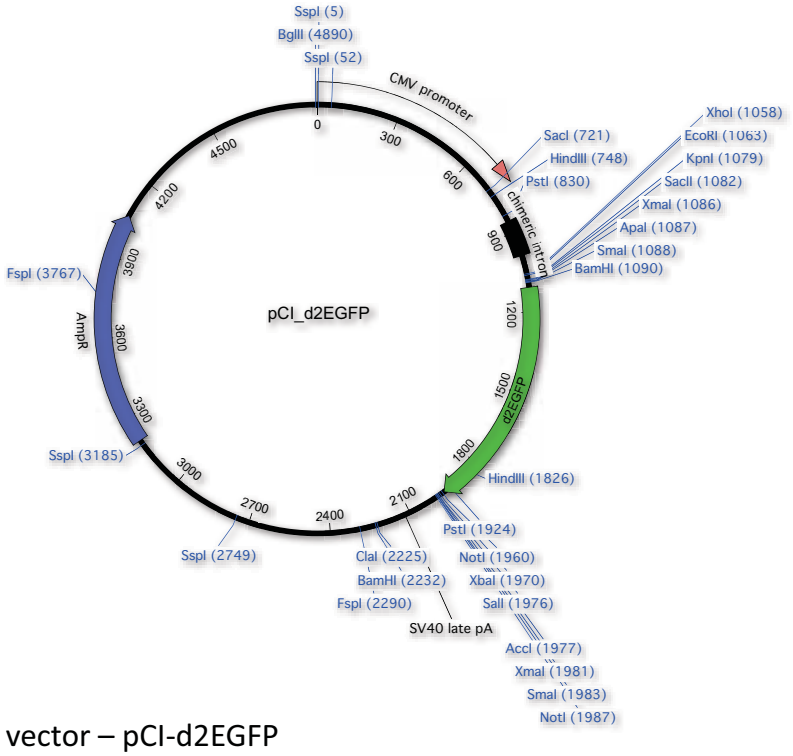


Figure 8. d2EGFP reporter vector – pCI-d2EGFP

pCI-d2EGFP was made by sub-cloning the d2EGFP coding sequence (including Kozak sequence) from pd2EGFP-N1 (Clontech) into pCI (Clontech) as described in the materials and methods.

| 3´ UTR | 1st pass primers | 2nd pass primers | | Cloning site | Insert size |
|---|---|---|---|---|---|
| rcdc42 | FWD - TAAACCGTTTTCTCCTTC | FWD - AATGCTAGCTAAACCGTTTTCTCCTTC | | NheI/XbaI destroyed - 1970 | 0.78kb |
| | REV - TAAACAAACAATTGTATAATT | REV - AATCTCGAGTAAACAAACAATTGTATAATT | | XhoI/SalI destroyed - 2750 | |
| rcofilin | FWD - TGGAGGGCAAGCCTTTG | FWD - ATTCTAGATGGAGGGCAAGCCTTTG | | XbaI - 1999 | 0.55kb |
| | REV - GTTAATTAGCCTTTTTATTGTG | REV - ATGTCGACGTTAATTAGCCTTTTTATTGTG | | SalI- 2552 | |
| zfCIRBP | FWD - CACACGAGTAAAAAAACCCCGATTG | FWD - GAGAAGTCTAGACACACGAGTAAAAAAACCCCGATTG | | XbaI - 1999 | 0.94kb |
| | REV - CGGAGGCAAAAGAAATCAGAGCG | REV - AGAGAAGTCGACGGAGGCAAAAGAAATCAGAGCG | | SalI -2939 | |

Table 2. Cloning 3´ UTR sequences into pCI-d2EGFP.

First pass PCR primers were designed to amplify predicted 3´ UTR sequences from cDNA template material reverse transcribed from total E18 rat embryo brain RNA.

Following purification, PCR products of the expected size were used as templates for a second PCR reaction using primers to incorporate appropriate restriction sites for cloning into pCI-FL

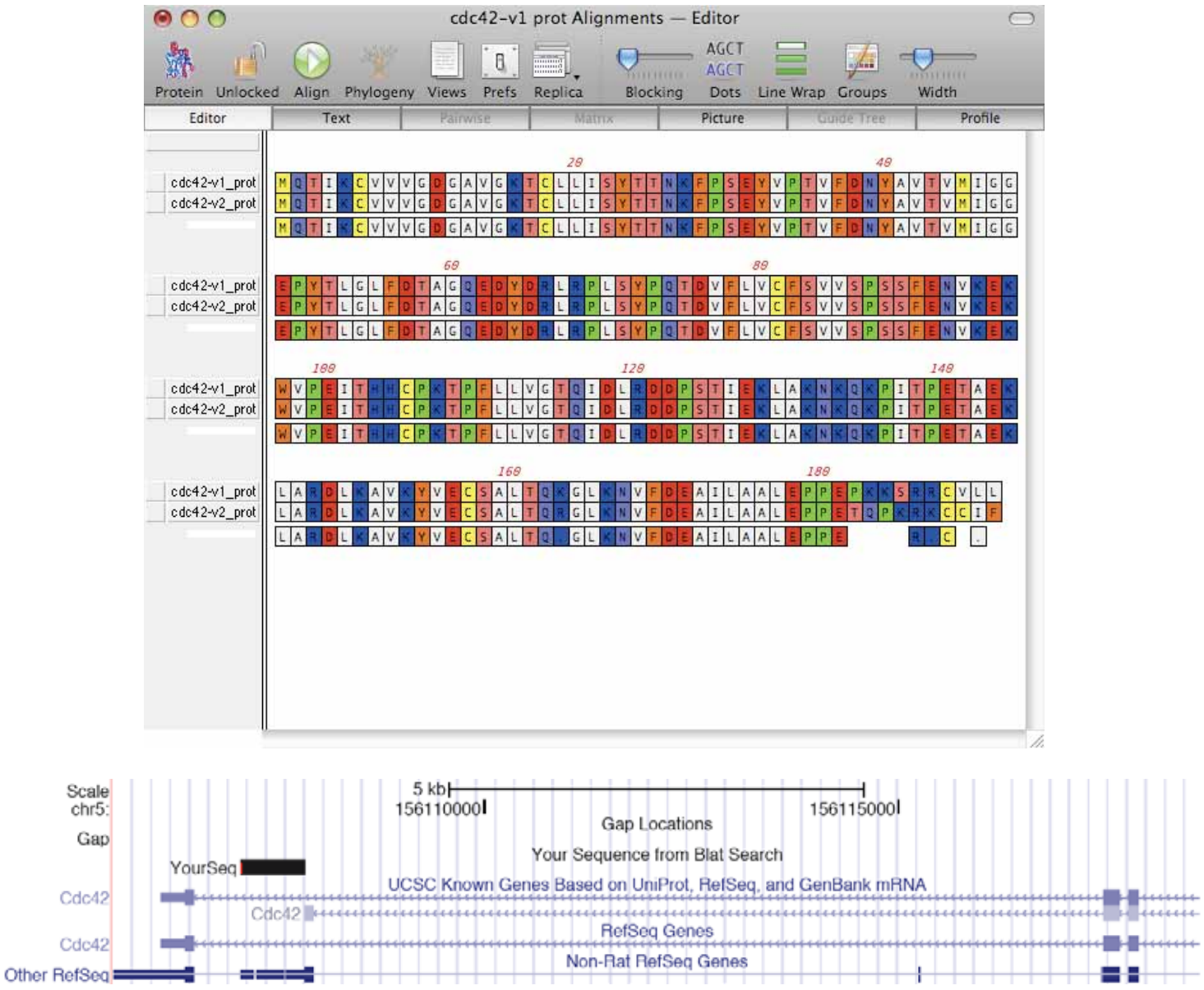


Figure 9. Alternative terminal exon splicing produces to highly similar cdc42 proteins differing only in their final 10 amino acids (figure 10a) and using alternative 3´UTR sequences (figure 10b).

Figure 9a. An alignment of the protein sequences for the rat cdc42 protein isoforms (cdc42-v1 and v2 respectively), is shown. Alignment was performed using sequences obtained from the UCSC genome database.

Figure 9b. A screen shot from the UCSC genome browser showing the two alternative terminal exons (including alternative 3´UTR sequences). The top cdc42 gene sequence is for cdc42-v1, the second sequence (shorter) encodes cdc42-v2.

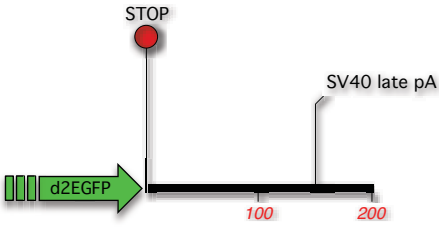


Control 3´UTR-reporter mRNA length ~1.3kb after splicing

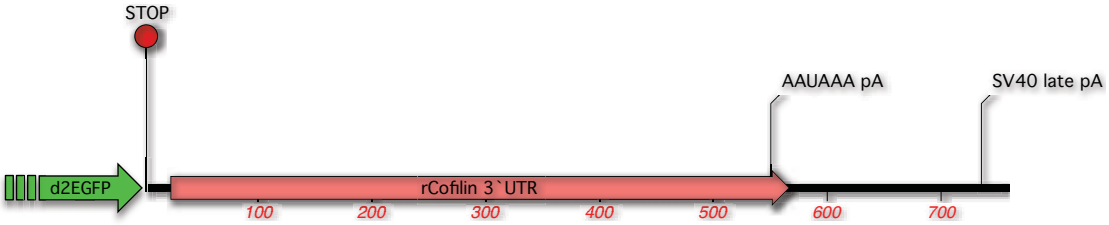


rCofilin 3´UTR-reporter mRNA length ~1.9kb after splicing

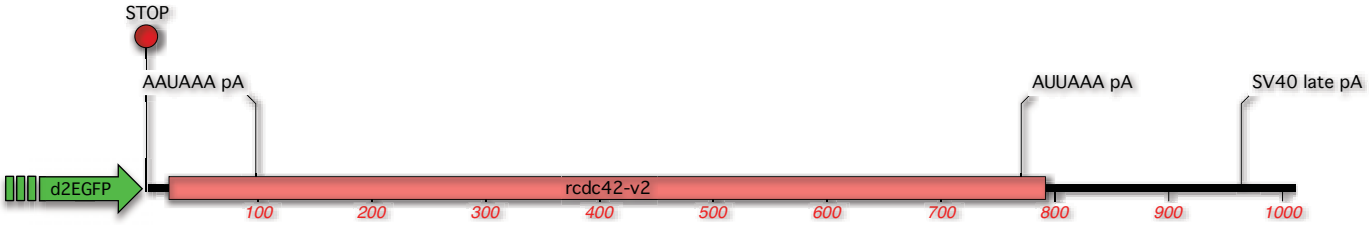


rcdc42-v2-reporter mRNA length ~2.1kb after splicing

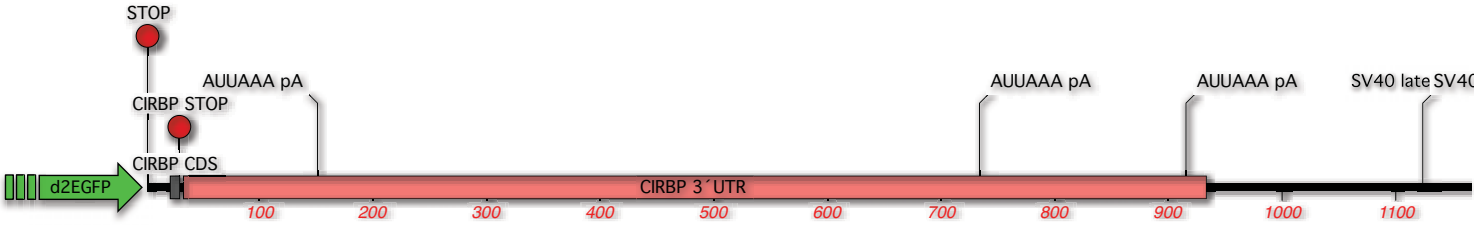


zfCIRBP-reporter mRNA length ~2.3kb after splicing

Figure 10. Putative target 3´UTR schematics

Schematic representations of the cloned rat 3´ UTR sequences are presented below. 3´ UTR sequences are shown as pink boxes. Included in the figures are the location and hexameric sequence of predicted polyadenylation sites (pA) and the location of translation stop codons (red circles) where primer design for a target 3´ UTR necessitated the inclusion of a small amount of coding sequence.

Scale (red) indicates length of cloned 3´UTR sequence. Total reporter mRNA lengths (after splicing but not accounting for polyadenylation) are indicated.

A

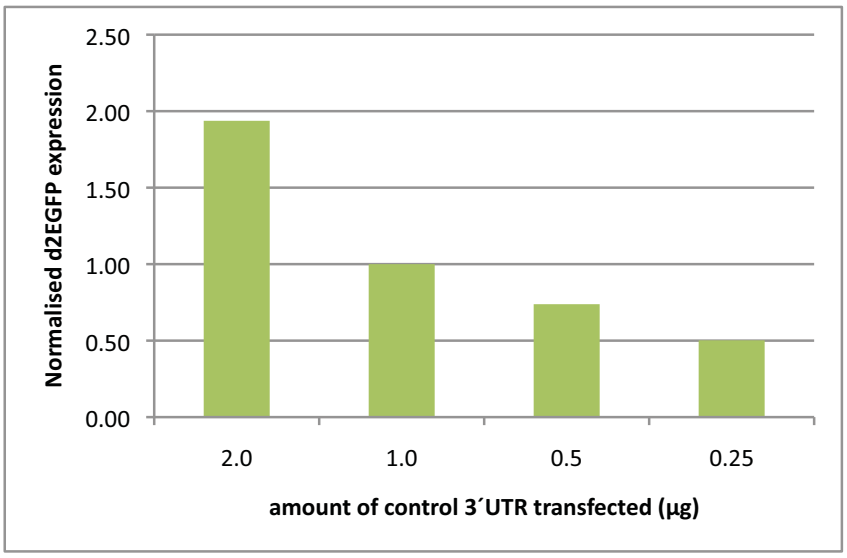


| | Raw amounts | | | normalised |
|---|---|---|---|---|
| Reporter: | d2EGFP | Actin | GFP/actin | GFP/actin |
| 2µg control 3´UTR | 1143 | 231 | 4.94 | 1.94 |
| 1µg control 3´UTR | 834 | 327 | 2.55 | 1.00 |
| 0.5µg control 3´UTR | 581 | 309 | 1.88 | 0.74 |
| 0.25µg control 3´UTR | 312 | 244 | 1.28 | 0.50 |
| | | | | |
| untransfected | | 220 | | |

B

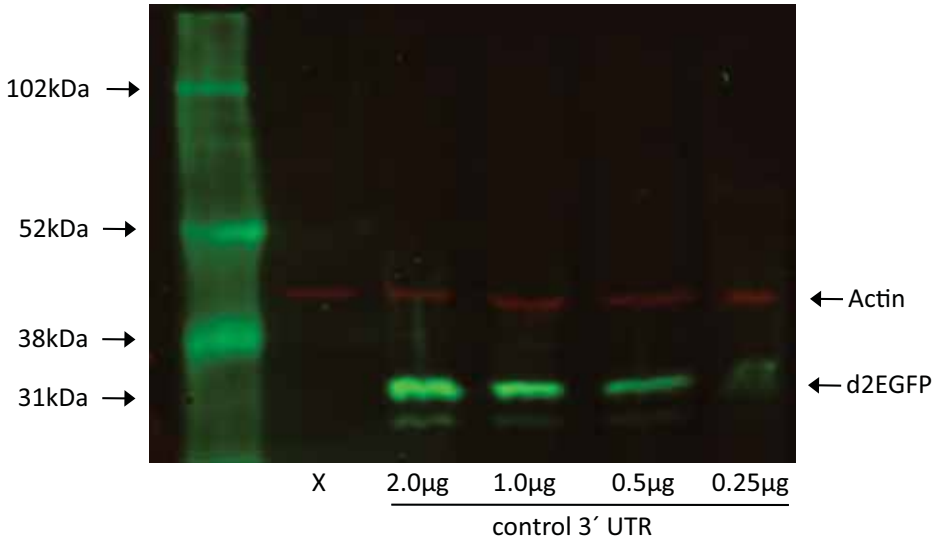


Figure 11. Examining EGFP expression from a range of pCI-control 3´UTR vector amounts.

Cells were transfected with a total of 2µg of plasmid DNA using 6µL of FuGENE. Where necessary, total DNA amounts were made up to 2µg using pcDNA3 (-HuCsv1).

a.) d2EGFP protein abundance shown normalised to Actin. The table shows the raw values obtained from analysis of the blot. Actin-normalised d2EGFP expression is shown relative to the 1µg control 3´UTR reporter condition in the final column (GFP/actin).

b.) Western blot image from which protein abundance values were obtained. Actin is shown in red, d2EGFP is shown in green. Amounts indicated (in µg) represent amount of control 3´UTR vector transfected. X indicates whole cell lysate from untransfected cells.

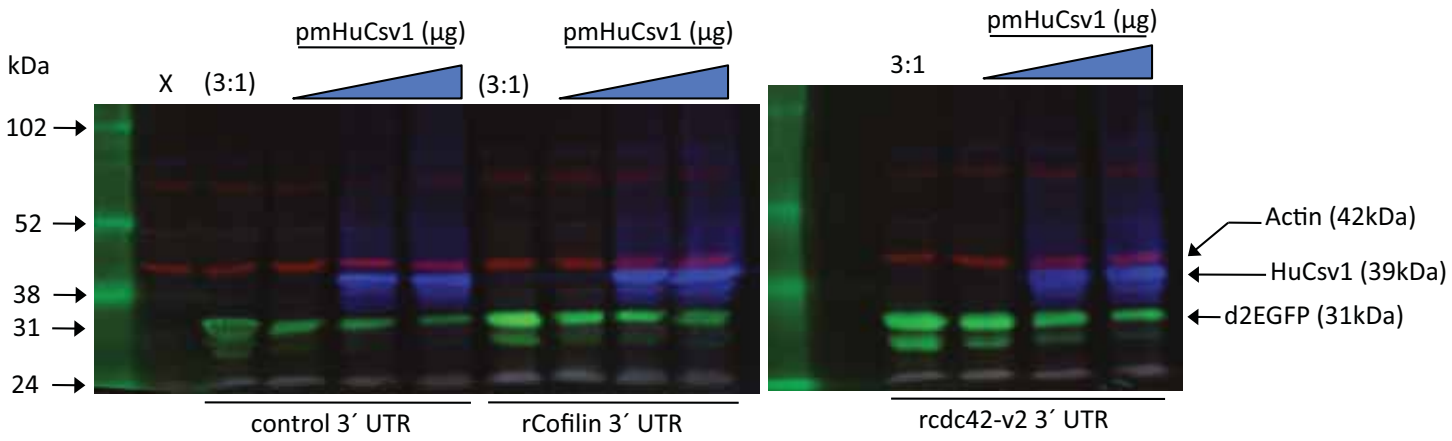


Figure 12a. Testing for an effect of HuCsv1 on putative target-3´UTR reporters

Cells were co-transfected with one of the 3´UTR reporters and either 0µg, 1µg or 2µg of pmHuCsv1 to a total of 2.25µg of plasmid DNA. Where necessary, total DNA amounts were made up to 2.25µg using pcDNA3.

Western blot image from which protein abundance values were obtained. Actin is shown in red, d2EGFP is shown in green and HuCsv1 shown in blue. The amount of pmHuCsv1 co-transfected increases moving left to right (blue triangle). X indicates untransfected lysate and lanes labeled 3:1 were loaded as for experimental lanes however only transfected with 1µg total DNA and 3µL FuGENE.

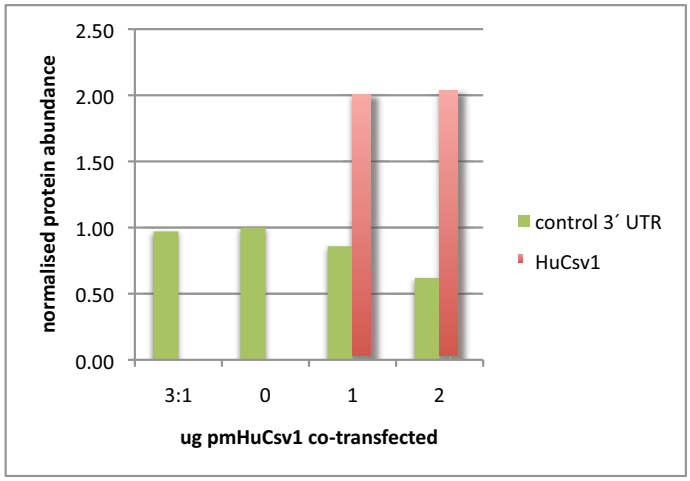


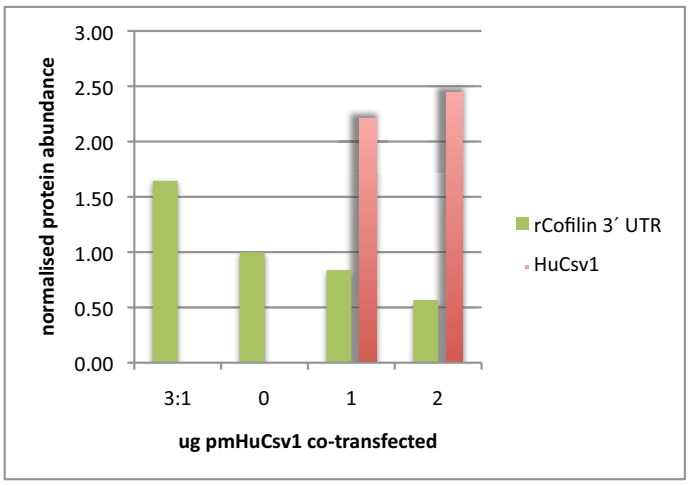


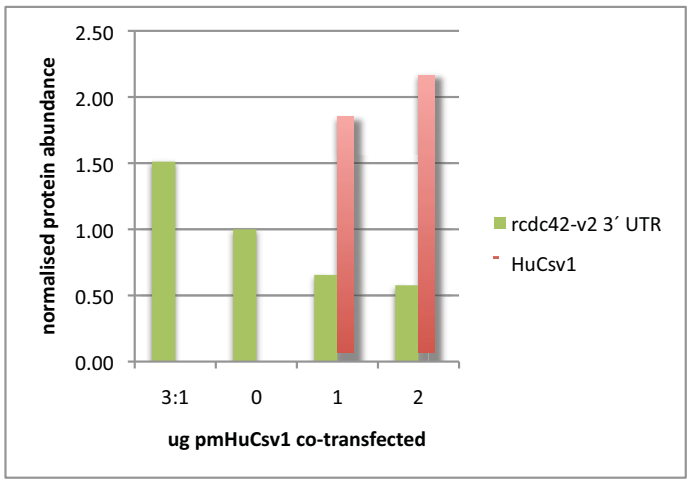


| | | Raw fluorescence values | | | | | normalised |
|---|---|---|---|---|---|---|---|
| Reporter: | (µg) HuCsv1 | d2EGFP | HuCsv1 | Actin | GFP/actin | HuCsv1/actin | GFP/actin |
| control | *3:1* | *578* | - | *125* | *4.63* | - | *0.97* |
| | 0µg | 808 | - | 169 | 4.77 | - | 1.00 |
| | 1µg | 765 | 374 | 187 | 4.10 | 2.01 | 0.86 |
| | 2µg | 544 | 375 | 184 | 2.95 | 2.03 | 0.62 |
| rCofilin | *3:1* | *1,860* | - | *178* | *10.43* | - | *1.64* |
| | 0µg | 1,103 | - | 174 | 6.34 | - | 1.00 |
| | 1µg | 1,001 | 429 | 189 | 5.31 | 2.28 | 0.84 |
| | 2µg | 799 | 558 | 222 | 3.60 | 2.51 | 0.57 |
| rcdc42-v2 | *3:1* | *1,819* | - | *122* | *14.88* | - | *1.51* |
| | 0µg | 1,637 | - | 166 | 9.85 | - | 1.00 |
| | 1µg | 1,325 | 380 | 205 | 6.45 | 1.85 | 0.66 |
| | 2µg | 1,060 | 404 | 187 | 5.68 | 2.17 | 0.58 |

Figure 12b. Testing for an effect of HuCsv1 on putative target-3´UTR reporters

Protein abundances normalised to Actin shown for d2EGFP (green) and HuCsv1 (red). The table shows the raw values obtained from analysis of the blot. Actin-normalised d2EGFP and HuCsv1 fluorescence values are shown (GFP/actin and HuCsv1/actin). Actin-normalised d2EGFP values relative to the 0µg HuCsv1 condition are graphed

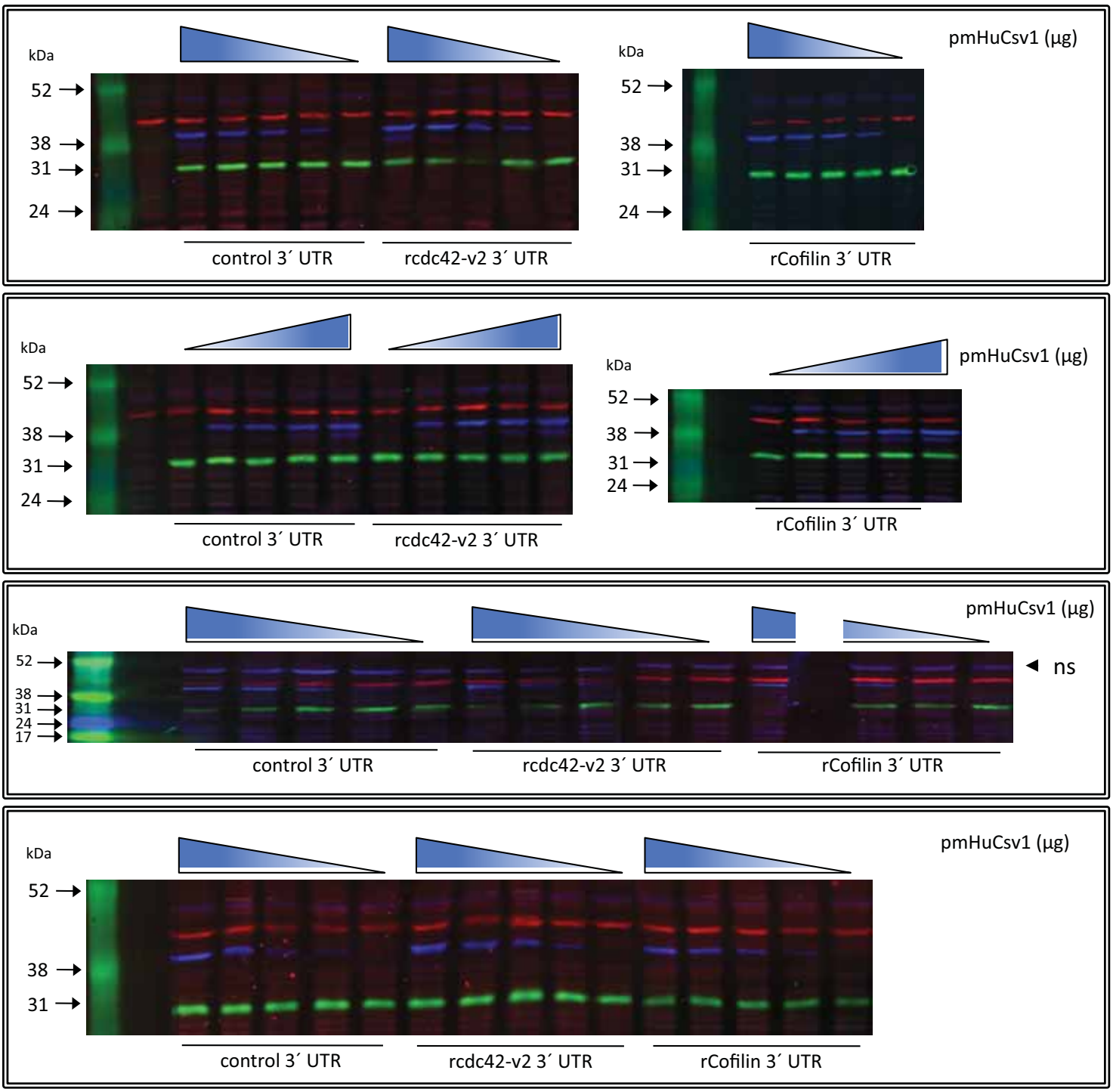


Figure 13. Western blots from four replicate experiments testing a range of pmHuCsv1 doses

Cells were co-transfected with one of the 3′UTR reporters and one of a range of amounts of pmHuCsv1 from 0µg to 2µg. Where necessary, total DNA amounts were made up to 2.25µg using pcDNA3.

Protein abundance values were obtained from these blots using digital image quantification software. Actin is shown in red, d2EGFP is shown in green and HuCsv1 shown in blue. The amount (µg) of pmHuCsv1 co-transfected is represented by the blue triangles and includes 0, 0.25, 0.5, 1.0 and 2.0µg. X indicates untransfected cell lysate.

The gels are arranged from top to bottom in chronological order with experiment 1 first followed by experiments 2, 3 and 4.

| | control 3´ UTR (GFP/actin) | | | | n=4 | | |
|---|---|---|---|---|---|---|---|
| pmHuCsv1 | Expt 1 | Expt 2 | Expt 3 | Expt 4 | average | STDEV | *p*<… |
| - | 7.60 | 4.51 | 3.42 | 1.31 | 4.21 | 2.62 | - |
| 0.25µg | 7.77 | 6.19 | 5.74 | 2.08 | 5.44 | 2.41 | 0.514291 |
| 0.5µg | 6.95 | 4.91 | 4.91 | 1.36 | 4.53 | 2.32 | 0.859848 |
| 1.0µg | 10.99 | 4.94 | 3.24 | 1.47 | 5.16 | 4.14 | 0.711736 |
| 2.0µg | 5.27 | 5.64 | 2.95 | 1.56 | 3.85 | 1.94 | 0.833208 |

| | control 3´ UTR (HuCsv1/actin) | | | | n=4 | |
|---|---|---|---|---|---|---|
| pmHuCsv1 | Expt 1 | Expt2 | Expt3 | Expt4 | average | STDEV |
| 0.25µg | 1.74 | 3.13 | 0.73 | 0.38 | 1.50 | 1.23 |
| 0.5µg | 3.45 | 3.41 | 1.44 | 0.63 | 2.23 | 1.42 |
| 1.0µg | 6.63 | 5.21 | 3.09 | 2.41 | 4.33 | 1.94 |
| 2.0µg | 7.82 | 8.98 | 3.52 | 3.96 | 6.07 | 2.74 |

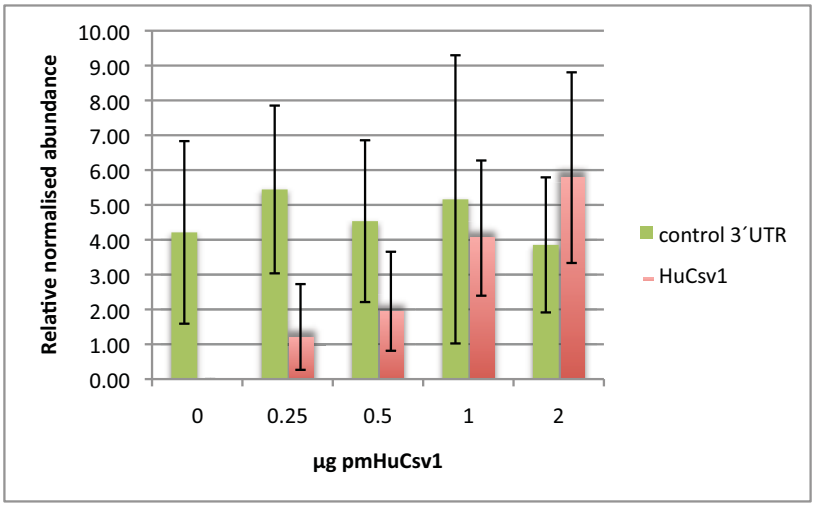


Figure 14a. Averaged results of four repeats testing for an effect of HuCsv1 on the **control 3´UTR-reporter**

The graph shows averaged protein abundances normalised to Actin for d2EGFP (green) and HuCsv1 (red) from n=4 experimental repeats  Error bars represent standard deviation values for each average.

The table shows normalised protein values for d2EGFP from each experiment as well as the average value, standard deviation (STDEV) and p-value as determined by 2-tailed homoschedastic Student's t-test.

| | control 3´ UTR (GFP/actin) | | | | n=4 | | |
|---|---|---|---|---|---|---|---|
| pmHuCsv1 | Expt 1 | Expt 2 | Expt 3 | Expt 4 | average | STDEV | *p*<… |
| - | 1.00 | 1.00 | 1.00 | 1.00 | 1.00 | - | - |
| 0.25µg | 1.02 | 1.37 | 1.68 | 1.58 | 1.41 | 0.29 | 0.029197 |
| 0.5µg | 0.91 | 1.09 | 1.44 | 1.04 | 1.12 | 0.22 | 0.325761 |
| 1.0µg | 1.45 | 1.10 | 0.95 | 1.12 | 1.15 | 0.21 | 0.198121 |
| 2.0µg | 0.69 | 1.25 | 0.86 | 1.19 | 1.00 | 0.26 | 0.986238 |

| | n=3 (Expt 1-3) | | |
|---|---|---|---|
| pmHuCsv1 | average | STDEV | *p*<… |
| - | 1.00 | - | - |
| 0.25µg | 1.36 | 0.33 | 0.132019 |
| 0.5µg | 1.15 | 0.27 | 0.393762 |
| 1.0µg | 1.16 | 0.26 | 0.33414 |
| 2.0µg | 0.93 | 0.29 | 0.712823 |

(i)

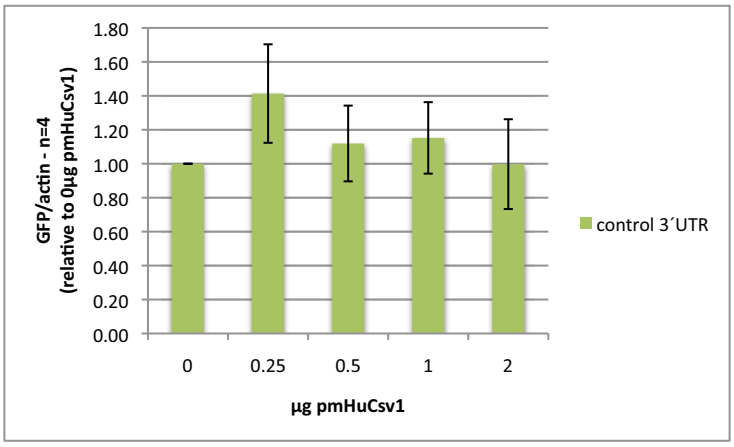


(ii)

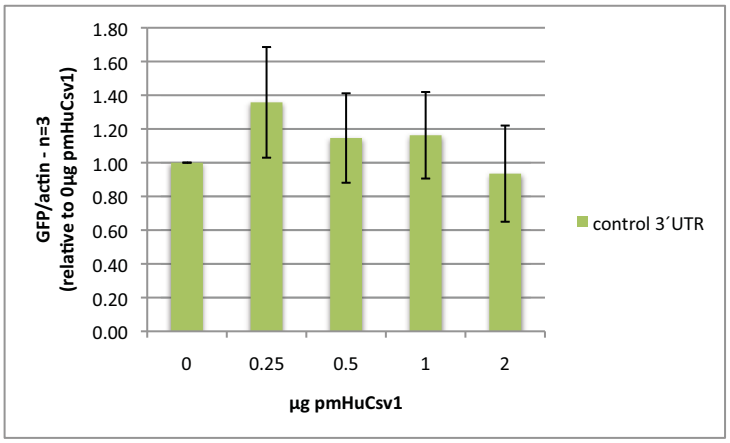


Figure 14b. Averaged results of four repeats testing for an effect of HuCsv1 on the **control 3´UTR-reporter**

Graph (i) shows averaged actin-normalised protein abundances for d2EGFP (green) , relative to the 0µg pmHuCsv1 condition from n=4 experimental repeats . Error bars represent standard deviation values for each average.

Graph (ii) shows averaged actin-normalised protein abundances for d2EGFP (green) , relative to the 0µg pmHuCsv1 condition from n=3 experimental repeats. For this graph, the results from the fourth experiment were omitted. Error bars represent standard deviation values for each average

The table shows actin normalised protein values for d2EGFP relative to the 0µg pmHuCsv1 condition from each experiment as well as the average value, standard deviation (STDEV) and p-value as determined by 2-tailed homoschedastic Student's t-test.

| | control 3´ UTR (HuCsv1/actin) | | | | n=4 | |
|---|---|---|---|---|---|---|
| pmHuCsv1 | Expt 1 | Expt2 | Expt3 | Expt4 | average | STDEV |
| 0.25µg | 0.34 | 0.64 | 0.54 | 0.34 | 0.46 | 0.15 |
| 0.5µg | 0.57 | 0.69 | 0.68 | 0.42 | 0.59 | 0.13 |
| 1.0µg | 1.00 | 1.00 | 1.00 | 1.00 | 1.00 | 0.00 |
| 2.0µg | 1.16 | 1.65 | 1.08 | 1.51 | 1.35 | 0.27 |

| | n=3 Expt 1-3 | |
|---|---|---|
| pmHuCsv1 | average | STDEV |
| 0.25µg | 0.51 | 0.16 |
| 0.5µg | 0.65 | 0.07 |
| 1.0µg | 1.00 | 0.00 |
| 2.0µg | 1.30 | 0.30 |

(i)

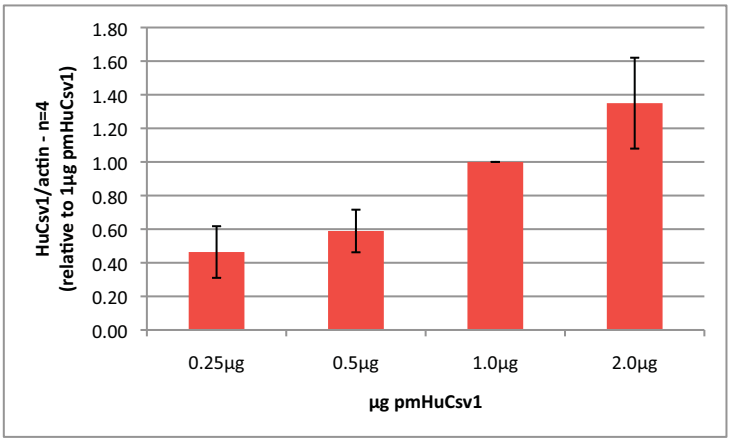


(ii)

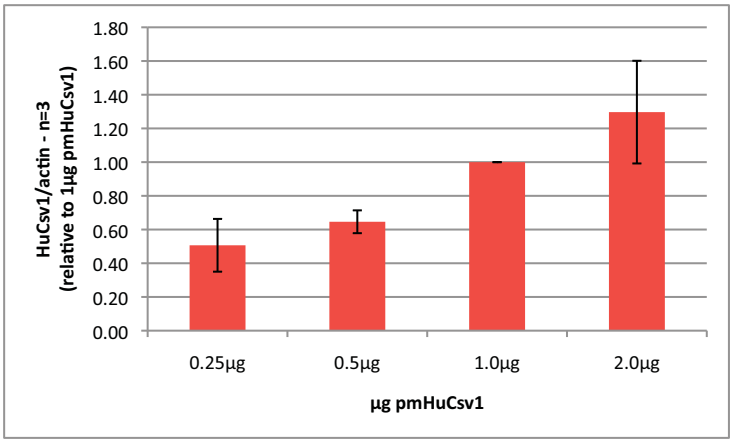


Figure 14c. Averaged results of four repeats testing for an effect of HuCsv1 on the **control 3´UTR-reporter**

Graph (i) shows averaged actin-normalised protein abundances for HuCsv1 (red) , relative to the 1µg pmHuCsv1 condition from n=4 experimental repeats Error bars represent standard deviation values for each average.

Graph (ii) shows averaged actin-normalised protein abundances for HuCsv1 (red) , relative to the 1µg pmHuCsv1 condition from n=3 experimental repeats. For this graph, the results from the fourth experiment were omitted. Error bars represent standard deviation values for each average

The table shows actin normalised protein values for HuCsv1 relative to the 1µg pmHuCsv1 condition from each experiment as well as the average value and standard deviation (STDEV).

| | rcdc42-v2 3´ UTR (GFP/actin) | | | | n=4 | | |
|---|---|---|---|---|---|---|---|
| pmHuCsv1 | Expt 1 | Expt 2 | Expt 3 | Expt 4 | average | STDEV | *p*<... |
| - | 5.18 | 5.32 | 6.00 | 1.29 | 4.45 | 2.13 | - |
| 0.25µg | 4.52 | 4.66 | 3.68 | 1.72 | 3.65 | 1.36 | 0.549961 |
| 0.5µg | 0.51 | 2.77 | 5.37 | 2.36 | 2.75 | 2.00 | 0.291334 |
| 1.0µg | 2.17 | 3.65 | 2.54 | 1.93 | 2.57 | 0.76 | 0.149191 |
| 2.0µg | 4.01 | 4.38 | 1.67 | 1.59 | 2.91 | 1.49 | 0.283103 |

| | rcdc42-v2 3´ UTR (HuCsv1/actin) | | | | n=4 | |
|---|---|---|---|---|---|---|
| pmHuCsv1 | Expt 1 | Expt2 | Expt3 | Expt4 | average | STDEV |
| 0.25µg | 2.03 | 2.79 | 0.60 | 0.61 | 1.51 | 1.08 |
| 0.5µg | 3.82 | 5.42 | 1.42 | 2.23 | 3.22 | 1.77 |
| 1.0µg | 8.83 | 6.51 | 1.58 | 3.50 | 5.10 | 3.21 |
| 2.0µg | 12.24 | 7.31 | 2.29 | 5.26 | 6.77 | 4.19 |

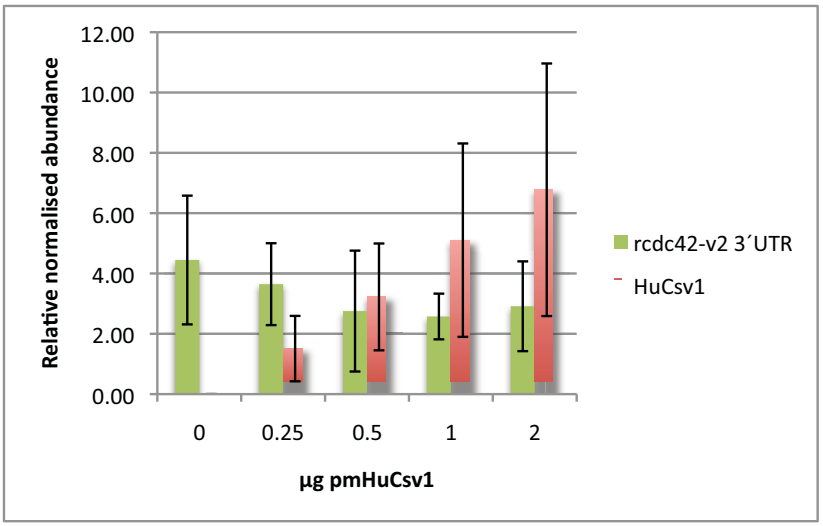


Figure 15a. Averaged results of four repeats testing for an effect of HuCsv1 on the **rcdc42-v2 3´UTR-reporter**

The graph shows averaged protein abundances normalised to Actin for d2EGFP (green) and HuCsv1 (red) from n=4 experimental repeats  Error bars represent standard deviation values for each average.

The table shows normalised protein values for d2EGFP from each experiment as well as the average value, standard deviation (STDEV) and p-value as determined by 2-tailed homoschedastic Student's t-test.

| | rcdc42-v2 3´ UTR (GFP/actin) | | | | n=4 | | |
|---|---|---|---|---|---|---|---|
| pmHuCsv1 | Expt 1 | Expt 2 | Expt 3 | Expt 4 | average | STDEV | *p*<… |
| - | 1.00 | 1.00 | 1.00 | 1.00 | 1.00 | - | - |
| 0.25µg | 0.87 | 0.88 | 0.61 | 1.33 | 0.92 | 0.30 | 0.62498 |
| 0.5µg | 0.10 | 0.52 | 0.90 | 1.83 | 0.84 | 0.74 | 0.669877 |
| 1.0µg | 0.42 | 0.69 | 0.42 | 1.50 | 0.76 | 0.51 | 0.37477 |
| 2.0µg | 0.78 | 0.82 | 0.28 | 1.23 | 0.78 | 0.39 | 0.298158 |

| | n=3 (Expt 1-3) | | |
|---|---|---|---|
| pmHuCsv1 | average | STDEV | *p*<… |
| - | 1.00 | - | - |
| 0.25µg | 0.79 | 0.15 | 0.072158 |
| 0.5µg | 0.51 | 0.40 | 0.097998 |
| 1.0µg | 0.51 | 0.15 | 0.005077 |
| 2.0µg | 0.63 | 0.30 | 0.098038 |

(i)

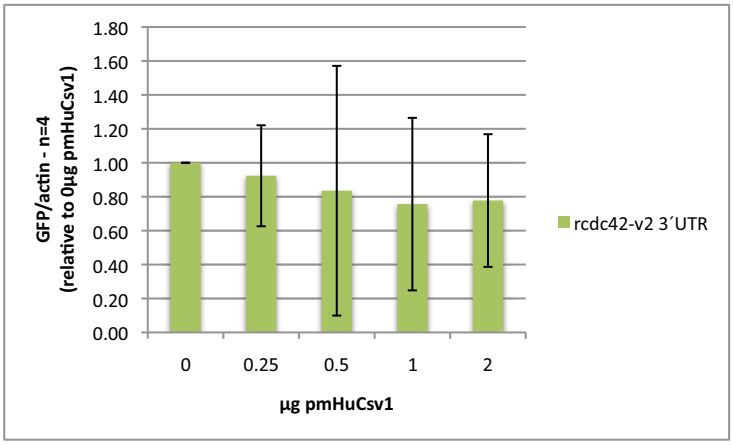


(ii)

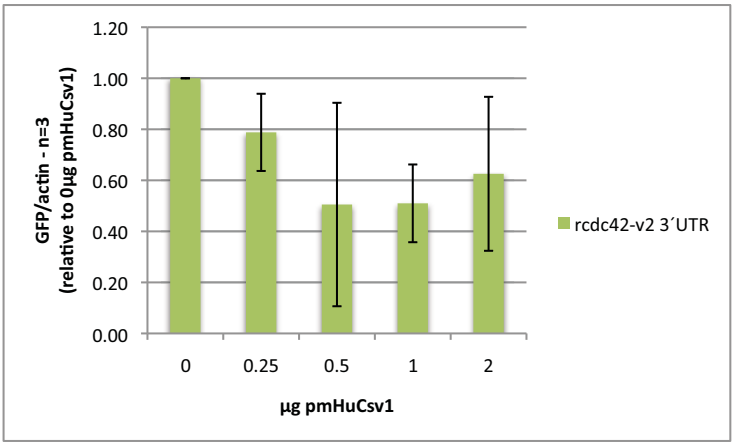


Figure 15b. Averaged results of four repeats testing for an effect of HuCsv1 on the **rcdc42-v2 3´UTR-reporter**

Graph (i) shows averaged actin-normalised protein abundances for d2EGFP (green) , relative to the 0µg pmHuCsv1 condition from n=4 experimental repeats . Error bars represent standard deviation values for each average.

Graph (ii) shows averaged actin-normalised protein abundances for d2EGFP (green) , relative to the 0µg pmHuCsv1 condition from n=3 experimental repeats. For this graph, the results from the fourth experiment were omitted. Error bars represent standard deviation values for each average

The table shows actin normalised protein values for d2EGFP relative to the 0µg pmHuCsv1 condition from each experiment as well as the average value, standard deviation (STDEV) and p-value as determined by 2-tailed homoschedastic Student's t-test.

| | rcdc42-v2 3´ UTR (HuCsv1/actin) | | | | n=4 | |
|---|---|---|---|---|---|---|
| pmHuCsv1 | Expt 1 | Expt2 | Expt3 | Expt4 | average | STDEV |
| 0.25µg | 0.29 | 0.48 | 0.73 | 0.30 | 0.45 | 0.20 |
| 0.5µg | 0.48 | 0.85 | 0.96 | 0.69 | 0.74 | 0.21 |
| 1.0µg | 1.00 | 1.00 | 1.00 | 1.00 | 1.00 | 0.00 |
| 2.0µg | 1.36 | 1.11 | 1.20 | 1.43 | 1.27 | 0.14 |

| | n=3 Expt 1-3 | |
|---|---|---|
| pmHuCsv1 | average | STDEV |
| 0.25µg | 0.50 | 0.22 |
| 0.5µg | 0.76 | 0.25 |
| 1.0µg | 1.00 | 0.00 |
| 2.0µg | 1.22 | 0.12 |

(i)

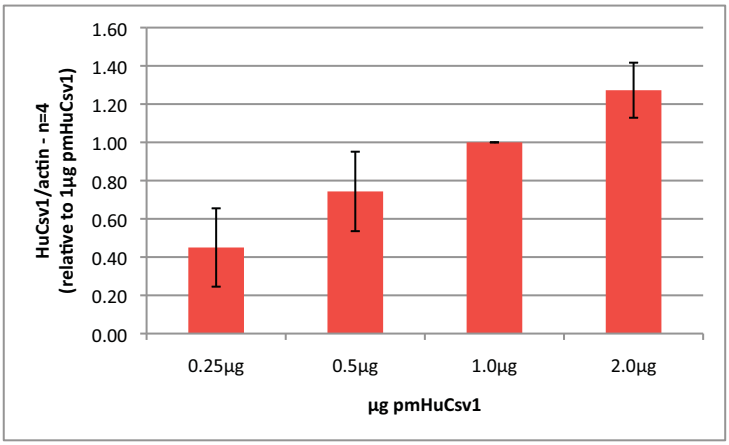


(ii)

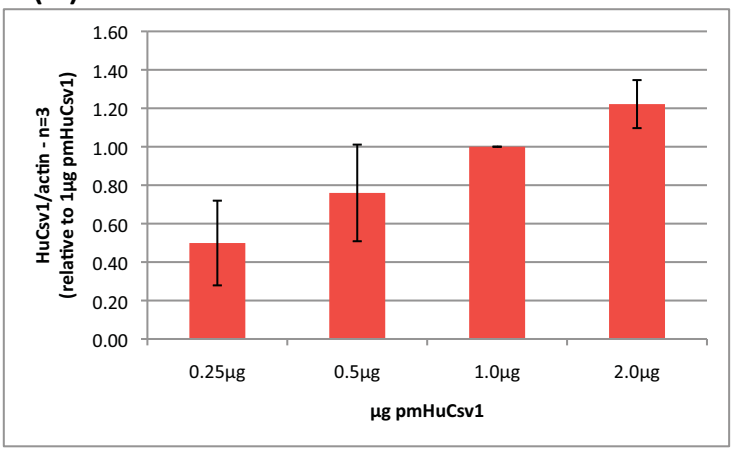


Figure 15c. Averaged results of four repeats testing for an effect of HuCsv1 on the **rcdc42-v2 3´UTR-reporter**

Graph (i) shows averaged actin-normalised protein abundances for HuCsv1 (red) , relative to the 1µg pmHuCsv1 condition from n=4 experimental repeats Error bars represent standard deviation values for each average.

Graph (ii) shows averaged actin-normalised protein abundances for HuCsv1 (red) , relative to the 1µg pmHuCsv1 condition from n=3 experimental repeats. For this graph, the results from the fourth experiment were omitted. Error bars represent standard deviation values for each average

The table shows actin normalised protein values for HuCsv1 relative to the 1µg pmHuCsv1 condition from each experiment as well as the average value and standard deviation (STDEV).

| | rCofilin 3´ UTR (GFP/actin) | | | | n=4 | | |
|---|---|---|---|---|---|---|---|
| pmHuCsv1 | Expt 1 | Expt 2 | Expt 3 | Expt 4 | average | STDEV | *p*<… |
| - | 3.05 | 1.91 | 5.57 | 0.47 | 2.75 | 2.15 | - |
| 0.25µg | 2.74 | 3.06 | 2.19 | 0.68 | 2.17 | 1.06 | 0.645373 |
| 0.5µg | 3.35 | 4.77 | 2.62 | 0.86 | 2.90 | 1.62 | 0.914582 |
| 1.0µg | 2.89 | 4.87 | - | 0.83 | 2.86 | 2.02 | 0.946417 |
| 2.0µg | 2.78 | 2.98 | 0.92 | 0.69 | 1.84 | 1.20 | 0.490905 |

| | rCofilin 3´ UTR (HuCsv1/actin) | | | | n=4 | |
|---|---|---|---|---|---|---|
| pmHuCsv1 | Expt 1 | Expt2 | Expt3 | Expt4 | average | STDEV |
| 0.25µg | 2.40 | 1.55 | 0.26 | 0.27 | 1.12 | 1.05 |
| 0.5µg | 5.45 | 3.15 | 0.83 | 1.08 | 2.63 | 2.15 |
| 1.0µg | 5.64 | 4.71 | - | 2.27 | 4.21 | 1.74 |
| 2.0µg | 7.41 | 6.95 | 1.94 | 3.37 | 4.92 | 2.68 |

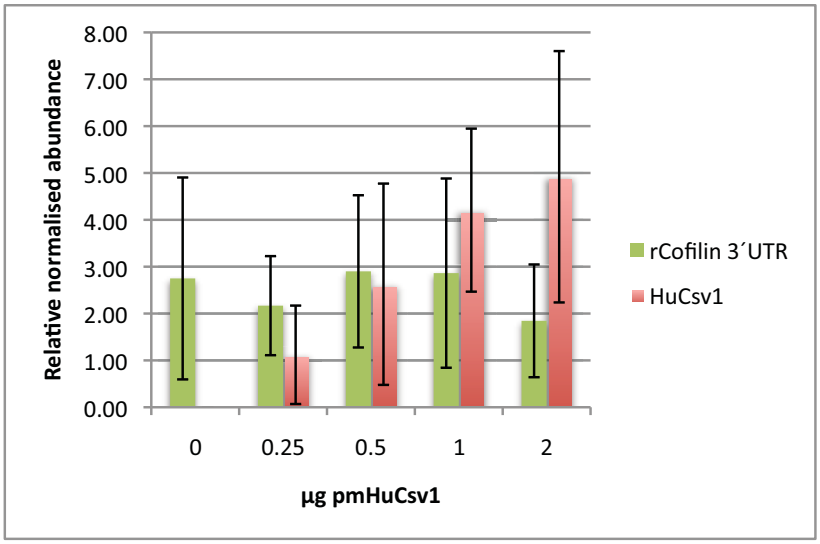


Figure 16a. Averaged results of four repeats testing for an effect of HuCsv1 on the **rCofilin 3´UTR-reporter**

The graph shows averaged protein abundances normalised to Actin for d2EGFP (green) and HuCsv1 (red) from n=4 experimental repeats  Error bars represent standard deviation values for each average.

The table shows normalised protein values for d2EGFP from each experiment as well as the average value, standard deviation (STDEV) and p-value as determined by 2-tailed homoschedastic Student's t-test.

| | rCofilin 3´ UTR (GFP/actin) | | | | n=4 | | |
|---|---|---|---|---|---|---|---|
| pmHuCsv1 | Expt 1 | Expt 2 | Expt 3 | Expt 4 | average | STDEV | *p*<… |
| - | 1.00 | 1.00 | 1.00 | 1.00 | 1.00 | - | - |
| 0.25µg | 0.90 | 1.60 | 0.39 | 1.43 | 1.08 | 0.55 | 0.774903 |
| 0.5µg | 1.10 | 2.50 | 0.47 | 1.82 | 1.47 | 0.88 | 0.323079 |
| 1.0µg | 0.95 | 2.55 | - | 1.75 | 1.75 | 0.80 | 0.109534 |
| 2.0µg | 0.91 | 1.56 | 0.17 | 1.47 | 1.03 | 0.64 | 0.937174 |

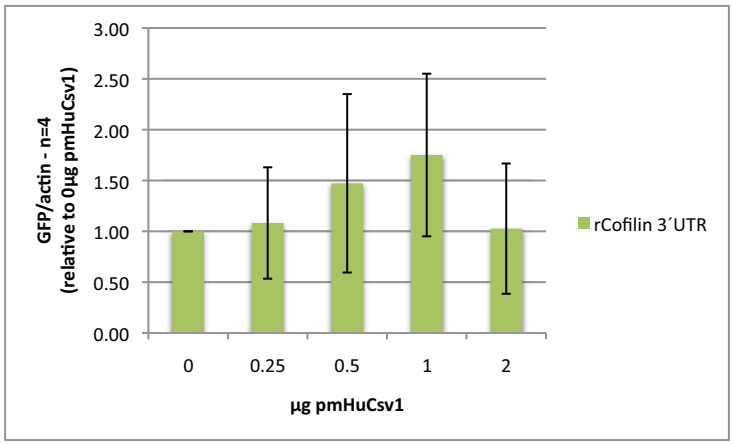


Figure 16b. Averaged results of four repeats testing for an effect of HuCsv1 on the **rCofilin 3´UTR-reporter**

The graph shows averaged actin-normalised protein abundances for d2EGFP (green) , relative to 0µg pmHuCsv1 condition from n=4 experimental repeats  Error bars represent standard deviation values for each average.

The table shows actin normalised protein values for d2EGFP relative to the 0µg pmHuCsv1 condition from each experiment as well as the average value, standard deviation (STDEV) and p-value as determined by 2-tailed homoschedastic Student's t-test.

| | rCofilin 3´ UTR (HuCsv1/actin) | | | | n=3 | |
|---|---|---|---|---|---|---|
| pmHuCsv1 | Expt 1 | Expt2 | Expt3 | Expt4 | average | STDEV |
| 0.25µg | 0.49 | 0.41 | - | 0.31 | 0.40 | 0.09 |
| 0.5µg | 0.97 | 0.71 | - | 0.59 | 0.76 | 0.19 |
| 1.0µg | 1.00 | 1.00 | - | 1.00 | 1.00 | 0.00 |
| 2.0µg | 1.28 | 1.42 | - | 1.38 | 1.36 | 0.07 |

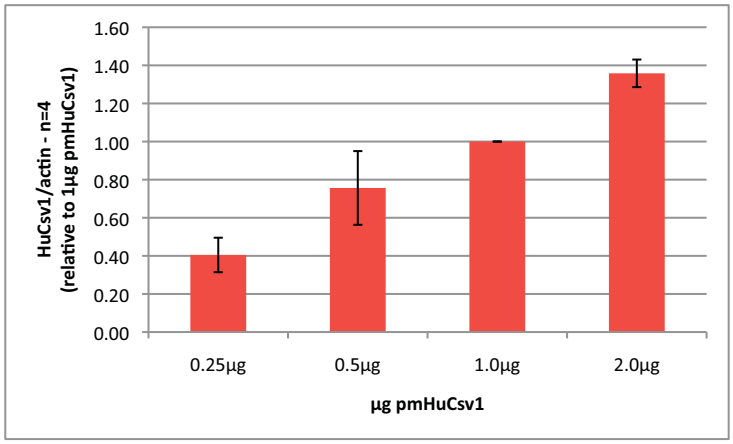


Figure 16c. Averaged results of four repeats testing for an effect of HuCsv1 on the **rCofilin 3´UTR-reporter**

The graph shows averaged actin-normalised protein abundances for HuCsv1 (red) , relative to 1µg pmHuCsv1 condition from n=3 experimental repeats Results for experiment 3 were omitted because no data was obtained for the 1µg HuCsv1 condition. Error bars represent standard deviation values for each average.

The table shows actin normalised protein values for HuCsv1 relative to the 1µg pmHuCsv1 condition from each experiment as well as the average value and standard deviation (STDEV).

| | control 3´UTR - Raw d2EGFP values | | | |
|---|---|---|---|---|
| µg pmHuCsv1: | Expt1 | Expt2 | Expt3 | Expt4 |
| - | 828,419 | 407,048 | 527,550 | 77,715 |
| 0.25 | 837,640 | 560,979 | 878,839 | 120,266 |
| 0.5 | 810,010 | 361,447 | 734,005 | 90,715 |
| 1.0 | 1,051,763 | 393,748 | 415,706 | 117,593 |
| 2.0 | 614,211 | 412,445 | 338,300 | 142,529 |

| | rcdc42-v2 3´UTR - Raw d2EGFP values | | | |
|---|---|---|---|---|
| µg pmHuCsv1: | Expt1 | Expt2 | Expt3 | Expt4 |
| - | 676,686 | 478,489 | 924,368 | 82,262 |
| 0.25 | 553,398 | 367,774 | 458,044 | 105,450 |
| 0.5 | 59,156 | 288,701 | 595,818 | 132,371 |
| 1.0 | 277,024 | 259,107 | 297,905 | 110,563 |
| 2.0 | 385,535 | 299,446 | 233,737 | 106,354 |

| | rCofilin 3´UTR - Raw d2EGFP values | | | |
|---|---|---|---|---|
| µg pmHuCsv1: | Expt1 | Expt2 | Expt3 | Expt4 |
| - | 159,927 | 187,670 | 954,005 | 28,392 |
| 0.25 | 124,558 | 327,186 | 455,081 | 42,592 |
| 0.5 | 148,703 | 355,842 | 560,391 | 54,522 |
| 1.0 | 136,137 | 308,158 | - | 57,702 |
| 2.0 | 127,101 | 180,690 | 175,156 | 46,030 |
| | | | | |
| BKG | 8,867 | 5,249 | 833,163 | 4,627 |

Figure 17a: Raw d2EGFP abundance values from 4 individual repeated experiments.

BKG = background signal from membrane.

| | control 3´UTR - Raw HuCsv1 values | | | |
|---|---|---|---|---|
| µg pmHuCsv1: | Expt1 | Expt2 | Expt3 | Expt4 |
| 0.25 | 267,459 | 285,596 | 421,977 | 59,342 |
| 0.5 | 488,296 | 336,333 | 517,798 | 84,744 |
| 1.0 | 705,555 | 456,729 | 657,037 | 243,444 |
| 2.0 | 997,225 | 566,643 | 636,224 | 421,122 |

| | rcdc42-v2 3´UTR - Raw HuCsv1 values | | | |
|---|---|---|---|---|
| µg pmHuCsv1: | Expt1 | Expt2 | Expt3 | Expt4 |
| 0.25 | 339,161 | 270,208 | 326,645 | 77,108 |
| 0.5 | 527,148 | 631,363 | 381,569 | 161,449 |
| 1.0 | 1,218,672 | 508,591 | 421,637 | 237,056 |
| 2.0 | 1,246,852 | 544,012 | 603,207 | 394,306 |

| | rCofilin 3´UTR - Raw HuCsv1 values | | | |
|---|---|---|---|---|
| µg pmHuCsv1: | Expt1 | Expt2 | Expt3 | Expt4 |
| 0.25 | 142,871 | 234,216 | 472,037 | 57,231 |
| 0.5 | 274,521 | 282,725 | 608,143 | 109,196 |
| 1.0 | 300,383 | 338,675 | - | 202,790 |
| 2.0 | 372,648 | 459,980 | 752,273 | 266,863 |
| | | | | |
| BKG | 31,136 | 31,394 | 2,880,001 | 23,725 |

Figure 17b: Raw HuCsv1 abundance values from 4 individual repeated experiments.

BKG = background signal from membrane.

| | control 3´UTR - Raw β-actin values | | | |
|---|---|---|---|---|
| µg pmHuCsv1: | Expt1 | Expt2 | Expt3 | Expt4 |
| - | 109,001 | 90,244 | 154,280 | 59,172 |
| 0.25 | 107,830 | 105,940 | 153,189 | 57,631 |
| 0.5 | 116,505 | 88,655 | 149,528 | 55,329 |
| 1.0 | 95,712 | 99,978 | 128,501 | 68,357 |
| 2.0 | 116,571 | 98,029 | 114,774 | 67,578 |

| | rcdc42-v2 3´UTR - Raw β-actin values | | | |
|---|---|---|---|---|
| µg pmHuCsv1: | Expt1 | Expt2 | Expt3 | Expt4 |
| - | 130,683 | 90,014 | 154,060 | 63,710 |
| 0.25 | 122,370 | 92,691 | 124,464 | 64,269 |
| 0.5 | 115,666 | 113,128 | 110,883 | 77,609 |
| 1.0 | 127,418 | 84,656 | 117,109 | 60,340 |
| 2.0 | 96,051 | 95,464 | 139,980 | 67,622 |

| | rCofilin 3´UTR - Raw β-actin values | | | |
|---|---|---|---|---|
| µg pmHuCsv1: | Expt1 | Expt2 | Expt3 | Expt4 |
| - | 52,513 | 98,265 | 171,309 | 60,098 |
| 0.25 | 45,462 | 103,782 | 207,386 | 59,709 |
| 0.5 | 44,382 | 90,170 | 213,653 | 68,712 |
| 1.0 | 47,089 | 89,973 | - | 75,057 |
| 2.0 | 45,712 | 88,296 | 189,840 | 66,854 |
| | | | | |
| FuGENE | 118,070 | 78,891 | - | - |
| BKG | 42,120 | 49,046 | 83,336 | 36,932 |

Figure 17c: Raw β-actin abundance values from 4 individual repeated experiments.

BKG = background signal from membrane.
FuGENE = actin abundance as measured from cells treated with FuGENE without plasmid DNA.

A

| control 3´UTR-reporter | | |
|---|---|---|
| | d2EGFP abundance | |
| incubation | - HuCsv1 | +HuCsv1 |
| 24hr | 2.52 | 1.81 |
| 28hr | 2.68 | 3.23 |
| 32hr | 1.71 | 2.16 |
| 35hr | 2.52 | 2.34 |
| 40hr | 3.47 | 2.29 |
| 44hr | 2.75 | 2.76 |
| 48hr | 3.15 | 2.91 |

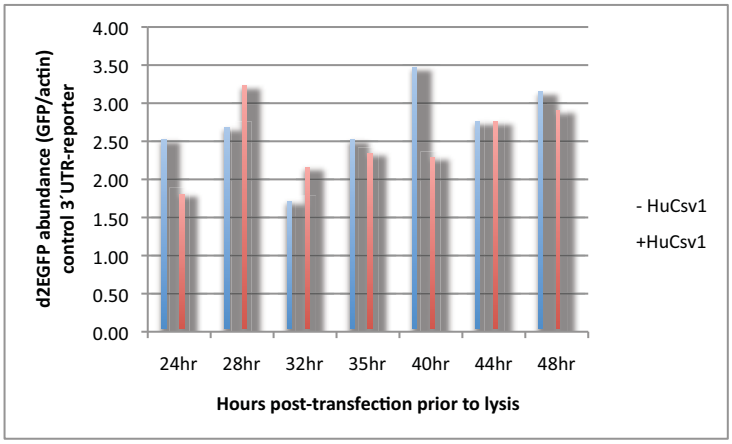


B

| rCofilin 3´UTR-reporter | | |
|---|---|---|
| | d2EGFP abundance | |
| incubation | - HuCsv1 | +HuCsv1 |
| 24hr | 1.22 | 1.57 |
| 28hr | 2.01 | 1.75 |
| 32hr | 0.66 | 0.86 |
| 35hr | 2.18 | 1.31 |
| 40hr | 1.61 | 1.12 |
| 44hr | 2.76 | 1.42 |
| 48hr | 3.32 | 2.12 |

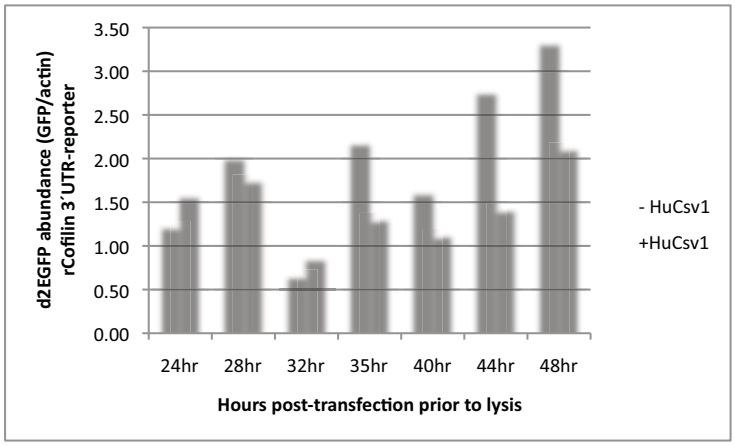


C

| rcdc42-v2 3´UTR-reporter | | |
|---|---|---|
| | d2EGFP abundance | |
| incubation | - HuCsv1 | +HuCsv1 |
| 24hr | 1.95 | 1.33 |
| 28hr | 4.82 | 3.52 |
| 32hr | 2.39 | 0.65 |
| 35hr | 3.73 | 1.78 |
| 40hr | 3.12 | 1.46 |
| 44hr | 5.63 | 1.86 |
| 48hr | 6.95 | 2.58 |

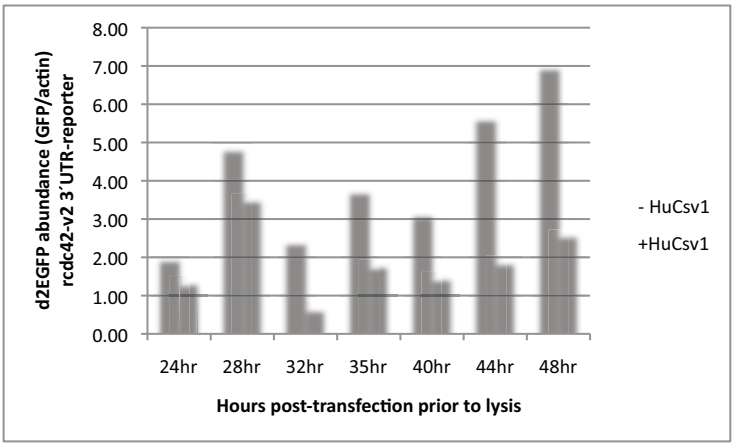


Figure 18. d2EGFP abundance in the presence or absence of HuCsv1. 24-hour time course results – BLOT 1

Graphs show d2EGFP abundances normalised to actin from cells co-transfected with either 1µg pmHuCsv1 (+HuCsv1) or 1µg pcDNA3 (-HuCsv1).

The tables show normalised d2EGFP abundance from each time point

| | HuCsv1 abundance | | |
|---|---|---|---|
| | 3´UTR-reporter | | |
| incubation | control | rCofilin | rcdc42-v2 |
| 24hr | 9.31 | 9.38 | 9.44 |
| 28hr | 12.68 | 11.16 | 17.14 |
| 32hr | 10.95 | 3.55 | 2.63 |
| 35hr | 2.76 | 3.38 | 3.33 |
| 40hr | 6.52 | 6.20 | 8.60 |
| 44hr | 8.52 | 9.72 | 9.97 |
| 48hr | 10.27 | 10.65 | 9.92 |

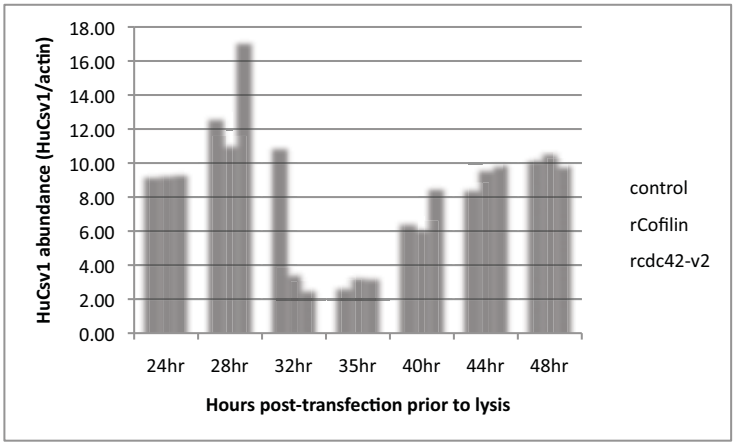


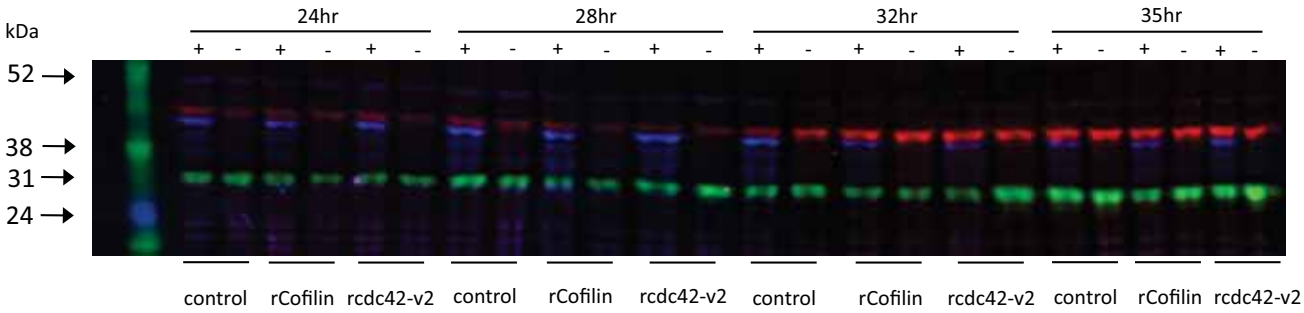


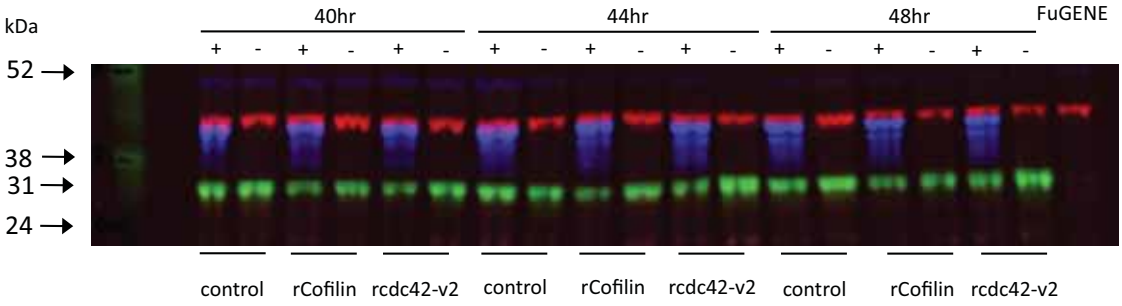


Figure 19. HuCsv1 abundances across 24-hour time course – BLOT 1

Graph and table show actin-normalised HuCsv1 abundances from cells co-transfected with 1µg pmHuCsv1 (+HuCsv1) and one of the three 3´UTR-reporter vectors.

Western blot images from the first blot shown below. d2EGFP (31kDa) shown in green, HuCsv1 (~41kDa) shown in blue and β-actin (~42kDa) shown in red. +/- represents co-transfection with (+) or without (-) pmHuCsv1. FuGENE lane corresponds to lysate from untransfected cells.

A

| control 3´UTR-reporter | | |
|---|---|---|
| | d2EGFP abundance | |
| incubation | - HuCsv1 | +HuCsv1 |
| 24hr | 2.09 | 1.94 |
| 28hr | 3.80 | 5.94 |
| 32hr | 5.07 | 4.22 |
| 36hr | 7.47 | 4.31 |
| 40hr | 7.39 | 4.22 |
| 44hr | 10.75 | 10.79 |
| 48hr | 8.45 | 4.78 |

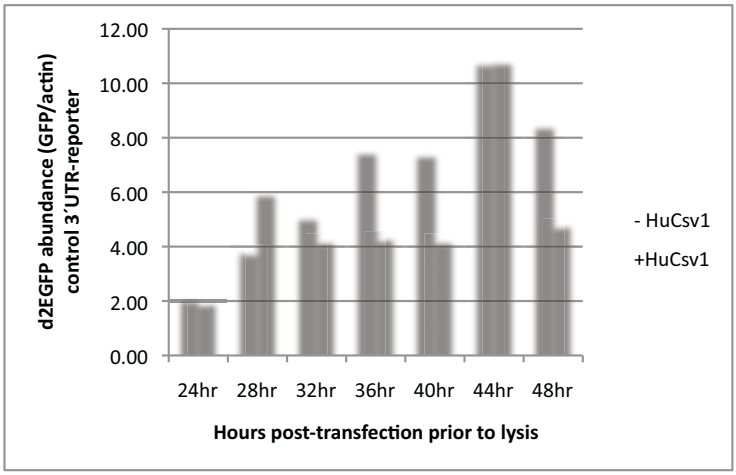


B

| rCofilin 3´UTR-reporter | | |
|---|---|---|
| | d2EGFP abundance | |
| incubation | - HuCsv1 | +HuCsv1 |
| 24hr | 2.81 | 1.30 |
| 28hr | 2.27 | 1.73 |
| 32hr | 3.13 | 2.07 |
| 36hr | 5.43 | 2.38 |
| 40hr | 6.21 | 3.13 |
| 44hr | 7.26 | 2.68 |
| 48hr | 6.41 | 4.02 |

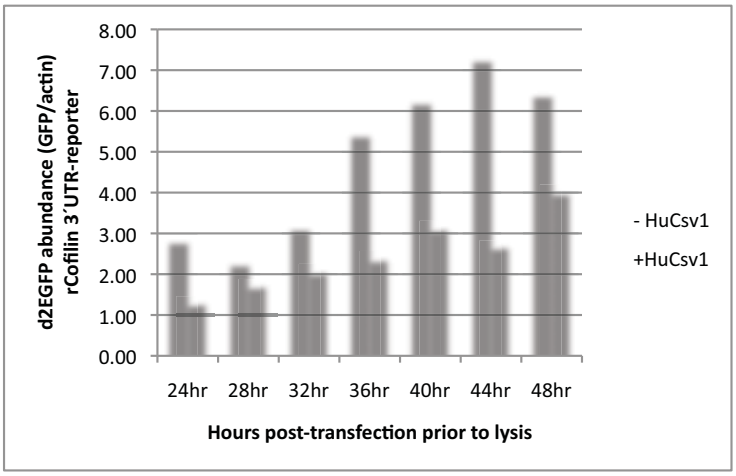


C

| rcdc42-v2 3´UTR-reporter | | |
|---|---|---|
| | d2EGFP abundance | |
| incubation | - HuCsv1 | +HuCsv1 |
| 24hr | 4.91 | 2.85 |
| 28hr | 4.26 | 2.34 |
| 32hr | 4.44 | 2.35 |
| 36hr | 4.17 | 2.21 |
| 40hr | 16.29 | 7.69 |
| 44hr | 8.19 | 4.73 |
| 48hr | 7.90 | 4.34 |

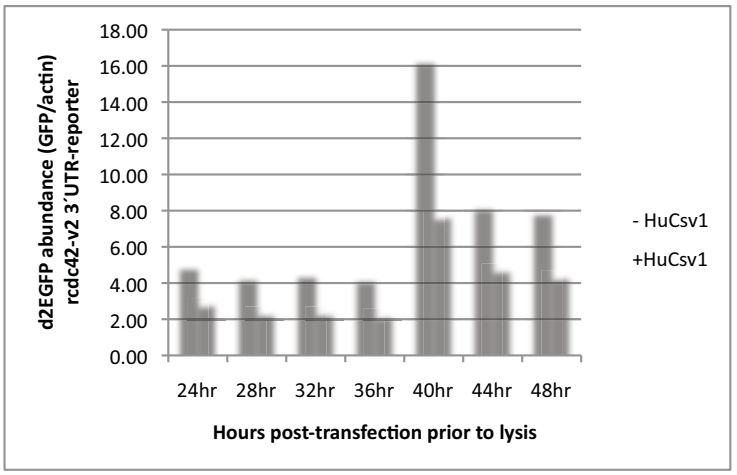


Figure 20. d2EGFP abundance in the presence or absence of HuCsv1. 24-hour time course results – BLOT 2

Graphs show d2EGFP abundances normalised to actin from cells co-transfected with either 1µg pmHuCsv1 (+HuCsv1) or 1µg pcDNA3 (-HuCsv1).

The table shows normalised d2EGFP abundance from each time point

| | HuCsv1 abundance | | |
|---|---|---|---|
| | 3´UTR-reporter | | |
| incubation | control | rCofilin | rcdc42-v2 |
| 24hr | 3.59 | 3.53 | 1.90 |
| 28hr | 3.32 | 7.84 | 5.72 |
| 32hr | 7.91 | 8.38 | 7.81 |
| 36hr | 9.68 | 7.69 | 8.10 |
| 40hr | 5.77 | 6.16 | 6.62 |
| 44hr | 6.36 | 5.82 | 6.07 |
| 48hr | 6.90 | 6.49 | 6.26 |

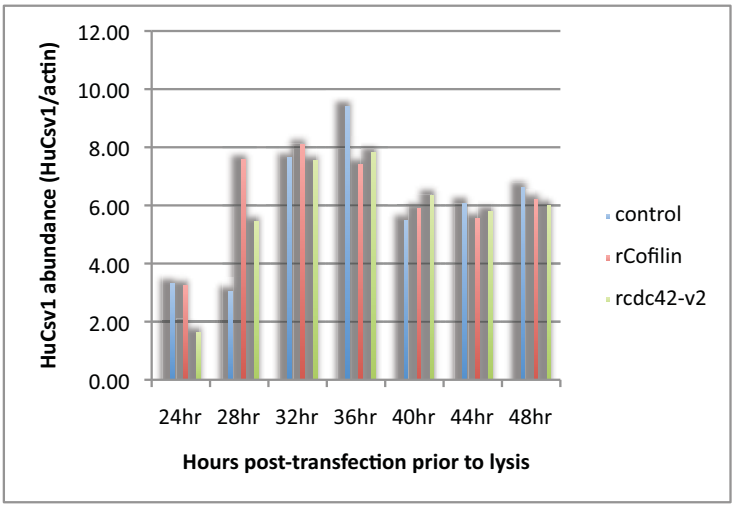


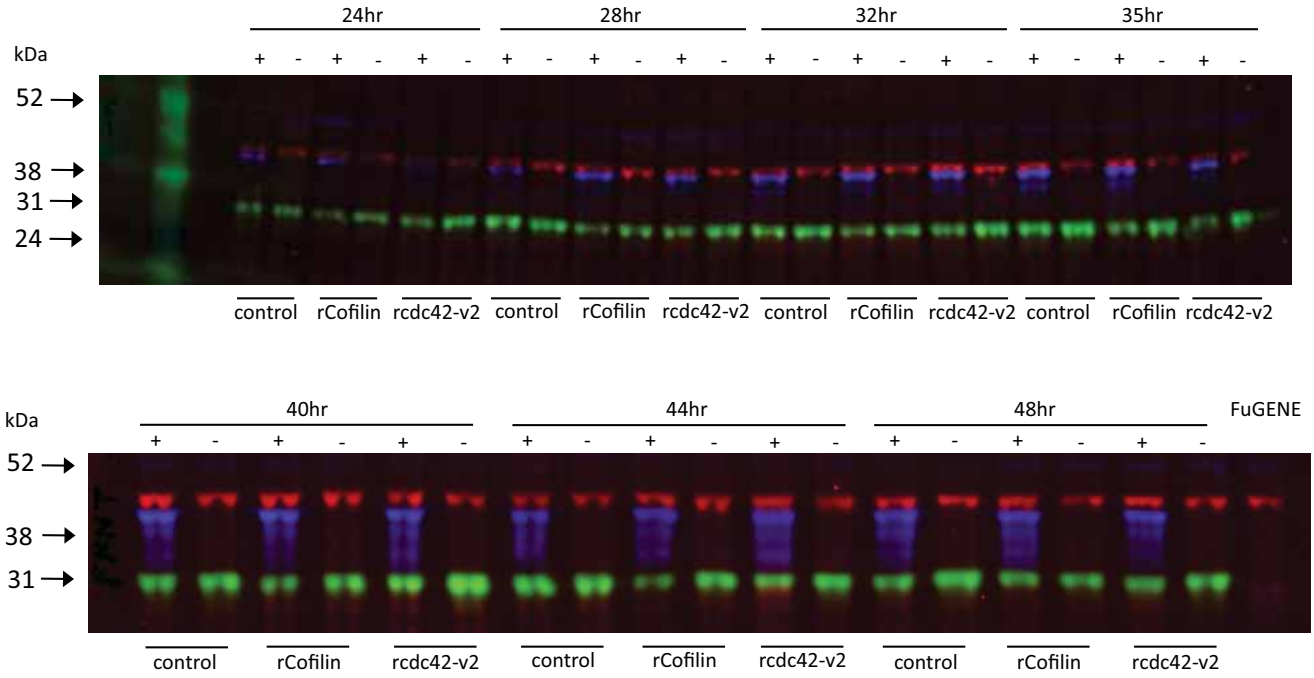


Figure 21. HuCsv1 abundances across 24-hour time course – BLOT 2

Graph and table show actin-normalised HuCsv1 abundances from cells co-transfected with 1µg pmHuCsv1 (+HuCsv1) and one of the three 3´UTR-reporter vectors.

Western blot images from the second blot shown below. d2EGFP (31kDa) shown in green, HuCsv1 (~41kDa) shown in blue and β-actin (~42kDa) shown in red. +/- represents co-transfection with (+) or without (-) pmHuCsv1. FuGENE lane corresponds to lysate from untransfected cells.

i.)

| | Raw Actin abundance values - control 3´UTR-reporter | | | | | | |
|---|---|---|---|---|---|---|---|
| | 24hr | 28hr | 32hr | 35hr | 40hr | 44hr | 48hr |
| -HuCsv1 | 17,962 | 21,397 | 34,080 | 50,656 | 64,071 | 52,634 | 72,731 |
| +HuCsv1 | 22,740 | 24,597 | 24,522 | 51,715 | 71,979 | 77,929 | 53,551 |

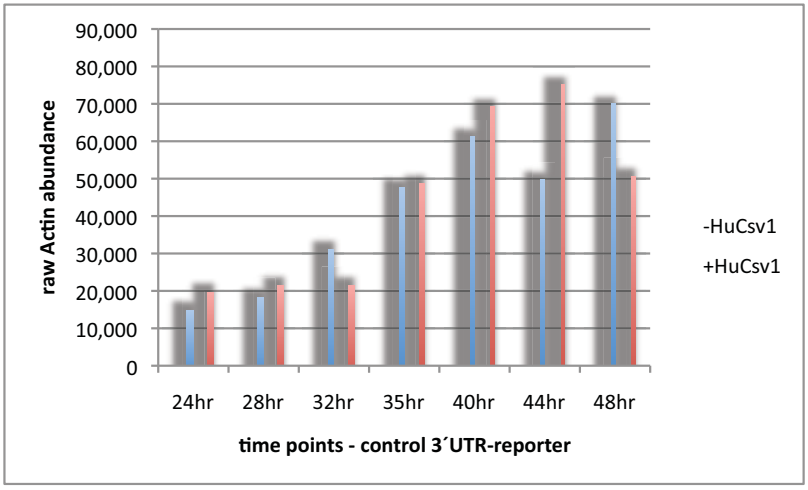


ii.)

| | Raw Actin abundance values - control 3´UTR-reporter | | | | | | |
|---|---|---|---|---|---|---|---|
| | 24hr | 28hr | 32hr | 35hr | 40hr | 44hr | 48hr |
| -HuCsv1 | 13,692 | 19,847 | 20,932 | 17,014 | 23,373 | 17,432 | 24,161 |
| +HuCsv1 | 12,198 | 15,665 | 18,792 | 22,531 | 29,658 | 17,381 | 23,250 |

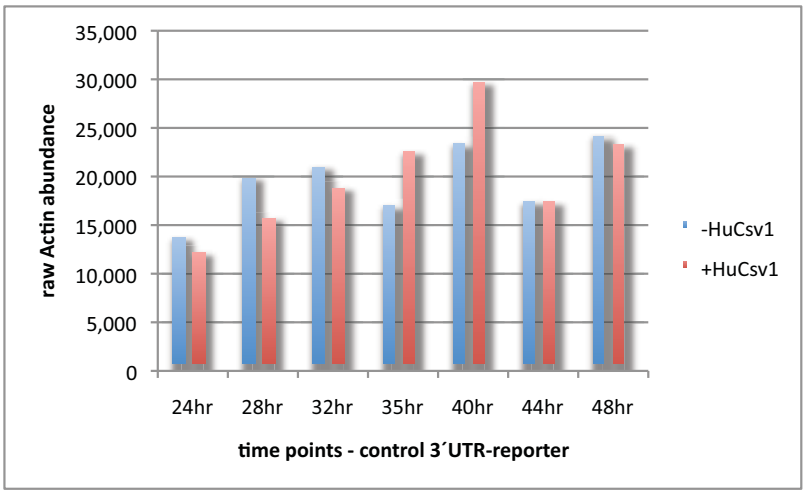


Figure 22a. Raw actin abundances from the time course HuCsv1 overexpression experiment

Raw actin abundance values from cells co-transfected with the control 3´UTR-reporter construct and either 1µg pmHuCsv1 (+HuCsv1) or 1µg pcDNA3 (-HuCsv1) and then incubated 24hr to 48hr post-transfection, prior to lysis.

i.) and ii.) represent raw actin abundances from the first and second western blots respectively.

i.)

| | Raw Actin abundance values - rCofilin 3´UTR-reporter | | | | | | |
|---|---|---|---|---|---|---|---|
| | 24hr | 28hr | 32hr | 35hr | 40hr | 44hr | 48hr |
| -HuCsv1 | 19,032 | 17,650 | 54,657 | 48,793 | 77,085 | 66,514 | 36,561 |
| +HuCsv1 | 19,842 | 20,264 | 45,671 | 44,405 | 76,172 | 52,964 | 45,131 |

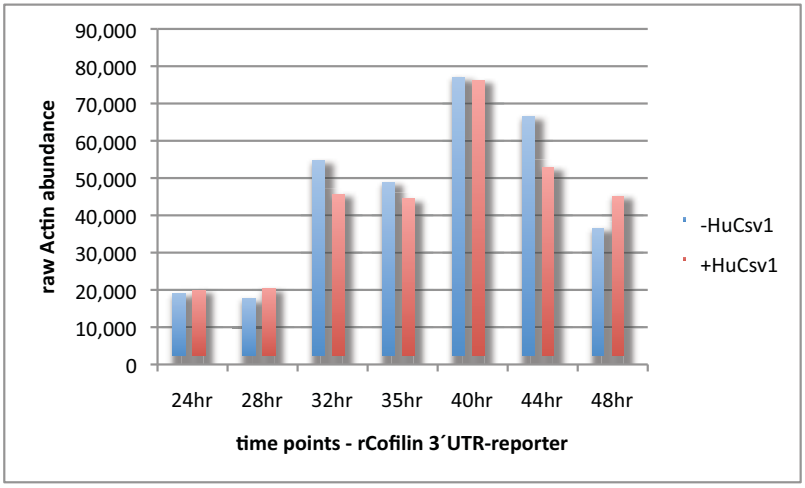


ii.)

| | Raw Actin abundance values - rCofilin 3´UTR-reporter | | | | | | |
|---|---|---|---|---|---|---|---|
| | 24hr | 28hr | 32hr | 35hr | 40hr | 44hr | 48hr |
| -HuCsv1 | 12,861 | 21,991 | 22,370 | 15,898 | 25,770 | 21,913 | 16,273 |
| +HuCsv1 | 13,521 | 18,810 | 22,345 | 21,776 | 28,690 | 21,384 | 23,790 |

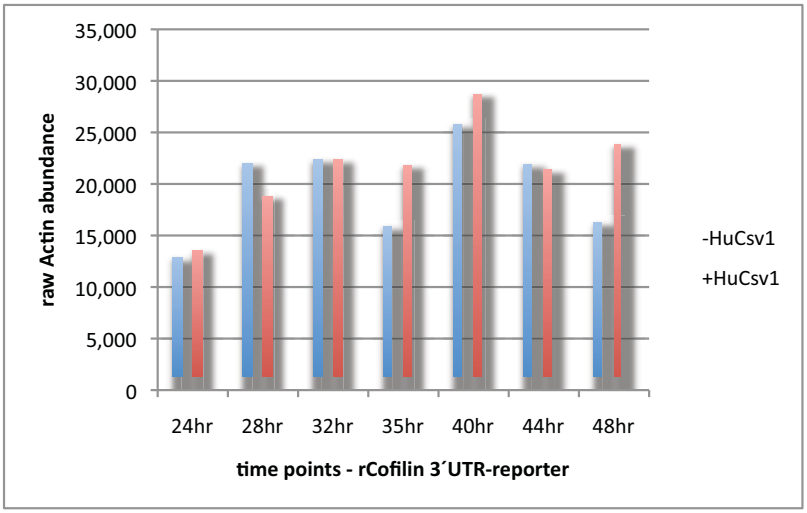


Figure 22b. Raw actin abundances from the time course HuCsv1 overexpression experiment

Raw actin abundance values from cells co-transfected with the rCofilin 3´UTR-reporter construct and either 1µg pmHuCsv1 (+HuCsv1) or 1µg pcDNA3 (-HuCsv1) and then incubated 24hr to 48hr post-transfection, prior to lysis.

i.) and ii.) represent raw actin abundances from the first and second western blots respectively.

i.)

| | Raw Actin abundance values - rcdc42-v2 3´UTR-reporter | | | | | | |
|---|---|---|---|---|---|---|---|
| | 24hr | 28hr | 32hr | 35hr | 40hr | 44hr | 48hr |
| -HuCsv1 | 17,998 | 18,604 | 48,915 | 38,763 | 60,653 | 53,368 | 36,682 |
| +HuCsv1 | 22,921 | 18,396 | 53,685 | 51,316 | 56,265 | 58,595 | 48,071 |

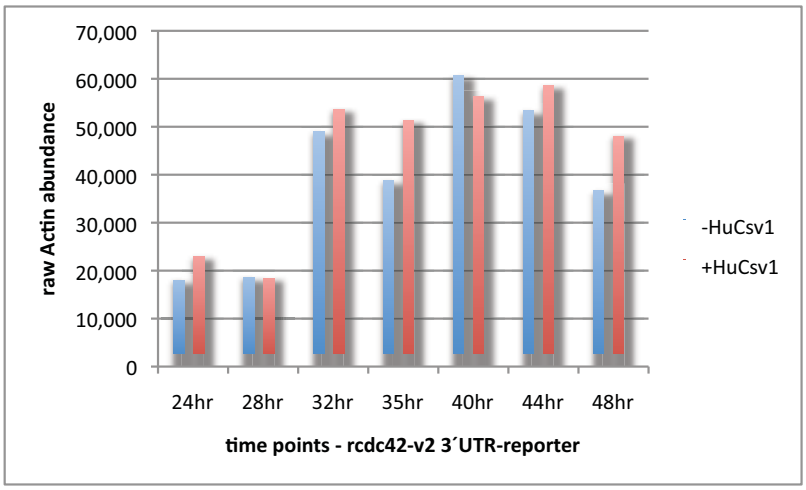


ii.)

| | Raw Actin abundance values - rcdc42-v2 3´UTR-reporter | | | | | | |
|---|---|---|---|---|---|---|---|
| | 24hr | 28hr | 32hr | 35hr | 40hr | 44hr | 48hr |
| -HuCsv1 | 13,372 | 19,285 | 26,583 | 14,298 | 19,106 | 18,961 | 20,434 |
| +HuCsv1 | 11,540 | 18,050 | 26,681 | 14,339 | 22,086 | 24,746 | 23,300 |

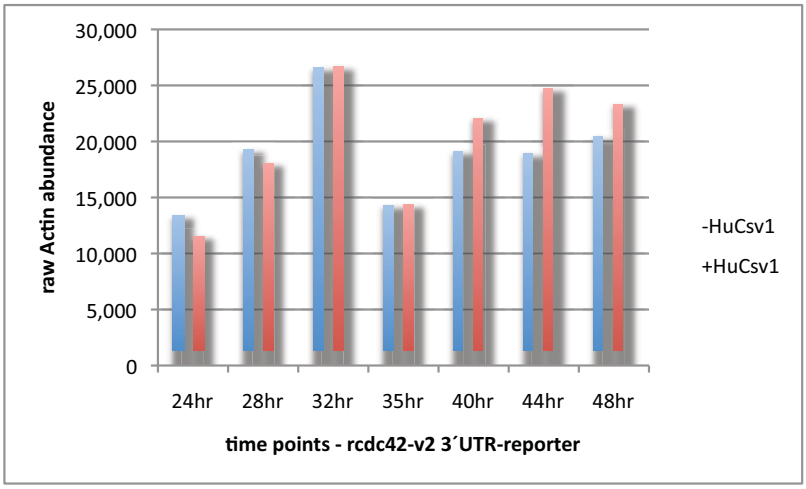


Figure 22c. Raw actin abundances from the time course HuCsv1 overexpression experiment

Raw actin abundance values from cells co-transfected with the rcdc42-v2 3´UTR-reporter construct and either 1µg pmHuCsv1 (+HuCsv1) or 1µg pcDNA3 (-HuCsv1) and then incubated 24hr to 48hr post-transfection, prior to lysis.

i.) and ii.) represent raw actin abundances from the first and second western blots respectively.

i.)

| | Blot 1: Raw HuCsv1 abundance values - control 3´UTR-reporter | | | | | | |
|---|---|---|---|---|---|---|---|
| | 24hr | 28hr | 32hr | 35hr | 40hr | 44hr | 48hr |
| +HuCsv1 | 2,117,438 | 3,118,720 | 2,685,483 | 1,427,531 | 46,924,223 | 66,393,181 | 55,010,390 |

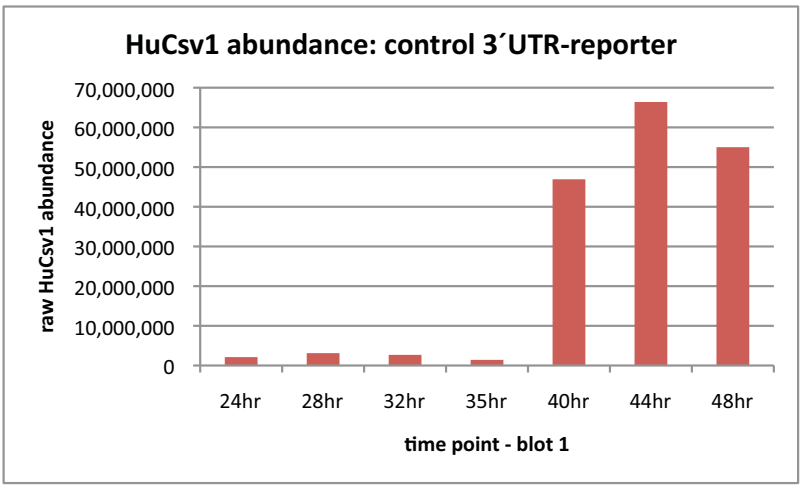


ii.)

| | Blot 2: Raw HuCsv1 abundance values - control 3´UTR-reporter | | | | | | |
|---|---|---|---|---|---|---|---|
| | 24hr | 28hr | 32hr | 35hr | 40hr | 44hr | 48hr |
| +HuCsv1 | 4,377,802 | 5,203,991 | 14,856,694 | 21,810,498 | 17,119,523 | 11,045,863 | 16,045,813 |

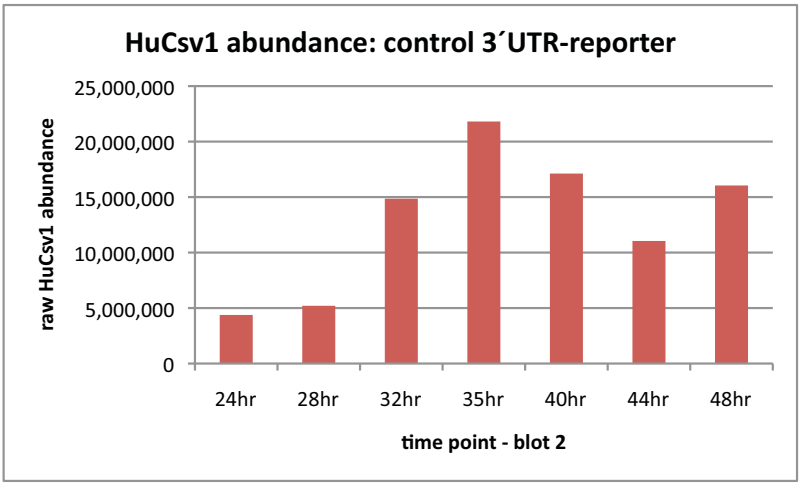


Figure 23a. Raw HuCsv1 abundances from the time course HuCsv1 overexpression experiment

Raw HuCsv1 abundance values from cells co-transfected with the control 3´UTR-reporter construct and 1µg of pmHuCsv1 (+HuCsv1) and then incubated 24hr to 48hr post-transfection, prior to lysis.

i.) and ii.) represent raw HuCsv1 abundances from the first and second western blots respectively.

i.)

| | Blot 1: Raw HuCsv1 abundance values - rCofilin 3´UTR-reporter | | | | | | |
|---|---|---|---|---|---|---|---|
| | 24hr | 28hr | 32hr | 35hr | 40hr | 44hr | 48hr |
| +HuCsv1 | 1,860,707 | 2,260,928 | 1,622,680 | 1,502,745 | 47,210,452 | 51,473,436 | 48,081,242 |

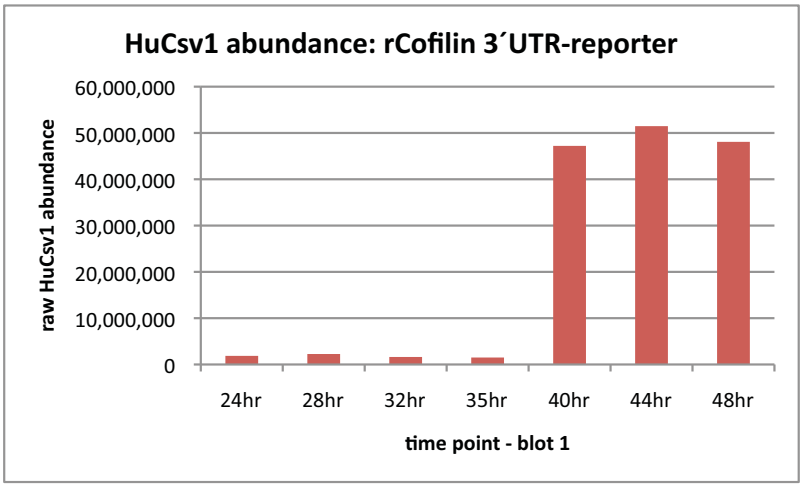


ii.)

| | Blot 2: Raw HuCsv1 abundance values - rCofilin 3´UTR-reporter | | | | | | |
|---|---|---|---|---|---|---|---|
| | 24hr | 28hr | 32hr | 35hr | 40hr | 44hr | 48hr |
| +HuCsv1 | 4,767,971 | 14,742,392 | 18,732,663 | 16,741,262 | 17,667,174 | 12,441,178 | 15,446,835 |

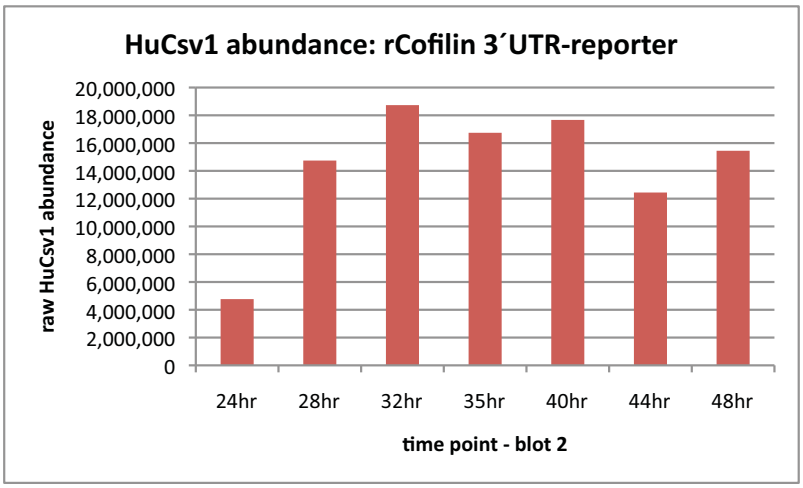


Figure 23b. Raw HuCsv1 abundances from the time course HuCsv1 overexpression experiment

Raw HuCsv1 abundance values from cells co-transfected with the rCofilin 3´UTR-reporter construct and 1µg of pmHuCsv1 (+HuCsv1) and then incubated 24hr to 48hr post-transfection, prior to lysis.

i.) and ii.) represent raw HuCsv1 abundances from the first and second western blots respectively.

i.)

| | Blot 1:Raw HuCsv1 abundance values - rcdc42-v2 3´UTR-reporter | | | | | | |
|---|---|---|---|---|---|---|---|
| | 24hr | 28hr | 32hr | 35hr | 40hr | 44hr | 48hr |
| +HuCsv1 | 2,162,784 | 3,153,265 | 1,409,897 | 1,710,499 | 48,404,424 | 58,406,017 | 47,667,758 |

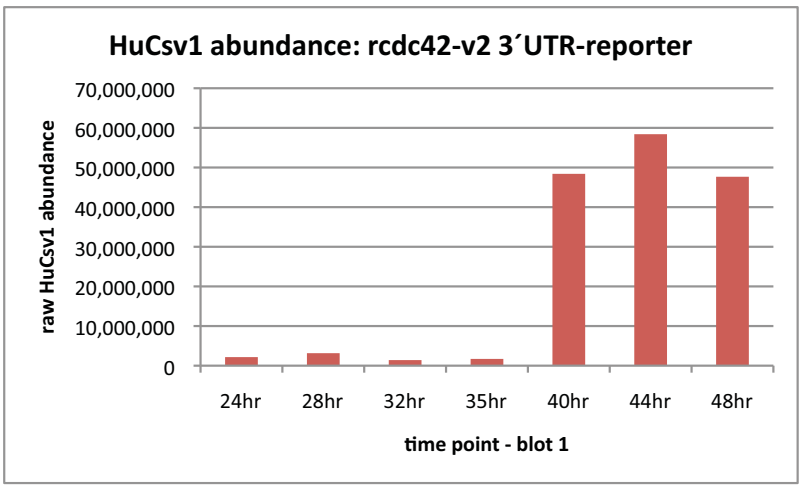


ii.)

| | Blot 2: Raw HuCsv1 abundance values - rcdc42-v2 3´UTR-reporter | | | | | | |
|---|---|---|---|---|---|---|---|
| | 24hr | 28hr | 32hr | 35hr | 40hr | 44hr | 48hr |
| +HuCsv1 | 2,192,248 | 10,315,732 | 20,840,665 | 11,613,019 | 14,615,071 | 15,010,075 | 14,591,235 |

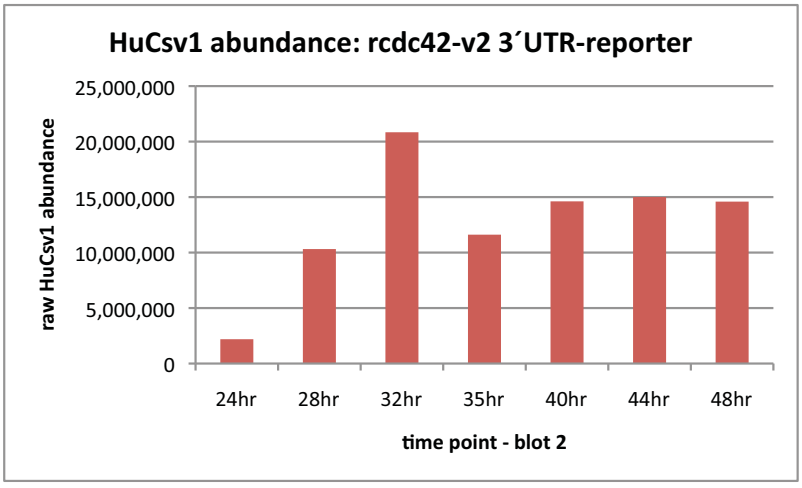


Figure 23c. Raw HuCsv1 abundances from the time course HuCsv1 overexpression experiment

Raw HuCsv1 abundance values from cells co-transfected with the rcdc42-v2 3´UTR-reporter construct and 1µg of pmHuCsv1 (+HuCsv1) and then incubated 24hr to 48hr post-transfection, prior to lysis.

i.) and ii.) represent raw HuCsv1 abundances from the first and second western blots respectively.

# Firefly luciferase-based reporter assays

## Introduction

### Dual Luciferase Assay format

The results from the fluorescence-based reporter assays suggested HuCsv1 had a negative effect on protein expression from mRNAs that contain 3′UTR sequences with putative nHu binding sites. However, this reporter assay was technically demanding, and it was difficult to achieve a high degree of reproducibility between and within experiments. Thus, it would be advantageous to develop a reporter assay that would overcome the technical challenges encountered with the fluorescence-based 3´UTR-reporter assays. The new reporter assay would be highly sensitive and would allow use of small amounts of transfected reporter plasmid (in an effort to keep a high molar ratio of nHu protein to reporter mRNA, thus ensuring nHu protein is never a limiting factor within the assay) and to enable more accurate and reproducible detection of small changes between reporter amounts and/or activities. Furthermore, the new assay would include an internal transfection control to enable reliable normalisation of reporter activity from each individual transfection and to more readily allow for direct comparison of data from different experiments. Finally, the new assay design would also minimise sample handling between transfection and data collection to reduce variation introduced by the investigator.

The Dual Luciferase Assay (Promega) is a genetic reporter system used to study eukaryotic gene expression [226]. It incorporates two distinct reporter enzymes; one from the insect *Photinus pyralis* (firefly), the other from the sea pansy *Renilla reniformis* (renilla). These luciferase enzymes catalyse the oxidation of specific substrates in a reaction that emits light. Because these two enzymes evolved independently, they utilise different enzyme substrates. As such, the abundance of both enzymes can be measured through the sequential addition of their respective substrates, in a single sample. In a given dual luciferase assay, firefly luciferase activity is measured first using its specific substrate, beetle luciferin. Once the light emission from firefly luciferase is recorded, renilla luciferase activity is measured by the addition of its substrate coelenterazine. Importantly, the coelenterazine solution rapidly quenches the first reaction, reducing firefly luciferase activity to less than 0.001% of its original activity, thus eliminating background light emission from the first measurement. Provided both luciferase substrates are in excess, the amount of luminescence given off from each oxidation reaction is linearly related

to the amount of luciferase enzyme present in the lysate over 6-7 orders of magnitude. Furthermore, Promega reports detection of luciferase activity from both reporters at amounts as low as $10^{-18}$ moles of enzyme. The linear relationship between enzyme abundance and light output, combined with the ability to detect attomolar amounts of reporter, make both luciferase enzymes highly useful for examining changes in expression of a given reporter when a highly sensitive assay is required.

### Improvements over GFP-based assay format

The Dual Luciferase Assay (DLA) addresses essentially all of the technical issues raised by the fluorescence-based reporter assay. By being significantly more sensitive, it allows for reductions in the amount of 3′UTR-reporter plasmid required in each experiment. Switching to the DLA also permits use of fewer cells per assay, meaning less transfection reagent, culture media and plasticware. Cell lysates are measured directly with no processing required, minimising variability introduced through handling and time taken to gather results. The obvious improvements in experiment throughput afforded by the DLA also mean that in principle, more 3′UTR-reporter constructs could be tested per experiment. Furthermore, all assays reported herein were conducted with a minimum of two replicate transfections. Finally, the ability to measure both the experimental reporter and an internal control reporter in the same sample, at the same time, provides the most faithful normalisation of experimental reporter presence relative to the internal control of any dual reporter method.

### A new generation of 3′UTR-reporter constructs

The move into a new assay system presented an opportunity to rethink reporter vector design. It was decided that the reporter assay system should more closely follow the data obtained from both the mouse and zebrafish nHu-CLIP data sets. As such, putative nHu target 3′UTR sequences as identified in the mouse and zebrafish nHu-CLIP experiments were used instead of the orthologous rat 3′UTR sequences used in the fluorescence-based 3′UTR-reporter vectors. This decision was not expected to affect the potential of these vectors to be used in subsequent experiments utilising cultured rat hippocampal neurons. As was the logic before, it is expected that any effect of neuronal Hu proteins on target 3′UTR-reporters would be conserved across different vertebrate species. The only perceived trade off in using a luciferase-based, rather than GFP-based reporter protein, was losing the capacity to observe potential differences in localised mRNA translation in unfixed, living cells. However, this could readily be addressed by reverting to the fluorescence-based reporter system, if deemed necessary.

Significantly, the vast improvement in assay efficiency prompted an increase in the number of 3′UTR s examined. Shown in table 3 are the 3′UTR sequences that were cloned into the vector pCI-FL immediately downstream of the stop codon in the firefly luciferase ORF, and upstream of the vector's SV-40-derived polyadenylation signal (see figure 24 for the vector description and map). For each cloned 3′UTR segment, the oligonucleotide sequences used to clone each 3′ UTR are shown, along with the identity of the restriction enzyme used to prepare the molecule for insertion into pFL-CMV. The position of the restriction site within the pCI-FL vector after ligation is included.

***3′UTR sequences tested in the firefly luciferase-based reporter system***

Figure 26 contains schematic representations of all seven putative target 3′UTR sequences cloned for use in the firefly luciferase-based reporter assays. The 3′UTR sequences are numbered such that the first nucleotide of the cloned sequence is labelled '1'. In a number of cases, the cloned 3′UTR segment contains a small remnant of the original message's ORF; these are indicated in grey in the schematics. Also shown are the relative positions of nHu-CLIP tag locations within the cloned segments (green boxes), along with the locations of all predicted polyadenylation sites (that is, pA sites supported by EST data).

One can see from the data in figure 26 that nHu CLIP-tags mapped to the 3′UTRs of both mouse and zebrafish *cofilin1* mRNA. These data support the idea that interactions between nHu proteins and target mRNA sequences would be conserved across different species. As a means of testing this idea, the orthologous 3′UTR sequences for the mouse and zebrafish *cdc42* mRNA were both cloned into the pCI-FL reporter vector. As stated in the Introduction, CLIP-tags corresponding to both alternative 3′UTR sequences of the alternatively spliced cdc42 mRNA were identified in the 4hpf and 24hpf zebrafish CLIP experiments. In the 24hpf CLIP experiment, a single CLIP tag was identified in the proximal 3′UTR (zfcdc42-v2), while in the 4hpf experiment, one CLIP tag matched the distal 3′UTR (zfcdc42-v1) (figure 7d). Both orthologous mRNA sequences are found in mouse and while neither 3′UTR was identified as a target for nHu proteins in the P4 mouse CLIP experiment, the 3′UTR sequences of both cdc42 splice variants were also cloned (denoted as mcdc42-v1 and mcdc42-v2). Finally, the *vasp* 3′UTR was identified as a potential nHu target sequence in the 24hpf zebrafish CLIP experiment. VASP or VAsodilator Stimulated Phosphoprotein is another factor known to be involved in modulating cytoskeletal dynamics and has been shown to be involved to axonogenesis [199].

All 3′UTRs incorporated into the firefly luciferase-based reporter plasmids were cloned using genomic DNA as a template. Primers were designed to amplify the complete 3′UTR sequence as judged from available EST data from the UCSC genome database. Importantly, the use of genomic DNA as the template allowed for incorporation of the complete terminal polyadenylation signal, including the 5′ hexanucleotide sequence, the cleavage site itself and the downstream uracil-rich element. This aspect of 3′UTR biology had been ignored in the original GFP-based 3′UTR reporters, which were cloned from cDNA templates and thus only include the 5′ hexanucleotide and cleavage site. Thus, the fluorescence-based reporters relied upon a vector encoded SV40 late polyadenylation element for proper 3′-end processing. The new cloning strategy resulted in each reporter having at least two polyadenylation sites: (at least) one from the cloned 3′UTR segment itself, and one encoded by the pCI-FL vector (the SV40 late polyadenylation signal), the pA cleavage site of which is found ~130nt downstream of the end of each cloned 3′UTR sequence. At the time, the presence of this additional vector encoded SV40 late polyadenylation signal was not given much consideration. This was mainly because it was expected that the 3′UTR-encoded pA signal would assume the role of directing cleavage and polyadenylation at the end of the reporter mRNA.

***"Non-target" negative-control 3′UTR-reporters***

The firefly luciferase-based reporter vector was made by exchanging the d2EGFP coding sequence in the pCI vector, for a firefly luciferase coding sequence (figure 24). The firefly luciferase coding sequence was sub-cloned from pGL3 (Promega) into the pCI (Clontech) multiple cloning site (see materials and methods). The firefly luciferase reporter protein has a half-life of approximately 3hrs [227], which is comparable to the approximately 2hr half-life of d2EGFP.

Two negative control vectors were generated for creating a non-target reporter mRNA sequences (figure 26). The first control vector used was the pCI-FL vector itself with no added 3′UTR sequence. This vector contains approximately 180nt of vector encoded untranslated sequence after the luciferase stop codon and before the SV40 late polyadenylation cleavage site. In the experiments presented herein, this vector is known as "control 3′UTR ". The second control vector, includes 140nt of the Xenopus β-globin 3′UTR (see materials and methods for cloning strategy). This vector is known as "Xβ-globin". Notably, the Xβ-globin vector was introduced later in the assay process and thus, does not feature in all data sets. Finally, the internal control vector used in these assays was the phRL_CMV vector (Promega), encoding

renilla luciferase (figure 25). This vector is essentially identical to the control 3′UTR reporter vector apart from the encoded reporter protein.

## Preliminary experiments:

### Basic experimental setup:

1. Firefly luciferase 3´UTR-reporter vector containing a CLIP-identified 3´UTR (figure 24)
2. Renilla luciferase internal control vector (figure 25)
3. Co-transfect both vectors into cells +/- pmHuCsv1 plasmid
4. Lyse cells and conduct dual luciferase assay. Normalise firefly luciferase activity to renilla luciferase activity. Each was condition conducted in triplicate. Normalised firefly luciferase activity averaged from three replicates constitutes one data point.

### Experimenting with assay parameters for 3'UTR-reporter assays

Once a set of firefly and renilla luciferase constructs are designed and constructed, there are only a few key variables within the dual luciferase assay that can be manipulated by the investigator. Three of these variables are: the amount of luciferase vectors used in a transfection, the amount of lysate, and the amount of luciferase substrate reagents required to accurately determine luciferase activity. These three parameters were tested in a series of pilot experiments. In the first pilot experiment, a range of firefly and renilla luciferase vector amounts were transfected to determine how much luciferase activity would be seen for a given amount of luciferase vector. With this information in hand, a second pilot experiment was carried out in which the amounts of sample lysate and luciferase assay reagent were varied, with the goal to ensure that within each sample, the amount of luciferase activity detected was directly proportional to luciferase reporter abundance.

***Testing amounts of reporter vector –***

As a starting point to testing the amount of luciferase activity for a given amount of luciferase vector, combinations of the control 3'UTR firefly luciferase vector ("control 3´UTR") and renilla luciferase transfection control vector (phRL-CMV) were co-transfected into 293T cells. Having never tested the vectors before, a small-scale experiment was performed using a relatively close series of different vector amounts spanning a range of amounts commonly reported in luciferase assays. In this experiment, 25ng, 50ng, 75ng and 100ng of the firefly vector were tested in combination with 10ng, 30ng or 50ng of the renilla vector. Notably, the amounts of firefly luciferase 3´UTR-reporter vector tested here are 3-10x lower than those used for the fluorescence-based 3´UTR-reporter vectors used for the fluorescence-based reporter assays. 293T cells were plated in 6 well plates to approximately 50% confluence and transfected the following day. The total amount of DNA transfected was brought up to 1µg using the

pcDNA3myc vector and complexed with 3µL of FuGENE. Cells were left for ~18hr prior to lysis with 500µL of Passive Lysis Buffer (PLB) per well. For the dual luciferase assay, 20µL of lysate was used with 100µL each of the luciferase assay reagents, Luciferase Assay Reagent II (LARII) and Stop and Glow (S&G).

The data for this first pilot experiment are shown in figure 27a and 27b. They show that high amounts of light output were detectable even at the lowest amounts of firefly and renilla luciferase vector tested (figure 27). Using the firefly luciferase vector at 100ng yielded $1.1x10^9$ relative light units (RLUs), which is essentially at the upper limit of the detectible range for the Glomax® 96 Microplate Luminometer used to detect luciferase activity in these assays. Reducing the amount of vector used in 25ng increments produced a near linear reduction in RLU output with the lowest amount of vector tested, 25ng, giving $2.9x10^8$ (figure 27a), still a very high reading. The renilla luciferase vector gave much more signal than firefly vector comparing weight to weight. For example, samples from cells co-transfected with 50ng of renilla luciferase vector had an average renilla luciferase activity of $3.5x10^9$ RLUs (figure 27b). Comparatively, the average activity for 50ng of the firefly luciferase vector was only $4.5x10^8$ RLUs. This is can partly be attributed to the fact that the renilla vector is smaller that the firefly vector (4.1kb vs 5.7kb). When considered in terms of number of molecules of vector, this equates to 13.5fmol of the firefly vector compared to 18.7fmol of the renilla vector, when 50ng of either vector is used. However, in this assay, light output from renilla luciferase almost 9-fold higher than firefly luciferase, indicating that in general renilla luciferase is significantly more active than firefly luciferase.

From the light outputs detected from the firefly and renilla luciferase vector amounts tested in this pilot assay, it appeared that the lowest amount of control 3´UTR-reporter vector tested (25ng) would provide ample signal for detection of firefly luciferase production from the 3´UTR-reporter mRNA. This amount of reporter vector equated to a >10-fold reduction in reporter vector used (per transfection) relative to the fluorescence-based reporter assay system. Furthermore, given the Glomax® 96 luminometer has a linear range of detection from $10^1$-$10^9$ relative light units (RLUs) the amount of 3´UTR-reporter vector co-transfected could <u>in principle</u> be reduced several orders of magnitude (from 25ng) if it appeared in subsequent tests that reporter activity was not responsive to HuCsv1 (*for instance*, if a molar excess of HuCsv1 protein to 3´UTR-reporter mRNA was not being achieved). Importantly, Promega recommend using a high firefly luciferase to renilla luciferase reporter vector ratio (in the order of 25-1; weight-to-

weight, firefly – renilla) to avoid variation in luciferase activities caused by promoter competition between the two vectors. Given luciferase activity appeared to be linearly related to the amount of reporter vector transfected, it was decided that the next optimisation stage would use 1ng of the renilla luciferase control vector. This was expected to produce an ~10-fold reduction in the amount of renilla luciferase activity relative to the 10ng condition tested, which would result in ~5x$10^7$ RLUs for the renilla luciferase control reporter.

***Comparing firefly luciferase activity of different 3'UTR-reporters***

The next experiment tested firefly luciferase activity for all of the experimental 3′UTR-reporters generated, using 25ng of each 3′UTR-reporter vector and 1ng of the renilla internal control vector. This experiment would demonstrate that the reporter constructs were working and indicate whether the conditions roughly defined using the control 3′UTR-reporter in the previous experiment would be suitable for all 3′UTR reporter vectors to be tested. In these assays, the amount of 3′UTR-reporter vector used was set to 6.25fmol (~25ng) and co-transfected with 1ng of the renilla vector, with the total amount of DNA co-transfected made up to 1µg with empty pcDNA3myc vector. Because of the high sensitivity of the luciferase assay, a set molar amount of firefly luciferase vector was used to help eliminate differences in reporter activity occurring simply because of slight differences in the number of vector molecules transfected. 293T cells were plated, transfected and harvested as before.

Analysis of luciferase activity from these lysates was initially different to the previous experiment. Specifically, it was suggested by several colleagues that the amount of LARII and S&G reagents used per assay could be reduced from 100µL to 50µL, without changing the amount of lysate tested, and still yield accurate measurements of luciferase activity. The benefit of reducing the amount of reagents used per assay was that it would increase the number of reactions that could be performed per assay kit, a desirable outcome given the cost of each DLA kit. Thus, in the first batch of measurements for this experiment, 50µL of each LARII and S&G reagents was used for analysis of 20µL of lysate in each assay.

The results from this experiment shown in figure 28, indicated that all eight firefly luciferase reporter vectors to be tested encoded functional firefly luciferase and that the normalised activities of firefly luciferase from each of these vectors were similar, differing by no more than ~2.5-fold (figure 28c). Interestingly though, the observed activity of both firefly and renilla luciferase in the 293T lysates from this experiment were lower than expected based on the previous experiment (figure 28). For the control 3′UTR-reporter, firefly luciferase activity was

over 7-fold lower (figure 28a) and renilla activity, which based on the previous experiment was expected to reach approximately 4-5x$10^7$ RLUs, was quite consistently around 3-fold lower than that (figure 28b). One possible explanation for the results in this experiment was that by reducing the amount of reagents used, the luciferase substrates were being exhausted, resulting in less observed light output. To test this possibility and look at the relationship between lysate amount and luciferase activity for a given amount of reagent, the luciferase assay was repeated using three different amounts of the VASP 3′UTR-reporter lysate, with three different amounts of LARII and S&G reagent.

***Testing the amount of lysate/reagents required to obtain accurate luciferase signal***

In this experiment, 5µL 10µL and 20µL of the VASP 3′UTR-reporter lysate from the previous assay were tested with 25µL, 50µL or 75µL of the LARII and S&G reagents (figure 29).

Looking first at the firefly luciferase activities (figure 29a), 25µL of reagent (LARII and S&G) is insufficient for accurately determining firefly luciferase activity in any of the samples. As lysate volume increases only a small increase in RLUs is detected. Furthermore, at all lysate volumes tested, using more of the DLA reagents (50µL and 75µL) resulted in more light output. Fitting a linear regression line to the three data points indicates that the increase in RLUs observed for each lysate volume tested with 25µL of reagents is not linear. These observations indicated that when only 25µL of the dual luciferase assay reagents were used, maximum activation of firefly luciferase within all samples tested was not achieved.

Using 50µL of reagent yields almost the same amount of signal (RLUs) as using 75µL of reagent when applied to 5µL of lysate, indicating that at this volume of lysate, 50µL of reagent is able to fully activate luciferase activity. Fitting a linear regression line to these three data points suggests the increase in light emitted as lysate volume increases using 50µL of reagent is close to linear up to 20µL of lysate ($R^2$ = 0.987). However, looking at the raw RLU values, it is clear the amount of light emitted at 20µL of lysate is not quite double that seen for 10µL of lysate, indicating 50µL of reagent is most likely the very minimum amount of reagent required for this particular reporter (VASP 3′UTR) and thus, is likely not a robust enough amount of reagent to use for subsequent tests.

Indeed, the best-behaved results in terms of the regression analysis are seen when 75µL of reagent is used. In these assays, as sample volume doubles, so does the amount of luciferase activity detected indicating a linear relationship exists between sample volume and light

produced at all sample volumes tested. This is further supported by the calculated linear regression value for these data points ($R^2$ = 0.9996), which is very close to 1.

However, the results for firefly luciferase activity using greater volumes of reagent do not immediately support the idea that exhaustion of the luciferin substrate is the cause of reduced activity. If substrate exhaustion were the cause, then for 50µL of reagent, 10µL of lysate would be expected to exhaust the available substrate, an effect not seen in these tests. In subsequent correspondence with a specialist technician for the Glomax® 96 luminometer from Promega, it was suggested that as well as providing sufficient substrate, greater volumes of LARII and S&G ensure thorough and more consistent mixing of lysate and reagent at the time of reagent injection (Teresa Lyons, Promega *pers comm*.). Because complete mixing of lysate and reagent is solely dependent on reagent injection, it is critical to inject a volume of reagent great enough to cause rapid and even dilution of the lysate into the reagent solution. As such, incomplete or inconsistent mixing of lysate and reagents is a likely explanation for the lower firefly luciferase activity results observed using 25µL of reagent. It was noted that Promega had anecdotal evidence that supported the use of lower amounts of reagent, but that this was largely dependent on specific reporter activity levels in each assay and also subject to constraint imposed by the requirement for complete mixing (Teresa Lyons, Promega *pers comm*.).

This idea is supported when looking at the renilla luciferase activity results (figure 29b). Despite the 17-fold molar difference in vector amount between firefly and renilla luciferase reporters, the behaviour of renilla luciferase in these assays is almost exactly the same as for firefly luciferase. As seen in the firefly luciferase data, when only 25µL of each reagent is used maximum renilla luciferase activity is not observed. Using 25µL of reagent, the amount of light emitted for each lysate does not double as lysate volumes double and the calculated linear regression for these values does not indicate light output is linearly related to lysate volume ($R^2$ = 0.827). However, using 50µL and 75µL of reagent, increases in sample volume correlate well with increased renilla luciferase activity, indicating a linear relationship between lysate amount and light output in both cases and when 75µL of reagent is used the linear regression calculated indicates a strong linear relationship between light output and lysate volume ($R^2$ = 0.998). Assuming that LARII and S&G contain equal molar amounts of firefly and renilla luciferase substrate, substrate exhaustion would not be expected to be the cause of the similarity in enzyme behaviour, given the 17-fold molar difference in reporter vectors. Accordingly,

incomplete mixing of lysate and reagents better explains the difference in reporter activity seen using lower volumes of reagent.

From this set of experiments, it was concluded that 75µL of the LARII and S&G reagents is sufficient to accurately determine luciferase activity for both enzymes in a lysate volume of 10µL. Finally, in the original for this transfection, the VASP reporter was previously found to produce comparatively high firefly luciferase activity among the reporter vectors to be tested. Thus, the combination of lysate volume and reagent volume identified in these optimisations was expected to be robust enough to accurately assay all the reporters to be tested using this assay.

## Results:

### Assaying for an effect of HuCsv1 on firefly luciferase expression from CLIP-identified 3'UTR-reporter mRNAs

With transfection conditions optimised for the 293T cell line, a series of experiments were carried out in which firefly luciferase expression from CLIP-identified and control 3'UTR-reporter mRNAs was examined in the presence or absence of HuCsv1. In these experiments, cells were plated in 12-well plates to reduce the amount of consumables required. The transition to a 12-well plate format led to a 2.5-fold reduction in the total amount of reporter vector used, in line with the approximately 2.5-fold reduction in surface area in a 12-well plate compared to a 6-well plate and in line with the transfection condition recommendations for the FuGENE 6 transfection reagent (Roche). As such, 2.5fmol of the 3'UTR reporter vectors was co-transfected with 400pg of the renilla control. The total amount of DNA added was made up to 500ng with either the pmHuCsv1 vector encoding HuCsv1 or the empty pcDNA3myc vector, in line with the recommended amount of total DNA for transfection according the FuGENE6 product specifications (Roche). Approximately 18hrs post-transfection cells were lysed in PLB according to the manufacturers instructions and luciferase activity from 10µL of lysate determined by DLA using 75µL of reagent (each) in the Glomax® 96 Microplate Luminometer (Promega).

Two additional cell lines were introduced at this point. Neuro-2a cells were selected because of their reported ease of transfection (ATCC – http://www.atcc.org, Roche - http://www.roche-applied-science.com/sis/transfection/index.jsp) and neuronal cell-like characteristics. Other neuronal-like cell lines such as P19 and PC12 cells were also tested, but found to be too difficult to transfect with high efficiency using the FuGENE6-based transfection conditions optimised for

293T cells (*data not shown*). HeLa cells were also tested because other experiments being conducted in the lab at that time to examine nHu subcellular localisation were utilising this cell line. The transfection conditions defined for 293T cells were directly applied to both the Neuro-2a and HeLa cell lines. It was expected and subsequently confirmed that the luciferase activity for both HeLa and Neuro-2a cell line experiments would be similar to that seen when employing 293T cells, although in both cases luciferase activity levels are typically lower, a result presumed to correspond to differences in the overall transfectability of these cell lines relative to 293T cells. For all cell lines tested, the averaged firefly luciferase activities (normalised to renilla luciferase), collected from at least three independent experiments are presented. Statistical significance was tested using a 2-tailed, unpaired homoschedastic student's t-test, *p*-values less than 0.01 were considered to indicate statistically significant differences between the two conditions (+/- HuCsv1).

## Testing for effects of HuCsv1 on 3'UTR-reporter activity – 293T cells

Four independent dual luciferase assays were conducted in 293T cells to test the effect of HuCsv1 on 3'UTR-reporter expression (see figure 30a-c). Each 3´UTR-reporter was co-transfected with the internal-control renilla luciferase reporter (phRL_CMV) along with either 500ng of pmHuCsv1 or "empty" pcDNA3 vector. In each case, the activities of both the firefly and renilla reporter enzymes were measured, and firefly luciferase activity normalised to that of renilla luciferase activities. Per experiment, every 3´UTR-reporter condition (*ie* + or – HuCsv1) was done in triplicate. For each assay (within the triplicate) firefly luciferase activity was normalised to renilla luciferase activity. These ratios were then averaged to produce a single normalised firefly luciferase activity value per condition, per experiment. The average of these values (*ie* n=4, from for separate experiments) are presented in figure 30a (as "Normalised firefly activity"). Error bars in the graph represent the standard deviation of these averages. The raw firefly and renilla luciferase activity data presented in Figure 30b (raw firefly luciferase activity) and Figure 30c (raw renilla luciferase activity) was treated in the same way but is not normalised. Finally, normalized firefly activities in the presence of HuCsv1 relative to that in the absence of HuCsv1 were expressed as a ratio (figure 30a – **[FL/RL (+HuCsv1)]/[FL/RL (-HuCsv1)]**), such that values above one would indicate increased reporter activity in the presence of HuCsv1, while values below one would indicate lower reporter activity when HuCsv1 is expressed.

***Raw firefly and renilla luciferase activity values***

The averaged raw renilla and firefly luciferase activities (figures 30b and 30c) from four independent experimental repeats indicate some potential general effects of HuCsv1 on expression of both reporter proteins. Each individual transfection contains an identical amount of renilla luciferase expression plasmid. Despite this, it is clear from the raw data in figure 30c that there is an approximately 30% reduction in renilla activity in the presence of HuCsv1. The magnitude of this reduction is quite consistent in each different transfection (+/- 4.5%). Looking at the raw firefly data (figure 30b), luciferase activity appears to diminish in the presence of HuCsv1 for all seven CLIP-identified 3´UTR-reporters as well as for the two "non-target" control reporters. With the exception of the zfcdc42-v2 3′UTR-reporter, the magnitude of the reductions in activity seen in raw renilla luciferase reporter activity in the presence of HuCsv1, are similar to those seen in the raw firefly luciferase activity data.

***Normalised firefly luciferase activity***

Averaged, normalised firefly luciferase activity from four independent experimental repeats agreed with initial optimisation experiments testing 3′UTR-reporter activity (figure 30a). Normalised firefly luciferase activities from all seven putative target 3′UTR-reporters were 2- to 3-fold higher than that of the two control reporters. However, with the exception of the zfcdc42-v2 3′UTR-reporter, co-expression with HuCsv1 did not significantly alter the normalised firefly luciferase activity of any of the nHu CLIP-identified target 3′UTR-reporters, as shown by the firefly luciferase activity ratios being very close to 1.00 (figure 30a). Interestingly, the zfcdc42-v2 3′UTR-reporter displayed a 33% increase in normalised firefly luciferase activity in the presence of HuCsv1. This effect was found to be statistically significant with a *p*-value of $p<0.001$ as measured by Student's t-test (figure 30a). However, the biological interpretation of this "increase" in normalised firefly luciferase activity from the zfcdc42-v2 3´UTR-reporter in the presence of HuCsv1 is unclear. Specifically, the increase in normalised firefly luciferase activity is actually due to the lack of reduction in raw firefly luciferase activity (in the presence of HuCsv1) for the zfcdc42-v2 3´UTR-reporter that was observed for every other luciferase vector (both firefly and renilla) (figure 30b and c)

## Testing for effects of HuCsv1 on 3′UTR-reporter activity – HeLa cells

Three independent replicate experiments, using identical transfection and analysis conditions as described above for 293T cells, were also conducted in HeLa cells using the seven 3′UTR-

reporter constructs and the pCI-FL "non-target" control 3′UTR-reporter (figures 5a-c) (NOTE: *the Xβ-globin 3'UTR-control reporter was not tested*).

***Raw firefly and renilla luciferase activity values***

Raw renilla and firefly luciferase activities for each reporter were significantly lower than seen for identically transfected amounts of plasmid in 293T cells. Comparison of renilla luciferase activity between HeLa and 293T cells is most informative for this difference, as in this case the only variable in the comparison is the cell line itself. In the absence of HuCsv1, averaged renilla luciferase activity in HeLa cells was 7-fold lower than in 293T cells (compare figure 30c with 31c). Averaged firefly luciferase activity for each of the 3′UTR-reporters was also greatly reduced in HeLa cells (compare figure 30b with 31b). However, the difference in activity between cell lines was somewhat dependent on the 3′UTR sequence involved ranging from 30 to 60-fold depending on which 3′UTR-reporter is compared. While the differences in raw renilla and firefly luciferase activities likely indicates differences in transfection efficiency between the two cell lines, it is curious that firefly luciferase activity is so much more greatly reduced in HeLa cells, compared to 293T cells. This may indicate some difference in the efficiency of expression, processing or general stability of this reporter mRNA or protein in HeLa cells compared to 293T cells.

This diminished activity was accompanied by somewhat larger variation in the replicate data, when compared to the 293T data set. There are a number of possible contributing factors to this variation including; differences in transfection efficiency between replicates and differences in cell density between replicates at the time of lysate collection.

In general, addition of HuCsv1 again showed a general repressive effect on both renilla and luciferase reporter activity (figure 31b & 31c). Renilla luciferase reporter activity in the presence of HuCsv1 was approximately 55% of that seen in cells lacking HuCsv1 (figure 31c). For individual firefly luciferase reporter activity, values ranged from a reduction of about 55% for the control sequence to around 70% for the VASP reporter when co-expressed with HuCsv1 (figure 31b).

***Normalised firefly luciferase activity***

However, unlike the 293T data, a statistically significant reduction in normalised firefly luciferase expression was observed for a number of 3′UTR-reporters in the presence of HuCsv1 (figure 31a). Importantly, no difference in normalised firefly luciferase activity was observed for

the control 3′UTR-reporter. Reductions in firefly luciferase activity from the zfcdc42-v2 (1.4-fold reduction) and VASP (1.8-fold reduction) 3′UTR-reporters were most the significant, with *p*-values of $p<0.002$ and $p<0.004$, respectively. Normalised firefly luciferase expression was also noticeably reduced for the zfCofilin (1.3-fold reduction), zfcdc42-v1 (1.4-fold reduction) and mcdc42-v1 (1.4-fold reduction) 3′UTR-reporters, however the *p*-values for these changes did not reach the $p<0.01$ threshold for statistical significance imposed ($p<0.028$, $p<0.043$ and $p<0.047$, respectively).

Importantly, despite the greater variation in raw firefly and renilla luciferase activities observed between replicate experiments from HeLa cells, normalised firefly luciferase activity was relatively consistent between experiments (*see standard deviations of normalised firefly luciferase activity values in figure 31a*). This result supports the idea that differences in raw activity levels between replicate experiments reflect differences abundance of the reporters in the presence AND absence of HuCsv1, possibly caused by general differences in transfection efficiency or cell density.

## Testing for effects of HuCsv1 on 3′UTR-reporter activity – Neuro-2a cells

Next, Neuro-2a (N2A) cells were employed as the cell line for an identical set of luciferase reporter transfections and assays (figure 32a-c).

***Raw firefly and renilla luciferase activity values***

Similarly to the reporter assay data set from HeLa cells, large differences in measured luciferase activities were observed between the four Neuro-2a experimental replicates. As for the HeLa cell data set, this was thought to have occurred through differences in cell density and/or transfection efficiency. Importantly though, within experiments raw renilla luciferase activity values were reasonably consistent. This was shown by calculating the difference in raw renilla luciferase values for each 3′UTR-reporter transfection compared to the raw renilla luciferase activity for the control 3′UTR-reporter (-HuCsv1 condition) and then calculating the average and standard deviation of these values across the four experimental replicates (figure 32d). This correction indicates that while large differences in raw renilla luciferase values between experiments were apparent (see error bars in figure 32c) across experiments; relative amounts of renilla luciferase activity were reasonably close (tighter error bars in figure 32d top graph). Importantly, taking the average of these differences in renilla luciferase activity (relative to control) for the (+HuCsv1) condition and the (-HuCsv1) condition, a significant reduction in

renilla luciferase activity is observed in cells co-transfected with HuCsv1 (approximately 30% reduction - $p<6 \times 10^{-10}$) (figure 32d bottom graph).

Interestingly, carrying out the same correction for the raw firefly luciferase activity values as presented for the renilla luciferase activities, averaged raw firefly luciferase activity from the control 3´UTR-reporter, in the presence of HuCsv1, did not show the same 30% reduction as seen for renilla luciferase activity (figure 32b bottom graph). In this case, the averaged difference in raw firefly luciferase activity for the control 3´UTR-reporter in the presence of HuCsv1 was only 5% lower compared to in the absence of HuCsv1 (figure 32b bottom graph). Consequently, in the presence of HuCsv1, the normalised firefly luciferase activity values indicate a small "increase" in firefly luciferase activity from the "non-target" control 3´UTR-reporter (presented below).

***Normalised firefly luciferase activity***

The normalised firefly luciferase activity of four independent Neuro-2a reporter assays showed a far more striking effect of HuCsv1 on several putative target 3′UTR-reporters, compared to the 293T and HeLa reporter assays (figure 32a). The VASP 3′UTR and both zebrafish cdc42 3′UTR-reporters showed a reduction in firefly luciferase expression that was highly significant. The greatest and most significant effect was seen on zfcdc42-v1 with a 1.8-fold decrease in normalised firefly luciferase activity ($p<8.4 \times 10^{-5}$). Next, the 3′UTR-reporters for VASP and zfcdc42-v2 both showed ~1.65-fold decreases in firefly luciferase activity in the presence of HuCsv1 ($p<0.0013$ and 0.0021 respectively). Expression of the mcdc42-v1 3′UTR-reporter was reduced by 1.54-fold ($p<0.0027$) while the mcdc42-v2 3′UTR-reporter was reduced by 1.38-fold. However, the calculated $p$-value for mcdc42-v2 of $p<0.029$, was higher than the chosen cut off of $p<0.01$. Interestingly, neither the mouse nor zebrafish cofilin 3′UTR-reporters, showed a statistically significant effect of HuCsv1 on their expression.

However, unexpectedly, normalised firefly luciferase activity from the "non-target" control 3′UTR-reporter was 1.3-fold higher in cells co-transfected with HuCsv1. Although this increase was small, it was found to be close to statistical significance with a $p$-value of 0.0355. Furthermore, the Xβ-globin 3´UTR-reporter showed an even greater increase in expression in the presence of HuCsv1 with normalised firefly luciferase expression increased by 1.9-fold. Notably, the Xβ-globin reporter was only tested in the final luciferase assay conducted, precluding any statistical analysis of this increase. Nevertheless, the effect is consistent with the observation for the control 3′UTR-reporter. Importantly, as was shown for the zfcdc42-v2

3′UTR-reporter results from the 293T transfections, the "increase" in normalised firefly luciferase activity for both of these "non-target" control reporters is actually due to a lack of reduction in raw firefly luciferase activity in the presence of HuCsv1, in a background of reduced renilla luciferase activity.

## Discussion of overall results from luciferase data

### General discussion

From a purely analytical perspective, the benefits of moving to a dual luciferase-based reporter format are obvious. While the overall experimental design is unchanged, the reduction in time and handling between sample preparation and sample analysis, combined with the sensitivity of the assay allowed for a significant increase in the number of constructs that could be tested as well as the amount of data that could be obtained per assay. Furthermore, through reducing handling steps and automating data collection, variation between experiments is also much lower, as evidenced by the standard deviations of averaged normalised firefly luciferase activities. This allowed for straightforward and direct comparison between independent experimental repeats.

### Effects of HuCsv1 on putative target 3′UTRs

The expression of firefly luciferase from several of the 3′UTR-reporters used in these experiments appeared to be influenced by co-expression with HuCsv1. In particular, the zebrafish cdc42-v2 3′UTR-reporter (zfcdc42-v2) was affected in all cell lines tested. Interestingly, while normalised firefly luciferase activity from this reporter was significantly reduced by co-expression with HuCsv1 in both Neuro-2a and HeLa cell lines (figures 31 and 32), no reduction was observed in 293T cells (figure 30a). Instead, an increase in normalised firefly luciferase was seen. Importantly, the observed "increase" in normalised firefly luciferase activity was not specifically indicative of increased raw firefly luciferase activity (compared to the –HuCsv1 condition), rather a lack of reduction in raw firefly luciferase activity that was generally seen for all reporters (including renilla luciferase) in all cell lines tested. A similar phenomenon was observed in Neuro-2a cells co-expressing HuCsv1 with the "non-target" control 3′UTR and Xβ-globin 3′UTR-reporters. While the small "increase" in normalised firefly luciferase activity seen for the control 3′UTR-reporter was not deemed statistically significant (based on the $p<0.01$ threshold), it was largely consistent and reproducible in the four experiments conducted. The unexpected effect of HuCsv1 on firefly luciferase activity for the control 3′UTR-reporters in

Neuro-2a cells potentially hinted at a 3′UTR-independent effect of HuCsv1 in these reporter assays that could confound any data obtained for the candidate target 3′UTR-reporters.

### Differences in raw luciferase activity values between + and – HuCsv1 conditions

Strikingly, in all cell lines tested, raw luciferase activity (both firefly and renilla) was consistently lower in cells co-expressing HuCsv1 compared to cells lacking HuCsv1 (-HuCsv1). The extent of this reduction varied between the different cell lines. In 293T cells, renilla luciferase activity was on average 30% lower in cells co-transfected with HuCsv1 (figure 30c). Likewise, averaged expression of the control 3′UTR and Xβ-globin 3′UTR-reporters was approximately 20% lower when co-transfected with HuCsv1 (figure 30b). In HeLa cells, renilla luciferase expression was 45% lower in cells co-transfected with HuCsv1 (figure 31c), while firefly luciferase activity from the control 3′UTR-reporter was 55% lower (figure 31b). Finally in Neuro-2a cells, renilla luciferase activity was on average 30% lower in cells co-transfected with HuCsv1 (figure 32d). Interestingly in this cell line, firefly luciferase activity from the control 3′UTR-reporter was essentially unchanged in the presence of HuCsv1 (figure 32b).

Because the reductions in firefly and renilla luciferase activity observed in cell co-expressing HuCsv1 (compared to –HuCsv1) were generally comparable this effect was initially considered to reflecting some difference in transfection efficiency between the + and – HuCsv1 conditions. However, upon comparing the data from the three cell lines tested as a whole, an idea emerged that the reductions in raw luciferase activity seen in cells co-transfected with HuCsv1 may actually be caused by a 3′UTR-independent effect of HuCsv1 on expression of both renilla and firefly luciferase. As a step towards addressing this possibility, it was decided that measuring mRNA abundance in each transfection condition (as well as luciferase activity) would provide insight into whether the observed differences in raw luciferase activity were the result of differences in transfection efficiency (and hence differences in luciferase mRNA abundance), or the manifestation of a 3′UTR-independent HuCsv1 effect in these assays.

### Taking the data from the firefly luciferase 3′UTR-reporter assays further

A number of possibilities could explain the effect of HuCsv1 on putative target 3′UTR-reporters observed in the dual luciferase assays. The most tempting possibility was that HuCsv1 was repressing target 3′UTR-reporter translation through an interaction within the CLIP-identified 3′UTR sequence. However, it was also possible that HuCsv1 was having an effect on the abundance or processing of the reporter mRNAs that resulted in a reduction in the amount of reporter protein produced per message. The most efficient way to look at all of these

possibilities was to carry out Northern analysis of mRNAs from cells co-transfected as before and look for changes in mRNA abundance or processing in the presence of HuCsv1 compared to in it's absence. Furthermore, in enabling quantification of mRNA abundance for each 3´UTR-reporter, Northern analysis would allow for determination of whether the changes in reporter protein expression observed for specific 3´UTR-reporters, were due to altered translation efficiency of reporter mRNA rather than mRNA abundance. This would be possible by normalising luciferase enzyme activity (a direct readout of reporter protein abundance) to the amount of reporter mRNA present in lysates (as determined by digital quantification of band intensities from a Northern). If altered translation efficiency of the reporter message were the cause of the reductions in reporter activity seen in the dual luciferase assays, then reductions in luciferase activity for a given 3'UTR-reporter would be greater than any reduction in reporter mRNA amount in cells co-transfected with HuCsv1. In this scenario, normalisation of firefly luciferase reporter to mRNA amounts would show lower reporter luciferase activity in the presence of HuCsv1. Conversely, if a reduction in the abundance of the reporter mRNA is the cause of reduced reporter protein expression, then normalisation to mRNA amounts would yield reporter luciferase activities that were approximately equal between cells co-transfected with or with HuCsv1.

## Analysis of 3´UTR-reporter mRNA expression by Northern blot

***Determining reporter mRNA abundance***

Calculating the translation efficiency of 3´UTR-reporter mRNAs relies on quantification of both reporter protein and 3´UTR-reporter mRNA abundance. To perform quantification of 3´UTR-reporter mRNA abundance, total RNA from cells co-transfected with pmHuCsv1 or pcDNA3 for each 3′UTR-reporter was collected and analysed by Northern blot, using randomly primed, radiolabelled DNA probes. For these Northerns, probes were made to detect the firefly and renilla luciferase coding sequences, as well as the endogenous transcript for GAPDH, for use as a Northern loading control. Northern blot was chosen because it is a highly sensitive and quantitative technique. Furthermore, because it provides a visual analysis of reporter mRNA, changes in mRNA abundance or processing events (such as alternative polyadenylation) can be observed directly. Northern analysis also eliminates the possibility of confounding effects from contaminating plasmid DNA, which could distort the results from RT-PCR-based techniques. This last point was considered important as the intron contained in the two reporter vectors is at the very 5´-end of the reporter mRNA, and as such, RT-PCR products that span the intronic sequence to distinguish cDNA products from plasmid contaminants may not be informative about whether the actual product is of the correct size to be from a complete mRNA. In the case where mRNA stability is affected, this could be a considerable problem.

Reporter mRNA abundance of each 3′UTR-reporter was determined from Northerns using the image analysis tool, ImageJ, a freely distributed program created by the National Institutes of Health [228]. As a first step, the background signal within each Northern blot was digitally subtracted using the rolling ball algorithm used by the ImageJ software [229] with a ball radius of 25 pixels. Following background subtraction, the minimum area required to surround each of the mRNA bands for a given 3′UTR-reporter was determined. This area is called the *measurement field.* This area was kept constant for all of the bands of a given 3′UTR-reporter. The measurement field was then placed around each mRNA band and the *integrated density* of each field was measured. The integrated density equals the mean of the grey values for all the pixels in the measurement field, multiplied by the area. All raw mRNA abundance values are presented as integrated density values.

Northern blots were carried out for both the Neuro-2a and 293T cell lines, using all the 3′UTR-reporters tested thus far (figures 33 and 34 respectively). Two striking effects were revealed in

the Northern experiments from both cell lines, which had a profound effect on the interpretation of the luciferase data gathered up until that point. These effects included; an obvious increase in firefly luciferase mRNA in the +HuCsv1 condition for all reporters including the controls, and unexpected differences in 3′UTR-reporter length and abundance between +/-HuCsv1 conditions for several of the 3′UTR-reporter mRNAs.

For this portion of the thesis, the reader is referred to figures 26 and 26b for supporting information regarding the interpretation of reporter mRNA sizes and the predicted locations of polyadenylation sites within the 3´UTRs of firefly luciferase reporter mRNAs

## Firefly luciferase mRNA is more abundant in HuCsv1 co-transfected cells

From both Northern blots, it was immediately obvious that samples from cells co-transfected with HuCsv1 showed higher steady-state levels of all 3′UTR-reporter mRNAs than their respective (pcDNA3) controls. After normalising for loading using the GAPDH mRNA abundance values, 3′UTR-reporter mRNAs showed increases in message abundances ranging from ~1.3-fold (VASP) to ~4.5-fold (zfcdc42-v2), in **Neuro-2a cells** co-transfected with HuCsv1 relative to –HuCsv1 (table 5). Similar increases were seen in **293T cells**, although generally the increases were more modest ranging from ~1.3-fold (VASP 3′UTR reporter) to 3-fold (control 3′UTR reporter) (table 6). Furthermore, in the Neuro-2a Northern, the presence of some reporter mRNA products appeared dependent on co-transfection with HuCsv1. For example, the smaller mRNA products present in the mcdc42-v1 and mcdc42-v2 samples (figure 33 lanes 7, 8, 9 and 10), and the longer product in the mCofilin sample (figure 33 lanes 15 and 16), all only appear in samples from cells co-transfected with HuCsv1.

Surprisingly, increases in firefly luciferase mRNA abundance were also obvious for the control reporters. For both the control 3′UTR and Xβ-globin 3′UTR-reporters, in both cell lines examined, there was a greater amount of reporter mRNA in the +HuCsv1 condition compared to –HuCsv1. In the case for the 293T Northern (figure 34), there was roughly 3x more control 3′UTR-reporter mRNA and 1.5x more Xβ-globin reporter mRNA in the +HuCsv1 condition. The results are similar in the Neuro-2a Northern (figure 33), with an ~3.8x increase for the control 3′UTR and an ~3x increase for Xβ-globin. The increase in abundance of firefly luciferase reporter mRNA in Neuro-2a cells co-transfected with HuCsv1 was not explained by an increase in transfection efficiency or amount of RNA loaded. Visually, in the Neuro-2a Northern, expression of the renilla luciferase mRNA for all reporters tested appears to be slightly lower in

the +HuCsv1 condition, in agreement with the raw renilla luciferase activity data gathered for this Northern (figure 33). Unfortunately, the signal generated with the renilla probe, is very low. This blot was re-probed several times in an attempt to obtain a better renilla luciferase Northern blot but in all attempts, the very low signal obtained from the probe resulted in significant increases in noise within the blot that affected the quality and quantification of the image. The low signal to noise ratio for the renilla luciferase mRNA made quantification of mRNA amounts difficult. Nevertheless, sufficient signal was obtained for renilla luciferase mRNAs from the control 3′UTR, Xβ-globin, mcdc42-v1, mcdc42-v2 and mCofilin co-transfections to permit an approximate quantification of renilla luciferase mRNA amounts (table 5). Despite the issues with signal intensity, it is fairly clear both visually and from the Northern quantification that unlike the firefly luciferase 3′UTR-reporter mRNAs, HuCsv1 did not cause an increase in renilla luciferase mRNA abundance. In fact, on average there appears to be slightly less renilla mRNA in cells co-transfected with HuCsv1. This result argues against the possibility that increased firefly luciferase mRNA in HuCsv1 co-transfected cells was caused by an increase in transfection efficiency. Likewise, probing for GAPDH in the Neuro-2a Northern also shows a preponderance of less mRNA in the +HuCsv1 condition, although in general the difference is slight (figure 33 and table 5). Again, this effect is at odds with the observations for the firefly luciferase mRNA and does not support the idea that increased firefly luciferase signal in samples from cells co-transfected with HuCsv1 was the result of increased mRNA loading.

In the 293T Northern (figure 34), due to the order in which the membrane was probed, no signal could be obtained for the renilla luciferase mRNA. This was due to the fact that the GAPDH mRNA, probed for second after the firefly luciferase mRNA probe, runs at approximately the same size as that expected for the renilla luciferase mRNA. Because the GAPDH probe produced such a strong signal that could not be completely removed by membrane stripping, no signal could be detected in the subsequent renilla luciferase mRNA blot that could be reliably attributed to the renilla luciferase mRNA. However, as for the Neuro-2a cells, the **raw renilla luciferase activity** values from the 293T experiment were lower in the +HuCsv1 condition (figure 30c), indicating the increase of firefly luciferase mRNA in the +HuCsv1 condition was unlikely to be due to higher transfection efficiency. Furthermore, the GAPDH blot ruled out the cause of the difference as coming from a difference in the amount of RNA loaded, in agreement with the Neuro-2a Northern (table 6 and figure 34).

In conclusion, the increase in total amount of 3´UTR-reporter mRNA in samples from cells co-transfected with HuCsv1 appeared to be the result of co-expression with the HuCsv1 protein. Furthermore, given the effect was also clearly evident for the two "non-target 3´UTR-reporter mRNAs, these increases appeared to occur in a manner that is independent of 3′UTR sequence and thus, is potentially the result of an interaction between HuCsv1 and some other sequence common to all the firefly luciferase reporters tested.

## Northerns suggest several 3´UTR-reporter mRNAs use multiple alternative polyadenylation sites

In cloning the 3′UTR sequences for the firefly luciferase 3′UTR reporter constructs, EST data from the UCSC genome database was examined to identify complete 3′UTR sequences for each putative target. PCR amplification of these sequences from genomic DNA was carried out using primers that deliberately included the predicted terminal polyadenylation hexanucleotide cleavage, site and approximately 100nt of downstream sequence to try and preserve 3′UTR-directed polyadenylation. In deciding on *bone fide* "complete" 3′UTR sequences, consideration was given to whether the identified sequence contained the CLIP identified target sequence(s) and where possible, whether the identified sequence was expressed in neuronal tissue.

Importantly, there was no way to predict how these 3′UTR sequences would be processed when expressed in the Neuro-2a and 293T cell lines. Somewhat naively, it was assumed that by default, a reporter mRNA containing the complete 3′UTR, as cloned into the firefly luciferase reporter vector, would be processed using the terminal polyadenylation signal encoded by the cloned 3´UTR sequence, in both cell lines tested. However, what the Northerns show is that in both the 293T and Neuro-2a cell lines, several of the 3′UTR reporter mRNAs use more than one polyadenylation site. Following this result, the 3′UTR sequences were re-examined and in conjunction with the Northern data, potential alternative polyadenylation sites were identified (figure 26). The predicted lengths for the reporter mRNAs, including mRNAs that may arise from alternative polyadenylation as judged from sequence data and the Northern results, are shown in (figure 26b) and indicated in schematics of each 3′UTR reporter mRNA in (figure 26).

Finally, measurements of migration rates for standard size markers were not obtained for either the 293T or Neuro-2a Northern. Predictions of mRNA length from the Northern have been made by comparison of migration rates of different products and their expected sizes. An explanation of how the different mRNA products were identified is provided below.

## Predicting the identity of mRNA products - Neuro-2a Northern

(*Refer also to figure 26 for a schematic of alternative mRNA product lengths*) Looking at the Neuro-2a Northern (figure 33), the control 3′UTR-reporter mRNA, which uses the vector-encoded SV40 late polyadenylation signal, has an estimated size of approximately 2.0kb. Thus, the reporter mRNA identified in the control 3′UTR-reporter mRNA samples should represent the distance travelled by a 2.0kb mRNA product. The Xβ-globin 3′UTR-reporter contains ~140nt of the Xenopus lavis β-globin 3′UTR. This 3′UTR includes a canonical polyadenylation sequence; AAUAAA$(N)_{13}$CA, but lacks downstream elements from the 3′UTR such as a conserved uracil-rich element, which are potentially necessary for proper polyadenylation using this signal. An mRNA product using this polyadenylation element is expected to be ~2.0kb in length. Downstream of the Xβ-globin 3′UTR is the vector encoded SV40 late polyadenylation sequence. Use of this polyadenylation element would produce a message of ~2.2kb in length. In the Northern, the Xβ-globin control reporter mRNA appears as a single mRNA product that runs slightly higher than the control 3′UTR-reporter mRNA. As such, it is reasonable to assume that the Xβ-globin control reporter, is exclusively using the SV40 late polyadenylation signal, and the observed message represents the distance travelled by a 2.2kb mRNA.

From these observations it is then possible to estimate the size of mCofilin 3′UTR-reporter mRNA products. In this case, cells co-transfected with HuCsv1 show two products, one of which runs at approximately the same height as the Xβ-globin control reporter and is thus ~2.2kb in size, while the other is slightly higher. Only one canonical polyadenylation signal is present in the mCofilin 3′UTR, corresponding to the predicted end of the 3′UTR sequence. A reporter mRNA using this sequence is predicted to be ~2.25kb in length. Thus, the smaller band present in the HuCsv1 co-transfected sample likely corresponds to this mRNA product. Use of the SV40 polyadenylation signal in this reporter is expected to yield an ~2.5kb message. As such, the larger band present in both + and – HuCsv1 conditions is predicted to correspond to this mRNA.

From this, the sizes of the zfCofilin and zfcdc42-v2 3′UTR-reporter mRNA products can be estimated. For zfCofilin, similarly to the mCofilin 3′UTR-reporter, two mRNA products are clearly detected in the Northern. Examination of the zfCofilin 3′UTR sequence reveals a canonical polyadenylation signal located approximately 850nt into the 3′UTR sequence. Interestingly, the EST data for the zfCofilin 3′UTR indicates this canonical polyadenylation signal is generally used by transcripts derived from non-neuronal tissues, such as myoblasts and germline related

tissues. Use of this canonical polyadenylation signal by the reporter mRNA would yield an mRNA of ~2.7kb. Comparison to the mCofilin mRNA products indicates that the smaller zfCofilin product is migrating at a size slightly longer than the largest mCofilin product. Thus it is likely that this is the polyadenylation site used by the smaller zfCofilin product observed in this Northern. No other canonical polyadenylation signals exist downstream of this site until the vector encoded SV40 late polyadenylation signal. However, the EST data does indicate a more distal non-canonical polyadenylation site exists ~350nt downstream of the canonical site. Furthermore, a significant number of these ESTs were obtained from a brain-derived cDNA library, suggesting this polyadenylation site might be favoured in neuronal tissues. A reporter-mRNA using this EST data–inferred polyadenylation site would run at ~3.0kb, which in comparison to other longer mRNA products in this Northern, agrees with the observed migration for the longer mRNA product detected in the zfCofilin 3´UTR-reporter RNA samples. Although, it is also possible that this mRNA is polyadenylated using the vector encoded SV40 late polyadenylation signal, which would yield a product of ~ 3.2kb.

The zfcdc42-v2 reporter yields three mRNA products, the smallest of which appears to run at around 2.0kb. Interestingly, there is no canonical polyadenylation signal present in the 3'UTR that would yield a product of this size. The first canonical polyadenylation sequence present in this sequence occurs ~350nt downstream from the firefly luciferase stop codon and would yield a reporter mRNA product of ~2.25kb, a size not seen in this Northern based on comparison with other reporter mRNAs. Looking at the EST data for this 3'UTR, a handful of shorter sequences, including a spliced mRNA sequence recently submitted to Genbank (mRNA ID - **AY865566** [230] – figure 35 ) are present that could indicate the presence of polyadenylation sites upstream of this first canonical sequence. The AY865566 mRNA sequence indicates that polyadenylation of the zfcdc42-v2 3´UTR sequence can occur approximately 45nt into the 3´UTR sequence. From this data, the most likely non-canonical polyadenylation signal being used is a UUUAAA sequence, which actually spans the STOP codon of the cdc42 coding sequence. The UUUAAA hexanucleotide sequence has been published as a *bone fide* non-canonical polyadenylation signal in a large-scale study of polyadenylation sequences in human and mouse genes [139]. However, it is intriguing that this signal sequence is comprised partly from the actual translation stop signal of the cdc42-v2 mRNA. Additionally, the human, mouse and Xenopus orthologs of cdc42-v2 all contain a canonical polyadenylation signal within 100nt of the STOP codon, the use of which is supported by EST data (as determined from the UCSC genome browser, *data not shown*). Conservation of an early polyadenylation site among other vertebrates supports the

possibility that such an upstream element might exist for the zebrafish cdc42-v2 3′UTR. Use of the UUUAAA site for polyadenylation would produce an ~1.95kb reporter mRNA.

The sizes of the larger two mRNAs present in the zfcdc42-v2 RNA sample from cells co-transfected with HuCsv1 are estimated by comparison with the mCofilin and zfCofilin mRNA products. The shorter of the two likely corresponds to an ~2.6kb product using the terminal 3′UTR polyadenylation site encoded by the 3′UTR. While the longer message is expected to be using the vector encoded SV40 late polyadenylation signal, producing a message ~2.9kb in length.

From these estimates, the sizes of the mcdc42-v2 mRNA products can also be predicted. The mcdc42-v2 3′UTR contains a canonical polyadenylation signal approximately 100nt downstream from the firefly luciferase STOP codon. Use of this signal would produce a message of ~2.0kb, which roughly agrees with the size of the smallest band observed in RNA from cells co-transfected with HuCsv1. The largest mRNA product detected, which is common to RNA from both + and – HuCsv1 transfections, appears to run at the same level as the largest product detected in the zfcdc42-v2 RNA samples. This would suggest the size of the largest mcdc42-v2 mRNA is also approximately 2.95kb, which would correspond to a reporter mRNA using the SV40 late polyadenylation signal. The mcdc42-v2 3′UTR also contains a more 3′ canonical polyadenylation signal ("terminal"), which if used, would yield an mRNA of ~2.7kb. However, from the Northern, this signal does not appear to be used in either the presence or absence of HuCsv1.

From this point, it is more difficult to be confident in predicting sizes of mRNA products. The zfcdc42-v1 3′UTR contains four canonical polyadenylation sites (excluding the vector encoded SV40 late polyadenylation signal). In RNA from cells co-transfected with HuCsv1, multiple reporter mRNA products are somewhat evident, however only the largest of these appears in RNA from cells co-transfected with the empty pcDNA3 vector. Based on comparison with the mcdc42-v2 mRNA products, this message is most likely polyadenylated using the terminal 3′UTR encoded polyadenylation signal, generating an ~3.2kb message. A further two smaller products are very weakly detected which, based on the location of polyadenylation sites within the 3′UTR and comparison to other reporter mRNAs in the Northern, are likely an ~2.4kb and ~2.1kb (or 2.15kb) mRNA (respectively) that use canonical polyadenylation elements. It is not possible to distinguish between the potential products of two canonical polyadenylation sites approximately

200nt into the zfcdc42-v1 3′UTR (see figure 26) by Northern blot. Notably, in determining abundance values for zfcdc42-v1 3′UTR-reporter mRNAs, the 2.4kb product was omitted due to the lack signal relative to background.

Comparing the zfcdc42-v1 reporter mRNA products to the mcdc42-v1 products, a similar pattern is observed. The mcdc42-v1 3′UTR-reporter mRNA contains three canonical polyadenylation signals (excluding the SV40 signal), with multiple products detected in RNA from cells co-transfect with HuCsv1. The largest product, which is also the only product detected in mRNA from cells co-transfected with the empty pcDNA3 vector, is predicted to represent mRNA of ~3.2kb in length, using the terminal 3′UTR encoded polyadenylation signal. This is based on comparison with the largest zfcdc42-v1 mRNA products. Upstream polyadenylation signals within the 3′UTR could also drive production of messages ~2.8kb ("middle") and 2.0kb ("very early") in size. The very early mRNA product is very weakly detected in RNA from cells co-transfected with HuCsv1 and essentially undetectable in the absence of HuCsv1. The ~2.8kb mRNA product is barely detectable in cells co-transfected with HuCsv1 and it's abundance was not sufficiently above background to allow for reliable quantification.

Finally, the VASP 3′UTR contains no canonical polyadenylation signal and examination of the UCSC genome browser for this gene reveals very few published ESTs. From the available EST data, a non-canonical polyadenylation site appears to drive polyadenylation approximately 1.1kb from the start of the 3′UTR sequence using the sequence AAGAAA. In the context of the reporter construct this polyadenylation site would yield a product of ~3.0kb. This predicted size does agree with the size of the observed VASP 3′UTR reporter mRNA when compared to the longest mRNA products detected in the mcdc42-v1 and zfcdc42-v1 RNA samples. It is also possible that the mRNA detected for the VASP 3′UTR reporter corresponds to a message polyadenylated using the vector encoded SV40 late polyadenylation signal. In this case, the predicted mRNA size would be ~3.3kb, although based on estimates of sizes for the other 3′UTR-reporter messages, this does not appear to be the polyadenylation site used.

### Identification of mRNA products: 293T Northern

The predicted mRNA products identified in the Neuro-2a Northern are largely present in the 293T Northern (figure 34). However, there are a number of differences regarding the presence and abundance of specific mRNA products, when compared to the Neuro-2A Northern. Firstly, the mCofilin reporter mRNA appears as only a single band in both the + and – HuCsv1 condition,

this band is expected to represent mRNAs polyadenylated using the SV40 polyadenylation signal (~2.5kb) based on comparison with the two control reporter mRNA bands (~2.0kb and 2.2kb, respectively) and the two bands present for the zfCofilin 3′UTR-reporter (2.7kb and 3.0kb respectively). Importantly, the zfCofilin 3′UTR is predicted to use the same two polyadenylation sites identified in the Neuro-2a Northern, being the 2.7kb "terminal" site and 3.0kb "non-canonical/late" site. Secondly, unlike the Neuro-2a cell line, only one longer mRNA product is detected in cells transfected with the zfcdc42-v2 3′UTR reporter. Based on comparison with the mCofilin and mcdc42-v2 3′UTR reporter mRNAs in the same gel, it is predicted that this band corresponds to the ~2.6kb zfcdc42-v2 reporter mRNA polyadenylated using the terminal 3′UTR-encoded polyadenylation signal. These observations suggest that in 293T cells there is possibly a difference in how the 3′UTRs of some reporter messages are processed.

### Predictions

The method described to identify different reporter mRNA products in these Northerns based on size predictions is by no means definitive. While the transcription start site of the CMV promoter has been defined [231], allowing for estimates of mRNA size to be made based on predicted polyadenylation sites; without reverse transcribing the reporter mRNA products from each transfection and then performing 3′-RACE to amplify each individual product from the 3′-end followed by sequencing each product, it is impossible to conclusively connect predicted polyadenylation sites with mRNA sequences observed in the Northerns. Regrettably, at the time, this level of investigation was not pursued because of time restrictions and the idea that the 3′UTR-independent interaction between HuCsv1 and reporter mRNAs that caused increases in mRNA abundance complicated other "HuCsv1-specific" effects observed on reporter mRNAs. In hindsight, this piece of information is critical to subsequent interpretations of HuCsv1 function in the 3′UTR-reporter assays reported in this thesis. In the absence of definitive evidence to identify particular polyadenylation sites, the identity of polyadenylation sites used by specific mRNA products reported in this thesis is based on predicted sizes of observed mRNA products, in conjunction with identification of canonical and non-canonical polyadenylation sites using available EST data where available and published descriptions of non-canonical sequences where EST data is unavailable.

## Inconsistencies in mRNA abundance suggest a potential effect of HuCsv1 on 3´-end formation of specific 3´UTR-reporter mRNAs - Neuro-2a Northern data

***Increased abundance of reporter mRNAs using proximal (early) polyadenylation sites in HuCsv1 co-transfected cells***

It was expected that if the only effect of HuCsv1 in these assays was a **3′UTR-independent** increase in firefly luciferase mRNA abundance, then roughly the same increases in abundance would be observed for all 3´UTR-reporter mRNAs produced in transfected cells (including 3´UTR-reporter mRNAs for which 2 or more products were observed). However, this expectation was challenged following quantification of 3´UTR-reporter mRNA abundances from the Northerns. The quantification revealed that several of the 3′UTR-reporters that produce multiple reporter mRNA variants, increases in abundance of alternative mRNA products were not always proportional to the increases seen for the control reporters (table 5). In some cases, the greatest increase in mRNA abundance was seen for transcripts polyadenylated closest to the firefly luciferase STOP codon. This was true for the mcdc42-v1, mcdc42-v2, zfcdc42-v1 and mCofilin 3′UTR-reporters.

There are a number of possible explanations for this observation. It is conceivable that the discrepancy in abundance between mRNAs from the same reporter occurs because those mRNA variants with longer 3′UTRs are more susceptible to other post-transcriptional regulatory events that counter-act the increase in abundance caused by HuCsv1. In this sense, HuCsv1 may be having a role in increasing the stability of the particular 3′UTR reporter mRNA through an interaction with a common sequence(s) outside of the 3′UTR which leads to increased stability of reporter mRNAs but that is countered in reporter messages that have longer 3′UTRs (arising from the use of more distal polyadenylation sites) due to other post-transcriptional regulatory mechanisms the are not necessarily dependent on HuCsv1. In this model, reporter mRNAs with short 3′UTRs (using early polyadenylation sites) would appear to be favoured compared to messages using later polyadenylation sites (pA sites). Alternatively, it is also possible that for 3′UTR-reporters with multiple polyadenylation sites, particularly those closest to the firefly luciferase coding sequence, HuCsv1 specifically increases the use of earlier polyadenylation sites either through an interaction with the 3′UTR sequence or firefly luciferase coding sequence. Unfortunately, the 3′UTR-independent increases in reporter mRNA abundance due to HuCsv1 seen for the two control 3′UTR reporters complicate interpretation of differences in reporter

mRNA variant abundance where earlier polyadenylation sites show greater usage compared to downstream sites.

***Reduced usage of proximal (early) polyadenylation sites in HuCsv1 co-transfected cells***

Intriguingly, for the zebrafish cdc42-v2 and cofilin 3′UTR-reporters, the opposite trend was observed (table 5). In these two cases, use of a 5´-proximal polyadenylation site appears to be less favoured in the presence of HuCsv1. A caveat to this interpretation is that the "reduction" is occurring in a background of generally increased reporter mRNA abundance. Thus, relative to when co-transfected with the empty pcDNA3 vector, the abundance of the shorter mRNA products does still increase (table 5 – zfcdc42-v2 "non-canonical early" fold change = 1.12, zfCofilin "terminal" fold change = 1.2). However, in both cases the increase is clearly less than that observed for the control reporters (Xβ-globin = 3-fold, control 3´UTR = 3.8-fold increased) and more importantly, less than that observed for mRNAs using more distal polyadenylation signals (zfcdc42-v2: "terminal" = 2.8-fold increased, SV40 pA = 4.5-fold increased. zfCofilin: "non-canonical late" = 3.34 increased.). Again, the cause of this observation cannot be pinpointed by Northern blot alone. It is possible these changes were the result of differential stability of the longer 3′UTR-reporter mRNA variants in the presence or absence of HuCsv1. Specifically, the data invites the possibility that HuCsv1 specifically increases the stability of zfcdc42-v2 3′UTR-reporter mRNAs that are polyadenylated using the terminal or SV40 late polyadenylation signals. However, given the abundance of reporter mRNAs using the "early" (non-canonical) polyadenylation signal appears to be negatively affected by HuCsv1 (based on a smaller increase in abundance relative to the control 3′UTR-reporters), this effect was tentatively interpreted as indicating HuCsv1 might be having an effect on alternative polyadenylation site usage for these two 3′UTRs. The details of the changes in abundance for these two reporters are presented below.

The effect described is most strikingly seen for the zfcdc42-v2 3′UTR-reporter. In this case, co-transfection with HuCsv1 results in only a 1.12-fold increase in abundance of reporter mRNAs using the "early/non-canonical" polyadenylation signal (table 5). This increase is less than half that seen for the controls and indicates that HuCsv1 may in some way be reducing the use of this early polyadenylation signal. Notably, while the abundance of mRNAs using the more distal polyadenylation signals is clearly greater than for the "early" signal; it is not markedly increased compared to the control reporters. Abundance of reporter mRNAs using the terminal

polyadenylation signal is ~2.8 times greater in the presence of HuCsv1, while mRNAs using the SV40 polyA signal are 4.5 times more abundant (table 5).

The zfCofilin 3′UTR-reporter shows a similar effect. Of the two reporter mRNAs detected, abundance of mRNAs using the more proximal polyadenylation site is increased by only 1.2-fold, while abundance of mRNAs using a more distal site is increased ~3.3-fold in the presence of HuCsv1.

Because of the 3′UTR-independent effect of HuCsv1 on control reporter abundance, it is not possible to tell whether the reduced usage of proximal polyadenylation signals leads to a corresponding increase in usage of distal signals. Compared to the control 3′UTR-reporters, the increases in abundance of mRNAs using more distal polyadenylation signals does not appear greater than that expected from the 3′UTR-independent effect of HuCsv1 on general reporter mRNA abundance. However, a possible explanation for this is that sequences present in the longer 3′UTR variants direct further post-transcriptional regulation of this message that affect mRNA abundance in a manner that is either dependent or independent of HuCsv1.

Following on from this, abundance of the VASP 3′UTR-reporter was not greatly increased in the presence of HuCsv1, showing only a 1.3-fold increase compared to in the absence of HuCsv1. Given this reporter would be expected to be subject to the same 3′UTR-independent effect seen for the other reporter mRNAs, the lack of a comparable increase in abundance suggests the VASP 3′UTR may influence reporter mRNA stability itself. If the VASP 3′UTR were able to reduce reporter mRNA stability, this may become more obvious under conditions where a second effect is acting to increase mRNA abundance. Notably, there are currently no available data regarding the mRNA half-life of the zebrafish VASP 3′UTR and only limited information regarding mammalian VASP mRNA half-life, which suggests a $t^{1/2}$ <4hr [232].

***Unexpected differences in reporter mRNA abundance for the 293T Northern***

Interestingly, the 293T Northern did not recapitulate the abundance differences seen in the Neuro-2a Northern for the zebrafish cdc42-v2 and cofilin 3′UTR-reporters. Generally speaking, in the 293T Northern, use of more proximal polyadenylation sites is less common among the 3′UTR-reporters in either the presence or absence of HuCsv1, with the bulk of reporter mRNAs appearing to use either terminal 3′UTR-encoded or SV40 late polyadenylation signals. Furthermore, increases in abundance of these longer mRNA variants in the presence of HuCsv1 are comparable for all 3′UTR-reporters ranging from 1.3-fold (VASP) to 1.87-fold (mcdc42-v1

"terminal"). Interestingly, the control 3′UTR-reporter, showed an increase in abundance of 4.7-fold in the presence of HuCsv1. This increase was by far the greatest seen from any of the 3′UTR-reporter mRNAs tested in 293T cells (table 6). Furthermore, this observation fits with the idea that the longer variants of 3´UTR sequences used in these reporter assays have some destabilising activity, particularly with respect to the VASP 3′UTR. This activity, appears to counter increases in message abundance due to co-expression with HuCsv1 and results in a lower fold increase in mRNA abundance, relative to the control 3′UTR-reporter.

Interestingly, in the presence of HuCsv1, the zebrafish cdc42-v2 3′UTR-reporter shows a strong **increase** in abundance of shorter reporter mRNA transcripts; presumed to be using a proximal ("early"), non-canonical polyadenylation signal, relative to in the absence of HuCsv1 (2.65-fold increase). Conversely, abundance of the longer mRNA variant (presumed to be polyadenylated at the terminal, 3´UTR-encoded pA site) was **decreased,** notably, to a level lower than observed even in the –HuCsv1 condition (~0.83-fold increase). This behaviour was in direct contrast to that seen for this reporter in Neuro-2a cells and suggested HuCsv1 may affect 3´-end processing of the zfcdc42-v2 3′UTR-reporter differently between the two cell lines.

From the data obtained, it is not possible to definitively explain the differential behaviour of the zfcdc42-v2 3′UTR-reporter in the two different cell lines. On the one hand, it is possible that HuCsv1 has no influence over alternative polyadenylation site usage for the zfcdc42-v2 3′UTR reporter in 293T cells. In this case, the discrepancy between abundance of the shorter versus longer mRNA variants is the result of post-transcriptional regulatory events that affect the longer 3′UTR variant, as explained for the VASP, mcdc42-v1, mcdc42-v2, zfcdc42-v1 and mCofilin 3´UTR-reporter results from the Neuro-2a Northern. In this case, increased abundance of the shorter zfcdc42-v2 3′UTR-reporter variant is caused by a 3′UTR-**independent** interaction between the zfcdc42-v2 3′UTR reporter mRNA and HuCsv1, which is countered by destabilising effects affecting the longer 3´UTR variant.

On the other hand, the fact that HuCsv1 does not appear to block the use of 5´-proximal ("early") polyadenylation sites in 293T cells may indicate that additional factors are involved in the effect(s) of HuCsv1 observed for the zfcdc42-v2 and zfCofilin 3′UTR-reporters seen in Neuro-2a cells. It is also possible that HuCsv1 itself behaves differently in the two different cell lines. These possibilities were motivating factors in the original decision to use additional cell lines such as neuronal-like Neuro-2a cells line, when the dual luciferase assay data suggested that

HuCsv1 was not causing any obvious effect to 3′UTR-reporter expression in 293T cells (figure 30a).

Importantly, looking back the normalised firefly luciferase reporter data (figure 30a) of all the reporters tested in the dual luciferase reporter assays from 293Ts, the only reporter to show a statistically significant effect was the zfcdc42-v2 3′UTR reporter. As shown, HuCsv1 caused a small increase in normalised firefly luciferase activity for this reporter, which contradicted the effect of HuCsv1 seen for the zfcdc42-v2 reporter in both HeLa and Neuro-2a cells. Importantly, this contradiction generally agrees with other observations of 3′UTR biology that show mRNAs with shorter 3′UTRs are generally more readily and efficiently translated than mRNAs with longer 3′UTRs ([233], [148]). In the assays described in this thesis, the increased expression of firefly luciferase from the zfcdc42-v2 3′UTR reporter in 293T cells corresponds to an increased abundance of reporter mRNAs carrying a shorter 3′UTR. Conversely, in Neuro-2a cells, a reduction in firefly luciferase from this reporter is associated with an apparent reduction in the use of more 5´-proximal ("early") polyadenylation sites. These differences were considered to be potentially indicative of a differential effect of HuCsv1 on polyadenylation site choice for the zfcdc42-v2 3′UTR reporter, between the two cell lines. If this were true, it could be possible to exploit these differences in behaviour to examine the requirements of HuCsv1 in regulation of polyadenylation site choice for the zfcdc42-v2 3′UTR reporter by looking for differences in proteins that interact with HuCsv1 or differences in other mRNA processing factors associating with the 3′UTR between the two cell lines.

In conclusion, Northern results for the firefly luciferase-based zfcdc42-v2 3′UTR-reporter potentially reveal an unexpected effect of HuCsv1 on 3´-end processing. Both the zfcdc42-v2 and zfCofilin 3´UTR-reporters indicate HuCsv1 might have an effect on alternative polyadenylation site choice for these 3′UTRs. While in these assays the 3′UTR-independent effect of HuCsv1 on 3′UTR reporter mRNA abundance prevented the formation of any definitive conclusions about effects of HuCsv1 on mRNA processing, this result was interpreted as a strong hint as to a potential and entirely unexpected function of HuCsv1.

## Conclusions from the firefly luciferase 3′UTR reporter Northerns

***Translation efficiency of 3′UTR-reporter mRNAs in the presence of HuCsv1***

Examination of 3′UTR-reporter mRNA expression was expected to allow determination of translational efficiency of the 3′UTR-reporters in the presence or absence of HuCsv1. Translation efficiency is calculated by normalising firefly luciferase expression for a given 3′UTR-reporter to the abundance of its respective mRNA. To compare translation efficiency of 3′UTR-reporters in the presence and absence of HuCsv1, it is then necessary to divide the normalised firefly luciferase activity values by the normalised renilla luciferase activity (normalised to mRNA amount as for firefly luciferase). This also allows for comparison between the different 3′UTR-reporters in a given assay. Determining the translation efficiency of the 3′UTR-reporters was deemed to be important because the results from the dual luciferase reporter assays indicated HuCsv1 was causing a small reduction in expression of the firefly luciferase reporter protein when it's encoding message carried one of several putative target 3′UTRs. As such, it was necessary to ascertain whether this change arose through a change in amount of the encoding mRNA, or as a result of a change in reporter mRNA translatability.

As shown, Northern analysis of 3′UTR-reporter mRNA abundance revealed a 3′UTR-independent effect of HuCsv1, which led to an increase in the abundance of all firefly luciferase reporter mRNAs, independent of 3′UTR sequence. As a consequence of this, translation efficiency calculations of all 3′UTR-reporters suggested HuCsv1 causes a significant reduction in translatability, in both Neuro-2a and 293T cell lines (figures 36 and 37), despite no obvious effect of HuCsv1 on control 3′UTR-reporter expression in the dual luciferase assays (figures 30a and 32a).

There are a number of caveats to the translation efficiency calculations presented here. Firstly, because of the very low signal intensity obtained for the renilla luciferase mRNA in the Neuro-2a Northern, translation efficiency was only calculated for reporters where reliable renilla luciferase mRNA quantification could be made. Secondly, in cases where 3′UTR-reporters had multiple mRNA variants, translation efficiency calculations we made using the summed mRNA abundance in any giving condition. This is not an ideal method for calculating translation efficiency because it is likely that the different mRNA variants do not contribute equally to the overall amount of firefly luciferase produced. Notably, of all the 3′UTR-reporters tested, the control, Xβ-globin and VASP 3′UTR-reporters showed only one reporter mRNA product by

Northern blot. As such, the translation efficiency calculations for these three reporters can be reliably attributed to represent a good approximation of reporter mRNA translatability. Thirdly, in the case of the 293T Northern, probing for GAPDH expression to normalise mRNA loading between samples inadvertently masked any renilla luciferase mRNA signal because these mRNAs run at approximately the same size and the GAPDH signal was too strong to allow for detection of the under lying renilla luciferase mRNA signal, despite multiple attempts to strip the membrane of the GAPDH probe. Nevertheless, an approximate calculation of translation efficiency was obtained by simply normalising firefly luciferase activity to mRNA amounts for each 3′UTR-reporter. Finally, transfections for Northern blot data were carried out independently of transfections for luciferase activity. As such, the Northern data does not strictly correspond to a specific luciferase assay data set and translation efficiency calculations were made using the averaged firefly and renilla luciferase activity values from 3´UTR-reporter dual luciferase assays. This was not expected to alter the interpretation of translation efficiency calculations, as the general trends of luciferase activity from 3´UTR-reporters in these assays had been consistent throughout.

In reality, the most important results of the translation efficiency calculations lie with the control reporters. From the Neuro-2a data, translation efficiency calculations for both the control and Xβ-globin 3′UTR-reporters indicate that HuCsv1 causes a reduction in translation efficiency of both of these reporters (figure 36). The control 3′UTR-reporter showed a 4.5-fold reduction in translatability, while for the Xβ-globin 3′UTR-reporter, translatability was reduced by more than 2-fold. Of the CLIP-identified 3′UTR-reporters, calculations were made for the VASP, mcdc42-v1 and mCofilin 3′UTR-reporters, all of which showed reductions in translatability between ~2.2 and 5.6-fold in the presence of HuCsv1.

Importantly, just looking at renilla luciferase activity normalised to mRNA abundance (figure 36), HuCsv1 does not appear to have a consistent effect (positive or negative) on the expression of this reporter. A homoschedastic Student's t-test comparing renilla luciferase activity normalised to mRNA between cells + and – HuCsv1 address with this conclusion ($p > 0.47$). Thus, from these results it appears as if the reductions in raw renilla luciferase activity observed for the dual luciferase assays (figure 32c) are the result of reduced mRNA abundance in these transfections and not some general effect of HuCsv1 on translation.

For the 293T data, normalisation of firefly luciferase activity to mRNA levels shows essentially the same thing (figure 37). Normalised firefly luciferase expression from all 3′UTR-reporters tested is reduced in the presence of HuCsv1. It is true that omitting the correction of these values to the normalised renilla luciferase values prevents accurate comparison of translation efficiency of a given 3′UTR between plus and minus HuCsv1 conditions. However, based on the normalised renilla luciferase values from the Neuro-2a cell line, this normalisation would not be expected to eliminate the observed reduction to 3′UTR-reporter translatability caused by HuCsv1 in 293T cells.

***Northerns reveal a 3′UTR-independent effect of HuCsv1 on firefly luciferase reporter expression***

The translation efficiency calculations for the Neuro-2a cell line highlight a confusing discrepancy between the 3′UTR-reporter luciferase activity data and mRNA abundance data. Specifically, while the abundance of all 3′UTR-reporter mRNAs tested is clearly increased in the presence of HuCsv1, a decrease in their respective luciferase activities is consistently observed. Following normalisation of luciferase activity reporter mRNA abundances, HuCsv1 is obviously reducing the translation of all 3′UTR-reporters in a manner that is independent of the 3′UTR sequence carried by the reporter message.

Looking back at the raw firefly and renilla luciferase activity. Reductions in activity of both luciferase enzymes, for all cell lines tested, were initially considered to be an artefact of transfection, as normalisation of firefly to renilla luciferase activity for the control 3′UTR-reporters corrected for any difference and no consistent effect of HuCsv1 was observed on normalised control 3′UTR-reporter activity. In the case for renilla luciferase this appears to be most likely, as after normalising renilla luciferase activity to mRNA abundance (from Neuro-2a cells) there is on average little difference between cells co-transfected with or without HuCsv1. As such, reduced renilla luciferase activities in cells co-transfected with HuCsv1 are likely the result of differences in transfection efficiency or cell number between the two conditions. However, the normalisation of firefly luciferase activity to mRNA abundance shows that while some difference in transfection efficiency may exist, the obvious increase in firefly luciferase reporter message abundance occurring in cells co-transfected with HuCsv1 does not translate into an increase in firefly luciferase activity. As such, reductions in raw firefly luciferase activity cannot be explained by differences in transfection efficiency alone.

This point is very hard to reconcile, as from the Northern data, firefly luciferase activity (in the presence of HuCsv1) would be expected to increase concordantly with the increases in reporter

mRNA. Why then do the firefly activities from 293T, HeLa and Neuro-2a cells (normalised to renilla luciferase activity – figure 30a, 31a and 32a) indicate there is little difference in activity between plus and minus HuCsv1 conditions? There is no clear answer to this question. Theoretically, HuCsv1 may be having a sequestering effect on the firefly luciferase reporter mRNA, binding and stabilising the mRNA but reducing its availability to the translation machinery. *If* the negative effect of HuCsv1 on firefly luciferase mRNA translation were only partial, then the net effect *could* lead to a reduced rate of 3´UTR-reporter mRNA translation (in the presence of) HuCsv1 which is in some way compensated for by the strong accumulation of reporter mRNA. *Italics* are used in describing this possibility because it one would have to be very lucky to essentially fluke transfection conditions in which this kind of effect results in the production of comparable amounts of (renilla luciferase-normalised) firefly luciferase reporter protein between the two HuCsv1 conditions (as determined by the dual luciferase assay – figure 30a, 31a and 32a).

Another possible explanation is that the stabilisation effect of HuCsv1 observed for the firefly luciferase reporter mRNAs occurs independently from reporter mRNA translation. Specifically, it is possible HuCsv1 is stabilising (or protecting) firefly luciferase mRNAs that are no longer being translated and have begun being turned over. An interesting visual feature of the Northern blot data itself is that there appears to be a subtle "sharpening" of reporter mRNA bands from samples co-expressing HuCsv1 (this is most obvious in the Neuro-2a Northern – figure 33 take the control 3´UTR and Xβ-globin as examples, lanes 1, 2 and 3, 4 respectively). This sharpening occurs with an equally subtle reduction in the apparent mean length of reporter mRNAs and possibly indicates the majority of mRNAs in these samples (*ie* +HuCsv1) have shorter polyA tails. Conceivably, in these experiments HuCsv1 may be stabilising translationally-inactive (de-adenylated) firefly luciferase reporter mRNAs through a 3´UTR-independent interaction with the firefly luciferase reporter mRNA. This effect would not necessary have any influence over firefly luciferase enzyme production (as it only retards complete mRNA turnover of already partially degraded mRNAs) thus no effect would necessarily be observed in the dual luciferase assays. However, mRNA abundance (as determined by Northern blot) would be clearly increased and confound any interpretation of changes in abundance of specific mRNA isoforms or calculations of mRNA translational efficiency.

***The firefly luciferase coding sequence; a likely target for HuCsv1 binding***

It seems likely that the increase in mRNA abundance in the presence of HuCsv1 is caused by something common to all firefly luciferase reporters. The most obvious possible culprit is the

firefly luciferase coding sequence. Looking at this sequence, there are eleven unique sites (figure 38) that satisfy the YUNNUUY binding sequence requirements for HuD, published in a crystallographic study of the interaction between the first two RRMs of the protein and the c-fos mRNA [38]. While no specific mRNA recognition element has been published for HuCsv1, it is generally accepted that the Hu RNA binding proteins interact with pyrimidine-rich sequences, particularly favouring uracil-rich sequences. There are a number of uracil-rich regions in the firefly luciferase coding sequence that could potentially serve as HuCsv1 interaction motifs. Furthermore, much of the published work looking at Hu RNA-binding proteins indicates they may have an effect on stabilising target mRNAs through interactions with uracil-rich sequences. As such, it is possible that through an interaction between HuCsv1 and the firefly luciferase coding sequence, the firefly luciferase mRNA is being artificially stabilised in a 3′UTR-independent manner for all of the reporters tested.

## A role for HuCsv1 in polyadenylation site choice?

Unexpectedly, the results from the Northern blot experiments performed using the firefly luciferase-based 3′UTR-reporters suggest that HuCsv1 may influence alternative polyadenylation site usage of the zebrafish mRNAs for both *cofilin1* and *cdc42-v2*.

Examination of the 3′UTR sequences for these mRNAs shows that in both cases, potential Hu binding sites in these 3′UTRs lie close to the predicted polyadenylation sites that show differential usage in the presence of HuCsv1 (figures 39a-b and 40a-b). For the zebrafish cofilin 3′UTR-reporter, the Northern data showed reduced usage of an earlier polyadenylation signal ("terminal") in favour of a later one (CAUAAA) when co-expressed with HuCsv1. The "terminal" polyadenylation site uses a canonical AAUAAA element, and yields a 3′UTR-reporter mRNA of 2.7kb (figure 39a). The more distal site uses a non-canonical sequence (CAUAAA) that yields a 3.0kb reporter mRNA transcript. Examination of available EST data for this gene shows both polyadenylation sites can be used. Interestingly, the CLIP-data for the zebrafish *cofilin* 3′UTR indicates neuronal Hu proteins bind within a uracil-rich element that spans ~350nt and ends roughly 200nt upstream of the "terminal" (AAUAAA) polyadenylation signal (figure 39b). From this information, it is difficult to see how HuCsv1 would be reducing use of this polyadenylation signal, given that this uracil-rich element is not located particularly close to the early polyA site. However, a second uracil-rich element is present in the zebrafish cofilin 3′UTR which spans an ~350nt region that includes the "terminal" polyadenylation signal. This site is also very close to the more distal non-canonical polyadenylation signal. The absence of CLIP-tags in this region does not exclude it as a potential nHu protein binding region, as the CLIP library has not been exhaustively sequenced, thus CLIP-tags may still be present in the library that map to this region. Furthermore, being rich in uracil residues theoretically satisfies the binding requirements for an Hu binding site. In the event of binding, HuCsv1 may cause a reduction in the use of the more proximal ("terminal") polyA site by physically blocking binding of cleavage and polyadenylation specific factors or through protein-protein interactions with factors involved in transcript cleavage and polyadenylation that accomplished this effect.

As was seen for the zebrafish cofilin 3′UTR, HuCsv1 also appears to reduce the usage of a 5′-proximal polyadenylation signal in the zebrafish cdc42-v2 3′UTR. What is interesting about this pA signal (UUUAAA) is that it is found within a 400nt stretch of 3′UTR that is particularly rich in uracil residues (figure 40b). The single CLIP tag available for the zfcdc42-v2 3′UTR identifies a nHu protein binding site at the 3′-boundary of this uracil-rich region, supporting the idea that

the high uracil content of this portion of the 3′UTR would support an interaction with HuCsv1. What is more interesting though, is that of the 45 residues including and immediately downstream of the UUUAAA sequence, 39 are either cytosine (x20) or uracil (x19). Based on known binding affinities of Hu proteins for uracil-rich sequences, it is highly probable that this pyrimidine-rich sequence would be favoured as Hu protein binding sites within the 3′UTR

Thus, it appears that for both the *cdc42-v2* and *cofilin* 3′UTRs, regions of high pyrimidine content immediately follow affected polyadenylation sites. Given the potential for these sites to serve as HuCsv1 binding sites, it is possible that the changes in polyadenylation site usage observed for these reporters in the presence of HuCsv1 are the result of an interaction with the reporter mRNA immediately downstream of the affect polyadenylation signal, which perturbs interactions with 3′-end processing factors that facilitate transcription termination and/or polyadenylation.

***Alternative possibilities to explain results from the Northern blots***

Importantly, while the differential expression of zfcdc42-v2 and zfCofilin 3′UTR-reporter mRNA variants seemed most likely due to alternative use of polyadenylation sites within the respective 3′UTR sequences, other possibilities could not be ruled out. Firstly, it was possible for the zfcdc42-v2 3′UTR-reporter that production of the smallest mRNA variant, for which no canonical polyadenylation signal could be identified, was not caused by use of an early/non-canonical polyadenylation event, but instead was the product of cryptic splicing between sequences in the firefly luciferase coding sequence and sequences present within the zfcdc42-v2 3′UTR. Such an event would be expected to cause a reduction in firefly luciferase activity (through a reduction in the amount of complete firefly luciferase encoding mRNA), as was observed in dual luciferase assays. And to produce an mRNA variant of smaller than expected size. To test this, it would be necessary to use a reporter other than firefly luciferase for the 3′UTR-reporter mRNAs and assay for reporter mRNA production by Northern blot. Production of the smaller mRNA variants from a 3′UTR-reporter vector using a different reporter coding sequence would rule out this possibility.

Secondly, it was also possible that the observed results arose through differential stabilisation of zfcdc42-v2 3′UTR-reporter mRNA variants. As a result of the 3′UTR-independent effect of HuCsv1 on mRNA abundance observed in the firefly luciferase-based 3′UTR-reporter Northern data, this possibility could not be ruled out. However, this possibility could also be ruled out

through use of an alternative reporter protein, for which the coding sequence does not show appreciable binding by HuCsv1.

Finally, the differential reporter mRNA abundance effects described for the Neuro-2a experiments usinf the firefly luciferase-based 3´UTR-reporter constructs are replicated in a second Northern from Neuro-2a cells (Appendix 2 - figure 7). Notably, this second Northern was obtained from an *essentially* identical experiment to those described for the firefly luciferase reporter assays thus far. The one exception to this being that following transfection, cells were treated with a membrane permeable analogue of cyclic AMP, dibutyryl cAMP (dbcAMP). This experiment is described in detail in Appendix 2. The results from this experiment are presented in some detail for completeness, although there are generally no solid conclusions from these data because of the general effect of HuCsv1 on firefly luciferase reporter mRNA abundance and subsequent transition to a different reporter assay system, which interrupted this line of investigation. Nevertheless, the reader is encouraged to examine the Northern blot data from Appendix 2 (Appendix 2 – figure 7 and table 1) as the results largely replicate those observed in the Northern data presented in this chapter.

## Taking the firefly luciferase data further

The conclusions from the firefly luciferase reporter assays were that HuCsv1 appeared to have a 3′UTR-independent interaction with the firefly luciferase reporter mRNA, which ultimately confounded any interpretation of 3′UTR-specific effects of HuCsv1 on reporter translation. However, despite the undesirable side-effects of the firefly luciferase reporter coding sequence, an unexpected and highly exciting effect of HuCsv1 on 3´-end processing of two of the 3′UTR-reporter messages appeared to have been identified by Northern blot. In the context of neuronal Hu protein biology, preferential enrichment of a particular 3′UTR variant of a target mRNA by HuCsv1 was an extremely exciting observation. Regulation of 3′UTR length through alternative polyadenylation site choice has more recently been recognised as an important factor in controlling gene expression [189]. Global analysis of 3′UTR length over development [148] and in comparison between quiescent cells/terminally differentiated cells and actively proliferating cancer cells [233] correlates changes in cell state from a less differentiated state (stem/progentiator/cancer cell) to more differentiated state (quiescent/terminally differentiated) with increasing 3′UTR length. Thus, as differentiation proceeds, a general lengthening in 3′UTR length is observed, primarily through use of alternative, downstream polyadenylation signals.

As such, an exciting prospect from the Northern data was that HuCsv1 might be involved in this aspect of cell biology as a sequence specific factor that promotes or maintains alternative processing of specific target mRNAs. In the case of the mRNA for *zfcdc42-v2*, HuCsv1 may drive increases in abundance of specific mRNAs bearing longer variants of the zfcdc42-v2 3′UTR. Based on the timing of neuronal Hu expression during the course of neuronal differentiation, nHu-specific changes in pre-mRNA processing of specific target messages could be of great importance in the transition of a neuronal precursor cell into a post-mitotic neuron or maintenance of the post-mitotic neuronal phenotype or function.

However, it was necessary to confirm this effect using a reporter assay system in which the 3´UTR-independent effect of HuCsv1 on reporter mRNA abundance had to be eliminated. This would allow for confirmation that the observed effect was not an artefact of the firefly luciferase-based reporter system, which was confounded by 3´UTR-independent interactions between HuCsv1 and 3´UTR-reporter mRNAs. In the final series of experiments for this project, a third generation of reporter vectors was constructed utilising renilla luciferase as the reporter protein. Renilla luciferase was chosen because in the dual luciferase assays described in this

chapter, steady state levels of the renilla luciferase mRNA did not appear to be affected by HuCsv1. As such, it was anticipated that this reporter would be suitable for looking at changes in reporter mRNA abundance.

Due to time constraints, only the control 3′UTR, Xβ-globin 3′UTR and zfcdc42-v2 3′UTR were tested using the renilla luciferase reporter. The zfcdc42-v2 3′UTR was chosen because it had shown some effect of HuCsv1 in both the dual luciferase assays and Northerns, for both the 293T and Neuro-2a cell lines.

Figure 24. Firefly luciferase reporter vector - pCI-FL

pCI-FL was made by sub-cloning the firefly luciferase coding sequence (including Kozak sequence) from pGL3 (Promega) into pCI (Clontech) as described in the materials and methods.

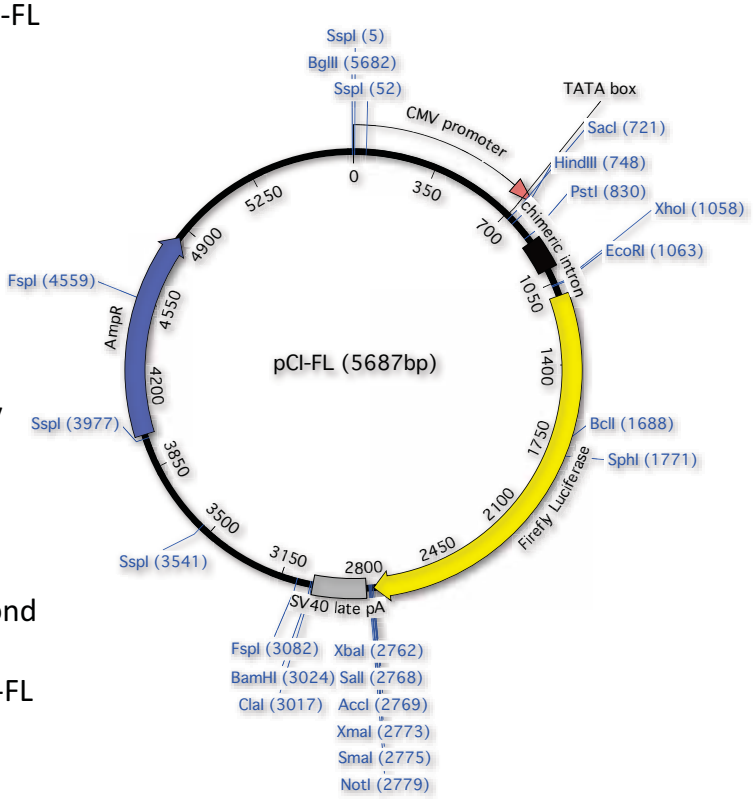


Table 3. Cloning 3´UTR sequences into pCI-FL.

First pass PCR primers were designed to amplify predicted 3´UTR sequences from genomic DNA (mouse or zebrafish).

Following purification, PCR products of the expected size were used as templates for a second PCR reaction using primers to incorporate appropriate restriction sites for cloning into pCI-FL

| 3´UTR | 1st pass primers | 2nd pass primers | | Cloning site | Insert size |
|---|---|---|---|---|---|
| VASP | FWD - CATAGTCCCACAGAAACTGATGG | AGAGGA**TCTAGA**CATAGTCCCAC AGAAACTGATGG | | XbaI - 2762 | 1.23kb |
| | REV - CAAACGTGTTAATGGCAAGG | AGAGGA**CCCGGG**CAAACGTGTT AATGGCAAGG | | XmaI - 3993 | |
| mcdc42-v1 | FWD - GTGTGTGCTGCTATGAACG | TTTTT**TCTAGA**GTGTGTGCTGCTA TGAACG | | XbaI - 2762 | 1.5kb |
| | REV - GTCACATTCTCATTTCTAAATACC | TTTTA**GCGGCCGC**GTCACATTCTC ATTTCTAAATACC | | NotI - 4255 | |
| mcdc42-v2 | FWD - GAAGTGCTGTATATTCTAAACC | TTGAGAAA**CCCGGG**GAAGTGCT GTATATTCTAAACC | | XmaI - 2777 | 0.88kb |
| | REV - CAAGGGGAGTCAAAGAAGC | TAGAGAAA**GCGGCCGC**CAAGGG GAGTCAAAGAAGC | | NotI - 3658 | |
| zfcdc42-v1 | FWD - GTAAATGTGTGCTGCTATGAGC | TTTTT**TCTAGA**GTAAATGTGTGCT GCTATGAGC | | XbaI - 2762 | 1.33kb |
| | REV - AGTGAGTGGAACATGATAAAGG | TTTTA**CCCGGG**AGTGAGTGGAAC ATGATAAAGG | | XmaI - 4099 | |
| zfcdc42-v2 | FWD - CTCCTGAAACGCAGCGAAAACG | AAGGGA**TCTAGA**CTCCTGAAAC GCAGCGAAAACG | | XbaI - 2762 | 0.8kb |
| | REV - GTGCAGCCCTAGTTCAAACC | AGAGAG**CCCGGG**GTGCAGCCCT AGTTCAAACC | | XmaI - 3569 | |
| mCofilin | FWD - GTTCTGGCCTTCCCAAACTGC | TTTTT**TCTAGA**GTTCTGGCCTTCC CAAACTGC | | XbaI - 2762 | 0.44kb |
| | REV - CTTACTAGGGACTGAACTAGAGG | TTTTA**CCCGGG**CTTACTAGGGAC TGAACTAGAGG | | XmaI - 3208 | |
| zfCofilin | FWD - GATTGAGGCTGACACATTTCAGG | TTTTT**TCTAGA**GATTGAGGCTGA CACATTTCAGG | | XbaI - 2762 | 1.17kb |
| | REV - CATCCCCAACGGAACCACTC | TTTTT**CCCGGG**CATCCCCAACGG AACCAC | | XmaI - 3934 | |

Figure 25. Renilla luciferase reporter vector – pCI-RL

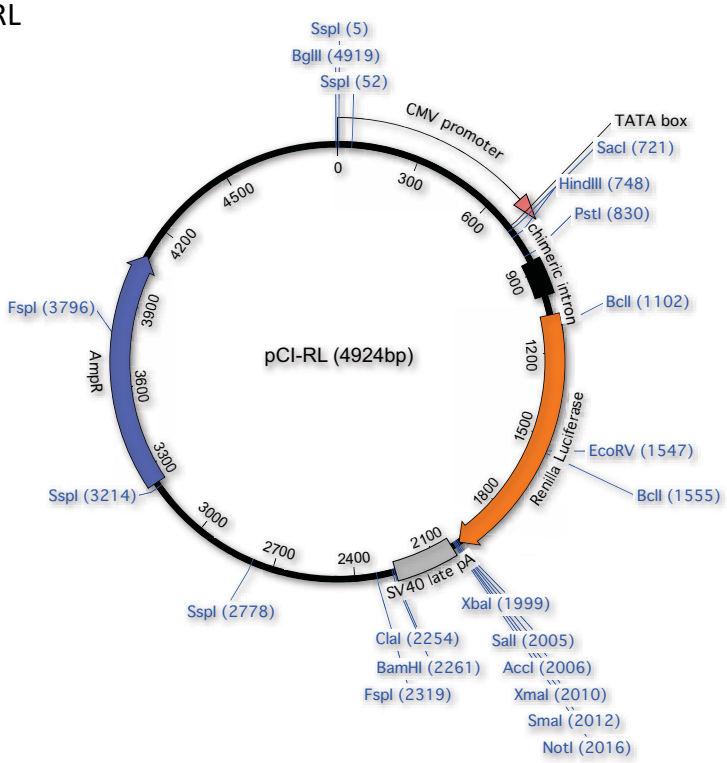


pCI-RL was made by sub-cloning the renilla luciferase coding sequence (including Kozak sequence) from phRL-CMV (Promega) into pCI (Clontech) as described in the materials and methods.

Table 4. Sub-cloning 3´UTR sequences into pCI-RL

Putative target 3´UTR sequences were sub-cloned from pCI-FL into pCI-RL using the restriction enzymes shown in the table.

| 3´UTR | pCI-FL cloning site | | pCI-RL cloning site | Insert size |
|---|---|---|---|---|
| Xβ-globin | XbaI - 2762 | | XbaI - 1999 | 0.15kb |
| | NotI - 2918 | | NotI - 2148 | |
| zfcdc42-v2 | XbaI - 2762 | | XbaI - 1999 | 0.8kb |
| | XmaI - 3569 | | XmaI - 2805 | |

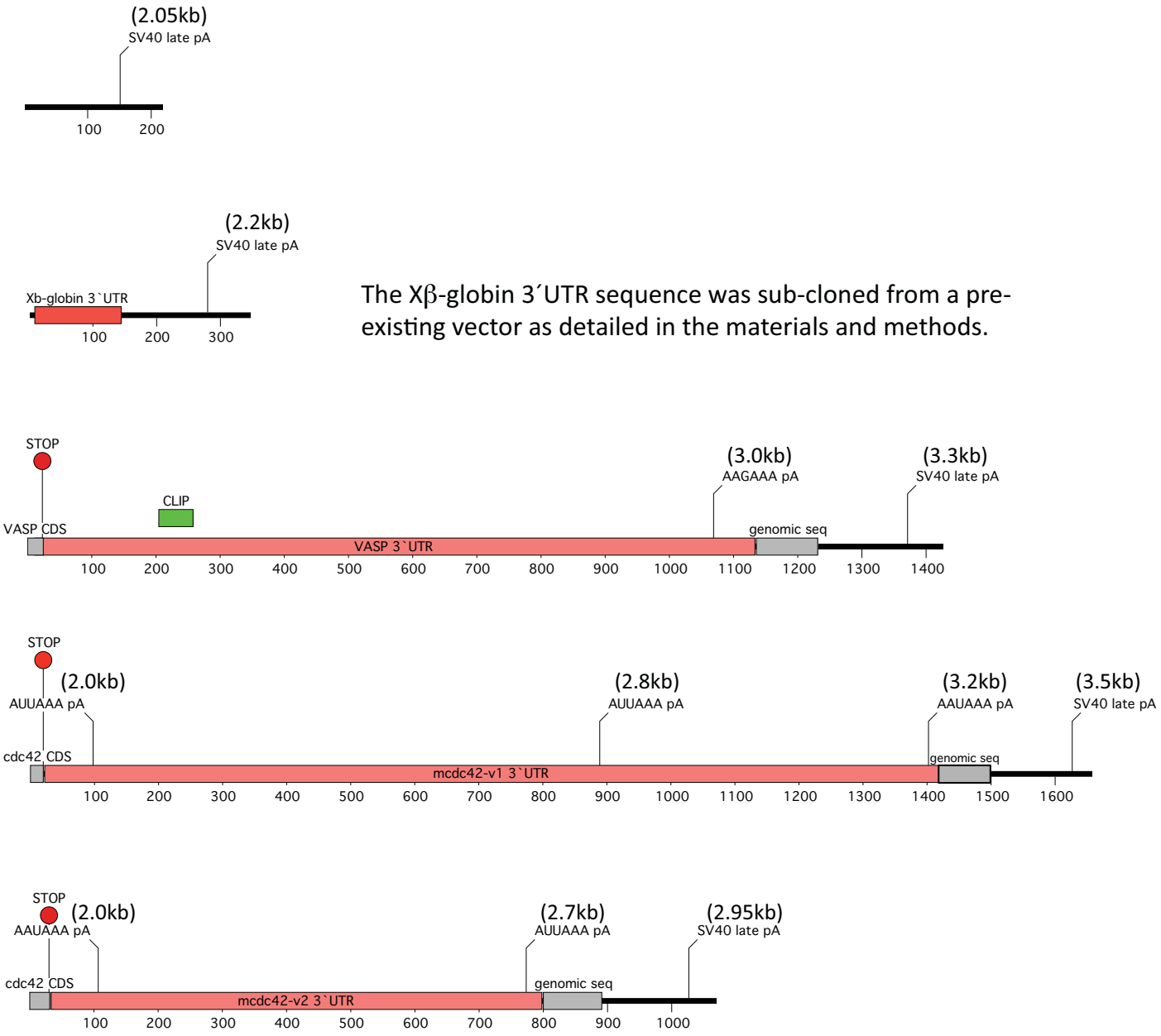


Figure 26. Putative target 3´UTR schematics.

Schematic representations of the cloned 3´UTR sequences are presented below. 3´UTR sequences are shown as pink boxes. Included in the figures are the location and hexameric sequence of predicted polyadenylation sites (pA), the location of CLIP-derived predicted nHu binding sites (green "CLIP" boxes), any included sequence up or downstream of the EST-derived 3´UTR sequence (grey boxes) and the location of translation stop codons (red circles) where primer design for a target 3´UTR necessitated the inclusion of a small amount of coding sequence.

The first two 3´UTRs shown are for the control and Xβ-globin 3´UTR "non-target" control reporters.

Lengths indicated at each polyA site are the predicted size based on a full transcript. The predicted length of each possible pA site variant includes 1.9kb of sequence constituting the full reporter mRNA from transcription start site to the beginning of the inserted 3´UTR-sequence.

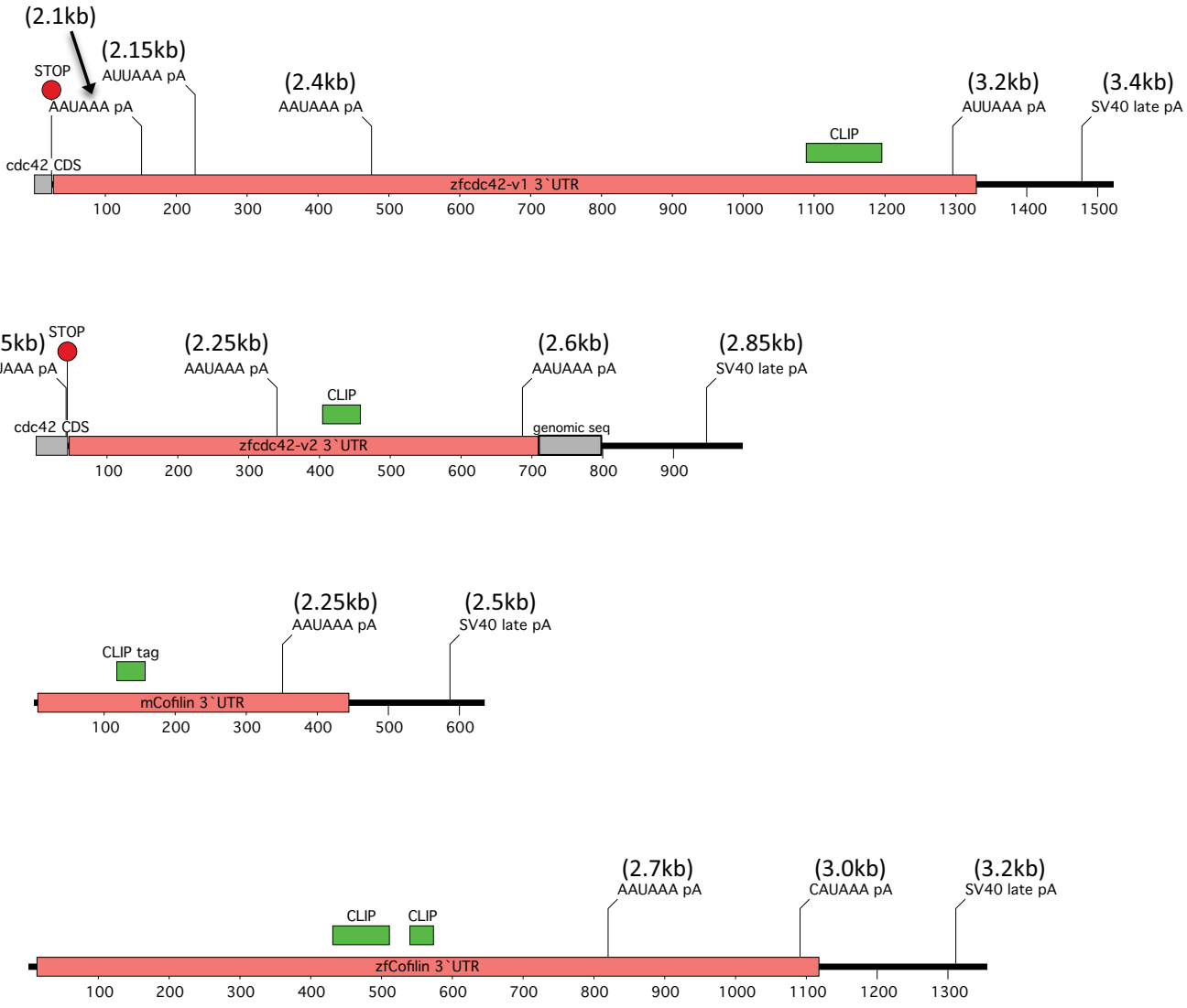


Figure 26. Putative target 3´UTR schematics. (…*continued*)

Figure 26b – Predicted 3`UTR reporter mRNA lengths (firefly luciferase)

| | | | | | |
|---|---|---|---|---|---|
| | | | | | SV40 late (AAUAAA) |
| control 3´UTR | | | | | 2.05kb |

| | | | | | |
|---|---|---|---|---|---|
| | | | | Terminal (AAUAAA) | SV40 late (AAUAAA) |
| Xβ-globin | | | | 2.05kb | 2.2kb |

| | | | | | |
|---|---|---|---|---|---|
| | | | | Terminal ** (AAGAAA) | SV40 late (AAUAAA) |
| VASP | | | | 3.0kb | 3.3kb |

| | | | | | |
|---|---|---|---|---|---|
| | Very Early (AUUAAA) | | Middle (AUUAAA) | Terminal (AUUAAA) | SV40 late (AAUAAA) |
| mcdc42-v1 | 2.0kb | | 2.8kb | 3.2kb | 3.5kb |

| | | | | | |
|---|---|---|---|---|---|
| | | Early (AAUAAA) | | Terminal (AUUAAA) | SV40 late (AAUAAA) |
| mcdc42-v2 | | 2.0kb | | 2.7kb | 2.9kb |

| | | | | | |
|---|---|---|---|---|---|
| | Very Early (AAUAAA) | Early (AUUAAA) | Middle (AAUAAA) | Terminal (AUUAAA) | SV40 late (AAUAAA) |
| zfcdc42-v1 | 2.1kb | 2.15kb | 2.4kb | 3.2kb | 3.4kb |

| | | | | | |
|---|---|---|---|---|---|
| | Early* (UUUAAA) | | Middle (AAUAAA) | Terminal (AAUAAA) | SV40 late (AAUAAA) |
| zfcdc42-v2 | 1.95kb | | 2.25kb | 2.6kb | 2.85kb |

| | | | | | |
|---|---|---|---|---|---|
| | | | | Terminal (AAUAAA) | SV40 late (AAUAAA) |
| mCofilin | | | | 2.25kb | 2.5kb |

| | | | | | |
|---|---|---|---|---|---|
| | | | Terminal (AAUAAA) | Late/non-canonical (CAUAAA) | SV40 late (AAUAAA) |
| zfCofilin | | | 2.7kb | 3.0kb | 3.2kb |

* use of the early polyadenylation site UUUAAA is supported by the mRNA AY865566 submitted to GenBank in June 2010 [209].
** the VASP terminal polyA site is derived from multiple ESTs from UCSC.

Predicted reporter mRNA sizes correspond to the length of each mRNA from the transcription start site (TATA-box of the CMV protomoter) to the cleavage site of the specified polyadenylation signal.

A

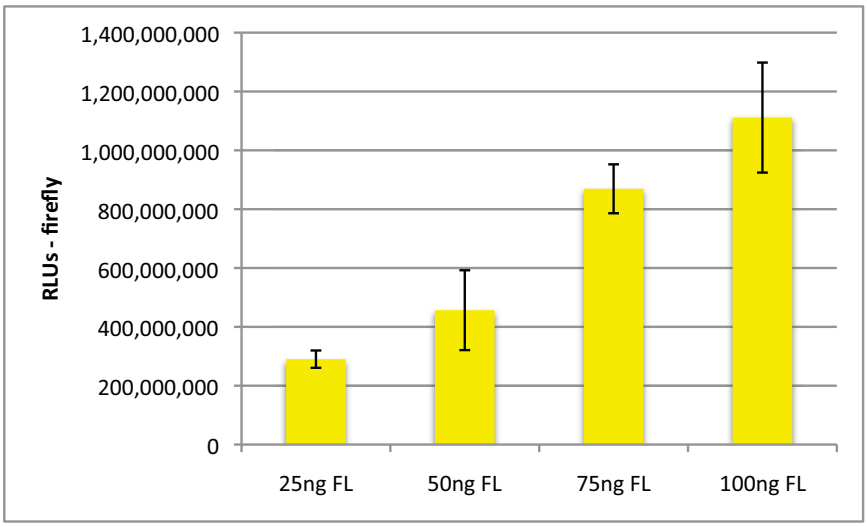


B

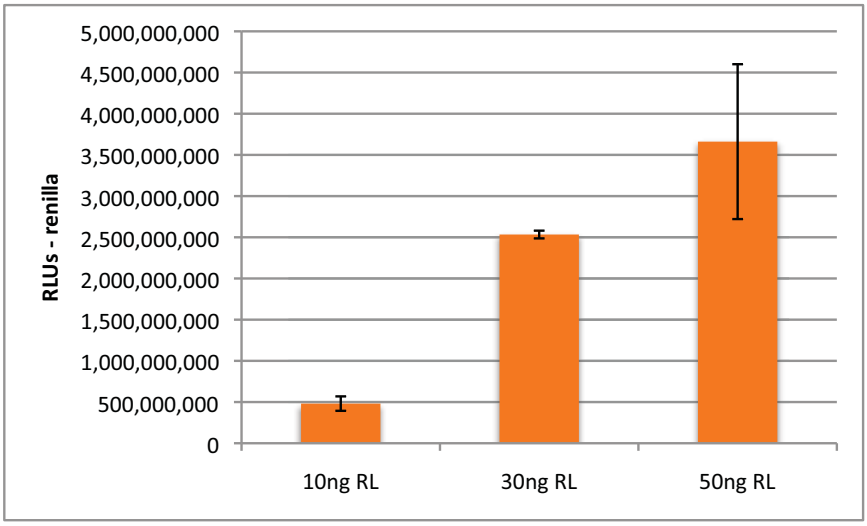


Figure 27. Testing FL and RL vector amounts:
Averaged firefly (a) and renilla (b) luciferase activities from three separate assays

Error bars represent standard deviation of the averages.

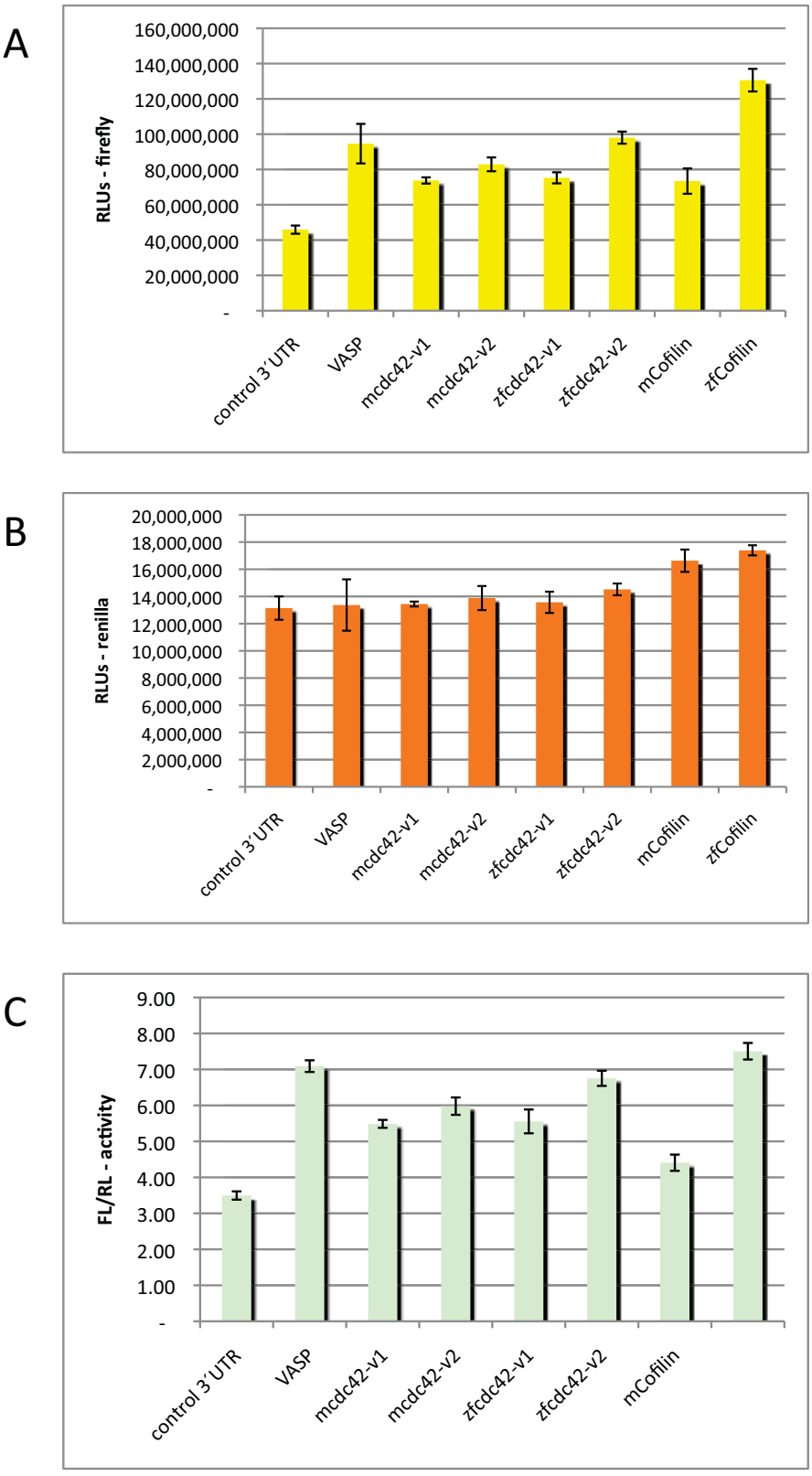


Figure 28. Testing FL and RL activity of all reporter vectors in 293T cells:
Averaged firefly (a) and renilla (b) luciferase activity of three replicates from a single assay. The average of the normalised firefly luciferase activity is shown in c.

Error bars represent standard deviation of the averages.

A

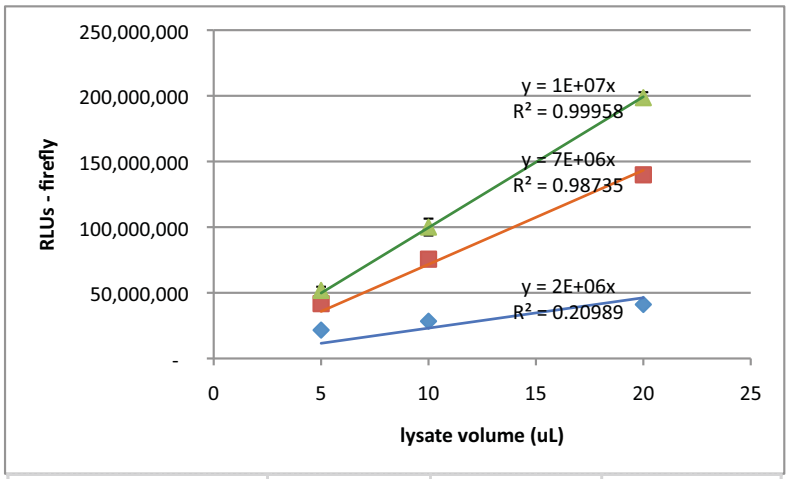


| | 5uL | 10uL | 20uL |
|---|---|---|---|
| 25uL LARII/S&G | 21,607,307 | 28,371,796 | 41,105,804 |
| 50uL LARII/S&G | 41,763,450 | 75,606,192 | 139,851,360 |
| 75uL LARII/S&G | 51,825,280 | 100,047,768 | 198,584,912 |

B

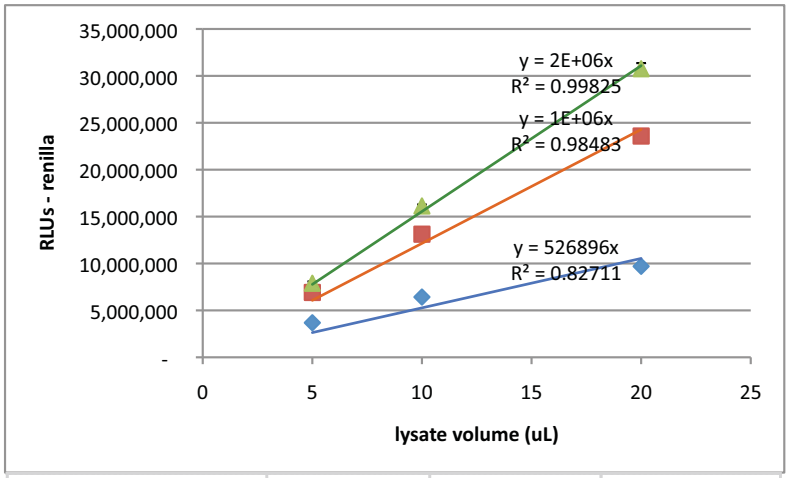


| | 5uL lysate | 10uL lysate | 20uL lysate |
|---|---|---|---|
| 25uL LARII/S&G | 3,682,526 | 6,423,828 | 9,698,488 |
| 50uL LARII/S&G | 6,912,527 | 13,123,189 | 23,587,800 |
| 75uL LARII/S&G | 7,895,844 | 16,132,558 | 30,761,560 |

Figure 29. Examining amount of lysate vs amount of reagents.
Averaged firefly (a) and renilla (b) luciferase activity of three replicates from a single assay.

Blue diamonds = 25uL of LARII and S&G reagent
Red squares = 50uL of LARII and S&G reagents
Green triangles = 75uL of LARII and S&G reagents

Error bars represent standard deviation of the averages.

A

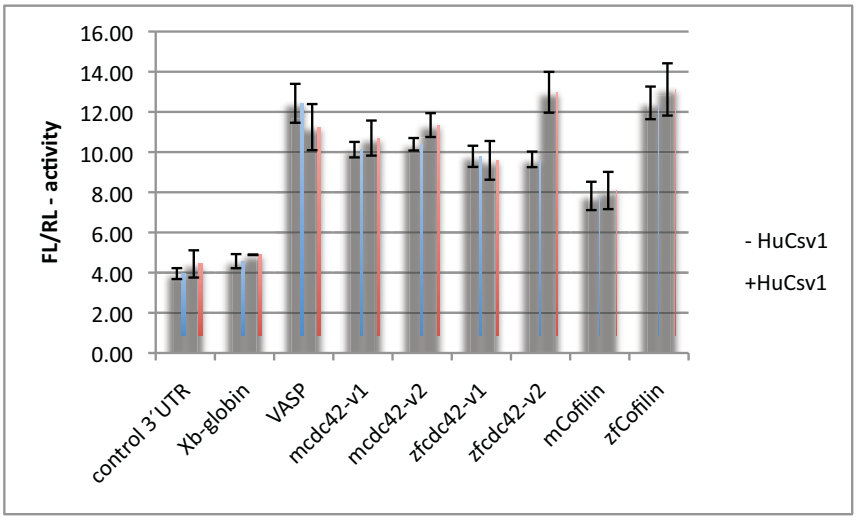


| Reporter: | Normalised firefly activity | | FL/RL (+HuC) / FL/RL (-HuC) | TTEST |
|---|---|---|---|---|
| | - HuCsv1 | +HuCsv1 | | |
| control 3´UTR | 3.95 | 4.43 | 1.12 | 0.23 |
| Xβ-globin | 4.57 | 4.89 | 1.07 | 0.33 |
| VASP | 12.43 | 11.24 | 0.90 | 0.17 |
| mcdc42-v1 | 10.12 | 10.70 | 1.06 | 0.27 |
| mcdc42-v2 | 10.39 | 11.34 | 1.09 | 0.03 |
| zfcdc42-v1 | 9.79 | 9.59 | 0.98 | 0.73 |
| zfcdc42-v2 | 9.64 | 12.98 | 1.35 | 0.00085 |
| mCofilin | 7.82 | 8.09 | 1.03 | 0.66 |
| zfCofilin | 12.45 | 13.12 | 1.05 | 0.42 |

B

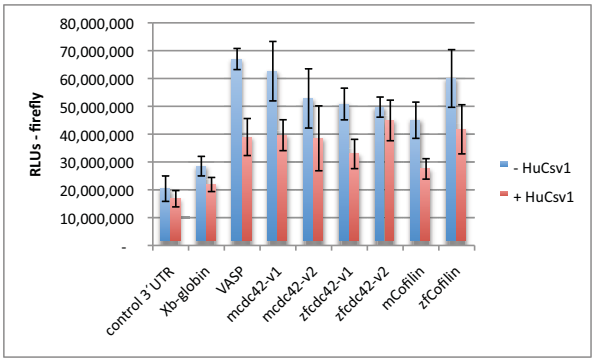


| Raw firefly luciferase values for each 3´UTR-reporter | | | |
|---|---|---|---|
| Reporter: | - HuCsv1 | +HuCsv1 | +HuC/- HuC |
| control 3´UTR | 20,398,409 | 16,786,999 | 0.82 |
| Xβ-globin | 28,490,391 | 21,898,179 | 0.77 |
| VASP | 66,992,833 | 38,959,761 | 0.58 |
| mcdc42-v1 | 62,622,433 | 39,617,873 | 0.63 |
| mcdc42-v2 | 52,828,922 | 38,497,146 | 0.73 |
| zfcdc42-v1 | 50,830,790 | 32,866,406 | 0.65 |
| zfcdc42-v2 | 49,721,379 | 44,924,032 | 0.90 |
| mCofilin | 44,999,012 | 27,508,674 | 0.61 |
| zfCofilin | 60,009,009 | 41,736,853 | 0.70 |

Figure 30a. Firefly luciferase 3´UTR-reporter assays. Averaged 3´UTR-reporter activity results from 293T transfections (n=4).

Figure 30b. Averaged raw firefly luciferase activity results from 293T transfections (n=4).

Error bars represent standard deviation of averages.

C

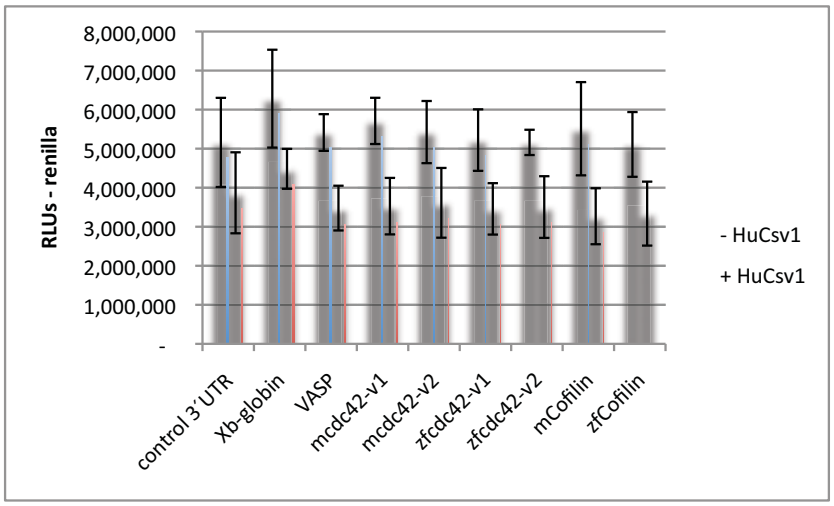


| Raw renilla luciferase values for each 3´UTR-reporter | | | |
|---|---|---|---|
| Reporter: | - HuCsv1 | +HuCsv1 | +HuC/- HuC |
| control 3´UTR | 5,159,621 | 3,869,262 | 0.75 |
| Xβ-globin | 6,280,710 | 4,483,288 | 0.71 |
| VASP | 5,413,789 | 3,477,445 | 0.64 |
| mcdc42-v1 | 5,710,715 | 3,527,409 | 0.62 |
| mcdc42-v2 | 5,424,493 | 3,612,607 | 0.67 |
| zfcdc42-v1 | 5,219,492 | 3,457,483 | 0.66 |
| zfcdc42-v2 | 5,160,301 | 3,504,210 | 0.68 |
| mCofilin | 5,510,473 | 3,268,898 | 0.59 |
| zfCofilin | 5,108,330 | 3,335,950 | 0.65 |
| | | | |
| average RL activity | 5,443,103 +/- 371,038 | 3,615,172 +/- 367,408 | 0.66 +/- 0.047 |

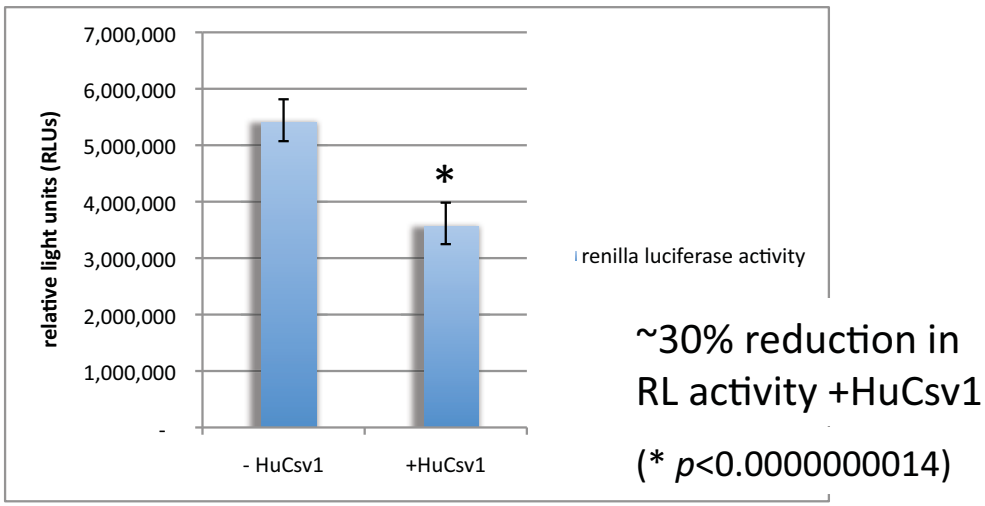


Figure 30c. Averaged raw renilla luciferase activity results for each 3´UTR-reporter from 293T transfections (n=4).

Error bars represent standard deviation of averages.

Bottom graph shows the averaged averages for renilla luciferase activity + or - HuCsv1

A

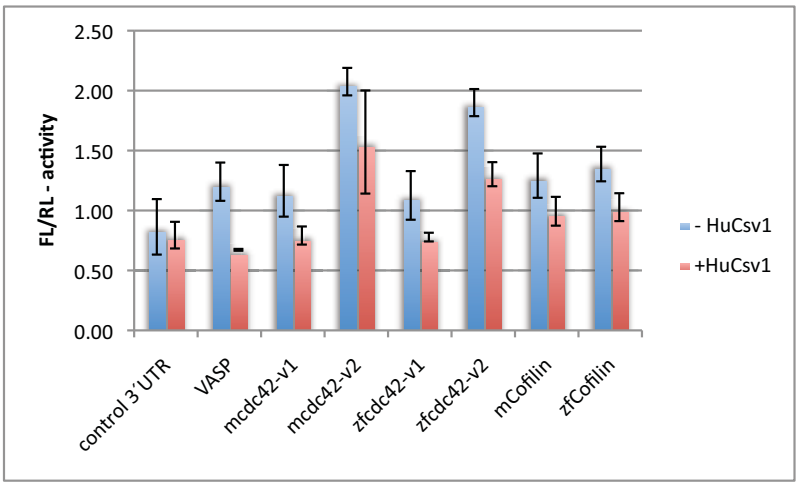


| Reporter: | Normalised firefly activity | | FL/RL (+HuC) / FL/RL (-HuC) | TTEST |
|---|---|---|---|---|
| | - HuCsv1 | +HuCsv1 | | |
| control 3´UTR | 0.86 | 0.79 | 0.92 | 0.665 |
| VASP | 1.24 | 0.67 | 0.54 | 0.004 |
| mcdc42-v1 | 1.16 | 0.79 | 0.68 | 0.047 |
| mcdc42-v2 | 2.07 | 1.57 | 0.76 | 0.122 |
| zfcdc42-v1 | 1.13 | 0.78 | 0.69 | 0.043 |
| zfcdc42-v2 | 1.90 | 1.30 | 0.69 | 0.002 |
| mCofilin | 1.29 | 0.99 | 0.77 | 0.080 |
| zfCofilin | 1.39 | 1.03 | 0.74 | 0.028 |

B

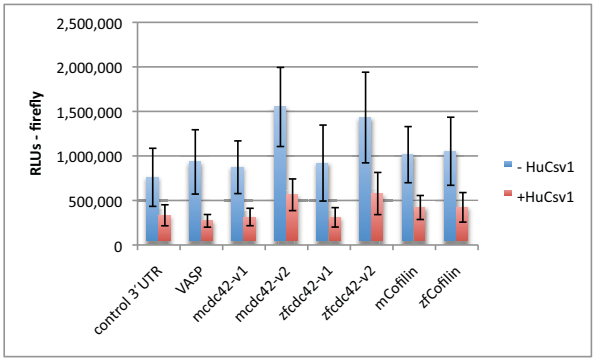


| Reporter: | - HuCsv1 | +HuCsv1 | +HuC/- HuC |
|---|---|---|---|
| control 3´UTR | 759,801 | 333,380 | 0.44 |
| VASP | 932,972 | 271,089 | 0.29 |
| mcdc42-v1 | 872,916 | 314,197 | 0.36 |
| mcdc42-v2 | 1,549,979 | 563,598 | 0.36 |
| zfcdc42-v1 | 920,171 | 310,219 | 0.34 |
| zfcdc42-v2 | 1,431,178 | 577,733 | 0.40 |
| mCofilin | 1,014,229 | 420,917 | 0.42 |
| zfCofilin | 1,052,510 | 422,781 | 0.40 |

Figure 31a. Firefly luciferase 3´UTR-reporter assays. Averaged 3´UTR-reporter activity results from HeLa transfections (n=3).

Figure 31b. Averaged raw firefly luciferase activity results from HeLa transfections (n=3).

Error bars represent standard deviation of averages.

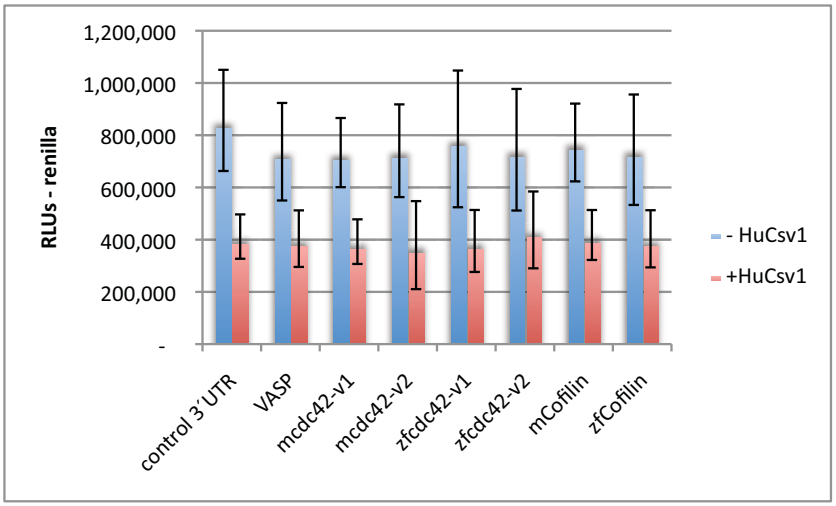


| Raw renilla luciferase values for each 3´UTR-reporter | | | |
|---|---|---|---|
| Reporter: | - HuCsv1 | +HuCsv1 | +HuC/- HuC |
| control 3´UTR | 856,679 | 411,827 | 0.48 |
| VASP | 736,802 | 403,912 | 0.55 |
| mcdc42-v1 | 733,440 | 392,419 | 0.54 |
| mcdc42-v2 | 740,522 | 379,099 | 0.51 |
| zfcdc42-v1 | 785,934 | 395,012 | 0.50 |
| zfcdc42-v2 | 744,386 | 437,403 | 0.59 |
| mCofilin | 772,134 | 417,916 | 0.54 |
| zfCofilin | 744,419 | 403,294 | 0.54 |
| | | | |
| average RL activity | 764,289 +/- 41,625 | 405,110 +/- 17,713 | 0.53 +/- 0.033 |

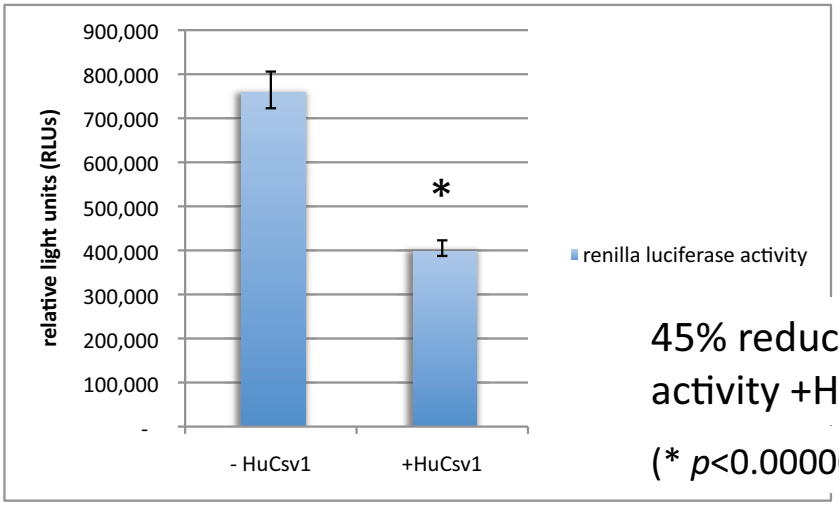


Figure 31c (top graph and table). Averaged raw renilla luciferase activity for each 3´UTR-reporter HeLa transfections (n=3).

Bottom graph shows the averaged averages for renilla luciferase activity + or - HuCsv1

Error bars represent standard deviation of averages.

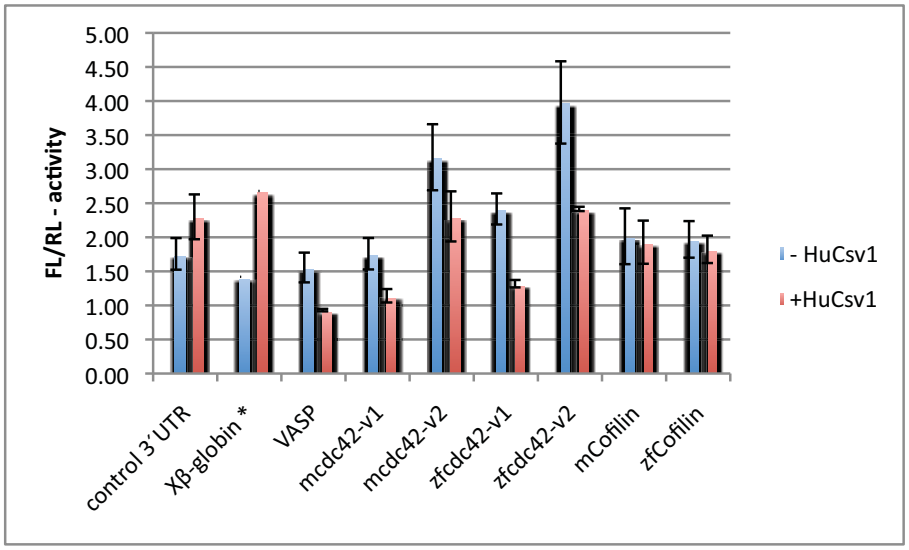


| Reporter: | Normalised firefly activity | | FL/RL (+HuC) / FL/RL (-HuC) | TTEST |
|---|---|---|---|---|
| | - HuCsv1 | +HuCsv1 | | |
| control 3´UTR | 1.76 | 2.30 | 1.31 | 0.035 |
| Xβ-globin * | 1.42 | 2.68 | 1.89 | - |
| VASP | 1.56 | 0.93 | 0.60 | 0.001 |
| mcdc42-v1 | 1.76 | 1.14 | 0.65 | 0.003 |
| mcdc42-v2 | 3.17 | 2.31 | 0.73 | 0.029 |
| zfcdc42-v1 | 2.42 | 1.32 | 0.55 | 0.000084 |
| zfcdc42-v2 | 3.98 | 2.42 | 0.61 | 0.002 |
| mCofilin | 2.01 | 1.93 | 0.96 | 0.749 |
| zfCofilin | 1.97 | 1.82 | 0.93 | 0.417 |

Figure 32a. Firefly luciferase 3´UTR-reporter assays. Averaged 3´UTR-reporter activity results from Neuro-2a transfections (n=4).

Error bars represent standard deviation of averages.

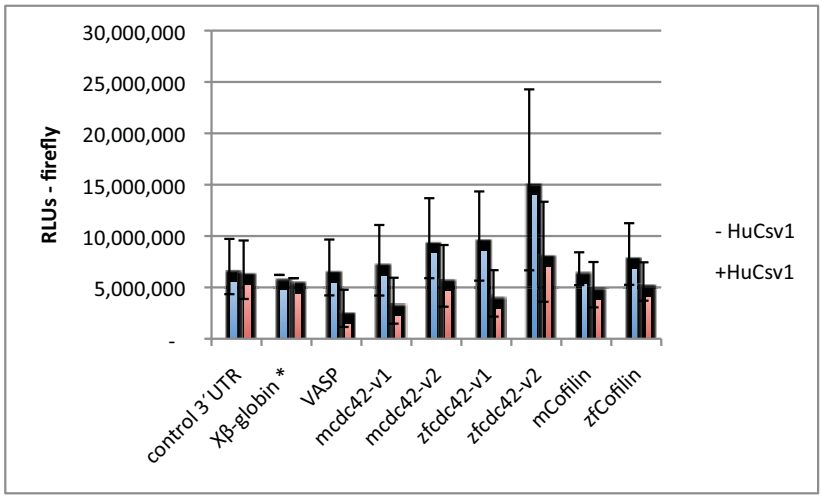


| Reporter: | - HuCsv1 | +HuCsv1 | +HuC/- HuC |
|---|---|---|---|
| control 3´UTR | 7,031,602 | 6,719,646 | 0.96 |
| Xβ-globin * | 6,213,817 | 5,900,604 | 0.95 |
| VASP | 6,941,446 | 2,960,344 | 0.43 |
| mcdc42-v1 | 7,641,748 | 3,705,213 | 0.48 |
| mcdc42-v2 | 9,791,525 | 6,123,516 | 0.63 |
| zfcdc42-v1 | 9,999,351 | 4,417,288 | 0.44 |
| zfcdc42-v2 | 15,469,685 | 8,470,659 | 0.55 |
| mCofilin | 6,821,658 | 5,263,596 | 0.77 |
| zfCofilin | 8,250,919 | 5,573,249 | 0.68 |

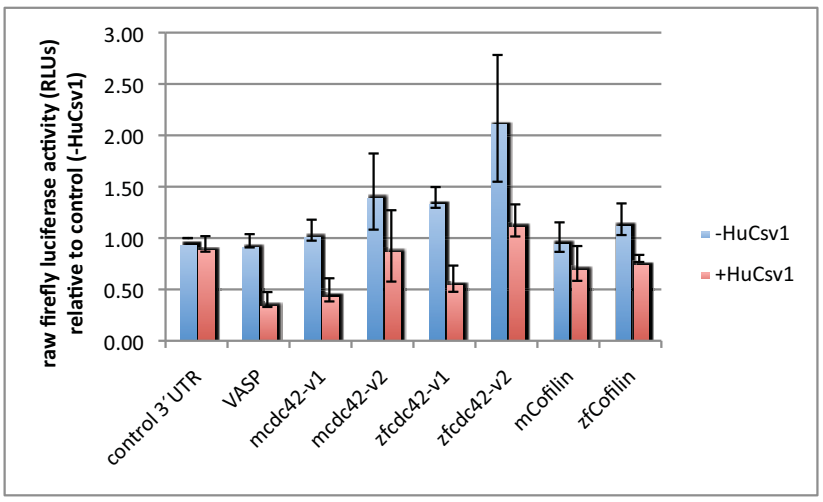


| raw firefly luciferase activity normalised to control 3´UTR (-HuCsv1) (n=4) | | |
|---|---|---|
| Reporter: | -HuCsv1 | +HuCsv1 |
| control 3´UTR | 1.00 | 0.94 |
| VASP | 0.97 | 0.40 |
| mcdc42-v1 | 1.08 | 0.50 |
| mcdc42-v2 | 1.45 | 0.92 |
| zfcdc42-v1 | 1.40 | 0.60 |
| zfcdc42-v2 | 2.17 | 1.17 |
| mCofilin | 1.01 | 0.75 |
| zfCofilin | 1.18 | 0.80 |

Figure 32b (top graph and table). Averaged raw firefly luciferase activity results from Neuro-2a transfections (n=4).

Figure 32b (bottom graph and table). Averaged difference in raw firefly luciferase activity values relative to the control 3´UTR (–HuCsv1 activity) value from each experiment (n=4).

Error bars represent standard deviation of averages.

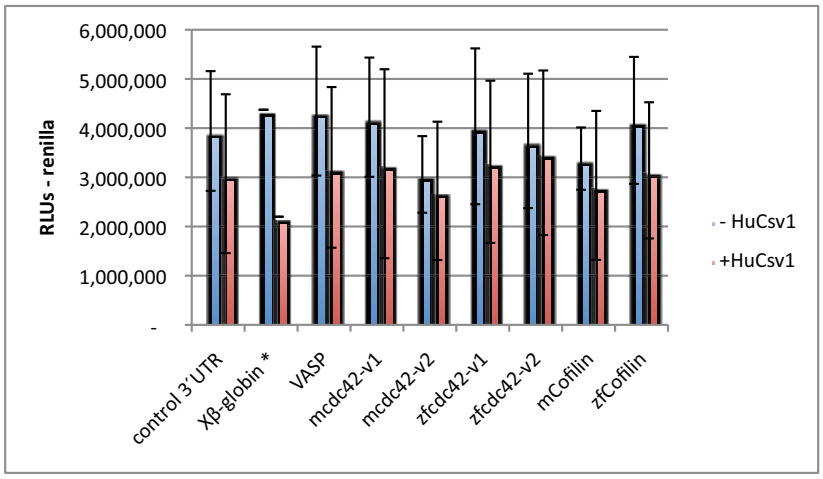


| Raw renilla luciferase values for each 3´UTR-reporter | | | |
|---|---|---|---|
| Reporter: | - HuCsv1 | +HuCsv1 | +HuC/- HuC |
| control 3´UTR | 3,941,936 | 3,073,655 | 0.78 |
| Xβ-globin * | 4,373,376 | 2,198,456 | 0.50 |
| VASP | 4,346,305 | 3,201,640 | 0.74 |
| mcdc42-v1 | 4,221,764 | 3,275,757 | 0.78 |
| mcdc42-v2 | 3,058,650 | 2,724,380 | 0.89 |
| zfcdc42-v1 | 4,036,951 | 3,315,589 | 0.82 |
| zfcdc42-v2 | 3,740,476 | 3,499,742 | 0.94 |
| mCofilin | 3,379,841 | 2,835,554 | 0.84 |
| zfCofilin | 4,157,214 | 3,141,193 | 0.76 |
| | | | |
| average RL activity | 3,917,391 +/- 449,254 | 3,029,552 +/- 391,953 | 0.78 +/- 0.123 |

Figure 32c. Averaged raw renilla luciferase activity results from Neuro-2a transfections (n=4).

Error bars represent standard deviation of averages.

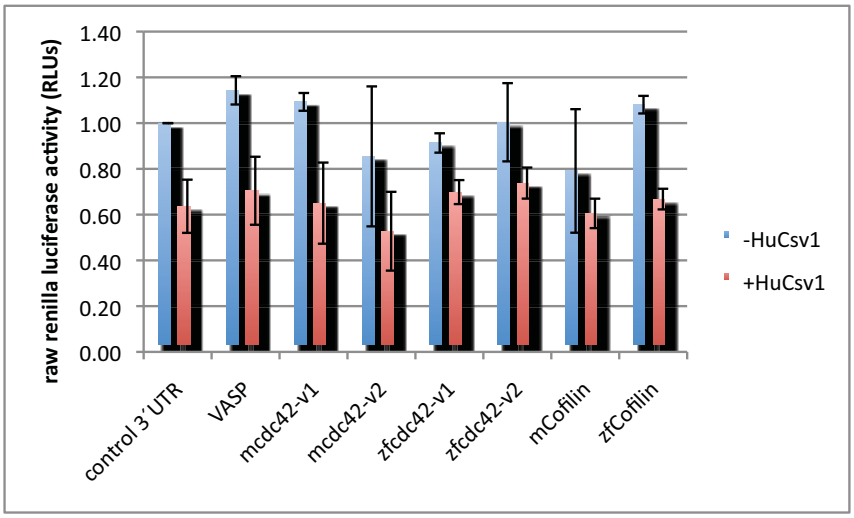


| raw renilla luciferase activity normalised to control 3´UTR (-HuCsv1) (n=4) | | |
|---|---|---|
| Reporter: | -HuCsv1 | +HuCsv1 |
| control 3´UTR | 1.00 | 0.64 |
| VASP | 1.14 | 0.70 |
| mcdc42-v1 | 1.09 | 0.65 |
| mcdc42-v2 | 0.85 | 0.53 |
| zfcdc42-v1 | 0.91 | 0.70 |
| zfcdc42-v2 | 1.00 | 0.74 |
| mCofilin | 0.79 | 0.61 |
| zfCofilin | 1.08 | 0.67 |
| | | |
| average | 0.98 | 0.65 |
| STDEV | 0.12 | 0.07 |

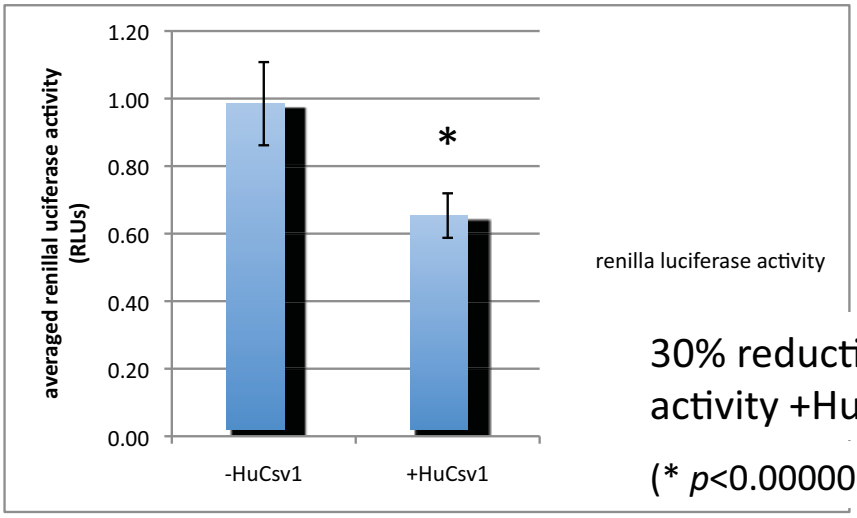


Figure 32d. Averaged difference in raw renilla luciferase activity values relative to the control 3´UTR-reporter (–HuCsv1 activity) value from each experiment (n=4).

(Bottom graph) - averaged averages (from raw renilla luciferase activity normalised to the RL value for the control 3´UTR-reporter for renilla luciferase activity + or - HuCsv1

Error bars represent standard deviation of averages.

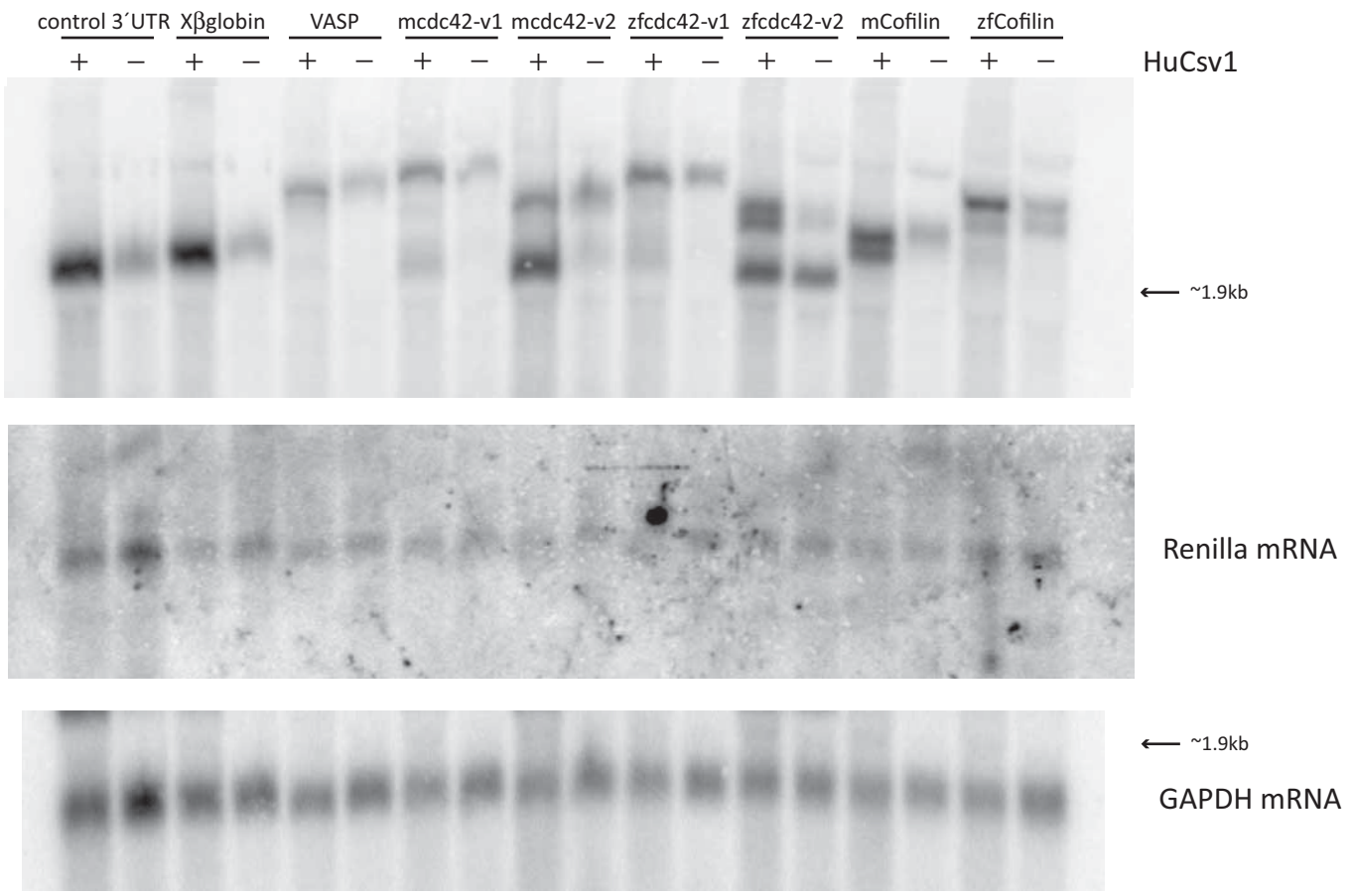


Figure 33. Firefly luciferase-based 3´UTR-reporter Northern experiment - Neuro-2a cells.

Total RNA from transfected Neuro-2a cells was probed with a radiolabelled DNA probe complementary to the firefly luciferase coding sequence (top image). A second probe was used to detect the coding sequence of the renilla luciferase transfection control reporter mRNA (middle image) and a third probe used to detect the GAPDH coding sequence (as a loading control - bottom image). The migration of size standards was not recorded for this Northern. The approximate location of the 28S ribosomal RNA (1.9kb) is indicated

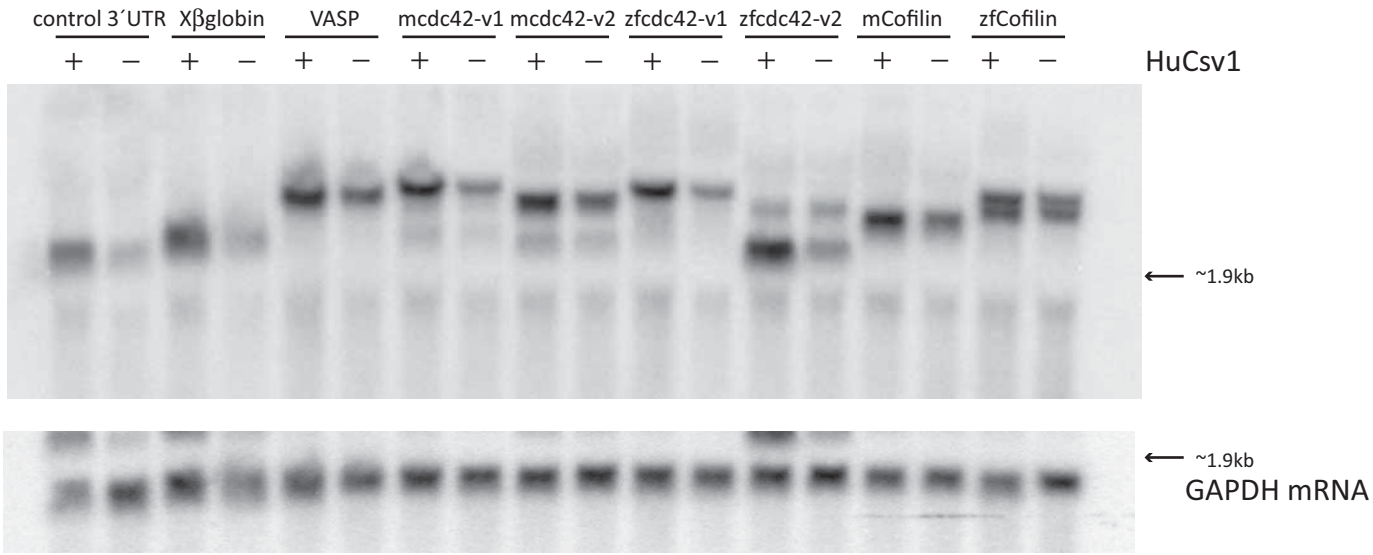


Figure 34. Firefly luciferase-based 3´UTR-reporter Northern experiment - 293T cells.

Total RNA from transfected 293T cells was probed with a radiolabelled DNA probe complementary to the firefly luciferase coding sequence (top image) and a second probe complementary to the GAPDH coding sequence (as a loading control - bottom image). The migration of size standards was not recorded for this Northern. The approximate location of the 18S ribosomal RNA (1.9kb) is indicated

| FL 3´UTR reporter mRNA Abundance (Int. Dens) | | | | Corrected to GAPDH | |
|---|---|---|---|---|---|
| Reporter: | - HuCsv1 | +HuCsv1 | | +HuCsv1 | fold change |
| control 3´UTR | 681 | 1,733 | | 2,568 | 3.77 |
| Xβ-globin 3´UTR | 566 | 1,583 | | 1,695 | 2.99 |
| VASP terminal | 465 | 533 | | 606 | 1.30 |
| mcdc42-v1 terminal | 468 | 727 | | 1,070 | 2.29 |
| mcdc42-v1 very early | 38 | 246 | | 362 | 9.61 |
| *mcdc42L (total)* | *506* | | | *1,433* | |
| mcdc42-v2 SV40 | 592 | 443 | | 638 | 1.08 |
| mcdc42-v2 early | 239 | 1,142 | | 1,644 | 6.89 |
| *mcdc42S (total)* | *831* | | | *2,282* | |
| zfcdc42-v1 terminal | 608 | 739 | | 937 | 1.54 |
| zfcdc42-v1 early | 59 | 193 | | 245 | 4.12 |
| *zfcdc42L (total)* | *667* | | | *1,183* | |
| zfcdc42-v2 SV40 | 112 | 509 | | 503 | 4.49 |
| zfcdc42-v2 terminal | 165 | 468 | | 462 | 2.80 |
| zfcdc42-v2 non-canonical early | 744 | 841 | | 830 | 1.12 |
| *zfcdc42S (total)* | *1,021* | | | *1,795* | |
| mCofilin SV40 | 309 | 579 | | 638 | 2.06 |
| mCofilin terminal | 91 | 535 | | 589 | 6.49 |
| *mCofilin (total)* | *400* | | | *1,227* | |
| zfCofilin non-canonical late | 223 | 545 | | 745 | 3.34 |
| zfCofilin terminal | 192 | 169 | | 231 | 1.20 |
| *zfCofilin (total)* | *415* | | | *976* | |

| RL mRNA Abundance (Int. Dens) | | | | Corrected to GAPDH | |
|---|---|---|---|---|---|
| Reporter: | - HuCsv1 | +HuCsv1 | | +HuCsv1 | fold change |
| control 3`UTR | 241 | 165 | | 244 | 1.01 |
| Xβ-globin | 130 | 101 | | 108 | 0.83 |
| VASP | 101 | 100 | | 114 | 1.13 |
| mcdc42-v1 | 107 | 87 | | 129 | 1.20 |
| mCofilin | 81 | 72 | | 79 | 0.97 |
| | | | | | |
| Average | 132 | 105 | | 135 | 1.03 |
| STDEV | 63 | 35 | | 64 | 0.14 |

| GAPDH mRNA Abundance (Int. Dens) | | | |
|---|---|---|---|
| Reporter: | - HuCsv1 | +HuCsv1 | fold change |
| control 3´UTR | 791 | 534 | 0.67 |
| Xβ-globin | 585 | 547 | 0.93 |
| VASP | 541 | 476 | 0.88 |
| mcdc42-v1 | 530 | 360 | 0.68 |
| mcdc42-v2 | 468 | 325 | 0.69 |
| zfcdc42-v1 | 482 | 380 | 0.79 |
| zfcdc42-v2 | 426 | 432 | 1.01 |
| mCofilin | 397 | 360 | 0.91 |
| zfCofilin | 470 | 344 | 0.73 |

Table 5. Firefly luciferase 3´UTR-reporter Neuro-2a cell line Northern – mRNA abundance

Values tabled represent mRNA abundance values (Integrated Density) minus background as determined from Northern analysis.

Fold changes = difference in mRNA abundance between +HuCsv1 and –HuCsv1 samples (+HuC/-HuC).

| FL 3´UTR reporter mRNA Abundance (Int. Dens) | | | | Corrected to GAPDH | |
|---|---|---|---|---|---|
| Reporter: | - HuCsv1 | +HuCsv1 | | +HuCsv1 | fold change |
| control 3´UTR | 239 | 488 | | 727 | 3.04 |
| Xβ-globin | 200 | 605 | | 306 | 1.53 |
| VASP | 491 | 595 | | 635 | 1.29 |
| mcdc42-v1 terminal | 299 | 627 | | 560 | 1.87 |
| mcdc42-v1 early | 56 | 86 | | 77 | 1.38 |
| *mcdc42-v1 (total)* | *355* | | | *637* | |
| mcdc42-v2 SV40 | 479 | 601 | | 634 | 1.32 |
| mcdc42-v2 early | 116 | 146 | | 154 | 1.32 |
| *mcdc42-v2 (total)* | *595* | | | *787* | |
| zfcdc42-v1 terminal | 297 | 573 | | 535 | 1.80 |
| zfcdc42-v1 middle | 61 | 59 | | 55 | 0.90 |
| zfcdc42-v1 early | 33 | 43 | | 40 | 1.21 |
| *zfcdc42-v1 (total)* | *392* | | | *630* | |
| zfcdc42-v2 terminal | 150 | 115 | | 125 | 0.83 |
| zfcdc42-v2 non-canonical early | 249 | 613 | | 662 | 2.65 |
| *zfcdc42-v2 (total)* | *399* | | | *787* | |
| mCofilin SV40 | 412 | 566 | | 595 | 1.44 |
| zfCofilin non-canonical late | 278 | 350 | | 515 | 1.85 |
| zfCofilin terminal | 340 | 377 | | 554 | 1.63 |
| *zfCofilin (total)* | *618* | | | *1,070* | |

| GAPDH mRNA Abundance (Int. Dens) | | | |
|---|---|---|---|
| Reporter: | - HuCsv1 | +HuCsv1 | fold change |
| control 3´UTR | 570 | 383 | 0.67 |
| Xβ-globin | 302 | 597 | 1.98 |
| VASP | 476 | 446 | 0.94 |
| mcdc42-v1 | 504 | 564 | 1.12 |
| mcdc42-v2 | 525 | 498 | 0.95 |
| zfcdc42-v1 | 421 | 451 | 1.07 |
| zfcdc42-v2 | 526 | 487 | 0.93 |
| mCofilin | 449 | 426 | 0.95 |
| zfCofilin | 523 | 356 | 0.68 |

Table 6. Firefly luciferase 3´UTR-reporter HEK293T cell line Northern – mRNA abundance

Values tabled represent mRNA abundance values (Integrated Density) minus background as determined from Northern analysis.

Fold changes = difference in mRNA abundance between +HuCsv1 and –HuCsv1 samples (+HuC/-HuC)

A

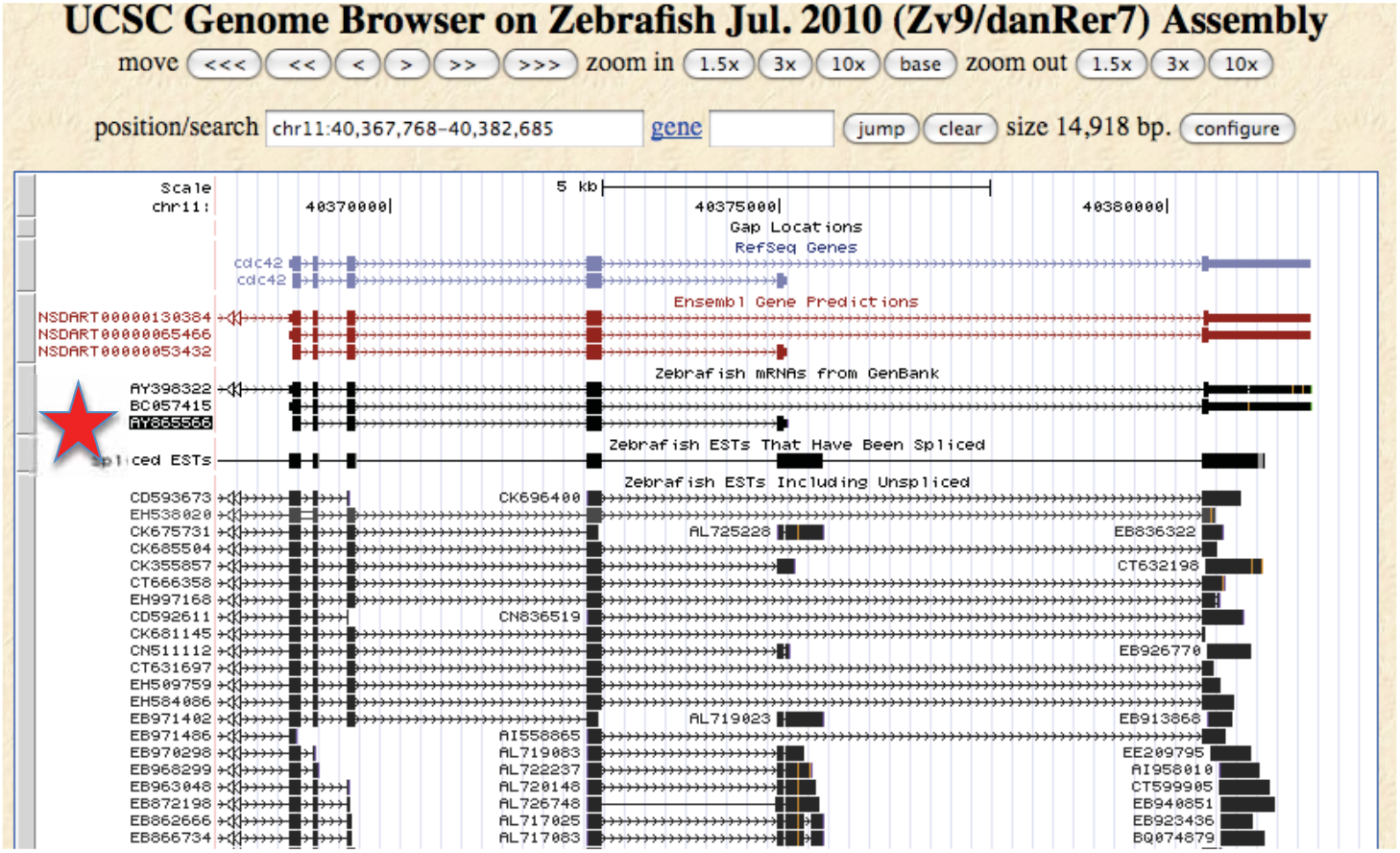


B

**cDNA AY865566**

```
ATGCAGACGA TCAAGTGCGT CGTTGTTGGT GATGGTGCAG TGGGTAAAAC  50
CTGTCTATTA ATCTCCTATA CAACTAATAA ATTCCCCTCC GAATATGTAC 100
CAACGGTCTT TGATAACTAT GCAGTTACGG TTATGATTGG TGGTGAGCCG 150
TACACCCTGG GGCTGTTTGA TACTGCAGGT CAGGAAGATT ACGATAGATT 200
ACGACCCCTG AGTTACCCTC AGACAGATGT CTTCTTAGTC TGTTTCTCAG 250
TTGTTTCACC TTCTTCATTT GAAAACGTCA AAGAAAAGTG GGTACCCGAG 300
ATCACCCACC ACTGTCCAAA GACCCCTTTC CTGCTGGTGG GGACGCAGAT 350
TGATCTGAGA GATGATCCTT CTACTATCGA AAAGCTTGCC AAGAACAAAC 400
AGAAACCCAT CACTCCAGAG ACGGCAGAGA AGCTGGCCCG CGATCTGAAG 450
GCTGTCAAAT ACGTGGAATG CTCCGCTCTG ACGCAGCGAG GTCTGAAGAA 500
TGTATTTGAT GAAGCTATCC TAGCTGCCCT CGAACCTCCT GAAACGCAGC 550
GAAAACGGAA GTGCTGTATA TTTTAAACCT CTCTCTCTCT CTTTCTCTCT 600
CTTTCTAACT CCCCACACTT tc
```

Figure 35. Screen shots from the UCSC genome browser showing the GenBank-submitted zfcdc42-v2 mRNA sequence AY865566 on a genome alignment (A – red star) and the complete mRNA sequence (B)

| FL activity / FL mRNA | | |
|---|---|---|
| Reporter: | - HuCsv1 | +HuCsv1 |
| control 3´UTR | 10,324.79 | 2,616.64 |
| Xβ-globin | 10,977.01 | 3,481.05 |
| VASP | 14,929.96 | 4,883.45 |
| mcdc42-v1 | 15,104.18 | 2,586.47 |
| mcdc42-v2 | 11,788.50 | 2,683.30 |
| zfcdc42-v1 | 14,989.22 | 3,734.99 |
| zfcdc42-v2 | 15,149.86 | 4,719.04 |
| mCofilin | 17,061.41 | 4,289.92 |
| zfCofilin | 19,866.87 | 5,713.09 |

| RL activity / RL mRNA | | | |
|---|---|---|---|
| Reporter: | - HuCsv1 | +HuCsv1 | fold change |
| control 3´UTR | 16,380 | 18,678 | 0.88 |
| Xβ-globin | 33,609 | 21,808 | 1.54 |
| VASP | 43,005 | 31,887 | 1.35 |
| mcdc42-v1 | 39,274 | 37,489 | 1.05 |
| mCofilin | 41,537 | 39,652 | 1.05 |
| Average | 34,761 | 29,903 | 1.17 |
| STDEV | 10,879 | 9,328 | 0.27 |
| TTEST (p-value) | 0.47015781 | | |

$$\text{Translation efficiency} = \frac{\text{(FL activity / FL mRNA abundance)}}{\text{(RL activity / RL mRNA abundance)}}$$

| Translation Efficiency | | |
|---|---|---|
| Reporter: | - HuCsv1 | +HuCsv1 |
| control 3´UTR | 0.63 | 0.14 |
| Xβ-globin | 0.33 | 0.16 |
| VASP | 0.35 | 0.15 |
| mcdc42-v1 | 0.38 | 0.07 |
| mCofilin | 0.28 | 0.07 |

| Translation Efficiency (vs: control 3`UTR - HuCsv1) | | | |
|---|---|---|---|
| Reporter: | - HuCsv1 | +HuCsv1 | fold change |
| control 3´UTR | 1.00 | 0.22 | 4.50 |
| Xβ-globin | 0.52 | 0.25 | 2.05 |
| VASP | 0.55 | 0.24 | 2.27 |
| mcdc42-v1 | 0.61 | 0.11 | 5.57 |
| mCofilin | 0.45 | 0.11 | 4.19 |

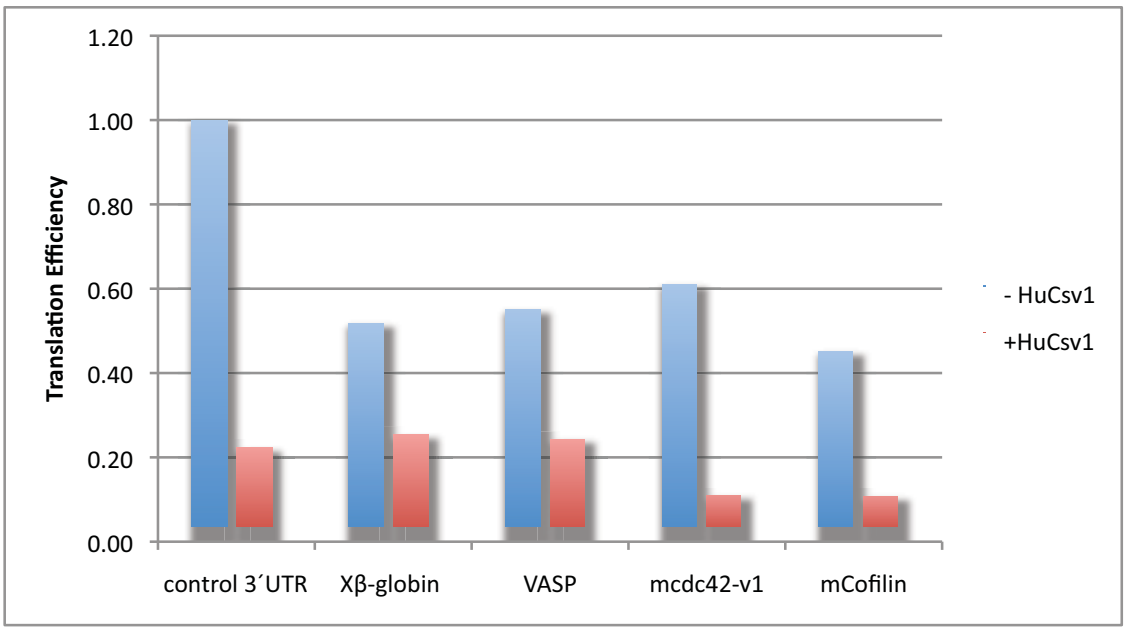


Figure 36. Translation efficiency calculation for firefly luciferase 3´UTR-reporters – Neuro-2a

Averaged (n=4) raw luciferase activities were divided by raw mRNA abundance values for each reporter. Where multiple mRNA products were present for a given 3´UTR-reporter, the total amount of mRNA detected was used.

Translation efficiency is shown relative to the control 3´UTR-reporter in the absence of HuCsv1.

Fold changes represent difference between (– HuCsv1) and (+HuCsv1) conditions

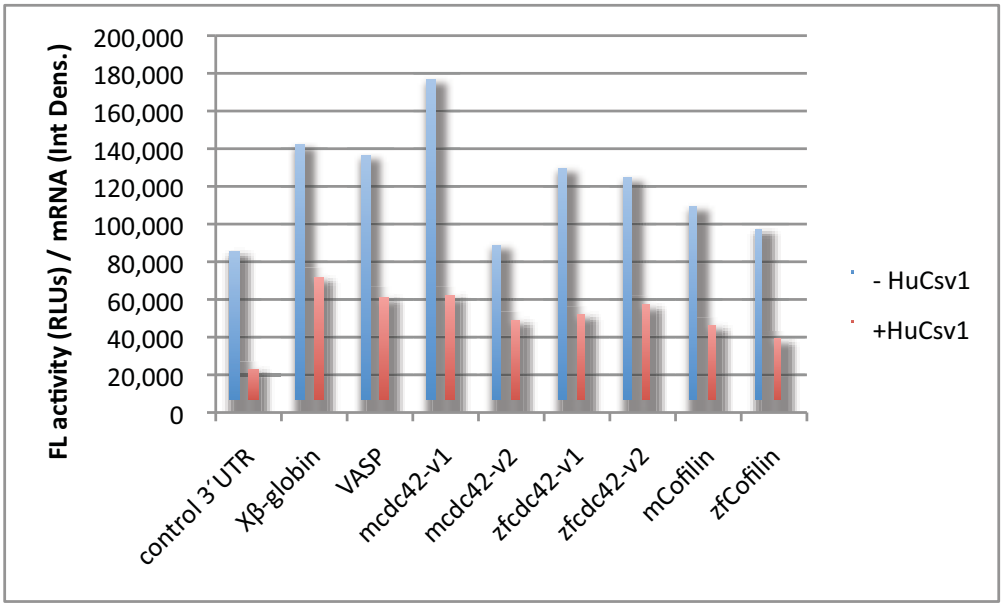


| FL activity / FL mRNA | | | |
|---|---|---|---|
| Reporter: | - HuCsv1 | +HuCsv1 | fold change |
| control 3´UTR | 85,406 | 23,089 | 3.70 |
| Xβ-globin | 142,173 | 71,618 | 1.99 |
| VASP | 136,395 | 61,306 | 2.22 |
| mcdc42-v1 | 176,595 | 62,206 | 2.84 |
| mcdc42-v2 | 88,860 | 48,911 | 1.82 |
| zfcdc42-v1 | 129,739 | 52,149 | 2.49 |
| zfcdc42-v2 | 124,496 | 57,115 | 2.18 |
| mCofilin | 109,114 | 46,206 | 2.36 |
| zfCofilin | 97,173 | 39,023 | 2.49 |

Figure 37. Firefly luciferase 3´UTR-reporter expression normalised to mRNA abundance – 293T

Fold change represents reduction in mRNA-normalised expression of averaged (n=4) firefly luciferase activity from 3´UTR-reporters in the presence of HuCsv1

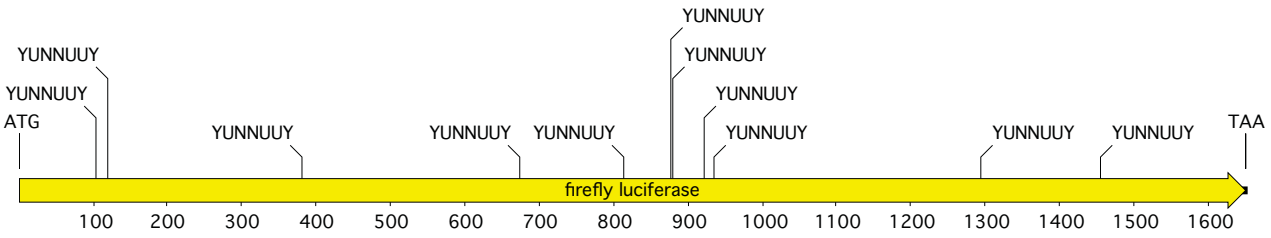


Figure 38. Location of potential HuCsv1 interaction sites within the firefly luciferase coding sequence.

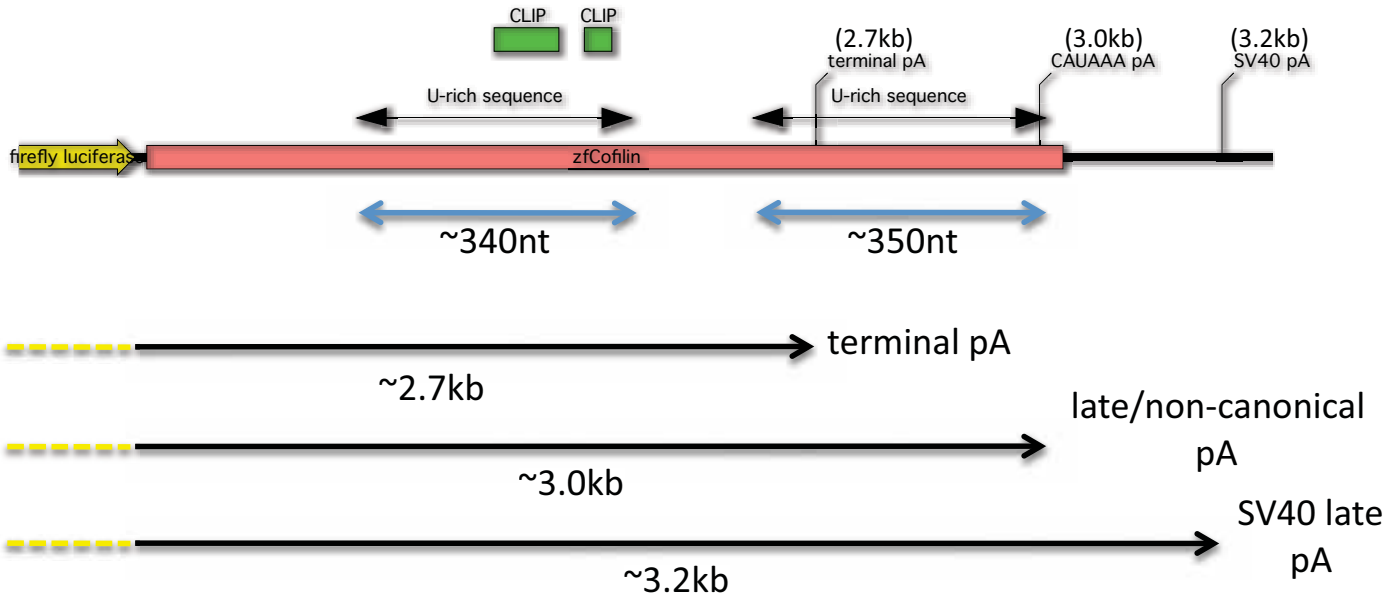


Figure 39a. Schematic representation of the zfCofilin 3´UTR within the firefly luciferase reporter vector

pA = predicted polyadenylation site
CLIP = region identified by CLIP isolation of putative target mRNAs of neuronal Hu proteins

Predicted sizes of reporter mRNAs are based on a full transcript including all sequence upstream of the firefly luciferase coding sequence beginning from the transcription start site (TATA-box of the CMV promoter). They do not account for polyA tail length.

zfCofilin 3´UTR

tgaGGCUGACACAUUUCAGGGGUUUAGCCGUUCAUUCCGACAUGGGUAGGGCAGAUGGGCACAGCACA

CCACUGUUCGUGGGCCAUGGGUGGGUUAAUGCGGGUGGGGAGGGUCGGGCAAAAGUGACAGUUUCC

AAACUCCACACGACGAAAGAUGUAGGCUGUCAUUCCAGUUCACACAUACAAUGAACAAGAACAAAAACA

CAAAAAGAGAAACAAAAAAAAAGAUCUUAAAAGACAAAAAUGAAGGAUGAUGAUUAUAAAAACAAAGU

AAUAUAACUGUAAAUGUGUACUGGCAGGUUUUCCUUCUUUCUGGGUUCCAUUAGAUUGUCAAUACG

AAAGACUGAGACAGCAGCCAUUACAAUUCAGCUAUACAACAUACUGUUUGUUCUUAAGAUUUAGUUU

UUUUUUUUUUUUUUUGCC***AAACGUCUAGUUAAGUUUAUUUUCUAAGUUUGUGUGUGU***

***UGCGACUAGGUAUAGUACAAAGUCACACAUUGUUAUCGGACC***AUUCUGGGAACACGAUCU

ACUCCCCUUU***CCCUCUUAUUUUAUUUUUGAGCAAGUUAUUUUAAU***GAUUCCAUCUGAUUU

AAAUCUUUCCAAACGUUCAGUCAAAAUCAUGGCACUGGUGUCAAGAAAUUGUACACAUUCCUUCUACC

UGUAUAAUCUGGGACCUAGUGGAUGAGCGGUCUGUUGAAGAAUUUGAAUUGAAGGACACGUAUGAA

GUUUAGAUGGGGAGAGCGAUAUAUUUGGGCAGCCUGUGUACAGAGCUUUGAUGGAUAUUGGUCAGU

GGAUGUUUUGUAUCGUCUCCUUAUCUCU**AAUAAA**AAAGCACUAAAUAACUCUGCUGUGUUACAA*CUU*

terminal

*UUUUUUGUUUCAUGUUGGGUGAAUUAUGUGAUAAGGGCUGUAACUUGUCUUUUUUUGGCCCUGGUU*

*GAAUCUAAUUUUACUCUUAGGUUUAAGUUAAGUCCAUAUGAGUUGAUCUUUUUAUAUUGGUUUAUAG*

*AAAUCUGCUUUACAUUUUGUGUCUGGAUAUUGUGCAUUUGUUGCUGUUUUAUCAGUGUUCAGCAUG*

*GUUUAUGCACUGGUAUAUGUGAUGGUUU*GCAACAUU**CAUAAA**GUUUCAAAUGGAUCCAAACAAAGA

Late/non-canonical

Figure 39b. Terminal exon of the zfCofilin mRNA.

The 3´UTR sequence is shown UPPER CASE. The cofilin stop codon is denoted in **red**. Predicted polyadenylation sites are underlined in **green**. Uracil-rich sequences are denoted in italicised **grey** with **grey underline**. The two CLIP-identified nHu binding sites are shown in **black** with **black underline**

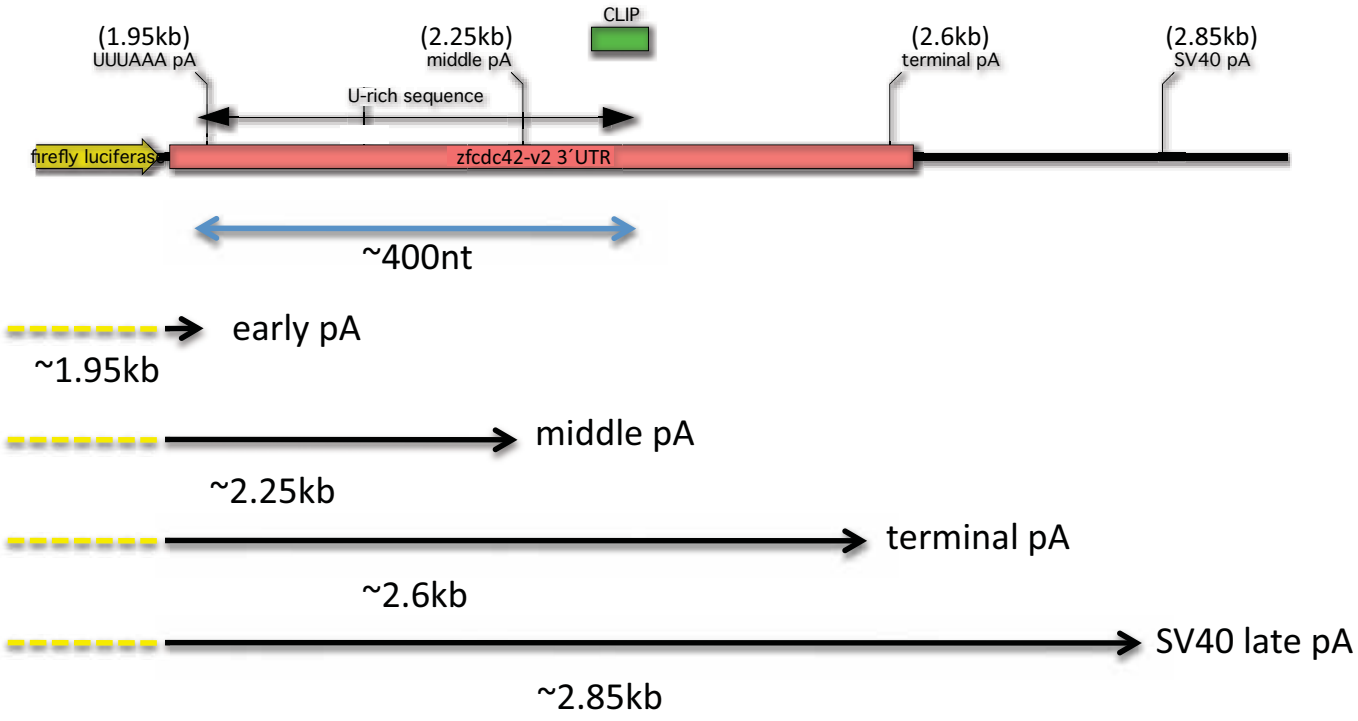


Figure 40a. Schematic representation of the zfcdc42-v2 3´UTR within the firefly luciferase reporter vector

pA = predicted polyadenylation site
CLIP = region identified by CLIP isolation of putative target mRNAs of neuronal Hu proteins

Predicted sizes of reporter mRNAs are based on a full transcript including all sequence upstream of the firefly luciferase coding sequence beginning from the transcription start site (TATA-box of the CMV promoter). They do not account for polyA tail length.

Penultimate exon

uggguacccgagaucacccaccacuguccaaagaccccuuuccugcuggugggacgcagauugaucugagagaugauccuucua

cuaucgaaaagcuugccaagaacaaacagaaacccaucacuccagagacggcagagaagcuggcccgcgaucugaaggcugucaaa

uacguggaaugcuccgcucugacgcag

Terminal exon

cgaggucugaagaauguauuugaugaagcuauccuagcugcccucgaaccuccugaaacgcagcgaaaacggaagugcuguauau

uu**uaa**A*CCUCUCUCUCUCUCUCUCUUUCUAACUCCCC*ACACUUCCCCAGAUGUUUGCUGCUUCCUUUAG

early

UUACCUCUUGCUCCACAGAAAAGACAAGUUUCCCGAUCUUAUAAGUGACGUCAUACCUGUGUAUCUUG

UUUCACAAAU**ACUAAA**GGAUUUGCUUUUGCUGGUUUUCUUUUUUUUUACUUUUUGUCGUGUUUGGA

early*

GACUGUUAAAGUUAAACCCAGCUCUUGGGAGUUCUGUUCGUCUCCAUUCUGCAGAUUAUUUUUAUUA

UUGCUAUUGGGUGCACUUUGAGUUUCAA**AAUAAA**ACAUGUGGAAGUUUACAAUGAAGGAUUGCAUA

middle

UAUAGUUUUGUUUUUUUUGCUUUAAGUG***CUAUUAUGUUGCUUUGGACUUUAUUUCGUCU***

***UACUGUUAUUUAAGAGCA***GACCAAGGUAAAAUAGUUGAGUUCAUUGCUGCUCGGUUUAUUUAC

AUUUCUAAAAAUCUUCUUUCCUUAUGUCAGUGUGUUUAUUUUGUACUUCAGCAGUUGUAUCAUAAA

AUUAAUUCUAAACUUAUUAAUGUAUGGCUACGGUUUGCAAUUUGGUGCCAUUCUUAUCCAUACAACG

UCUUGAGAGUUUAAAUGGCUUAAUAUAAUCCUGUGAAAAAUGAUUUGUGCCAUU**AAUAAA**GGACAG

terminal

CUGCAAUUGCCAU

Figure 40b. Penultimate and terminal exons of the zfcdc42-v2 pre-mRNA.

Coding sequence is shown in lower case and 3´UTR sequence in UPPER CASE. The cdc42 stop codon is denoted in **red**. Predicted polyadenylation sites are underlined in **green**. The pyrimidine-rich sequence proximal to the predicted UUUAAA polyadenylation site is shown in italicised **grey** with **grey underline**. The 24hpf CLIP-identified nHu binding site is shown in **black** with **black underline**

## Renilla luciferase-based 3´UTR-reporter assays

Other than using a different reporter coding sequence, the reporter vectors used in the renilla luciferase-based 3´UTR-reporter assays were identical to the firefly luciferase vectors described thus far (figure 25). However, because firefly luciferase could not be used in these reporter assays, the general assay format had to be altered. A vector encoding β-galactosidase (lacZ) was used in place of renilla luciferase as the transfection control reporter. As such, it was no longer possible to obtain reporter activity data simultaneously for both the 3′UTR-reporter and transfection control reporter. Instead, renilla luciferase activities were obtained using the Glomax96® luminometer as before, while lacZ activity was determined by colourimetric assay using a plate reader set to detect absorbance at 407nm. The Northern assay format was essentially unchanged except that more 3′UTR-reporter vector was transfected per cell to increase the signal for mRNA variants detected by Northern blots. In these assays, 50fmol of 3′UTR reporter vector (~160-170ng) was transfected per well in a 6-well dish, an 8-fold increase over the firefly luciferase reporter transfections. The amount of β-galactosidase reporter vector transfected per well was 80ng. To accommodate the increased amounts of reporter vector(s) used, the total amount of HuCsv1 or empty vector (for the -HuCsv1 condition) transfected were reduced to accommodate the extra reporter vector amounts. In these assays, 750ng of HuCsv1 or empty vector were co-transfected with reporter vectors per well (table 7).

For experiments in which both luciferase activity and mRNA data were collected, transfections were performed using the same transfection cocktails for either assay. This would allow direct correlation between mRNA abundances as determined by Northern and luciferase activity data. Transfections for reporter activity assays were carried out in 12-well plates, as such the total amount of DNA added per well for these assays was one fifth ($1/5^{th}$) that used for the Northerns.

## Northern analysis of the renilla luciferase-based zfcdc42-v2 3′UTR-reporter

Northern analysis of the effect of HuCsv1 on the renilla luciferase-based zfcdc42-v2 3′UTR-reporter was attempted in both 293T and Neuro-2a cell lines. While no significant technical problems were encountered in the 293T experiments, unexpected difficulties were had using the Neuro-2a cell line. Specifically, despite increasing the amount of reporter vectors used, both renilla luciferase and β-galactosidase activities were considerably lower in Neuro-2a cell lysates, than that seen for comparable 293T transfections. This was most evident in the time taken to develop the colourimetric LacZ assay between the two cell lines. For 293T cells, OD readings between 0.1 – 0.9 were attained within 7 minutes of addition of the β-galactosidase substrate, with incubation at room temperature. However, assays for β-galactosidase activity from Neuro-2a cell transfections were consistently slower to develop, typically requiring 20 – 30 minutes at 37°C to reach a comparable optical density. While the reduction in reporter activity did not prevent acquisition of reporter activity data, no Neuro-2a Northern data could be obtained because in all attempts, no signal was reliably observed for either the renilla luciferase or β-galactosidase reporter mRNAs. A cause for the apparent change in Neuro-2a cell transfection efficiency was not identified. As a result of these difficulties only the data from the 293T renilla luciferase reporter assays is presented. Three separate experiments were conducted using the 293T cell line. For the first experiment only Northern analysis was carried out. For the second and third experiments, reporter mRNA abundance (as determined by Northern) and renilla luciferase/β-galactosidase enzyme activity data were obtained.

### *Identity of the early/non-canonical polyadenylation site*

Importantly, the renilla luciferase-based 3′UTR-reporter Northerns provided some support to the prediction that the smallest reporter mRNA transcript observed for the zfcdc42-v2 3′UTR-reporter uses the non-canonical polyadenylation signal UUUAAA hexanucleotide sequence also used for the **AY865566** mRNA submitted to Genbank in June 2010. In all three Northerns (figure 41, 42 and 43), the smallest zfcdc42-v2 3′UTR-reporter mRNA variant clearly migrates faster than the control 3′UTR-reporter mRNA. The greater resolution of this difference in size is likely due to the fact that the renilla luciferase coding sequence is substantially shorter than that of the firefly luciferase sequence (935nt vs 1.65kb) and as such, could be separated with higher resolution in the 1.5% formaldehyde/agarose gels used in these Northerns. In these assays, the predicted length of the control 3′UTR-reporter without polyadenylate tail, is ~1.31kb (figure 44). Looking at the Northerns, the control 3′UTR-reporter appears to run at a size slightly smaller than 1.5kb, which is consistent with a normal polyadenylate tail length of 100-200nt. For the

zfcdc42-v2 3′UTR-reporter (figure 41, 42 and 43), the smallest mRNA variant runs at ~1.3kb in the Northerns. Reporter mRNA cleavage and polyadenylation driven by the UUUAAA hexanucleotide sequence would yield a message with a very short (<50nt) 3′UTR sequence, plus polyadenylate tail. The predicted length of a reporter mRNA using this signal is 1.22kb (minus the polyA tail) (figure 44), which when looking at the Northern is conceivable, given a polyA tail length of 100-200nt. Thus, while the identity of the polyadenylation signal used by the early/non-canonical zfcdc42-v2 reporter mRNA variant has not been conclusively shown, the UUUAAA sequence appears to be the most likely candidate given the available data.

***The early polyadenylation site is contained within a highly uracil-rich region***

Examination of the zfcdc42-v2 3′UTR sequence reveals a higher than expected uracil content throughout the entire 3′UTR, particularly within the first ~450nt. The single CLIP-identified nHu-binding site is found at the very 3′-end of this region (figures 40a-b). However, binding of nHu proteins within this entire region could be expected, based purely on high content of uracil residues. Interestingly, the pyrimidine content of the sequence including and immediately downstream of the proposed UUUAAA polyadenylation signal is remarkably high (figure 40a-b). Specifically, of the 45 residues including and immediately downstream of the UUUAAA sequence, 39 are either cytosine (x20) or uracil (x19), a feature that would be highly likely to support an interaction with HuCsv1. Given the high uracil content of sequences proximal to the UUUAAA sequence, and the observed effect of HuCsv1 on abundance of the smallest zfcdc42-v2 3′UTR-reporter mRNA, any interaction with HuCsv1 would potentially have the capacity to perturb binding of cleavage and/or polyadenylation specific factors necessary to facilitate termination of transcription at this point.

***No 3′UTR-independent accumulation of reporter mRNA using renilla luciferase-based reporters***

As expected, switching to renilla luciferase eliminated the 3′UTR-independent increases in abundance of control and Xβ-globin 3′UTR-reporter mRNAs in the presence of HuCsv1, that were seen in the firefly luciferase reporter Northerns (figure 45). The averaged mRNA abundances from three independent transfections for the two control 3′UTR-reporters were within 10% of each other and were not found to be significantly different by homoscedastic two-tail Student's t-test ($p < 0.11$ and $p < 0.41$ for control 3′UTR and Xβ-globin 3′UTR, respectively). This result confirmed that the cause of the increased reporter mRNA abundance seen in the firefly luciferase reporter Northerns was indeed the firefly luciferase coding sequence.

***HuCsv1 does not affect translation efficiency of control 3'UTR-reporters***

With the 3′UTR-independent effect of HuCsv1 on reporter mRNA abundance removed, it was possible to ask whether HuCsv1 had any effect on translational efficiency of the either the control or Xβ-globin 3′UTR-reporters.

Looking firstly at the raw renilla luciferase and β-galactosidase activity values from experiments 2 and 3 (figure 49), it is immediately clear that the reductions in 3′UTR-reporter and internal control reporter activity seen in the firefly luciferase-based 3′UTR reporter assays are not occurring in the renilla luciferase reporter-based assays. In fact, lysates from cells co-transfected with HuCsv1 appear to have higher levels of activity for both reporter enzymes. Importantly, renilla luciferase activity normalised to mRNA abundance shows no obvious effect of HuCsv1 on renilla luciferase translation. This is also true for the β-galactosidase control. From these calculations, it appears that reporter activity is directly proportional to reporter mRNA abundance, drawing the conclusion that in these assays HuCsv1 does not appear to have a non-specific effect on translation of either reporter. Furthermore, normalisation of renilla luciferase activity to β-galactosidase activity for both control reporters does not indicate an obvious effect of HuCsv1 on renilla luciferase activity, demonstrating that differences in reporter activity are proportional comparing cells with or without HuCsv1. Finally, the calculated translation efficiencies for both the control and Xβ-globin 3′UTR-reporters in the presence versus absence of HuCsv1 do not reveal an obvious effect on the translation efficiency of either of these two reporters. Thus, in these assays, there is no obvious effect of HuCsv1 on general translation.

Notably, raw mRNA abundance values for the 3´UTR-reporters and β-galactosidase are consistently higher in cells co-transfected with HuCsv1 compared to in the absence of HuCsv1 (figure 46 - 48). While the translation efficiency calculations show that the increases in reporter activity observed are not due to an effect of HuCsv1 on translation of the reporters, they cannot rule out an effect on reporter mRNA abundance. It is possible that in these assays, HuCsv1 is generally increasing the stability or reducing the rate of turnover of both the renilla luciferase and β-galactosidase mRNA and that this is in turn allowing for a greater amount of reporter to be translated. While no evidence was gathered to investigate this possibility, it seems unlikely given no increase in renilla luciferase mRNA abundance was seen in the firefly luciferase-based 3′UTR-reporter Northerns. The most straightforward explanation in this case is that cells co-transfected with HuCsv1 are achieving higher rates of transfection efficiency than those in the minus HuCsv1 condition.

## HuCsv1 negatively influences use of a 5´-proximal polyadenylation site within the zfcdc42-v2 3´UTR

Importantly, the switch from firefly to renilla luciferase as the reporter protein did not result in a loss of production of the smallest zfcdc42-v2 3´UTR-reporter mRNA variant. This result indicated that cryptic splicing between sequences in the firefly luciferase coding sequence and the zfcdc42-v2 3´UTR was not likely to be responsible for production of this mRNA variant. Unexpectedly though, in changing to a renilla luciferase-based 3´UTR-reporter message, a distinct change was seen in the behaviour of the zfcdc42-v2 3′UTR-reporter, in the presence of HuCsv1 compared to its behaviour in 293T cells using the firefly luciferase-based 3´UTR-reporter.

In the three Northern blots presented, HuCsv1 clearly reduces the abundance of the smallest reporter mRNA variant (Northern figures 41 – 43, quantification of mRNA abundances shown in figures 45 - 48). Following quantification of reporter mRNA band intensities (figures 46 - 48), the averaged abundance of the smallest mRNA variant (early/non-canonical polyA site), normalised to the abundance of the β-galactosidase transfection control mRNA, was less than half that seen in the absence of HuCsv1 (+HuCsv1 condition versus –HuCsv1 condition in figure 45). Furthermore, this effect was consistent and the difference in abundance between cells co-transfected with versus without HuCsv1 across the three experiments was found to be statistically significant using a homoscedastic two-tail Student's t-test ($p$<0.01) (figure 45). This result agreed with the observed behaviour of the zfcdc42-v2 3′UTR-reporter (firefly luciferase) in Neuro-2a cells and suggests that the behaviour of the firefly luciferase-based zfcdc42-v2 3′UTR reporter in 293Ts may have been complicated by the 3′UTR-independent effect of HuCsv1 on firefly luciferase reporter abundance.

In addition to this, the reduction in abundance of the smallest mRNA product is most consistent with the notion that HuCsv1 is negatively influencing usage of an early polyadenylation site, as opposed to stabilising longer mRNA variants. Notably, abundance of longer mRNA variants, predicted to be using the SV40 late polyadenylation signal, did show a small increase (figure 45). The averaged abundance of SV40 late polyadenylated messages was found to be 1.4-fold greater in the presence of HuCsv1 ($p$<0.017). Averaged abundance of the terminal 3′UTR-encoded polyadenylation site was neither increased nor decreased in the presence of HuCsv1 (1.07-fold increase, $p$ < 0.79). While the increased abundance of longer 3′UTR variants does not appear to

account for the reduction in abundance of the short 3′UTR variant, it is entirely possible that longer variants of the zfcdc42-v2 3′UTR are susceptible to other posttranscriptional regulatory effects that increase their turnover, as already proposed. As such these data appear to be most consistent with the idea that HuCsv1 is specifically reducing the use of an early/non-canonical polyadenylation site within the zfcdc42-v2 3´UTR.

## Summary of results from 3´UTR-reporter experiments examining HuCsv1 function

***How did we end up here?***

In all honesty, at the start of this PhD thesis, the idea that HuCsv1 would be involved in alternative polyadenylation site choice of target messages was not seriously considered. As detailed in the introduction, several lines of evidence appeared to correlate well with a role for nHu proteins in the regulation of translation of target mRNAs. The sub-cellular localisation of nHu proteins to the growth cone of actively migrating neurons was a key instigator for this train of thought. This was largely because of recently published evidence showing local translation within the migrating axonal growth cone (of cytoskeleton components and modifying proteins, in particular) is fundamentally required for responses to chemotactic factors involved in axon guidance. Given several independent examples that nHu proteins can associate with actively translating polysomes and an association between nHu protein expression and increased protein expression from target mRNAs a role of nHu proteins in regulating translation at the growth cone seemed entirely plausible. This idea was greatly strengthened when data emerged from nHu-CLIP experiments conducted in our lab, revealing nHu proteins bind to mRNAs encoding cytoskeleton components and modifying factors, many of which had previously been demonstrated to localise to, or at least encode proteins that localised to the axonal growth cone. In particular, binding of nHu proteins to these mRNAs was found to occur within the 3´-untranslated region, an observation that was interpreted as being in agreement with a role in control of mRNA translation, stability or localisation. As such, the 3´UTR of several CLIP-identified mRNAs encoding cytoskeleton-modifying proteins were used in a series of reporter-based assays with the intention of showing (or not) that nHu proteins are in fact involved in regulating the translation (or localisation) of target mRNAs with known roles in the axonal growth cone during axon migration. However, despite initial indications that translation from several of these 3´UTR-reporter mRNAs was modestly reduced in the presence of HuCsv1, the results from these assays do not indicate HuCsv1 has any direct effect on translation of the target mRNAs tested in these assays. That said, it is acknowledged that the reporter assays used for testing a role for HuCsv1 in regulation of target mRNA translation do not fully recapitulate the cellular context in which nHu proteins would naturally be found. Most specifically, the cell lines used are not true neuronal cells. As such, it is entirely possible that in these assays, some factor(s) or parameters that are necessary for other potential nHu protein functions (such as a role in translational control) have not been satisfied. While the results from these experiments

do provide an example of a role forHuCsv1 in alternative polyadenylation site choice, a role in translational control of other target mRNAs, by nHu proteins has not been ruled out.

***If not translation, then what?***

Northern analysis of mRNAs produced from firefly luciferase-based 3′UTR-reporter constructs indicated that nearly all tested reporter mRNAs produced multiple mRNA variants when expressed in the cell lines tested. Based on examination of mRNA product sizes, 3′UTR sequence composition and available EST data, these products were concluded to result from use of alternative polyadenylation sites, present within the specific 3′UTR sequences. Unexpectedly, use of specific alternative polyadenylation sites for a number of 3′UTR-reporter mRNAs appeared to be affected by co-expression with HuCsv1. However, because of an unrelated and confounding 3′UTR-independent effect of HuCsv1 on firefly luciferase reporter mRNA abundance in these experiments, it was not possible to be confident that the observed differences in mRNA abundance revealed a 3′UTR-specific effect of HuCsv1. To overcome this problem, a final set of experiments in which the firefly luciferase reporter was replaced with renilla luciferase was carried out using just the zfcdc42-v2 3′UTR-reporter. The zfcdc42-v2 3′UTR was chosen because, of the other affected reporter mRNAs, the effect observed on the zfcdc42-v2 3′UTR-reporter mRNA was the most convincing in spite of the confounding effects of the firefly luciferase reporter sequence.

Use of renilla luciferase in the final 3′UTR-reporter assays eliminated the 3′UTR-independent effect of HuCsv1 on reporter mRNA abundance. More importantly though, the negative effect of HuCsv1 on abundance of specific zfcdc42-v2 3′UTR-reporter mRNAs, predicted to be using an early polyadenylation site, seen in the firefly luciferase-based 3′UTR-reporter Northern blots was replicated in the renilla luciferase data. As such, collectively, the data from the 3′UTR-reporter assays presented in this thesis are tentatively interpreted as revealing a role for HuCsv1 in modulation of polyadenylation site choice.

## Preliminary data examining molecular requirements of HuCsv1 for its effect on zfcdc42-v2 3´UTR processing

Due to time constraints, a very limited exploration of the molecular requirements for the negative effect of HuCsv1 on polyadenylation site choice of the zfcdc42-v2 3´UTR-reporter mRNA was conducted within the renilla luciferase-based 3´UTR-reporter assays presented in this thesis. As such, the results and discussion for these experiments are highly preliminary. However, the reader is encouraged to consider the data presented, as several ideas for how HuCsv1 influences production of the small zfcdc42-v2 3´UTR-reporter mRNA product are raised. Note that only the processed data is presented for this discussion, raw quantification of mRNA abundances for these two Northerns is presented as supplementary figure (figure S1 and S2)

***Is mRNA abundance still reduced when RNA-binding activity of HuCsv1 is impaired?***

Following the result from the first renilla luciferase-based 3´UTR reporter Northern, the two subsequent reporter experiments included an extra condition to test the requirement for RNA-binding activity of HuCsv1 in its effect on polyA site usage for the zfcdc42-v2 3′UTR. For this condition, the 3′UTR-reporter constructs were co-transfected with an HuCsv1 overexpression construct that had been altered using a previously reported targeted mutagenesis strategy, such that the RNA-binding activity of all three RRMs was impaired.

Specifically, site-directed mutagenesis was used to convert a critical aromatic residue (phenylalanine) within one of the two highly conserved RNP motifs present within all three RRMs found in the Hu proteins, to an aspartate. In the wildtype situation, the side chain of the targeted phenylalanine extends into the solvent-exposed RNA-binding pocket of the RRM and forms a key stacking interaction with bound RNA [38] (figure 51a). Mutation of the phenylalanine residue to aspartate changes the amino acid side chain in this position from an aromatic residue to an acidic (negatively charged) residue. Removing the aromatic side chain is predicted to eliminate the important stacking interaction that occurs between the target RNA and RRM and the added influence of the negative charge on the aspartate side chain would be further expected to reduce the affinity of the RRM for RNA by repulsive forces between the negative charge of the side chain and negatively charged phosphate backbone of the RNA. Additionally, alanine substitutions were made to the two amino acid residues preceding the common phenylalanine in the RNP1 of each RRM. In the case of the first RRM this changes a tyrosine to alanine, for the second RRM this changes a valine to an alanine and for the third RRM alanine replaces another phenylalanine residue (figure 51b). The alanine substitutions were

made to help prevent these amino acids from compensating for the mutation of the common phenylalanine residue.

Importantly, because the side-chain of the common phenylalanine exists within the solvent exposed RNA binding pocket of the RRM, mutation to a negatively charged amino acid is not predicted to cause a gross alteration in RRM structure [234], [41]. However, it is important to note that no direct structural analysis has been published that verifies the overall folding of the mutated RRM(s) is unaffected. Various *in vivo* and *in vitro* assays of mutated protein function have been described. Use of this mutagenesis strategy for the Drosophila Hu protein homolog *elav*, has previously been reported to abolish protein function in a larvae survival-based assay [234]. In these experiments, larvae expressing the mutated Elav protein showed the same survival characteristics through development as $elav^{-/-}$ flies and the mutant Elav protein was unable to compensate for a temperature sensitive hypomorphic *elav* mutant. Biochemical experiments testing the RNA-binding characteristics of mammalian Hu proteins mutated using the same or highly similar strategies show strong reductions in RNA-binding [118], [41], [40].

In the context of the zfcdc42-v2 3′UTR message, co-expression with an HuCsv1 protein incapable of RNA binding would test whether the negative effect of HuCsv1 on polyadenylation at the early/non-canonical site was dependent on a direct interaction between the zfcdc42-v2 3′UTR-reporter mRNA and HuCsv1. If it were, then co-transfection of the HuCsv1 RRM mutant (RRMmut) with the zfcdc42-v2 3′UTR-reporter would not be expected to lead to a reduction in abundance of reporter mRNAs using the early/non-canonical polyadenylation site. In this case, it could be inferred that the effect of alternative polyA site usage by the zfcdc42-v2 3′UTR in the presence of HuCsv1 was contingent on the ability of HuCsv1 to physically interact with the zfcdc42-v2 3′UTR sequence.

***Loss of mRNA binding activity for HuCsv1 increases the abundance of the smallest zfcdc42-v2 3′UTR-reporter mRNA***

Interestingly, in both experiments, co-expression of the HuCsv1 RRMmut with the zfcdc42-v2 3′UTR-reporter construct led to a strong increase in use of the early/non-canonical polyadenylation site when compared to in the absence of any HuCsv1. In the first experiment testing the RRM mutant version of HuCsv1, abundance of the early/non-canonical polyadenylated reporter mRNA was ~1.75-fold higher in the presence of the HuCsv1 RRMmut compared to in the absence of HuCsv1 (Northern figure 42 and figure 52 - ii). Interestingly, in this experiment a comparable effect is also seen for the Xβ-globin 3′UTR-reporter, with an

almost 2-fold increase in mRNA abundance in the presence of the RRM mutant HuCsv1. Notably, no effect is observed on the abundance of the control 3′UTR-reporter.

In the final experiment, the results were considerably more clear-cut. Firstly, an even greater increase in abundance of the smallest zfcdc42-v2 3′UTR-reporter mRNA product was observed when co-expressed with the HuCsv1 RRM mutant (Northern figure 43 and figure 53 - ii). In this case, use of the early/non-canonical polyadenylation site is 3.15-fold greater in the presence of the RRM mutant HuCsv1 compared to in the absence of HuCsv1. Secondly, no effect of the RRM mutant HuCsv1 (or wildtype HuCsv1) is observed for either of the two control 3′UTR-reporters.

***Does the RRM-mutant HuCsv1 provide evidence for an interaction between HuCsv1 and HuR?***

Co-transfection of the zfcdc42-v2 3′UTR-reporter with the RRM mutant HuCsv1 was not predicted to cause an increase in the usage of the early/non-canonical polyA site. However, this result may provide an additional clue to help explain the behaviour of the zfcdc42-v2 3`UTR-reporter in 293T cells. Firstly, the behaviour of the zfcdc42-v2 3′UTR-reporter in the presence of the HuCsv1 RRM mutant suggests RNA-binding activity is required for HuCsv1 to alter polyadenylation site choice for that 3′UTR. Why though is usage of the early polyadenylation site greater in the presence of the RRM mutant HuCsv1, than in the absence of wildtype HuCsv1? While there is no clear answer for this question it is important to consider that all of the cell lines tested in these experiments endogenously express HuR. Although there is currently no specific evidence available to show HuR has any direct role in regulating alternative polyadenylation of 3′UTRs, there is sufficient evidence to suggest both are able to bind uracil-rich RNA sequences. As such, it is possible that in these reporter assays, some reduction in usage of the early polyadenylation site of the zfcdc42-v2 3′UTR-reporter is occurring simply through an interaction between the zfcdc42-v2 3′UTR and HuR.

How then does the RRM-mutant HuCsv1 cause an apparent increase in abundance of the short zfcdc42-v2 3`UTR variant? As described in the introduction, an increasing body of evidence suggests that Hu proteins (and ELAV) are able to physically interact in dimers and/or multimers [42], [41], [44], [45]). Importantly, multimerisation of these proteins (into homo- and/or hetero-meric Hu complexes or homomeric ELAV complexes) was shown to be possible in the absence of mRNA binding [41], [45]). Furthermore, in the case of the Hu proteins, interactions between Hu proteins are not necessarily homomeric, with GST-tagged versions of all three neuronal Hu proteins able to bind S35-labelled HuD, even in the presence of RNAse A [41].

Notably, some evidence for an interaction between exogenous HuCsv1 (transiently overexpressed) and endogenous HuR was obtained from firefly luciferase reporter-based experiments conducted in HeLa cells (Appendix 3). In these experiments, HeLa cells were co-transfected with either the VASP or zfcdc42-v2 3´UTR-reporter vectors (firefly luciferase-based) and HuCsv1. Following transfection, cells were briefly exposed to formaldehyde to reversibly cross-link HuCsv1 to any interacting mRNAs. HuCsv1 was then immunoprecipitated using an antibody that specifically recognises the neuronal Hu proteins **but not HuR**. Co-precipitating mRNA was then isolated by organic extraction using Trizol (Invitrogen) and reverse transcribed to cDNA. RT-PCR was then used to detect the presence of either the VASP or zfcdc42-v2 3´UTR-reporter mRNAs. Importantly, accompanying Western data to examine efficiency of the immunoprecipitation reaction reveals HuR co-immunoprecipitates with HuCsv1 in cross-linked samples (see Appendix 3 – figure 1 and associated text for details). Because the antibody used to immunoprecipitate HuCsv1 **does not** recognise HuR, the presence of HuR in the IP material is most reasonably explained by either a direct interaction between HuR and HuCsv1, or an indirect interaction mediated by a common intermediate (such as a common mRNA target) that was captured by cross-linking.

Taking these ideas into consideration, a possible explanation for why usage of the early/non-canonical polyadenylation site increases in the presence of the RRM mutant HuCsv1 emerges. The mutation strategy used to produce the RRM-mutant HuCsv1 does not alter amino acids involved in RRM3-mediated multimerisation [234], [41], [45]. As such, the RRM-mutant HuCsv1 protein should retain some capacity for multimerisation. If multimerisation occurs between HuCsv1 and HuR, this may allow the HuCsv1 RRM-mutant proteins to function as a dominant negative, sequestering away endogenous HuR proteins and thus reducing any effect of HuR on polyadenylation site choice for the zfcdc42-v2 3′UTR.

Finally, as well as HuCsv1, HuCsv4 was also included in the second HuCsv1 RRM mutant experiment (figure 18) to examine whether the effect observed on polyadenylation site choice for the zfcdc42-v2 3′UTR in the presence of HuCsv1 was unique to this splice variant or a more general effect of HuC binding. Interestingly, the Northern data suggests co-expression of HuCsv4 with the zfcdc42-v2 3′UTR reporter has the opposite to that seen for HuCsv1 and is more similar to that observed for the HuCsv1 RRM mutant (figure 53 and Northern figure 43). Although this experiment was only tested once, it warrants further investigation. One possibility from this result is that HuCsv4 operates in opposition to HuCsv1, binding to the same mRNA targets, but

causing the opposite functional outcome. Notably, preliminary results from examination of different nHu family members during the *in vitro* differentiation of P19 cells into neuron-like cells using retinoic acid, indicates expression of the short nHu family members (*ie* splice variants 3 and 4) is higher in undifferentiated cells and gradually transitions to expression of longer splice variants (*ie* splice variants 1 and 2) as differentiation proceeds (*unpublished data - Jensen*). This transition in splice variant expression may correspond with a transition in how pre-mRNA processing of nHu target mRNAs is regulated.

## Preliminary deletion analysis experiments aimed at identifying HuCsv1 binding regions within the zfcdc42-v2 3´UTR-reporter mRNA

As a first step towards identifying sequences in the zfcdc42-v2 3´UTR responsible for the HuCsv1-mediated reduction in early polyadenylation site use, the final renilla luciferase experiment (figure 43) also included a series of zfcdc42-v2 3´UTR deletion constructs (see figure 54 - expected mRNA lengths shown in figure 44b). The deletion constructs were generated prior to Northern analysis of any of the 3´UTR-reporter messages and were intended to crudely identify regions involved in the small negative influence HuCsv1 appeared to have on normalised firefly luciferase activity observed in the firefly luciferase-based 3´UTR-reporter assays (figure 31a and 32a). In total, three deletion constructs were generated (figure 54) using an overlapping PCR strategy (see materials and methods). The deletion-1 construct was designed to essentially remove the first third of the zfcdc42-v2 3´UTR sequence. As such, the resulting construct lacks approximately 250nt of uracil-rich sequence (figure 54c). More importantly though, this reporter message lacks the early polyadenylation signal and thus is forced to use the more distal terminal and SV40 late polyA sites. The deletion-2 reporter message carries both the early and terminal/SV40 late polyadenylation sites but lacks the CLIP-identified putative neuronal Hu binding site and a significant portion of uracil-rich sequence distal from the early polyadenylation site (figure 54b). This construct was considered to be potentially the most interesting of the three in the context of polyadenylation site choice because it removes a putative neuronal Hu binding site but retains the early polyadenylation site that appears to be influenced by HuCsv1. Finally deletion-3 contains all polyadenylation signals and the CLIP-identified putative binding site, but lacks a 120nt uracil-rich stretch immediately 3´ to the CLIP-identified neuronal Hu binding site (figure 54d).

***Results for the deletion-1 3´UTR-reporter***

The results for the deletion-1 reporter are not striking in the context of HuCsv1 influencing alternative polyA site usage. There is a roughly a 2-fold increase in abundance of reporter mRNA variants using the 3´UTR-encoded terminal polyadenylation signal, relative to the full-length reporter in all co-transfection conditions (compare red columns from figure 55a – "terminal" mRNA abundance = 1.85 - and figure 55c - "terminal" mRNA abundance = 3.59). The most likely explanation for this outcome is that the absence of any upstream polyadenylation signals forces use of the distal polyadenylation sites. Importantly, no considerable difference in abundance of the zfcdc42-v2 3´UTR-reporter mRNA is observed comparing cells co-transfected with versus without HuCsv1 (or HuCsv4) (figure 55c. -HuCsv1 = 4.32, +HuCsv1 = 3.59, +HuCsv4 = 4.78; *all*

*values relate to mRNA abundance relative to the SV40 late polyA terminating reporter mRNA in the –HuCsv1 condition*). While this result does not add any direct information to the hypothesis that HuCsv1 is driving the use of later polyadenylation sites in the zfcdc42-v2 3´UTR, it is still valuable in an indirect way. Specifically, it argues against a role for HuCsv1 in stabilising longer 3´UTR variants.

***Results for the deletion-2 construct - deletion of the CLIP-identified HuCsv1 binding region in the zfcdc42-v2 3´ UTR reverses its effect on early polyadenylation site usage***

The deletion-2 construct however, may provide additional information that helps to appreciate the complexity of the apparent effect of HuCsv1 on alternative polyadenylation site usage. Specifically, looking at the abundance of each zfcdc42-v2 3´UTR-reporter mRNA variant for deletion-2 reveals an interesting difference in behaviour relative to the full-length reporter. For the full-length reporter, co-expression with HuCsv1 causes an ~2.1-fold reduction in abundance of the early polyadenylation site relative to the –HuCsv1 condition (figure 55a – compare purple columns. –HuCsv1 = 2.27, +HuCsv1 = 1.05; *all values relate to mRNA abundance relative to the SV40 late polyA terminating reporter mRNA in the –HuCsv1 condition*). However, for the deletion-2 3´UTR reporter, the opposite effect is seen, with over a 5-fold increase in the abundance of reporter mRNAs using the early polyadenylation site in the presence of HuCsv1 (figure 55b – compare purple columns. –HuCsv1 = 1.07, +HuCsv1 = 5.4). The pattern of abundance of the early and late (terminal and SV40 late) polyadenylation signals is also reversed when compared to the full-length reporter. In the **absence** of HuCsv1, abundance of zfcdc42-v2 (deletion-2) reporter mRNAs using the terminal polyadenylation site is almost 2-fold greater compared to the full-length 3´UTR-reporter (compare red columns for –HuCsv1 condition between figures 55a and 55b. –HuCsv1 [full length reporter] = 2.42, –HuCsv1 [deletion 2 reporter] = 4.62). Likewise, abundance of reporter mRNAs using the early polyadenylation site in the absence of HuCsv1 is reduced 2-fold (compare purple columns for –HuCsv1 condition between figures 55a and 55b. –HuCsv1 [full length reporter] = 2.27. –HuCsv1 [deletion 2 reporter] = 1.07).

This result suggests that the region deleted in the deletion-2 3´UTR-reporter message contains sequences that exert effects on polyA site choice for the zfcdc42-v2 3´UTR. Importantly, even in the absence of HuCsv1, removal of this sequence clearly alters use of the early polyA site, suggesting this decision is regulated in a more complex manner than a simple on or off switch governed by the presence of HuCsv1. What seems more likely is that other factors influence the use of the early polyA signal through interactions with mRNA sequences within the deletion-2 region. One possibility is that for the full-length 3´UTR sequence, in the absence of HuCsv1,

factors binding within the deletion-2 sequence promote usage of the early polyadenylation site. In the presence of HuCsv1 the ability of these factors to promote polyadenylation at the early polyadenylation site is reduced. This could occur as a result of HuCsv1 physically restricting access of these other factors to their binding site (competition) or as a result of protein-protein interactions between HuCsv1 and these other factors that reduce their ability to promote polyadenylation at the early pA site (sequestration).

***Deletion-2 results hint at interactions between HuCsv1 and polyadenylation factors***

As shown, use of the early polyadenylation site by the deletion-2 3´UTR-reporter is reduced in the absence of HuCsv1. This suggests that the deleted sequence is recognised by factors that promote use of the early polyadenylation site. Remarkably, co-expression with HuCsv1 reverses this, with a strong increase in use of the early polyA site compared to both the absence of HuCsv1 for the deletion-2 reporter, and the presence of HuCsv1 for the full-length reporter. Given published evidence that nHu proteins (and ELAV) can interact directly with at least one component of the cleavage and polyadenylation machinery (CstF64) [126], [135]) this observation may indicate that in the case of the zfcdc42-v2 3´UTR-reporter, HuCsv1 influences where polyadenylation occurs within the 3´UTR, through direct interactions with components of the polyadenylation machinery. In the case of the deletion-2 reporter, the first 300nt of the 3´ UTR sequence is very uracil-rich (~38% uracil). It is possible that the full-length 3´UTR contains multiple nHu binding sites within the uracil-rich region in the proximal half of the sequence. As such, it may be that nHu protein function within the context of the zfcdc42-v2 3´UTR is highly dependent on the arrangement and/or proportion of nHu proteins distributed across that sequence. Removing nHu-binding sites more 3´ from the early polyadenylation site may cause a shift in the pattern or prevalence of HuCsv1 binding across this uracil-rich region, favouring binding of HuCsv1 to more proximal sequences (closer to the early polyA site). If HuCsv1 does influence polyadenylation site usage through an interaction with components of the polyadenylation machinery (such as CstF64), an increase in Hu protein binding at sites closer to the early polyadenylation signal (or conversely a reduction in Hu binding further away from the early polyA signal) could inadvertently promote increased use of that signal. Importantly, while the reported interactions between CstF64 and (either) nHu proteins [135]or ELAV [126] occur in a context of reduced polyadenylation site usage, neither paper reveals mechanistically how this interaction causes reduced polyA site usage.

***Results for the deletion-3 3´UTR-reporter***

Finally, the deletion-3 construct behaves similarly to the full-length 3´UTR with respect to HuCsv1 (figure 55d). Upon co-expression with HuCsv1, the abundance of messages using the early polyadenylation signal is reduced ~3-fold while no change is seen in abundance of messages using the later polyadenylation sites (terminal and SV40) relative to in the absence of HuCsv1 (figure 55d - compare red and blue columns from +/–HuCsv1). In a simple way, the results from the deletion-3 3´UTR-reporter support the findings presented thus far that HuCsv1 appears to reduce usage of an early polyadenylation site in the zfcdc42-v2 3´UTR. Furthermore, the deletion 3 construct indicates that this activity does not depend on interactions with sequences distal to the CLIP-identified nHu protein binding sequence.

Notably, compared to the full-length 3´UTR-reporter in the absence of HuCsv1, use of the early polyadenylation site is more strongly favoured over use of more distal polyadenylation sites (compare figures 55d and 55a). In the –HuCsv1 condition, abundance of reporter mRNAs using the early polyA site = 3.29 [deletion 3 reporter] compared to 2.27 [full length reporter]. Furthermore, the abundance of reporter mRNAs using more distal polyadenylation sites ("terminal" or "SV40 late") is reduced for the deletion 3 construct (compared to the full length reporter). These results suggest that sequences deleted in the deletion-3 mRNA may have some role in use of the terminal polyA site.

***Results from co-expression of HuCsv4 and the RRM-mut HuCsv1 with deletion constructs***

Finally, within this experiment the HuCsv4 and HuCsv1 RRM-mutant constructs were also co-transfected with the deletion constructs. However, with the limited amount of testing done using these two HuC isoforms (*ie* in any other reporter experiments presented in this thesis) there is little that can be concluded from these results.

Notably, the effect of HuCsv4 on use of the early polyA site in the deletion-2 3´UTR-reporter construct was similar to how it affected the full-length 3´UTR-reporter (figure 55b versus figure 55a). In both cases, an ~3-fold increase in early polyA site use was observed for HuCsv4 compared to the –HuCsv1 condition. There is no definitive explanation for this difference in behaviour between HuCsv4 and HuCsv1 with respect to the zfcdc42-v2 3´UTR-reporter. Conceivably, this result indicates some difference in binding sequence specificity between the two HuC splice variants. This interpretation may be supported by the results from the deletion-3 reporter, which suggest HuCsv4 loses its ability to increase use of the early polyadenylation site (as was seen for the full length zfcdc42-v2 3´UTR-reporter relative to in the absence of HuCsv4)

when sequences 3′ of the CLIP-identified nHu-binding site are deleted (figure 55d). Given this data, it may be interesting to examine whether the different HuC splice variants display differential sequence specificity, or if binding to different regions of the zfcdc42-v2 3′UTR sequence is driven by interactions with other factors.

For the HuCsv1 RRM-mutant, the results are not entirely consistent with expectations. Particularly for the deletion-2 mutant; if the HuCsv1 RRM-mutant does work as a dominant-negative Hu protein, then the expectation would be that the abundance of messages using the early polyadenylation site would be more like that for when HuCsv1 is absent (*ie* reduced). However, as is seen, the deletion-2 3′UTR-reporter mRNA behaves similarly to the full-length 3′UTR when co-transfected with HuCsv1 RRM-mutant, with a comparable increase in abundance of the early polyadenylated message relative to the full-length 3′UTR-reporter (compare purple bars for RRM-mut, figures 55a and b). Without a better understanding of how the HuCsv1 RRM-mutant is actually behaving in the context of the full-length zfcdc42-v2 3′UTR-reporter it is difficult to identify an explanation for this behaviour. While the results for HuCsv4 and the HuCsv1 RRM-mutant are potentially interesting and warrant further investigation, the lack of experimental repeats for each condition precludes any greater conclusions to be drawn from these results, than the suppositions given here.

## Missing piece of the puzzle

One conspicuous omission from the results of this thesis is confirmation of the identity of zfcdc42-v2 3′UTR-reporter mRNA products observed by Northern analysis. While mRNA product identities have been predicted with some degree of confidence based on comparison of mRNA product size to the location of predicted polyadenylation sites within 3′UTR sequences (derived from EST data where available), it is not possible to definitively know the identity of observed products without specifically sequencing each reporter mRNA product. To do this, total RNA from reporter transfected cells would first be reverse transcribed using oligo dT primers containing unique anchor sequences (specifically a stoichiometrically equal mix of oligo dT sequences that have either an A, G, C or T as the most 3′ nucleotide) to generate cDNA predominantly composed of sequences beginning with the immediate 3′-ends of all polyadenylated mRNAs from the RNA sample (*ie* beginning from the start of the polyA tail of the template mRNA with a polyT sequence only as long as the initial oligo dT primer). Following reverse transcription, PCR using a primer pair comprised of a forward primer complementary to sequences within the renilla luciferase coding sequence and an oligo dT reverse primer would be used to specifically amplify the 3′-ends of all zfcdc42-v2 3′UTR-reporter mRNAs present in the cDNA. Finally, all resulting products from this reaction would be sequenced and the identity of each product revealed. The experimental protocol outlined above is commonly known as 3′-RACE (rapid amplification of 3′-ends) and is commonly used in the identification of unknown polyadenylation sites of specific mRNAs [235].

Notably, there are two reasons why the identification of specific mRNA products of the zfcdc42-v2 3′UTR-reporter mRNA was not carried out prior to completing work for this thesis. Firstly, confirmation that HuCsv1 affects mRNA production from the renilla luciferase-based reporter zfcdc42-v2 3′UTR reporter as was first noticed using the firefly luciferase-based reporter construct, came in the final stages of this PhD work. Due to strict time restrictions faced by the author, it was not possible to pursue the results of the renilla luciferase Northern data any further than has been presented in this thesis. In hindsight, the author acknowledges that identification of reporter mRNA products should have been conducted earlier on, (*ie* immediately following the results of the firefly luciferase-based Northern assays). However, at the time this aspect of the data was overlooked, for the most part because the 3′UTR-independent effect of HuCsv1 apparent for all 3′UTR-reporter mRNAs was confounding and as such, the data from these assays was not deemed sufficiently reliable to justify deeper interrogation.

Future work examining an effect of HuCsv1 on polyadenylation site use in the zfcdc42-v2 3′UTR-reporter mRNA, is contingent on conclusive identification of all mRNA products produced from this reporter in the results presented in this thesis. As the data currently stands, while alternative polyadenylation is the most supported explanation for production the smallest mRNA product of the zfcdc42-v2 3′UTR-reporter, alternative mechanisms such as cryptic reporter mRNA splicing (see below) and spurious premature transcription termination are also potential causes. Importantly, mRNA products arising from either of these alternative explanations will not produce products by 3′-RACE. In the event that no product corresponding to the predicted smallest zfcdc42-v2 3′UTR-reporter mRNA is identified, either of these two alternative possibilities may be pursued.

***Ruling out cryptic splicing as an alternative source of the smallest zfcdc42-v2 3′UTR-reporter mRNA product***

As stated; in the absence of data identifying the mRNA products of the zfcdc42-v2 3′UTR-reporter observed by Northern blot, a role for HuCsv1 in regulation of polyadenylation site use by the zfcdc42-v2 3′UTR has not been conclusively demonstrated. What the data do show is that co-expression of HuCsv1 with the zfcdc42-v2 3′UTR-reporter alters the processing of the zfcdc42-v2 3′UTR-reporter mRNA in a manner that specifically reduces the abundance of an as yet, unidentified mRNA variant. Assuming the zfcdc42-v2 3′UTR-reporter mRNA is behaving as expected, the most likely explanation for this effect is that HuCsv1 reduces the use of a non-canonical polyadenylation site located very close to the 5′-end of the zfcdc42-v2 3′UTR. However, it is possible that the zfcdc42-v2 3′UTR-reporter mRNA could behave in a manner not anticipated that would result in the production of an mRNA of the size observed for the smallest mRNA variant. While cryptic splicing within the firefly luciferase reporter as an explanation for the production of the smallest zfcdc42-v2 3′UTR-reporter mRNA variant was excluded following the results of the renilla luciferase-based reporter Northerns, it is theoretically possible that splicing between the splice donor site of the chimeric intron present at the very 5′-end of the reporter mRNA, and a splice acceptor site at the very 5′-end of the zfcdc42-v2 3′UTR sequence could occur and yield a product of approximately the size observed for the smallest zfcdc42-v2 3′UTR-reporter mRNA variant (figure 56). The splicing donor site of the chimeric intron is located approximately 100nt downstream of the transcription start site of the reporter mRNA. Splicing to a cryptic acceptor site at the very 5′-end of the zfcdc42-v2 3′UTR would yield an mRNA that contained ~100nt of sequence between the transcription start site and intron, plus some amount of the zfcdc42-v2 3′UTR sequence. Reporter mRNAs terminating at the terminal

polyadenylation site encoded by the zfcdc42-v2 3´UTR would measure approximately 800 – 1000nt, depending on polyA tail length; a size that appears too small from the Northern results. However, mRNAs using the SV40 late polyadenylation site would measure between 1000 – 1200nt; which could agree with the size observed for the smallest mRNA variant produced from the zfcdc42-v2 3´UTR-reporter.

Importantly, while this possibility cannot be ruled out, two observations from these experiments count against this possibility. Firstly, if HuCsv1 were blocking a cryptic splicing event as described above, a strong increase in abundance of the longer mRNA variants (assumed to mRNAs spliced correctly) would be anticipated, as normal splicing would be forced to occur. Contrary to this, while a >4 fold reduction in abundance of the smallest mRNA variant is observed in the presence of HuCsv1 in the second experiment (figure 47), the abundance of longer mRNA variants is collectively increased by less than 3-fold. In the third experiment, where a >2-fold reduction in abundance of the smallest zfcdc42-v2 3´UTR-reporter mRNA variant is observed, abundance of both larger mRNA variants is observed to decrease slightly (~25% for mRNAs predicted to use the SV40 late polyA site, with no change in abundance of the predicted terminal polyA site using variant) (figure 48). Furthermore, a reduction in cryptic splicing by HuCsv1 would also be expected to result in an increase in normalised renilla luciferase activity, as a greater amount of mRNA containing the renilla luciferase coding sequence should be produced. However, in the presence of HuCsv1, no increase in normalised renilla luciferase activity is observed (figure 57).

In summary, in the absence of definitive proof for the identity of the smallest zfcdc42-v2 3´UTR-reporter mRNA product; the available data are most supportive of a model in which this mRNA arises through use of an early polyadenylation site, located within the first 150nt of the 3´UTR sequence.

## How does the 3´UTR-reporter assay data fit with what is currently understood about neuronal Hu proteins and RNA-processing biology

***Existing evidence for a role of nHu proteins in regulating polyadenylation site choice***

As detailed in the introduction of this thesis, a limited number of studies into ELAV and nHu protein function have provided evidence for a role for neuronal Hu proteins in modulating polyadenylation site usage [126], [130], [135]). In all cases, nHu proteins (or ELAV) were shown to reduce cleavage and polyadenylation at polyadenylation sites upstream of uracil-rich sequences, to which the proteins bound. While a mechanism for this activity has yet to be conclusively identified, evidence of a specific protein-protein interaction between nHu/ELAV and CstF64, a key component of the cleavage and polyadenylation machinery has been shown [126], [135]). In both papers, the authors conclude that direct interactions between nHu/ELAV and a given target mRNA, in addition to direct interactions between nHu/ELAV and factors involved in cleavage and polyadenylation, are likely involved in the negative effect of both (nHu/ELAV) on use of specific polyadenylation sites. As such, two possible mechanisms may explain the reduction in abundance of the smallest zfcdc42-v2 mRNA product observed in this thesis. Firstly, nHu proteins may act as regulators of alternative splicing in the cdc42 pre-mRNA. Secondly, nHu proteins (or more specifically HuCsv1) may specifically modulate 3´UTR length of the cdc42-v2 mRNA through alternative polyadenylation site choice.

***HuCsv1 as a regulator of alternative splicing of the terminal exon of cdc42***

Importantly, while the published examples mentioned above provide one potential model of how regulation of polyadenylation site use by nHu proteins (or ELAV) might it influence target mRNA processing, it is not clear how applicable they are in considering a role for HuCsv1 in the production of alternative cdc42 mRNA variants. Specifically, the papers from Soller *et al* and Zhu *et al* indicate that nHu proteins (and ELAV) can reduce non-neuronal splicing of their particular mRNA targets by preventing polyadenylation at sites present in alternatively spliced, early terminal exons. By reducing polyadenylation site use through binding to uracil-rich sequences located downstream of the affected polyadenylation site, nHu proteins (and ELAV) promote exon skipping of an early terminal exon resulting in production of neuron-specific isoforms of their target mRNAs.

Conversely to both the *ewg* and *CGRP/calcitonin* examples, the neuron-specific cdc42-v2 mRNA variant arises from splicing that incorporates the early terminal exon into the final mRNA

product, while the ubiquitously expressed cdc42-v1 mRNA variant arises through alternative splicing that skips this exon (figure 35). Furthermore, both cdc42 mRNA variants are expressed (at comparable levels) in neuronal tissues [212]. As such, while the production of the cdc42-v2 mRNA variant is unique to neurons, it is not exclusive to production of the cdc42-v1 mRNA variant, in neurons.

Functionally, very little has been reported on how alternative splicing influences cdc42 behaviour within the cell, making it difficult to predict how or when alternative splicing of the cdc42 pre-mRNA might be important. Both cdc42-v1 and cdc42-v2 produce protein products capable of modulating actin cytoskeleton dynamics with no reported difference in activity. Where they do differ is in the type of post-translational lipid-modification that can be attached at their C-terminal end, with proposed effects on membrane localisation [214] (explained in the section describing cdc42, starting from page 60). This difference appears to specialise cdc42-v2 function, and likely diversifies the roles in which both proteins can serve [214]. Briefly, while both cdc42-v1 and cdc42-2 are involved in the formation of dendrites by neuronal cells, cdc42-v2 appears to be involved in specific changes in actin cytoskeleton arrangement necessary for the formation of dendritic spines (small neuritic outgrowths extending a short distance away from the main dendritic branch) during the formation of neuronal synapses [214].

Speaking very generally then, nHu proteins may act to differentially regulate splicing of the cdc42 pre-mRNA to yield either the cdc42-v1 or cdc42-v2 mRNA product, as required, during neuronal development. The data from the zfcdc42-v2 3´UTR-reporter experiments presented in this thesis suggest that HuCsv1 acts to block early polyadenylation site usage in the cdc42-v2 3´UTR. Given the general requirement for interactions between the splicing machinery and polyadenylation site binding factors in the recognition of terminal exonic sequence [236], these experiments may indicate that HuCsv1 favours the production of zfcdc42-v1 by specifically interfering with components of the polyadenylation machinery (such as CstF64), resulting in a reduction in the use of polyadenylation sites present in the zfcdc42-v2 terminal exon. Importantly, the reporter assay used in the experiments presented here cannot properly address a possible influence of HuCsv1 on cdc42 mRNA splicing/terminal exon usage. It is equally possible that HuCsv1 promotes use the early terminal exon (formation of cdc42-v2) but that the components necessary for examining such a function (*ie* a reporter that included the complete sequence from the penultimate exon splice donor site, to the end of the second terminal exon [end of the cdc42-v1 3´UTR]) were not present in the 3´UTR-reporter transcript. In their

absence, binding of HuCsv1 to the zfcdc42-v2 3´UTR sequence may have a specific, but not necessarily biologically relevant, effect on 3´UTR polyadenylation site choice.

***HuCsv1 as a regulator of 3´UTR length through modulation of polyadenylation site use***

The second possible mechanism to explain the effect of HuCvs1 on abundance of the smallest zfcdc42-v2 mRNA in these reporter assays is that HuCsv1 is specifically involved in blocking use of 5´-proximal polyadenylation sites, in favour of more distal polyadenylation sites present within the targeted 3´UTR sequence. As detailed in the introduction, the progression of both embryonic development and cellular differentiation has been correlated with a general phenomenon of increasing 3´UTR length. When taken with the evidence showing nHu expression first comes on in neuronal cells as they make the transition from neuronal precursor to immature neuron, a role for nHu proteins in promoting lengthening of the zfcdc42-v2 3´UTR in differentiated neurons through blocking early polyadenylation site choices, could be supported. Importantly though, the data from the zfcdc42-v2 3´UTR-reporter experiments presented here suggest that any involvement of HuCsv1 in alternative polyadenylation site use within the zfcdc42-v2 3´UTR is restricted to the molecular decision to use or not use the early polyadenylation site, as a reciprocal increase in abundance of longer mRNA variants was not observed in HuCsv1 co-transfected cells. It may be that as a result of using a non-neuronal, mitotically active human embryonic kidney cell line (HEK293T), factors necessary for stabilisation of longer zfcdc42-v2 mRNA variants are not present or alternatively, factors directly reducing the abundance of longer mRNA variants are.

## Limitations of the current reporter assay design – looking ahead

***Testing for a role of nHu proteins in regulating target mRNA translation***

The functional assays presented in this thesis were primarily designed to ascertain whether HuCsv1 post-transcriptionally regulates target mRNA translation through direct interactions with sequences present in the 3´UTR of target mRNAs. However, of the 3´UTR sequences tested, no role for HuCsv1 in regulation of target mRNA translation has been identified. Importantly, this does not exclude a role for nHu proteins in regulation of target mRNA translation. It is possible that the specific mRNA targets selected for use in these assays are not affected in this way by binding of HuCsv1, despite the correlative evidence available to support such a role. Alternatively, it is possible that nHu proteins do not work autonomously, and that effects on target mRNA translation depend on additional, as yet unidentified parameters that have not

been properly addressed in these assays. It is not clear how to proceed with cell culture-based assays for effects of nHu proteins on target mRNA translation. While it would be desirable to assay for effects of nHu proteins on target mRNA translation in a more neuronal system, such as cultured E18 rat hippocampal neurons, the technical caveats associated with achieving efficient transgene transfection restrict the utility of this system. Furthermore, the expression of multiple different nHu protein isoforms would complicate attribution of any effect on 3′UTR-reporter mRNA translation to a specific nHu family member short of carrying out complicated siRNA knockdown experiments, in conjunction with reporter assays. In the end, the amount of work that would be required to show that loss of nHu protein expression in these assays was directly responsible for any change in 3′UTR-reporter translation (or even translation of endogenously expressed putative target mRNAs) is considerable, and prohibitive in the absence of data that directly supports a role for nHu proteins in regulating the translation of a specific target message. Future experiments focussed on identifying factors that interact with nHu proteins in neurons may be helpful in identifying important parameters that have not been considered in the reporter assays thus far.

***Testing for a role of nHu proteins in regulating target pre-mRNA processing***

The reduction in abundance of the smallest zfcdc42-v2 3′UTR-reporter mRNA, observed in these assays requires further confirmation before mechanistic interrogation of this phenomenon can be pursued. As stated, 3′-RACE followed by specific amplification and sequencing of all zfcdc42-v2 3′UTR-reporter mRNA products observed in these assays must be performed. Provided the results from this experiment confirm the expectation that the smallest zfcdc42-v2 3′UTR-reporter mRNA product observed corresponds to a reporter mRNA using the non-canonical (UUUAAA) polyadenylation site present at the very 5′-end of the zfcdc42-v2 3′UTR, a series of experiments to examine how and why HuCsv1 reduces the apparent abundance of mRNAs using this polyadenylation site could be conducted. In the absence of actual data to show how HuCsv1 influences 3′-end processing of the cdc42 mRNA, a series of thought experiments that would in principle provide this data are presented below.

## Thought experiments to examine a proposed role for HuCsv1 in 3′-end processing of target mRNAs

***Testing for a role in alternative splicing of the cdc42 pre-mRNA***

The simplest and most clear-cut method to determine if HuCsv1 influences alternative splicing of the cdc42 pre-mRNA, would be an RNAse protection assay (RPA). Briefly, because the RNA

sequences of the two cdc42 mRNA variants differ only at the terminal exon, a complementary, isotopically-labelled ($^{32}P$) RNA sequence (probe) could be synthesised that would bind to some amount of common mRNA sequence upstream of the cdc42-v2 terminal exon (the final 100nt of the penultimate exon, for instance) and then be specifically complementary to the coding region of the cdc42-v2 terminal exon (figure 58a). The expected products of an RPA carried out using this probe would be a 100nt sequence representing the total amount of cdc42-v1 mRNA present in the RNA sample tested, and a190nt product representing the total amount of cdc42-v2 mRNA present (there are 90nt of coding sequence contained within the terminal cdc42-v2 exons of zebrafish, mouse and human cdc42-v2 = 190nt RPA product). Using this RPA format, it would then be possible to compare abundance of both (**endogenously expressed**) cdc42 splice variants in equal amounts of total RNA obtained from non-neuronal and/or neuronal cells (such as the 293T, HeLa and Neuro-2a cell lines tested in this thesis) transiently transfected to overexpress HuCsv1 (or any one of the nHu proteins) with cells lacking any nHu expression. If HuCsv1 (or any of the nHu proteins) does cause alternative splicing of the cdc42 pre-mRNA, this would be exemplified by a difference in the abundance of either RPA product between the two conditions.

The advantages of using an RPA over Northern blot are two-fold. Firstly, the RPA is empirically a more sensitive assay than Northern blot, meaning detection of endogenously expressed cdc42 mRNA variants would be less likely to be hampered in a the case where these mRNAs are only lowly abundant. Secondly, the RPA is easily multiplexed allowing for the abundance of a variety of different mRNA sequences to be measured from a single sample, simultaneously. The only consideration that needs to be made when multiplexing is to ensure that each protected probe fragment is sufficiently unique in size (following nuclease treatment) to allow reliable detection following separation by denaturing polyacrylamide gel electrophoresis. In the case of the experiments planned here, multiplexing would enable measurement of nHu transcript abundance (as a control to show nHu expression, or lack there of, in transfected cells) in addition to abundance of a general housekeeping gene product (*ie* GAPDH, β-actin or TATA box-binding protein etc) to control for differences in RNA loading. In these experiments, using a probe to produce an RPA product of 150nt for the loading control transcript and 500nt for the nHu transcript would be a good starting point as the signal from the overexpressed nHu transcript would be expected to be significantly stronger than that of any of the endogenously expressed mRNAs probed for.

**Redesigning the reporter assay to examine effects on alternative splicing**

If the data from the RNAse protection assays outlined above did reveal a role for HuCsv1 (or any nHu protein) in altering alternative splicing of the cdc42 pre-mRNA, a new reporter assay format would be required. Without going into extensive detail, the splicing-reporter assay would be designed to replicate as closely as possible, the alternative splicing decision of the cdc42 terminal exon(s). This in itself would not necessary be a straightforward task, as the amount of sequence spanning (and including) the penultimate and terminal exon of zebrafish cdc42-v1 is ~9.5kb. Interestingly, the human sequence is considerably smaller, at ~6.5kb, while the mouse sequence is similar in size to zebrafish at ~9.2kb. However, the general idea would be to clone these sequences into an expression vector, in frame with a sequence encoding a myc-tag (to produce an N-terminally myc-tag protein product). This expression vector would be anticipated to recapitulate the alternative splicing behaviour of the cdc42 terminal exon choice when expressed in cells and thus, could be used in experiments identifying sequences within the cloned region that are critical in the terminal exon splicing decision. Depending on the behaviour of each reporter in the presence and absence of HuCsv1, one or all of the splicing reporter constructs could be applied to subsequent experiment. A brief account of potential applications of these reporter constructs is presented.

Importantly, at the time of writing, a high-throughput sequencing CLIP experiment (HITS-CLIP) for nHu proteins is being conducted in our lab. To date, no such experiment has been published for the neuronal Hu proteins and it is anticipated that the results of this experiment will be enormously helpful in pinpointing key nHu protein binding sites within target mRNAs. With respect to the hypothetical splicing reporter assay mentioned above, this data will be invaluable in honing in on likely sites within the cdc42 pre-mRNA that

1. Are bound by nHu proteins.
2. Would be most likely to influence an alternative splicing decision to include or exclude the early terminal exon on the cdc42-v2 mRNA product.

Using these data, (and following confirmation that the splicing reporter behaves as expected by transfection with and without HuCsv1, followed by RPA or Northern blot), it would be possible to test each CLIP-identified nHu protein binding site within the splicing reporter, for a role in regulating alternative splicing of the reporter transcript. This would be done by carrying out targeted mutagenesis of CLIP-identified nHu binding sequences and then assaying for changes in

alternative splicing of the reporter in the presence of nHu proteins, compared to the "wildtype" reporter sequence (using the RPA experiment outlined above).

"Rescue" experiments for mutant reporters could also be conducted by way of confirmation that changes in alternative splicing of the mutant cdc42 reporter construct result from loss of nHu protein binding to specific mutated sequences. To rescue mutants, nHu proteins could be artificially "tethered" to the mutated nHu binding site to show that splicing changes mediated by nHu proteins could be restored to the mutant reporter by enabling nHu protein binding to the mutant binding site. Tethering of RNA-binding proteins to specific RNA sequences is an increasingly common method used in the study of RNA-binding protein function (comprehensively reviewed in [237]). While several methods can be used to tether proteins to RNA sequences, a single hypothetical example is provided to outline how rescue experiments might be performed. Firstly, a tethering sequence, such as the 19nt long boxB RNA hairpin loop, would be cloned into the mutated nHu-binding site of the cdc42 splicing reporter construct. The boxB hairpin loop is recognised and tightly bound by the N-protein of bacteriophage λ, a 22 amino acid arginine-rich peptide sequence that binds the boxB hairpin at a $K_d$ of ~20nM [238]. Fusion of the N-protein sequence to the N-terminus of the nHu protein would be necessary to create a nHu-fusion protein capable of binding the boxB RNA hairpin. By overexpressing the mutant cdc42 splicing reporter construct with the N-protein/nHu fusion-protein, it would be possible to restore nHu protein binding at the mutated binding site and (conceivably) demonstrate rescue of nHu-directed alternative splicing of the (mutant) cdc42 splicing reporter.

From this point, experiments to examine the mechanism of nHu-mediated changes in cdc42 alternative splicing would be required. Discussion of how these experiments might be carried out is largely beyond the scope of this thesis. Although obviously, the first line of investigation would focus on exploring for a connection between nHu protein-mediated splicing changes and the cleavage and polyadenylation machinery (provided the results of the nHu HITS-CLIP experiment and subsequent examination of mutant cdc42 splicing reporters were supportive of such a possibility). Experiments exploring the mechanism by which nHu proteins mediate alternative splicing decisions of the cdc42 reporter construct would be assisted by companion experiments aimed at identifying interactions between nHu proteins and other factors. Such experiments could involve co-immunoprecipitation of nHu proteins from non-neuronal cells overexpressing specific nHu proteins or from brain lysates, followed by mass spectrometry, to isolate and identify interacting factors.

**Testing for a role in alternative polyadenylation site choice in the cdc42 3´UTR**

Testing for a role of HuCsv1 in alternative polyadenylation site choice in the cdc42-v2 3´UTR would also utilise the RNAse protection assay. However, in this case, the probe sequence would be designed to span the entire terminal exon of the cdc42-v2 mRNA, including the 3´UTR. In the first instance, RPAs would be conducted using a similar zfcdc42-v2 3´UTR-reporter construct as used in the renilla luciferase-based reporter assays of this thesis (figure 58b). However, this reporter would be re-designed to eliminate the SV40 late polyadenylation signal currently present within this vector, and apparently used to some extent in reporter mRNA products. Furthermore, the entire terminal exon sequence from zfcdc42-v2 (including 90nt of terminal exon coding sequence, plus ~700nt of 3´UTR; altogether ~800nt in total) would be cloned into the reporter vector, in-frame with the renilla luciferase coding sequence (immediately before the renilla luciferase STOP codon, such that the zfcdc42-v2 STOP codon is used. These changes in the renilla luciferase-based zfcdc42-v2 3´UTR-reporter would be made as a first-pass attempt at presenting HuCsv1 with a faithful recapitulation of the entire terminal exon of zfcdc42-v2, as accurately as possible.

For these RPAs, the probe sequence would span the entire terminal exon. Based on the predicted polyadenylation sites used from the available zfcdc42-v2 3´UTR-reporter data, the smallest zfcdc42-v2 3´UTR-reporter mRNA product (using the UUUAAA polyadenylation site), would yield a product of 100 - 130nt (90nt of coding sequence, plus an estimated 10 - 40nt of 3´UTR sequence. The terminal 3´UTR-encoded polyadenylation site would produce a product of ~750nt (90nt of coding sequence, plus ~660nt of 3´UTR). There is also potentially a third product using a canonical (AAUAAA) polyadenylation site located roughly in the middle of the zfcdc42-v2 3´UTR (referred to as "middle" through this thesis). Polyadenylation at this site would produce a product of ~400nt (90nt of coding sequence, plus 315 nt of 3´UTR)

Transfections would be carried out identically to how they are described in the renilla luciferase-based 3´UTR-reporter assays of this thesis (see materials and methods for details). RPAs would be carried out on total RNA prepared from transfected cells and multiplexed with a probe to determine abundance of the β-galactosidase transcript (as a measure of transfection efficiency and to normalise the abundance of RPA products for the zfcdc42-v2 3´UTR-reporter) and a probe to measure nHu transcript abundance as outlined in the splicing RPA thought-experiments above. An effect of HuCsv1 (or any nHu protein) on polyadenylation site use for the zfcdc42-v2

3´UTR reporter would be reflected in a difference in normalised abundance of specific RPA products (for the reporter) comparing cells with and with HuCsv1 overexpression.

Provided some effect of HuCsv1 (or any nHu protein) were observed in these assays, a similar mutagenesis strategy as described in the splicing RPA experimental outline could be employed to identify sequences within the 3´UTR required for HuCsv1 activity. These would be supported by nHu-tethering experiments (also as indicated in the splicing RPA experiments) to try and rescue nHu-mediated polyadenylation choices and thus show that changes in polyadenylation site choice are caused by binding of HuCsv1 to the specific element(s) identified in the mutagenesis experiments.

Importantly, the results from preliminary deletion analysis of the zfcdc42-v2 3´UTR-reporter suggest that the HuCsv1 may share a common binding site in the 3´UTR with other factors that promote production of the smallest zfcdc42-v2 3´UTR-reporter variant. As such, it is not immediately obvious what the results of mutagenesis and "rescue" experiments would be. It is possible that as well as reducing binding of HuCsv1 to the 3´UTR, mutagenesis of putative HuCsv1-binding sites would also disrupt binding of factors that promote use of the early polyadenylation site, that share the HuCsv1 binding site or bind in its immediate vicinity. Given the relatively loose sequence binding requirements of nHu proteins (essentially only dependent on high uracil content), it is likely that mutagenesis experiments would require several rounds of refinement to ascertain whether HuCsv1 binding to the zfcdc42-v2 3´UTR can in fact be reduced, without a concomitant reduction in binding of factors also involved in the use of the early polyadenylation site.

In the face of this problem, it may be necessary to turn to the use of HuCsv1-mutants, as a means of interfering with HuCsv1 regulation of polyadenylation site use. Such experiments might compare polyadenylation site use in the presence of HuCsv1-mutants for which either RNA-binding activity is specifically disrupted (targeted mutagenesis of RRMs as described for the HuCsv1 RRM mutant), or the capacity for protein-protein interactions is reduced (such as through mutagenesis of amino acid residues in RRM3 that have been previously reported to support protein-protein interactions between ELAV/Hu proteins). Depending on the outcome of these experiments, overexpression of HuCsv1-mutant proteins could be combined with tethering assays to show a number of things, including

1. *A direct interaction between HuCsv1 and the zfcdc42-v2 3´UTR is required to cause changes in polyadenylation site use.* This could be tested by firstly co-transfecting the 3´UTR-reporter with the HuCsv1 RRM-mutant and showing the RRM-mutant protein is unable to reduce polyadenylation site use by the zfcdc42-v2 3´UTR-reporter mRNA (by RPA). To demonstrate that this effect arises because of the specific loss of HuCsv1 binding to the zfcdc42-v2 3´UTR-reporter mRNA, a tethering site could be incorporated at putative HuCsv1 binding sites within the 3´UTR. Co-expression of the 3´UTR-reporter (containing the tethering site) with an RRM-mutant HuCsv1 (λ N-protein fusion protein) could then be used to determine whether restoration of binding by the HuCsv1-mutant to the 3´UTR restores the negative effect of HuCsv1 on early polyadenylation site use.
2. *HuCsv1 participates in protein-protein interactions that mediate changes in polyadenylation site use.* This experiment would be somewhat more difficult, as currently very little is known about which residues or domains of nHu proteins participate in protein-protein interactions. Some evidence is available to suggest that RRM3 is an interface for protein-protein interactions between members of the Hu protein family [45]. The "spacer" domain has also been proposed to be a site of protein-protein interactions [40]. A variety of mutants designed to perturb interactions at potential interaction sites could be tested for loss of HuCsv1 function (with respect to zfcdc42-v2 3´UTR-reporter mRNA variant abundance). If specific mutants were identified that lost the capacity to negatively affect early polyadenylation site usage, it would be necessary to show this was because of loss of protein-protein binding and not just loss of overall protein structure or stability. In the event that a protein-protein interaction mutant were identified, it could be used to show that loss of protein-protein interaction activity; specifically at the zfcdc42-v2 3´UTR, is responsible for loss of the negative effect of HuCsv1 on early polyadenylation site usage. Specifically, a third HuCsv1 mutant type could be generated in which the RNA-binding mutant and protein-protein interaction mutant were combined to produce an HuCsv1 protein unable to bind RNA **or** form protein-protein interactions identified as being necessary for regulating alternative polyadenylation site use. This HuCsv1 double-mutant would be expressed as a fusion-protein with the λ N-peptide sequence and co-transfected into cells with the same tethering 3´UTR-reporter construct used in the loss of RNA-binding activity studies of point 1.) (*above*). Because the HuCsv1 double mutant would be specifically targeted to the zfcdc42-v2 3´UTR, it would be theoretically possible to show that the loss of protein-protein interactions by HuCsv1, bound to the zfcdc42-v2 3´UTR, is responsible for its inability to reduce polyadenylation at the early polyadenylation site.

If the results of these experiments did indicate a specific role for HuCsv1 (or any nHu protein) in controlling use of the early polyadenylation site of the zfcdc42-v2 3´UTR, it would then be necessary to examine mechanistically how this occurs. Again, without knowing the results of these thought-experiments, extensive proposals of experiments to examine such an outcome are somewhat premature. However, as for investigations into a mechanism of alternative splicing, identification of interacting factors would be of significant benefit.

One question that needs to be addressed is what would drive 3´UTR lengthening of the cdc42-v2 3´UTR. If a biological context could be identified under which 3´UTR length (or alternative splicing) of the cdc42-v2 mRNA is differentially modulated, this may be of assistance in identifying factors involved in its regulation and mechanisms by which nHu activity is controlled. An obvious potential biological context would be the process of neuronal differentiation. As discussed, the process of cellular differentiation has previously been correlated with global increases in 3´UTR length [149], [148]. Neuronal differentiation can be modelled *in vitro* using a number of different neuronal-like cell lines using chemical stimuli. For example, P19 cells (a pluripotent mouse cell line derived from an embryonic teratocarcinoma) are a well-characterised, highly stereotypical, *in vitro* model of neuronal differentiation [239], [240]). Following treatment with retinoic acid, P19 cells differentiate into quiescent, neuron-like cells with gene expression (including expression of nHu family members) and general morphology that is highly similar to *bone fide* neurons [240]. As such, P19 cells, or a comparable *in vitro* model of neuronal differentiation, could be useful in providing a system in which alternative polyadenylation site choice or alternative splicing of the cdc42-v2 mRNA could be triggered. Such as system would then enable experiments that test for effects of removing or supplying factors potentially involved in regulation of cdc42-v2 mRNA processing with a view to identifying factors (such as nHu proteins) necessary and/or sufficient for this process.

## Final word from the author

Even at the very beginning of this project, it was clear that while our hypothesis; *that neuronal Hu proteins are involved in regulating the translation of target mRNAs*, was supported by correlative and empirically derived evidence, no obvious system existed by which this hypothesis could be mechanistically tested. As such, while not technically pioneering, the practical aims of the experiments undertaken in this project were as much about constructing a robust system with which to test for the effects of neuronal Hu proteins on target messages, as they were about understanding how these effects influence neuronal differentiation and neural development. In this sense, while no single conclusion with respect to the function of neuronal Hu proteins in the process of neuronal differentiation has hitherto been provided, the work conducted in this project has been instrumental in developing and refining a system with which to better address these aims. In testimony to the value of this refinement, results from the final iteration of reporter experiments presented, suggest an entirely unexpected function of nHu proteins, as modulators of alternative polyadenylation site choice of at least one target message. Importantly, a role for nHu proteins in modulating polyadenylation site choice was in no way considered likely at the outset of this project and one that has to date, only been (recently) suggested by one other group. Unfortunately, the allotted time for this PhD project did not permit further examination of this exciting observation. However, in lieu of experimental confirmation the HuCsv1 does indeed modulate polyadenylation of the zfcdc42-v2 3´UTR, a discussion of future experiments designed to address is question has been provided. While ultimately the work presented in this thesis has not conclusively confirmed or refuted the originally stated hypothesis, it has contributed greatly to guiding and focussing future experiments in the Jensen lab aimed at understanding the function of neuronal Hu proteins, an outcome that is, in itself, a satisfying conclusion for the author.

a.)

| | amount of vector/transfection | |
|---|---|---|
| Vector: | fmoles | nanograms |
| 3`UTR reporter | 50 | 130 - 160 |
| β-galactosidase | 15.7 | 80 |
| +/-HuCsv1 | 195.5 | 750 |
| Total | 261.2 fmoles | 960 - 990ng |

b.)

| | amount of vector/transfection | |
|---|---|---|
| Vector: | fmoles | nanograms |
| 3`UTR reporter | 10 | 26 - 32 |
| β-galactosidase | 3.14 | 16 |
| +/-HuCsv1 | 39.1 | 150 |
| Total | 52.24 fmoles | 192 - 198ng |

Table 7. Renilla luciferase reporter assay transfections

Tables show amounts of vector used in transfections for either Northern analysis of mRNA abundance (a.) or reporter activity analysis (b.).

All transfections were carried out using FuGENE6® at a 3:1 ratio to DNA.

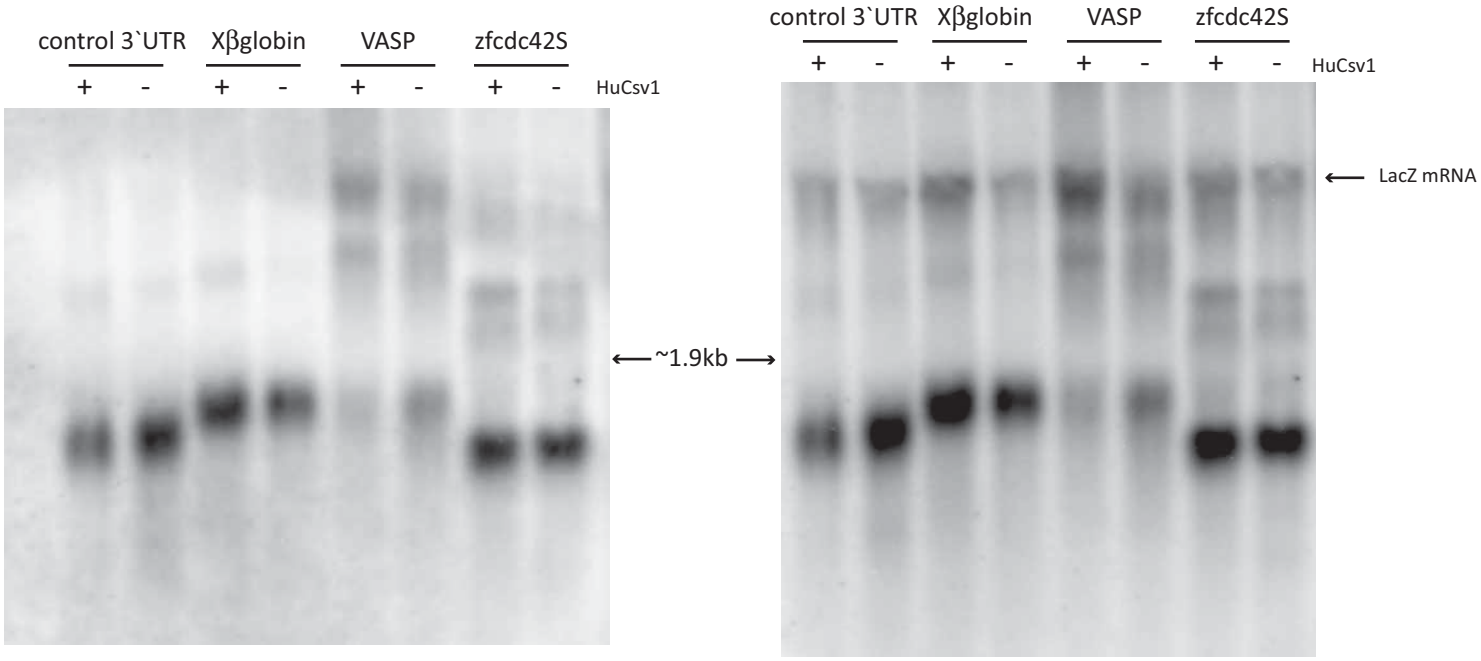


Figure 41. Renilla luciferase-based 3´UTR-reporter Northern - 293T Exp.1

Total RNA from transfected 293T cells was probed with a radiolabelled DNA probe complementary to the renilla luciferase coding sequence and a second probe complementary to the LacZ coding sequence (as a loading control). The migration of size standards was not recorded for this Northern. The approximate location of the 18S ribosomal RNA (1.9kb) is indicated.

Note - By eye there does not appear to be a reduction in the abundance of the smallest reporter mRNA product for the zfcdc42-v2 3´UTR-reporter in the presence of HuCsv1. However, normalisation to LacZ mRNA abundance (which is greater for the +HuCsv1 condition in this Northern) reveals a reduction relative to in the -HuCsv1 condition as shown in figure 46.

A VASP 3´UTR-reporter was also tested in this Northern. However, the sequence of this vector was subsequently found to be incorrect. No further testing with this vector was carried out.

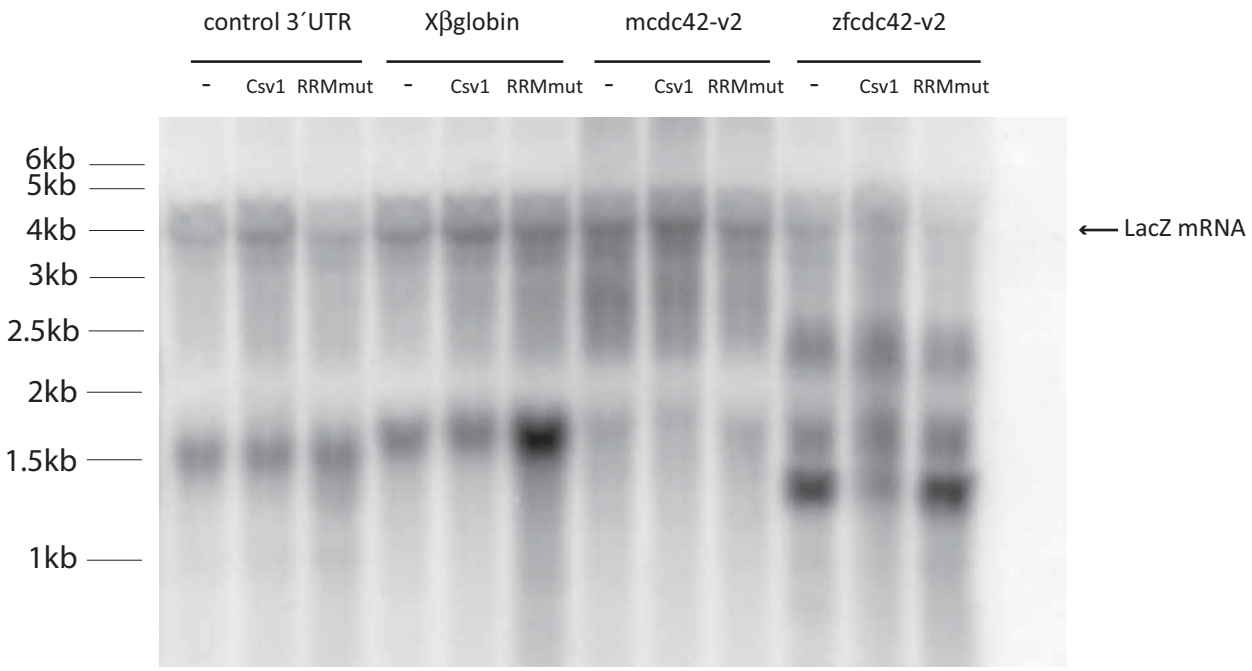


Figure 42. Renilla luciferase-based 3´UTR-reporter Northern - 293T Exp.2

Total RNA from transfected 293T cells was probed with a radiolabelled DNA probe complementary to the renilla luciferase coding sequence and a second probe complementary to the LacZ coding sequence (as a loading control). RNA size markers were run with this experiment. The migration of RNAs of known size is indicated on the left of the figure.

An mcdc42-v2 3´UTR-reporter was also tested in this Northern. However, the sequence of this vector was subsequently found to be incorrect. No further testing with this vector was carried out.

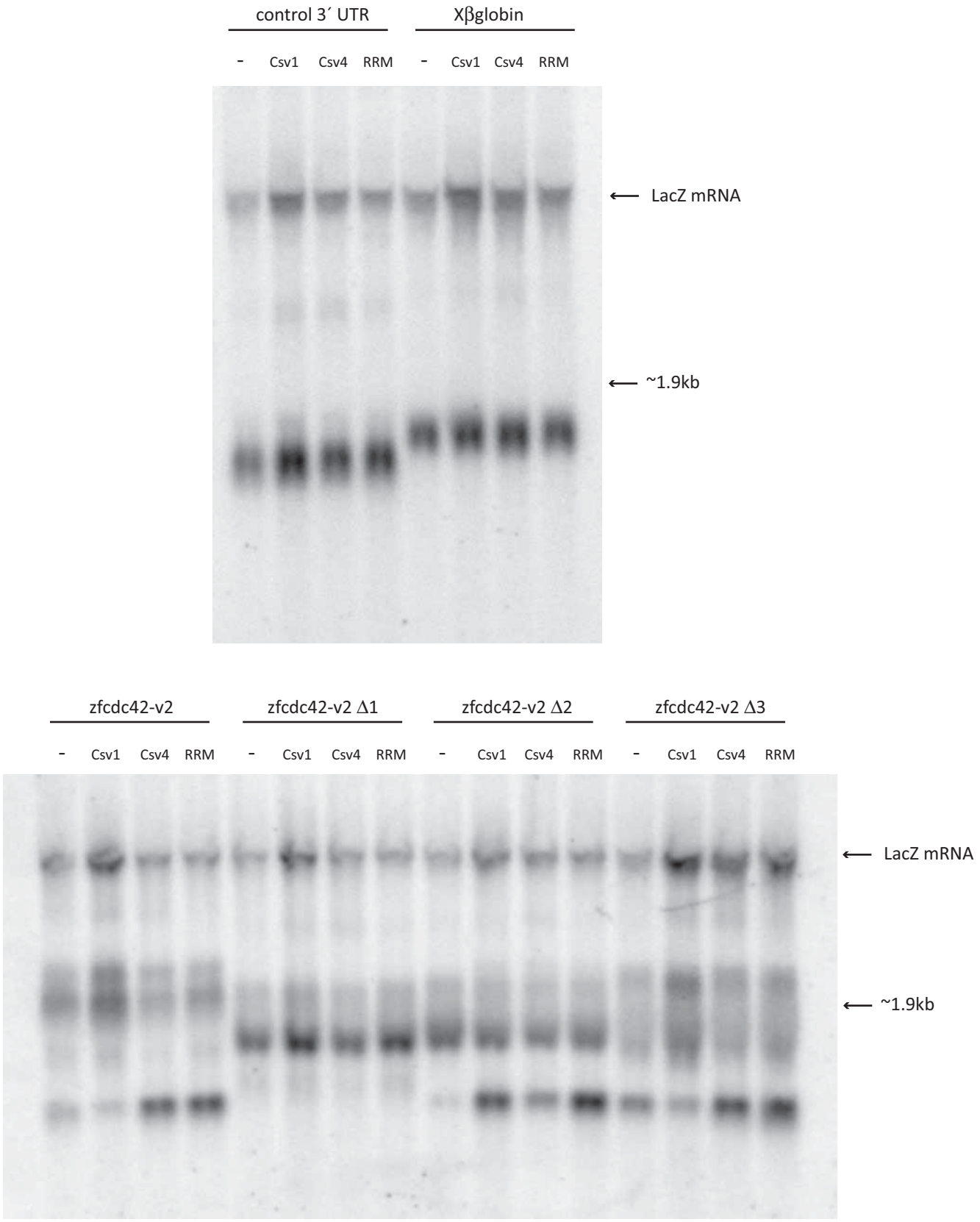


Figure 43. Renilla luciferase-based 3´UTR-reporter Northern - 293T Exp. 3

Total RNA from transfected 293T cells was probed with a radiolabelled DNA probe complementary to the renilla luciferase coding sequence and a second probe complementary to the LacZ coding sequence (as a loading control). The migration of size standards was not recorded for this Northern. The approximate location of the 18S ribosomal RNA (1.9kb) is indicated.

This experiment also included a series of zfcdc42-v2 deletion constructs (Δ1, Δ2, Δ3). In order to run the deletion constructs on the same gel as the full length zfcdc42-v2 reporter, it was necessary to run the two control reporters on a separate gel.

Figure 44 – Predicted 3`UTR reporter mRNA lengths (renilla luciferase)

| | | | | | |
|---|---|---|---|---|---|
| | | | | | SV40 late (AAUAAA) |
| control 3´UTR | | | | | 1.31kb |

| | | | | | |
|---|---|---|---|---|---|
| | | | | | SV40 late (AAUAAA) |
| Xβ-globin | | | | | 1.45kb |

| | | | | | |
|---|---|---|---|---|---|
| | Early* (UUUAAA) | | Middle (AAUAAA) | Terminal (AAUAAA) | SV40 late (AAUAAA) |
| zfcdc42-v2 | 1.22kb | | 1.51kb | 1.86kb | 2.1kb |

Figure 44b - Predicted 3`UTR reporter mRNA lengths for zfcdc42S 3`UTR deletion constructs

| | | | | | |
|---|---|---|---|---|---|
| | | | Middle (AAUAAA) | Terminal (AAUAAA) | SV40 late (AAUAAA) |
| zfcdc42-v2 Δ1 | | | 1.27kb | 1.615kb | 1.87kb |

| | | | | | |
|---|---|---|---|---|---|
| | Early* (UUUAAA) | | Middle (AAUAAA) | Terminal (AAUAAA) | SV40 late (AAUAAA) |
| zfcdc42-v2 Δ2 | 1.22kb | | | 1.675kb | 1.915kb |

| | | | | | |
|---|---|---|---|---|---|
| | Early* (UUUAAA) | | Middle (AAUAAA) | Terminal (AAUAAA) | SV40 late (AAUAAA) |
| zfcdc42-v2 Δ3 | 1.22kb | | 1.51kb | 1.74kb | 1.98kb |

Length of β-galactosidase internal control mRNA

| | | | | | |
|---|---|---|---|---|---|
| | | | | | SV40 late (AAUAAA) |
| β-galactosidase | | | | | 4.3kb |

Predicted reporter mRNA sizes correspond to the length of each mRNA from the transcription start site (TATA-box of the CMV promoter) to the cleavage site of the specified polyadenylation signal.

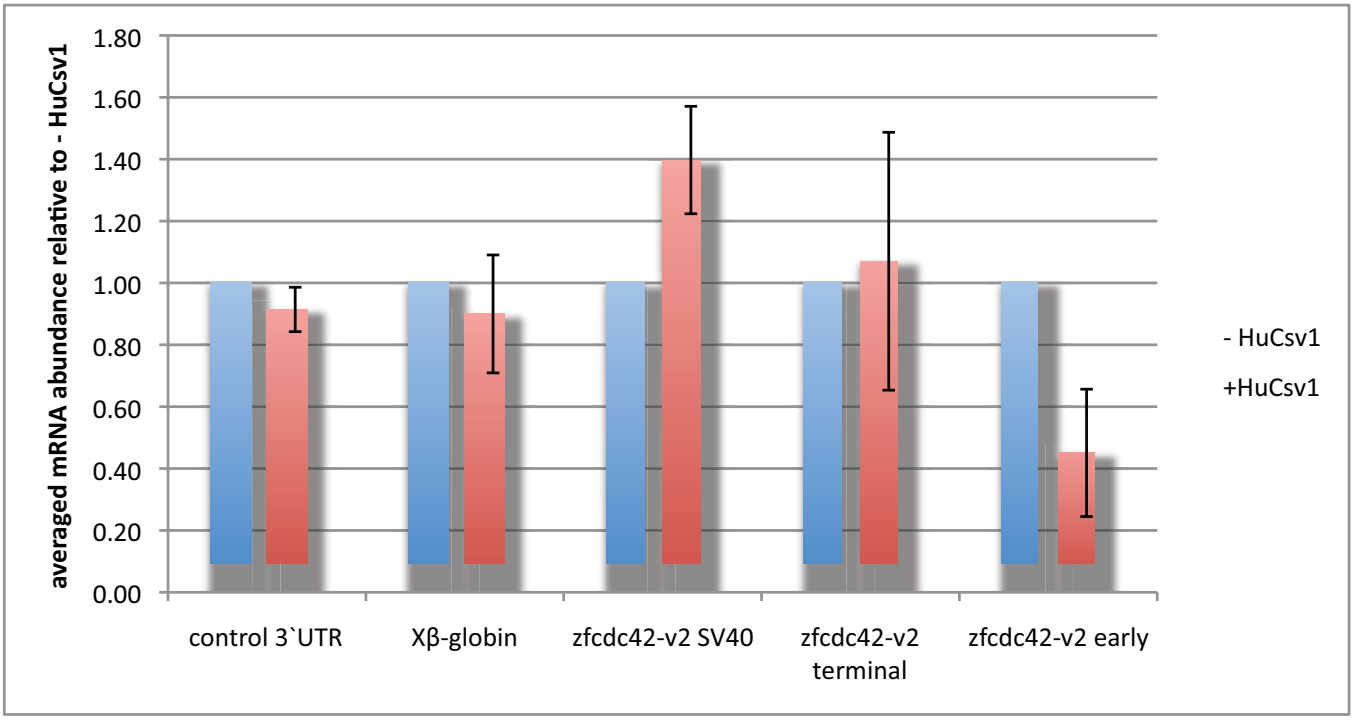


| Averaged difference in reporter mRNA abundance | | | |
|---|---|---|---|
| Reporter: | - HuCsv1 | +HuCsv1 | TTEST (*p*-VALUE) |
| control 3`UTR | 1.00 | 0.91 | 0.107 |
| Xβ-globin | 1.00 | 0.90 | 0.414 |
| zfcdc42-v2 SV40 | 1.00 | 1.40 | 0.017 |
| zfcdc42-v2 terminal | 1.00 | 1.07 | 0.785 |
| zfcdc42-v2 early | 1.00 | 0.45 | 0.010 |

Figure 45. mRNA abundance values from 3´UTR-reporter Northerns - 293T cell line

mRNA abundance in the presence of HuCsv1 compared to –HuCsv1 for each 3´UTR-reporter
Results for each 3´UTR-reporter are the average from three independent experiments.

Homoschedastic Student's t-test was used to determine the statistical significance of the difference in reporter mRNA abundance between the two HuCsv1 condition

| RL 3`UTR reporter mRNA abundance (Int. Dens) | | |
|---|---|---|
| Reporter: | - HuCsv1 | +HuCsv1 |
| control 3`UTR | 2,228 | 1,614 |
| Xβ-globin | 1,635 | 2,261 |
| zfcdc42-v2 SV40 | 170 | 385 |
| zfcdc42-v2 terminal | 162 | 222 |
| zfcdc42-v2 early | 2,097 | 2,061 |

| β-galactosidase mRNA abundance (Int. Dens) | | |
|---|---|---|
| Reporter: | - HuCsv1 | +HuCsv1 |
| control 3`UTR | 892 | 678 |
| Xβ-globin | 794 | 1,243 |
| zfcdc42-v2 | 668 | 1,011 |

| 3`UTR reporter mRNA abundance | | |
|---|---|---|
| Reporter: | - HuCsv1 | +HuCsv1 |
| control 3`UTR | 1.00 | 0.95 |
| Xβ-globin | 0.82 | 0.73 |
| zfcdc42-v2 SV40 | 0.10 | 0.15 |
| zfcdc42-v2 terminal | 0.10 | 0.09 |
| zfcdc42-v2 early | 1.26 | 0.82 |

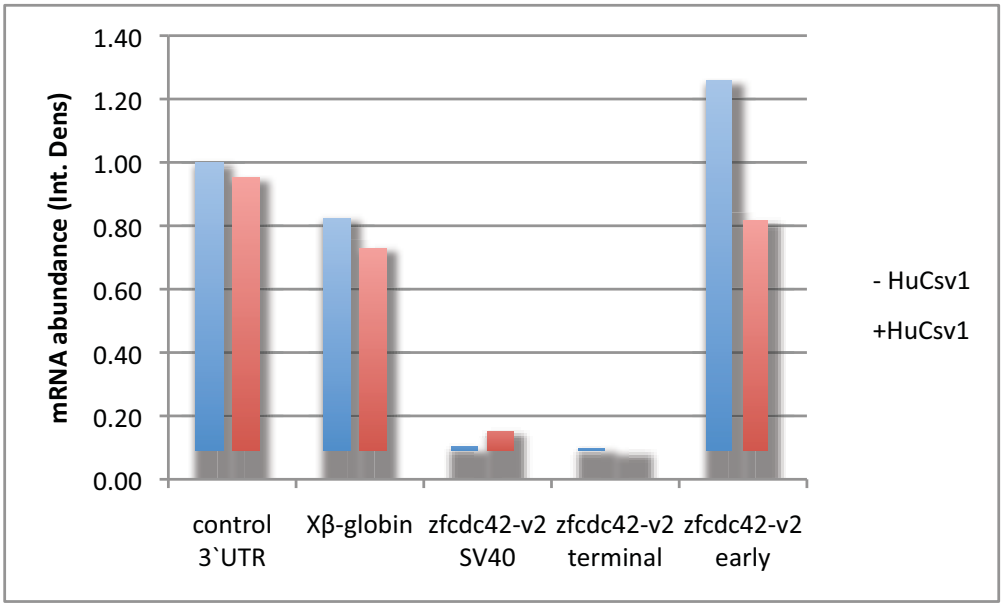


Figure 46. mRNA abundance values from 3´UTR-reporter Northerns - 293T cell line. Experiment 1.

The first two tables present raw mRNA abundance values (integrated density - Int. Dens) for both the 3´UTR-reporter mRNAs and β-galactosidase mRNAs.

Abundance of the 3´UTR-reporter mRNA was then determined by normalising to β-galactosidase mRNA abundance. These values are shown relative to abundance of the control 3´UTR-reporter mRNA from cells –HuCsv1 and are shown in the third table and following graph

| RL 3´UTR reporter mRNA abundance (Int. Dens) | | |
|---|---|---|
| Reporter: | - HuCsv1 | +HuCsv1 |
| control 3`UTR | 807 | 769 |
| Xβ-globin | 846 | 1,050 |
| zfcdc42-v2 SV40 | 727 | 815 |
| zfcdc42-v2 terminal | 663 | 901 |
| zfcdc42-v2 early | 1,646 | 701 |

| β-galactosidase mRNA abundance (Int. Dens) | | |
|---|---|---|
| Reporter: | - HuCsv1 | +HuCsv1 |
| control 3`UTR | 519 | 570 |
| Xβ-globin | 654 | 807 |
| zfcdc42-v2 | 417 | 476 |

| 3´UTR reporter mRNA abundance | | |
|---|---|---|
| Reporter: | -HuCsv1 | +HuCsv1 |
| control 3`UTR | 1.00 | 0.83 |
| Xb-globin | 0.91 | 1.00 |
| zfcdc42-v2 SV40 | 0.96 | 1.44 |
| zfcdc42-v2 terminal | 1.03 | 1.60 |
| zfcdc42-v2 early | 3.65 | 0.87 |

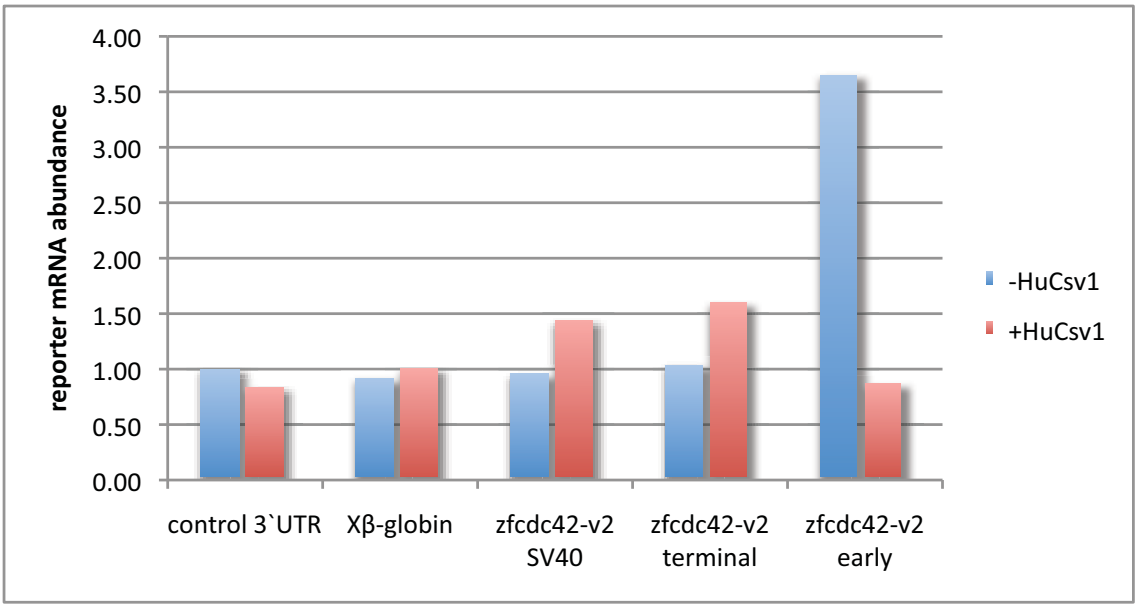


Figure 47. mRNA abundance values from 3´UTR-reporter Northerns - 293T cell line. Experiment 2.

The first two tables present raw mRNA abundance values (integrated density - Int. Dens) for both the 3´UTR-reporter mRNAs and β-galactosidase mRNAs.

Abundance of the 3´UTR-reporter mRNA was then determined by normalisation to β-galactosidase mRNA abundance. These values are shown relative to abundance of the control 3´UTR mRNA from cells –HuCsv1 and are shown in the third table and following graph

| RL 3`UTR reporter mRNA abundance (Int. Dens) | | |
|---|---|---|
| Reporter: | -HuCsv1 | +HuCsv1 |
| control 3`UTR | 942 | 1,793 |
| Xβ-globin | 1,155 | 1,117 |
| zfcdc42-v2 SV40 | 163 | 314 |
| zfcdc42-v2 terminal | 395 | 485 |
| zfcdc42-v2middle | 129 | 198 |
| zfcdc42-v2 early | 369 | 277 |

| β-galactosidase mRNA abundance (Int. Dens) | | |
|---|---|---|
| Reporter: | -HuCsv1 | +HuCsv1 |
| control 3`UTR | 192 | 381 |
| Xβ-globin | 287 | 387 |
| zfcdc42-v2 | 514 | 828 |

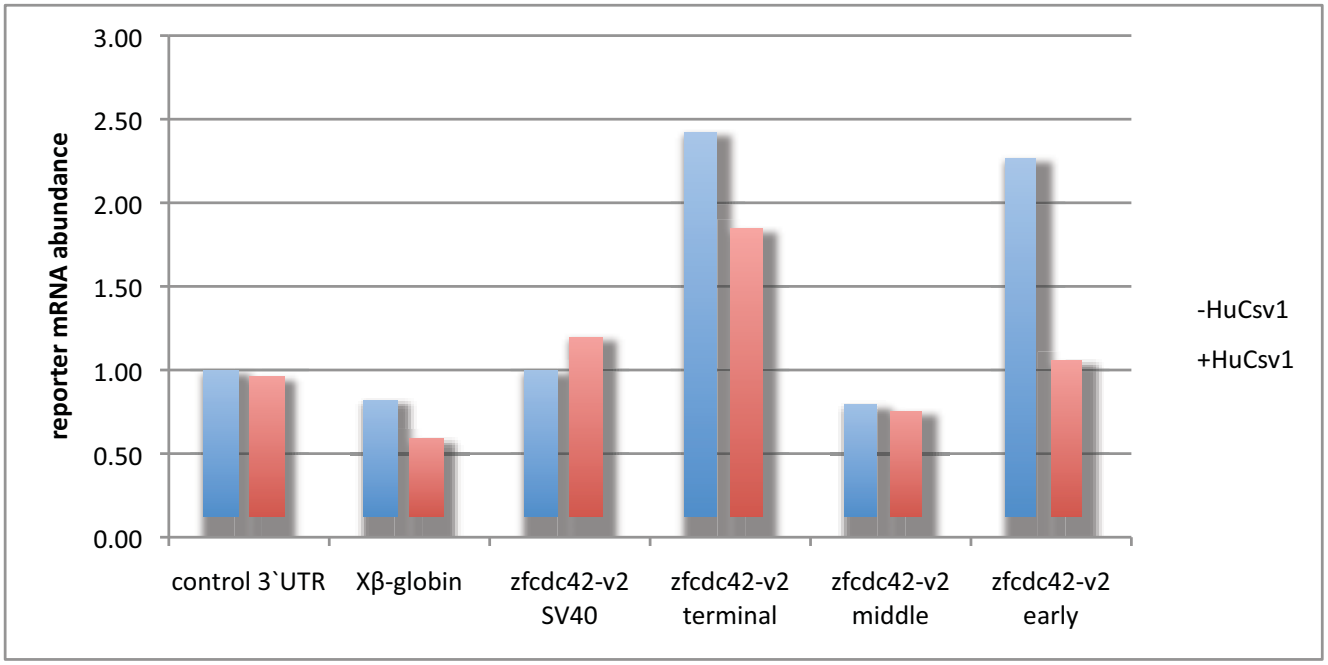


| 3`UTR reporter mRNA abundance | | |
|---|---|---|
| Reporter: | -HuCsv1 | +HuCsv1 |
| control 3`UTR | 1.00 | 0.96 |
| Xβ-globin | 0.82 | 0.59 |
| zfcdc42-v2 SV40 | 1.00 | 1.20 |
| zfcdc42-v2 terminal | 2.42 | 1.85 |
| zfcdc42-v2 middle | 0.79 | 0.75 |
| zfcdc42-v2 early | 2.27 | 1.05 |

Figure 48. mRNA abundance values from 3´UTR-reporter Northerns - 293T cell line. Experiment 3.

The first two tables present raw mRNA abundance values (integrated density - Int. Dens) for both the 3´UTR-reporter mRNAs and β-galactosidase mRNAs.

Abundance of the 3´UTR-reporter mRNA was then determined by normalisation to β-galactosidase mRNA abundance. These values are shown relative to abundance of the control 3´UTR mRNA from cells –HuCsv1 and are shown in the third table and following graph. Notably, reporter mRNAs were run on a separate Northern to the experimental reporter. Consequently, in comparing abundance values relative to – HuCsv1, for the zfcdc42-v2 reporter mRNAs values were made relative to zfcdc42-v2 (SV40) – HuCsv1

## Experiment 2

| | Raw RL activity | |
|---|---|---|
| Reporter: | -HuCsv1 | +HuCsv1 |
| control 3`UTR | 200,720,592 | 279,780,672 |
| Xβ-globin | 192,732,312 | 244,917,072 |

| | RL activity / RL mRNA | |
|---|---|---|
| Reporter: | -HuCsv1 | +HuCsv1 |
| control 3`UTR | 38,353,032 | 47,756,366 |
| Xβ-globin | 28,456,814 | 33,454,046 |

| | Raw LacZ activity | |
|---|---|---|
| Reporter: | -HuCsv1 | +HuCsv1 |
| control 3`UTR | 0.4106 | 0.66205 |
| Xβ-globin | 0.4609 | 0.68265 |

| | LacZ activity / LacZ mRNA | |
|---|---|---|
| Reporter: | -HuCsv1 | +HuCsv1 |
| control 3`UTR | 0.4700 | 0.5542 |
| Xβ-globin | 0.3733 | 0.4287 |

| | RL activity / LacZ activity | |
|---|---|---|
| Reporter: | -HuCsv1 | +HuCsv1 |
| control 3`UTR | 488,847,034 | 422,597,496 |
| Xβ-globin | 418,165,138 | 358,774,001 |

| | translation efficiency | |
|---|---|---|
| Reporter: | -HuCsv1 | +HuCsv1 |
| control 3`UTR | 1.00 | 1.06 |
| Xβ-globin | 1.00 | 1.02 |

## Experiment 3

| | Raw RL activity | |
|---|---|---|
| Reporter: | -HuCsv1 | +HuCsv1 |
| control 3`UTR | 101,062,456 | 186,983,656 |
| Xβ-globin | 86,396,964 | 137,246,972 |

| | RL activity / RL mRNA | |
|---|---|---|
| Reporter: | -HuCsv1 | +HuCsv1 |
| control 3`UTR | 61,585,896 | 43,402,812 |
| Xβ-globin | 37,449,919 | 42,274,063 |

| | Raw LacZ activity | |
|---|---|---|
| Reporter: | -HuCsv1 | +HuCsv1 |
| control 3`UTR | 0.161 | 0.329 |
| Xβ-globin | 0.200 | 0.305 |

| | LacZ activity / LacZ mRNA | |
|---|---|---|
| Reporter: | -HuCsv1 | +HuCsv1 |
| control 3`UTR | 0.25 | 0.20 |
| Xβ-globin | 0.19 | 0.18 |

| | RL activity / LacZ activity | |
|---|---|---|
| Reporter: | -HuCsv1 | +HuCsv1 |
| control 3`UTR | 629,672,623 | 568,253,019 |
| Xβ-globin | 431,337,813 | 450,507,047 |

| | translation efficiency | |
|---|---|---|
| Reporter: | -HuCsv1 | +HuCsv1 |
| control 3`UTR | 1.00 | 0.89 |
| Xβ-globin | 1.00 | 1.20 |

Figure 49. Translation efficiency calculations from the second and third renilla luciferase-based 3´UTR-reporter experiments

Top: Experiment 2
Bottom: Experiment 3

Translation efficiency in the presence of HuCsv1 is presented relative to the -HuCsv1 condition for all 3´UTR-reporters.

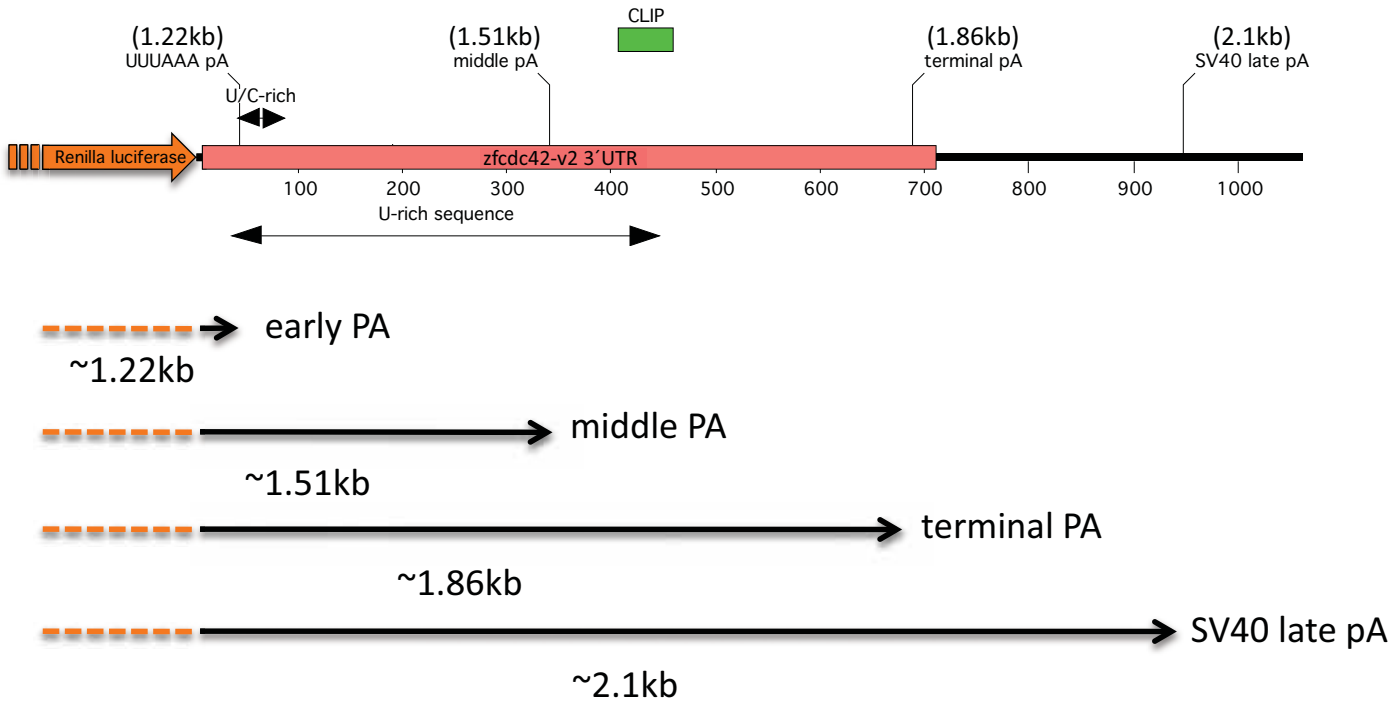


Figure 50. Schematic representation of the zfcdc42-v2 3´UTR within the renilla luciferase reporter vector

pA = predicted polyadenylation site
CLIP = region identified by CLIP isolation of putative target mRNAs of neuronal Hu proteins

Predicted sizes of reporter mRNAs are based on a full transcript including all sequence upstream of the renilla luciferase coding sequence. They do not account for polyA tail length.

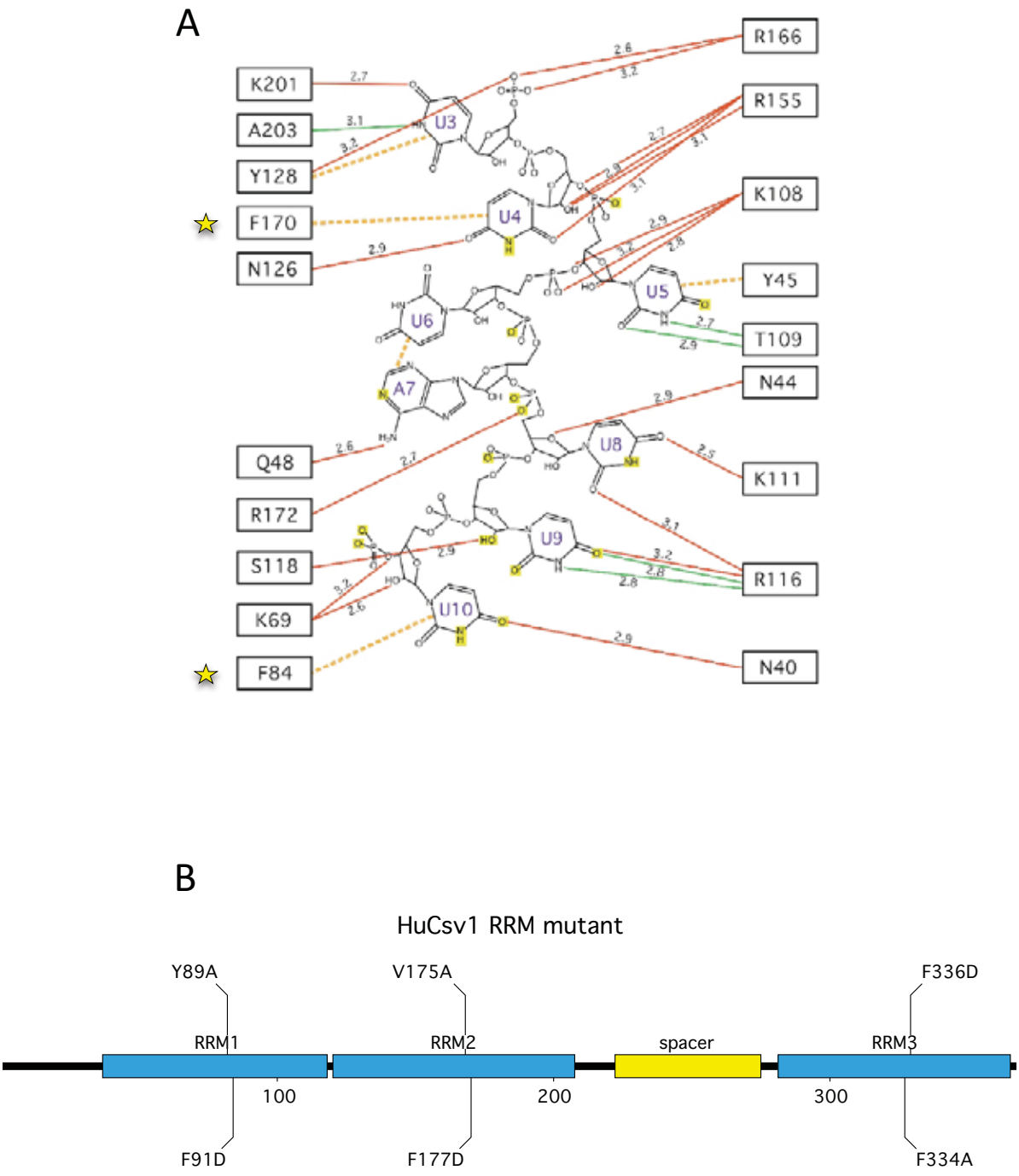


Figure 51. Targeted mutagenesis of phenylalanine residue in RRMs of Hu proteins abolishes RNA-binding activity.

a.) Key stacking interactions (orange dashed line) between a phenylalanine in RNP1 of RRM 1 (F84) and RRM2 (F170) from HuD have been shown by X-ray crystallography for HuD in complex with a target mRNA sequence. The corresponding phenylalanine residues of RRMs 1, 2 and 3 of HuCsv1 were mutated to alanine by PCR-based, site directed mutagenesis. Figure adapted from Wang X 2001.

b.) Schematic showing location of amino acid substitutions for the HuCsv1 RRM mutant.

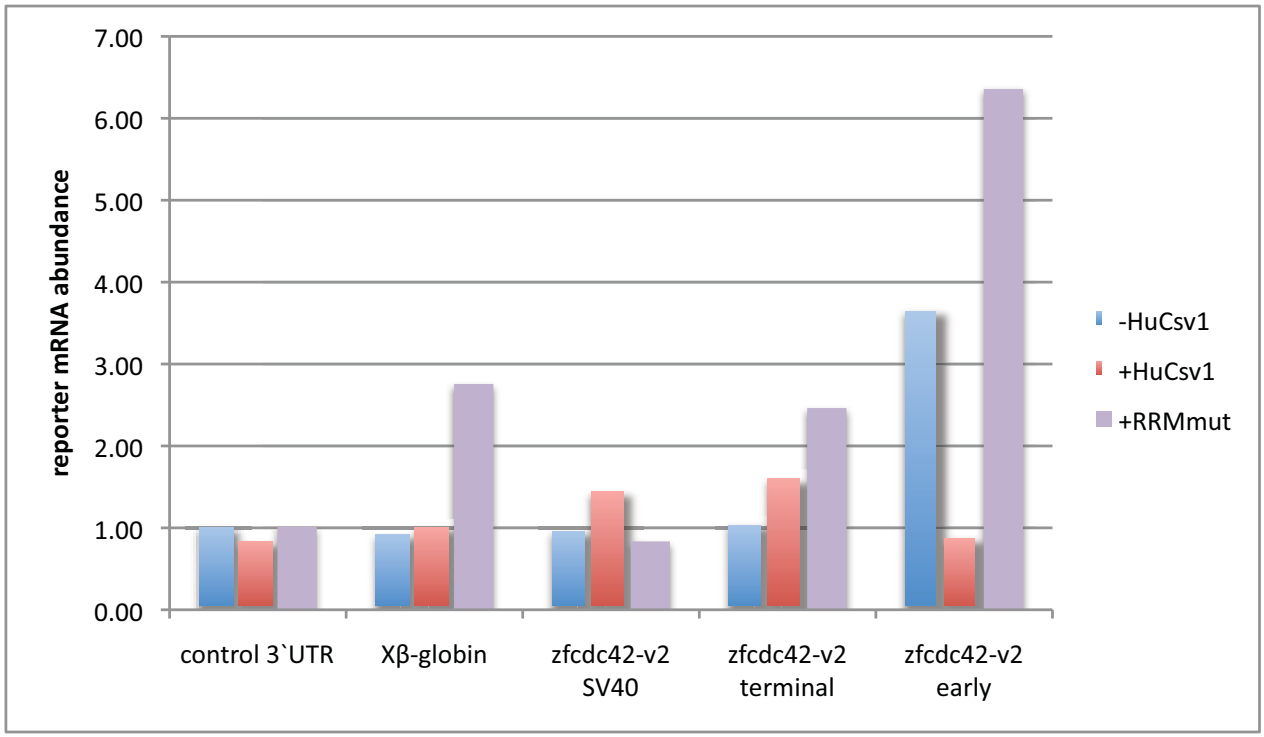


(i.)

| | 3´UTR reporter mRNA abundance | | |
|---|---|---|---|
| Reporter: | -HuCsv1 | +HuCsv1 | +RRMmut |
| control 3´UTR | 1.00 | 0.83 | 1.01 |
| Xβ-globin | 0.91 | 1.00 | 2.76 |
| zfcdc42-v2 SV40 | 0.96 | 1.44 | 0.83 |
| zfcdc42-v2 terminal | 1.03 | 1.60 | 2.46 |
| zfcdc42-v2 early | 3.65 | 0.87 | 6.36 |

(ii.)

| | abundance relative to -HuCsv1 | | |
|---|---|---|---|
| Reporter: | -HuCsv1 | +HuCsv1 | +RRMmut |
| control 3´UTR | - | 0.83 | 1.01 |
| Xβ-globin | - | 1.10 | 3.01 |
| zfcdc42-v2 SV40 | - | 1.50 | 0.87 |
| zfcdc42-v2 terminal | - | 1.54 | 2.38 |
| zfcdc42-v2 early | - | 0.24 | 1.74 |

Figure 52. mRNA abundance values for 3´UTR-reporters in the presence of HuCsv1 and the HuCsv1 RRM mutant. Corresponds to Northern figure G.

Graph and (i.) - mRNA abundance is shown relative to the abundance of the control 3´UTR-reporter in the –HuCsv1 condition

(ii.) – mRNA abundance for each reporter mRNA in the presence of HuCsv1 **or** HuCsv1 RRMmut relative to in the –HuCsv1 condition.

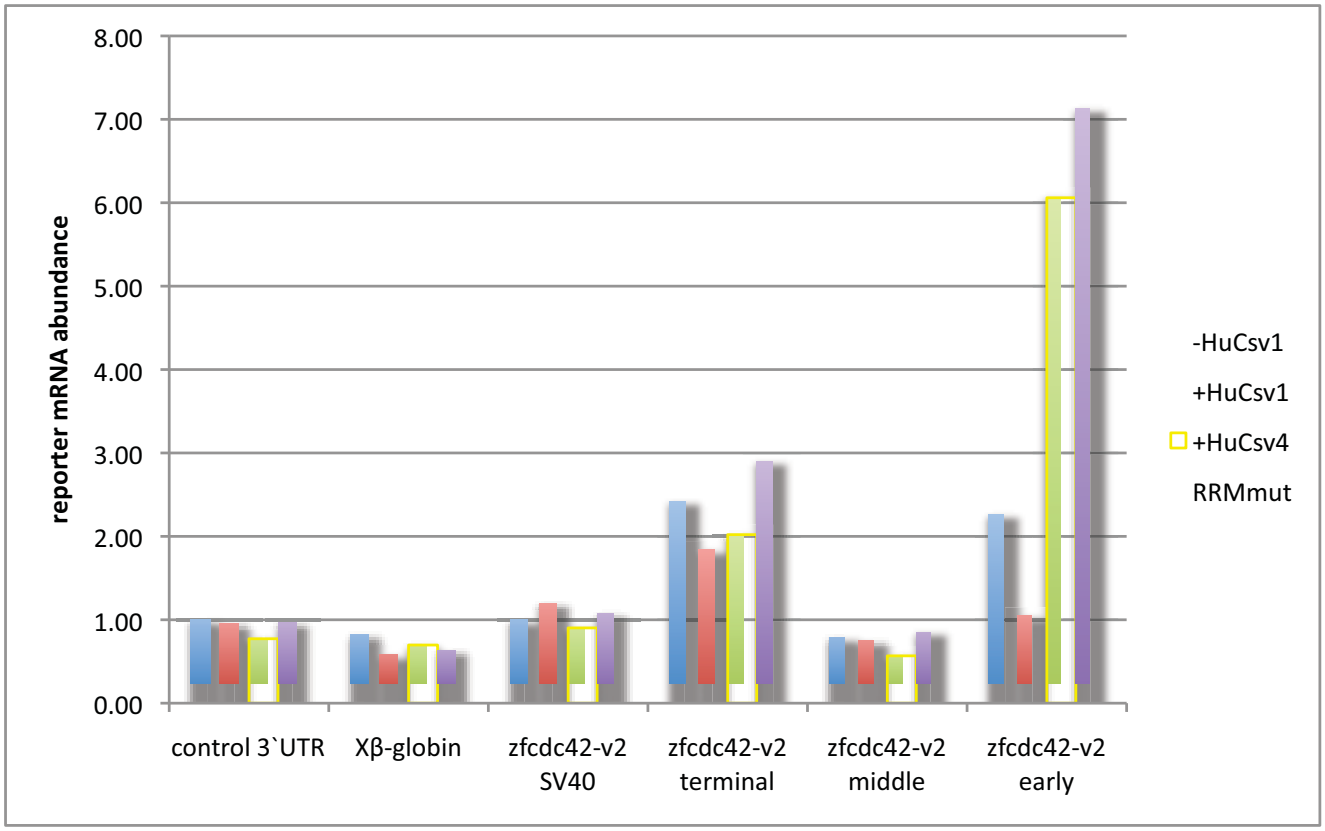


(i.)

| | 3`UTR reporter mRNA abundance | | | |
|---|---|---|---|---|
| Reporter: | -HuCsv1 | +HuCsv1 | +HuCsv4 | RRMmut |
| control 3´UTR | 1.00 | 0.96 | 0.77 | 0.96 |
| Xβ-globin | 0.82 | 0.59 | 0.70 | 0.63 |
| zfcdc42-v2 SV40 | 1.00 | 1.20 | 0.90 | 1.07 |
| zfcdc42-v2 terminal | 2.42 | 1.85 | 2.02 | 2.90 |
| zfcdc42-v2 middle | 0.79 | 0.75 | 0.57 | 0.85 |
| zfcdc42-v2 early | 2.27 | 1.05 | 6.06 | 7.13 |

(ii.)

| | abundance relative to -HuCsv1 | | | |
|---|---|---|---|---|
| Reporter: | -HuCsv1 | +HuCsv1 | +HuCsv4 | +RRMmut |
| control 3´UTR | - | 0.96 | 0.77 | 0.96 |
| Xβ-globin | - | 0.72 | 0.85 | 0.77 |
| zfcdc42-v2 SV40 | - | 1.20 | 0.90 | 1.07 |
| zfcdc42-v2 terminal | - | 0.76 | 0.83 | 1.20 |
| zfcdc42-v2 middle | - | 0.95 | 0.72 | 1.08 |
| zfcdc42-v2 early | - | 0.46 | 2.67 | 3.15 |

Figure 53. mRNA abundance values for 3´UTR-reporters in the presence of HuCsv1, HuCsv4 and the HuCsv1 RRM mutant. Corresponds to Northern figure H

Graph and (i.) - mRNA abundance is shown relative to the abundance of the control 3´UTR-reporter in the –HuCsv1 condition

(ii.) – mRNA abundance for each reporter mRNA in the presence of HuCsv1, HuCsv4 **or** HuCsv1 RRMmut relative to in the –HuCsv1 condition.

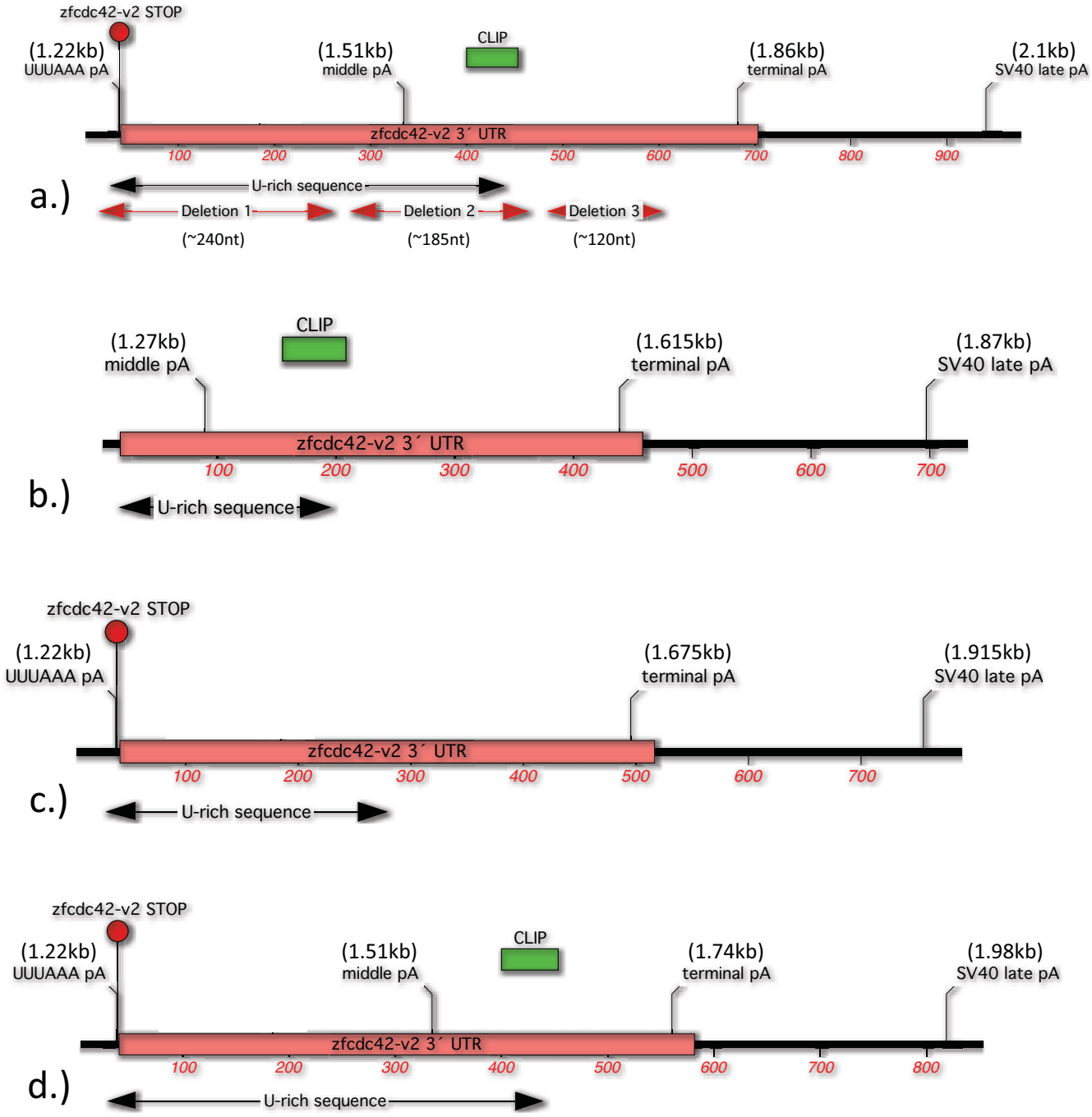


Figure 54. Schematic representation of the zfcdc42-v2 3´UTR deletion reporter mRNAs

pA = predicted polyadenylation site
CLIP = region identified by CLIP isolation of putative target mRNAs of neuronal Hu proteins

a.) Full length reporter mRNA with deleted regions indicated by red arrows
b.) deletion-1 mRNA – lacks the first two predicted polyadenylation sitesand ~200nt of U-rich sequence
c.) deletion-2 mRNA – lacks the predicted middle polyadenylation signal, CLIP identified nHu binding site and ~!50nt of U-rich sequence
d.) deletion-3 mRNA – all polyadenylation sites are present as is CLIP identified nHu binding site

a.)

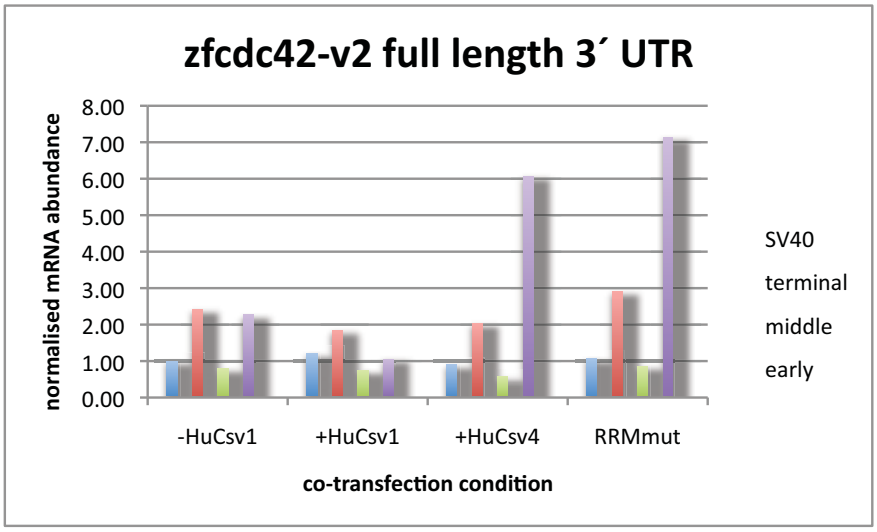


| 3`UTR reporter mRNA abundance | | | | |
|---|---|---|---|---|
| zfcdc42-v2 - Full Length | | | | |
| polyA site: | -HuCsv1 | +HuCsv1 | +HuCsv4 | RRMmut |
| SV40 | 1.00 | 1.20 | 0.90 | 1.07 |
| terminal | 2.42 | 1.85 | 2.02 | 2.90 |
| middle | 0.79 | 0.75 | 0.57 | 0.85 |
| early | 2.27 | 1.05 | 6.06 | 7.13 |

b.)

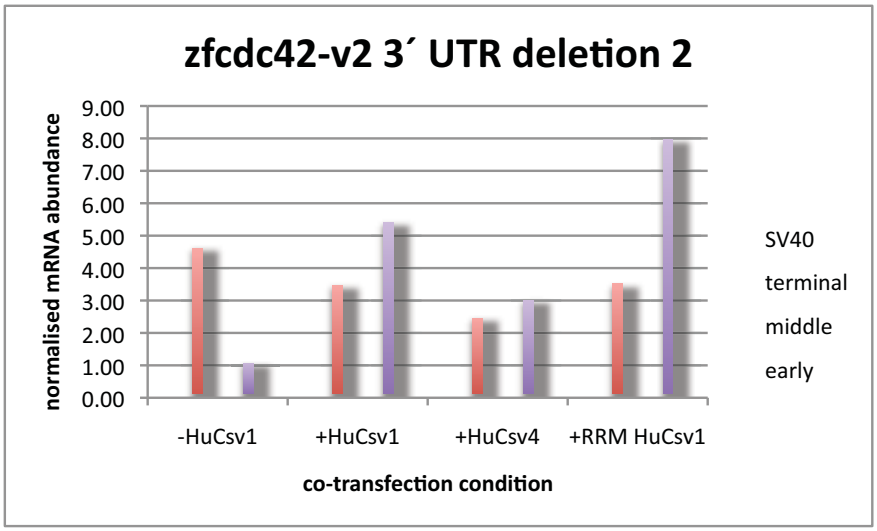


| 3`UTR reporter mRNA abundance | | | | |
|---|---|---|---|---|
| zfcdc42-v2 - Deletion 2 | | | | |
| polyA site: | -HuCsv1 | +HuCsv1 | +HuCsv4 | -RRM HuCsv |
| *SV40* | | | | |
| terminal | 4.62 | 3.47 | 2.46 | 3.51 |
| middle | | | | |
| *early* | 1.07 | 5.40 | 3.00 | 7.98 |

Figure 55. Schematic representation of the zfcdc42-v2 3´UTR deletion reporter mRNAs

a.) Full length reporter mRNA variant abundances
b.) deletion-2 mRNA variant abundances

RL mRNA abundances were normalised to GAPDH mRNA values and then corrected to the abundance of reporter mRNAs using the SV40 late polyA site in the –HuCsv1 condition for the full length reporter.

c.)

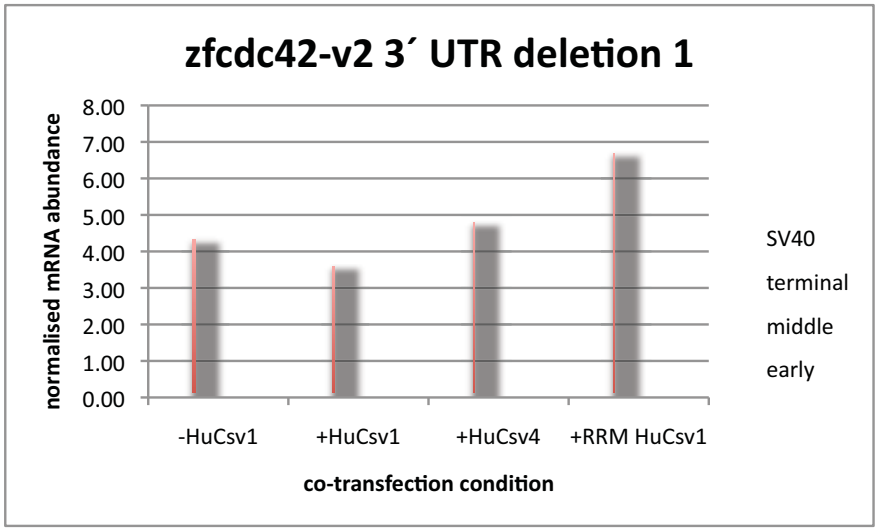


| 3`UTR reporter mRNA abundance | | | | |
|---|---|---|---|---|
| zfcdc42-v2 - Deletion 1 | | | | |
| polyA site: | -HuCsv1 | +HuCsv1 | +HuCsv4 | -RRM HuCsv |
| *SV40* | | | | |
| terminal | 4.32 | 3.59 | 4.78 | 6.67 |
| middle | | | | |
| *early* | | | | |

d.)

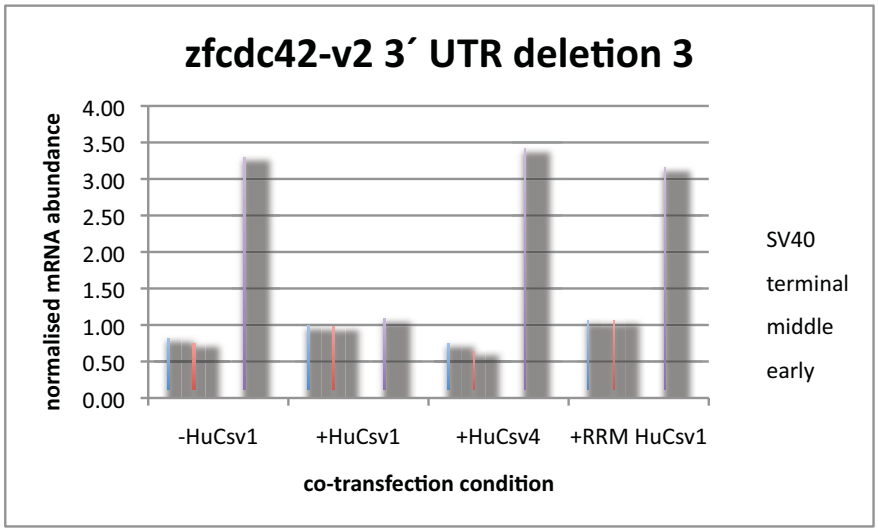


| 3`UTR reporter mRNA abundance | | | | |
|---|---|---|---|---|
| zfcdc42-v2 - Deletion 3 | | | | |
| polyA site: | -HuCsv1 | +HuCsv1 | +HuCsv4 | -RRM HuCsv |
| *SV40* | 0.82 | 0.99 | 0.75 | 1.06 |
| terminal | 0.75 | 0.97 | 0.63 | 1.06 |
| *middle* | | | | |
| early | 3.29 | 1.08 | 3.41 | 3.15 |

Figure 55. Schematic representation of the zfcdc42-v2 3´UTR deletion reporter mRNAs

c.) deletion-1 reporter mRNA variant abundances
d.) deletion-3 mRNA variant abundances

RL mRNA abundances were normalised to GAPDH mRNA values and then corrected to the abundance of reporter mRNAs using the SV40 late polyA site in the –HuCsv1 condition for the full length reporter.

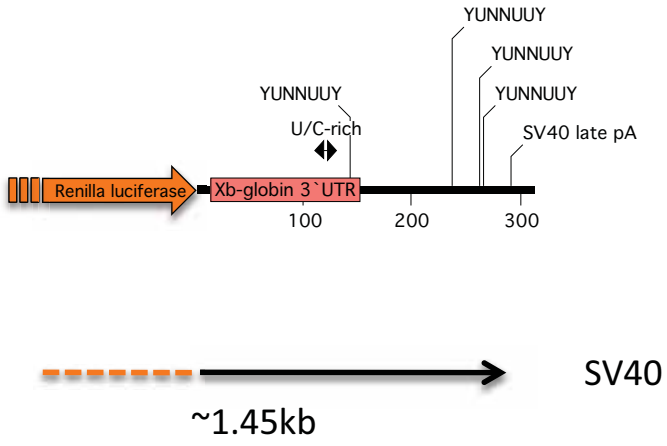


Figure 14. Schematic representation of the Xβ-globin 3´UTR within the renilla luciferase reporter vector

pA = predicted polyadenylation site
YUNNUUY = possible Hu protein interaction site. (Y = pyrimidine, U = uracil, N = any ribonucleotide)

Predicted sizes of reporter mRNA is based on a full transcript including all sequence upstream of the renilla luciferase coding sequence beginning from the transcription start site (TATA-box of the CMV protomoter). This does not account for polyA tail length.

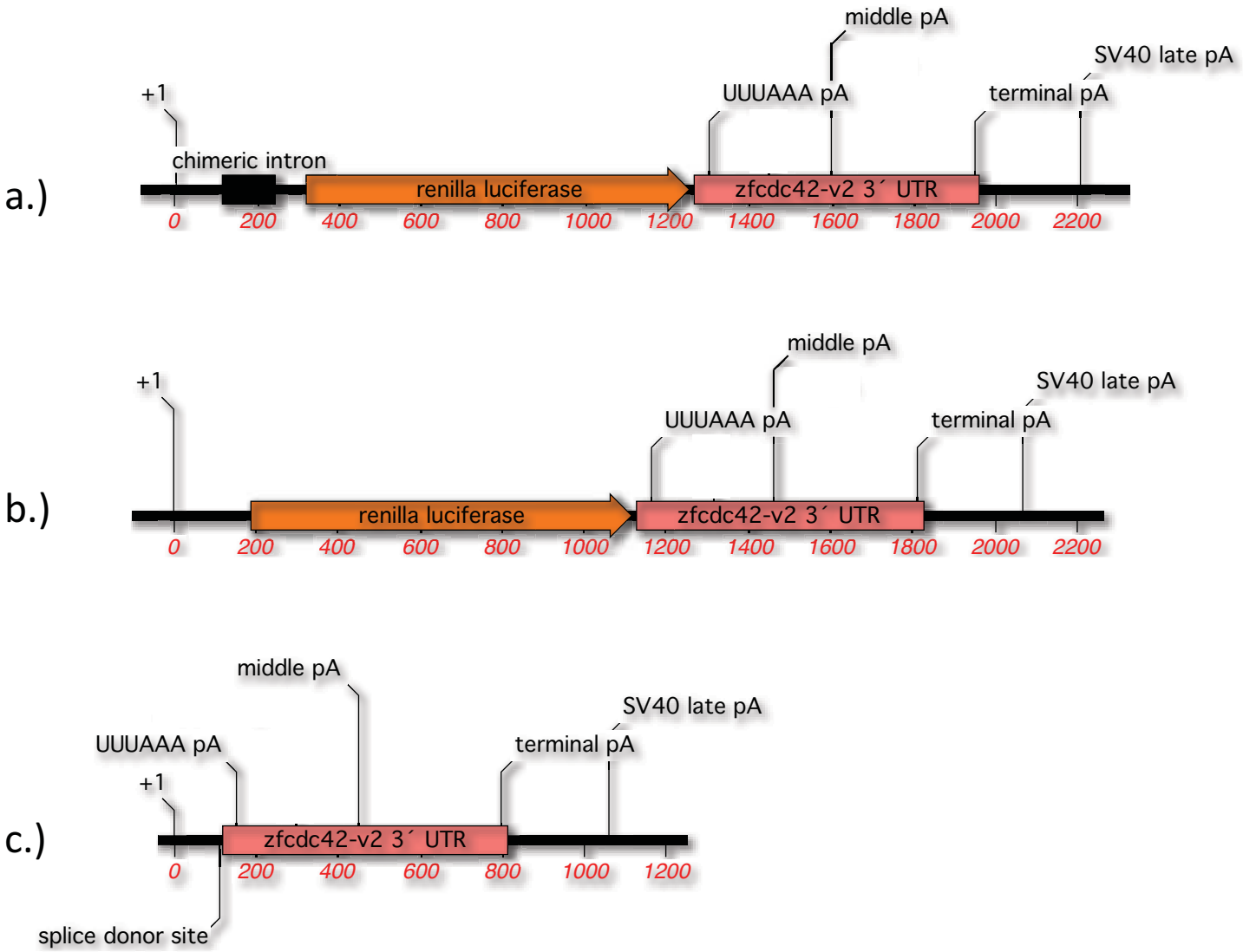


Figure 56. Schematic representation of how cryptic splicing within the zfcdc42-v2 3´UTR-reporter mRNA could yield an mRNA product of a similar size to that observed for the smallest mRNA product in the renilla (and firefly) luciferase-based reporter Northern blots.

a.) represents the un-processed zfcdc42-v2 3´UTR-reporter mRNA, showing the location of the chimeric intron within the mRNA sequence.

b.) Correct splicing of the zfcdc42-v2 3´UTR-reporter mRNA would produce a transcript containing the renilla luciferase coding sequence, and would be polyadenylated at one of the indicated polyadenylation sites (pA)

c.) Cryptic splicing of the 5´-donor site from the chimeric intron to an unidentified 3´-acceptor site at the start of the zfcdc42-v2 3´UTR would yield a reporter mRNA lacking the renilla luciferase coding sequence. Based on the Northern blot data, this mRNA would be polyadenylated at the SV40 late polyadenylation site to yield a transcript of approximately 1000 – 1200nt depending on polyA tail length.

Indicated sizes are in nucleotides and begin from the CMV promoter transcription start site.

a.)

| | RL activity/lacZ activity (normalised to -HuCsv1) | | | |
|---|---|---|---|---|
| | Experiment 2 | | Experiment 3 | |
| Reporter: | -HuCsv1 | +HuCsv1 | -HuCsv1 | +HuCsv1 |
| control 3`UTR | 1.00 | 0.86 | 1.00 | 0.79 |
| Xβ-globin | 1.00 | 0.86 | 1.00 | 0.79 |
| zfcdc42-v2 | 1.00 | 0.59 | 1.00 | 0.96 |

b.)

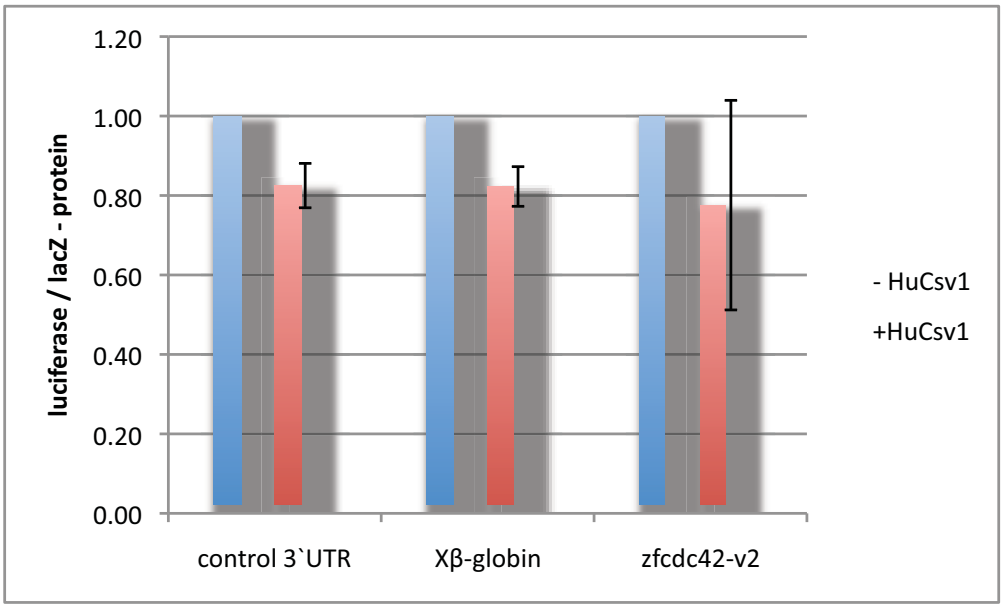


| | average RL/lacZ | | STDEV |
|---|---|---|---|
| | - HuCsv1 | +HuCsv1 | |
| control 3`UTR | 1.00 | 0.82 | 0.06 |
| Xβ-globin | 1.00 | 0.82 | 0.05 |
| zfcdc42-v2 | 1.00 | 0.78 | 0.26 |

Figure 57. Renilla luciferase (RL) activity normalised to β-galactosidase (lacZ) activity collected from the second and third experiments does not reliably indicate whether a reduction in renilla luciferase activity is observed for the zfcdc42-v2 3´UTR-reporter in the presence of HuCsv1

a.) normalised RL activity from experiments 2 and 3. Normalised activity for each 3´UTR-reporter is shown relative to the –HuCsv1 condition.

b.) averaged normalised RL activity relative to the –HuCsv1 condition. Error bars indicate standard deviation (STDEV) for each average.

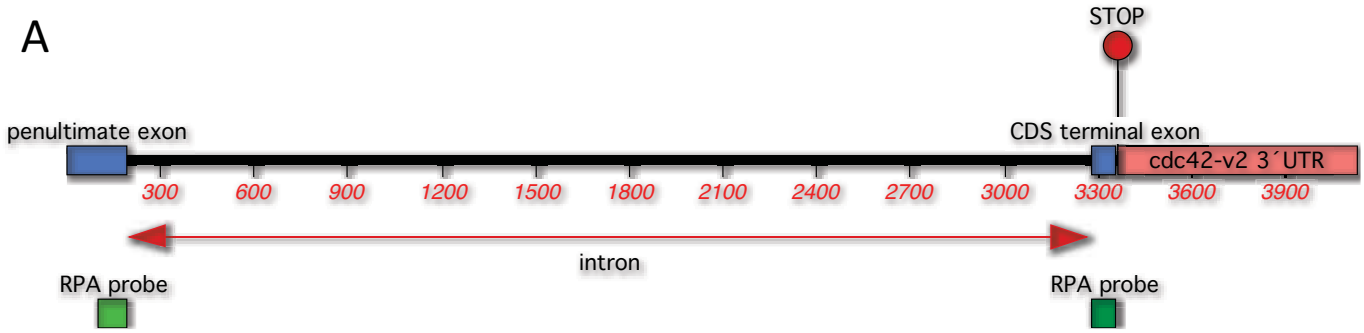


| splice isoform | RPA product |
|---|---|
| cdc42-v1 | 100nt |
| cdc42-v2 | 190nt |
| total probe length= 190nt | |

Figure 58a. An RPA probe sequence complementary to a stretch of nucleotides in the cdc42-v2 mRNA that spanned the terminal (alternatively spliced) intron could be used to ascertain if HuCsv1 influences alternative splicing of the cdc42 mRNA to favour production of the cdc42-v2 message. In the schematic, the probe recognises 100nt of the penultimate exon which is present in both the cdc42-v1 and –v2 mRNAs and cdc42-v2 transcript. The full 190nt of the probe however is only present in the cdc42-v2 mRNA. Using this probe it would be possible to compare the abundance of the cdc42-v2 product (relative to the cdc42-v1 product) in the presence and absence of HuCsv1.

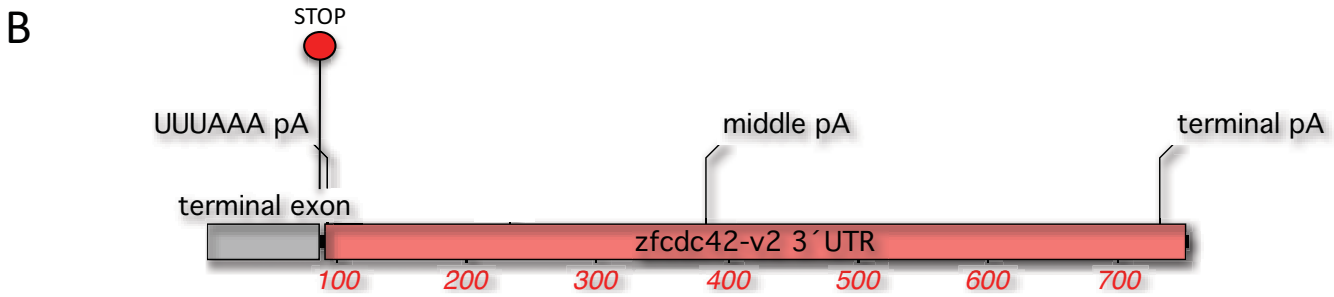


| polyA site used | RPA product size |
|---|---|
| early/UUUAAA | ~90nt |
| middle | ~380nt |
| terminal | ~740nt |
| total probe length | 900nt |

Figure 58b. An RPA probe sequence complementary to the entire zfcdc42-v2 3´UTR (including ~90nt of coding sequence) could be used to compare the relative abundance of zfcdc42-v2 reporter mRNAs using each of the possible polyadenylation sites present within the 3´UTR sequence. Any change in use of a specific polyadenylation sequence (*ie.* Reduced usage of the early /UUUAAA polyadenylation site) in the presence of HuCsv1 would be evident by changes in abundance of the corresponding RPA product. Approximate sizes of RPA products using a probe spanning the mRNA sequence shown in the schematic are presented in the accompanying table.

## *Supplementary figure 1*

| RL 3`UTR reporter mRNA abundance (Int. Dens) | | | |
|---|---|---|---|
| Reporter: | - HuCsv1 | +HuCsv1 | +RRMmut |
| control 3`UTR | 807 | 769 | 735 |
| Xβ-globin | 846 | 1,050 | 1,751 |
| zfcdc42-v2 SV40 | 727 | 815 | 615 |
| zfcdc42-v2 terminal | 663 | 901 | 788 |
| zfcdc42-v2 early | 1,646 | 701 | 1,547 |

| β-galactosidase mRNA abundance (Int. Dens) | | | |
|---|---|---|---|
| Reporter: | - HuCsv1 | +HuCsv1 | +RRMmut |
| control 3`UTR | 519 | 570 | 430 |
| Xβ-globin | 654 | 807 | 642 |
| zfcdc42-v2 | 417 | 476 | 228 |

| 3`UTR reporter mRNA abundance | | | |
|---|---|---|---|
| Reporter: | -HuCsv1 | +HuCsv1 | +RRMmut |
| control 3`UTR | 1.00 | 0.83 | 1.01 |
| Xb-globin | 0.91 | 1.00 | 2.76 |
| zfcdc42-v2 SV40 | 0.96 | 1.44 | 0.83 |
| zfcdc42-v2 terminal | 1.03 | 1.60 | 2.46 |
| zfcdc42-v2 early | 3.65 | 0.87 | 6.36 |

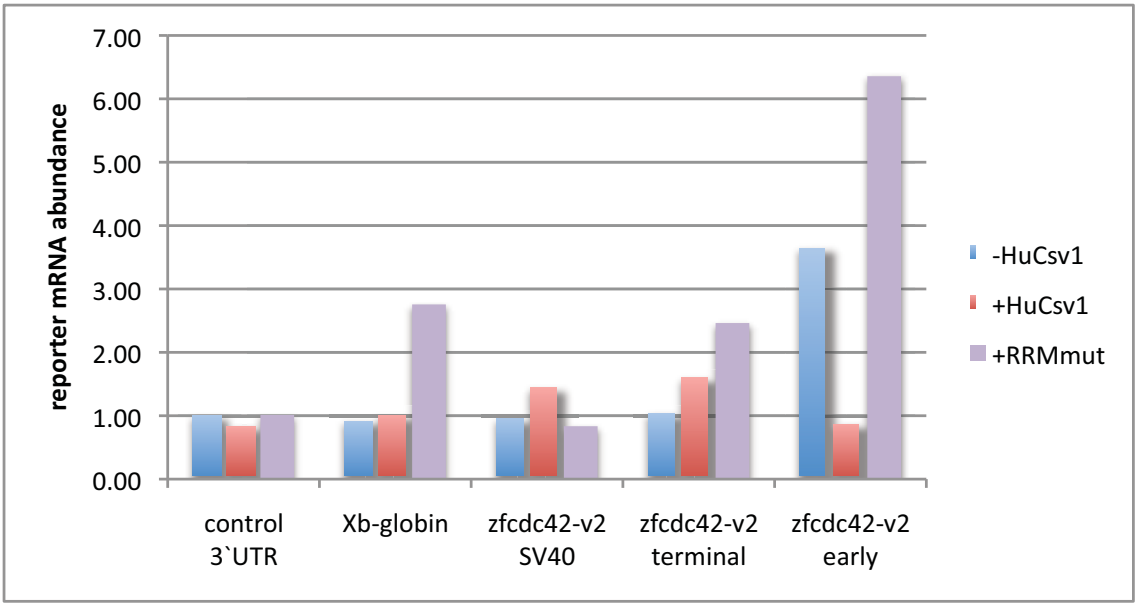


Figure S1. mRNA abundance values from 3´UTR-reporter Northerns - 293T cell line. Experiment 2.

The first two tables present raw mRNA abundance values ( integrated density - Int. Dens) for both the 3´UTR-reporter mRNAs and β-galactosidase mRNAs.

Abundance of the 3´UTR-reporter mRNA was then determined by normalisation to β-galactosidase mRNA abundance. These values are shown relative to abundance of the control 3´UTR mRNA from cells –HuCsv1 and are shown in the third table and following graph

*Supplementary figure 2*

| RL 3`UTR reporter mRNA abundance (Int. Dens) | | | | |
|---|---|---|---|---|
| Reporter: | -HuCsv1 | +HuCsv1 | +HuCsv4 | +RRMmut |
| control 3`UTR | 942 | 1,793 | 1,219 | 1,384 |
| Xβ-globin | 1,155 | 1,117 | 1,163 | 1,020 |
| zfcdc42-v2 SV40 | 163 | 314 | 119 | 137 |
| zfcdc42-v2 terminal | 395 | 485 | 266 | 371 |
| zfcdc42-v2middle | 129 | 198 | 75 | 109 |
| zfcdc42-v2 early | 369 | 277 | 798 | 910 |

| β-galactosidase mRNA abundance (Int. Dens) | | | | |
|---|---|---|---|---|
| Reporter: | -HuCsv1 | +HuCsv1 | +HuCsv4 | +RRMmut |
| control 3`UTR | 192 | 381 | 322 | 293 |
| Xβ-globin | 287 | 387 | 340 | 328 |
| zfcdc42-v2 | 514 | 828 | 415 | 403 |

| 3`UTR reporter mRNA abundance | | | | |
|---|---|---|---|---|
| Reporter: | -HuCsv1 | +HuCsv1 | +HuCsv4 | RRMmut |
| control 3`UTR | 1.00 | 0.96 | 0.77 | 0.96 |
| Xβ-globin | 0.82 | 0.59 | 0.70 | 0.63 |
| zfcdc42-v2 SV40 | 1.00 | 1.20 | 0.90 | 1.07 |
| zfcdc42-v2 terminal | 2.42 | 1.85 | 2.02 | 2.90 |
| zfcdc42-v2 middle | 0.79 | 0.75 | 0.57 | 0.85 |
| zfcdc42-v2 early | 2.27 | 1.05 | 6.06 | 7.13 |

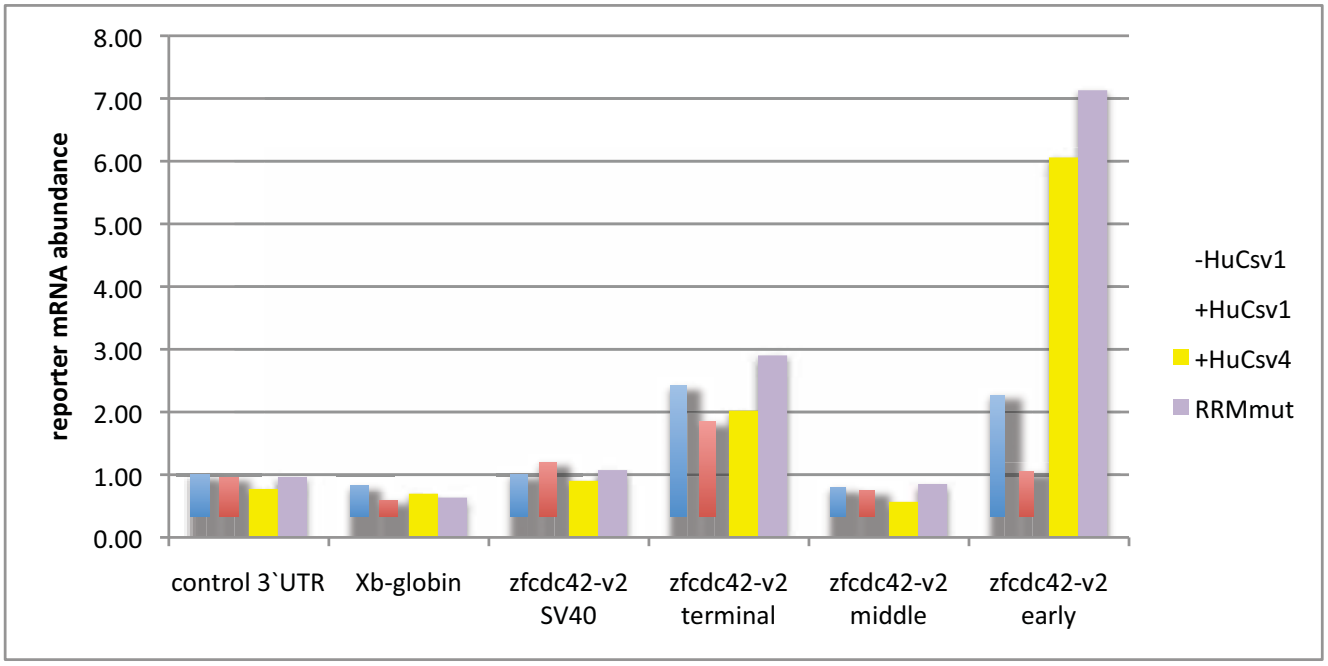


Figure S2. mRNA abundance values from 3´UTR-reporter Northerns - 293T cell line. Experiment 3.

The first two tables present raw mRNA abundance values ( integrated density - Int. Dens) for both the 3´UTR-reporter mRNAs and β-galactosidase mRNAs.

Abundance of the 3´UTR-reporter mRNA was then determined by normalisation to β-galactosidase mRNA abundance. These values are shown relative to abundance of the control 3´UTR mRNA from cells –HuCsv1 and are shown in the third table and following graph. Notably, reporter mRNAs were run on a separate Northern to the experimental reporter. Consequently, in comparing abundance values relative to – HuCsv1, for the zfcdc42-v2 reporter mRNAs values were made relative to zfcdc42-v2 (SV40) – HuCsv1

# Appendix 1 - Rat hippocampal neuron culture system

In considering methods for testing the general hypothesis that neuronal Hu proteins are involved in regulation of growth cone localised mRNAs, it was seen as desirable to establish a primary neuron culturing system. Such a system would enable examination of the effects of nHu-mediated mRNA regulation in a neuronal context, while retaining the advantages of conducting experiments in an *in vitro* cell system. For example, by using an *in vitro* neuron culturing system, effects on axon growth, guidance or synapse formation resulting from perturbed nHu function (either RNA binding or growth cone localisation) could be visualised. Furthermore, dissecting the function of nHu proteins at the growth cone could be carried out to ascertain what role nHu proteins play at the growth cone. Possible roles included (but were not limited to), localisation of mRNAs, regulation of mRNA translation stability at the growth cone either generally or in response to specific signals such as those arising from responses to chemotactic factors or cell-cell contact. Importantly, previous immunofluorescence analysis of nHu expression in hippocampal neurons cultured from day 18 embryonic rat (E18) brains had revealed nHu proteins present within the growth cones of neurons during early stages of culture as the axon migrates away from the cell body (figure 5). Published expression analysis of nHu proteins in mouse hippocampi had also revealed strong nHu expression, indicating all three proteins were present, but that different hippocampal regions appeared to express more or less of particular family members [20]. As such, methods for culturing and transfecting E18 rat hippocampal neurons were developed in anticipation of using this system to examine nHu protein function.

## Why use embryonic rat hippocampal neurons?

Primary cultures of embryonic day 18 (E18) rat hippocampal neurons are an archetypal culturing system for studying the processes of neuronal polarisation, axon and dendrite outgrowth and synapse formation [241], [242], [243], [244]. The process of isolating dissociated hippocampal neurons results in a loss of all axonal and dendritic connections that existed in the hippocampus, *in vivo*. Consequently, when plated, E18 rat hippocampal neurons are effectively returned to their unpolarised immature neuron morphology and must re-establish their axonal and dendritic processes. In doing so, cultured hippocampal neurons recapitulate the *in vivo* processes of axon specification, axonogenesis and synaptogenesis, *in vitro*. These processes are

divided into five separate stages [241], which are represented in cartoon form in Appendix 1 – figure 1.

***The first stage*** occurs within the first 6 hours of plating with neurons extending lamellipodia uniformly around the cell body, contacting the substrate to which they are attached. After some time, the lamellipodia become more isolated, separating into discrete motile regions from which minor neuritic processes extend.

The formation of small neurites marks ***the second stage*** and occurs between 12 and 24 hours after plating. The neurites are highly motile extending to a length of approximately 10-15μm. They can remain this length for up to 24 hours (2 days post-plating), extending and retracting short distances.

***The third stage*** commences when one of the neurites breaks from this cycle and undergoes a rapid period of growth, extending away from the cell body 5-10 times faster than any of the other neurites. This transition is caused by the specification of the neuronal axon from one of the minor neuritic processes. Exclusive elongation of the axon continues for up to 60 hours (during the period 1.5-4 days post-plating).

***The fourth stage*** is marked by the initiation of dendrite outgrowth, whereby the remaining neuritic process begin sustained outgrowth. As axons and dendrites they are able to make connections and form functional synapses.

Synapse formation is ***the final stage*** of *in vitro* growth. The majority of synapses form about 1 week following plating. Neurons will survive in culture, under the conditions used in this thesis in excess of one month [245].

In summary, E18 rat hippocampal neuron cultures are a robust and versatile *in vitro* model for a number of important biological processes that occur during neuronal development.

## Cultured primary neurons versus immortalised cell lines

Importantly, at the start of this project very little was known as to how nHu proteins affected their target mRNA sequences. The hypothesis that nHu proteins regulate translation of growth cone localised mRNAs was based on connections between observations of related biological phenomena. Primarily these included the demonstration that local translation is required at the growth cone of migrating axons for responses to guidance cues [164], that nHu proteins localise to the growth cone of migrating axons [159], (figure 5), that nHu proteins associate with the translation machinery, particularly with polysomes [115] and finally that a number of CLIP-identified mRNA targets of nHu proteins were indeed known to localise to neuronal growth

cones (*Kate Dredge unpublished CLIP data*). However, the lack of any information connecting nHu protein localisation at the growth cone and a specific functional outcome meant that this project was working essentially in the dark with respect to knowing how to best assay effects of nHu proteins on target mRNAs. In light of this, while the idea of testing nHu function in the most representative *in vitro* neuronal context sounded good, the reality was that with no clear idea as to the effect(s) of nHu proteins on target mRNAs, primary neuron cultures would be a considerably more costly method of examining neuronal Hu protein function compared to using immortalised cell lines, both ethically through the potential requirement for a large number of animals and in terms of labour, time and materials required for each culture and experiments conducted therein. Consequently, functional studies on the effects of nHu proteins (particularly HuCsv1) on target mRNA sequences were carried out in cell lines. The advantages of using cell lines over cultured primary neurons are clear. Compared to cultured neurons, cell lines are substantially less expensive and labour intensive per experiment. They are also much easier to transfect. Finally, non-neuronal cell lines such as the HEK293T and HeLa cell lines used in this thesis do not endogenously express neuronal Hu proteins, allowing for investigation of the effects of specific nHu family members on CLIP-identified target mRNA sequences. However, it was anticipated that should the investigation of nHu protein function in cell lines provide insights into molecular mechanisms of nHu protein behaviour that supported a role for in regulation of growth cone localised mRNAs (such as regulation of mRNA translation or stability), demonstration and dissection of that mechanism in a primary neuron culturing system would be necessary to understand the functional outcomes of nHu protein activity in a true neuronal context.

***Establishing a protocol for the dissection, culture and transfection of E18 rat hippocampal neurons***

In anticipation of exciting results from the 3´UTR-reporter assays, efforts were made to establish an E18 rat hippocampal neuron culturing system in the lab. A complete protocol for dissection and culturing is included in this appendix as well as a calcium phosphate transfection protocol, which achieved some level of transfection (~1%). Furthermore, a selection of immunofluorescence images are also included showing nHu expression (detected using the Hu-PND patient antiserum *Gu*) in combination with an antibody directed against acetylated α-tubulin, which stains stabilised microtubules. Different time points were stained from very early (12hr post-plating) to approximately 3.5 days in culture. Throughout this time the isolated neurons are re-establishing axons, which will eventually form functioning synapses with neighbouring cells. The observations from these antibody stains reveal the subcellular localisation of nHu proteins during the *in vitro* recapitulation of axon specification and growth by cultured hippocampal neurons. Finally, data from a reverse-transcription PCR (RT-PCR) using primers spanning the alternatively spliced HNS region of the nHu mRNA for all three neuronal Hu family members is included. This PCR was carried out to ascertain which splice variants are present in cultured E18 rat hippocampal neurons.

## Immunofluorescence results

***Gu-PND antiserum shows nHu proteins in growing neuronal processes of cultured neurons***

Immunofluorescent detection of nHu protein and acetylated α-tubulin was carried out for several stages during E18 rat hippocampal neuron culture (Appendix 1 – figures 2 – 5). Materials and methods for the staining protocol are presented in the materials and methods. Images were obtained using a Zeiss Axioplan epifluorescence microscope and manipulated using Photoshop CS (Adobe). As expected, nHu protein expression was strongly detected in the nucleus and cytoplasm at all time points examined. Two interesting features of this staining were observed, which agree with the published literature regarding nHu protein subcellular distribution in neuronal cells. Firstly, at all stages, nHu proteins were found to be present in discrete cytoplasmic puncta that were also present throughout neuronal processes (axonal and dendritic). Secondly, nHu immunoreactivity was observed at the growth cone of neuronal processes. Interestingly, staining of neurons prior to the specification of the axonal process (before 36 hours) revealed nHu protein localisation at the growth cone of all neuritic processes (Appendix 1 – Figure 3) and even earlier at the ends of microtubules extending into the lamellipodia surrounding recently plated neurons (Appendix 1 – Figure 2). The presence of nHu proteins at these sites at these early time points may suggests a fundamental role in the growth or neuronal processes. Later time-points show nHu protein localising to actively migrating growth cones (Appendix 1 – Figures 4 and 5) as previously reported. Staining in axons from a stage four neuron indicate theat at least some of the nHu proteins present within axons co-localise with microtubules (Appendix 1 – Figure 5) a feature that has been reported to be necessary for their association with polysomes [151], [115], [159].

## Calcium Phosphate transfection results

Low efficiency transfection (<1%) of E18 rat hippocampal neurons was achieved using a calcium phosphate protocol (provided). Neurons were transfected with the pCI-d2EGFP vector using in the fluorescence-based reporter assays (control 3´UTR) ~24 hours after plating. Expression of d2EGFP was then examined at 1, 3 and 5 days post-transfection. The images presented are representative of three separate transfection attempts (Appendix 1 – Figures 6). Average transfection efficiency was estimated at being <1% based on the number of transfected cells observed relative to that plated. Transfection using FuGENE6 (Roche) was also carried out. However, the transfection efficiency was no better than the calcium phosphate protocol. Additionally, based on morphology, FUGENE6 appeared to transfect a greater number of non-neuronal cells compared to the calcium phosphate protocol (Appendix 1 – figure 7). One possibility was that FuGENE6 was preferentially transfecting non-neuronal, cells within the culture such as astrocytes or contaminating endothelial cells (introduced through incomplete removal of meningial tissue). Alternatively, FuGENE6 may elicite morphological changes in neurons through toxicity.

The results from neuron transfection assays indicated the non-viral methods tested would not be suitable for carrying out the reporter assay-style experiments presented in this thesis using cell lines, in the primary neuron culture system. Viral vector delivery was not pursued for a number of reasons. Primarily, the amount of workup involved in establishing this method was deemed too great. The simplicity of using cell lines, both in terms of ease of transfection and lack of endogenous nHu proteins (excluding Neuro-2a cells) made these a more desirable choice for initial reporter assay experiments, aimed at identifying a nHu-specific effect on target mRNA sequences. In addition to this, the ethical, financial and labour-associated costs in using primary neuronal cultures rendered this method of investigation somewhat inappropriate at a time when so little was known about how nHu proteins affect their target sequences. As stated, depending on the results of the cell line-based reporter assays, the time and effort invested in establishing E18 rat hippocampal neuron culturing methods could easily be capitalised on to test for effects of disrupted nHu-target mRNA interactions on axon growth, axon specification and even axon guidance.

## Characterising nHu expression in E18 rat hippocampal neurons.

Finally, in deciding which nHu protein to study in the 3´UTR-reporter assays, an RT-PCR was performed using RNA isolated from E18 rat hippocampal neurons (dissected, not cultured) to determine which family members and HNS-splice variants were expressed. To do this, primers were designed to specifically amplify a small region spanning the alternatively spliced exon 6 region of the mRNAs encoding HuB, HuC and HuD. Because the difference in product sizes for the different splice variants was potentially quite small PCRs were carried out using radiolabeled primers and resulting amplification products separated by electrophoresis through a denaturing 8% polyacrylamide gel. A schematic showing the location of primers in the context of the amplified region is provided (Appendix 1 – Figure 8a-c) as well as a table indicating the predicted sizes of potential products for each splice variant of each family member (Appendix 1 – Figure 9).

The results of the PCR (Appendix 1 – Figure 9) indicated HuBsv2 is the most abundant isoform of HuB expressed in hippocampal neurons, with weak expression of HuBsv4 also detected. For HuC, splice variants 1 and 2 were most strongly detected with splice variants 3 and 4 detected only weakly. Expression of HuDsv1 and 2 was also detected, with expression of HuDsv4 also present but again, weaker that either of the two longer isoforms. The sizes of PCR products for all three nHu family members appear slightly smaller than expected when compared to the ϕX174 DNA ladder. However, sequences of predicted splice variant PCR products were confirmed by gel extraction of the relevant PCR products followed by dideoxy chain-termination sequencing.

## Conclusions from work using cultured E18 rat hippocampal neurons

As shown, protocols for dissecting, culturing and transfecting E18 rat hippocampal neurons were developed in conjunction with the work presented in this thesis. These cultures were used to demonstrate growth cone localisation of nHu proteins and to identify which nHu isoforms are expressed in cultured hippocampal neurons at the E18 developmental time point. The results from the RT-PCR contributed to the decision to use HuCsv1 in the 3´UTR-reporter assays conducted in cell lines.

From the 3´UTR-reporter assays, it may be interesting to revisit the hippocampal neuron cultures. The Nothern results from the firefly and renilla luciferase-based 3´UTR-reporter assays suggest HuCsv1 influences 3´-end processing of the zfcdc42-v2 mRNA. While it is not currently known by what mechanism this occurs, one possibility is that HuCsv1 interacts with the 3´UTR of the zfcdc42-v2 mRNA and directs the use of alternative, distal polyadenylation sites. Depending on how much redundancy exists between different nHu family members, it may be possible to employ virally delivered siRNA knockdown constructs to specifically reduce expression of nHu family members individually or en masse and then assay for changes in polyadenylation site choice for putative nHu protein target mRNAs (such as cdc42-v2) by 3´RACE using a combination of oligo-dT reverse primers ending in either A, G, C or T plus a forward primer common to both long and short 3´UTR sequences. The "lock-docking" reverse primer allows for amplification of cDNA ends from the start of the polyadenylate tail [246], [247], simplifying analysis of PCR products and subsequent isolation for di-deoxy chain termination sequencing. Additionally, Northern analysis for alternative mRNA products (such as for cdc42) would also be necessary to determine whether differences in abundance of a particular 3´UTR variant were caused by alternative terminal exon splicing, as is possible for the cdc42 transcript.

## Culturing hippocampal neurons from E18 rat embryos

***Dissecting out the hippocampi***

1. Humanely kill the mother by $CO_2$ asphyxiation
2. Place the mother on an absorbent disposable mat so that her belly is facing up.
3. Using large scissors, open the mother up from the vagina to the bottom of the rib cage. This may be easiest if first the skin is cut and then the underlying fat and muscle is cut.
4. The pups are found in the uterus, a long purple/red tube that sits on either side of the internal organs.
5. Cut the pups out, and quickly remove them from the sac they are in and decapitate them.
6. The heads are placed into ice-cold 1xHBSS

You can expect to obtain anywhere from 1-14 heads but typically each head provides ~ 500,000 cells so only get as many heads as you require (over estimate a bit), time is very much of the essence. Also, when choosing which heads to keep it is probably best to use those from the largest pups.

7. Take the heads (in 1x HBSS) to the dissecting microscope and place them on ice.
8. Place fresh, ice-cold 1xHBSS into another petri dish and place this under the scope.
9. Transfer one of the heads into this dish and begin the dissection.
10. Firstly, open the head up using fine scissors to cut along the midline from the back of the head where the spine met with the skull along and over to the nose (see below).

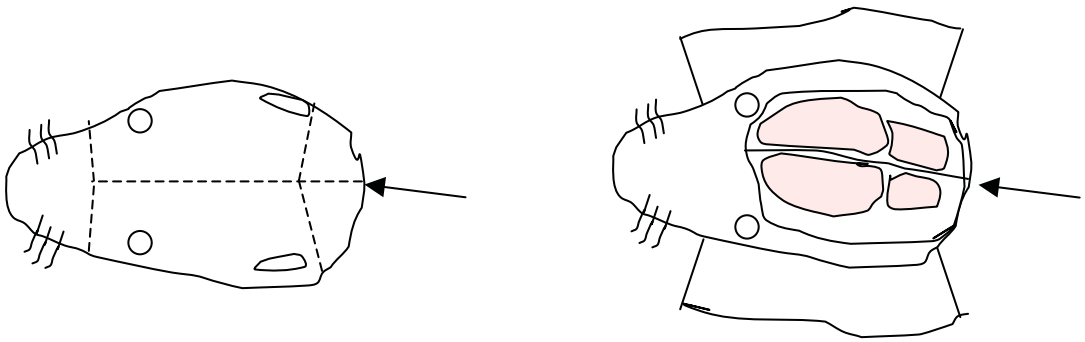

11. Insert the scissors under the bone but be very careful to keep them above the brain, they will fit between the skull and the brain but when first trying this it can be easier to first

cut away the skin and cut the skull open once you have a clear view of the underlying brain.

12. Once cut, hold the skull open using the tweezers and gently roll the brain out of the skull using the scissors.
13. Remove the head from the dish and place the brain, ventral side up under the scope.


14. Increase magnification so that the brain takes up the entire field of view,

15. To remove each cortical hemisphere, place the brain dorsal side up. Make one cut between the two cortices from the olfactory bulbs down to where the pineal gland would be (figure i above).
16. Next, place the brain ventral side up; you should be able to see a physical structure known as the Circle of Willis (named after Thomas Willis [b.1621-d.1675] who gave a complete description of it along with an illustration of the vascular network at the base of the brain in his publication *Cerebri anatome: cui accessit nervorum descriptio et usus.* [T Willis London, 1664]) where the cortices meet the diencephalon on the underside of the brain. There is a distinctive ring of veins that designate this spot (indicated by dashed lines in figure ii above).
17. Cut the cortices away from the brain with one linear cut along the base of the cortex, using the Circle of Willis as a guide

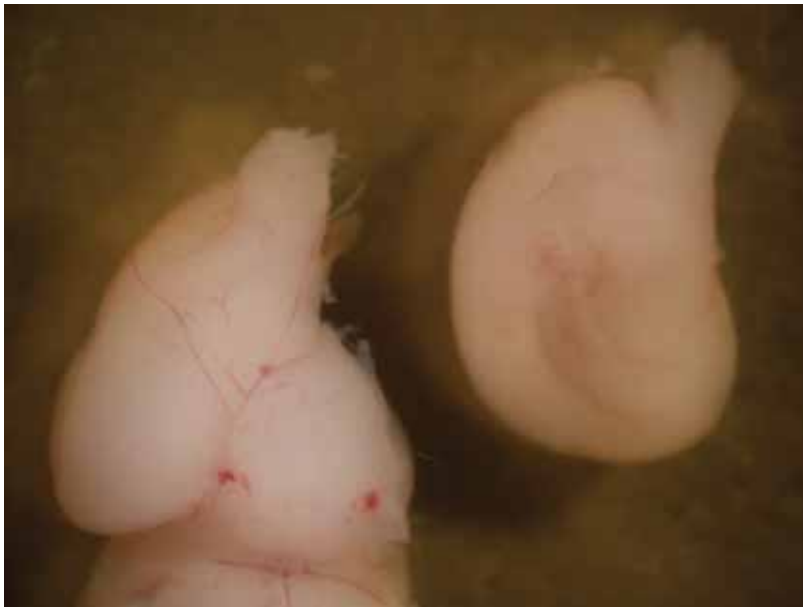

18. With the cortical hemisphere separated from the rest of the brain the next task is to remove the meningeal tissue overlying the brain to leave only the white and grey matter of the brain. This is likely the most time consuming aspect of the dissection next to obtaining the pups as the brain is very fragile at this stage of development and can tear in the process of removing the meningial tissue.
19. To remove the meningies first cut the olfactory bulb at it's base leaving only the cortical tissue.
20. Place the hemisphere lateral side down and carefully get between the meningial tissue and the brain with the tip of the scissors. This is usually easiest along the ventral side of the hemisphere where the meningies terminate with a flap leading into the interior of the hemisphere.

21. With the tip of the scissors pinning the meninges to the dish, gently roll/peel the hemisphere out starting from the anterior end and peeling posteriorly.

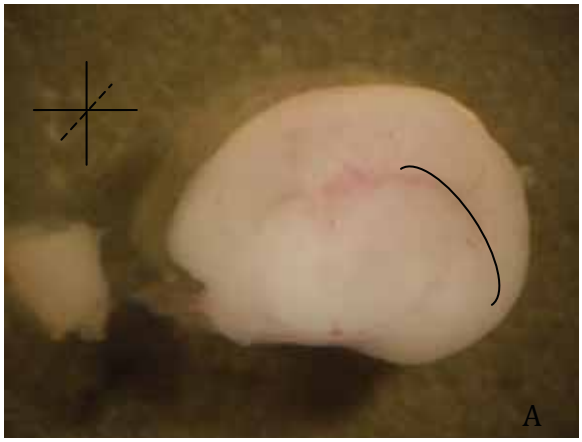


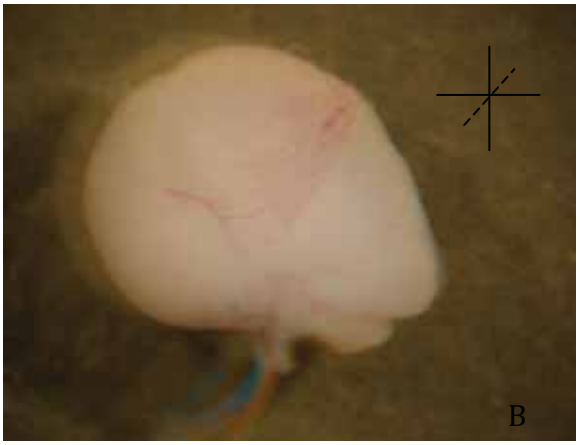


**A.** Medial side of the right cortical hemisphere, the ventral side is towards the bottom, anterior side is to the left. The olfactory bulb has been cut but the meninges have not yet been removed. The meninges wraps around the lateral (outer) side of the hemisphere like a bag with its opening where the hemisphere connected to the diencephalon. The edge of this bag at the ventral side of the hemisphere is the easiest point of access for removing the hemisphere from the bag. Use caution, the meninges are tucked into the hemisphere at the hippocampus (obscured at this point, however location demarcated by darker crescent shape and bracket) therefore take care when pulling them away from the tissue to ensure the hippocampus is not damaged.

**B.** The lateral side of the hemisphere showing the meninges pulled halfway off. Removal of the meninges began at the ventral side holding the meninges down with a point and rolling the anterior side of the hemisphere out. Once at this point the scissors can be placed between the meninges and cortex and peeled away by holding the hemisphere down gently and pulling the meningeal tissue away.

**C and D.** Liberated hemisphere. The hippocampus is now visible.

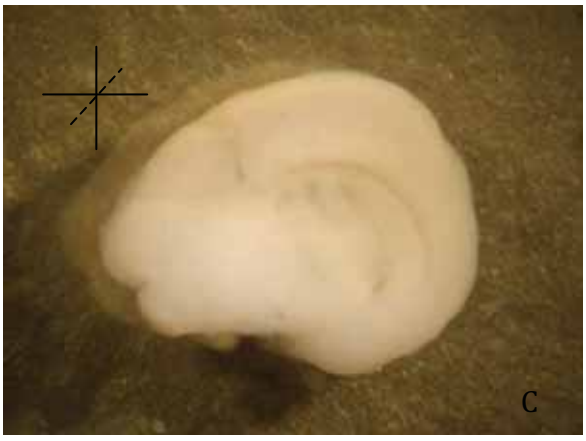


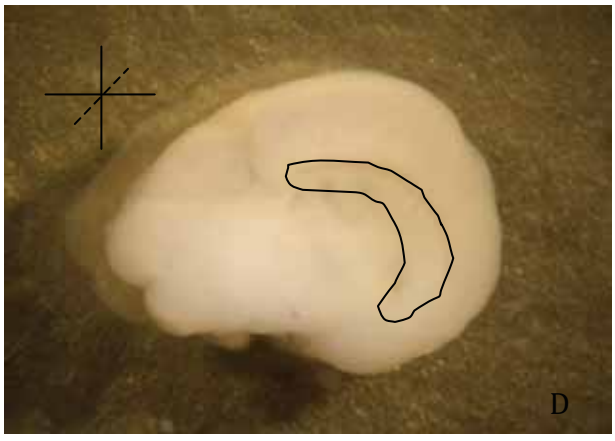


22. Once the hippocampus is exposed, it can be easily dissected out using fine scissors.

23. Place dissected hippocampi into ice-cold Hibernate + B27 or Neurobasal + B27 + PenStrep and keep on ice until dissociation.
24. Once sufficient hippocampi have been recovered, aspirate media and replace with neat 4.5mL Neurobasal .
25. Add 500uL of 10x trypsin, mix and incubate for 15minutes at 37°C swirling every 5min.
26. Aspirate dissociation solution and wash (2x) in 1mL NeuroBasal + B27 + 10%FCS + PenStrep media.
27. Resuspend in ~800µL NBasal + B27 + 10%FCS + PenStrep media and dissociate cells by trituration (12x) using a blue tip/P1000. Do not over dissociate hippocampi, there will always be clumps…get used to it.
28. Allow the dissociated cells to sit for 3 minutes to ensure clumps settle at the bottom.
29. Transfer the supernatant to a new eppendorf tube and determine the number of cells/µL
30. Plate 15,000 – 20,000 cells on poly-D-lysine coated coverslips and make up media to 500uL/well with NBasal + B27 + 10%FCS + PenStrep + Glutamine + 25µM Glutamate
31. Grow cells at 37°C/5%$CO_2$ for 4-6hrs to allow time to plate.
32. Replace media with NBasal + B27 + PenStrep + Glutamine. Neurons can be cultured for up to 4 days without media change, after 4days replace half the media (~250µL) with fresh media.

***Calcium-Phosphate transfection protocol.***

The calcium phosphate transfection protocol has been used for 18,000 to 100,000 cell/well transfections. It seems that the greater the amount of DNA used the higher the transfection, but to what limit that applies is unclear. Using 5µg of DNA/transfection I have achieved up to an estimated 1% efficiency (of total culture population)

For each well:

1. Place 2-5µg of DNA into 60µL of 250mM $CaCl_2$ solution (filter sterilised)
2. Allow DNA solution to incubate for 5 minutes at room temp.
3. Add 60µL of 2xBES buffered saline.
4. Incubate at room temp for 5min
5. Add drop-wise to well, swirling dish while adding
6. Incubate 45min – 1.5 hours at 37°C with 5%$CO_2$. Wells should be monitored for precipitate formation .Do not allow particles to become too large. Large particles are cytotoxic.
7. Aspirate media and wash 2x in prewarmed media
8. Add 500µL media to wells and incubate overnight at 37°C with 5%$CO_2$.

Dotti et al J Neurosci. 8(4) 1454 (1988)

Appendix 1 – Figure 1. The five stages of *in vitro* cultured hippocampal neuron growth.

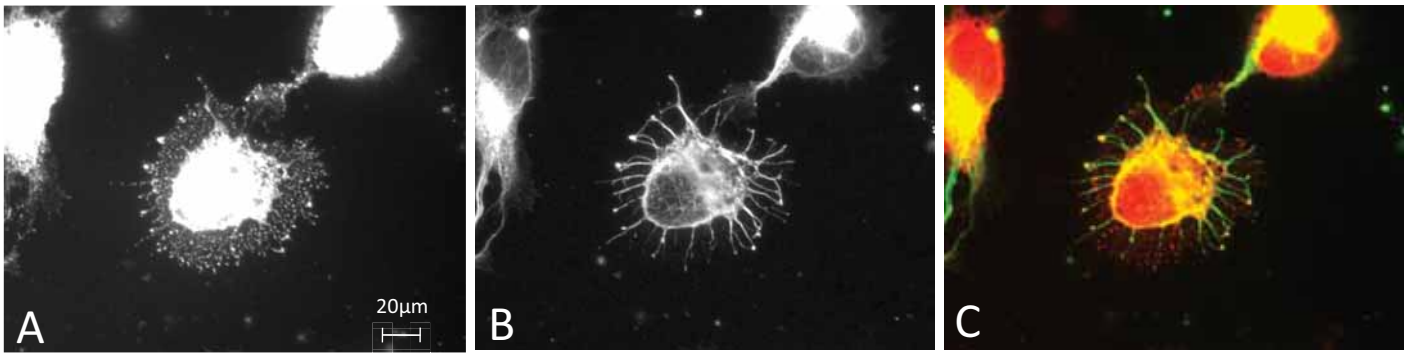


Appendix 1 – Figure 2. Images of a single dual-stained E18 rat hippocampal neuron cultured for 12 hours *in vitro* (stage 1). Image taken at 100x magnification.

Figure 2a – Gu PND antiserum staining. nHu immunoreactivity is present within the nucleus and cytoplasm as well as in discrete granules throughout the lamellipodia

Figure 2b – acetylated α-tubulin staining. Microtubules are observed extending into the lamellipodia.

Figure 2c – nHu (red) and acetylated α-tubulin (green) images merged. nHu staining is observed at the ends of microtubules extending into lamellipodia.


Appendix 1 – Figure 3. Images of a single dual-stained E18 rat hippocampal neuron cultured for 18 hours *in vitro* (stage 2). Image taken at 100x magnification. False colouring swapped

Figure 3a – Gu PND antiserum staining. nHu immunoreactivity is present within the nucleus and cytoplasm as well as in discrete granules throughout all minor neurites.

Figure 3b – acetylated α-tubulin staining.

Figure 3c – nHu (green) and acetylated α-tubulin (red) images merged. nHu staining is observed at the growth cones of all neurites.

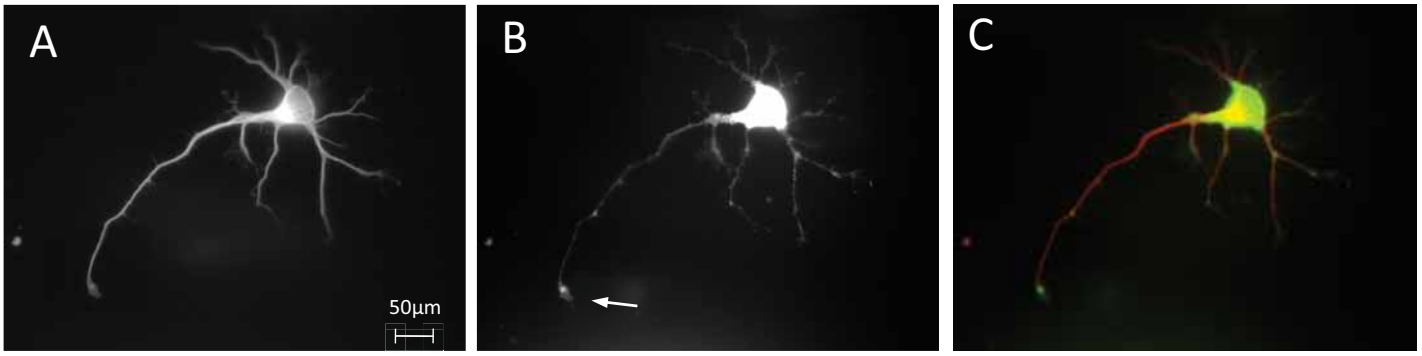


Appendix 1 – Figure 4. Images of a single dual-stained E18 rat hippocampal neuron cultured for 68 hours *in vitro* (stage 3). Image taken at 60x magnification.

Figure 4a – acetylated α-tubulin staining.

Figure 4b –Gu PND antiserum staining is observed at the axonal growth cone (arrow).

Figure 4c – nHu (green) and acetylated α-tubulin (red) images merged. The merged image is not perfect because of a small difference in focal depth between the two images.

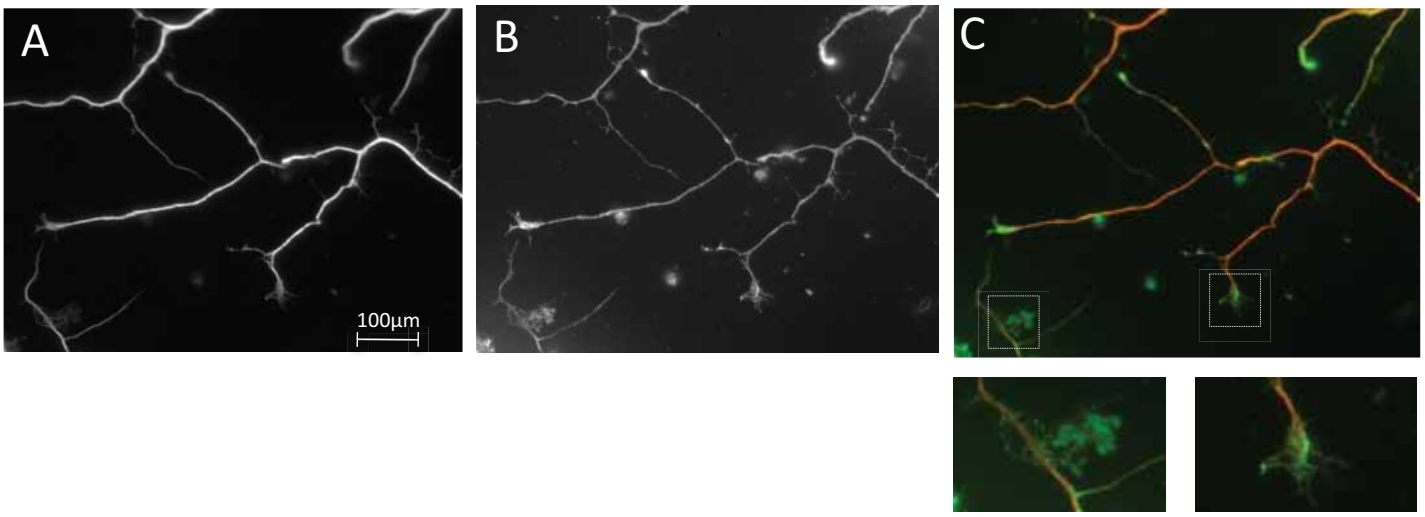


Appendix 1 – Figure 5. Images of a single dual-stained E18 rat hippocampal neuron cultured for 68 hours *in vitro* (stage 3). Image taken at 60x magnification.

Figure 5a – Gu PND antiserum staining. nHu immunoreactivity is present in discrete granules throughout the axon and at the axonal growth cone.

Figure 5b – acetylated α-tubulin staining.

Figure 5c – nHu (green) and acetylated α-tubulin (red) images merged. nHu staining is observed in association with microtublues (exemplified in the two close up images)

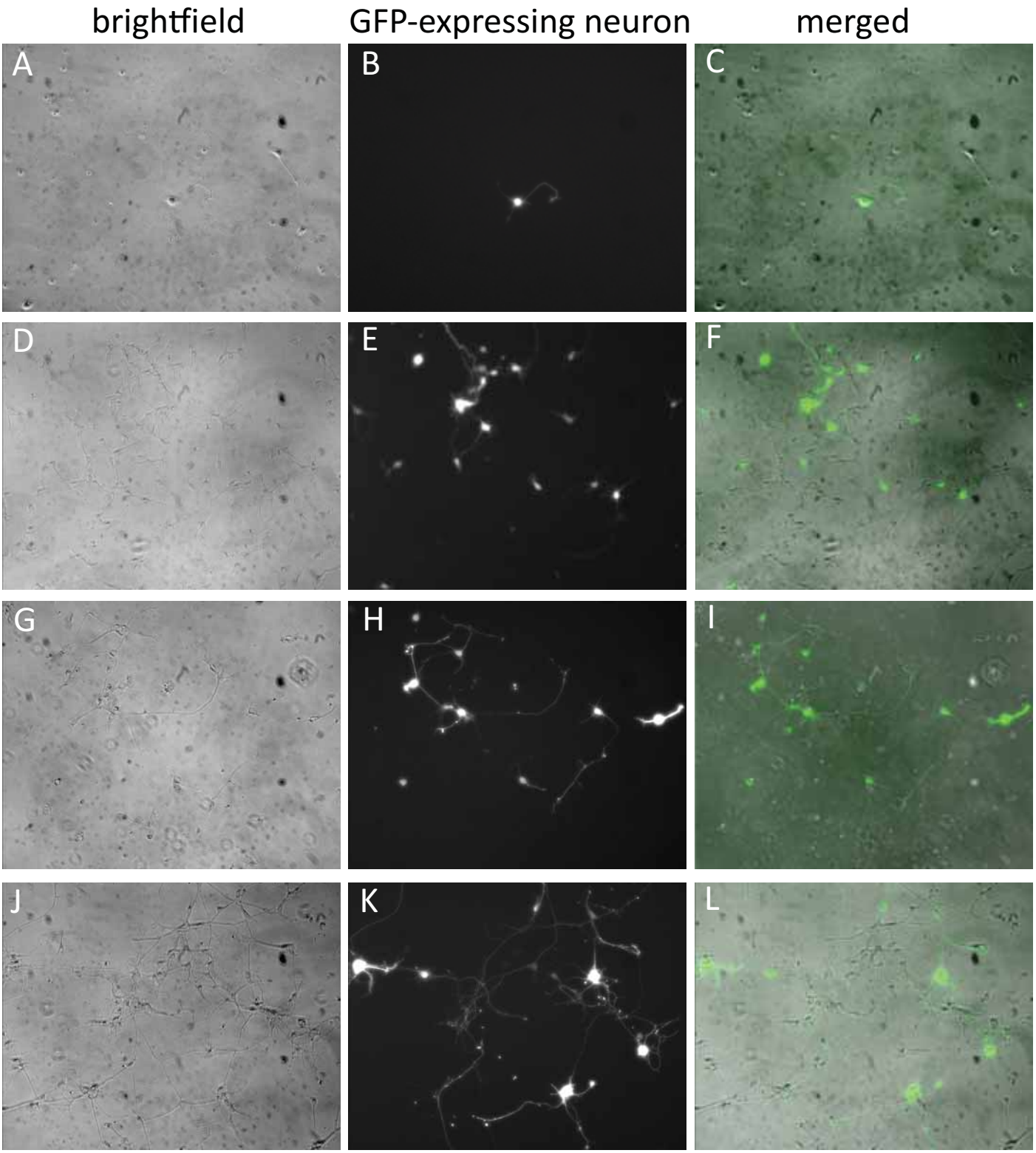


Appendix 1 – Figure 6. Images of calcium phosphate transfected E18 rat hippocampal neurons expressing d2EGFP). Images acquired at 20x magnification.

Figure 6a-c. 24 hours post-transfection (2 days *in vitro* – DIV
Figure 6d-f. 2 days post-transfection (3 days *in vitro* – DIV)
Figure 6g-i. 3 days post-transfection (4 days *in vitro* – DIV)
Figure 6j-l. 4 days post-transfection (5 days *in vitro* – DIV)

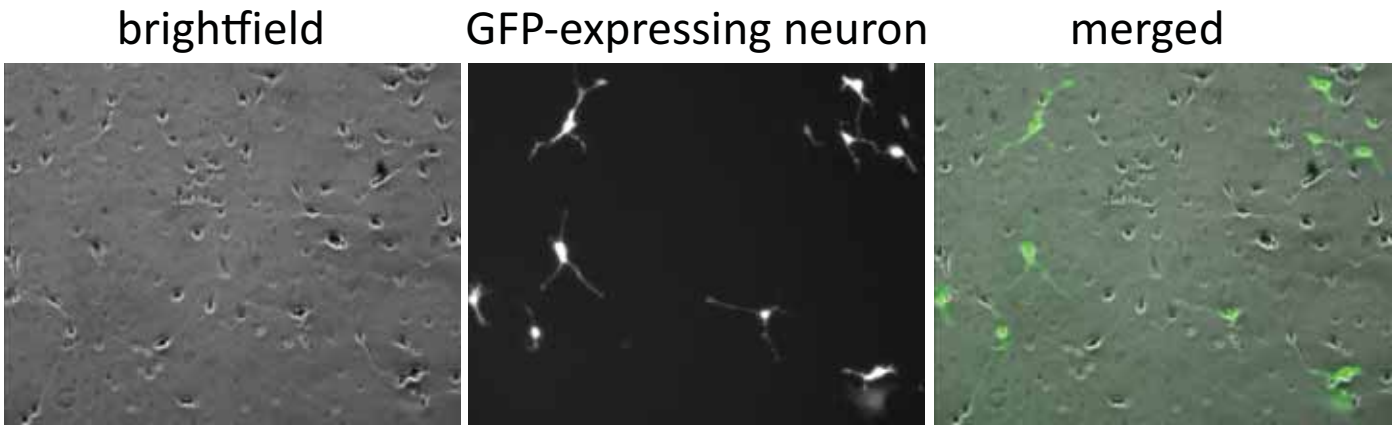


Appendix 1 – Figure 7. Images of FuGENE6 transfected E18 rat hippocampal neurons expressing d2EGFP 24 hours post-transfection (2 days *in vitro* – DIV). Images acquired at 20x magnification.

Notably, the general morphology of transfected cells is not indicative of healthy neurons. d2EGFP expressing cells appear to have less neuronal processes. And in some cases appear thicker than axons/ dendrites of hippocampal neurons possibly indicating they are not neurons but astrocytes.

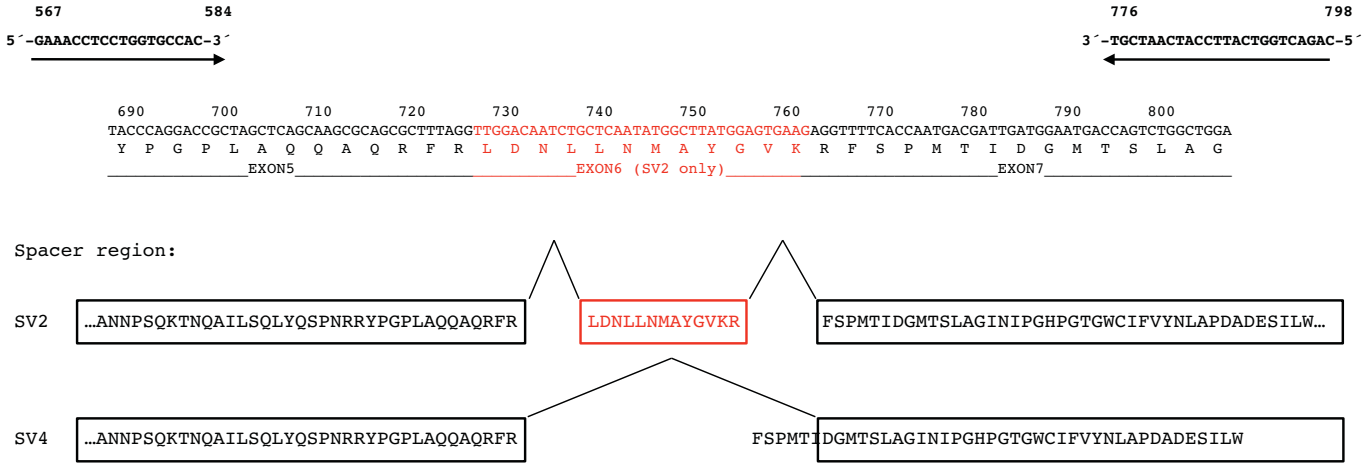


Appendix 1 – Figure 8a. Alternative splicing in the spacer region of HuB. Primer sequences and position within the HuB coding sequence are shown above. Nucleotide position (beginning from the ATG start codon; A = 1st nucleotide) are shown. Forward primer binds within exon5, reverse primer binds within exon7.

Alternative splicing within the spacer region of HuB results in the inclusion of a short leucine-rich sequence (exon6). This splice variant is called HuBsv2. Skipping of exon6 produces HuBsv4.

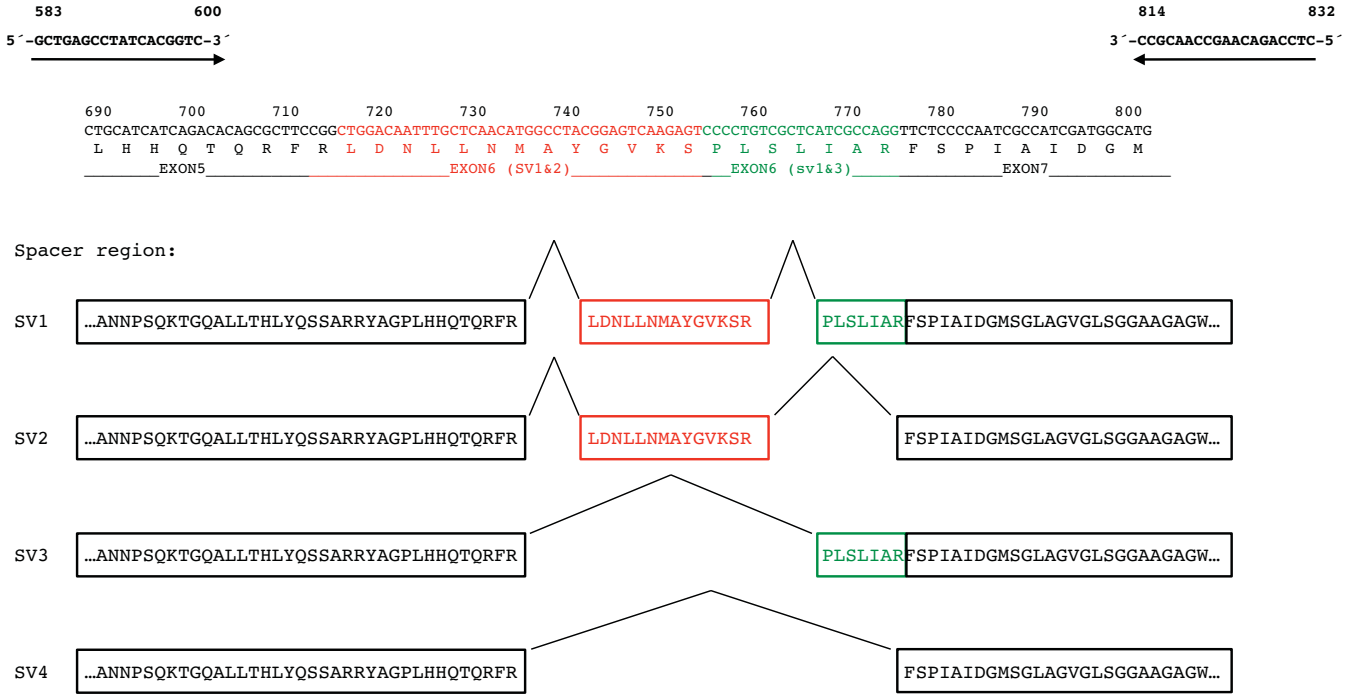


Appendix 1 – Figure 8b. Alternative splicing in the spacer region of HuC. Primer sequences and position within the HuC coding sequence are shown above. Nucleotide position (beginning from the ATG start codon; A = 1st nucleotide) are shown. Forward primer binds within exon5, reverse primer binds within exon7.

Splicing of exon5 to exon6 is requisite for HuCsv1 and HuCsv2 production. Alternative splice acceptor sites in exon7 distinguish the two isoforms, as indicated. Exon6 is skipped in both HuCsv3 and HuCsv4 and the two products arise from differential use of the two splice acceptor sites in exon7.

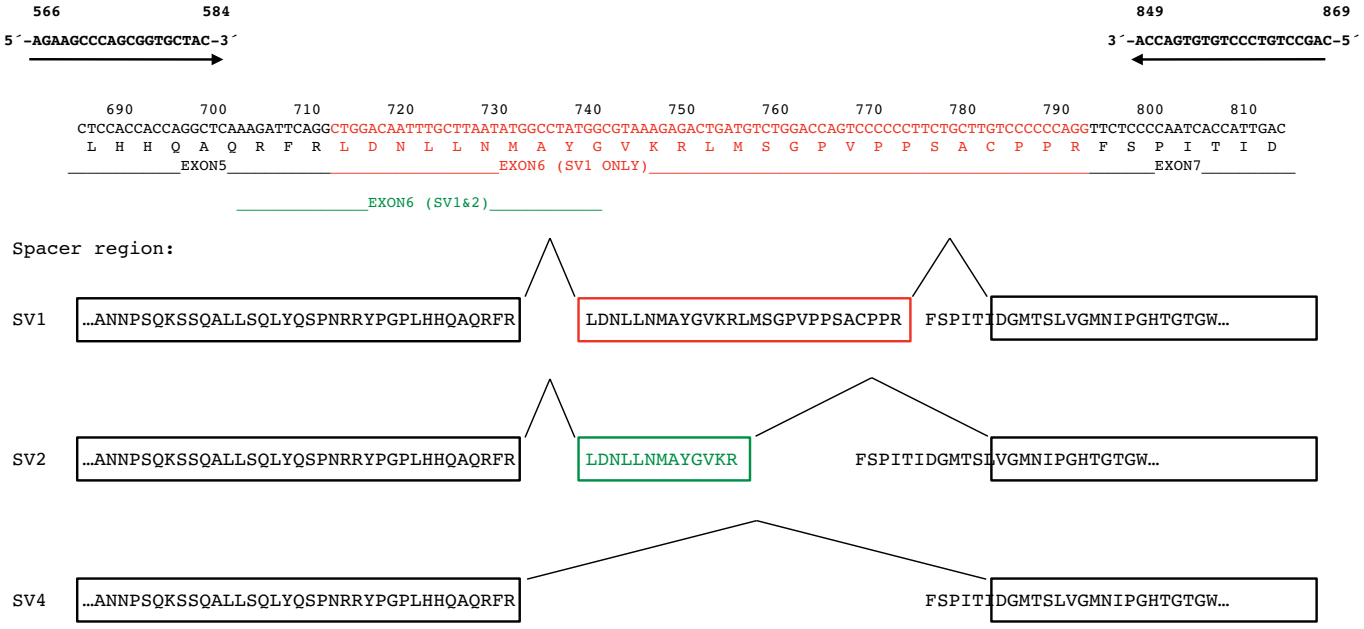


Appendix 1 – Figure 8c. Alternative splicing in the spacer region of HuD. Primer sequences and position within the HuD coding sequence are shown above. Nucleotide position (beginning from the ATG start codon; A = 1st nucleotide) are shown. Forward primer binds within exon5, reverse primer binds within exon7.

Splicing of exon5 to exon6 is requisite for HuDsv1 and HuDsv2 production. However, unlike HuC, alternative splice donor sites in exon6 splice to a common splice acceptor site in exon7 as indicated. HuDsv4 is produced by skipping of exon6.

Appendix 1 – Figure 9. Auto-rad from RT-PCR to detect the expression of all nHu HNS splice variants in total mRNA obtained from E18 rat hippocampi. PCR was carried out using primers labeled at the 5´-end with 32-P using T4 Polynucleotide kinase.

The ϕX ladder was very weak compared to PCR products. Intersity of ladder was brought by increasing output levels in Photoshop.

Asterisks indicate PCR products of sizes not predicted for the primers used. Furthermore, the two highest bands in the HuB PCR lanes do not correspond to any predicted PCR product size. These bands were not sequenced.

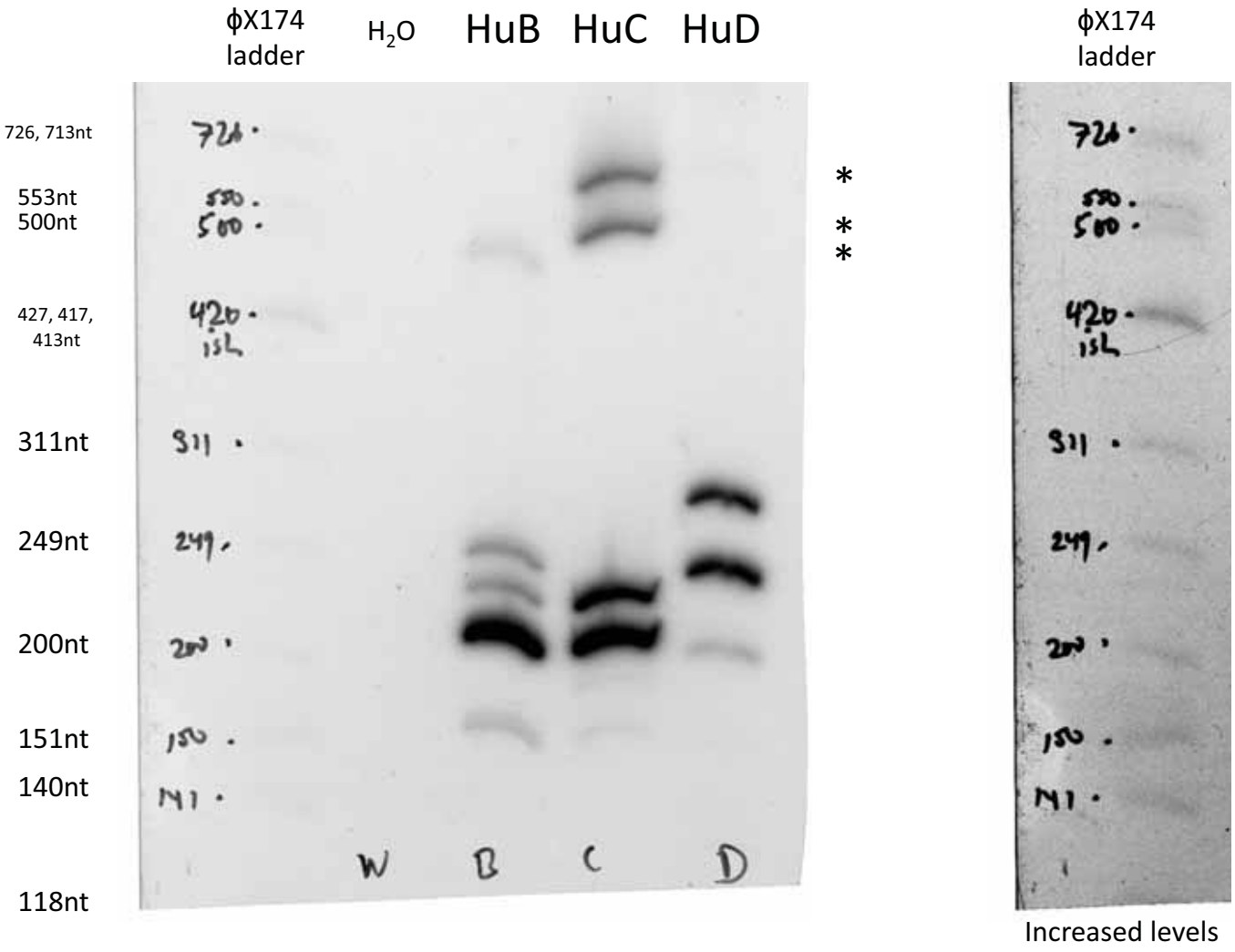


| | | PCR product size (nt) per neuronal Hu family member | | |
|---|---|---|---|---|
| Splice variant | | HuB | HuC | HuD |
| sv1 | | - | 250nt | 300nt |
| sv2 | | 225nt | 230nt | 260nt |
| sv3 | | - | 210nt | - |
| sv4 | | 180nt | 190nt | 220nt |

## Appendix 2 - Dibutyryl cyclic AMP treatment of Neuro-2a cells

This appendix presents data from the firefly luciferase reporter experiments in which Neuro-2a cells, co-transfected with firefly luciferase-based 3´UTR-reporter and HuCsv1 constructs (as described) were exposed to the membrane permeable analog of cyclic AMP (cAMP) dibutyryl cyclic AMP (dbcAMP).

Cyclic AMP is a direct regulator of protein kinase A (PKA). Binding of cAMP to PKA activates PKA allowing it to phosphorylate target proteins. The targets and outcomes of PKA activation in neuronal cells are numerous and are generally beyond the scope of this thesis. However, signalling through cAMP to PKA has well-documented and powerful effects in neuronal cells, particularly during development. PKA activation leads to significant changes in gene expression that are associated with neuronal differentiation [248], [249]. Gene expression changes resulting from PKA activation are also responsible for controlling synaptic plasticity in learning and memory paradigms and loss of PKA function in mice is known to reduce long-term memory and learning [250]. Furthermore, changes in cAMP levels in the growth cone of neurons during axonogenesis have important consequences on how the growth cone responds to different signalling cues [251], [252], [253].

In the context of Neuro-2a cells, exposure to high concentrations of dbcAMP has been shown to cause neurite extension in Neuro2a cells [254] and subsequent differentiation into neuronal-like cells. Neuro-2a cells differentiated in this manner have recently been shown to express low levels of tyrosine hydroxylase and dopamine [255], two signature markers of dopaminergic neurons. While neither HuR nor any of the neuronal Hu proteins have been described as direct targets of PKA or cAMP signalling, these lines of evidence suggest that cAMP signalling could potentially promote an environment in which neuronal Hu protein function might be more distinctly observed.

Neuro-2a cells co-transfected with or without HuCsv1 and the firefly luciferase 3´ UTR reporter constructs (as described) were treated with cAMP in two separate side experiments to see whether enhancing the neuronal-characteristics of the transfected Neuro-2a cells caused any changes to the activity of HuCsv1 observed in these assays. Of the two data sets obtained, only the second contains both luciferase activity data and mRNA abundance data as determined by Northern blot. This experimental approach was not pursued further because treatment of

transfected Neuro-2a cells with dbcAMP led to increases in firefly and renilla luciferase reporter activity that were completely blocked by HuCsv1. The mechanism by which HuCsv1 blocked the increase in luciferase activity observed in dbcAMP-treated cells (lacking HuCsv1) was not pursued. However, Northern analysis of co-transfected cells treated with dbcAMP did provide another piece of data that indicates usage of an early polyadenylation site within the zfcdc42-v2 3′UTR is blocked by co-expression with HuCsv1. The results are provided and discussed in this appendix.

## Luciferase reporter activity in response to cAMP

Neuro-2a cells, co-transfected as described, were treated with dbcAMP in two separate experiments. The experiments were conducted in parallel to transfections in which cells were not treated with dbcAMP (these were treated as vehicle controls). In the first experiment, cells were transfected and then left for 8 hours prior to removal of media and replacement with either media containing or lacking dbcAMP at a final concentration of 1mM. Cells were then left for 16 hours prior to collection of lysates for luciferase activity analysis. In the second experiment, the procedure was repeated however the final concentration of cAMP added was doubled to 2mM. The reason for doubling the concentration of cAMP is explained.

The results from the first experiment showed dbcAMP generally caused a strong upregulation in expression of both firefly and renilla luciferase in the absence of HuCsv1. Relative to untreated cells, raw firefly luciferase activity was on average ~3.2-fold higher in the absence of HuCsv1 (Appendix 2 - figure 1a –HuCsv1 column). Likewise, raw renilla luciferase activity was ~2.3-fold higher (Appendix 2 - figure 1b – HuCsv1 column). In both cases, the increases were shown to be highly statistically significant.

This in itself turns out not to be surprising. A paper published in 1989 by Fickenscher et al, indicates that the immediate early CMV enhancer promoter sequence, present in both the firefly and renilla luciferase reporter vectors, contains several putative cAMP responsive elements and is activated by treatment with 8-Bromo-cAMP, a membrane permeable cAMP analog similar to dbcAMP [256]. Looking further back in the literature, the CMV promoter used is likely activated by treatments that stimulate PKA and protein kinase C (PKC) activity [257], [258] in that it contains binding sites for transcription factors known to be activated by both PKA and PKC signalling. Based on these studies, it appears that in this assay a general increase in expression from both reporter vectors and the HuCsv1 overexpression vector would be expected.

What was interesting though, was that cells co-transfected with HuCsv1 did not show the same 2-3 fold increases in luciferase activity following treatment with 1mM dbcAMP as seen for cells lacking HuCsv1 (Appendix 2 - figure 1a and 1b). In fact, co-transfection with HuCsv1 appeared to block any response of either firefly or renilla luciferase to dbcAMP.

Looking at the normalised firefly luciferase activity data from cells treated with 1mM dbcAMP versus untreated cells. Fold reductions in normalised 3′ UTR reporter activity in the presence of HuCsv1 are not greatly different between cells treated with versus without dbcAMP, with a slightly stronger repressive effect observed in cells treated with 1mM dbcAMP (Appendix 2 - figure 2). Notably, this effect does not appear to be due to a change in HuCsv1 activity. For essentially every 3′ UTR reporter, raw firefly luciferase activity in dbcAMP-treated cells lacking HuCsv1 shows a >3-fold increase in firefly luciferase activity compared to untreated cells (Appendix 2 - figure 1a and 1c). In the same context, only an ~2-fold increase is seen for renilla luciferase activity (Appendix 2 - figure 1b and 1d). The difference in increase observed most likely comes down to differences in molar amounts of the respective firefly and renilla luciferase encoding vectors. Importantly, because no change is seen in activity of either luciferase enzyme in cells co-transfected with HuCsv1 **and** treated with dbcAMP, the greater normalised firefly luciferase activity from the dbcAMP treated group (lacking HuCsv1) falsely suggests HuCsv1 is causing a greater reduction in normalised 3′ UTR reporter activity (see Appendix 2 - figure 2a – graph shows fold reduction of normalised 3′UTR-reporter expression in the presence of HuCsv1).

***Treatment with 1mM dbcAMP reveals a possible general effect of HuCsv1 on translation***

From these results, treatment with 1mM dbcAMP did not appear to have an obvious effect on HuCsv1 activity in the context of 3′ UTR-specific regulation of reporter expression. However, an obvious general effect of HuCsv1 on reporter expression was observed following dbcAMP treatment (Appendix 2 - figure 1). Given the strong effect of HuCsv1 in blocking any increase in luciferase reporter expression in dbcAMP-treated cells, it was pertinent to ascertain whether the effect was arising from a change in the amount of firefly and renilla luciferase transcript present in cells co-expressing HuCsv1, or through changes in the translatability of the reporter mRNAs. Northern blot analysis of co-transfected cells (+/- HuCsv1) would reveal whether differences in mRNA abundance between +/- HuCsv1 samples explained the observed differences in reporter activity. If no difference in mRNA abundance were observed then the differences in reporter

activity would likely be due to some reduction in the translatability of these reporter mRNAs (or translation generally).

## Investigating a post-transcriptional mechanism for reductions in non-target mRNA translation caused by HuCsv1

To examine post-transcriptional regulation of luciferase reporter expression in dbcAMP-treated cells, Neuro-2a cells were transfected as before but measurements of both luciferase activity and RNA abundance were acquired. In this assay, the amount of dbcAMP used to treat cells was increased to 2mM. This change was made to examine whether the repressive effect of HuCsv1 on dbcAMP-induced increases in luciferase activity was sensitive to dose. If it were then an even greater reduction in luciferase activity would be expected (compared to untreated cells) in HuCsv1 co-transfected cells. A dose-sensitive response of the luciferase reporters in HuCsv1 co-transfected cells might also suggest dbcAMP was changing or augmenting some activity in HuCsv1 that drove its activity in reducing reporter activity.

### *Increasing the dbcAMP concentration increases raw luciferase activity in cells lacking HuCsv1*

As in the first dbcAMP experiment, activity of both firefly and renilla luciferase was increased in cells treated with dbcAMP and lacking HuCsv1. Notably, the extent of the increase was also greater in this experiment (Appendix 2 - figure 3 compared to Appendix 2 - figure 1), indicating that increasing the concentration of dbcAMP was driving a greater increase in the amount of observed luciferase activity, compared to the previous experiment (Appendix 2 - figure 3a and 3b). Firefly luciferase activity values ranged but were consistently 3-fold greater than untreated cells (the average increase was 4.5-fold), with the increase found to be highly statistically significant ($p<8.8\text{x}10^{-5}$). Renilla luciferase activity also showed a greater increase compared to the previous experiment with averaged activity up 3-fold. This effect was also highly significant ($p<8.3\text{x}10^{-12}$). Importantly, luciferase activities from cells co-transfected with HuCsv1 were again essentially unchanged between dbcAMP-treated and untreated cells. This result indicated that the repressive effect of HuCsv1 on dbcAMP-mediated increases in luciferase reporter activity was repeatable but that it was not obviously dose-dependent.

In saying this, it should be pointed out that in 2mM dbcAMP-treated cells, the actual difference in renilla luciferase reporter activity between cells co-transfected with versus without HuCsv1 is

greater than in the previous experiment where only 1mM dbcAMP was used (~2.8-fold reduced in the presence of HuCsv1 in the 1mM treatment experiment compared to 4.75-fold reduced in the 2mM treatment (see Appendix 2 - figure 4). This comparison on its own could imply that HuCsv1 is actually having a stronger repressive effect on renilla luciferase activity levels in the 2mM treatment group. However, the fact that renilla luciferase levels remain comparable between HuCsv1 co-transfected cells treated with either 2mM dbcAMP or vehicle control suggests another mechanism is at work. One possibility is that assuming the activity of the CMV–promoter (used by all the vectors in these assays) is increased by cAMP-dependent signalling pathways, increased expression from the luciferase reporter vector(s) should be accompanied by a proportional increase in expression from the HuCsv1 overexpression vector. As such, comparing differences in renilla luciferase activities from HuCsv1 overexpressing versus HuCsv1 lacking cells between different dbcAMP concentrations would be misleading, in that changes in the amount of HuCsv1 present within the cell are going to follow changes in the amount of luciferase reporter vector expression (all driven by dbcAMP). If dbcAMP were having no effect on HuCsv1 activity and HuCsv1 levels changed proportionally to changes in luciferase reporter vector expression, then one would expect to see a similar pattern for differences in luciferase activities from cells co-transfected with HuCsv1 and treated with dbcAMP at all cAMP concentrations, as appears to be the case in these experiments. That the fold difference in renilla luciferase activity between cells co-transfected with versus without HuCsv1 looks greater in the 2mM dbcAMP treated cells is most likely because treated cells lacking HuCsv1 have greater renilla luciferase reporter activity following 2mM dbcAMP treatment compared to 1mM dbcAMP treatment. In this way, the greater difference in renilla luciferase between HuCsv1 overexpressing versus lacking cells in the 2mM dbcAMP treatment group compared to the 1mM dbcAMP treatment group is explained the a greater level of renilla luciferase activity in HuCsv1-lacking cells from the 2mM group relative to the 1mM group.

As in the 1mM dbcAMP treatment group, 2mM dbcAMP was not found to greatly change differences in normalised firefly luciferase reporter activity between HuCsv1 overexpressing and HuCsv1 lacking cells (Appendix 2 - figure 5 - graph shows fold reduction of normalised 3´UTR-reporter expression in the presence of HuCsv1). Interestingly, unlike for renilla luciferase activity, increasing the dbcAMP dose from 1mM to 2mM did not increase the fold difference in averaged raw firefly luciferase activity between HuCsv1 overexpressing and HuCsv1 lacking cells (Appendix 2 - figure 6A – compare top two tables). It is not immediately clear why firefly luciferase reporter activity would not respond in a similar way to renilla luciferase activity in

comparing the two dbcAMP doses. Looking at the averaged raw firefly luciferase activities from untreated cells (Appendix 2 - figure 6B – compare two bottom tables), the averaged fold difference in reporter activity between HuCsv1 +/- cells in the 1mM dbcAMP experiment was almost 2-fold. However, from untreated cells in the 2mM dbcAMP experiment the fold difference in reporter activity was only 1.6-fold. Thus, it is conceivable that the 1mM dbcAMP experiment was already working in a background of greater reduction in raw firefly luciferase activity in the presence of HuCsv1 and as such, the 5.36-fold reduction seen in the 1mM dbcAMP-treated cells is not directly comparable to the 5.5-fold reduction seen in the 2mM dbcAMP-treated cells. Repeating the experiment could aid in determining whether the reduction in firefly luciferase activity in dbcAMP-treated cells from the first experiment is unusually high, or conversely unusually low in the second experiment. However, further complicating this comparison is the issue of HuCsv1 having a direct effect on firefly luciferase mRNA abundance (figure 33), presumably through a 3´UTR-independent interaction with the reporter mRNA. As a consequence of this interaction it is difficult to draw any conclusions about the effect of HuCsv1 on firefly luciferase reporter activity because the interaction between HuCsv1 and the reporter mRNA introduces another variable for which there is no control to compare.

### Luciferase reporter mRNA abundance relative to activity in dbcAMP-treated cells

While the firefly luciferase data is complicated by a non-specific interaction with HuCsv1, the renilla luciferase activity data raises a compelling possibility that HuCsv1 is in fact having a general, negative effect on translation. In the course of the firefly luciferase experiments, Northern blot had been used to determine mRNA abundances for reporter mRNAs from **untreated** cells co-transfected with or without HuCsv1. By knowing relative abundances of mRNAs in either condition, it was possible to measure (approximately) relative translation efficiency of the reporter mRNAs by simply normalising reporter activity to encoding mRNA. In experiments looking at cells **not** treated with dbcAMP, HuCsv1 causes an increase in abundance of the firefly luciferase reporter mRNA that is independent of 3´ UTR sequence and is not co-incident with an increase in reporter activity. This observation suggested that a common sequence among the firefly luciferase reporter messages, which was most likely the firefly luciferase coding sequence; promoted an interaction with HuCsv1 which led to the accumulation of translationally inactive (potentially deadenylated) reporter mRNAs. However, for the renilla luciferase reporter, translational efficiency did not appear to be strongly affected by co-expression with HuCsv1 in cells **not** treated with dbcAMP (see figure 36 and 33 luciferase chapter, supported by results from renilla luciferase-based 3´ UTR experiments figure 49). As such, it was curious as to whether the observed differences in renilla luciferase reporter activity

between HuCsv1 expressing versus HuCsv1 lacking cells treated with dbcAMP were arising due to some effect of HuCsv1 on abundance of the reporter mRNAs or if dbcAMP treatment was augmenting some effect of HuCsv1 on general translation that was not apparent in untreated cells.

***Translation efficiency of the renilla luciferase reporter is reduced in dbcAMP-treated cells***

On average, renilla luciferase activity normalised to mRNA was reduced 4.5-fold ($p$<0.00004) when co-expressed with HuCsv1, compared to HuCsv1-lacking cells (Appendix 2 - figure 8b). From previously described data in this thesis, cells co-transfected with HuCsv1 but **not** treated with dbcAMP **do not** indicate that the renilla luciferase reporter (phRL_CMV) is translationally regulated by HuCsv1 (figure 36 and figure 49). As such, it is possible the data from this dbcAMP-treatment experiment indicates following particular stimuli (*ie* dbcAMP treatment in this case), HuCsv1 can be activated or induced to have a general, non-specific effect on cellular translation. However, because of the apparent effect of HuCsv1 on pre-mRNA processing of the zfcdc42-v2 3´UTR reporter mRNA, and the lack of any obvious 3´UTR-dependent effect of HuCsv1 on candidate target reporter mRNA translation, no effort was made to investigate how this dbcAMP-dependent effect of HuCsv1 on general translation might be occurring. Conceivably, given dbcAMP activates members of the PKA and PKC families of protein kinases, which have been reported to directly phosphorylate nHu proteins and influence their activity [67], [182], [183].

***Northern results for dbcAMP-treated cells show similar effect of HuCsv1 on pre-mRNA processing of specific candidate 3´UTR-reporter mRNAs***

Finally, the most relevant piece of data to come out of these dbcAMP treatment studies was the observation from the Northern blot (Appendix 2 - figure 7) that showed a similar effect of HuCsv1 on the alternative pre-mRNA processing of the zfcdc42-v2 3´UTR-reporter mRNA as was seen in the Northern from Neuro-2a cells **not** treated with dbcAMP (figure 33). Specifically, as seen in the untreated Neuro-2a cells (figure 46), abundance of the control 3´UTR-reporter mRNAs was increased 2-3-fold in the presence of HuCsv1 (Appendix 2 - table 1). However, no increase in abundance of the non-canonical early zfcdc42-v2 3´UTR-reporter mRNA transcript was observed, despite an ~2.9-fold increase in abundance of the longer mRNA product (denoted terminal/SV40 in this Northern because it was not possible to distinguish the two different bands). This recapitulation of this effect in these experiments lend strength to the validity of the original observation and motivated subsequent investigation of a role for HuCsv1 in alternative pre-mRNA processing of this reporter mRNA in the renilla-luciferase reporter-based experiments presented in this thesis.

a.)

| fold change FL activity +1mM cAMP | | |
|---|---|---|
| Reporter: | - HuCsv1 | +HuCsv1 |
| control 3`UTR | 3.14 | 1.02 |
| VASP | 3.23 | 1.11 |
| mcdc42-v1 | 3.29 | 0.92 |
| mcdc42-v2 | 3.28 | 0.98 |
| zfcdc42-v1 | 3.47 | 1.23 |
| zfcdc42-v2 | 3.13 | 1.20 |
| mCofilin | 3.98 | 2.18 |
| zfCofilin | 2.23 | 0.95 |
| Average | 3.22 | 1.20 |
| STDEV | 0.48 | 0.41 |
| TTEST ($p$<…) | 0.000196 | 0.43 |

b.)

| fold change RL activity +1mM cAMP | | |
|---|---|---|
| Reporter: | - HuCsv1 | +HuCsv1 |
| control 3`UTR | 2.00 | 1.00 |
| VASP | 2.33 | 1.00 |
| mcdc42-v1 | 2.23 | 1.24 |
| mcdc42-v2 | 1.78 | 0.86 |
| zfcdc42-v1 | 2.36 | 1.07 |
| zfcdc42-v2 | 2.37 | 1.09 |
| mCofilin | 2.64 | 1.14 |
| zfCofilin | 2.60 | 1.05 |
| Average | 2.29 | 1.06 |
| STDEV | 0.29 | 0.11 |
| TTEST ($p$<…) | 2.88E-10 | 0.2941642 |

c.)

| Raw firefly luciferase activity (+1mM cAMP) | | |
|---|---|---|
| Reporter: | - HuCsv1 | +HuCsv1 |
| control 3`UTR | 29,839,023 | 9,739,351 |
| VASP | 32,759,667 | 4,609,089 |
| mcdc42-v1 | 37,861,604 | 6,881,558 |
| mcdc42-v2 | 52,108,647 | 10,793,975 |
| zfcdc42-v1 | 50,072,916 | 6,641,089 |
| zfcdc42-v2 | 84,701,261 | 13,173,140 |
| mCofilin | 45,870,529 | 11,969,354 |
| zfCofilin | 41,873,468 | 9,150,054 |

| Raw firefly luciferase activity | | |
|---|---|---|
| Reporter: | - HuCsv1 | +HuCsv1 |
| control 3`UTR | 9,509,787 | 9,553,616 |
| VASP | 10,134,426 | 4,166,845 |
| mcdc42-v1 | 11,501,992 | 7,484,128 |
| mcdc42-v2 | 15,881,457 | 11,015,265 |
| zfcdc42-v1 | 14,435,622 | 5,381,430 |
| zfcdc42-v2 | 27,030,245 | 11,012,777 |
| mCofilin | 11,525,231 | 5,494,178 |
| zfCofilin | 18,751,512 | 9,649,356 |

d.)

| Raw renilla luciferase activity (+1mM cAMP) | | |
|---|---|---|
| Reporter: | - HuCsv1 | +HuCsv1 |
| control 3`UTR | 10,823,412 | 4,164,064 |
| VASP | 13,436,190 | 4,504,784 |
| mcdc42-v1 | 12,899,850 | 4,978,227 |
| mcdc42-v2 | 11,677,186 | 4,558,190 |
| zfcdc42-v1 | 12,800,686 | 4,238,037 |
| zfcdc42-v2 | 13,668,785 | 4,859,034 |
| mCofilin | 14,861,591 | 5,293,352 |
| zfCofilin | 13,080,122 | 4,528,794 |

| Raw renilla luciferase activity | | |
|---|---|---|
| Reporter: | - HuCsv1 | +HuCsv1 |
| control 3`UTR | 5,409,770 | 4,154,501 |
| VASP | 5,759,794 | 4,482,437 |
| mcdc42-v1 | 5,776,608 | 4,023,624 |
| mcdc42-v2 | 6,573,037 | 5,313,854 |
| zfcdc42-v1 | 5,423,360 | 3,971,974 |
| zfcdc42-v2 | 5,759,597 | 4,476,795 |
| mCofilin | 5,620,666 | 4,635,215 |
| zfCofilin | 5,027,096 | 4,294,796 |

Appendix 2 - Figure 1. Luciferase reporter activity results from Neuro-2a transfections.

Tables a.) and b.) show fold-increases of raw firefly (FL) and renilla (RL) luciferase activity (respectively) in the presence or absence of HuCsv1, following treatment with 1mM dbcAMP (compared to untreated cells. Homoschedastic Student's t-test was used to determine the statistical significance of the difference in activity between treated and untreated cells for each HuCsv1 condition (TTEST – $p$<…).

Tables c.) and d.) show raw luciferase activity values (FL and RL respectively) used to generate the tables 1a and 1b. FL and RL activity from cells treated with 1mM cAMP for 16hr are shown in the top two tables, respective luciferase activities are shown in the bottom two tables. Activity values are the average of three replicate assays from one experiment.

a.)

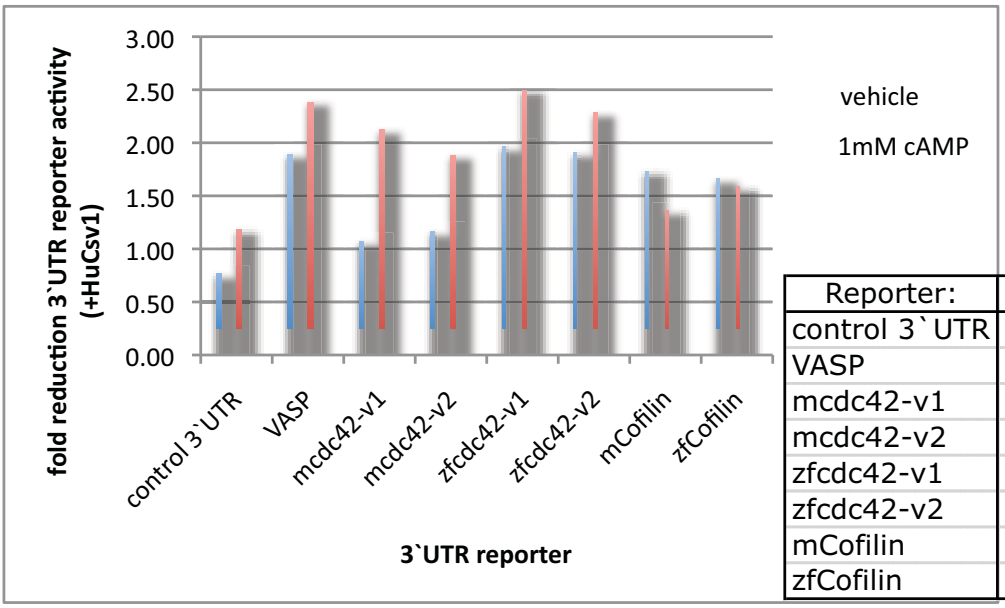


| Reporter: | vehicle | 1mM cAMP |
|---|---|---|
| control 3`UTR | 0.76 | 1.18 |
| VASP | 1.89 | 2.38 |
| mcdc42-v1 | 1.07 | 2.12 |
| mcdc42-v2 | 1.17 | 1.88 |
| zfcdc42-v1 | 1.96 | 2.50 |
| zfcdc42-v2 | 1.91 | 2.29 |
| mCofilin | 1.73 | 1.36 |
| zfCofilin | 1.66 | 1.58 |

b.)

| Normalised FL activity (+1mM cAMP) | | | |
|---|---|---|---|
| Reporter: | - HuCsv1 | +HuCsv1 | fold change |
| control 3`UTR | 2.76 | 2.34 | 1.18 |
| VASP | 2.44 | 1.02 | 2.38 |
| mcdc42-v1 | 2.94 | 1.38 | 2.12 |
| mcdc42-v2 | 4.46 | 2.37 | 1.88 |
| zfcdc42-v1 | 3.91 | 1.57 | 2.50 |
| zfcdc42-v2 | 6.20 | 2.71 | 2.29 |
| mCofilin | 3.09 | 2.26 | 1.36 |
| zfCofilin | 3.20 | 2.02 | 1.58 |

| Normalised FL activity | | | |
|---|---|---|---|
| Reporter: | - HuCsv1 | +HuCsv1 | fold change |
| control 3`UTR | 1.76 | 2.30 | 0.76 |
| VASP | 1.76 | 0.93 | 1.89 |
| mcdc42-v1 | 1.99 | 1.86 | 1.07 |
| mcdc42-v2 | 2.42 | 2.07 | 1.17 |
| zfcdc42-v1 | 2.66 | 1.35 | 1.96 |
| zfcdc42-v2 | 4.69 | 2.46 | 1.91 |
| mCofilin | 2.05 | 1.19 | 1.73 |
| zfCofilin | 3.73 | 2.25 | 1.66 |

Figure 2. Firefly luciferase 3' UTR reporter assays. Reporter activity results from Neuro-2a transfections.

a.) Graph shows the fold reduction in normalised 3' UTR reporter activity from cells co-transfected with HuCsv1 (relative to – HuCsv1), either in the presence or absence of 1mM dbcAMP.

b.) Tables showing firefly luciferase (FL) activity normalised to renilla luciferase activity in either the presence or absence of 1mM dbcAMP. Fold changes represent the difference in normalised FL activity in cells lacking HuCsv1 compared to cells expressing HuCsv1.

a.)

| fold change FL activity +2mM cAMP | | |
|---|---|---|
| Reporter: | - HuCsv1 | +HuCsv1 |
| control 3`UTR | 4.10 | 1.53 |
| Xβ-globin | 3.80 | 1.25 |
| VASP | 3.72 | 1.12 |
| mcdc42-v1 | 4.49 | 1.31 |
| mcdc42-v2 | 6.23 | 1.29 |
| zfcdc42-v1 | 3.59 | 1.45 |
| zfcdc42-v2 | 6.85 | 1.27 |
| mCofilin | 4.42 | 1.39 |
| zfCofilin | 3.27 | 1.10 |
| Average | 4.50 | 1.30 |
| STEDEV | 1.23 | 0.14 |
| TTEST ($p$<…) | 8.8352E-05 | 0.19 |

b.)

| fold change RL activity +2mM cAMP | | |
|---|---|---|
| Reporter: | - HuCsv1 | +HuCsv1 |
| control 3`UTR | 3.08 | 1.17 |
| Xβ-globin | 2.37 | 0.95 |
| VASP | 2.89 | 0.88 |
| mcdc42-v1 | 2.76 | 1.11 |
| mcdc42-v2 | 3.78 | 0.94 |
| zfcdc42-v1 | 2.78 | 1.16 |
| zfcdc42-v2 | 4.18 | 0.93 |
| mCofilin | 2.97 | 1.07 |
| zfCofilin | 2.60 | 0.78 |
| Average | 3.04 | 1.00 |
| STDEV | 0.58 | 0.13 |
| TTEST ($p$<…) | 8.3393E-12 | 0.91 |

c.)

| Raw firefly luciferase activity (+2mM cAMP) | | |
|---|---|---|
| Reporter: | - HuCsv1 | +HuCsv1 |
| control 3`UTR | 20,564,308 | 7,561,791 |
| Xβ-globin | 23,634,556 | 7,380,650 |
| VASP | 17,828,324 | 1,859,310 |
| mcdc42-v1 | 24,755,362 | 2,951,056 |
| mcdc42-v2 | 42,596,980 | 8,696,269 |
| zfcdc42-v1 | 23,289,146 | 4,008,341 |
| zfcdc42-v2 | 53,914,784 | 7,221,375 |
| mCofilin | 24,150,952 | 6,321,203 |
| zfCofilin | 16,787,330 | 4,617,421 |

| Raw firefly luciferase activity | | |
|---|---|---|
| Reporter: | - HuCsv1 | +HuCsv1 |
| control 3`UTR | 5,020,956 | 4,945,739 |
| Xβ-globin | 6,213,817 | 5,900,604 |
| VASP | 4,794,137 | 1,665,076 |
| mcdc42-v1 | 5,516,200 | 2,258,696 |
| mcdc42-v2 | 6,835,889 | 6,740,030 |
| zfcdc42-v1 | 6,482,080 | 2,768,380 |
| zfcdc42-v2 | 7,873,709 | 5,675,925 |
| mCofilin | 5,459,737 | 4,533,518 |
| zfCofilin | 5,134,042 | 4,201,230 |

d.)

| Raw renilla luciferase activity (+2mM cAMP) | | |
|---|---|---|
| Reporter: | - HuCsv1 | +HuCsv1 |
| control 3`UTR | 10,007,603 | 2,269,325 |
| Xβ-globin | 10,349,809 | 2,092,357 |
| VASP | 10,738,197 | 1,562,480 |
| mcdc42-v1 | 9,166,890 | 1,990,950 |
| mcdc42-v2 | 9,512,635 | 2,228,861 |
| zfcdc42-v1 | 8,290,318 | 2,579,842 |
| zfcdc42-v2 | 10,230,166 | 2,179,126 |
| mCofilin | 10,828,360 | 2,109,560 |
| zfCofilin | 8,435,430 | 1,826,193 |

| Raw renilla luciferase activity | | |
|---|---|---|
| Reporter: | - HuCsv1 | +HuCsv1 |
| control 3`UTR | 3,253,534 | 1,933,214 |
| Xβ-globin | 4,373,376 | 2,198,456 |
| VASP | 3,717,830 | 1,774,437 |
| mcdc42-v1 | 3,326,977 | 1,793,133 |
| mcdc42-v2 | 2,514,472 | 2,380,898 |
| zfcdc42-v1 | 2,986,440 | 2,232,514 |
| zfcdc42-v2 | 2,447,065 | 2,354,809 |
| mCofilin | 3,641,106 | 1,965,842 |
| zfCofilin | 3,239,486 | 2,331,638 |

Figure 3. Luciferase reporter activity results from Neuro-2a transfections.

Tables a.) and b.) show fold-increases of raw firefly (FL) and renilla (RL) luciferase activity (respectively) in the presence or absence of HuCsv1, following treatment with 2mM dbcAMP (compared to untreated cells. Homoschedastic Student's t-test was used to determine the statistical significance of the difference in activity between treated and untreated cells for each HuCsv1 condition (TTEST – $p$<…).

Tables c.) and d.) show raw luciferase activity values (FL and RL respectively) used to generate the tables 3a and 3b. FL and RL activity from cells treated with 2mM cAMP for 16hr are shown in the top two tables, respective luciferase activities are shown in the bottom two tables. Activity values are the average of three replicate assays from one experiment.

a.)

| Averaged raw renilla luciferase activity (+1mM cAMP) | | | |
|---|---|---|---|
| | - HuCsv1 | +HuCsv1 | fold change |
| Average | 12,905,978 | 4,640,560 | 2.78 |
| STDEV | 1,229,162 | 380,727 | 0.18 |
| TTEST ($p$<…) | 3.9384E-11 | | |

| Averaged raw renilla luciferase activity (+2mM cAMP) | | | |
|---|---|---|---|
| | - HuCsv1 | +HuCsv1 | fold change |
| Average | 9,728,823 | 2,093,188 | 4.75 |
| STDEV | 938,561 | 286,642 | 1.02 |
| TTEST ($p$<…) | 8.7266E-14 | | |

b.)

| Averaged raw renilla luciferase activity (-1mM cAMP) | | | |
|---|---|---|---|
| | - HuCsv1 | +HuCsv1 | fold change |
| Average | 5,668,741 | 4,419,149 | 1.29 |
| STDEV | 445,169 | 430,352 | 0.08 |
| TTEST ($p$<…) | 5.4071E-05 | | |

| Averaged raw renilla luciferase activity (-2mM cAMP) | | | |
|---|---|---|---|
| | - HuCsv1 | +HuCsv1 | fold change |
| Average | 3,277,810 | 2,107,216 | 1.59 |
| STDEV | 600,839 | 242,448 | 0.42 |
| TTEST ($p$<…) | 5.6668E-05 | | |

c.)

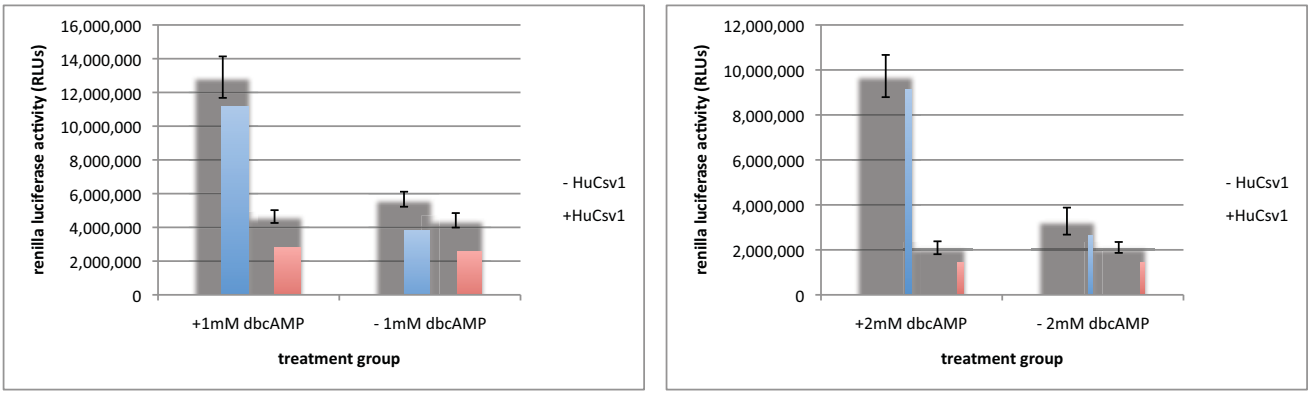


Figure 4. Firefly luciferase 3' UTR reporter assays. Reporter activity results from Neuro-2a transfections.

a.) The top two tables show the averaged raw renilla luciferase activity in the presence or absence of HuCsv1, following treatment with either 1mM or 2mM dbcAMP for 16hr prior to harvest.

b.) The bottom two tables show the averaged raw renilla luciferase activity in the presence or absence of HuCsv1, from the vehicle control experiments conducted at the same time as the respective dbcAMP experiments.

Homoschedastic Student's t-test was used to determine the statistical significance of the difference in luciferase activity between the two HuCsv1 conditions in each treatment group.

c.) Graphs show the averaged renilla luciferase activity from +/- HuCsv1 cells in the two different treatment groups

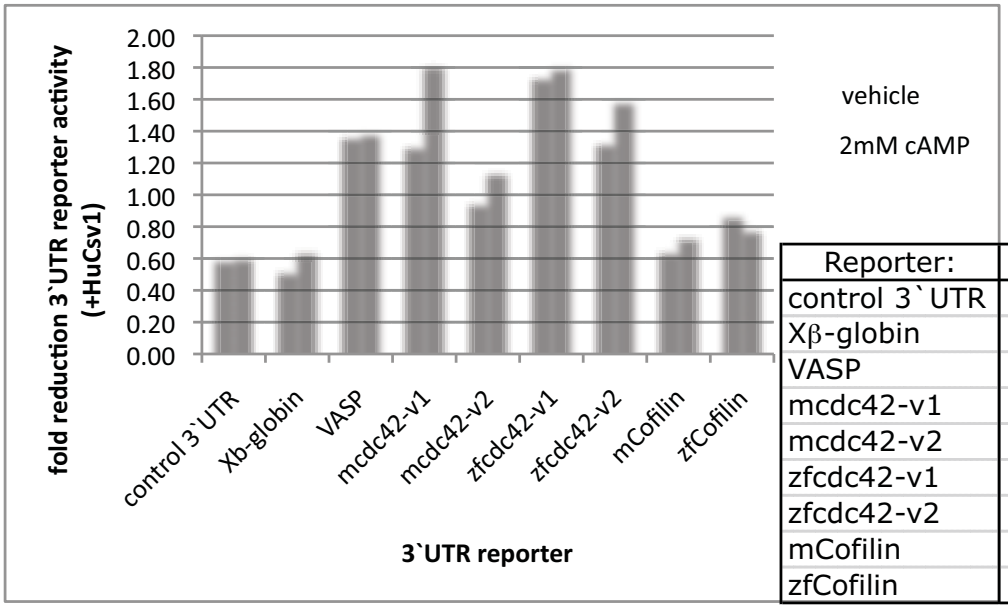


a.)

| Reporter: | vehicle | 2mM cAMP |
|---|---|---|
| control 3`UTR | 0.60 | 0.62 |
| Xβ-globin | 0.53 | 0.65 |
| VASP | 1.37 | 1.40 |
| mcdc42-v1 | 1.32 | 1.82 |
| mcdc42-v2 | 0.96 | 1.15 |
| zfcdc42-v1 | 1.75 | 1.81 |
| zfcdc42-v2 | 1.33 | 1.59 |
| mCofilin | 0.65 | 0.74 |
| zfCofilin | 0.88 | 0.79 |

b.)

| Normalised FL activity (+2mM cAMP) | | | |
|---|---|---|---|
| Reporter: | - HuCsv1 | +HuCsv1 | fold change |
| control 3`UTR | 2.05 | 3.33 | 0.62 |
| Xβ-globin | 2.28 | 3.53 | 0.65 |
| VASP | 1.66 | 1.19 | 1.40 |
| mcdc42-v1 | 2.70 | 1.48 | 1.82 |
| mcdc42-v2 | 4.48 | 3.90 | 1.15 |
| zfcdc42-v1 | 2.81 | 1.55 | 1.81 |
| zfcdc42-v2 | 5.27 | 3.31 | 1.59 |
| mCofilin | 2.23 | 3.00 | 0.74 |
| zfCofilin | 1.99 | 2.53 | 0.79 |

| Normalised FL activity | | | |
|---|---|---|---|
| Reporter: | - HuCsv1 | +HuCsv1 | fold change |
| control 3`UTR | 1.54 | 2.56 | 0.60 |
| Xβ-globin | 1.42 | 2.68 | 0.53 |
| VASP | 1.29 | 0.94 | 1.37 |
| mcdc42-v1 | 1.66 | 1.26 | 1.32 |
| mcdc42-v2 | 2.72 | 2.83 | 0.96 |
| zfcdc42-v1 | 2.17 | 1.24 | 1.75 |
| zfcdc42-v2 | 3.22 | 2.41 | 1.33 |
| mCofilin | 1.50 | 2.31 | 0.65 |
| zfCofilin | 1.58 | 1.80 | 0.88 |

Figure 5. Firefly luciferase 3' UTR reporter assays. Reporter activity results from Neuro-2a transfections.

a.) Graph shows the fold reduction in normalised 3' UTR reporter activity from cells co-transfected with HuCsv1 (relative to – HuCsv1), either in the presence or absence of 2mM dbcAMP.

b.) Tables showing firefly luciferase (FL) activity normalised to renilla luciferase activity in either the presence or absence of 2mM dbcAMP. Fold changes represent the difference in normalised FL activity in cells lacking HuCsv1 compared to cells expressing HuCsv1.

a.)

| Averaged raw firefly luciferase activity (+1mM cAMP) | | | |
|---|---|---|---|
| | - HuCsv1 | +HuCsv1 | fold change |
| Average | 46,885,889 | 9,119,701 | 5.36 |
| STDEV | 17,176,294 | 2,909,035 | 1.58 |
| TTEST ($p$<…) | 2.5986E-05 | | |

| Averaged raw firefly luciferase activity (+2mM cAMP) | | | |
|---|---|---|---|
| | - HuCsv1 | +HuCsv1 | fold change |
| Average | 27,502,416 | 5,624,157 | 5.50 |
| STDEV | 12,417,166 | 2,352,086 | 2.39 |
| TTEST ($p$<…) | 8.8781E-05 | | |

b.)

| Averaged raw firefly luciferase activity (-1mM cAMP) | | | |
|---|---|---|---|
| | - HuCsv1 | +HuCsv1 | fold change |
| Average | 14,846,284 | 7,969,699 | 1.95 |
| STDEV | 5,828,911 | 2,709,524 | 0.58 |
| TTEST ($p$<…) | 0.00907403 | | |

| Averaged raw firefly luciferase activity (-2mM cAMP) | | | |
|---|---|---|---|
| | - HuCsv1 | +HuCsv1 | fold change |
| Average | 5,925,619 | 4,298,800 | 1.62 |
| STDEV | 1,007,862 | 1,744,481 | 0.74 |
| TTEST ($p$<…) | 0.02765524 | | |

c.)

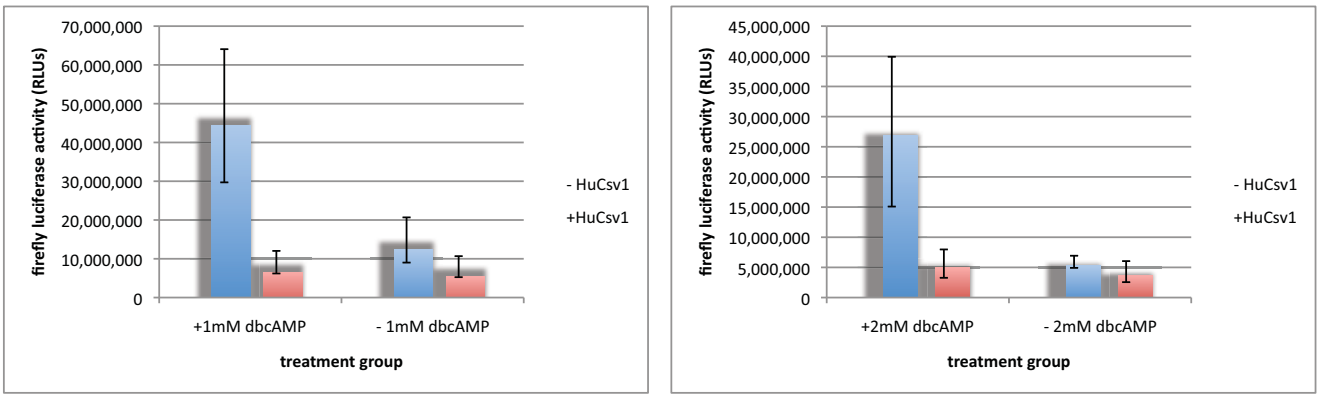


Figure 6. Firefly luciferase 3' UTR reporter assays. Reporter activity results from Neuro-2a transfections.

a.) The top two tables show the averaged raw firefly luciferase activity in the presence or absence of HuCsv1, following treatment with either 1mM or 2mM dbcAMP for 16hr prior to harvest.

b.) The bottom two tables show the averaged raw firefly luciferase activity in the presence or absence of HuCsv1, from the vehicle control experiments conducted at the same time as the respective dbcAMP experiments.

Homoschedastic Student's t-test was used to determine the statistical significance of the difference in luciferase activity between the two HuCsv1 conditions in each treatment group.

c.) Graphs show the averaged renilla luciferase activity from +/- HuCsv1 cells in the two different treatment groups

Firefly Northern Neuro - 2a +cAMP

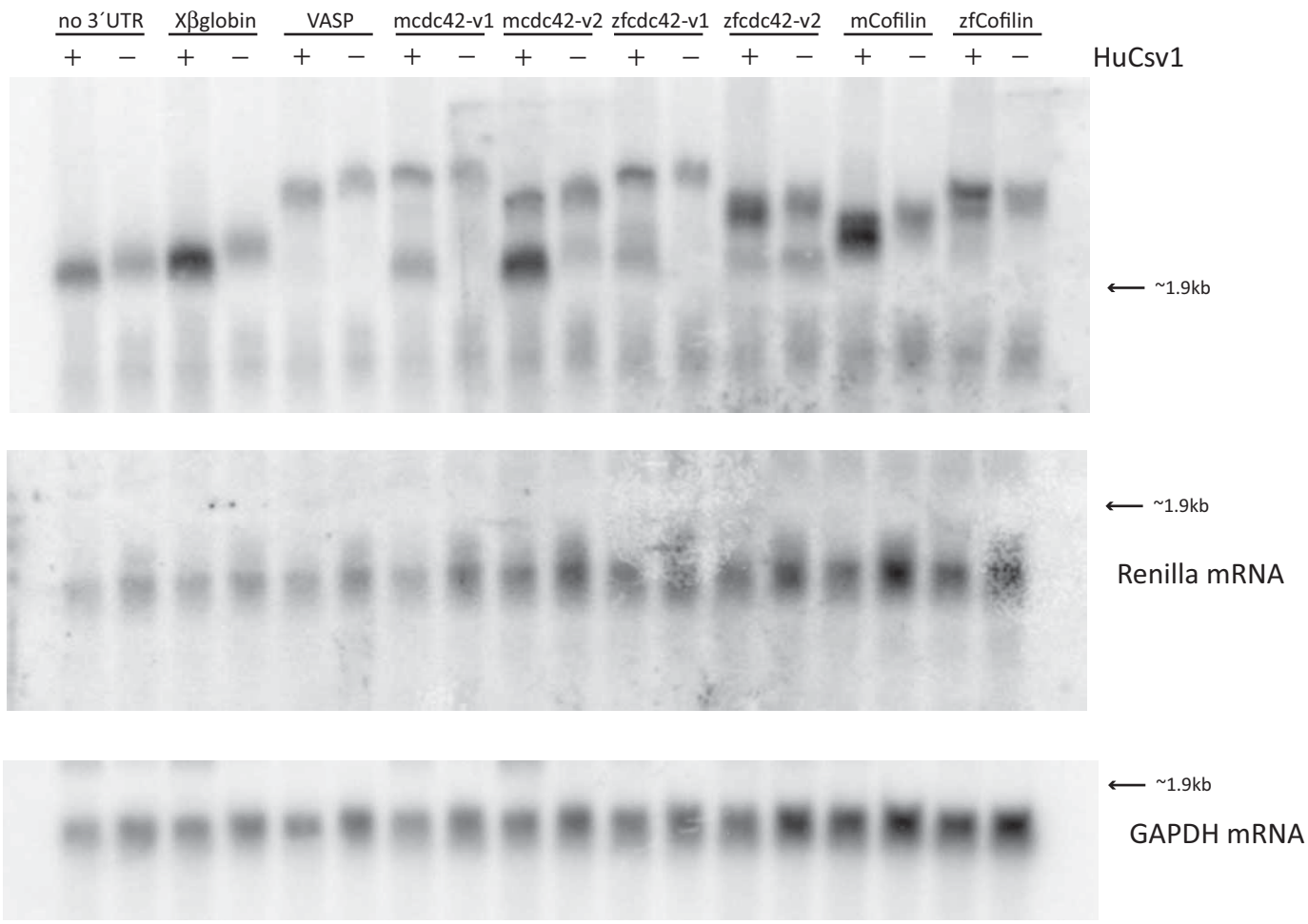


Appendix 2 - Figure 7. Firefly luciferase-based 3´UTR-reporters - Neuro-2a cells + 2mM dbcAMP.

Total RNA from transfected Neuro-2a cells was probed with a radiolabelled DNA probe complementary to the firefly luciferase coding sequence (top image). A second probe was used to detect the coding sequence of the renilla luciferase transfection control reporter mRNA (middle image) and a third probe used to detect the GAPDH coding sequence (as a loading control - bottom image). The migration of size standards was not recorded for this Northern. The approximate location of the 28S ribosomal RNA (1.9kb) is indicated

| FL 3`UTR reporter mRNA Abundance (Int. Dens) | | | | Corrected to GAPDH | |
|---|---|---|---|---|---|
| Reporter: | - HuCsv1 | +HuCsv1 | | +HuCsv1 | fold change |
| control 3`UTR | 401 | 673 | | 833 | 2.08 |
| Xβ-globin | 357 | 1,007 | | 1,170 | 3.27 |
| VASP | 338 | 383 | | 574 | 1.70 |
| mcdc42-v1 terminal | 256 | 345 | | 538 | 2.10 |
| mcdc42-v1 very early | | 268 | | 418 | |
| *mcdc42-v1 total* | *256* | | | *956* | 3.73 |
| mcdc42-v2 SV40 | 335 | 342 | | 499 | 1.49 |
| mcdc42-v2 early | 180 | 642 | | 936 | 5.19 |
| *mcdc42-v2 total* | *515* | | | *1,434* | 2.79 |
| zfcdc42-v1 terminal | 360 | 484 | | 606 | 1.68 |
| zfcdc42-v1 early | 51 | 178 | | 224 | 4.40 |
| *zfcdc42-v1 total* | *411* | | | *830* | 2.02 |
| zfcdc42-v2 terminal/SV40 | 436 | 630 | | 1,273 | 2.92 |
| zfcdc42-v2 non-canonical early | 295 | 153 | | 309 | 1.05 |
| *zfcdc42-v2 total* | *731* | | | *1,582* | 2.16 |
| mCofilin SV40 | 363 | 302 | | 451 | 1.24 |
| mCofilin terminal | 166 | 509 | | 760 | 4.59 |
| *mCofilin total* | *529* | | | *1,211* | 2.29 |
| zfCofilin non-canonical late | 223 | 441 | | 559 | 2.50 |
| zfCofilin terminal | 180 | 261 | | 331 | 1.84 |
| *zfCofilin total* | *404* | | | *890* | 2.21 |

| RL mRNA Abundance (Int. Dens) | | | | Corrected to GAPDH | | |
|---|---|---|---|---|---|---|
| Reporter: | - HuCsv1 | +HuCsv1 | | - HuCsv1 | +HuCsv1 | fold change |
| control 3`UTR | 211 | 124 | | 211 | 153 | 0.73 |
| Xβ-globin | 208 | 177 | | 176 | 174 | 0.99 |
| VASP | 238 | 154 | | 178 | 172 | 0.97 |
| mcdc42-v1 | 281 | 141 | | 293 | 229 | 0.78 |
| mcdc42-v2 | 334 | 264 | | 284 | 326 | 1.15 |
| mCofilin | 400 | 281 | | 252 | 265 | 1.05 |
| | | Average | | 232 | 220 | 0.94 |
| | | STDEV | | 52 | 67 | 0.16 |
| | | TTEST ($p$<…) | | | | 0.729 |

| GAPDH mRNA Abundance (Int. Dens) | | | |
|---|---|---|---|
| Reporter: | - HuCsv1 | +HuCsv1 | fold change |
| control 3`UTR | 643 | 520 | 0.81 |
| Xβ-globin | 762 | 656 | 0.86 |
| VASP | 861 | 575 | 0.67 |
| mcdc42-v1 | 617 | 395 | 0.64 |
| mcdc42-v2 | 757 | 519 | 0.69 |
| zfcdc42-v1 | 640 | 511 | 0.80 |
| zfcdc42-v2 | 1,039 | 515 | 0.50 |
| mCofilin | 1,019 | 682 | 0.67 |
| zfCofilin | 977 | 770 | 0.79 |

Appendix 2 - Table 1. Firefly luciferase 3' UTR reporter – mRNA abundance

Values tabled represent mRNA abundance values (Integrated Density) minus background as determined from Northern analysis.

Fold changes = difference in mRNA abundance between +HuCsv1 and –HuCsv1 samples (+HuC/-HuC).

Figure 7. Firefly luciferase 3' UTR reporter assays. Reporter activity results from Neuro-2a transfections.

a.) Firefly luciferase reporter activity normalised to mRNA abundance.

b.) Renilla luciferase reporter activity normalised to mRNA abundance. Graph shows averaged (mRNA normalised) renilla luciferase activity. Error bars represent standard deviation of averaged values.

Homoschedastic Student's t-test was used to determine the statistical significance of the difference in renilla luciferase activity between the +HuCsv1 and – HuCsv1 conditions.

a.)

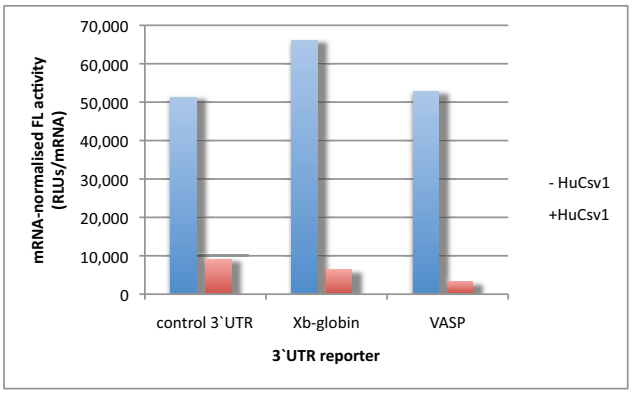


b.)

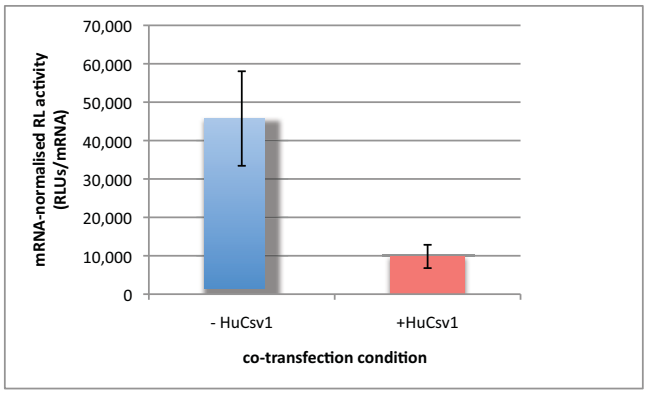


| mRNA-normalised FL activity +cAMP | | |
|---|---|---|
| Reporter: | - HuCsv1 | +HuCsv1 |
| control 3`UTR | 51,292 | 9,082 |
| Xβ-globin | 66,122 | 6,309 |
| VASP | 52,736 | 3,241 |

| mRNA-normalised RL activity +cAMP | | |
|---|---|---|
| Reporter: | - HuCsv1 | +HuCsv1 |
| control 3`UTR | 47,329 | 14,798 |
| Xβ-globin | 58,884 | 12,051 |
| VASP | 60,465 | 9,073 |
| mcdc42-v1 | 31,329 | 8,693 |
| mcdc42-v2 | 33,506 | 6,827 |
| mCofilin | 42,911 | 7,496 |
| | | |
| Average | 45,737 | 9,823 |
| STDEV | 12,308 | 3,032 |
| TTEST ($p$<…) | | 4.0E-05 |

Figure 8. Firefly luciferase 3' UTR reporter assays. Reporter activity results from Neuro-2a transfections.

Translation efficiency (mRNA normalised FL activity / mRNA normalised RL activity) was determined for the two control 3' UTR reporters and the VASP 3' UTR reporter.

Homoschedastic Student's t-test was used to determine the statistical significance of the difference in renilla luciferase activity between the +HuCsv1 and – HuCsv1 conditions.

| 3`UTR translation efficiency +cAMP | | |
|---|---|---|
| Reporter: | - HuCsv1 | +HuCsv1 |
| control 3`UTR | 1.08 | 0.61 |
| Xβ-globin | 1.12 | 0.52 |
| VASP | 0.87 | 0.36 |

| 3`UTR translation efficiency +cAMP | | |
|---|---|---|
| Reporter: | - HuCsv1 | +HuCsv1 |
| control 3`UTR | 1.00 | 0.57 |
| Xβ-globin | 1.04 | 0.48 |
| VASP | 0.80 | 0.33 |

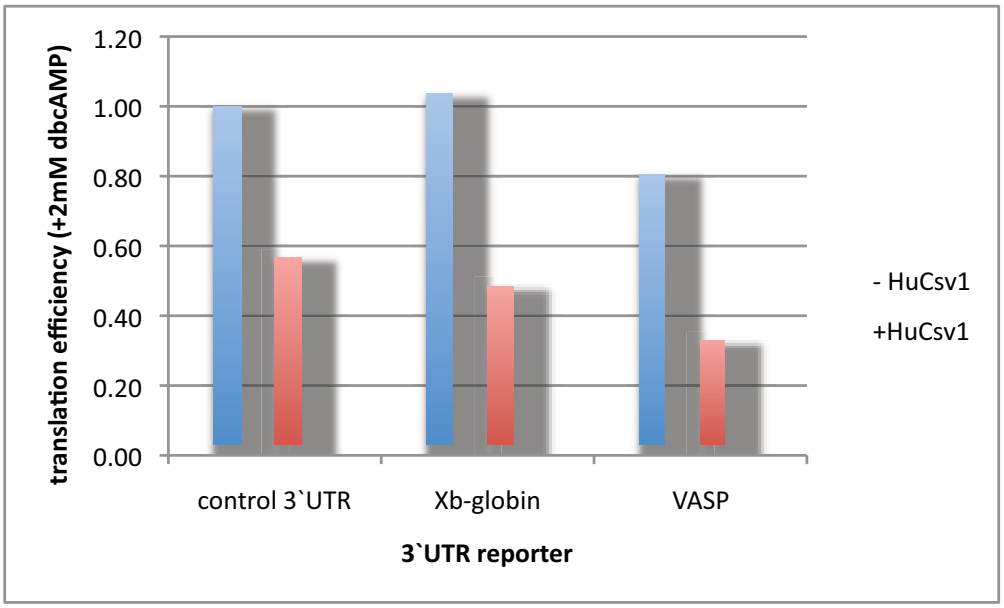

Figure 9. GAPDH-normalised firefly luciferase mRNA abundances from 2mM dbcAMP-treated and untreated Neuro-2a cells

a.) results from Northern for untreated cells

b.) results from Northern for 2mM dbcAMP-treated cells

a.)

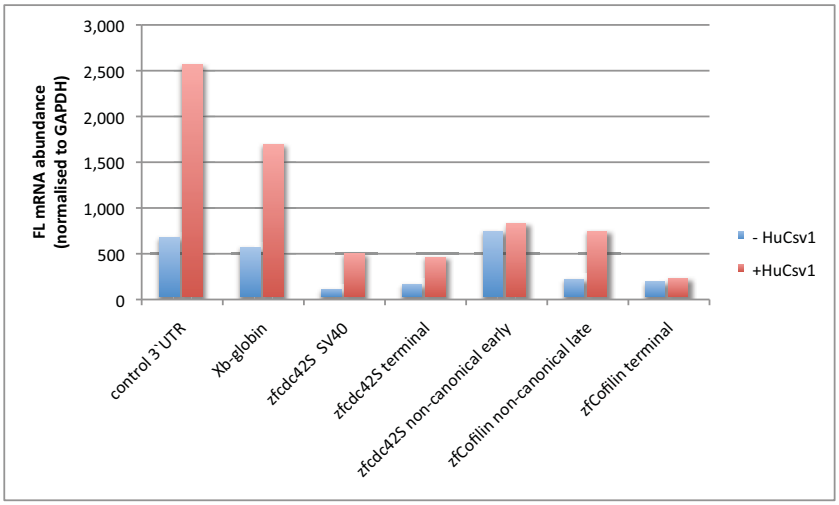


| Reporter: | - HuCsv1 | +HuCsv1 |
|---|---|---|
| control 3`UTR | 681 | 2,568 |
| Xβ-globin | 566 | 1,695 |
| zfcdc42S SV40 | 112 | 503 |
| zfcdc42S terminal | 165 | 462 |
| zfcdc42S non-canonical early | 744 | 830 |
| zfCofilin non-canonical late | 223 | 745 |
| zfCofilin terminal | 192 | 231 |

b.)

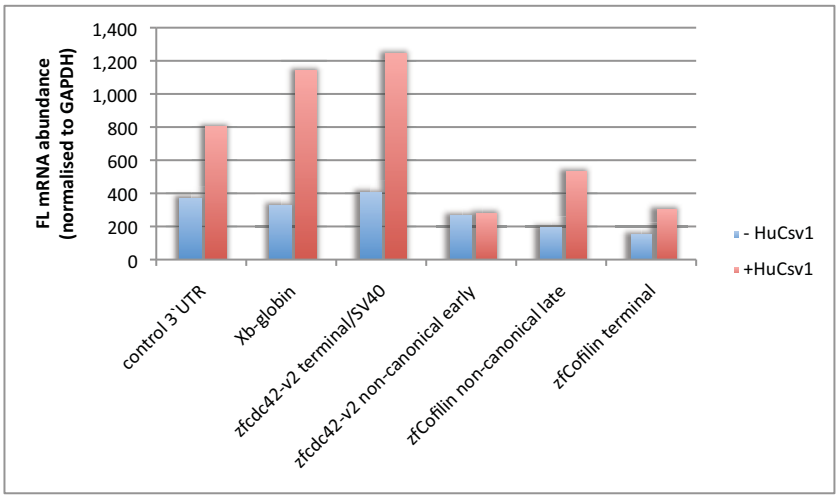


| Reporter: | - HuCsv1 | +HuCsv1 |
|---|---|---|
| control 3`UTR | 401 | 833 |
| Xβ-globin | 357 | 1,170 |
| zfcdc42-v2 terminal/SV40 | 436 | 1,273 |
| zfcdc42-v2 non-canonical early | 295 | 309 |
| zfCofilin non-canonical late | 223 | 559 |
| zfCofilin terminal | 180 | 331 |

## Appendix 3 – Developing an RNA-IP protocol to identify interactions between HuCsv1 and 3´UTR-reporter mRNAs

Another technique optimised while conducting the firefly luciferase-based 3´UTR-reporter assays was a cross-linking immunoprecipitation protocol to specifically isolate RNA products interacting with HuCsv1 in co-transfected cells. The protocol, known as RNA-IP is similar to a ChIP assay, in that formaldehyde is used to form reversible cross-links between primary amino groups in proteins (typically side chains of basic amino acids) and nearby nitrogen atoms in other proteins or nucleic acids, within living cells. Immunoprecipitation in then used to capture the RNA-binding protein of interest (in this case HuCsv1). Importantly, the formation of cross-links ensures interactions occurring in the cell, prior to cell lysis are captured and allows for more stringent washing of immunoprecipitated material to eliminate non-specific interactions that may occur following cell lysis. The reversibility of the formaldehyde-generated cross-links following mild heating in an aqueous solution enables any RNA co-immunoprecipitating with the RNA-binding protein of interest (HuCsv1) could be liberated and subsequently purified and analysed by RT-PCR.

In these experiments, Neuro-2a cells were co-transfected with pmHuCsv1 and either the control 3´UTR-reporter, zfcdc42-v2 3´UTR-reporter or the VASP 3´UTR-reporter. Approximately 18 hours after transfection, cells were briefly exposed to a weak solution of formaldehyde. Following cross-linking, cells were lysed and the myc-tagged HuCsv1 protein specifically immunoprecipitated using a commercially available α-myc antibody. Immunoprecipitated material was washed and then heated to reverse cross-linking and co-precipitating mRNA was then extracted using TRI Reagent (Ambion) and reverse transcribed to generate cDNA. The resulting cDNA was used in PCRs in combination with 3´UTR-specific primers to ascertain whether the 3´UTR-reporter mRNA co-immunoprecipitated out specifically with HuCsv1.

In the context of the experiments occurring at the time, development of this RNA-IP assay started shortly before the first Northern results from the firefly luciferase-based reporter assays were generated. At the time, the luciferase activity data indicated HuCsv1 had a small but reproducible negative effect on firefly luciferase activity from the zfcdc42-v2 and VASP 3´UTR-reporters. One piece of evidence that was lacking though, was proof that this effect was being caused by a direct interaction between HuCsv1 and either of the two reporter mRNAs. It was possible that rather than interacting directly; overexpressed HuCsv1 was altering either the

expression or function of other factors specifically involved in regulating the zfcdc42-v2 or VASP 3´UTR-reporters. For instance, by interfering with other *trans*-acting factors that would normally bind to the zfcdc42-v2 or VASP 3´UTR sequence, or by altering the expression of such factors through effects on their encoding mRNAs. As such, efforts to develop this protocol were undertaken to show that the negative effects of HuCsv1 on luciferase activity from the zfcdc42-v2 and VASP 3´UTR-reporters, were the result of a direct interaction between HuCsv1 and its target reporter mRNAs.

Unfortunately, once the data from the firefly luciferase reporter Northerns was obtained, the relevance of any data generated from these assays was brought into question. Specifically, the Northern data indicated that HuCsv1 could specifically stabilise all firefly luciferase-based 3´UTR reporter mRNAs, presumably through a direct interaction between these mRNAs and HuCsv1. In part, the data obtained from the RNA-IP experiments supports this conclusion, showing that both the zfcdc42-v2 and VASP 3´UTR reporter mRNAs could be specifically co-immunoprecipitated with HuCsv1. However, because of the non-specific interaction between HuCsv1 and the firefly luciferase reporter sequence, experiments using the firefly luciferase-based reporter constructs were dropped and replaced with renilla luciferase-based constructs. Due to time constraints, co-immunoprecipitation of renilla luciferase-based reporter mRNAs with HuCsv1 was never attempted. Because of the apparent interaction between HuCsv1 and the firefly luciferase coding sequence, the data from these RNA-IP experiments cannot be used to demonstrate a direct interaction between HuCsv1 and CLIP-identified target 3´UTR sequences, as intended. Nevertheless, the interactions identified with this assay to support the conclusion that HuCsv1 does specifically interact with both the VASP and zfcdc42-v2 3´UTR-reporter mRNAs. Furthermore, the results here provide a basic proof of principle that this protocol could be used to test for direct interactions between myc-tagged HuCsv1 and target mRNAs in future work.

## Optimising the RNA-IP protocol for myc-HuCsv1

RNA-immunoprecipitation has been used in a number of published papers [259], [260], [261]. In general, the protocol used by these papers follows the protocol published in 2002 by Niranjanakumari *et al* [262]. This was the protocol used as the basis for the RNA-IP experiments performed herein.

***Testing immunoprecipitation from formaldehyde cross-linked lysates***

As a starting point for these assays, rabbit polyclonal anti-myc antibody (C3956 – Sigma) was tested for its ability to immunoprecipitate myc-tagged HuCsv1 from cell lysates following formaldehyde cross-linking. For this experiment, $5.8x10^5$ HeLa cells were plated in 10cm tissue culture dishes and transfected at ~60% confluency with 38fmol of the control 3′UTR-reporter construct (~15x greater than used in 12-well dishes for luciferase activity assays, to account for 15-fold increase in surface area/number of cell plated) and 6μg of either pmHuCsv1 or empty pcDNA3 vector. The amount of pmHuCsv1 or empty pcDNA3 vector was only increased 6-fold inline with the recommended total amounts of plasmid DNA to transfect indicated for FuGENE6 (Roche). The protocol for cross-linking transfected cells is provided at the end of this appendix. For antibody testing, the protocol was only carried through as far as the immunoprecipitation step. Following immunoprecipitation samples for the input lysate, depleted lysate (ie, the supernatant from the IP) and the immunoprecipitated material from the beads were separated by SDS-PAGE and myc-HuCsv1 abundance in the different samples determined using a mouse monoclonal antibody reactive against all Hu proteins (3A2 – Santa Cruz Biotech). Detection was carried out using Enhanced ChemiLuminescence (ECL) (Western Lightning – Perkin Elmer) followed by exposure of the membrane to autoradiographic film (AGFA).

The results from this experiment indicated that the rabbit α-myc antibody retained the ability to immunoprecipitate myc-tagged HuCsv1 (Appendix 3 – figure 1) from formaldehyde cross-linked cell lysates. Comparing equally loaded pre-cleared sample and depleted sample lanes, a modest reduction in the amount of HuCsv1 was observed (compare lanes 2 and 3). Interestingly, several higher molecular weight products were also immunoprecipitated from the lysate (lanes 4-6). These products were captured as a result of the formaldehyde cross-linking and in addition to HuCsv1 may contain mRNA and/or other proteins. Notably, the western blot was probed using the 3A2 monoclonal antibody reactive against all Hu proteins (including HuR). Importantly, HuR is also detected in immunoprecipitates (running at ~36kDa, slightly below HuCsv1). As such, it is also possible these complexes contain HuR.

***Testing wash buffers***

Additionally, within this experiment, a number of different stringency wash buffers were tested. The reason for doing this was that the Niranjanakumari paper tested a range of stringency wash buffers consisting of lysis buffer supplemented with some amount of urea. At the lowest stringency, washes were done simply in lysis buffer alone. Stringency was increased by addition of urea to the lysis buffer at final concentrations ranging from 1M to 4M (medium to high

stringency). In their paper, Niranjanakumari *et al* indicate that the presence of urea in the wash buffers prevented co-immunoprecipitation of target mRNA from non-cross-linked cell lysates, but had no effect on samples from cross-linked cells. They conclude that higher stringency wash buffers are presumably more reliable in that they are more likely to eliminate false positive results arising from co-immunoprecipitation of mRNA that is not cross-linked to the RNA-binding protein of interest.

For the HuCsv1 co-IP, three different stringency washes were tested. At the highest stringency, lysis buffer was supplemented with 2M urea (final concentration). For the medium stringency wash, lysis buffer alone was tested. Low stringency washing was done using 1xPBS+0.1% tween20. Following incubation with the cell lysate, antibody conjugated protein G bead slurry was washed four times (10min/wash). Interestingly, a reduction in the amount of higher molecular weight, 3A2-reactive, material was observed in the lysate washed under high stringency conditions, when compared to low stringency conditions (compare lanes 4 and 6). This reduction was matched by an increase in the amount of monomeric (~42.1kDa) HuCsv1 protein, suggesting that 2M urea may disrupt cross-linking, resulting in reduced complex formation. The medium stringency conditions also showed slightly higher abundance of monomeric myc-HuCsv1 compared to the low stringency conditions (compared lanes 5 and 6). However, the relative presence and abundance of higher molecular weight products between the medium and low stringency conditions was similar. Although the lowest stringency conditions appeared to best preserve the formation of higher molecular weight complexes (which presumably contained Hu protein in complexes with either other proteins or mRNA), subsequent RNA-IP experiments were conducted using the medium stringency wash conditions. This was done because of concern that the low stringency wash would not be sufficiently stringent to remove any contaminating reporter mRNA not specifically cross-linked to myc-HuCsv1, which would produce, false positive results in the final RT-PCR.

### RNA IP identifying HuCsv1 interactions with 3´UTR-reporter mRNAs

With the antibody and IP wash conditions finalised, a number of RNA-IP experiments were attempted. Initially, no interaction between myc-HuCsv1 and target mRNA sequences could be detected. Given the nature of the experiment it was very difficult to know how to trouble shoot this outcome, as there is no positive control to demonstrate successful co-IP of cross-linked mRNA. A number of different PCR conditions were attempted in which the number of PCR cycles was progressively increased from 25 cycles to 40 cycles in the final experiment. Additionally, higher amounts of RNAse inhibitor and a DNAse I step were included in the protocol to avoid

problems with RNA degradation and plasmid DNA contamination respectively. In the final RNA-IP experiment conducted, PCR products of the correct predicted size for both the zfcdc42-v2 and VASP 3´UTR reporter were obtained from reverse transcribed RNA, co-immunoprecipitated with HuCsv1 (Appendix 3 – figure 2). No PCR products were observed in the –RT samples or pcDNA3 control samples for the VASP 3´UTR-reporter, while a weak band was observed in several –RT samples from the zfcdc42-v2 co-transfections. These bands are likely due to a low level of contaminating 3´UTR-reporter plasmid either co-immunoprecipitating with the mRNA or accidentally introduced following RNA isolation. Because of the relatively large number of PCR cycles (40) in this final experiment, it is not surprising that a low level of contaminating reporter plasmid might be detected in –RT samples. Overall, the results from these RT-PCRs indicated both the VASP and zfcdc42-v2 3´UTR-reporter mRNA were specifically immunoprecipitated with myc-tagged HuCsv1 from co-transfected cells. As such, these data support the idea that HuCsv1 interacts specifically with both of these 3´UTR-reporter mRNAs.

Notably, this experiment was conducted both with and without formaldehyde cross-linking. The reason for this was that in order to reverse the cross-links generated by formaldehyde, it was necessary to heat the IP'd-material or the beads (following washing) at 70°C for 50 minutes. In light of the negative results obtained from previous RT-PCRs from RNA-IP experiments, it seemed possible that this heating step was causing immunoprecipitated mRNA to degrade prior to reverse transcription. To test this, in the final experiment cells were transfected and then immediately prior to formaldehyde treatment (*ie* following tyrpsinisation) cell suspensions were divided in half. One half was subjected to formaldehyde treatment, while the other was lysed immediately and then kept on ice until both sets of lysates were ready for immunoprecipitation (approximately 1hr). Immunoprecipitated material from non-cross-linked samples was **not** heat-treated.

Interestingly, the results for the two different nHu-target 3´UTR-reporter mRNAs are slightly different. While the zfcdc42-v2 3´UTR reporter was found to co-IP with mycHuCsv1 in both cross-linked and non-cross-linked cell lysates, the VASP 3´UTR-reporter mRNA appeared to only immunoprecipitate when cells were cross-linked with formaldehyde (Appendix 3 – figure 2). This result highlighted the need for formaldehyde cross-linking in this experiments to capture intracellular, molecular interactions prior to lysis as without cross-linking, this interaction appears to be lost. It also indicated that heat-treatment of lysates can be used to reverse formaldehyde cross-links without completely degrading the immunoprecipitated mRNA.

Frustratingly, PCR products of the correct predicted size were observed in both +RT and –RT samples for the control 3´UTR-reporter samples from both cross-linked and non-cross-linked cell lysates. (Appendix 3 – figure 3). Given the similar intensity of PCR products in the + and – RT samples, it seems likely the purified RNA (following extraction) was contaminated with control 3´UTR-reporter plasmid, prior to its reverse transcription. In an attempt to overcome this problem, PCR using primers specific for the endogenously expressed TATA box-Binding Protein (TBP) was performed on cDNA from cross-linked cell lysates of cells co-transfected with HuCsv1 (Appendix 3 – figure 3: *bottom gel*). The mRNA encoding TBP is a highly abundant transcript in mammalian cells and is commonly used as a normalisation control in real-time and semi-quantitative RT-PCRs (QIAGEN – *see reference at end of section*). A highly expressed, non-target, endogenous mRNA was chosen in an effort to replicate as closely as possible the high abundance of the 3´UTR-reporter mRNAs present in cell lysates. It was expected that given the TBP mRNA is not a predicted nHu protein target, negative results for this PCR, from cDNA samples positive for an interaction with the reporter mRNA, would provide some evidence to support the conclusion that the interaction between HuCsv1 and 3´UTR-reporter mRNA was specific and not the result of either general RNA binding by HuCsv1 at the time of cross-linking, or insufficient washing of IP'd material prior to RNA recovery.

Indeed, the results for the TBP RT-PCR do not show an interaction between HuCsv1 and the TBP mRNA. As such, at the time, the results for the two predicted target 3´UTR-reporter mRNAs were thought to be indicative of specific interactions between HuCsv1 and the 3´UTR sequences of the reporter mRNAs. However, as described, the Northern results questioned the validity of these results, suggesting an interaction would be expected to occur; regardless of the 3´UTR sequence present in the reporter mRNA, through an interaction with the firefly luciferase coding sequence. Frustratingly, the plasmid contamination in the control 3´UTR-reporter prevents definitive confirmation of this. Importantly, the results from the TBP RT-PCR were encouraging as they suggest the interactions detected by the RNA-IP experiment are genuine, and did not arise from non-specific RNA interactions at the time of cross-linking or insufficient washing prior to RNA recovery. However, the TBP data was also mis-leading in that it did not control for interactions occurring between HuCsv1 and reporter mRNA sequences other than the CLIP-identified 3´UTRs.

In conclusion, shortly after the final RNA-IP experiment, it became clear from the firefly luciferase Northern experiments that 3´UTR-independent interactions between HuCsv1 and the firefly luciferase reporter sequence were occurring in co-transfected cells. As such while the RNA-IP experiments cannot be used to show 3´UTR-specific interactions between HuCsv1 and either the VASP or zfcdc42-v2 3´UTR-reporters (firefly luc), these experiments go most of the way to showing that this protocol does work and are a proof of principle that RNA-IP can be used to specifically identify interactions between HuCsv1 and predicted mRNA targets.

QIAGEN reference for TBP -
http://www.qiagen.com/products/pcr/quantitect/housekeepinggenes.aspx#Human

Web page first accessed July 2008. Information current and correct at 11th March 2011.

## Final RNA-IP protocol for myc-tagged HuCsv1

1. Plate cells the night before transfection so that cell density at time of transfection is ~60%. In the case of Neuro-2a cells this corresponded to ~1x$10^6$ cells/10cm tissue culture dish.
2. Cells transfected with 3´UTR-reporter vector (38fmol) and 6µg of either pmHuCsv1 or empty pcDNA3 vector complexed with 20µL of FuGENE6 (Roche). *All plasmids prepared by cesium chloride purification as described in main methods*.
3. Approximately 18 hours post-transfection aspirate media and wash cells once with pre-warmed (37°C) 1xPBS (Gibco). Aspirate 1xPBS and add 1mL of trypsin (Gibco) per dish.
4. Incubate cells for 5 minutes at 37°C and then add 2mL of pre-warmed media containing 10% fetal calf serum to inactivate the trypsin. Gently lift cells from the dish by drawing up media with a 10mL pipette and washing across the surface of the dish. Collect resuspended cells in a 30mL yellow capped tube and pellet by centrifugation for 2 minutes at 1,200rpm (~240 x g).
5. Aspirate media and wash once with 10mL pre-warmed 1xPBS. Pellet, aspirate and resuspend cells in 7.5mL 1% formaldehyde (Merck) made up in 1xPBS. Incubate at room temp for 10 minutes to cross-link. After 10 minutes add 2.5mL of 1M glycine pH 7.5 (0.25M final concentration) and then pellet cells by centrifugation for 2 minutes at 240 x g (at 4°C).
6. Aspirate and wash twice with ice-cold 1xPBS (10mL/wash). After the second wash resuspend cells in 1mL 1xPBS and transfer to a 1.5mL microcentrifuge tube and pellet cells by centrifugation for 2 minutes at 240 x g (at 4°C).
7. Aspirate and resuspend cells in 150µL of Sonication buffer containing protease and RNAse inhibitors. Sonicate cell suspensions for 8 minutes (30 seconds on, 30 seconds off) using a Bioruptor (Diagenode) set to HIGH.
8. Following sonication, make up lysates to 1500µL with RNA-IP buffer containing protease and RNAse inhibitors and then centrifuge for 10 minutes at 16,000 x g (4°C).
9. In a new 1.5mL microcentrifuge tube wash 25µL of Protein G coated sepharose beads (Sigma) twice with RNA-IP buffer plus inhibitors. Aspirate wash solution after second wash and add lysate.
10. Preclear lysate against Protein G beads by incubation at 4°C for two hours on a nutator.

11. While lysate pre-clears, complex 75µL of (washed) Protein G beads with 3µg of anti-myc antibody (Sigma – C3956) in 300µL of RNA-IP buffer plus inhibitors. Allow beads/antibody to complex at 4°C for two hours on a nutator.
12. After 2 hours wash beads four times with 500µL RNA-IP buffer plus inhibitors. Aspirate buffer after fourth wash and add pre-cleared lysate. Incubate lysate with antibody-coated beads overnight at 4°C on a nutator.
13. The following day, aspirate (and save) depleted lysate and wash beads three times with RNA-IP buffer plus inhibitors. After the third wash in RNA-IP buffer, wash beads once with 500uL of 1x Turbo DNAse buffer (Ambion).
14. Resuspend beads in 100uL 1x Turbo DNAse buffer and add 2µL Turbo DNAse. Incubate at 37°C for 30 minutes.
15. Aspirate DNAse solution and wash three times with RNA-IP buffer + inhibitors. After third wash, resuspend beads in 100µL Collection buffer.
16. Incubate beads for 50 minutes at 70°C (this step reverse the formaldehyde cross-linking).
17. Collect supernatant (this should be the co-immunoprecipitated RNA). Beads can be stored at -80°C for western analysis to confirm immunoprecipitation.
18. Extract RNA from supernatant using TRI Reagent (Ambion). Briefly, to 100µL RNA solution, add 300µL TRI reagent and 80µL chloroform. Vortex and incubate for 10 minutes at room temperature.
19. Centrifuge samples at 13,200 x g for 10 minutes at 4°C.
20. Collect aqueous (top) phase and precipitate RNA using 300µL isopropanol (original volume of TRI reagent) with 1µL of glycogen. Allow precipitation to occur for one hour at room temperature.
21. Pellet RNA by centrifugation at 16,000 x g for 10 minutes at 4°C. Wash once with 75% ethanol. Briefly dry RNA – a pellet may or may not be visible. And resuspend in 5µL of RNAse-free MQ $H_2O$.
22. Reverse transcribe all 5µL of RNA using Superscript III (Invitrogen) with random hexamers as per the manufacturers instructions.
23. PCR reactions performed using 3´UTR-specific primers and 3µL of cDNA template with Taq DNA polymerase (Invitrogen). PCR primers and cycling conditions given in the table below.
24. PCR products separated in a 2% agarose gel (containing ethidium bromide) and PCR products visualised using the Typhoon Trio variable mode imager using the ethidium bromide setting in fluorescence detection mode.

***3´UTR-specific primers***

VASP forward primer – CACACACACACAATCACCCAGG

VASP reverse primer – TGTTTTAGCCTCTTCAGTGCTGC

:: expected product size of 355nt

zfcdc42-v2 forward primer – TGAAACGCAGCGAAAACGG

zfcdc42-v2 reverse primer – AGACGAACAGAACTCCCAAGAGC

:: expected product size of 277nt

control 3´UTR forward primer – GCAGAAGTTGGTCGTGAGG

control 3´UTR reverse primer – CAGGGCGTATCTCTTCATAGC

:: expected product size of 180nt

***TBP-specific primers***

Forward – AGGCAACACAGGGAACCTCAGG

Reverse – TATTCGGCGTTTCGGGCACG

:: expected product size of 350nt

***PCR conditions***

Denaturing -94°C 1 minute

Followed by 40 cycles of:

94°C – 15 seconds

62°C – 15 seconds

72°C – 1 minute

Final elongation step at 72°C for 5 minutes

| Lanes: | |
|---|---|
| 1 = 1% input | 4 = 15% (rel. to input) IP material + high stringency wash |
| 2 = 1% pre-cleared input | 5 = 15% (rel. to input) IP material + medium stringency wash |
| 3 = 1% depleted | 6 = 15% (rel. to input) IP material + low stringency wash |

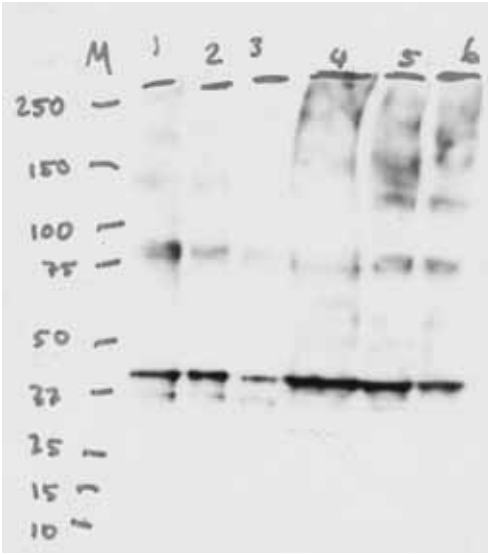


IP: Rb-αmyc (C3956)

WB: Mus-αHuR (3A2)

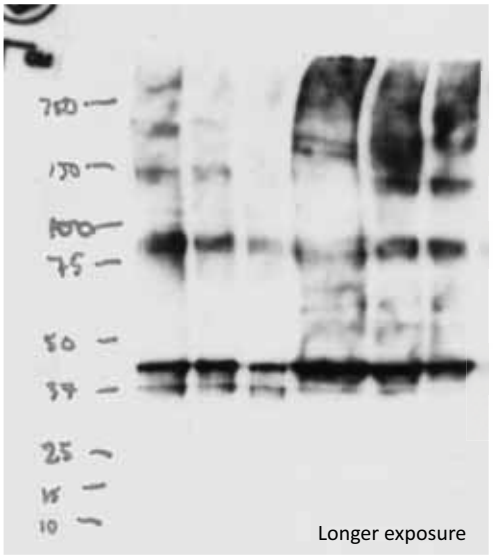


High MW HuCsv1/HuR complexes

myc-HuCsv1 (42.1 kDa)

HuR (36.2 kDa)

4-12% tris-glycine gel

Appendix 3 – Figure 1. Western blot results for IP using the rabbit α-myc antibody (C3956 – Sigma). Transfected HeLa cells were formaldehyde cross-linked prior to lysis. Lysates were precleared against proteinA/G sepharose. Precleared lysates were then added to antibody-coated beads and immunoprecipitation carried out for 2 hours at room temperature. Depleted lysate was collected and then beads divided into three lots and washed under high, medium or low stringency conditions.

1% of total lysate, precleared lysate and depleted lysate and 50% of IP material was used for western analysis. IP material/wash = 30% of total, 50% of this was run per sample, therefore 15% of total IP'd material per wash condition.

Western blot probed with an α-HuR monoclonal (3A2 – Santa Cruz Biotech). Short and long exposures of the same blot are presented.

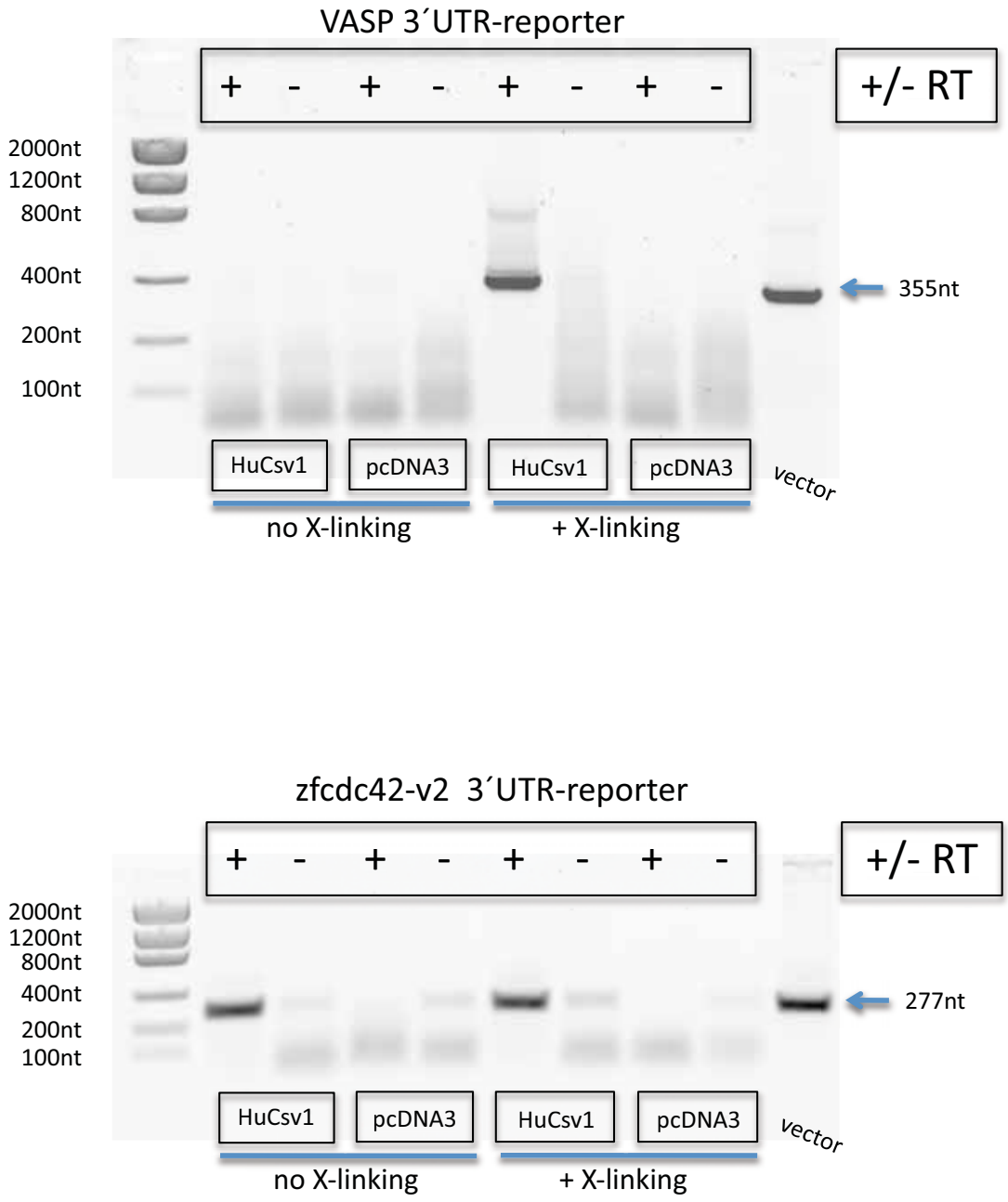


Appendix 3 – Figure 2. Digital scans of RT-PCR results from final RNA-IP for VASP and zfcdc42-v2 3´UTR-reproters. Reverse transcription and 3´UTR-specific PCR was carried out on immunoprecipitated RNA from both cross-linked and non-cross-linked cell lysates. A positive control (3´UTR-reporter plasmid – called **vector** in figures) was used to indicate the expected size of PCR products from experimental samples.

TOP GEL - VASP 3´UTR-reporter: a PCR product of the expected size was obtained from HuCsv1 co-transfected cells that had been cross-linked prior to lysis.

BOTTOM GEL - zfcdc42-v2 3´UTR-reporter: a PCR product of the expected size was obtained from HuCsv1 co-transfected cells that had been cross-linked prior to lysis and from non-cross-linked cell lysate.

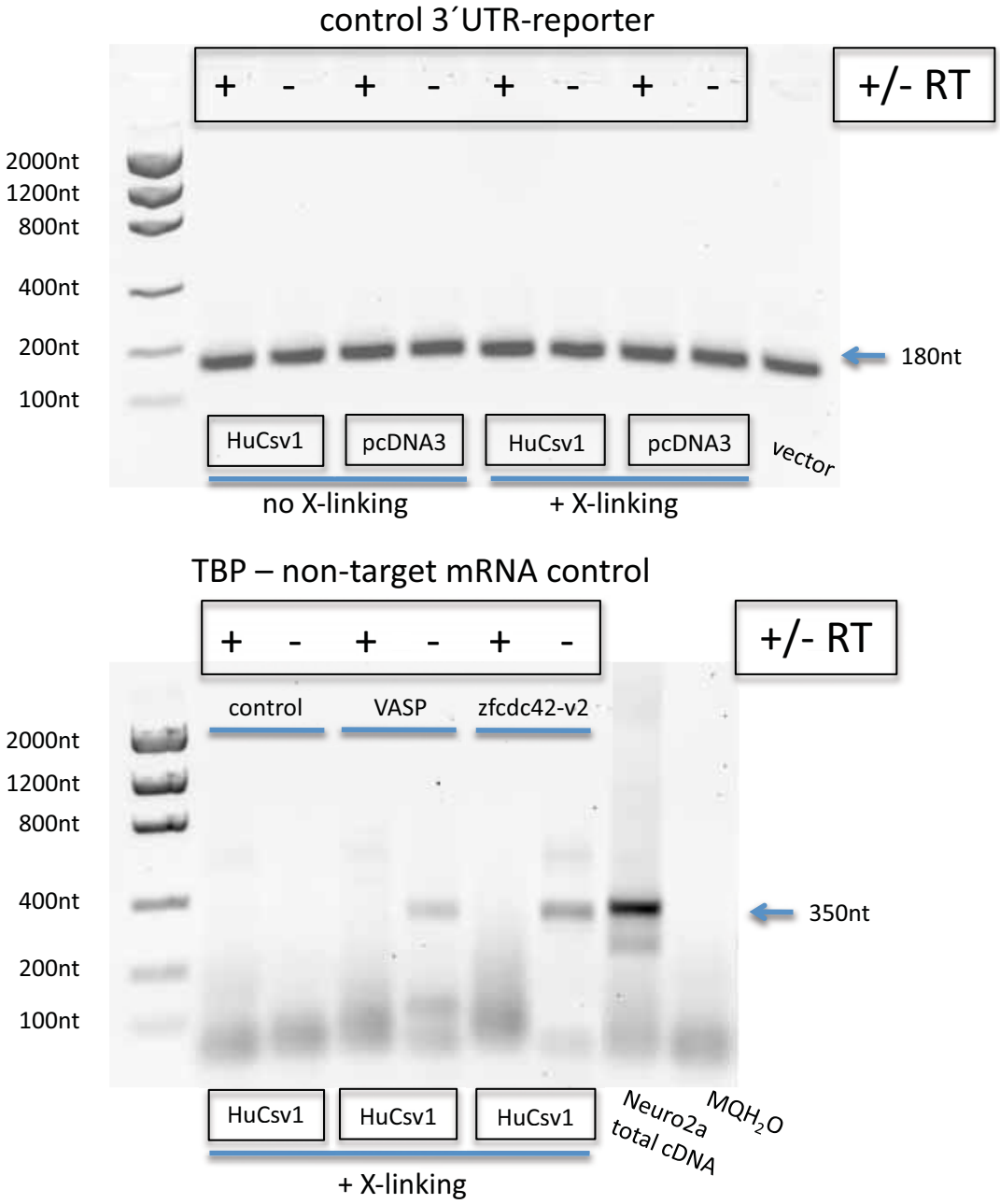


Appendix 3 – Figure 3. Digital scans of RT-PCR results from the final RNA-IP experiment testing for the presence of mRNAs encoding either the control 3´UTR-reporter or TATA-box Binding Protein (endogenous expression) in the indicated samples. Reverse transcription and 3´UTR-specific PCR was carried out on immunoprecipitated RNA from both cross-linked and non-cross-linked cell lysates. For the TBP RT-PCR, only samples from cross-linked cells co-transfected with HuCsv1 were tested. The 3´UTR-reporter plasmid was used as a positive control and to indicate expected PCR product size (top gel; last lane – **vector**). Reverse transcribed total RNA from Neuro-2a cells was used as template for the TBP positive control (bottom gel; 2nd to last lane – **total cDNA**).

TOP GEL - control 3´UTR-reporter: a PCR product of the expected size was obtained for all samples. This result appears to be due to vector contamination.

BOTTOM GEL – TATA-box Binding Protein negative control: a PCR product of the expected size was obtained from Neuro-2a total cDNA. Additionally, weak bands were detected in the non-reverse transcribed (RT-) samples for the VASP and zfcdc42-v2 samples.

## Materials and Methods

### 3´UTR cloning and reporter vector design

The HuCsv1 overexpression construct was obtained using primers to amplify the open reading frame from mouse P4 brain total RNA reverse transcribed into cDNA using Superscipt III (Invitrogen). This cloned sequence was ligated into the pcDNA3 (Invitrogen) vector such that an N-terminal myc tag was added. This vector was called pmHuCsv1 and was used for all HuCsv1 overexpression experiments.

### Fluorescence-based 3´UTR-reporter vectors

The d2EGFP open reading frame including Kozak sequence from pd2EGFP (Clontech) was cloned into pCI (Clontech) using Kpn1 and XbaI restriction sites. This vector was called pCI_d2EGFP and was used as the control 3´UTR reporter vector for the fluorescence-based 3´UTR-reporter assays.

The 3´UTR sequences for rat cdc42, cofilin and zebrafish cold-inducible RNA-binding protein were cloned using the primer sequences provided below. 3´UTR sequences from rat were cloned from cDNA reverse transcribed from total brain RNA from E18 rat embryos. Zebrafish 3´UTR sequences were cloned from total genomic DNA. All PCRs to amplify 3´UTR sequences used Accuprime I Supermix (Invitrogen). 3´UTR sequences were cloned in a two-step process. The first round of PCR employed 3´UTR-specific primers to amplify the complete 3´UTR sequences.

***Primers for rcdc42-v2:***

Fwd = TAAACCGTTTTCTCCTTC

Rev = TAAACAAACAATTGTATAATT

***Primers for rCofilin:***

Fwd = TGGAGGGCAAGCCTTTG

Rev = GTTAATTAGCCTTTTTATTGTG

***Primers for zfCIRBP:***

Fwd = CACACGAGTAAAAAAACCCCGATTG

Rev = CGGAGGCAAAAGAAATCAGAGCG

Amplified 3´UTR sequences were isolated by gel extraction (QIAGEN) following separation by agarose gel electrophoresis in 1% agarose gels.

Purified 3´UTR amplification products were then used in a second round of PCR to attach specific restriction sites to the 5´ and 3´ ends.

***Primers for rcdc42-v2:***

Fwd = AAT**GCTAGC**TAAACCGTTTTCTCCTTC; *adds NheI site*

Rev = AAT**CTCGAG**TAAACAAACAATTGTATAATT; *adds XhoI site*

***Primers for rCofilin:***

Fwd = AT**TCTAGA**TGGAGGGCAAGCCTTTG; *adds XbaI site*

Rev = AT**GTCGAC**GTTAATTAGCCTTTTTATTGTG; *adds SalI site*

***Primers for zfCIRBP:***

Fwd = GAGAAG**TCTAGA**CACACGAGTAAAAAAACCCCGATTG; *adds XbaI site*

Rev = AGAGAA**GTCGAC**GGAGGCAAAAGAAATCAGAGCG; *adds SalI site*

Amplified 3´UTR sequences were isolated by gel extraction (QIAGEN) following separation by agarose gel electrophoresis in 1% agarose gels.

Following gel extraction purified PCR products were subjected to restriction digestion using restriction enzymes (New England Biolabs). The pCI_d2EGFP vector was digested with XbaI and SalI to generate compatible ends for ligation with digested PCR-amplified 3´UTR sequences. Following digestion the vector was treated with calf intestinal phosphatase (New England Biolabs) to prevent re-ligation of incompletely digested vector. Digested 3´UTR sequences and vector sequence were purified by separation in a 1% agarose gel and gel extracted (QIAGEN). Ligation was carried out using T4 DNA ligase (New England Biolabs) as per the manufacturers instructions. **NOTE//** It was not possible to amplify the rcdc42-v2 3´UTR with primers incorporating XbaI or SalI sites, as sequences for both of these enzymes were present in the rcdc42-v2 3´UTR sequence. As such, NheI and XhoI were used which make compatible ends for XbaI and SalI respectively. Ligation products were transformed into DH5α heat-shock competent bacteria and plated on solid L-agar containing 50ug/mL Ampicillin. The vectors produced from this ligation were called pCI_d2EGFP-rcdc42-v2 and pCI_d2EGFP-rcofilin.

## Firefly luciferase-based 3´UTR-reporter vectors

The cloning of firefly luciferase from pGL3 (Promega) into pCI (Clontech) was not as straight forward as for d2EGFP because of a lack of compatible restriction sites. As such a two-step, sequential digestion reaction was performed for both vectors.

***Obtaining the firefly luciferase coding sequence from pGL3***

The pGL3 vector was digested using HindIII (New England Biolabs) for 2.5hr at 37°C followed by heat killing at 65°C for 20min. DNA polI, large (Klenow) fragment was then added to the heat-inactivated digestion reaction (supplemented with dNTPs at a final concentration of 33μM) to blunt the HindIII liberated DNA ends by 5´ to 3` end-filling. After 30min at ~22°C, the digest reaction was heat inactivated at 75°C for 5min. Following heat-inactivation, XbaI was added to the reaction and incubated for 3hr at 37°C to free the blunt-ended firefly luciferase coding sequence from pGL3. The firefly luciferase coding sequence was isolated by agarose gel electrophoresis using a 1%-agarose gel and purified by gel extraction (QIAGEN).

***Generating a pCI vector backbone with compatible ends for the firefly luciferase fragment***

pCI was digested, first with MluI for 2.5hr at 37°C followed by heat-inactivation, blunt-ending and digestion with XbaI as above. Following digestion, purified pCI was isolated by agarose gel electrophoresis using a 1%-agarose gel followed by gel extraction (QIAGEN). The firefly luciferase coding sequence was ligated into pCI using T4 DNA ligase as per the manufacturers instructions. Ligation products were transformed into DH5α heat-shock competent bacteria and plated on solid L-agar containing 50ug/mL Ampicillin. The vector produced from this ligation was called pCI-FL and was used as a control 3´UTR reporter vector for the firefly luciferase-based 3´UTR-reporter assays.

The 3´UTR sequences for mouse and zebrafish 3´UTR-reporter vectors were amplified from genomic DNA templates using Accuprime I Supermix (Invitrogen). As previous, primers were designed to amplify 3´UTR sequences in a two-step process. 3´UTR-specific primers were used first to amplify the complete 3´UTR sequences, followed by identical primers to which specific restriction sites were included.

***Primers for VASP***

Fwd = CATAGTCCCACAGAAACTGATGG

Rev = CAAACGTGTTAATGGCAAGG

Fwd = AGAGGA**TCTAGA**CATAGTCCCACAGAAACTGATGG; *adds XbaI site*

Rev = AGAGGA**CCCGGG**CAAACGTGTTAATGGCAAGG; *adds XmaI site*

***Primers for mcdc42-v1***

Fwd = GTGTGTGCTGCTATGAACG

Rev = GTCACATTCTCATTTCTAAATACC

Fwd = TTTTT**TCTAGA**GTGTGTGCTGCTATGAACG; *adds XbaI site*

Rev = TTTTA**GCGGCCGC**GTCACATTCTCATTTCTAAATACC; *adds NotI site*

***Primers for mcdc42-v2***

Fwd = GAAGTGCTGTATATTCTAAACC

Rev = CAAGGGGAGTCAAAGAAGC

Fwd = TTGAGAAA**CCCGGG**GAAGTGCTGTATATTCTAAACC; *adds XmaI site*

Rev = TAGAGAAA**GCGGCCGC**CAAGGGGAGTCAAAGAAGC; *adds NotI site*

***Primers for zfcdc42-v1***

Fwd = GTAAATGTGTGCTGCTATGAGC

Rev = AGTGAGTGGAACATGATAAAGG

Fwd = TTTTT**TCTAGA**GTAAATGTGTGCTGCTATGAGC; *adds XbaI site*

Rev = TTTTA**CCCGGG**AGTGAGTGGAACATGATAAAGG; *adds XmaI site*

***Primers for zfcdc42-v2***

Fwd = CTCCTGAAACGCAGCGAAAACG

Rev = GTGCAGCCCTAGTTCAAACC

Fwd = AAGGGA**TCTAGA**CTCCTGAAACGCAGCGAAAACG; *adds XbaI site*

Rev = AGAGAG**CCCGGG**GTGCAGCCCTAGTTCAAACC; *adds XmaI site*

***Primers for mCofilin***

Fwd = GTTCTGGCCTTCCCAAACTGC

Rev = CTTACTAGGGACTGAACTAGAGG

Fwd = TTTTT**TCTAGA**GTTCTGGCCTTCCCAAACTGC; *adds XbaI site*

Rev = TTTTA**CCCGGG**CTTACTAGGGACTGAACTAGAGG; *adds XmaI site*

***Primers for zfCofilin***

Fwd = GATTGAGGCTGACACATTTCAGG

Rev = CATCCCCAACGGAACCACTC

Fwd = TTTTT**<u>TCTAGA</u>**GATTGAGGCTGACACATTTCAGG; *adds XbaI site*

Rev = TTTTT**<u>CCCGGG</u>**CATCCCCAACGGAACCAC; *adds XmaI site*

Following PCR amplification products were gel extracted, digested with their respective enzymes and ligated into pCI-FL as described above.

**NOTE//** The Xβ-globin 3´UTR reporter (control) was generated by subcloning the Xβ-globin 3´UTR from pXT7 (a gift from J Eisen) into the pCI-FL vector.

## Renilla luciferase-based 3´UTR-reporter vectors

Renilla luciferase 3´UTR-reporter vectors were generated by subcloning the 3´UTR sequences from the Xβ-globin, zfcdc42-v2 and zfCofilin firefly luciferase-based reporter vectors into the phRL-CMV (Promega) vector which is essentially identical to the pCI-FL vector designed here, with the firefly luciferase coding sequence replaced with that of renilla luciferase. The internal control vector used was pCMV-sport-βgal (Invitrogen). Transfections for RNA extraction (Northern) used 80ng/well; this was scaled down to 32ng/well for reporter activity assays in 12-well plates.

***For all vectors***, following confirmation of correct ligation by dideoxy chain termination DNA sequencing, reporter vectors were re-transformed into DH5α cells and spread on L-agar plates containing 50μg/mL ampicillin. Individual colonies for each vector were picked and grown in small volume, agitated liquid cultures (4mL luria broth containing 50μg/mL ampicillin) for ~8 hours at 37°C to get them to logarithmic phase growth. Large volume cultures (300mL luria broth containing 50μg/mL ampicillin) were then inoculated with 300μL of the starter culture and grown overnight (~16hrs) at 37°C. Cultures were spun down and plasmid obtained by alkaline lysis followed by phenol/chloroform/isoamyl alcohol (25:24:1) extraction. Plasmid DNA was then precipitated and further purified by cesium chloride isopycnic density gradient ultracentrifugation. The cesium chloride plasmid purification protocol is included at the end of this section.

A stock vector solution was stored at -20°C at high concentration. All reporter assays were performed using working stocks diluted with1xTE down to 1μg/μL for nHu vectors and 100ng/μL for 3´UTR-reporter vectors.

## Fluorescence-based 3´UTR-reporter assays in 293T cells

***Cell culture***

Very low passage number HEK293T cell stocks (3-5 passages) were expended for use in these assays. Expanded stocks were maintained for a maximum of 20 passages and then discarded and freshly expanded from original stocks. Cells were passaged every three to four days and maintained in DMEM (Gibco) supplemented with 10% fetal calf serum and 1% penicillin/streptomycin. Cells were grown at 37°C and 5% $CO_2$. Approximately 24 hours prior to transfection, cells were passaged and plated in 6-well dishes (Falcon) at 200,000 cells/well. 18-24hrs later cells were transfected (at 50%-70% confluence) using FuGENE6 (Roche).

***Transfections and lysate collection***

A variety of DNA/FuGENE6 amounts were used throughout the course of the experiments, as described in relevant results sections. In general, transfection complexes were made up and left 30min prior to addition to cells. Duration of culturing following transfection was also variable ranging from 24hr to 48hr as indicated in relevant results sections. For lysate collection, whole cell lysates were obtained by aspirating media followed by a gentle resuspension of cells in 1mL pre-warmed (37°C) filter-sterilised 1xPBS (-$Mg^{2+}$/$Ca^{2+}$ - Gibco). Cells were transferred to a 1.5mL microfuge tube and pelleted at 4,000rpm (1,500x*g*). The supernatant was then aspirated and cells lysed in 40µL PXL2 lysis buffer (1xPBS, 0.5% DOC, 1% NP-40), containing Complete Protease Inhibitor (Roche). Following lysis, lysates were spun down at 16.1x$10^3$xg and clarified lysates transferred to a new microfuge tube.

***Serum starvation***

For serum starvation conditions, cells were transfected as described and left to take up FuGENE6/DNA complexes for 12hrs. Following incubation, media was aspirated, cells washed 2x with pre-warmed 1xPBS and then media replaced with pre-warmed DMEM lacking fetal calf serum and supplemented with 1% penicillin/streptomycin. Cells were left for 24hrs under these conditions and then harvested directly, as indicated.

***Cold-shock***

For cold-shock conditions, cells were transfected as described and incubated for 24hrs. Following incubation cells were transferred to a 32°C incubator (no $CO_2$ injection) and incubated for a further 1hr prior to lysis as described.

***Determination of total protein amounts in lysates***

Total protein concentrations for each sample were determined by Bradford analysis. Briefly, 1µL of lysate was added to 999µL of 1xBradford reagent (Bio-Rad) and transferred to a spectrophotometer cuvette. Three standard protein amounts (10µg, 2.5µg and 0.5µg) were made up using bovine serum albumin and used to calibrate the Bradford assay function of a Biophotometer (Eppendorf). Bradford reagent/lysate (or BSA for calibrations) mixtures were left for ~15 minutes prior to measurement. Following calibration, all measurements were taken sequentially and in the order of their making to minimise variation due to differences in incubation time.

***SDS-PAGE and fluorescent western blot***

Several different types of polyacrylamide gel were tested during throughout the fluorescence-based reporter assays. Best results were obtained using pre-poured 4%-12% gradient NuPAGE gels (Invitrogen) run in 1xMOPS buffer. Other gels used were pre-poured 4%-12% gradient Criterion gels (BioRad) run in 1xMOPS buffer as well as homemade 10 and 12% denaturing bis-tris acrylamide gels run in 1xGTS buffer. In all cases, gels were run at 150V for 1-2hours as necessary.

Prior to SDS-PAGE, 4µL of 5x SDS-load buffer was added to 20µg of lysate (as determined by Bradford assay) and total volumes made up to 20µL using neat lysis buffer as required. ECL-plex fluorescent size markers (Amersham) were run in every gel.

Following separation, proteins were transferred onto Hybond-LFP PVDF membrane (Amersham) by semi-dry transfer. Briefly, Whatman paper cut into gel-sized portions was soaked for 3 minutes in semi-dry transfer buffer (24mM Tris, 192mM glycine, 20% methanol). PVDF membrane, also cut to gel-size, was wetted (5 seconds) with 100% methanol and then soaked for 5 minutes in semi-dry transfer buffer. On the semi-dry transfer apparatus (Transblot SD - BioRad), 4 pieces of soaked whatman were laid out followed by the PVDF membrane and then the gel containing the separated proteins, followed by 4 more pieces of soaked whatman. Transfer was conducted at 15V for 45min. After transfer the membrane was blocked for 30min at room temperature in 1xPBST (1xPBS+0.1% Tween20).

***Antibodies***

Antibodies used for immunofluorescent detection included; mouse monoclonal anti-EGFP (JL-8 - Clontech) at 1:1500, human Hu-syndrome PND patient antiserum “Cs” (a gift from Dr Robert

Darnell) at 1:3000 and rabbit polyclonal anti-Actin (A2066 - Sigma) at 1:1500. Primary antibodies dilutions were made up in 3mL of 1xPBST and used simultaneously. Secondary antibodies used include; anti-mouse (715-165-150), anti-rabbit (711-495-152) and anti-human (709-485-149) antibodies all raised in donkey and conjugated with Cy3, Cy5 or FITC fluorophores (Jackson). Secondary antibodies were all diluted 1:1000 in 3mL of 1xPBST and used simultaneously. Following blocking, membranes were incubated with primary antibody solutions overnight at 4°C. Following incubation with the primary antibodies membranes washed 4x in 1xPBST for 15 minutes/wash. Membranes were then incubated with secondary antibodies for 1 hour at room temperature in the dark. Membranes washed as described and then dried at room temperature overnight in the dark.

***Membrane imaging and fluorescence quantification***

Dried membranes were scanned using a Typhoon Trio 9410 Variable Mode Imager (GE Lifesciences) to image and quantify antibody staining. For detection, the scanner was set to detect fluorescence and the specific channels for detection selected (ie Cy3, Cy5 and/or FITC). As a starting point the PMT (photomultiplier threshold) for all channels was set to 450, this value was increased where signal was too low (rare) or decreased when signal was too high. Scans were taken at 100µm/pixel resolution. Quantification of band fluorescence intensity was carried out using the Typhoon-associated Image Quant software package for PC **(**GE Lifesciences**)**. Briefly, for each channel scanned, fluorescence intensity was determined using the Volume Report feature for each band. Under the western blotting conditions used (excess primary and secondary antibody for blotting relative to antigen; fluorescence intensity is linearly related to protein quantity. This information was then exported to Excel (Microsoft) for generation of graphs and statistical analysis.

For visual reproduction of scanned membranes, the ".gel" files generated by the Typhoon Imaging software were saved and a duplicate file converted to ".tif". These files could then be opened and manipulated using Photoshop CS (Adobe). Files were left as 16-bit Greyscale images. The only manipulation performed to membrane scans using Photoshop was to set the intensity levels of each channel to the first detected pixel at both the white and black end of the light spectrum. For membranes in which data was collect in multiple channels (*ie*. 2 or more proteins detected) individual channels were processed as described and then combined as individual channels in a separate RGB file for simultaneous visualisation of channels. This manipulation false colours each channel to red, green or blue.

## Firefly luciferase reporter assays

***Cell culture***

Three cell lines were used in the firefly luciferase reporter assays; HEK293T, HeLa and Neuro-2a. HEK293T cell stocks were as described, Neuro-2a cell were also from very low passage number (3-5 passages) stocks. As for HEK293T cells, Neuro-2a cells were maintained for 20 passages and then discarded and freshly expanded. HeLa cell stocks were of unknown passage number and maintained for 20 passages before discarded and freshly expanded. Expanded lines were maintained in DMEM supplemented with 10% fetal calf serum and 1% penicillin. Cells were passaged every 3-4 days. For transfections cells were split 18-24hrs prior to transfections and seeded at densities to obtain ~50% confluence 24hr after seeding. When seeding into 12-well plates for luciferase assays this equated to approximately $7x10^4$ HEK293T or Neuro-2a cells and $6x10^4$ HeLa cells. When seeding into 6-well plates for RNA extraction this equated to approximately $1.8x10^5$ HEK293T or Neuro-2a cells and $1.5x10^5$ HeLa cells.

***Transfections***

A variety of DNA/FuGENE6 amounts were used throughout the course of the experiments, as described in relevant results sections. In general, transfection complexes were made up and left 30min prior to addition to cells. Duration of culturing following transfection was kept to approximately 18hrs.

***Dual Luciferase Assays***

Cells were plated in 12-well plates as described above. Collection of lysates for dual luciferase assays (Promega) was as follows. Media from transfected cells was aspirated and cells washed once with pre-warmed 1xPBS – $Mg^{2+}$, $Ca^{2+}$ (Gibco). Cells were then lysed directly in the plate using Passive Lysis Buffer (Promega). Cells were left 15min at room temp for lysis and then frozen down at -20°C for a minimum of 2hrs and no longer than overnight. Dual luciferase assays were conducted as per the manufacturers instructions using lysate and reagent amounts as stated in the relevant results sections. ***NOTE:*** Both the LARII and Stop&Glo reagents used for the dual luciferase assay were kept a frozen stocks at -80°C for up to 6 months with no apparent loss in activity. Dual luciferase assays were conducted using the Glomax96® luminometer (Promega) as per the manufacturers instructions. Luciferase activity data was exported directly to Excel (Microsoft) and all normalisation and statistical analysis conducted using Excel.

***RNA extraction - Northerns***

Cells were plated in 6-well plates as described above. For RNA extraction media was aspirated and 1mL of Trireagent (Ambion or Sigma) added directly to cells. Because prolonged incubation of Trireagent is tissue culture plasticware is not recommended, cells were quickly scraped and transferred into 1.5mL microfuge tubes. Once transferred, RNA extraction was as per the manufacturers instructions. Purified RNA was resuspended in 10uL of RNAse-free MQ$H_2O$ and stored at -20°C. RNA concentration was determined using an Eppendorf Biophotometer.

***Northern Blot***

Full Northern protocol as described by Sambrook and Russell ([263] Chapter 7.42). Briefly, 20ug of total RNA was separated by formaldehyde/agarose gel electrophoresis in 2%agarose gels. RNA was transferred to Hybond N+ nylon membrane (GE Lifesciences) by non-alkaline upward capillary transfer overnight. Following transfer, RNA was UV cross-linked to the membrane using a Stratalinker (Stratagene) set to auto cross-link. Following cross-linking the membrane was dried until ready for probing.

***α-$^{32}$P-labelled probe synthesis***

Probe labelling was as described by Sambrook and Russell ([263] chapter 9.7). Briefly, pCI-FL was digested with SphI and XbaI followed by agarose gel electrophoresis and gel extraction to isolate an ~1kb fragment of the firefly luciferase coding sequence. Likewise an ~1kb fragment from the renilla luciferase coding sequence was digested from the phRL-CMV vector by digestion with NheI and XbaI. A 600nt PCR fragment of a conserved region of the mouse GAPDH coding sequence was kindly donated by Dr James Hughes and used as a template for synthesis of the GAPDH probe. ~25ng of either the firefly or renilla luciferase DNA fragment or the mGAPDH PCR fragment was then used as template for random priming using random hexamers to incorporate α-32P ATP (specific activity 3000Ci/nmol – Perkin Elmer) into DNA probes using DNA polI Large (Klenow) fragment (3´=>5´ exo-) (New England Biolabs). Reactions were incubated at 37°C for 1hr and then purified from unincorporated nucleotides using a G-25 sephadex quick-spin column (Roche). 1µL of newly synthesised probe was used to measure specific activity of probe using a scintillation counter. Yields ranged from $1.5x10^5$ – $4x10^5$ counts from a 30second read.

***Membrane probing***

Membrane probing was also according to the Ultrahyb (Ambion) manufacturers instructions. Briefly, membranes were placed in rotating HybAid glass incubation tubes and wetted with

2xSSC at 68°C, once wetted, 2xSSC was replaced with 4mL of Ultrahyb (Ambion) and membranes prehybridised for 1hr. After 1hr of prehybridisation, total probe reactions (50µL) were heated to 95°C for 4 minutes and then mixed directly into HybAid tubes with prehybridised membranes. Membranes were hybridised with probe overnight (minimum 12hrs) and then washed, wrapped in plastic wrap and placed inside a Kodak storage phosphorscreen cassette, probe side facing the intensifier screen. Screens were scanned using the Typhoon Trio 9410 Variable Mode Imager (GE Lifesciences) set to phosphorscreen. Scans were taken at 100µm/pixel resolution and saved as ".gel" files. Quantification of band intensities was performed using ImageJ64 (freely available from http://rsbweb.nih.gov/ij/) as described in the relevant results sections.

For firefly/renilla luciferase mRNA blots, hybridisation with the relevant probes was done sequentially with no stripping of the membrane until both firefly and renilla had been probed. The firefly and renilla luciferase mRNAs were sufficiently different in size (FL ≈ 2.0kb – 3.5kb // RL = 1.3kb) to not require stripping, however marked differences in signal strength (very low for RL) required sequential probing to allow for long/short enough exposure for linear results. GAPDH was probed for last because the signal strength was very high and not fully removed by stripping. This was a problem because the GAPDH mRNA migrates at approximately the same size as the renilla luciferase mRNA (~1.3kb). Stripping by boiling the membrane for 5 min in 10mM Tris (pH 7.5) plus 0.1% SDS removed most of the renilla luciferase signal.

***Dibutyryl cAMP treatment of Neuro-2a cells***

For dbcAMP treatments, Neuro-2a cells were plated and transfected as described. 8hrs after transfection, media was aspirated and replaced with pre-warmed media containing dbcAMP to a final concentration of 1mM. To make stocks of dbcAMP (Sigma – A6885-25mg), 25mg (powder) was dissolved in 675µL of $MQH_2O$ to bring to a final concentration of 100mM and stored frozen at -20°C. To avoid freeze/thawing, 10µL aliquots were dispensed. One 10µL aliquot would provide enough dbcAMP one well of a 6-well plate (containing 500µL media) at a final concentration of 2mM.

## Renilla luciferase reporter assays

***Cell culture***

Only HEK 293T and Neuro-2a cells were used in the renilla luciferase reporter assays. Plating densities, transfection conditions and lysis were as described or as indicated in the relevant results section.

***Renilla Luciferase/β-galactosidase activity assays***

Renilla luciferase and β-galactosidase activity assays were carried out as follows. 5µL of lysate was used for detection of renilla luciferase activity using the Glomax96 luminometer (Promega). For these reactions only the Stop&Glo (Promega) reagent was used and measurements taken as described. Measurement of β-galactosidase activity from lysates was carried out according to Sambrook and Russell ([263] chapter 17.48). Briefly, reactions were set up in flat, clear plastic 96-well trays. Each well contained 201µL sodium phosphate buffer (0.1M, pH 7.5), 30µL of cell lysate, 3µL of 10mM $MgCl_2$. Once set up, a multichannel pipette was used to rapidly dispense 66µL ONPG (4mg/mL stock made fresh). Reactions were incubated at room temp unless otherwise indicated and allowed to proceed until yellow colour was obvious. Optical densities (OD) for each reaction were measured using a plate reader set to detect absorbance at 414nm. β-galactosidase activity data was exported directly to Excel (Microsoft) and all normalisation and statistical analysis conducted using Excel.

***RNA extraction - Northerns***

Cells were plated in 6-well plates as described above. RNA extraction conducted as described above.

***Northern Blot***

Full Northern protocol as described above.

***α-$^{32}$P-labelled probe synthesis***

Probe labelling was as described above. Key differences lie with the probe template. Renilla luciferase probe template was as described. β-galactosidase probe template was generated by digestion of the pCMV-Sport-β-gal with SacI and PvuII to liberate an ~700nt DNA fragment from the β-galactosidase coding sequence. Template fragment was purified as described.

***Membrane probing***

Membrane probing was performed as described above. For renilla luciferase/β-galactosidase mRNA blots, hybridisation with the relevant probes was done simultaneously. The renilla luciferase and β-galactosidase mRNAs were sufficiently different in size (RL ≈ 1.3 – 2.1kb // β-gal ~4.3kb) to not require stripping.

## Cesium Chloride DNA preps from 100 – 200mL bacterial cultures.

Notes:

- Inoculate 5mL of LB from a freshly spread plate and grow to log-phase (~8hr).
- Use this starter culture at 1 in 500 to 1 in 1000 to inoculate the plasmid prep culture. (ie 200 – 400µL of starter into 200mL LB)
- Grow at 37°C for 12-16 hours with 200rpm shaking.

1. Spin down cultures in 500mL centrifuge bottles (do not fill to the top) at 4000rpm, 10min at 4°C in the refrigerated Sigma 6K15 centrifuge (MLW lab). Pour off cleared LB.
2. Resuspend bacteria in **2.4mL solution I** by pipetting up and down until no clumps are visible. Transfer to a 50mL Falcon tube and add **0.6mL 20mg/mL lysozyme** in solution I. Incubate at RT for 10min
3. Lyse bacteria by adding **5.5 solution II** and immediately swirling gently. Incubate on ice 5min.
4. Stop lysis reaction and precipitate protein/cell debris etc by adding **2.8mL solution III** and **mixing gently by inverting the tube several times**. Incubate on ice 15min.
5. To remove white precipitate, transfer supernatant to an Oakridge tube and spin at 15,000 rpm for 10min at 4°C (JA-25 rotor in new centrifuge in the Rathjen lab).
6. Pour the cleared supernatant through a 70µm cell strainer (Falcon 2350) into a new 50mL tube.
7. Add 10mL of phenol/chloroform/isoamyl alcohol (25:24:1) and vortex then spin at 4K for 5min to separate phases.
8. Transfer aqueous (TOP) phase to an Oakridge tube and precipitate the DNA by adding 0.6 volumes of isopropanol. Vortex and leave at RT for minimum of 10min.
9. Spin at 18,000 rpm for 15min at 4°C. There should be an obvious pellet of DNA at the bottom of the tube. Pour off isopropanol wash with 5mL 70% ethanol. Spin at 10K for 5min.
10. Pour off ethanol and dry pellet by draining over kimwipe. Wipe away excess ethanol in tube with a fresh kimwipe being careful to avoid touching the DNA!

11. Resuspend pellet in 4.0mL 1xTE. For every gram of DNA solution, add 4.5grams of solid cesium chloride. As cesium chloride dissolves into the solution it causes an endothermic reaction making the solution quite cool. To speed the reaction up and ensure complete dissolution, heat the solution gently in a 37°C water bath and mix gently until all the salt is dissolved.
12. Add 200µL of 10mg/mL ethidium bromide and confirm that the refractive index of the DNA/cesium/ethidium solution is now 1.386.
13. After addition of the EtBr a fine, dark-coloured precipitate may form in the solution. If this occurs spin the solution at maximum speed in the 5810R eppendorf centrifuge (Jensen lab) for 10 minutes to clear the solution.
14. Load the cleared solution into a TLA100.4 centrifuge tube and plug the tube ensuring **no air bubbles are present.** Top up with 52% cesium solution if required.
15. With each tube capped, spin at 90,000 rpm in the ultracentrifuge for 4 hours at 22°C.

Depending on how much plasmid is present there may be a visible band in the upper to middle part of the tube distinguishable by its red colour. Conversely, it may be necessary to use a UV lamp to visualise the position of the bands with in the tube. Also, often there are two distinct bands; the upper band consists of nicked circular plasmid DNA while the lower (generally thicker) band corresponds to supercoiled (desirable) plasmid DNA.

16. Extract the banded DNA by unplugging the tube and puncturing just below the level of the band using an 18gauge needle and 5mL syringe.

(*Note: Only pull the lower band if it can be obviously identified and proceed from step 19, otherwise just pull all the DNA and go to step 17*)

17. Transfer DNA into a new TLA100.4 centrifuge tube and top up with 52% CsCl. Seal and spin at 60,000rpm in the ultracentrifuge for 12 hours at 22°C.
18. Extract band as above but this time, take care to only remove the lower, supercoiled plasmid DNA. Place extracted DNA in a 15mL plastic tube.
19. Remove ethidium from the DNA by extraction with 4mL CsCl saturated isopropanol. Once added, the ethidium moves into the upper (pink) phase and the DNA remains in the lower (slightly cloudy) phase. Remove the upper phase and repeat until no longer pink.
20. Precipitate the DNA from the CsCl containing solution by adding 2 volumes of 1xTE and 3 original volumes of isopropanol. Mix and incubate at room temp for 5min.

21. Spin at 3000rpm for 10min at room temp in Eppendorf 5810R centrifuge (KJ lab). Discard supernatant.

22. Dissolve DNA in 400µL of 1xTE and transfer to a 1.5mL eppendorf tube. Precipitate again by adding 20µL 3M NaAc and 800µL ethanol. Incubate 1min and then spin at 13,200rpm.
23. Depending on expected yield, resuspend DNA in 50 – 400µL of 1xTE (more if very high yield) and determine concentration by spectrophotometry.
24. Dialyse DNA against 1xTE to remove any residual CsCl from the solution.

**Solution 1: 0.05M glucose, 0.025M Tris pH 8.0, 0.01M EDTA**

| | **100mL** | **500mL** |
|---|---|---|
| Glucose | 0.9g | 4.5g |
| 1.0M Tris, pH8.0 | 2.5mL | 12.5mL |
| 0.5M EDTA | 2.0mL | 10.0mL |
| $H_2O$ | 95.0mL | 475.0mL |

**Solution 2: 0.2M NaOH, 1% SDS**

| | **100mL** | **500mL** |
|---|---|---|
| 5M NaOH | 4.0mL | 20.0mL |
| 20% SDS (Xi) (36/37/38) (26) | 5.0mL | 25mL |
| $H_2O$ | 91.0mL | 455.0mL |

***CAUTION*** 5M NaOH is highly caustic and can cause burns

**Solution 3: 5M KAc, pH4.8**

| | **100mL** |
|---|---|
| Glacial acetic acid(C)(10-35)(23-26-45) | 11.5mL |
| 5.0M KAc (36/37/38)(26-36) | 60.0mL |
| $H_2O$ | 28.5mL |

**52% (w/w) Cesium chloride solution:**

To 52grams of cesium chloride add **48mL TE.** Density should be ~1.55 (check refractive index 1.386)

**Isopropanol/CsCl solution:**

Add $H_2O$, solid CsCl and isopropanol so there is still some solid CsCl left at he bottom of the bottle. Two phases will form, use ONLY the top phase.

100g CsCl/75mL $H_2O$ + 500mL isopropanol

***CAUTION*** Isopropanol is FLAMMABLE

HAZARD CODE, RISK PHRASE and SAFETY PHRASE numbers refer to those listed on the Sigma-Aldrich website and found in the PDF titled **RISK AND SAFETY – SIGMA ALDRICH** on the lab server in the methods & recipes folder of the common lab items_ folder.

## Bibliography


1. Darnell RB, Posner JB (2003) Paraneoplastic syndromes involving the nervous system. N Engl J Med 349: 1543-1554.
2. Darnell RB (1996) Onconeural antigens and the paraneoplastic neurologic disorders: at the intersection of cancer, immunity, and the brain. Proc Natl Acad Sci USA 93: 4529-4536.
3. Roberts WK, Darnell RB (2004) Neuroimmunology of the paraneoplastic neurological degenerations. Curr Opin Immunol 16: 616-622.
4. Anderson NE, Rosenblum MK, Graus F, Wiley RG, Posner JB (1988) Autoantibodies in paraneoplastic syndromes associated with small-cell lung cancer. Neurology 38: 1391-1398.
5. Graus F, Cordon-Cardo C, Posner JB (1985) Neuronal antinuclear antibody in sensory neuronopathy from lung cancer. Neurology 35: 538-.
6. Dalmau J, Furneaux HM, Gralla RJ, Kris MG, Posner JB (1990) Detection of the anti-Hu antibody in the serum of patients with small cell lung cancer--a quantitative western blot analysis. Ann Neurol 27: 544-552.
7. Dalmau J, Graus F, Rosenblum MK, Posner JB (1992) Anti-Hu--associated paraneoplastic encephalomyelitis/sensory neuronopathy. A clinical study of 71 patients. Medicine 71: 59-72.
8. Szabo A, Dalmau J, Manley G, Rosenfeld M, Wong E, et al. (1991) HuD, a paraneoplastic encephalomyelitis antigen, contains RNA-binding domains and is homologous to Elav and Sex-lethal. Cell 67: 325-333.
9. Campos AR, Rosen DR, Robinow SN, White K (1987) Molecular analysis of the locus elav in Drosophila melanogaster: a gene whose embryonic expression is neural specific. EMBO J 6: 425-431.
10. Robinow S, White K (1988) The locus elav of Drosophila melanogaster is expressed in neurons at all developmental stages. Dev Biol 126: 294-303.
11. Robinow S, White K (1991) Characterization and spatial distribution of the ELAV protein during Drosophila melanogaster development. J Neurobiol 22: 443-461.
12. Campos AR, Grossman D, White K (1985) Mutant alleles at the locus elav in Drosophila melanogaster lead to nervous system defects. A developmental-genetic analysis. J Neurogenet 2: 197-218.
13. Homyk T, Jr., Isono K, Pak WL (1985) Developmental and physiological analysis of a conditional mutation affecting photoreceptor and optic lobe development in Drosophila melanogaster. J Neurogenet 2: 309-324.
14. Sakai K, Gofuku M, Kitagawa Y, Ogasawara T, Hirose G, et al. (1994) A hippocampal protein associated with paraneoplastic neurologic syndrome and small cell lung carcinoma. Biochem Biophys Res Commun 199: 1200-1208.
15. Manley GT, Smitt PS, Dalmau J, Posner JB (1995) Hu antigens: reactivity with Hu antibodies, tumor expression, and major immunogenic sites. Ann Neurol 38: 102-110.
16. Levine TD, Gao F, King PH, Andrews LG, Keene JD (1993) Hel-N1: an autoimmune RNA-binding protein with specificity for 3' uridylate-rich untranslated regions of growth factor mRNAs. Mol Cell Biol 13: 3494-3504.
17. King PH, Levine TD, Fremeau RT, Keene JD (1994) Mammalian homologs of Drosophila ELAV localized to a neuronal subset can bind in vitro to the 3' UTR of mRNA encoding the Id transcriptional repressor. J Neurosci 14: 1943-1952.
18. Good PJ (1995) A conserved family of elav-like genes in vertebrates. Proc Natl Acad Sci USA 92: 4557-4561.
19. Ma WJ, Cheng S, Campbell C, Wright A, Furneaux H (1996) Cloning and characterization of HuR, a ubiquitously expressed Elav-like protein. J Biol Chem 271: 8144-8151.

20. Okano HJ, Darnell RB (1997) A hierarchy of Hu RNA binding proteins in developing and adult neurons. J Neurosci 17: 3024-3037.
21. Fan XC, Steitz JA (1998) Overexpression of HuR, a nuclear-cytoplasmic shuttling protein, increases the in vivo stability of ARE-containing mRNAs. EMBO J 17: 3448-3460.
22. Fan XC, Steitz JA (1998) HNS, a nuclear-cytoplasmic shuttling sequence in HuR. Proc Natl Acad Sci USA 95: 15293-15298.
23. Kasashima K, Terashima K, Yamamoto K, Sakashita E, Sakamoto H (1999) Cytoplasmic localization is required for the mammalian ELAV-like protein HuD to induce neuronal differentiation. Genes Cells 4: 667-683.
24. Hing F (2011) PhD Thesis. Adelaide: University of Adelaide.
25. Maris C, Dominguez C, Allain FH-T (2005) The RNA recognition motif, a plastic RNA-binding platform to regulate post-transcriptional gene expression. FEBS J 272: 2118-2131.
26. Adam SA, Nakagawa T, Swanson MS, Woodruff TK, Dreyfuss G (1986) mRNA polyadenylate-binding protein: gene isolation and sequencing and identification of a ribonucleoprotein consensus sequence. Mol Cell Biol 6: 2932-2943.
27. Swanson MS, Nakagawa TY, LeVan K, Dreyfuss G (1987) Primary structure of human nuclear ribonucleoprotein particle C proteins: conservation of sequence and domain structures in heterogeneous nuclear RNA, mRNA, and pre-rRNA-binding proteins. Mol Cell Biol 7: 1731-1739.
28. Dreyfuss G, Swanson MS, Piñol-Roma S (1988) Heterogeneous nuclear ribonucleoprotein particles and the pathway of mRNA formation. Trends Biochem Sci 13: 86-91.
29. Bandziulis RJ, Swanson MS, Dreyfuss G (1989) RNA-binding proteins as developmental regulators. Genes Dev 3: 431-437.
30. Kenan DJ, Query CC, Keene JD (1991) RNA recognition: towards identifying determinants of specificity. Trends Biochem Sci 16: 214-220.
31. Birney E, Kumar S, Krainer AR (1993) Analysis of the RNA-recognition motif and RS and RGG domains: conservation in metazoan pre-mRNA splicing factors. Nucleic Acids Res 21: 5803-5816.
32. Park S, Myszka DG, Yu M, Littler SJ, Laird-Offringa IA (2000) HuD RNA recognition motifs play distinct roles in the formation of a stable complex with AU-rich RNA. Mol Cell Biol 20: 4765-4772.
33. Liu J, Dalmau J, Szabo A, Rosenfeld M, Huber J, et al. (1995) Paraneoplastic encephalomyelitis antigens bind to the AU-rich elements of mRNA. Neurology 45: 544-550.
34. Abe R, Sakashita E, Yamamoto K, Sakamoto H (1996) Two different RNA binding activities for the AU-rich element and the poly(A) sequence of the mouse neuronal protein mHuC. Nucleic Acids Research 24: 4895-4901.
35. Chung S, Jiang L, Cheng S, Furneaux H (1996) Purification and properties of HuD, a neuronal RNA-binding protein. J Biol Chem 271: 11518-11524.
36. Ma WJ, Chung S, Furneaux H (1997) The Elav-like proteins bind to AU-rich elements and to the poly(A) tail of mRNA. Nucleic Acids Research 25: 3564-3569.
37. Inoue M, Muto Y, Sakamoto H, Yokoyama S (2000) NMR studies on functional structures of the AU-rich element-binding domains of Hu antigen C. Nucleic Acids Research 28: 1743-1750.
38. Wang X, Tanaka Hall TM (2001) Structural basis for recognition of AU-rich element RNA by the HuD protein. Nat Struct Biol 8: 141-145.
39. Iyaguchi D, Yao M, Tanaka I, Toyota E (2009) Cloning, expression, purification and preliminary crystallographic studies of the adenylate/uridylate-rich element-binding protein HuR complexed with its target RNA. Acta Crystallogr F Struct Biol Cryst Commun 65: 285-287.

40. Fukao A, Sasano Y, Imataka H, Inoue K, Sakamoto H, et al. (2009) The ELAV protein HuD stimulates cap-dependent translation in a Poly(A)- and eIF4A-dependent manner. Mol Cell 36: 1007-1017.
41. Kasashima K, Sakashita E, Saito K, Sakamoto H (2002) Complex formation of the neuron-specific ELAV-like Hu RNA-binding proteins. Nucleic Acids Research 30: 4519-4526.
42. Fialcowitz-White EJ, Brewer BY, Ballin JD, Willis CD, Toth EA, et al. (2007) Specific protein domains mediate cooperative assembly of HuR oligomers on AU-rich mRNA-destabilizing sequences. J Biol Chem 282: 20948-20959.
43. Meisner N-C, Hintersteiner M, Mueller K, Bauer R, Seifert J-M, et al. (2007) Identification and mechanistic characterization of low-molecular-weight inhibitors for HuR. Nat Chem Biol 3: 508-515.
44. Soller M, White K (2005) ELAV multimerizes on conserved AU4-6 motifs important for ewg splicing regulation. Mol Cell Biol 25: 7580-7591.
45. Toba G, White K (2008) The third RNA recognition motif of Drosophila ELAV protein has a role in multimerization. Nucleic Acids Research 36: 1390-1399.
46. Fornerod M, Ohno M, Yoshida M, Mattaj IW (1997) CRM1 is an export receptor for leucine-rich nuclear export signals. Cell 90: 1051-1060.
47. Cullen BR (2003) Nuclear RNA export. J Cell Sci 116: 587-597.
48. Brennan CM, Gallouzi IE, Steitz JA (2000) Protein ligands to HuR modulate its interaction with target mRNAs in vivo. J Cell Biol 151: 1-14.
49. Fukuda M, Asano S, Nakamura T, Adachi M, Yoshida M, et al. (1997) CRM1 is responsible for intracellular transport mediated by the nuclear export signal. Nature 390: 308-311.
50. Gallouzi IE, Steitz JA (2001) Delineation of mRNA export pathways by the use of cell-permeable peptides. Science 294: 1895-1901.
51. Rebane A, Aab A, Steitz JA (2004) Transportins 1 and 2 are redundant nuclear import factors for hnRNP A1 and HuR. RNA 10: 590-599.
52. Pollard VW, Michael WM, Nakielny S, Siomi MC, Wang F, et al. (1996) A novel receptor-mediated nuclear protein import pathway. Cell 86: 985-994.
53. Siomi MC, Eder PS, Kataoka N, Wan L, Liu Q, et al. (1997) Transportin-mediated nuclear import of heterogeneous nuclear RNP proteins. J Cell Biol 138: 1181-1192.
54. Güttinger S, Mühlhäusser P, Koller-Eichhorn R, Brennecke J, Kutay U (2004) Transportin2 functions as importin and mediates nuclear import of HuR. 101: 2918-2923.
55. Levy NS, Chung S, Furneaux H, Levy AP (1998) Hypoxic stabilization of vascular endothelial growth factor mRNA by the RNA-binding protein HuR. J Biol Chem 273: 6417-6423.
56. Peng SS, Chen CY, Xu N, Shyu AB (1998) RNA stabilization by the AU-rich element binding protein, HuR, an ELAV protein. EMBO J 17: 3461-3470.
57. Ford LP, Wilusz J (1999) An in vitro system using HeLa cytoplasmic extracts that reproduces regulated mRNA stability. Methods 17: 21-27.
58. Chen CY, Shyu AB (1995) AU-rich elements: characterization and importance in mRNA degradation. Trends Biochem Sci 20: 465-470.
59. Chen CY, Shyu AB (1994) Selective degradation of early-response-gene mRNAs: functional analyses of sequence features of the AU-rich elements. Mol Cell Biol 14: 8471-8482.
60. Bakheet T, Frevel M, Williams BR, Greer W, Khabar KS (2001) ARED: human AU-rich element-containing mRNA database reveals an unexpectedly diverse functional repertoire of encoded proteins. Nucleic Acids Research 29: 246-254.
61. Chen CY, Gherzi R, Ong SE, Chan EL, Raijmakers R, et al. (2001) AU binding proteins recruit the exosome to degrade ARE-containing mRNAs. Cell 107: 451-464.
62. Shyu AB, Belasco JG, Greenberg ME (1991) Two distinct destabilizing elements in the c-fos message trigger deadenylation as a first step in rapid mRNA decay. Genes Dev 5: 221-231.

63. Chen CY, Xu N, Shyu AB (1995) mRNA decay mediated by two distinct AU-rich elements from c-fos and granulocyte-macrophage colony-stimulating factor transcripts: different deadenylation kinetics and uncoupling from translation. Mol Cell Biol 15: 5777-5788.
64. Wang W, Furneaux H, Cheng H, Caldwell MC, Hutter D, et al. (2000) HuR regulates p21 mRNA stabilization by UV light. Mol Cell Biol 20: 760-769.
65. Gallouzi IE, Brennan CM, Stenberg MG, Swanson MS, Eversole A, et al. (2000) HuR binding to cytoplasmic mRNA is perturbed by heat shock. 97: 3073-3078.
66. Westmark CJ, Bartleson VB, Malter JS (2005) RhoB mRNA is stabilized by HuR after UV light. Oncogene 24: 502-511.
67. Pascale A, Amadio M, Scapagnini G, Lanni C, Racchi M, et al. (2005) Neuronal ELAV proteins enhance mRNA stability by a PKCalpha-dependent pathway. Proc Natl Acad Sci USA 102: 12065-12070.
68. Kim HH, Yang X, Kuwano Y, Gorospe M (2008) Modification at HuR(S242) alters HuR localization and proliferative influence. Cell Cycle 7: 3371-3377.
69. Atasoy U, Watson J, Patel D, Keene JD (1998) ELAV protein HuA (HuR) can redistribute between nucleus and cytoplasm and is upregulated during serum stimulation and T cell activation. J Cell Sci 111 ( Pt 21): 3145-3156.
70. Kim HH, Kuwano Y, Srikantan S, Lee EK, Martindale JL, et al. (2009) HuR recruits let-7/RISC to repress c-Myc expression. Genes Dev 23: 1743-1748.
71. Wang W, Caldwell MC, Lin S, Furneaux H, Gorospe M (2000) HuR regulates cyclin A and cyclin B1 mRNA stability during cell proliferation. EMBO J 19: 2340-2350.
72. Lafarga V, Cuadrado A, Lopez de Silanes I, Bengoechea R, Fernandez-Capetillo O, et al. (2009) p38 Mitogen-activated protein kinase- and HuR-dependent stabilization of p21(Cip1) mRNA mediates the G(1)/S checkpoint. Mol Cell Biol 29: 4341-4351.
73. Ghosh M, Aguila HL, Michaud J, Ai Y, Wu M-T, et al. (2009) Essential role of the RNA-binding protein HuR in progenitor cell survival in mice. The Journal of Clinical Investigation 119: 3530-3543.
74. Cho SJ, Zhang J, Chen X (2010) RNPC1 modulates the RNA-binding activity of, and cooperates with, HuR to regulate p21 mRNA stability. Nucleic Acids Res 38: 2256-2267.
75. Dixon DA, Tolley ND, King PH, Nabors LB, McIntyre TM, et al. (2001) Altered expression of the mRNA stability factor HuR promotes cyclooxygenase-2 expression in colon cancer cells. J Clin Invest 108: 1657-1665.
76. Nabors LB, Gillespie GY, Harkins L, King PH (2001) HuR, a RNA stability factor, is expressed in malignant brain tumors and binds to adenine- and uridine-rich elements within the 3' untranslated regions of cytokine and angiogenic factor mRNAs. Cancer Res 61: 2154-2161.
77. Sengupta S, Jang BC, Wu MT, Paik JH, Furneaux H, et al. (2003) The RNA-binding protein HuR regulates the expression of cyclooxygenase-2. J Biol Chem 278: 25227-25233.
78. Champelovier P, Pautre V, Elatifi M, Dupre I, Rostaing B, et al. (2006) Resistance to phorbol ester-induced differentiation in human myeloid leukemia cells: a hypothetic role for the mRNA stabilization process. Leuk Res 30: 1407-1416.
79. Kakuguchi W, Kitamura T, Kuroshima T, Ishikawa M, Kitagawa Y, et al. (2010) HuR knockdown changes the oncogenic potential of oral cancer cells. Mol Cancer Res 8: 520-528.
80. Mrena J, Wiksten JP, Thiel A, Kokkola A, Pohjola L, et al. (2005) Cyclooxygenase-2 is an independent prognostic factor in gastric cancer and its expression is regulated by the messenger RNA stability factor HuR. Clin Cancer Res 11: 7362-7368.
81. Denkert C, Weichert W, Winzer KJ, Muller BM, Noske A, et al. (2004) Expression of the ELAV-like protein HuR is associated with higher tumor grade and increased cyclooxygenase-2 expression in human breast carcinoma. Clin Cancer Res 10: 5580-5586.

82. Niesporek S, Kristiansen G, Thoma A, Weichert W, Noske A, et al. (2008) Expression of the ELAV-like protein HuR in human prostate carcinoma is an indicator of disease relapse and linked to COX-2 expression. Int J Oncol 32: 341-347.
83. Doller A, Pfeilschifter J, Eberhardt W (2008) Signalling pathways regulating nucleo-cytoplasmic shuttling of the mRNA-binding protein HuR. Cell Signal 20: 2165-2173.
84. Leandersson K (2006) Wnt-5a mRNA translation is suppressed by the Elav-like protein HuR in human breast epithelial cells. Nucleic Acids Research 34: 3988-3999.
85. Mazan-Mamczarz K, Galbán S, López de Silanes I, Martindale JL, Atasoy U, et al. (2003) RNA-binding protein HuR enhances p53 translation in response to ultraviolet light irradiation. Proc Natl Acad Sci USA 100: 8354-8359.
86. Kim HH, Abdelmohsen K, Lal A, Pullmann R, Yang X, et al. (2008) Nuclear HuR accumulation through phosphorylation by Cdk1. Genes Dev 22: 1804-1815.
87. Abdelmohsen K, Pullmann R, Lal A, Kim HH, Galban S, et al. (2007) Phosphorylation of HuR by Chk2 regulates SIRT1 expression. Mol Cell 25: 543-557.
88. Kuwano Y, Kim HH, Abdelmohsen K, Pullmann R, Martindale JL (2008) MKP-1 mRNA Stabilization and Translational Control by RNA-Binding Proteins HuR and NF90 28: 4562.
89. Yaman I, Fernandez J, Sarkar B, Schneider RJ, Snider MD, et al. (2002) Nutritional control of mRNA stability is mediated by a conserved AU-rich element that binds the cytoplasmic shuttling protein HuR. J Biol Chem 277: 41539-41546.
90. Bhattacharyya SN, Habermacher R, Martine U, Closs EI, Filipowicz W (2006) Relief of microRNA-mediated translational repression in human cells subjected to stress. Cell 125: 1111-1124.
91. Buscemi G, Perego P, Carenini N, Nakanishi M, Chessa L, et al. (2004) Activation of ATM and Chk2 kinases in relation to the amount of DNA strand breaks. Oncogene 23: 7691-7700.
92. Brunet A, Sweeney LB, Sturgill JF, Chua KF, Greer PL, et al. (2004) Stress-dependent regulation of FOXO transcription factors by the SIRT1 deacetylase. Science 303: 2011-2015.
93. Baldin V, Lukas J, Marcote MJ, Pagano M, Draetta G (1993) Cyclin D1 is a nuclear protein required for cell cycle progression in G1. Genes Dev 7: 812-821.
94. Pagano M, Pepperkok R, Verde F, Ansorge W, Draetta G (1992) Cyclin A is required at two points in the human cell cycle. EMBO J 11: 961-971.
95. Karapetian RN, Evstafieva AG, Abaeva IS, Chichkova NV, Filonov GS, et al. (2005) Nuclear oncoprotein prothymosin alpha is a partner of Keap1: implications for expression of oxidative stress-protecting genes. Mol Cell Biol 25: 1089-1099.
96. Sherr CJ, Roberts JM (1999) CDK inhibitors: positive and negative regulators of G1-phase progression. Genes Dev 13: 1501-1512.
97. Bashir T, Pagano M (2005) Cdk1: the dominant sibling of Cdk2. Nat Cell Biol 7: 779-781.
98. Pillai RS (2005) MicroRNA function: Multiple mechanisms for a tiny RNA? RNA 11: 1753-1761.
99. Katsanou V, Milatos S, Yiakouvaki A, Sgantzis N, Kotsoni A, et al. (2009) The RNA-binding protein Elavl1/HuR is essential for placental branching morphogenesis and embryonic development. Mol Cell Biol 29: 2762-2776.
100. Levine AJ (1997) p53, the cellular gatekeeper for growth and division. Cell 88: 323-331.
101. Yi J, Chang N, Liu X, Guo G, Xue L, et al. (2010) Reduced nuclear export of HuR mRNA by HuR is linked to the loss of HuR in replicative senescence. Nucleic Acids Research 38: 1547-1558.
102. Copp AJ, Greene NDE, Murdoch JN (2003) The genetic basis of mammalian neurulation. Nat Rev Genet 4: 784-793.
103. Marusich MF, Furneaux HM, Henion PD, Weston JA (1994) Hu neuronal proteins are expressed in proliferating neurogenic cells. J Neurobiol 25: 143-155.
104. Kim CH, Ueshima E, Muraoka O, Tanaka H, Yeo SY, et al. (1996) Zebrafish elav/HuC homologue as a very early neuronal marker. Neurosci Lett 216: 109-112.

105. Park HC, Hong SK, Kim HS, Kim SH, Yoon EJ, et al. (2000) Structural comparison of zebrafish Elav/Hu and their differential expressions during neurogenesis. Neurosci Lett 279: 81-84.
106. Wakamatsu Y, Weston JA (1997) Sequential expression and role of Hu RNA-binding proteins during neurogenesis. Development 124: 3449-3460.
107. Miyata T, Kawaguchi A, Saito K, Kawano M, Muto T, et al. (2004) Asymmetric production of surface-dividing and non-surface-dividing cortical progenitor cells. Development 131: 3133-3145.
108. Miyata T, Kawaguchi A, Okano H, Ogawa M (2001) Asymmetric inheritance of radial glial fibers by cortical neurons. Neuron 31: 727-741.
109. Noctor SC, Martínez-Cerdeño V, Ivic L, Kriegstein AR (2004) Cortical neurons arise in symmetric and asymmetric division zones and migrate through specific phases. Nat Neurosci 7: 136-144.
110. Barami K, Iversen K, Furneaux H, Goldman SA (1995) Hu protein as an early marker of neuronal phenotypic differentiation by subependymal zone cells of the adult songbird forebrain. J Neurobiol 28: 82-101.
111. García-Verdugo JM, Ferrón S, Flames N, Collado L, Desfilis E, et al. (2002) The proliferative ventricular zone in adult vertebrates: a comparative study using reptiles, birds, and mammals. Brain Research Bulletin 57: 765-775.
112. Sakakibara S, Okano H (1997) Expression of neural RNA-binding proteins in the postnatal CNS: implications of their roles in neuronal and glial cell development. J Neurosci 17: 8300-8312.
113. Alvarez-Buylla A, Lois C (1995) Neuronal stem cells in the brain of adult vertebrates. Stem Cells 13: 263-272.
114. Sakakibara S, Imai T, Hamaguchi K, Okabe M, Aruga J, et al. (1996) Mouse-Musashi-1, a neural RNA-binding protein highly enriched in the mammalian CNS stem cell. Dev Biol 176: 230-242.
115. Antic D, Lu N, Keene JD (1999) ELAV tumor antigen, Hel-N1, increases translation of neurofilament M mRNA and induces formation of neurites in human teratocarcinoma cells. Genes Dev 13: 449-461.
116. Andrews PW (1984) Retinoic acid induces neuronal differentiation of a cloned human embryonal carcinoma cell line in vitro. Dev Biol 103: 285-293.
117. Gao FB, Keene JD (1996) Hel-N1/Hel-N2 proteins are bound to poly(A)+ mRNA in granular RNP structures and are implicated in neuronal differentiation. J Cell Sci 109 ( Pt 3): 579-589.
118. Akamatsu W, Okano HJ, Osumi N, Inoue T, Nakamura S, et al. (1999) Mammalian ELAV-like neuronal RNA-binding proteins HuB and HuC promote neuronal development in both the central and the peripheral nervous systems. Proc Natl Acad Sci USA 96: 9885-9890.
119. Mobarak CD, Anderson KD, Morin M, Beckel-Mitchener A, Rogers SL, et al. (2000) The RNA-binding protein HuD is required for GAP-43 mRNA stability, GAP-43 gene expression, and PKC-dependent neurite outgrowth in PC12 cells. Mol Biol Cell 11: 3191-3203.
120. Akamatsu W, Fujihara H, Mitsuhashi T, Yano M, Shibata S, et al. (2005) The RNA-binding protein HuD regulates neuronal cell identity and maturation. Proc Natl Acad Sci USA 102: 4625-4630.
121. Fox WM (1965) Reflex-ontogeny and behavioural development of the mouse. Anim Behav 13: 234-241.
122. Carter RJ, Hunt MJ, Morton AJ (2000) Environmental stimulation increases survival in mice transgenic for exon 1 of the Huntington's disease gene. Mov Disord 15: 925-937.
123. Baquet ZC, Gorski JA, Jones KR (2004) Early striatal dendrite deficits followed by neuron loss with advanced age in the absence of anterograde cortical brain-derived neurotrophic factor. J Neurosci 24: 4250-4258.
124. Koushika SP, Lisbin MJ, White K (1996) ELAV, a Drosophila neuron-specific protein, mediates the generation of an alternatively spliced neural protein isoform. Curr Biol 6: 1634-1641.
125. Koushika SP, Soller M, White K (2000) The neuron-enriched splicing pattern of Drosophila erect wing is dependent on the presence of ELAV protein. Mol Cell Biol 20: 1836-1845.

126. Soller M, White K (2003) ELAV inhibits 3'-end processing to promote neural splicing of ewg pre-mRNA. Genes Dev 17: 2526-2538.
127. Wilusz J, Shenk T, Takagaki Y, Manley JL (1990) A multicomponent complex is required for the AAUAAA-dependent cross-linking of a 64-kilodalton protein to polyadenylation substrates. Mol Cell Biol 10: 1244-1248.
128. Gilmartin GM, Nevins JR (1991) Molecular analyses of two poly(A) site-processing factors that determine the recognition and efficiency of cleavage of the pre-mRNA. Mol Cell Biol 11: 2432-2438.
129. Keller W, Bienroth S, Lang KM, Christofori G (1991) Cleavage and polyadenylation factor CPF specifically interacts with the pre-mRNA 3' processing signal AAUAAA. EMBO J 10: 4241-4249.
130. Zhu H, Hasman RA, Barron VA, Luo G, Lou H (2006) A nuclear function of Hu proteins as neuron-specific alternative RNA processing regulators. Mol Biol Cell 17: 5105-5114.
131. Adema GJ, van Hulst KL, Baas PD (1990) Uridine branch acceptor is a cis-acting element involved in regulation of the alternative processing of calcitonin/CGRP-l pre-mRNA. Nucleic Acids Research 18: 5365-5373.
132. Lou H, Gagel RF, Berget SM (1996) An intron enhancer recognized by splicing factors activates polyadenylation. Genes Dev 10: 208-219.
133. Zhu H, Hasman RA, Young KM, Kedersha NL, Lou H (2003) U1 snRNP-dependent function of TIAR in the regulation of alternative RNA processing of the human calcitonin/CGRP pre-mRNA. Mol Cell Biol 23: 5959-5971.
134. Berget SM (1995) Exon recognition in vertebrate splicing. J Biol Chem 270: 2411-2414.
135. Zhu H, Zhou H-L, Hasman RA, Lou H (2007) Hu proteins regulate polyadenylation by blocking sites containing U-rich sequences. J Biol Chem 282: 2203-2210.
136. Keene JD (2007) RNA regulons: coordination of post-transcriptional events. Nat Rev Genet 8: 533-543.
137. Filipowicz W, Bhattacharyya SN, Sonenberg N (2008) Mechanisms of post-transcriptional regulation by microRNAs: are the answers in sight? Nat Rev Genet 9: 102-114.
138. Martin KC, Ephrussi A (2009) mRNA localization: gene expression in the spatial dimension. Cell 136: 719-730.
139. Tian B, Hu J, Zhang H, Lutz CS (2005) A large-scale analysis of mRNA polyadenylation of human and mouse genes. Nucleic Acids Research 33: 201-212.
140. Zhang H, Lee JY, Tian B (2005) Biased alternative polyadenylation in human tissues. Genome Biol 6: R100.
141. Wallace AM, Dass B, Ravnik SE, Tonk V, Jenkins NA, et al. (1999) Two distinct forms of the 64,000 Mr protein of the cleavage stimulation factor are expressed in mouse male germ cells. Proc Natl Acad Sci USA 96: 6763-6768.
142. Takagaki Y, Manley JL, MacDonald CC, Wilusz J, Shenk T (1990) A multisubunit factor, CstF, is required for polyadenylation of mammalian pre-mRNAs. Genes Dev 4: 2112-2120.
143. Wagner EJ, Garcia-Blanco MA (2001) Polypyrimidine tract binding protein antagonizes exon definition. Mol Cell Biol 21: 3281-3288.
144. Castelo-Branco P, Furger A, Wollerton M, Smith C, Moreira A, et al. (2004) Polypyrimidine tract binding protein modulates efficiency of polyadenylation. Mol Cell Biol 24: 4174-4183.
145. Ashiya M, Grabowski PJ (1997) A neuron-specific splicing switch mediated by an array of pre-mRNA repressor sites: evidence of a regulatory role for the polypyrimidine tract binding protein and a brain-specific PTB counterpart. RNA 3: 996-1015.
146. Gunderson SI, Beyer K, Martin G, Keller W, Boelens WC, et al. (1994) The human U1A snRNP protein regulates polyadenylation via a direct interaction with poly(A) polymerase. Cell 76: 531-541.

147. Calvo O, Manley JL (2001) Evolutionarily conserved interaction between CstF-64 and PC4 links transcription, polyadenylation, and termination. Mol Cell 7: 1013-1023.
148. Ji Z, Lee JY, Pan Z, Jiang B, Tian B (2009) Progressive lengthening of 3' untranslated regions of mRNAs by alternative polyadenylation during mouse embryonic development. Proc Natl Acad Sci USA 106: 7028-7033.
149. Sandberg R, Neilson JR, Sarma A, Sharp PA, Burge CB (2008) Proliferating cells express mRNAs with shortened 3' untranslated regions and fewer microRNA target sites. Science 320: 1643-1647.
150. Shi Y, Di Giammartino DC, Taylor D, Sarkeshik A, Rice WJ, et al. (2009) Molecular architecture of the human pre-mRNA 3' processing complex. Mol Cell 33: 365-376.
151. Antic D, Keene JD (1998) Messenger ribonucleoprotein complexes containing human ELAV proteins: interactions with cytoskeleton and translational apparatus. J Cell Sci 111 ( Pt 2): 183-197.
152. Aranda-Abreu GE, Behar L, Chung S, Furneaux H, Ginzburg I (1999) Embryonic lethal abnormal vision-like RNA-binding proteins regulate neurite outgrowth and tau expression in PC12 cells. J Neurosci 19: 6907-6917.
153. Beckel-Mitchener AC, Miera A, Keller R, Perrone-Bizzozero NI (2002) Poly(A) tail length-dependent stabilization of GAP-43 mRNA by the RNA-binding protein HuD. J Biol Chem 277: 27996-28002.
154. Quattrone A, Pascale A, Nogues X, Zhao W, Gusev P, et al. (2001) Posttranscriptional regulation of gene expression in learning by the neuronal ELAV-like mRNA-stabilizing proteins. Proc Natl Acad Sci U S A 98: 11668-11673.
155. Manohar CF, Short ML, Nguyen A, Nguyen NN, Chagnovich D, et al. (2002) HuD, a neuronal-specific RNA-binding protein, increases the in vivo stability of MYCN RNA. J Biol Chem 277: 1967-1973.
156. Pascale A, Gusev PA, Amadio M, Dottorini T, Govoni S, et al. (2004) Increase of the RNA-binding protein HuD and posttranscriptional up-regulation of the GAP-43 gene during spatial memory. Proc Natl Acad Sci USA 101: 1217-1222.
157. Ratti A, Fallini C, Cova L, Fantozzi R, Calzarossa C, et al. (2006) A role for the ELAV RNA-binding proteins in neural stem cells: stabilization of Msi1 mRNA. J Cell Sci 119: 1442-1452.
158. Ratti A, Fallini C, Colombrita C, Pascale A, Laforenza U, et al. (2008) Post-transcriptional regulation of neuro-oncological ventral antigen 1 by the neuronal RNA-binding proteins ELAV. J Biol Chem 283: 7531-7541.
159. Aronov S, Aranda G, Behar L, Ginzburg I (2002) Visualization of translated tau protein in the axons of neuronal P19 cells and characterization of tau RNP granules. J Cell Sci 115: 3817-3827.
160. Smith CL, Afroz R, Bassell GJ, Furneaux HM, Perrone-Bizzozero NI, et al. (2004) GAP-43 mRNA in growth cones is associated with HuD and ribosomes. J Neurobiol 61: 222-235.
161. Aronov S, Aranda G, Behar L, Ginzburg I (2001) Axonal tau mRNA localization coincides with tau protein in living neuronal cells and depends on axonal targeting signal. J Neurosci 21: 6577-6587.
162. Chung S, Eckrich M, Perrone-Bizzozero N, Kohn DT, Furneaux H (1997) The Elav-like proteins bind to a conserved regulatory element in the 3'-untranslated region of GAP-43 mRNA. J Biol Chem 272: 6593-6598.
163. Anderson KD, Morin MA, Beckel-Mitchener A, Mobarak CD, Neve RL, et al. (2000) Overexpression of HuD, but not of its truncated form HuD I+II, promotes GAP-43 gene expression and neurite outgrowth in PC12 cells in the absence of nerve growth factor. J Neurochem 75: 1103-1114.

164. Campbell DS, Holt CE (2001) Chemotropic responses of retinal growth cones mediated by rapid local protein synthesis and degradation. Neuron 32: 1013-1026.
165. Brunet I, Weinl C, Piper M, Trembleau A, Volovitch M, et al. (2005) The transcription factor Engrailed-2 guides retinal axons. Nature 438: 94-98.
166. Wu KY, Hengst U, Cox LJ, Macosko EZ, Jeromin A, et al. (2005) Local translation of RhoA regulates growth cone collapse. Nature 436: 1020-1024.
167. Leung K, Van Horck F, Lin A, Allison R, Standart N, et al. (2006) Asymmetrical β-actin mRNA translation in growth cones mediates attractive turning to netrin-1. Nat Neurosci 9: 1247-1256.
168. Yao J, Sasaki Y, Wen Z, Bassell G, Zheng J (2006) An essential role for β-actin mRNA localization and translation in Ca2+-dependent growth cone guidance. Nat Neurosci 9: 1265-1273.
169. Piper M, Anderson R, Dwivedy A, Weinl C, van Horck F, et al. (2006) Signaling mechanisms underlying Slit2-induced collapse of Xenopus retinal growth cones. Neuron 49: 215-228.
170. Van Kesteren R (2006) Local Synthesis of Actin-Binding Protein -Thymosin Regulates Neurite Outgrowth. Journal of Neuroscience 26: 152-157.
171. Lin AC, Holt CE (2008) Function and regulation of local axonal translation. Curr Opin Neurobiol 18: 60-68.
172. Wang DO, Martin KC, Zukin RS (2010) Spatially restricting gene expression by local translation at synapses. Trends Neurosci 33: 173-182.
173. Ross AF, Oleynikov Y, Kislauskis EH, Taneja KL, Singer RH (1997) Characterization of a beta-actin mRNA zipcode-binding protein. Mol Cell Biol 17: 2158-2165.
174. Hüttelmaier S, Zenklusen D, Lederer M, Dictenberg J, Lorenz M, et al. (2005) Spatial regulation of β-actin translation by Src-dependent phosphorylation of ZBP1. Nature 438: 512-515.
175. Sasaki Y, Welshhans K, Wen Z, Yao J, Xu M, et al. (2010) Phosphorylation of zipcode binding protein 1 is required for brain-derived neurotrophic factor signaling of local beta-actin synthesis and growth cone turning. J Neurosci 30: 9349-9358.
176. Darnell JC, Jensen KB, Jin P, Brown V, Warren ST, et al. (2001) Fragile X mental retardation protein targets G quartet mRNAs important for neuronal function. Cell 107: 489-499.
177. Antar LN, Dictenberg JB, Plociniak M, Afroz R, Bassell GJ (2005) Localization of FMRP-associated mRNA granules and requirement of microtubules for activity-dependent trafficking in hippocampal neurons. Genes Brain Behav 4: 350-359.
178. Napoli I, Mercaldo V, Boyl PP, Eleuteri B, Zalfa F, et al. (2008) The fragile X syndrome protein represses activity-dependent translation through CYFIP1, a new 4E-BP. Cell 134: 1042-1054.
179. Bolognani F, Perrone-Bizzozero NI (2008) RNA-protein interactions and control of mRNA stability in neurons. J Neurosci Res 86: 481-489.
180. Benowitz LI, Routtenberg A (1997) GAP-43: an intrinsic determinant of neuronal development and plasticity. Trends Neurosci 20: 84-91.
181. Bolognani F, Qiu S, Tanner DC, Paik J, Perrone-Bizzozero NI, et al. (2007) Associative and spatial learning and memory deficits in transgenic mice overexpressing the RNA-binding protein HuD. Neurobiol Learn Mem 87: 635-643.
182. Doller A, Huwiler A, Müller R, Radeke HH, Pfeilschifter J, et al. (2007) Protein Kinase C alpha-dependent phosphorylation of the mRNA-stabilizing factor HuR: implications for posttranscriptional regulation of cyclooxygenase-2. Mol Biol Cell 18: 2137-2148.
183. Doller A, Schlepckow K, Schwalbe H, Pfeilschifter J, Eberhardt W (2010) Tandem phosphorylation of serine 221 and 318 by PKC{delta} coordinates mRNA binding and nucleo-cytoplasmic shuttling of HuR. Mol Cell Biol.
184. Ule J, Jensen KB, Ruggiu M, Mele A, Ule A, et al. (2003) CLIP identifies Nova-regulated RNA networks in the brain. Science 302: 1212-1215.

185. Ule J, Jensen K, Mele A, Darnell RB (2005) CLIP: a method for identifying protein-RNA interaction sites in living cells. Methods 37: 376-386.
186. Mili S, Steitz JA (2004) Evidence for reassociation of RNA-binding proteins after cell lysis: implications for the interpretation of immunoprecipitation analyses. RNA 10: 1692-1694.
187. Jensen KB, Dredge BK, Stefani G, Zhong R, Buckanovich RJ, et al. (2000) Nova-1 regulates neuron-specific alternative splicing and is essential for neuronal viability. Neuron 25: 359-371.
188. Dredge BK, Darnell RB (2003) Nova regulates GABA(A) receptor gamma2 alternative splicing via a distal downstream UCAU-rich intronic splicing enhancer. Mol Cell Biol 23: 4687-4700.
189. Licatalosi DD, Darnell RB (2010) RNA processing and its regulation: global insights into biological networks. Nat Rev Genet 11: 75-87.
190. Licatalosi DD, Mele A, Fak JJ, Ule J, Kayikci M, et al. (2008) HITS-CLIP yields genome-wide insights into brain alternative RNA processing. Nature 456: 464-469.
191. Yeo GW, Coufal NG, Liang TY, Peng GE, Fu X-D, et al. (2009) An RNA code for the FOX2 splicing regulator revealed by mapping RNA-protein interactions in stem cells. Nat Struct Mol Biol 16: 130-137.
192. Sanford JR, Wang X, Mort M, Vanduyn N, Cooper DN, et al. (2009) Splicing factor SFRS1 recognizes a functionally diverse landscape of RNA transcripts. Genome Res 19: 381-394.
193. Chi SW, Zang JB, Mele A, Darnell RB (2009) Argonaute HITS-CLIP decodes microRNA-mRNA interaction maps. Nature.
194. Hafner M, Landthaler M, Burger L, Khorshid M, Hausser J, et al. (2010) Transcriptome-wide identification of RNA-binding protein and microRNA target sites by PAR-CLIP. Cell 141: 129-141.
195. Wiszniak S (2011) Investigating mechanisms of post-transcriptional gene regulation in the germ cells of zebrafish. [PhD]. Adelaide: University of Adelaide.
196. Brown MD, Cornejo BJ, Kuhn TB, Bamburg JR (2000) Cdc42 stimulates neurite outgrowth and formation of growth cone filopodia and lamellipodia. J Neurobiol 43: 352-364.
197. Garvalov BK, Flynn KC, Neukirchen D, Meyn L, Teusch N, et al. (2007) Cdc42 regulates cofilin during the establishment of neuronal polarity. J Neurosci 27: 13117-13129.
198. Gehler S (2004) Brain-Derived Neurotrophic Factor Regulation of Retinal Growth Cone Filopodial Dynamics Is Mediated through Actin Depolymerizing Factor/Cofilin. Journal of Neuroscience 24: 10741-10749.
199. Lebrand C, Dent EW, Strasser GA, Lanier LM, Krause M, et al. (2004) Critical role of Ena/VASP proteins for filopodia formation in neurons and in function downstream of netrin-1. Neuron 42: 37-49.
200. Gatlin JC, Estrada-Bernal A, Sanford SD, Pfenninger KH (2006) Myristoylated, alanine-rich C-kinase substrate phosphorylation regulates growth cone adhesion and pathfinding. Mol Biol Cell 17: 5115-5130.
201. Lee H, Engel U, Rusch J, Scherrer S, Sheard K, et al. (2004) The microtubule plus end tracking protein Orbit/MAST/CLASP acts downstream of the tyrosine kinase Abl in mediating axon guidance. Neuron 42: 913-926.
202. Yao KM, Samson ML, Reeves R, White K (1993) Gene elav of Drosophila melanogaster: a prototype for neuronal-specific RNA binding protein gene family that is conserved in flies and humans. J Neurobiol 24: 723-739.
203. Schramm M, Falkai P, Pietsch T, Neidt I, Egensperger R, et al. (1999) Neural expression profile of Elav-like genes in human brain. Clin Neuropathol 18: 17-22.
204. Perron M, Furrer MP, Wegnez M, Théodore L (1999) Misexpression of the RNA-binding protein ELRB in Xenopus presumptive neurectoderm induces proliferation arrest and programmed cell death. Int J Dev Biol 43: 295-303.

205. Amato MA, Boy S, Arnault E, Girard M, Della Puppa A, et al. (2005) Comparison of the expression patterns of five neural RNA binding proteins in the Xenopus retina. J Comp Neurol 481: 331-339.
206. Carruthers S, Mason J, Papalopulu N (2003) Depletion of the cell-cycle inhibitor p27(Xic1) impairs neuronal differentiation and increases the number of ElrC(+) progenitor cells in Xenopus tropicalis. Mech Dev 120: 607-616.
207. Huang MT, Gorman CM (1990) Intervening sequences increase efficiency of RNA 3' processing and accumulation of cytoplasmic RNA. Nucleic Acids Research 18: 937-947.
208. Evans MJ, Scarpulla RC (1989) Introns in the 3'-untranslated region can inhibit chimeric CAT and beta-galactosidase gene expression. Gene 84: 135-142.
209. Le Hir H, Nott A, Moore MJ (2003) How introns influence and enhance eukaryotic gene expression. Trends Biochem Sci 28: 215-220.
210. Heasman SJ, Ridley AJ (2008) Mammalian Rho GTPases: new insights into their functions from in vivo studies. Nat Rev Mol Cell Biol 9: 690-701.
211. Gallo G, Letourneau PC (2004) Regulation of growth cone actin filaments by guidance cues. J Neurobiol 58: 92-102.
212. Marks PW, Kwiatkowski DJ (1996) Genomic organization and chromosomal location of murine Cdc42. Genomics 38: 13-18.
213. Lee CJ, Irizarry K (2003) Alternative splicing in the nervous system: an emerging source of diversity and regulation. Biol Psychiatry 54: 771-776.
214. Kang R, Wan J, Arstikaitis P, Takahashi H, Huang K, et al. (2008) Neural palmitoyl-proteomics reveals dynamic synaptic palmitoylation. Nature 456: 904.
215. Govek EE, Newey SE, Van Aelst L (2005) The role of the Rho GTPases in neuronal development. Genes Dev 19: 1-49.
216. Ridley AJ (2006) Rho GTPases and actin dynamics in membrane protrusions and vesicle trafficking. Trends Cell Biol 16: 522-529.
217. Bamburg JR (1999) Proteins of the ADF/cofilin family: essential regulators of actin dynamics. Annu Rev Cell Dev Biol 15: 185-230.
218. Meberg PJ, Ono S, Minamide LS, Takahashi M, Bamburg JR (1998) Actin depolymerizing factor and cofilin phosphorylation dynamics: response to signals that regulate neurite extension. Cell Motility and the Cytoskeleton 39: 172-190.
219. Meberg PJ, Bamburg JR (2000) Increase in neurite outgrowth mediated by overexpression of actin depolymerizing factor. J Neurosci 20: 2459-2469.
220. Marsick BM, Flynn KC, Santiago-Medina M, Bamburg JR, Letourneau PC (2010) Activation of ADF/cofilin mediates attractive growth cone turning toward nerve growth factor and netrin-1. Devel Neurobio 70: 565-588.
221. Aizawa H, Wakatsuki S, Ishii A, Moriyama K, Sasaki Y, et al. (2001) Phosphorylation of cofilin by LIM-kinase is necessary for semaphorin 3A-induced growth cone collapse. Nat Neurosci 4: 367-373.
222. Lee S (2003) Organization and translation of mRNA in sympathetic axons. J Cell Sci 116: 4467-4478.
223. Willis D, Li KW, Zheng J-Q, Chang JH, Smit A, et al. (2005) Differential transport and local translation of cytoskeletal, injury-response, and neurodegeneration protein mRNAs in axons. J Neurosci 25: 778-791.
224. Aranda-Abreu GE, Hernández ME, Soto A, Manzo J (2005) Possible Cis-acting signal that could be involved in the localization of different mRNAs in neuronal axons. Theoretical biology & medical modelling 2: 33.
225. AmershamBioscience (2005) Application note 28-4015-40 AB.
226. Sherf B (1996) Dual-Luciferase® reporter assay: An advanced co-reporter

technology integrating firefly and Renilla luciferase assays. Promega Notes 57: 2-9.
227. Thompson JF, Hayes LS, Lloyd DB (1991) Modulation of firefly luciferase stability and impact on studies of gene regulation. Gene 103: 171-177.
228. Rasband W (1997-2009) ImageJ. U.S. National Institutes id Health.
229. Sternberg S (1983) Biomedical Image Processing. Computer 16: 22-34.
230. Tay HG, Ng YW, Manser E (2010) A vertebrate-specific Chp-PAK-PIX pathway maintains E-cadherin at adherens junctions during zebrafish epiboly. PLoS ONE 5: e10125.
231. Boshart M, Weber F, Jahn G, Dorsch-Häsler K, Fleckenstein B, et al. (1985) A very strong enhancer is located upstream of an immediate early gene of human cytomegalovirus. Cell 41: 521-530.
232. Rosenberger P, Khoury J, Kong T, Weissmüller T, Robinson AM, et al. (2007) Identification of vasodilator-stimulated phosphoprotein (VASP) as an HIF-regulated tissue permeability factor during hypoxia. The FASEB Journal 21: 2613-2621.
233. Mayr C, Bartel DP (2009) Widespread shortening of 3'UTRs by alternative cleavage and polyadenylation activates oncogenes in cancer cells. Cell 138: 673-684.
234. Lisbin MJ, Gordon M, Yannoni YM, White K (2000) Function of RRM domains of Drosophila melanogaster ELAV: Rnp1 mutations and rrm domain replacements with ELAV family proteins and SXL. Genetics 155: 1789-1798.
235. Scotto-Lavino E, Du G, Frohman MA (2006) 3' end cDNA amplification using classic RACE. Nature Protocols 1: 2742-2745.
236. Millevoi S, Vagner S (2009) Molecular mechanisms of eukaryotic pre-mRNA 3' end processing regulation. Nucleic Acids Research.
237. Keryer-Bibens C, Barreau C, Osborne HB (2008) Tethering of proteins to RNAs by bacteriophage proteins. Biol Cell 100: 125-138.
238. Tan R, Frankel AD (1995) Structural variety of arginine-rich RNA-binding peptides. Proc Natl Acad Sci USA 92: 5282-5286.
239. Jones-Villeneuve EM, McBurney MW, Rogers KA, Kalnins VI (1982) Retinoic acid induces embryonal carcinoma cells to differentiate into neurons and glial cells. J Cell Biol 94: 253-262.
240. Bain G, Gottlieb DI (1998) Neural cells derived by in vitro differentiation of P19 and embryonic stem cells. Perspect Dev Neurobiol 5: 175-178.
241. Dotti CG, Sullivan CA, Banker GA (1988) The establishment of polarity by hippocampal neurons in culture. J Neurosci 8: 1454-1468.
242. Da Silva JS, Dotti CG (2002) Breaking the neuronal sphere: regulation of the actin cytoskeleton in neuritogenesis. Nat Rev Neurosci 3: 694-704.
243. Wiggin GR, Fawcett JP, Pawson T (2005) Polarity proteins in axon specification and synaptogenesis. Dev Cell 8: 803-816.
244. Barnes AP, Polleux F (2009) Establishment of axon-dendrite polarity in developing neurons. Annu Rev Neurosci 32: 347-381.
245. Brewer GJ (1995) Serum-free B27/neurobasal medium supports differentiated growth of neurons from the striatum, substantia nigra, septum, cerebral cortex, cerebellum, and dentate gyrus. J Neurosci Res 42: 674-683.
246. Thweatt R, Goldstein S, Shmookler Reis RJ (1990) A universal primer mixture for sequence determination at the 3' ends of cDNAs. Anal Biochem 190: 314-316.
247. Borson ND, Salo WL, Drewes LR (1992) A lock-docking oligo(dT) primer for 5' and 3' RACE PCR. PCR Methods Appl 2: 144-148.
248. Stork PJS, Schmitt JM (2002) Crosstalk between cAMP and MAP kinase signaling in the regulation of cell proliferation. Trends Cell Biol 12: 258-266.

249. Impey S, McCorkle SR, Cha-Molstad H, Dwyer JM, Yochum GS, et al. (2004) Defining the CREB regulon: a genome-wide analysis of transcription factor regulatory regions. Cell 119: 1041-1054.
250. Abel T, Nguyen PV, Barad M, Deuel TA, Kandel ER, et al. (1997) Genetic demonstration of a role for PKA in the late phase of LTP and in hippocampus-based long-term memory. Cell 88: 615-626.
251. Lohof AM, Quillan M, Dan Y, Poo MM (1992) Asymmetric modulation of cytosolic cAMP activity induces growth cone turning. J Neurosci 12: 1253-1261.
252. Piper M, van Horck F, Holt C (2007) The role of cyclic nucleotides in axon guidance. Adv Exp Med Biol 621: 134-143.
253. Song HJ, Poo MM (1999) Signal transduction underlying growth cone guidance by diffusible factors. Curr Opin Neurobiol 9: 355-363.
254. Krylova O, Messenger MJ, Salinas PC (2000) Dishevelled-1 regulates microtubule stability: a new function mediated by glycogen synthase kinase-3beta. J Cell Biol 151: 83-94.
255. Tremblay RG, Sikorska M, Sandhu JK, Lanthier P, Ribecco-Lutkiewicz M, et al. (2009) Differentiation of mouse Neuro 2A cells into dopamine neurons. Journal of Neuroscience Methods.
256. Fickenscher H, Stamminger T, Rüger R, Fleckenstein B (1989) The role of a repetitive palindromic sequence element in the human cytomegalovirus major immediate early enhancer. J Gen Virol 70 ( Pt 1): 107-123.
257. Imagawa M, Chiu R, Karin M (1987) Transcription factor AP-2 mediates induction by two different signal-transduction pathways: protein kinase C and cAMP. Cell 51: 251-260.
258. Mitchell PJ, Wang C, Tjian R (1987) Positive and negative regulation of transcription in vitro: enhancer-binding protein AP-2 is inhibited by SV40 T antigen. Cell 50: 847-861.
259. Vasudevan S, Steitz JA (2007) AU-rich-element-mediated upregulation of translation by FXR1 and Argonaute 2. Cell 128: 1105-1118.
260. Danckwardt S, Kaufmann I, Gentzel M, Foerstner KU, Gantzert A-S, et al. (2007) Splicing factors stimulate polyadenylation via USEs at non-canonical 3' end formation signals. EMBO J 26: 2658-2669.
261. West S, Proudfoot NJ, Dye MJ (2008) Molecular dissection of mammalian RNA polymerase II transcriptional termination. Mol Cell 29: 600-610.
262. Niranjanakumari S, Lasda E, Brazas R, Garcia-Blanco MA (2002) Reversible cross-linking combined with immunoprecipitation to study RNA-protein interactions in vivo. Methods 26: 182-190.
263. Sambrook JR, David (2001) Molecular Cloning: a laboratory manual. Cold Spring Harbor, New York: Cold Spring Harbor Laboratory Press. 2,2344 p.

## Addendum

Corrections to the original thesis document are listed below.

1.) Figure legends from figures 33, 34 and Appendix 2 figure 7 all incorrectly state that the 28S ribosomal RNA migrates at 1.9kb in the Northern blots presented. The sentence should read:

> The approximate location of the *18S* ribosomal RNA (1.9kb) is indicated.

2.) Figure legends for figures 41, 42 and 43 incorrectly label the LacZ transfection control as the "loading control". The sentence should read:

> Total RNA from transfected 293T cells was probed with a radiolabelled DNA probe complementary to the renilla luciferase coding sequence and a second probe complementary to the LacZ coding sequence (as a *transfection control*).